

Discomfort glare from daylight in classrooms

Abreu Vieira Viula, R.J.

DOI

[10.7480/abe.2022.14](https://doi.org/10.7480/abe.2022.14)

Publication date

2022

Document Version

Final published version

Citation (APA)

Abreu Vieira Viula, R. J. (2022). *Discomfort glare from daylight in classrooms*. [Dissertation (TU Delft), Delft University of Technology]. A+BE | Architecture and the Built Environment.
<https://doi.org/10.7480/abe.2022.14>

Important note

To cite this publication, please use the final published version (if applicable).
Please check the document version above.

Copyright

Other than for strictly personal use, it is not permitted to download, forward or distribute the text or part of it, without the consent of the author(s) and/or copyright holder(s), unless the work is under an open content license such as Creative Commons.

Takedown policy

Please contact us and provide details if you believe this document breaches copyrights.
We will remove access to the work immediately and investigate your claim.



Discomfort glare from daylight in classrooms

Raquel Viula

Discomfort glare from daylight in classrooms

Raquel Viula



22#14

Design | Sirene Ontwerpers, Véro Crickx

Cover photo | # Ceiling of the Forum of the Eckenberg Gymnasium by Ecker Architekten. Image by John Ruffolo.

Keywords | #Daylighting, discomfort glare, metrics, classrooms.

ISBN 978-94-6366-591-9

ISSN 2212-3202

© 2022 Raquel Viula

This dissertation is open access at <https://doi.org/10.7480/abe.2022.14>

Attribution 4.0 International (CC BY 4.0)

This is a human-readable summary of (and not a substitute for) the license that you'll find at:
<https://creativecommons.org/licenses/by/4.0/>

You are free to:

Share — copy and redistribute the material in any medium or format

Adapt — remix, transform, and build upon the material
for any purpose, even commercially.

This license is acceptable for Free Cultural Works.

The licensor cannot revoke these freedoms as long as you follow the license terms.

Under the following terms:

Attribution — You must give appropriate credit, provide a link to the license, and indicate if changes were made. You may do so in any reasonable manner, but not in any way that suggests the licensor endorses you or your use.

Unless otherwise specified, all the photographs in this thesis were taken by the author. For the use of illustrations effort has been made to ask permission for the legal owners as far as possible. We apologize for those cases in which we did not succeed. These legal owners are kindly requested to contact the author.

Discomfort glare from daylight in classrooms

Dissertation

for the purpose of obtaining the degree of doctor
at Delft University of Technology
by the authority of the Rector Magnificus, prof.dr.ir. T.H.J.J. van der Hagen
chair of the Board for Doctorates
to be defended publicly on
Wednesday 7 September 2022 at 17:30 o'clock

by

Raquel José ABREU VIEIRA VIULA
Master of Advanced Environmental and Energy Studies,
University of East London, UK
born in Funchal, Portugal

This dissertation has been approved by the promotor.

Composition of the doctoral committee:

Rector Magnificus, Dr. R.M.J. Bokel Dr.ir. M.J. Tenpierik	chairperson Delft University of Technology, promotor Delft University of Technology, promotor
---	---

Independent members:

Prof.dr. S.C. Pont	Delft University of Technology
Prof.ir. M.F. Asselbergs	Delft University of Technology
Prof.dr. L. Bellia	University of Naples Federico II, Italy
Prof.dr. M. Overend	Delft University of Technology
Dr. E. Brembilla	Delft University of Technology

This research was funded by the Portuguese Foundation for Science and Technology (Fundação para a Ciência e a Tecnologia) under the POCH and QREN programmes with funds from the Portuguese Ministry of Education and Science and from the European Social Fund, with an individual doctoral research grant for the period 12/2014 to 12/2018 (SFRH/BD/93536/2013), which is thankfully acknowledged.



To Jorge

Acknowledgements

This work would have never been possible without the direct or indirect support from many individuals that I would like to thank:

- Peter Luscuere and Truus Hordjik, for accepting me as a PhD student and for their tutoring in the initial part of my research.
- My promotors, Regina Bokel and Martin Tenpierik, for their courage to dive into the subject of this dissertation with myself, for their suggestions and advice in many tutoring sessions, for giving me the time I needed to complete the different PhD tasks and for their help with the mathematical aspects of this dissertation.
- The members of the PhD defense committee, for taking the time to read this dissertation and provide their comments.
- My colleagues at the TU Delft AE+T department, Dadi Zhang, Marco Ortiz Sanchez, Tatiana Armijos Moya, Marjolein Overtoom, Michiel Fremouw, Tiantian Du, Xiaoyu Du, Minyoung Kwon, Joana Gonçalves and Nick ten Caat, for their companionship and for the experiences we shared within and outside PhD life.
- All the participants in my experimental work and those that helped me in sourcing participants.
- Jan Wienold, for the interest showed on my research since the beginning, for the advice provided throughout the years, for sharing his pf2pic tool that become crucial in speeding up the analysis and for his availability to respond to my questions on the use of *evalglare*.
- Sylvia Jansen for always being available to respond to my questions on statistics.
- Jorge Gil, whom I owe so much in the form of both personal and professional support, for taking care of the domestic aspects of our life when I wasn't available, for always offering a positive outlook on my work, for helping me with the scripting in this work, but above all for his intellectual honesty and generosity that provided me with the best example I could possibly have as an aspiring researcher.
- The student assistants Jasper Vos, Tom Scholten and Kjell-Erik Prins, for assisting me in setting up and conducting the experimental work.
- Frans van der Meij from Spectra Partners, for providing me with the illuminant standard that was used to conduct the extended calibration of the LMK system.
- The administrative staff of the TU Delft AE+T department for their hospitality over the years, and particularly the friendship and support that I received from Bo Song.
- My colleagues in the building Physics Group of the AE+T department that have always been very kind and helpful.

- My colleagues at the DAYKE project, particularly Frederica Giulliani, Aicha Diakite-Kortlever and Natalia Sokól, for the opportunity they offered me to do research beyond the PhD.
- Many other researchers whom I met personally and that gave useful feedback, asked relevant questions, made suggestions, or gave encouragement to carry on.
- My friends in Den Haag, Cristina Lago da Silva, Joana Volkmann, Ana Luiza Hutton, Johanna Prieto and Inês Garrett, for welcoming my children and I into to their lives and their homes, and making my life as a working mother in a foreign country a easier one.
- Verena Balz for hosting me in so many occasions, for the many conversations we had on the struggles of the PhD life and for her friendship and kind advice.
- All my family for their unconditional love and support, at every stage of my life and academic career.
- And my daughters, Clara and Alice, for their patience and understading in the times we had to be apart or that I was simply not available; they won't be seeing me staring at colourful circles (as they would say) again for while, and I suspect that will make them happy.

Contents

List of Tables	17
List of Figures	20
List acronyms, abbreviations and symbols	27
Summary	29
Samenvatting	31

1 Introduction 33

1.1	Daylighting	33
1.2	Glare	34
1.3	Prediction of discomfort glare	36
1.4	Applicability of the EN 17037	37
1.5	Visual environment of classrooms	38
1.6	Research questions	40
1.7	Thesis layout	41

2 Discomfort glare metrics 43

2.1	Introduction	43
2.2	Glare index	45
2.2.1	British Glare Index (BGI)	45
2.2.2	Daylight Glare Index (DGI)	46
2.2.3	CIE Glare Index (CGI)	47
2.2.4	Unified Glare Rating (UGR)	48
2.2.5	Early studies comparing BGI, DGI, CGI and UGR	49
2.2.6	Visual Comfort Probability (VCP)	50
2.2.7	Predicted Glare Sensation Vote (PGSV)	51
2.2.8	New Daylight Glare Index (DGI _N)	53
2.2.9	Daylight Glare Index modified (DGI _{mod}) and experimental Unified Glare Rating (UGR _{exp})	54
2.2.10	Daylight Glare Probability (DGP)	56
2.2.11	Unified Glare Probability (UGP)	59

2.2.12	Perceived Glare Level (PGL)	60
2.2.13	Glare Sensation Vote (GSV)	61
2.2.14	Daylight Glare Probability Modified (DGPmod)	62
2.3	Simple luminance metrics	63
2.3.1	Contrast ratios	63
2.3.1.1	Window-based contrast ratios	64
2.3.1.2	Glare source-based contrast ratios	64
2.3.2	Region-based metrics	65
2.3.2.1	Window-based metrics	65
2.3.2.2	The 40° horizontal band	65
2.3.2.3	Combined regions	66
2.3.2.4	Luminance of the visual field	66
2.4	Vertical eye illuminance (E_v)	67
2.5	Illuminance of the glare source (E_{dir})	67
2.6	Daylight Glare Probability simplified (DGPs)	68
2.7	Glare_{Ev}	69
2.8	Useful Daylight Illuminance (UDI)	70
2.9	Annual sunlight hours (ASH)	71
2.10	Cross-validation of existing glare metrics	71
2.11	Physiological response to discomfort glare	72
2.12	Discussion	73
2.13	Conclusion	77

3 Measurement of discomfort glare 79

3.1	Introduction	79
3.2	Image-based luminance measurement	81
3.3	High dynamic range imaging	82
3.4	Image-based luminance measuring devices	83
3.5	Measuring the luminance of the visual-field	86
3.6	Conclusion	89

4 Experimental method 91

4.1	Introduction	91
4.2	Experiment set-up	92
4.3	Experiment design	94

4.4	Measurements	97
4.4.1	Luminance measurement	97
4.4.2	The LMK luminance-acquisition system	97
4.4.2.1	Extended calibration of the LMK for daylight glare measurements	100
4.4.2.2	Fish-eye lens projection estimation	102
4.4.3	Luminance capture in the experiments	103
4.4.4	Pairing luminance measurement and evaluation of glare	104
4.4.5	Illuminance measurements	107
4.4.5.1	Task surface illuminance	107
4.4.5.2	Vertical eye illuminance	108
4.4.6	Other measurements	109
4.4.6.1	Degree of eye opening	109
4.4.6.2	Room temperature	110
4.5	Questionnaire	110
4.6	Visual activity	114
4.7	General equipment	116
4.8	Experiments workflow	118
4.9	Experiment population	121
4.10	Sky conditions	123
4.11	Data processing	123
4.11.1	Matching luminance and illuminance measurement	123
4.11.2	Luminance image pixel saturation correction	124
4.11.3	Comparison of measured and image-derived illuminance	124
4.11.4	Metrics calculation	125
4.12	Statistical analysis method	128
4.12.1	Ability of a metric to describe the full glare scale	128
4.12.2	Accuracy of a metric	129

5 Experimental study I 133

5.1	Introduction	133
5.2	Population	133
5.3	Metrics	135
5.4	Data processing	136
5.4.1	Luminance overflow correction	136
5.4.2	Measurement selection	137
5.4.3	Comparison of measured and image-derived illuminance	137

5.5	Metrics calculation	139
5.5.1	Glare source detection method in DGP	139
5.5.2	Region and mask-based calculation	142
5.6	Results	142
5.6.1	Reported visual comfort and glare	142
5.6.2	Glare metrics	145
5.7	Analysis	147
5.7.1	Analysis criteria	147
5.7.2	Two-zone approach	148
5.7.3	Glare metrics and evaluations reported by zone	149
5.7.4	Spearman correlation analysis	150
5.7.5	ROC curve analysis	153
5.7.6	Borderline between comfort and discomfort (BCD)	157
5.7.7	Performance analysis	158
5.8	Conclusion	160

6 Experimental study II 163

6.1	Introduction	163
6.2	Population	163
6.3	Metrics	165
6.4	Data processing	166
6.4.1	Evaluation of the validity of the glare question	166
6.4.2	Light variation during glare assessment	167
6.4.3	Luminance overflow correction	168
6.4.4	Comparison of measured and image-derived illuminance	168
6.5	Metrics calculation	169
6.6	Results	170
6.6.1	Reported visual comfort and glare	170
6.6.2	Glare metrics	176

6.7	Analysis	178
6.7.1	Analysis sample	178
6.7.2	Glare metrics and evaluations reported by zone	178
6.7.3	Spearman correlation analysis	182
6.7.4	ROC curve analysis	185
6.7.4.1	ROC's AUC	185
6.7.4.2	ROC's TPR, TNR and 'shortest distance'	189
6.7.4.3	Borderline between comfort and discomfort (BCD)	191
6.7.5	Performance analysis	192
6.8	Discussion	194
6.9	Conclusion	197

7 Identifying successful glare parameters 199

7.1	Introduction	199
7.2	Glare parameters in the study	201
7.2.1	Basic parameters	201
7.2.2	Adaptation ratio parameters	202
7.2.3	Contrast parameters	203
7.3	Method	204
7.4	Results	206
7.4.1	Descriptive statistics	206
7.4.2	ROC curve and Spearman correlation	209
7.4.2.1	Full room	210
7.4.2.2	Position 1	213
7.4.2.3	Position 2	216
7.4.2.4	Position 3	219
7.4.2.5	Position 4	222
7.4.2.6	Window zone	225
7.4.2.7	Wall zone	228
7.4.2.8	Front zone	231
7.4.2.9	Back zone	234
7.5	Analysis	237
7.6	Conclusion	241

8 A metric-based discomfort glare equation 243

- 8.1 **Introduction** 243
- 8.2 **Method** 245
 - 8.2.1 Equation definition 245
 - 8.2.2 Linear regression 246
 - 8.2.3 Transformation of the variables 247
 - 8.2.4 The analysis models 248
 - 8.2.5 Grouping the variables 249
 - 8.2.6 Assumptions of linear regression 250
- 8.3 **Results and analysis** 251
- 8.4 **Conclusion** 259

9 Developing a discomfort glare model based on a modified metric 261

- 9.1 **Introduction** 261
- 9.2 **Metrics and their components** 262
- 9.3 **Method** 264
 - 9.3.1 Optimisation goal 264
 - 9.3.2 Model development approach 265
 - 9.3.3 Optimisation approach 267
 - 9.3.4 Analysis models 270
 - 9.3.5 Statistical power analysis 271
- 9.4 **Results** 272
 - 9.4.1 Testing the parameters of the optimisation 272
- 9.5 **Optimisation** 274
 - 9.5.1 Optimisation results 276
- 9.6 **Analysis** 277
 - 9.6.1 Magnitude of the improvement 277
 - 9.6.2 Fitness of the optimised models 278
 - 9.6.3 Deriving the equations 282
 - 9.6.3.1 $DGP_{\log(Ev)_{\text{new}}}$ 282
 - 9.6.3.2 DGP_{new} 285
 - 9.6.3.3 UGP_{new} 287

- 9.7 **Discussion** 289
- 9.7.1 DGP_{new} in comparison to DGP 289
- 9.7.2 $DGPlog(Ev)_{new}$ in comparison to DGP 291
- 9.7.3 UGP_{new} in comparison to UGP 295

- 9.8 **Conclusion** 295

- 10 **Design strategies for a discomfort glare free classroom** 297

- 10.1 **Introduction** 297

- 10.2 **Design strategies** 299

- 10.3 **Classroom walls** 302

- 10.3.1 Increasing the reflectance of the walls 302

- 10.3.2 Increasing the illuminance of the walls 305

- 10.3.2.1 Room lighting 305

- 10.3.2.2 Illuminated walls 306

- 10.4 **Classroom windows** 309

- 10.4.1 Avoiding a view of the window 309

- 10.4.1.1 Roof-lights with occluded windows 309

- 10.4.1.2 Side-windows with occluding baffles 310

- 10.4.1.3 Repositioning of the visual task 311

- 10.4.1.4 Teacher situation 312

- 10.4.2 Avoiding a view of the window within the central visual field 313

- 10.4.3 Reducing the window luminance 315

- 10.5 **Avoiding secondary glare sources** 317

- 10.6 **Summary** 320

- 10.7 **Conclusion** 322

- 11 **Discussion** 325

- 11.1 **Luminance measurement** 325

- 11.2 **Data range** 326

- 11.3 **Evaluation of discomfort glare** 327

- 11.4 **Tested metrics** 328

- 11.5 **Contrast glare in the window zone** 328

- 11.6 **Variability of gaze** 329

11.7	Produced model and future developments	329
11.8	Design guidelines	331

12	Conclusion	333
----	-------------------	-----

12.1	Experimental conditions	333
12.2	Performance of existing discomfort glare metrics (RQ1)	334
12.3	Development of a new discomfort glare metric (RQ2)	335
12.3.1	Method 1: predictive power of individual glare parameters	336
12.3.2	Method 2: metric based on the current DGP and UGP	337
12.3.3	Method 3: metric based on a modified DGP or UGP	338
12.4	Architectural design guidelines (RQ3)	340
12.5	Future research	341

	Appendices	343
--	-------------------	-----

Appendix A	Experimental method	344
Appendix B	Experimental study I	379
Appendix C	Experimental study II	392
Appendix D	Parameters' analysis	409
Appendix E	Model based on a metric	415
Appendix F	Model based on modified metric	424
Appendix G	Design guidelines	451
Appendix H	Data and code repository	457

	References	459
	Biography	465
	Publications	467

List of Tables

- 2.1 Summary of presented metrics, their characterization, and conditions of their development. 76
- 3.1 The equations for different fisheye image projection methods (Bettonvil, 2005). 86
- 4.1 Light properties of the room's surfaces. Reflectance measured with one illuminance and luminance meter. Transmittance measured with two illuminance meters. 93
- 4.2 Simulated field-of-view luminance, L (cd/m²), and glare indices DGP, DGI and UGR, in the subject's position and in a position of 75 cm from the subject, in sitting positions 1 and 3. 106
- 4.3 Experiment workflow for the Study I experiment. 119
- 4.4 Experiment workflow for the Study II experiment. 120
- 5.1 Metrics, their borderline between comfort and discomfort (BCD) threshold and label used in the study. 135
- 5.2 Spearman correlation coefficient (ρ) and significance for different DGP calculation methods for the full, window positions and wall positions samples. 141
- 5.3 Performance criteria (Spearman). 150
- 5.4 Spearman correlation results and ranks for the full dataset. 151
- 5.5 Spearman correlation results and ranks for the window zone. 151
- 5.6 Spearman correlation results and ranks for the wall zone. 152
- 5.7 Performance criteria (ROC). 154
- 5.8 AUC test results and ranks for the full room. 154
- 5.9 AUC test results and ranks for the window zone. 155
- 5.10 AUC test results and ranks for the wall zone. 155
- 5.11 TPR and TNR test results and ranks for the full room. 156
- 5.12 TPR and TNR test results and ranks for the window zone. 156
- 5.13 TPR and TNR test results and ranks for the wall zone. 157
- 5.14 Passed statistical tests for the full room sample. 158
- 5.15 Passed statistical tests for the window zone sample. 159
- 5.16 Passed statistical tests for the wall zone sample. 159
- 6.1 Metrics, their borderline between comfort and discomfort (BCD) threshold and label used in the study. 165
- 6.2 Counts of votes for the 'would you want to put the blinds down' question, by level of glare. 173
- 6.3 Counts of votes for the 'discomfort due to reflections on the screen' question, by level of glare. 174
- 6.4 Performance criteria (Spearman). 182
- 6.5 Spearman correlation and ranks for the full room dataset (mean measurement). 183
- 6.6 Spearman correlation and ranks for the window dataset (mean measurement). 183

6.7	Spearman correlation and ranks for the wall dataset (mean measurement).	184	7.9	AUC-ranked ROC curve for disturbing glare for position 1	215
6.8	Performance criteria (ROC).	186	7.10	ρ -ranked Spearman correlation for position 2	216
6.9	AUC test and ranks for the full room (mean measurement).	187	7.11	AUC-ranked ROC curve results for any glare for position 2	217
6.10	AUC test and ranks for the window zone (mean measurement).	187	7.12	AUC-ranked ROC curve for disturbing glare for position 2	218
6.11	AUC test and ranks for the wall zone (mean measurement).	188	7.13	ρ -ranked Spearman correlation for position 3	219
6.12	TPR and TNR test and ranks for full room (mean measurement).	189	7.14	AUC-ranked ROC curve results for any glare for position 3	220
6.13	TPR and TNR test and ranks for window zone (mean measurement).	190	7.15	AUC-ranked ROC curve for disturbing glare for position 3	221
6.14	TPR and TNR test and ranks for wall zone (mean measurement).	190	7.16	ρ -ranked Spearman correlation for position 4	222
6.15	Passed statistical tests for the full room sample, 'mean measurement'.	192	7.17	AUC-ranked ROC curve results for any glare for position 4	223
6.16	Passed statistical tests for the window sample, 'mean measurement'.	193	7.18	AUC-ranked ROC curve for disturbing glare for position 4	224
6.17	Passed statistical tests for the wall sample, 'mean measurement'.	193	7.19	ρ -ranked Spearman correlation for the window zone	225
7.1	Glare classifications used in the ROC curve definition.	204	7.20	AUC-ranked ROC curve results for any glare for the window zone	226
7.2	Performance criteria (Spearman).	209	7.21	AUC-ranked ROC curve for disturbing glare for the window zone	227
7.3	Performance criteria (ROC).	209	7.22	ρ -ranked Spearman correlation for the wall zone	228
7.4	ρ -ranked Spearman correlation for the full room.	210	7.23	AUC-ranked ROC curve results for any glare for the wall zone	229
7.5	AUC-ranked ROC curve results for any glare for the full room	211	7.24	AUC-ranked ROC curve for disturbing glare for the wall zone	230
7.6	AUC-ranked ROC curve for disturbing glare for the full room	212	7.25	ρ -ranked Spearman correlation for the front zone	231
7.7	ρ -ranked Spearman correlation for position 1	213	7.26	AUC-ranked ROC curve results for any glare for the front zone	232
7.8	AUC-ranked ROC curve results for any glare for position 1	214			

7.27	AUC-ranked ROC curve for disturbing glare for the front zone	233	9.9	Detailed results of the linear regressions for DGP for optimisation 2.	278
7.28	ρ -ranked Spearman correlation for the back zone	234	9.10	Descriptive statistics for DGPlot(Ev)new, for the two zones and the two definitions of glare.	291
7.29	AUC-ranked ROC curve results for any glare for the back zone	235	10.1	Requirements to reduce the contrast effect in relation to the DGPlot(Ev)new.	298
7.30	AUC-ranked ROC curve for disturbing glare in the back zone	236	10.2	Discomfort glare strategies.	299
7.31	Classification of the parameters' performance for the full dataset and for the positions' subsamples.	239	10.3	Reflectance requirements for classrooms. Source: (The Society of Light and Lighting, 2011).	302
7.32	Classification of the parameters' performance for the zones' subsamples.	240	10.4	Typical reflectance of a range of reflective diffusive wall finishes. Source: (IESNA, 2000).	303
8.1	Regression models in the analysis.	248	10.5	Design strategies to prevent discomfort glare in the classroom.	322
8.2	Coefficient of determination r^2 and maximum standard deviation for the different grouping approaches.	250	12.1	Design strategies to prevent discomfort glare in the classroom.	341
8.3	Linear regression results for the 20 models.	256			
9.1	Analysis models.	270			
9.2	Tests to the parameters of the genetic algorithm optimisation, 1 to 5.	272			
9.3	Tests to the parameters of the genetic algorithm optimisation, 6 to 13.	273			
9.4	Results of the first optimisation run: r^2 and resulting components c1, c2, c3, c4.	274			
9.5	Parameters of the final optimisation runs.	275			
9.6	Results of the optimisation 1: r^2_{optim} and components c1, c2, c3 and c4 in comparison with the coefficient of determination obtained before optimisation, r^2_{before} .	276			
9.7	Results of the optimisation 2: r^2_{optim} and components c1, c2, c3 and c4 in comparison with the coefficient of determination obtained before optimisation, r^2_{before} .	276			
9.8	Detailed results of the linear regressions for optimisation 1.	278			

List of Figures

- 1.1 A situation that can result in disability glare (left) (source: by the author) and a situation that can result in discomfort glare (right) (source: Dubois et al., 2019). In the left image, the extreme brightness of the reflected light patch can impair seeing for an observer looking in the direction of the window. On the right image, the very bright windows in the direct view of the observer in this meeting room, creates visual discomfort. 35
- 1.2 Luminance maps showing the increase of luminance contrast in a daylit room as a function of room depth (cd/m²). Source: (New Buildings Institute et al., 2021). 37
- 1.3 Critical positions in a classroom in relation to discomfort glare (circled in red), for a classroom with a "U" layout (left) and for subjects engaged on a board task (right). 38
- 1.4 Three primary school classrooms of the same typology and same orientation with varying layouts. Source: by the author. 39
- 1.5 Thesis outline and outputs. 42
- 2.1 Visual representation of luminance and illuminance. Source: (Dubois et al., 2019). 44
- 3.1 A modern version of the discomfort glare measuring set-up used by Luckiesh and Guth in 1949 for the development of the glare sensation formula, showing the dome used for measuring the background luminance and the movable glare source. Source: (Kim and Kim, 2010). 79
- 3.2 A cosine-corrected illuminance meter (source: (Konica Minolta Sensing Americas, Inc, 2020) and field-of-view luminance measurement set-up using unshielded and shielded illuminance metres. Source: (Fisekis et al., 2003). 80
- 3.3 A field-of-view measurement of discomfort glare set-up using image-based luminance capture (Wienold, 2010). 80
- 3.4 Sequence of low dynamic range photographs captured with different exposures (aperture fixed at F2.6, ISO 100, shutter speed range 1/60"- 15") and the resulting high dynamic range image. Source: (Jacobs, 2007). 82
- 3.5 The CIE photopic luminous efficiency curve, data source: (Stockman, 2020) plotted against the electromagnetic spectrum, data source: (Zwinkels, 2016). 83
- 3.6 Spectral mismatch of an absolute-calibrated Canon EOS700 DSLR camera, based on the V(λ) curve of the CIE 1931 2° standard modified photopic observer. Source: (Technoteam, 2016). 84
- 3.7 Estimated vignetting effect for apertures F4, F5, F8 and F11 (left to right) for an LMK mobile air system. Source: Technoteam. 85
- 3.8 The human binocular visual field, or area that is seen by both eyes simultaneously (in white) and the monocular visual field (in grey). Source: (Boyce, 2014). 86
- 3.9 The four commonly used methods for projecting fisheye images, showing the curves for theta angles, θ , from 10° to 90°. Source: (Wagdy et al., 2019). 87
- 3.10 Region definitions in a fisheye luminance image for the purpose of calculating discomfort glare metrics with *evalglare*. 88

4.1	Experiment room in four photographs.	93	4.13	Vertical eye illuminance measurement set-ups used: a) and b) adapters in Study I and c) adapter in Study II.	109
4.2	Plan view of the room in Study I, with view direction from each position.	94	4.14	Visual activity from Study I.	115
4.3	The four visual conditions of Study I.	94	4.15	Visual activity for Study II (desk task). An adaptation stage text (top) and the character search task (bottom).	117
4.4	Four room layouts for two different visual tasks. From left to right: 'U' layout (desk task), regular layout (desk task), diagonal layout (desk task) and the layout used for the board task.	95	4.16	Participants in the experiment of Study I.	121
4.5	The sixteen visual conditions of Study II (images with adjusted exposure).	96	4.17	Room set-up for the screen task and participant performing a desk task, in the experiment Study II.	121
4.6	A typical LMK $\pm 3EV$ sequence.	98	4.18	Luminance data processing workflow, from luminance capture to the calculation of the glare metrics.	127
4.7	Comparison of the LMK calibrated shutter speed and aperture range with the ranges used in other two studies using Canon DSLR cameras and fisheye lenses (Stumpfel et al., 2004) (Van Den Wymelenberg, 2012) for the measurement of daylight. Stumpfel et al. captured the luminance of the sun with an aperture of F16, shutter speed of 0.00013" and an additional neutral density filter. Van Den Wymelenberg captured a daylit scene over 90 days in a cellular office space with aperture F5.6 and a shutter speed as low as 0.00025".	99	4.19	ROC curve definition. Source: by the author.	130
4.8	Luminance capture with luminance overflow in the indicated area (F22, shutter speed 0.001" to 0.062").	101	5.1	Counts of the self-reported 'sensitivity to bright light'.	134
4.9	Luminance capture with luminance overflow in the indicated areas (F22, shutter speed 0.001" to 0.062").	101	5.2	Counts of the 'importance of a view out in the workplace'.	134
4.10	Figure 1-minute vertical eye illuminance measured at eye level near the window in the experiment room for an hour, in a clear sky day in June with a few scattered clouds and a light breeze.	104	5.3	Examples of images with luminance overflow (in pink).	136
4.11	Camera location and view direction in the two positions.	105	5.4	Some of the eliminated measurements: a) movement in front of camera, b) sun in the edge of a window, c) sun incident on task, d) sun on the task area.	137
4.12	Variation of light between the sitting position and the point of illuminance measurement. Illuminance meter is circled in red.	108	5.5	Luminance-derived versus externally measured vertical illuminance (Ev) for the initial sample of 199 cases (top) and for the study sample of 185 cases (bottom).	138
			5.6	Region and masks used in the study (position 1). From left to right: 40° band region, task and window masks.	142
			5.7	Distribution of the 'how well is screen seen' responses.	143
			5.8	Distribution of the 'discomfort due to sunlight' responses.	143

- 5.9 Distribution of the 'discomfort due to reflections on screen / screen washed out' responses. 144
- 5.10 Distribution of the 'overall visual discomfort' responses. 144
- 5.11 Distribution of the 'discomfort due to glare' responses 145
- 5.12 Distributions for the glare metrics, by position. 146
- 5.13 Distributions of DGP, E_v , DGI and UGR, per glare level and per zone. Boxplots for all other metrics can be found in the Appendix B, section3. 149
- 5.14 ROC curve of the metrics for the full room dataset. 153
- 5.15 ROC curve of the metrics for the window zone. 153
- 5.16 ROC curve of the metrics for the wall zone. 153
- 6.1 Counts of the self-reported 'sensitivity to bright light'. 164
- 6.2 Counts of the 'importance of a view out in the workplace'. 164
- 6.3 Percentage difference (%) and illuminance difference (Lux) of the measured E_v , between the start and end measurements. 167
- 6.4 Luminance-derived versus externally measured E_v for the 256 measurements (2 measurements per case, measurement at the start and at the end of the evaluation). 'Corrected' refers to the images that were corrected for luminance overflow, 'excluded' refers to images that showed a difference above 25% (1 case) and 'unchanged' relates to all other data points. 168
- 6.5 Region and masks used in the study for the four studied layouts and position 1. From top to bottom: 'U' layout, 'regular' layout, 'diagonal' layout and 'board-task' layout; From left to right: 40° band region, task mask and window mask mask. 169
- 6.6 Distribution of '(in)satisfaction with visual conditions' responses. 171
- 6.7 Distribution of '(dis)comfort due to glare' responses. 171
- 6.8 Distribution of 'level of glare' responses. 172
- 6.9 Distribution of 'would have wanted to put the window blinds down' responses. 172
- 6.10 Distribution of 'reflections on screen / screen washed out' responses. 174
- 6.11 Distribution of 'discomfort due to sun' responses. 175
- 6.12 Distributions of the metrics based on the 'mean' measurement, by position. 177
- 6.13 Distributions of the metrics for the 'mean' measurement, by zone. 179
- 6.14 ROC curve for the full room (mean measurement). 185
- 6.15 ROC curve for the window zone (mean measurement). 185
- 6.16 ROC curve for the wall zone (mean measurement). 185
- 6.17 Vertical illuminance (E_v) distribution in Study I and in Study II (Log scale). 194
- 6.18 Luminance distribution in position 1 (left) and in position 4 (right), in the same session and for a clear sky. 196
- 7.1 Adaptation and contrast terms in two equations. Note that in UGR_{exp} , L_{avg} is replaced by L_b in the contrast part of the equation. 200
- 7.2 Areas corresponding to the dataset subsamples: position 1 (P1), position 2 (P2), position 3 (P3), position 4 (P4), window zone (window), wall zone (wall), front zone (front) and back zone (back). 205
- 7.3 Box plots for the basic parameters (complete dataset). 207

- 7.4 Box plots of the adaptation ratios E_v/L_b and E_v/L_t (complete dataset). 208
- 7.5 Box plots of L_{s_mean}/E_v , L_{s_mean}/L_{avg} and L_{s_mean}/L_t (complete dataset). 208
- 8.1 Scatter plots of the linear regressions for DGP and DGPlot(E_v) with and without low light correction and for UGP, in the window zone; 'disturbing glare' regressions on the left and 'any glare' regressions on the right. 252
- 8.2 Scatter plots of the linear regressions for DGP and DGPlot(E_v) with and without low light correction and for UGP, in the wall zone; 'disturbing glare' regressions on the left and 'any glare' regressions on the right. 254
- 9.1 Components of the DGP equation. 262
- 9.2 Flow chart of the genetic algorithm search process (Scrucca, 2013b). 268
- 9.3 Flow chart of the optimisation and fitness algorithms. 269
- 9.4 Components' plots for DGP, in the wall zone: 'disturbing glare' (left) and 'any glare' (right). The vertical black line shows the iteration from which the r^2 does not change. The plots show the components obtained for every improvement of the r^2 . As an improved r^2 is not always found for all the iterations, the number of data points in these plots (x-axis) is much smaller than the total number of iterations. 275
- 9.5 DGP optimised in comparison to the DGP non-optimised (before) versus the percentage of persons that report glare, for the wall zone. Left: 'disturbing' glare definition; right: 'any glare' definition. Before optimisation (in blue) and after optimisation (in black). 279
- 9.6 DGPlot(E_v) optimised in comparison to the DGPlot(E_v) non-optimised (before) versus the percentage of persons that report glare, for the wall zone. Left: 'disturbing' glare definition; right: 'any glare' definition. Before optimisation (in blue) and after optimisation (in black). 279
- 9.7 UGP optimised in comparison to the UGP non-optimised (before) versus the percentage of persons that report glare, for the wall zone. Left: 'disturbing' glare definition; right: 'any glare' definition. Before optimisation (in blue) and after optimisation (in black). 280
- 9.8 DGP optimised in comparison to the DGP non-optimised (before) versus the percentage of persons that report glare, for the window zone. Left: 'disturbing' glare definition; right: 'any glare' definition. Before optimisation (in blue) and after optimisation (in black). 280
- 9.9 DGPlot(E_v) optimised in comparison to the DGPlot(E_v) non-optimised (before) versus the percentage of persons that report glare, for the window zone. Left: 'disturbing' glare definition; right: 'any glare' definition. Before optimisation (in blue) and after optimisation (in black). 281
- 9.10 UGP optimised in comparison to the UGP non-optimised (before) versus the percentage of persons that report glare, for the window zone. Left: 'disturbing' glare definition; right: 'any glare' definition. Before optimisation (in blue) and after optimisation (in black). 281
- 9.11 Scatter plots of the new DGPlot(E_v) model. Results before optimisation (in blue) and results for the DGPlot(E_v)_{new} model (in black). 284
- 9.12 Scatter plots of the new DGP model. Results before the optimisation (in blue) and results for the DGP_{new} (in black). 286
- 9.13 Scatter plots of the new UGP model. Results before the optimisation (in blue) and results for the UGP_{new} (in black). 288
- 9.14 Calculated contrast and adaptation terms of DGP_{new} and of DGP, based on the Study I data. 290
- 9.15 Distributions of DGPlot(E_v)_{new} for the 'any glare' definition (left) and for the 'disturbing glare' definition (right), per zone. 292

- 9.16 Calculated contrast and adaptation terms of $DGPlog(E_v)_{new}$, based on Study I data. 293
- 10.1 A typical classroom setting with walls and four critical sitting positions – P1, P2, P3 and P4 and zones, studied in this research. 300
- 10.2 Luminance distribution in the side-lit classroom of this research for a situation where discomfort glare is reported on (a) an overcast day and (b) on a sunny day. The images refer to the situation where the walls of the room are very visible to the observer (position 1 / board task). 301
- 10.3 Sightlines and respective binocular visual field for the four critical positions of the classroom P1, P2, P3 and P4, for students engaged on a board task and for a teacher looking at critical student positions (P2 and P3): Plan and longitudinal section for (a) board task and (b) desk task. 301
- 10.4 A colour wheel, showing hue, chroma and value. Source: based on <https://www.britannica.com/science/Munsell-color-system>. 303
- 10.5 CIBSE colour chart (a), source: (Society of Light and Lighting, 2001); RAL colour fan (b), source: https://en.wikipedia.org/wiki/RAL_colour_standard. 304
- 10.6 Wall visibility from the four critical positions and from the teacher sitting position. Lighter grey represents the less visible part of the room. 305
- 10.7 Example of a scene where glare is reported for a low illuminance: (a) the identified glare sources in colour (image exposure reduced to -5.5) and (b) the luminance distribution of the scene. 306
- 10.8 Increasing illuminance of W4 with artificial lighting. 307
- 10.9 Increasing illuminance of W4 with additional window. 307
- 10.10 Increasing W4 illuminance using daylight with (a) a sky-light, (b) a light-well and (c) a monitor window. 308
- 10.11 Roof-lights with 'view-shaded' windows. 309
- 10.12 A baffle system that offers a fully shaded view of the window in the central part of the visual field for all the sitting positions. The zones correspond to four different baffle arrangements. 311
- 10.13 Repositioning the board. 312
- 10.14 Sightlines and central visual field of the teacher, for the critical point of observation (looking at P2) when sitting in the window zone and when sitting in the wall zone. 312
- 10.15 Position Index (1-15) overlaid on view angles 15° to 90°. 313
- 10.16 Curves for a Position Index of 7.7 and of 2.6. 313
- 10.17 High window totally located outside the 45° central view cone, combined with a semi-raised ceiling: (a) longitudinal and (b) cross-section. The high window can be extended to the back of room wall (W1) and to the 'inner' wall (W4), as shown in (b). 314
- 10.18 High window partially located outside the 45° central view cone, with a raised slanted ceiling: (a) longitudinal and (b) cross-section. The visible part of the window will require a reduction of window luminance (see 10.4.2). 314
- 10.19 Light redirection with Retrolux window shading technology. Source: (Köster, 2004). 316
- 10.20 Identified glare sources in positions P1 and P2 (a) and for positions P3 and P4 (b), showing the window glare source mostly situated in the upper half of the visual field and other large glare source areas in the bottom half of the visual field. (Image exposure set to -5.5). 317

- 10.21 Avoiding secondary glare sources: interaction of the room with typical solar angles for a Northern Europe location and (a) a window of normal height, with (b) a high window and a light-shelf and with (c) a “in-use” solution for a window of normal height, by changing position of desks and using window blinds when required. In the images, a darker shading of grey indicates an area that is less affected by solar reflections all year around. 319
- 10.22 Design workflow to minimise discomfort glare. 321
- 12.1 Discomfort glare ‘in space’, experimental conditions of this research in comparison to other discomfort glare studies: a) modern version of the artificial light set-up used in the early glare index studies by Luckiesh and Guth in 1949 (Kim and Kim, 2010), b) an artificial window set-up used in laboratory glare research (Kent et al., 2019), c) the cellular office testing facility of the DGP investigation (Wienold, 2010) and d) the classroom set-up of this research. 342

List acronyms, abbreviations and symbols

Acronyms and abbreviations	
ASH	Annual Sunlight Hours metric
AUC	Area under the ROC curve
BGI	British Glare Index
CGI	CIE Glare Index
CI	Confidence interval. Refers to the lower or upper bound of the 95% confidence interval of a statistic; a statistic with a lower confidence interval of 0.76 and an upper confidence interval of 0.85 means that there is a 95% chance that the value of the statistic varies between 0.76 and 0.85.
DGI	Daylight Glare Index
DGI _{mod}	Daylight Glare Index modified
DGI _N	New Daylight Glare Index
DGP	Daylight Glare Probability index
DGP _{mod}	Daylight Glare Probability Modified index
DGPs	Daylight Glare Probability simplified index
E _{dir}	Direct Illuminance [Lux]: the part of the illuminance reaching the eye (E _v) from the glare sources only; equivalent to the mean luminance of the glare sources, (L _s).
E _{ind}	Indirect illuminance [Lux]: the part of the illuminance reaching the eye (E _v) from the background only; equivalent to the mean luminance of the background, (L _b).
E _v	Vertical eye illuminance [lux]: total illuminance reaching the eye
GSV	Glare Sensation Vote metric
HDRI	High dynamic range imaging
L _s	Mean luminance of the glare source [cd/m ²]. For metrics developed before HDRI, it can correspond to the mean luminance of the window.
L _b	Mean luminance of the background [cd/m ²], corresponding to the area of the field of view excluding the glare sources.
L _{avg}	Mean luminance of the field of view [cd/m ²]; it is equivalent to L _{180°} when referring to the mean luminance of a field-of-view extending to a 180° view angle.
L _{180°}	Mean luminance of the field-of-view extending to a 180° view angle (used in the context of luminance measured in 180° fish-eye images).

>>>

Acronyms and abbreviations

ASH	Annual Sunlight Hours metric
L_{win}	Luminance of the window [cd/m^2].
L_{task}, L_t	Luminance of the task [cd/m^2].
L_{40°	Luminance of the region within the 40° horizontal band of the visual field, along the central horizontal axis [cd/m^2].
ω_s	Solid angle subtended by the glare source [steradians]: the portion of the field-of-view occupied by a glare source, measured from the eye.
Ω_s	Weighted solid angle subtended by the glare source [steradians]: the portion of the field-of-view occupied by a glare source, measured from the eye, modified by the position of the source with respect to the field of view and Guth's position index.
P	Position index [-]: a value between 1 and 15 that expresses the change in discomfort glare experienced relative to the angular displacement of the glare source from the observer's line of sight.
PGL	Perceived Glare Level metric
PGSV	Predicted Glare Sensation Vote index
ROC	Receiver operating characteristic curve statistic
TNR	True negative rate of a ROC curve statistic
TPR	True positive rate of a ROC curve statistic
UDI	Useful Daylight Illuminance metric
UGP	Unified Glare Probability index
UGR	Unified Glare Rating index
UGRexp	Experimental Unified Glare Rating index
VCP	Visual Comfort Probability index

symbols

i	Summation index
n	Number of glare sources
avg. mean	Mean
max	Maximum
min	Minimum
med	Median
std	Standard deviation
ω	Solid angle of the glare source
total	Sum
cov	Coefficient of variation (standard deviation divided by the mean)
ρ	Spearman rank correlation coefficient, measuring the effect size of the statistic
r^2	Coefficient of determination of the linear regression, measuring the effect size of the statistic
r	Pearson correlation coefficient
p	p-value, or significance of a statistic
N	Sample size

Summary

As children, adolescents or young adults we tend to spend a long time if not most of our time inside classrooms, the quality of the physical environment of these spaces being increasingly regarded of high importance to our learning success and development.

Provision of daylight without the risk of discomfort glare is one of the aspects that determine the quality of classroom environment and is the overall focus of this research.

Although discomfort glare from windows is under investigation for a long time, a knowledge gap concerning the applicability of the existing discomfort glare metrics to the spatial conditions of the classroom space was identified and forms the basis of this work. This thesis is in the first place an investigation on the applicability of existing metrics to the prediction of discomfort glare in classrooms. This investigation is based on two experimental studies that consisted of collecting subjective glare evaluations and objective luminance and illuminance measurements in a classroom space. The statistical analysis of this data shows that the existing discomfort glare metrics have poor predictive ability regarding the reported discomfort glare particularly in the sitting positions away from the window light source. This is attributed to the specific conditions of position and view direction of the classroom when compared to the conditions in the cellular office space in which the existing metrics have been developed and validated.

A study is then carried out with the intention of investigating how can more appropriate predictive models of discomfort glare be developed, based on the data collected in this work. Three different development methods are tested: the statistical analysis of a range of relevant glare parameters, a linear regression based on the DGP and the UGP metrics and a modification of the DGP and UGP equations. The modification of the DGP equation produced a significantly better discomfort glare model than any of the metrics that have been studied in this thesis and than the DGP itself. The analysis of the newly produced predictive model shows that this improvement results in a group of equations where the contribution of the contrast term is higher than the contribution of what is called the adaptation term of the DGP equation. This outcome indicates that the discomfort glare in the studied conditions results from a contrast rather than from a saturation glare effect. The study also

shows that a logarithmic rather than a linear form of the adaptation term of the DGP equation results in a better prediction of the reported discomfort glare. Based on this, a new model, $DGPlog(Ev)_{new}$, is presented as the best model of discomfort glare resulting from this investigation. The $DGPlog(Ev)_{new}$ model is based on four equations corresponding to two definitions of glare, 'disturbing glare' and 'any glare', and two classroom zones, the 'window zone' and the 'wall zone'. This result suggests that an improved model of discomfort glare for the classroom is better defined based on a range of equations for different sitting positions or that new variables that account for sitting position need to be included in a predictive model of discomfort glare for classrooms.

The $DGPlog(Ev)_{new}$ set of equations suggest that a reduction of the risk of discomfort glare in the classroom is achieved by an overall reduction of the luminance contrast in these spaces. A set of architectural design guidelines towards a discomfort glare-free classroom is then proposed, based on the newly produced model and on the collected data.

Samenvatting

Kinderen, pubers en jong volwassenen brengen heel veel tijd door in een klaslokaal. De kwaliteit van het fysieke binnenklimaat van de ruimtes wordt daarom steeds belangrijker geacht voor het studiesucces en de ontwikkeling van deze kinderen, pubers en jong volwassenen. Voorzien in daglicht zonder risico op verblinding is een van de aspecten die de kwaliteit van een leeromgeving bepalen en daarmee het overkoepelende doel van dit onderzoek. Hoewel hinderlijke verblinding al lang onderwerp van onderzoek is, is er een gebrek aan kennis over de toepassing van de bestaande maten voor verblinding in de specifieke ruimtelijke omstandigheden van een klaslokaal. Deze kennislacune vormt de basis van dit onderzoek.

Dit proefschrift is in eerste instantie een onderzoek naar hoe goed bestaande maten verblinding kunnen voorspellen in klaslokalen. Het onderzoek is gebaseerd op twee experimentele studies die bestonden uit het verzamelen van subjectieve beoordelingen van verblinding samen met objectief gemeten luminanties en verlichtingssterktes in een klaslokaal. De statistische analyse van deze data laat zien dat bestaande verblindingsmaten de subjectief ervaren verblinding slecht voorspellen, vooral in zitposities ver weg van de bron van het daglicht, het raam. Deze slechte voorspelling van verblinding wordt toegeschreven aan de specifieke omstandigheden, d.w.z. posities en kijkrichtingen, in een klaslokaal die anders zijn dan de omstandigheden in een cellenkantoor waarvoor de bestaande verblindingsmaten zijn ontwikkeld en gevalideerd.

Gebaseerd op de gemeten data in klaslokalen is er gekeken of beter voorspellende modellen gemaakt kunnen worden. Drie verschillende methodes zijn daarbij toegepast: Een statistische analyse van een reeks van relevante verblindingsparameters, een lineaire regressie gebaseerd op de bestaande DPG en UPG maten voor verblinding en als laatste een aanpassing van de DGP en UGP vergelijkingen. De aanpassing van de DGP vergelijking zorgde voor een significant beter verblindingsmodel dan elk van de bestaande maten en de DGP zelf. Het nieuwe verblindingsmodel bestaat uit een aantal vergelijkingen. In deze vergelijkingen is de bijdrage van de contrastterm hoger dan de bijdrage van wat de adaptatieterm wordt genoemd in de DGP vergelijking. Dit betekent dat onder de omstandigheden van deze studie in klaslokalen de verblinding vooral wordt veroorzaakt door het ervaren contrast en minder door verzadiging van het netvlies. Deze studie laat ook zien dat een logaritmische vorm van de adaptatieterm van de DGP vergelijking een betere voorspeller is van de ervaren verblinding dan een lineaire vorm van de adaptatieterm.

Gebaseerd op de resultaten van het onderzoek wordt een nieuw model, $DGPlog(Ev)_{new}$, gepresenteerd als beste model om verblinding te voorspellen. Het $DGPlog(Ev)_{new}$ model bestaat uit 4 vergelijkingen die overeenkomen met twee definities van verblinding, 'storende verblinding' en 'alle verblinding' en twee zones in het klaslokaal, de 'raamzone' en de 'wandzone'. Dit resultaat suggereert dat een verbeterd model voor het voorspellen van verblinding moet bestaan uit verschillende vergelijkingen voor verschillende zitposities of dat het model onderscheid moet maken tussen verschillende zitposities in een klaslokaal.

De $DGPlog(Ev)_{new}$ set van vergelijkingen suggereert dat een vermindering van het risico op verblinding wordt bereikt door een algehele reductie van het luminantiecontrast in deze ruimtes. Een set van architectonische ontwerprichtlijnen voor verblindingsvrije klaslokalen is vervolgens opgesteld, gebaseerd op het nieuwe model en de verzamelde data.

1 Introduction

1.1 Daylighting

Lighting constitutes the second major energy expenditure of non-residential buildings after space heating worldwide (International Energy Agency, 2018), even though LED-based illumination systems have increasingly been used in recent years. There is a general expectation that a building's lighting expenditure can be reduced to a certain degree by the use of daylight, a free, non-polluting and natural source of lighting energy and illumination. Daylighting can minimise the need for electric lighting particularly when combined with adequate control systems, as has been demonstrated in several studies (Onaygıl and Güler, 2003) (Li et al., 2006) (Roisin et al., 2008) (Lee and Selkowitz, 2006). Strong evidence of energy savings from daylighting have also been found in a large study involving the refurbishment and design of schools in the US, resulting in a reduction of peak cooling loads ranging from 9% to 27% and savings in lighting energy from 6% to 64%, equating a total energy consumption reduction of 10% to 25% (Lighting Research Center, 2004). Daylighting presents a great opportunity for saving energy in schools given that the highest lighting energy demand occurs during the day when daylight is generally available. Most school design codes and best practice recommendations across Europe and US specify that the main source of light in the classroom should be daylight (Society of Light and Lighting, 2011) (The Collaborative for High Performance Schools, 2006), with several country-specific design codes stipulating that a fraction of the classroom illumination is to be provided by daylight (Parque Escolar EPE, 2017) (Rijksdienst voor Ondernemend Nederland, 2014) (Department for Education and Skills, 2003).

The importance of designing classrooms for daylighting, as any other working space for that matter, extends far beyond its energy benefits. Daylight is a flicker-free, high intensity source of illumination with excellent colour rendering properties and expected positive impacts on human health and well-being. In addition, daylighting was found to have a significantly positive impact on student

performance, resulting in an improvement of 21% in learning outcomes (Heschong Mahone Group, Inc., 2003a) and to an increase of children's progress in primary school (Barrett et al., 2015). However, daylighting poses a far bigger challenge to classroom illumination than artificial lighting. Daylight is a highly variable and often unpredictable light source and its full potential will only be achieved if any associated problems such as heat and glare from windows are appropriately dealt with.

In possibly the largest study carried out to date on the effects of daylighting on a student population, glare from daylighting was found to have a significant impact on the quality of the visual environment and to negatively impact student learning (Heschong Mahone Group, Inc., 2003b). This impact was particularly related for the disciplines that resort to instruction using vertical task areas, such as the classroom board. In that study, direct sun penetration and lack of control of blinds to prevent intermittent sources of glare were also found to be associated with negative student performance. Additionally, teachers in daylit rooms were found to be more likely to report problems with glare, expressing a desire to have more daylight in their classrooms, provided that these problems were resolved.

Glare from daylight can indeed create visually poor and possibly harmful learning environments. The response to glare is often drawing the blinds and switching on the electric light, a behaviour that undermines the use of daylight and its benefits.

1.2 Glare

Glare is a form of visual discomfort defined as “a condition of vision in which there is discomfort or a reduction in the ability to see details or objects, caused by an unsuitable distribution or range of luminance, or to extreme contrasts” (Society of Light and Lighting, 2018). In interior spaces, glare occurs either in the form of disability glare or discomfort glare. Disability glare is caused by light scattered in the eye, a condition that results in the loss of luminance contrast of the retinal image of what is being observed and therefore impairs seeing. Disability glare is generally produced in the presence of glare sources of extreme brightness (Figure 1.1). Because it causes a clear physical response in the eye, disability glare can be predicted with accuracy based on what is known as the equivalent veiling luminance (Boyce, 2014). The equivalent veiling luminance is a measure of the visibility of an object in the presence of a glare source compared to the visibility of the same object

seen through a uniform veil, where the luminance of the veil is a measure of the amount of disability provoked by the glare source. The prediction of disability glare is relatively straightforward and does not present a particular challenge to current lighting design practice. This will therefore not be investigated in this dissertation.

Contrary to disability glare, discomfort glare does not directly interfere with the ability to see but it causes annoyance, irritation and/or distraction (Figure 1.1). Hopkinson and others (1966) explain that discomfort glare from daylight can result from a 'contrast' effect, when windows are seen against a much lower brightness background or from a 'saturation' effect, when the high overall brightness of the scene leads to the saturation of the human visual response mechanism. The 'saturation' effect is believed to arise because the luminance of the visual field is bright beyond the limit within which the eye can function efficiently whereas the 'contrast' effect occurs when most of the visual field is well within the adaptation range of the eye, but the glare source is beyond the range to which the eye is adapted to (Hopkinson and Collins, 1970). Although discomfort glare is believed to cause a state of imbalance in the eye in the form of contraction of the muscles of the iris it is not exactly known how is this muscular activity produced and how it is processed by the human brain (Hopkinson and Collins, 1970). For this reason the study of discomfort glare and its measuring method has to date been almost exclusively based on the study of subjective evaluations of discomfort. As a result, several discomfort glare metrics have been produced and are currently in use.



FIG. 1.1 A situation that can result in disability glare (left) (source: by the author) and a situation that can result in discomfort glare (right) (source: Dubois et al., 2019). In the left image, the extreme brightness of the reflected light patch can impair seeing for an observer looking in the direction of the window. On the right image, the very bright windows in the direct view of the observer in this meeting room, creates visual discomfort.

1.3 Prediction of discomfort glare

The study of glare started more than 70 years ago pertaining the relationship between the brightness of a glare source and subsequent effect upon human vision (Luckiesh and Holladay, 1925). It started by addressing the problem of glare from artificial light sources and for that reason the original mathematical formulations, in the form of what is called the glare index (Luckiesh and Guth, 1949), were for a very long time lacking a definition that would apply to glare from windows. The initial formulas, developed based on glare from very small lighting appliances were not directly applicable to what is now understood as the large non-uniform glare sources that result from windows.

In the second half of the twentieth century, Hopkinson initiated the study of discomfort glare from daylight after demonstrating that both disabling and discomfort effects of glare were a major cause of dissatisfaction in naturally lit buildings (Hopkinson, 1949). Since then several studies have been conducted to adapt, develop and improve existing discomfort glare metrics or simply to test existing and newly proposed metrics to the context of the daylit working environment. It is interesting to find that most studies done in recent years have pointed towards very different directions in terms of what a successful discomfort glare metric is (Wienold, 2010) (Jakubiec and Reinhart, 2013) (Van Den Wymelenberg and Inanici, 2014) (Hirning et al., 2014) (Konis, 2014) (Mahić et al., 2017), in some cases justifying the proposal for a whole range of new metrics and assessment criteria (Van Den Wymelenberg and Inanici, 2015).

In the case of classrooms, the methods proposed for the prediction of discomfort glare from daylight remain either simply qualitative (Society of Light and Lighting, 2011) (Parque Escolar EPE, 2017), based on the horizontal (desk) illuminance (Education Funding Agency, 2014) or on task-based luminance methods (Rijksdienst voor Ondernemend Nederland, 2014). Nonetheless, two very important developments regarding the standardization of the discomfort glare assessment methods have occurred in the recent years, with the publication of the IES LM-83-12 in the US (IESNA, 2012) and of the EN 17037 – Daylight in buildings in Europe (Comité Européen de Normalisation, 2018).

1.4 Applicability of the EN 17037

After several years under development, the EU standard EN 17037 - Daylight in buildings (Comité Européen de Normalisation, 2018) was finally published in 2018, providing a much needed framework for the evaluation of the daylighting of buildings. The standard applies to any daylight-oriented indoor space which is mainly side-lit and where the expected activities are comparable to reading, writing or using display devices. The standard adopted the Daylight Glare Probability (DGP) index (Wienold and Christoffersen, 2006) as the discomfort glare method assessment, specifying either maximum annual DGP thresholds or expected annual DGP performance criteria for spaces with shading devices and for a range of pre-defined conditions in tabulated form. However, the standard also indicates that the DGP method should not be applied to the positions of a space that are far away from the daylight openings or have low daylight levels. Although it is not stated exactly what “far away” means in this context, it seems that the metric is not directly applicable to the positions of a room where the light levels tend to be much lower than by a window. This stems from the fact that the DGP is a metric that has been developed under the conditions of close proximity to a window (Wienold, 2010), a situation leading to saturation glare (Wienold et al., 2019), a condition whereby the field-of-view of the subject is dominated by an overall high brightness. Glare from daylight however can result not only from high brightness but also from high contrast (Hopkinson et al., 1966), a condition that will tend to occur in the inner parts of a room (Figure 1.2), and as it has been pointed out by other authors (Hirning et al., 2014) (Konis, 2014). A question therefore emerges regarding the applicability of the EU standard and of DGP to the classroom space, where subjects can sit at a variety of distances to the window light source.

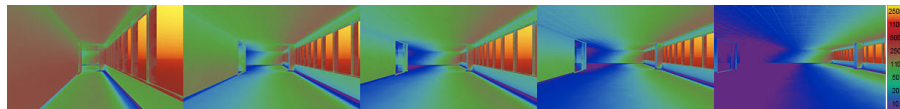


FIG. 1.2 Luminance maps showing the increase of luminance contrast in a daylit room as a function of room depth (cd/m^2). Source: (New Buildings Institute et al., 2021).

It also appears that in the case of a typical classroom with a depth of 6.5 m, at least half of the room falls outside the scope of the simplified annual glare evaluation defined in the EU standard, which is applicable to distances to a window from 1 to 3 meters.

The critical positions in terms of discomfort glare in the classroom can easily occur at a depth beyond 3 meters, for some common classroom layouts or when the subjects sitting in areas deeper in the room look in the direction of the classroom board (Figure 1.3).

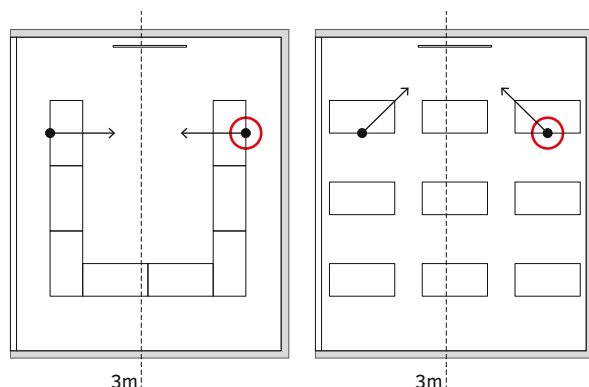


FIG. 1.3 Critical positions in a classroom in relation to discomfort glare (circled in red), for a classroom with a “U” layout (left) and for subjects engaged on a board task (right).

1.5 Visual environment of classrooms

Classrooms are naturally multi-activity spaces where subjects sit in a variety of positions and orientations in relation to the window daylight source (Figure 1.4). In informal interviews to primary school teachers and students done by the author it was found that a classroom layout changes at least two to three times during the year and sometimes on the same day. The reasons for these changes are entirely pedagogical and might therefore come unaccounted for at daylighting design and assessment stage. Perhaps for this reason, there is a lack of studies investigating the perception of discomfort glare for the variety of sitting positions and orientations that an occupant can have in a classroom. Field-of-view luminance distribution however changes dramatically depending on distance and orientation in relation to the window light source. Most of the research done in recent years investigating perception of discomfort glare in deeper spaces indicate that the predictive power of the DGP and a wide range of other metrics is not as high as could be expected in those conditions (Hirning et al., 2014) (Konis, 2014) (Jakubiec and Reinhart, 2013) (Mahić et al., 2017) and in some cases new metrics have been proposed. The applicability of these metrics on the prediction of discomfort glare from daylight in classrooms is, however, still unknown.

On the other hand, for most of the time, occupants of classrooms look towards a vertical task located in the centre of a room and at a distance from the subject. This situation very much differs from the conditions of a desk task, which has been the focus of most discomfort glare research to date. There is a lack of studies investigating the impact that these field-of-view conditions have on the perception of glare and on how applicable existing glare metrics are in this situation. There is a need to understand how existing glare metrics, particularly the metrics in current standards, perform 'in space' and in particular in the classroom space.



FIG. 1.4 Three primary school classrooms of the same typology and same orientation with varying layouts. Source: by the author.



1.6 Research questions

Many of the existing metrics have been developed in conditions of close proximity to a window and task and therefore their applicability to the classroom space has not been systematically studied to date. This problem is the object of the present investigation that focuses on three main research questions and their sub-questions:

RQ 1 To what extent are existing metrics appropriate to capture the problem of discomfort glare in the visual conditions of classrooms?

- 1.1 How are metrics defined and how is discomfort glare measured?
- 1.2 How well do existing and newly proposed metrics predict reported discomfort glare for different positions in space and view direction in the classroom?

RQ 2 How can better predictive models of discomfort glare for classrooms be defined?

- 2.1 Are there glare parameters that have more predictive power than others and in that way are more appropriate for the definition of a new model of discomfort glare for the classroom?
- 2.2 Can a successful relationship be established between the reported discomfort glare in the classroom and the current definitions of existing metrics?
- 2.3 Can adequate models of discomfort glare for classrooms be developed based on a modification of the existing metrics?

RQ 3 What aspects of the architectural design and what design strategies should be considered in order to reduce the risk of discomfort glare in classrooms?

A literature review will be conducted to identify what the existing discomfort glare metrics are and how they have been developed (chapter II), followed by an investigation on the technique of glare measurement and calculation (chapter III). This information produces the basis for an analysis of the performance of the existing metrics, which is investigated experimentally based on subjective evaluations and objective measurements carried out in a classroom space (chapters V and VI). This will be followed by an investigation on the definition of a new predictive model of discomfort glare for the classroom, based on the collected discomfort glare data and using a range of statistical analysis.

Three different methods are used for the investigation of a new predictive model of glare for the classroom: identification of successful glare parameters, definition of a model based on an existing metric and optimisation of an existing metric (chapters VII, VIII and IX, respectively). Architectural design guidelines for a discomfort glare free classroom are then proposed (chapter X), based on the collected data and on the new model of discomfort glare that is developed in this work.

1.7 Thesis layout

This thesis contains twelve chapters. The first part of the thesis corresponds to the theoretical background of the work (chapters II and III), the second part refers to the experimental part of the work (chapters IV, V and VI) and the third part refers to the development of a discomfort glare model for classrooms and design guidance towards a glare free classroom (chapters VII, VIII, IX and X). Chapters XI and XII correspond to the final discussion and conclusion of the work. An overview of the thesis layout and content can be found in Figure 1.5.

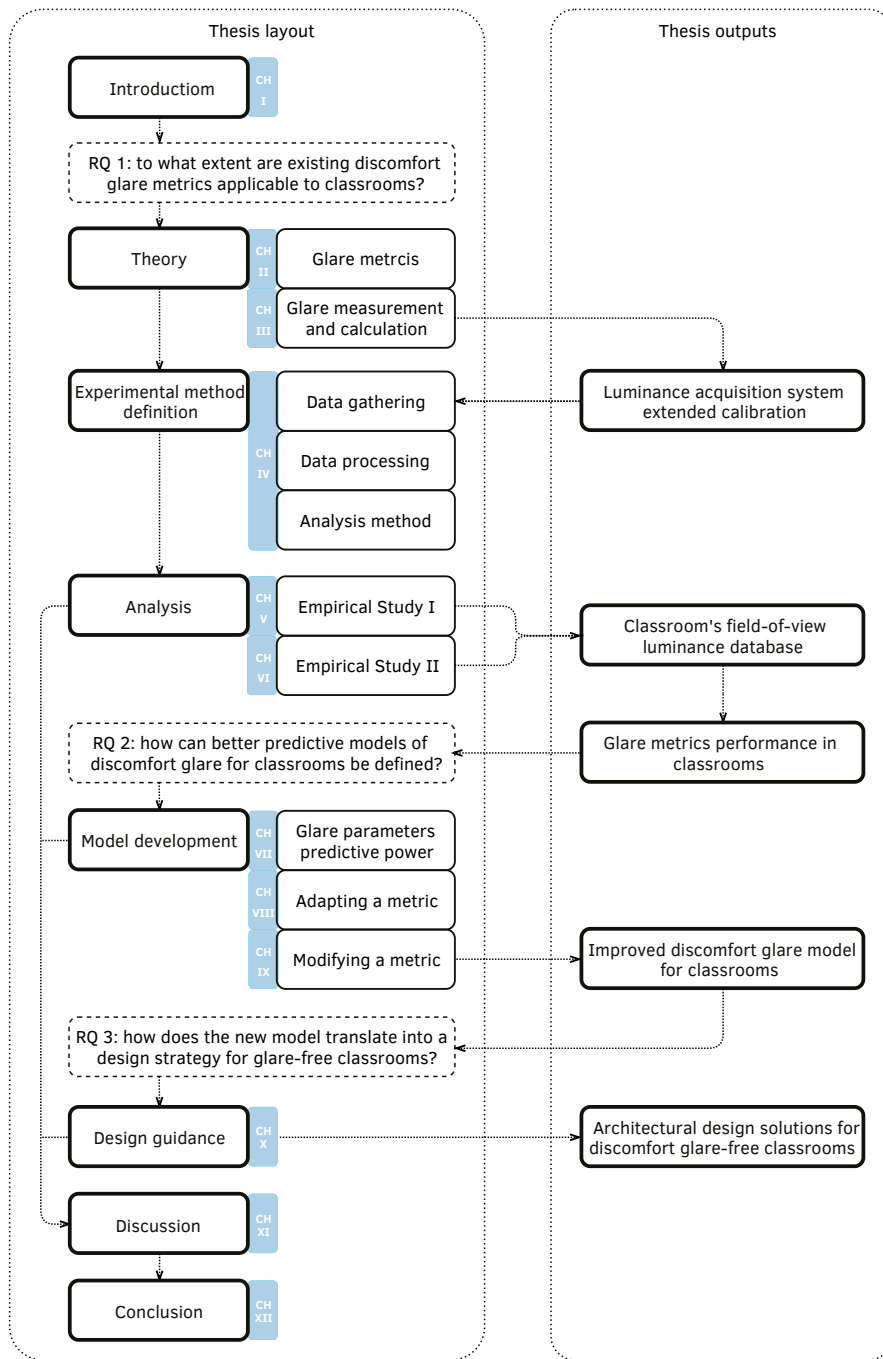


FIG. 1.5 Thesis outline and outputs.

2 Discomfort glare metrics

2.1 Introduction

The study of discomfort glare in buildings and its quantification started in the middle of the twentieth century with the work of Luckiesh and Guth (1946) in the US and Petherbridge and Hopkinson in the UK (1950). Based on these early studies, several discomfort glare metrics have been created and published in different parts of the world and as a result, a wide range of different equations exist. This chapter presents a review of the discomfort glare metrics from the early glare indices to the simplified metrics that have been in use, particularly in recent times.

Discomfort glare metrics are generally based on one or two different ways of quantifying the amount of light in a visual scene, namely as luminance and illuminance. Illuminance corresponds to the luminous flux density on a point or surface. Luminance corresponds to the light emitted or reflected in a given direction from a surface element, divided by the projected area of the element in the same direction (Figure 2.1). Illuminance, measured in lumens/m² or lux, is the light quantity that is generally used when determining the level of illumination of a surface. Luminance, measured in candelas/m², is more directly associated with the perception of brightness in the visual field.

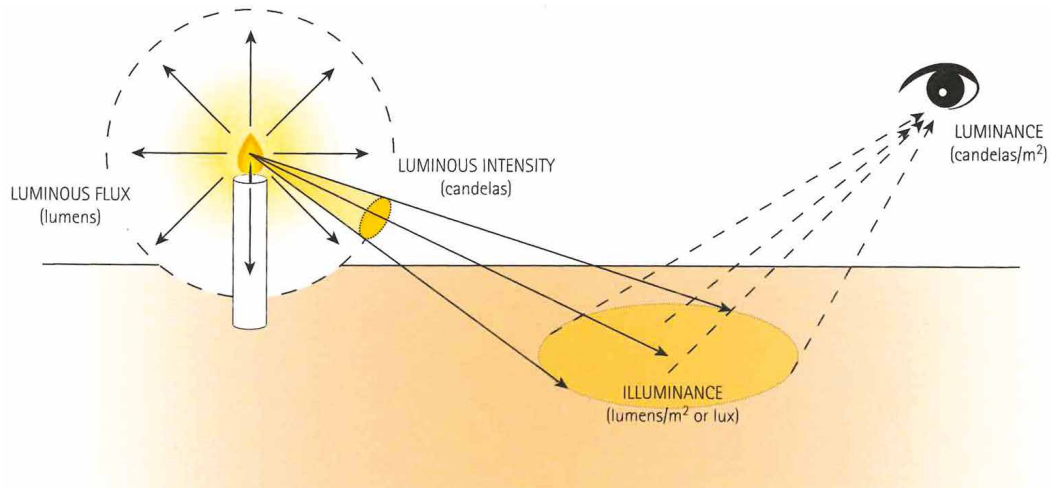


FIG. 2.1 Visual representation of luminance and illuminance. Source: (Dubois et al., 2019).

The discomfort glare metrics review that is here presented resulted from a selection of articles from a range of Google Scholar searches using the following keywords: *daylight metrics*, *glare metrics* and *discomfort glare metrics* and for publications up to June 2018. A recent cross-validation study of discomfort glare metrics from Weinold et al. (Wienold et al., 2019) was also consulted. Articles that were referenced within certain sources that were considered to contain relevant information were also consulted when available. References to two existing literature reviews are also included, one on the specific subject of discomfort glare metrics (Marty et al., 2003) and another on the general subject of visual discomfort that includes glare metrics (Carlucci et al., 2015). The review includes the consultation of a range of relevant international codes and standards related to the lighting of the working environment, two international green building certification systems and Boyce's reference book on the subject of human factors in lighting (Boyce, 2014).

A detailed description of the variables and symbols in the equations are given in the List of Acronyms and List of Symbols in the beginning of the thesis. Variables that are specific to a particular metric are described in the context of that metric.

The discomfort glare metrics have initially the form of a glare index, with several alternatives to the index being developed subsequently. These alternative metrics have been developed with the main purpose of simplifying the calculation and measurement of discomfort glare.

2.2 Glare index

A glare index is an empirical formula connecting directly measurable physical quantities, such as glare source luminance, solid angle or background luminance, to the experience of glare by a subject. Although the actual form of the various discomfort glare indices differ, they are generally constructed around four main variables of an expression that, for a single small glare source, can be generalised as (Boyce, 2014):

$$G = \left(\frac{L_s^a \cdot \omega_s^b}{L_b^c \cdot P^d} \right)$$

Where a, b, c and d are exponents that differ between the glare index systems.

The discomfort glare sensation formula, as it is generally known, expresses the subjective sensation of glare. It was developed after experiments involving human response to glare, measured in terms of the luminance that a subject reports to be on the borderline between comfort and discomfort (Luckiesh and Guth, 1949). The equation indicates that an increase in the luminance of the glare source, an increase of the solid angle subtended by the glare source, a decrease of the luminance of the background and a decrease of the deviation of the glare source from the line of sight will all increase the discomfort glare sensation, while changes of these components in the opposite direction will decrease that sensation. The glare sensation formula forms the basis of the glare indices that have been produced over the years and that are presented next.

2.2.1 British Glare Index (BGI)

The British Glare Index (BGI) was created by Petherbridge and Hopkinson at the Building Research Station in England (Petherbridge and Hopkinson, 1950), after studying the effect of the background luminance and of a glare source of subtended solid angle up to $2.7 \cdot 10^{-2}$ steradians on glare sensation.

$$\text{BGI} = 10 \cdot \log_{10} 0.478 \cdot \sum_{i=1}^n \frac{L_s^{1.6} \cdot \omega_s^{0.8}}{L_b \cdot P^{1.6}} \quad \text{EQ 01}$$

Citing several studies, Marty et al. (2003) explain that the equation does not predict glare accurately for large sources, does not take into account the effect of eye adaptation and that it was found that the formula consistently predicted more severe glare than what was reported in several studies. These results were attributed to the fact that BGI was originally developed for the prediction of glare from point sources rather than large sources of glare.

According to the classification in Wienold et al. (2019), BGI is a metric that is based on the contrast effect of glare only.

2.2.2 Daylight Glare Index (DGI)

The Daylight Glare index (DGI) is the Hopkins–Cornell large-source glare formula that was created in 1972 (Hopkinson, 1972), based on a modification of the BGI glare index. It was developed to address the problem of glare from large sources such as windows and is therefore called the Daylight Glare Index. It constitutes the first attempt to define a metric for problems of discomfort glare from windows. The metric was developed using a stack of packed fluorescent lights arranged behind an opal diffusing screen, set in a separately illuminated white surface extending to the limits of the observer's view.

$$\text{DGI} = 10 \cdot \log_{10} 0.478 \cdot \sum_{i=1}^n \frac{L_{s,i}^{1.6} \cdot \Omega_{s,i}^{0.8}}{L_b + 0.07 \cdot \omega_{s,i}^{0.5} \cdot L_{s,i}} \quad \text{EQ 02}$$

Marty et al. (2003) provide an extensive review of studies where DGI has been investigated. The findings of these studies indicate shortcomings regarding the applicability of DGI to the prediction of glare from actual windows (Chauvel et al., 1982) (Iwata et al., 1990) (Boubekri and Boyer, 1992) (Gall et al., 2000), to the wider range of window sizes (Iwata et al., 1990), to non-uniform sources of glare (Waters et al., 1995) and to situations where the glare source is not directly in the line of sight of the observer (Iwata et al., 1990) (Chauvel et al., 1982). The lack of a

term to account for the eye adaptation in the equation is also considered a limitation of the metric by several authors (Iwata et al., 1990) (Osterhaus and Bailey, 1992).

The metric has nevertheless been studied further in recent years. In the study by Wienold (2010), DGI showed a medium correlation with to the percentage of people disturbed by glare and to be outperformed by metrics such as the vertical eye illuminance (E_v) and the average luminance of the visual field (L_{avg}). In contrast, DGI was found to produce a high correlation with reported discomfort in (Hirning, 2014).

In the cross-validation study performed by Wienold et al. (2019), DGI was found to perform very poorly, failing four of the six statistical tests that were carried out.

DGI is considered a metric that is based on the contrast effect only, according to the classification in Wienold et al. (2019).

2.2.3 CIE Glare Index (CGI)

The CIE Glare Index (CGI) is the metric adopted by the Commission International de L'Éclairage in 1979, after studies performed by Einhorn (1969) (1979).

$$CGI = 8 \cdot \log_{10} 2 \cdot \frac{\left[1 + \frac{E_{dir}}{500}\right]}{E_{dir} + E_{ind}} \cdot \sum_{i=1}^n \frac{L_{s,i}^2 \cdot \omega_{s,i}}{P_i^2} \quad EQ\ 03$$

According to Marty et al. (2003), the CGI was developed in order to correct the mathematical inconsistency of the BGI formula for multiple glare sources.

In (Iwata et al., 1990), the authors showed that the CGI was less accurate than DGI to predict the glare vote from large glare sources. This result however was obtained based on experiments with an artificial window. They also maintained that the formula is not adequate because it does not take into consideration the eye adaptation condition. The metric was found to perform similarly to DGI in (Wienold, 2010) producing an relatively lower correlation to reported glare, while Hirning (2014) found the metric to produce a good correlation to glare.

The CGI is classified as a metric based on the contrast effect only in (Wienold et al., 2019). In that study, CGI was found to be the best performing from all studied metrics within that category. The authors suggest that is because the metric uses the E_{dir} (illuminance induced by the glare source) to enlarge the effect of the product of $L_s^2 \cdot \omega_s$.

2.2.4 Unified Glare Rating (UGR)

The Unified Glare Rating (UGR) system is the glare index calculation method that has been adopted by the CIE in 1995 (CIE, 1995). The UGR incorporates aspects of the CGI and BGI equations to evaluate glare from artificial lighting systems, restricted to sources subtending a solid angle at the eye from $3 \cdot 10^{-4}$ to 10^{-1} steradians.

$$UGR = 8 \cdot \log_{10} \left(\frac{0.25}{L_b} \cdot \sum_{i=1}^n \frac{L_{s,i}^2 \cdot \omega_{s,i}}{P_i^2} \right) \quad \text{EQ 04}$$

In relation to CGI, it can be seen that in the UGR equation the contribution from the direct illuminance of the glare source (E_{dir}) as well as the contribution of the illuminance of the background (E_{ind}) were dropped in favor of the luminance of the background (L_b).

It has been noted by several authors that the formula is intended for the prediction of glare from small glare sources of artificial light and therefore not directly applicable to daylight glare problems. However, the metric has been studied by several researchers in that context, producing successful results in (Hirning et al., 2014) (Konstantzos and Tzempelikos, 2017). In (Hirning et al., 2014), that result is attributed to the contrast-glare prevailing conditions that were verified in the open-plan offices of the study. In contrast, the UGR performed rather poorly in the study from Wienold (2010).

UGR is still the current proposed method of glare assessment by the CIE (2002), it has been adopted in several lighting codes in Europe (The Society of Light and Lighting, 2012) (The Society of Light and Lighting, 2011) and is used worldwide for the prediction of glare from artificial light sources.

The UGR is considered a contrast effect only metric by Wienold et al. (2019). In that study, the metric was found to have a poor performance, failing five of the six types of statistical tests that were performed.

2.2.5 Early studies comparing BGI, DGI, CGI and UGR

Iwata et al. (1990) conducted a glare study in an environmental test chamber, equipped with an artificial window of 80 × 80 cm, illuminated by a bank of metal halide lamps, where the intensity of the light was adjusted by a number of sheets of paper that also served to diffuse the light. The subjects sat either parallel or perpendicular to a window at a distance of 2.5 m doing a paper-based task and were asked to raise their sight to the window before doing the glare evaluation. Each subject repeated the test at five different luminances: 40,000, 13,000, 7,000, 4,000 and 2,500 cd/m². For these conditions, the authors found that DGI produced the best agreement with the reported glare sensation whereas CGI and BGI tended to over-predict it.

In 1992, Iwata et al. (1992) conducted an experiment in 2 rooms with real windows (one facing north and the other facing south), with 46 subjects. Each subject assessed 12 different lighting conditions (2 desk illuminances × 3 positions in space × 2 rooms). The three positions in space corresponded to a distance of 2 m, 4 m and 6 m from the window, for a window perpendicular to the line of sight. Subjects were asked to rate glare when looking directly at the window after performing a reading task. By comparing DGI and UGR to the subjective glare evaluations, the authors concluded that both metrics were insufficient at predicting the glare sensation in all the studied conditions. The authors suggest that the weight of the background luminance L_b in those equations might be too big and propose a change of the exponent of L_b to a ratio of exponents that would apply to different ranges of lighting conditions. They maintain that the effect of the total amount of light on the visual field of the observer cannot be neglected in the case of large light sources. The authors propose that three effects must be considered in the measurement of discomfort glare: the contrast in the visual field, the total amount of light coming into the eye (adaptation) and the transition of the adaptation level of the eye. They indicate that each of these three effects might have a variable influence in the sensation of glare, depending on different ranges of lighting conditions. The authors also indicate that the luminance distribution of the window and of the line of sight relative to the window should be further investigated.

2.2.6 Visual Comfort Probability (VCP)

The Visual Comfort Probability (VCP) (CIE, 1983), is a glare index that is widely used in North-America for the prediction of discomfort glare from artificial lighting that is based on the work carried out by Guth in 1963. The VCP is expressed as a percentage and its scale is inverted relative to the other glare indices in that high levels of VCP predict a higher level of comfort. The index is based on the calculation of the discomfort glare rating (DGR) that expresses the summation of the glare sensation produced by multiple glare sources. The VCP equation, as defined in the (IESNA, 2000) is as follows:

$$\text{VCP} = \frac{100}{\sqrt{2\pi}} \int_{-\infty}^{6.374-1.3227 \ln \text{DGR}} e^{-t^2/2} dt$$

with

$$\text{DGR} = \left(\sum_{i=1}^n M_i \right)^{n^{-0.0914}}$$

EQ 05

$$M_i = \left(\frac{0.5 \cdot L_{s,i} \cdot (20.4 \cdot \omega_{s,i} + 1.52 \cdot \omega_{s,i} - 0.075)}{P_i \cdot F_v^{0.44}} \right)$$

$$F_v = \left(\frac{L_w \cdot \omega_w + L_f \cdot \omega_f + L_c \cdot \omega_c + L_s \cdot \omega_s}{5} \right)$$

With average luminance of the walls (L_w), floor (L_f), ceiling (L_c) and source (L_s) and with solid angle of walls (ω_w), floor (ω_f), ceiling (ω_c) and source (ω_s).

In the review done by Marty et al. (2003), the authors explain that VCP is not applicable to the prediction of glare from very small sources such as incandescent and high intensity discharge lamps, from very large sources such as the ceiling-based indirect systems or from non-uniform sources. The authors state that Veitch and Newsham (1998) considered that several features of the VCP model limit its applicability as an indicator of discomfort glare since the original model was developed using flat-bottomed recessed luminaires only and was initially restricted to that application. In the same study it is argued that evidence from perceptual differences between uniform and non-uniform sources found in Water et al. (1995) render the VCP model ineffective in predicting glare ratings for non-uniform sources.

The VCP produced a low correlation with reported glare in the studies by Hirning (2014) and by Wienold (2010). The metric is considered a contrast glare only metric in (Wienold et al., 2019). In that study, it performs at the lowest end of all the studied metrics failing four of the six performed statistical tests and showing a non-significant statistical effect for five of the seven studied datasets.

2.2.7 Predicted Glare Sensation Vote (PGSV)

After the low correlation found between reported glare and the BGI and CGI (Iwata et al., 1990) and concluding that DGI was inadequate to a range of wide-source glare conditions, Tokura et al. (1996) developed the Predicted Glare Sensation Vote (PGSV) formula, which is based on the results from experiments carried out in Japan with 240 subjects, encompassing 120 different test conditions. The experiment was carried out in a test room with an artificial window of 2 m width with a luminance ranging from 2,000 to 20,000 cd/m². The subjects sat at a variety of distances to the window light source, looking at two view directions: a direction parallel to the window plane, at distances between 0.75 and 1.5 m from the window and a direction perpendicular to the window plane, at distances varying between 1.5 m and 3 m. The wall surfaces of the test room were finished with black, white or gray paper creating three different wall contrast conditions. The subjects performed a paper task and were asked to look straight in front before evaluating the glare conditions.

Using statistical regression, the authors developed the new PGSV index that produced a reasonable correlation with reported glare. The authors showed that PGSV performed better than DGI and concluded that PGSV was more adequate than DGI at predicting glare for a relatively large window. In the same study, the PGSV formula was tested against datasets collected in previous experiments with actual windows, a study presented in (Iwata, 1992). It was found that the PGSV equation produced more plausible results regarding the reported glare sensation than DGI, but that it still predicted higher values of glare than reported. The authors attributed this to the fact that the PGSV does not cover the effect of the luminance distribution of a real window surface and to the fact that the luminance distribution of actual windows or the view out from the windows could bring some psychophysical comfort to the subjects.

Wienold, Iwata and others (Wienold et al., 2019) provide a version of the PGSV equation with separate applications for contrast and saturation glare. They define these conditions as:

$$\text{PGSV} = \text{PGSV}_{\text{con}} \text{ if } \frac{L_s}{L_b} > \frac{L_{\text{avg}}}{L_{\text{adapt}}} \text{ (contrast glare)}$$

$$\text{PGSV} = \text{PGSV}_{\text{sat}} \text{ if } \frac{L_s}{L_b} \leq \frac{L_{\text{avg}}}{L_{\text{adapt}}} \text{ (saturation glare)}$$

with

$$L_{\text{adapt}} = L_t \text{ and } L_{\text{avg}} = \frac{E_v}{\pi}$$

For the contrast glare version of the equation, the authors in (Wienold et al., 2019) refer to the original equation from (Tokura and Iwata, 1996):

$$\text{PGSV}_{\text{con}} = 3.2 \cdot \log L_{\text{win}} + (0.79 \cdot \log \omega_{\text{win}} - 0.61) \cdot \log L_b - 0.64 \cdot \log \omega_{\text{win}} - 8.2 \quad \text{EQ 06}$$

For the saturation glare version of the equation, they refer to the equation provided by (Iwata and Osterhaus, 2010):

$$\text{PGSV}_{\text{sat}} = \frac{-0.57 - 3.3}{1 + \left(\frac{L_{\text{avg}}}{1250} \right)^{1.7}} + 3.3 \quad \text{EQ 07}$$

In contrast with the DGI, the PGSV takes into consideration the luminance adaptation level of the eyes. However, Boyce (2014) notes that there is no term relating to the deviation of the glare source from the line of sight because it is assumed the observer is looking directly at the window. Previously, Velds (1999) has also stated that because PGSV does not include the position index, it can only aim at evaluating glare from windows located perpendicular to the line of sight.

As the equations and definitions indicate, $PGSV_{sat}$ is a metric based on the saturation effect only whereas $PGSV_{con}$ is a metric based on the contrast effect only. In (Wienold et al., 2019), $PGSV_{sat}$ along with E_v were found to perform quite similarly and to be more robust than the other studied saturation glare metrics. The authors note that $PGSV_{sat}$ and E_v only fail for the dataset in which all data points included the presence of the sun in the visual field, the impact of which gets dissipated due to the small solid angle of the solar disc. The authors advance though that these metrics have an intrinsic disadvantage when it comes to the analysis of contrast glare-prone situations.

2.2.8 New Daylight Glare Index (DGI_N)

Stating that existing glare index equations are not adequate to real daylight conditions, Nazzal proposed a new Daylight Glare Index (DGI_N) (Nazzal, 2000), an equation that is built upon Chauvel's revision of the DGI formula (Chauvel et al., 1982).

$$DGI_N = 8 \cdot \log_{10} 0.25 \cdot \left[\frac{\sum_{i=1}^n L_{ext}^2 \cdot \Omega_{pN}}{L_{adapt} + 0.07 \cdot \left(\sum_{i=1}^n L_{win}^2 \cdot \omega_N \right)^{0.5}} \right] \quad \text{EQ 08}$$

Where

L_{ext} is the average vertical unshielded luminance of the outdoors [cd/m^2]

L_{win} is the average vertical shielded luminance of the windows [cd/m^2]

L_{adapt} is the average vertical unshielded luminance of the surroundings [cd/m^2]

ω_N is the solid angle subtended by the glare source (window) to the point of observation [steradians]

Ω_{pN} is a position factor depending on the geometry of the window and the distance from the observation place to the centre of the window area

In DGI_N , the solid angle subtended by the window is modified to include the effect of the point of observation and a window configuration factor. The author explains that the weight of the background luminance in the DGI equation is too large and that a large glare source such as a window covers an area that is too large to be clearly distinguished from the background. For that reason, he rejects the background luminance variable of the original DGI equation (L_b) in favour of what he calls the adaptation luminance, i.e. the total luminance of the visual field including the window (L_{adapt}).

The metric, which corresponds to a simple theoretical transformation of the DGI equation, has not been tested in any way and therefore its validity remains to be demonstrated.

2.2.9 Daylight Glare Index modified (DGI_{mod}) and experimental Unified Glare Rating (UGR_{exp})

A study on the suitability of the DGI and UGR to the prediction of discomfort glare from daylight was conducted by Fisekis et al. (2003). The study is based on data collected over a 10-month period under real sky conditions in a purpose-built test cell, using a group of 10 subjects sitting at a distance of 3 m from the window with a line of sight perpendicular to it. The subjective assessment of glare was made based on the DGI glare criteria scale.

Pointing out the lack of reliability of the DGI when the glare source extends to the whole visual field and when the background luminance equals that of the source, the authors developed the Daylight Glare Index modified (DGI_{mod}) which is a modified version of DGI, based on a new interpretation of background luminance and of visual adaptation.

The authors state that the problem with the background luminance (L_b) when calculated according to the DGI equation is that when the source is increased in size the visual field becomes governed only by the contribution of the source which leads to an overestimated DGI. They explain that a large glaring source such as a window can cover a very large area of the visual field and for that reason cannot be clearly distinguished from the background. The authors therefore propose the replacement of the background luminance by the average luminance (L_{avg}) of the whole visual field.

The results of the study indicated that mild degrees of glare could be predicted with relative accuracy with the use of the average luminance L_{avg} in the denominator of the equation without considering any extra contribution from the source. The authors state that as the source luminance rises, the saturation process takes place and the influence of the average luminance in the adaptation function has a declining effect, which can be accommodated into the formula by raising L_{avg} to an exponent ($x < 1$). They found that when the explicit contribution of the source in the denominator is kept constant, the best fit for that exponent was $x = 0.85$. The DGI_{mod} equation thus takes the form:

$$DGI_{mod} = 10 \cdot \log_{10} 0.478 \cdot \sum_{i=1}^n \frac{L_{s,i}^{1.6} \cdot \Omega_{s,i}^{0.8}}{L_{avg}^{0.85} + 0.07 \cdot \omega_{s,i}^{0.5} \cdot L_{s,i}}$$

with

EQ 09

$$L_{avg} = \frac{E_v}{\pi}$$

Using the same experimental data, the authors tested the ability of UGR to predict discomfort glare from daylight with the aim of developing a possible general index applicable to environments that would include both daylight and electric lighting. They propose a modification of the UGR equation that they call experimental UGR (UGR_{exp}), by replacing L_b by L_{avg} and by including L_b in the denominator of the second term of the equation to account for the fact that they found a better agreement when the contrast effect, represented as the ratio between the source and the background luminance (L_s/L_b), was included. The UGR_{exp} equation thus takes the form:

$$UGR_{exp} = 8 \cdot \log_{10} L_{avg} + 8 \cdot \log_{10} \sum_{i=1}^n \frac{L_{s,i} \cdot \omega_{s,i}}{L_b \cdot P_i^2}$$

with

EQ 10

$$L_{avg} = \frac{E_v}{\pi}$$

In (Wienold et al., 2019), DGI_{mod} performed only slightly better than DGI while the UGR_{exp} performed rather poorly, failing five of the six statistical tests. The authors suggest that this behaviour is caused by the smaller influence of the glare sources in the equation in comparison to other glare equations, where L_s^2 is more commonly used instead of L_s . Since in (Wienold, 2010) it was found that the logarithm of E_v had a lower correlation to the ratio of people disturbed by glare than the linear form of E_v , the authors in (Wienold et al., 2019) conclude that the logarithmic function applied to the average luminance L_{avg} in the UGR_{exp} might be disadvantageous.

The DGI_{mod} is considered a metric based on the contrast effect only, according to (Wienold et al., 2019) while UGR_{exp} is considered a metric that is based on both the contrast and saturation effects.

2.2.10 Daylight Glare Probability (DGP)

In the context of a EU-project starting in the early two-thousands, Wienold and Christoffersen developed the Daylight Glare Probability index (Wienold and Christoffersen, 2006). The experimental set-up for this study was carefully investigated and addressed several issues identified in previous studies, both at experimental and at the glare index development level. The metric is based on an experiment with 70 subjects that took place in two identical experimental rooms located in Copenhagen and Freiburg, used three window configurations and three shading systems for a total of 349 data points. The experiment was run under daylighting only and stable clear sky conditions. The subjects sat at 1.5 m from the window, conducting three-typical office tasks that included reading and working on a computer. The viewing direction was either parallel to the window (90°) or facing diagonally towards the window (45°).

Testing the correlation of several metrics with the subjective assessments of glare, the authors found that from all the metrics analysed (including DGI and CGI), the linear function of vertical eye illuminance (E_v) had the strongest correlation with the probability of persons disturbed by glare, a finding that was in line with results from previous research (Velds, 1999). They considered that the E_v was a better variable for the adaptation term in the glare equation, a hypothesis that was also supported by achieving a somewhat higher correlation for E_v than for L_{avg} .

The basic idea towards an improved metric was therefore to combine the vertical eye illuminance with the general glare source term of the glare index formula. This led to the definition of a basic structure for the equation as:

$$DGP = c1 \cdot E_v + c2 \cdot \log_{10} \left(1 + \sum_{i=1}^n \frac{L_{s,i}^2 \cdot \omega_{s,i}}{E_v^{c3} \cdot P_i^2} \right) + c4$$

It can be seen that the logarithmic function, associated with the eye adaptation level (and saturation) in previous glare models was dropped in favour of a linear function of vertical eye illuminance. This results from the fact that, in the study, a much higher correlation for the linear form of E_v was found than for a logarithmic form.

DGP has separate terms for 'adaptation' and 'contrast' but it has the particularity of using the adaptation variable (E_v) in the contrast part of the equation, where the background luminance or illuminance variables were generally used. This means that for the DGP contrast is understood as the contrast within the overall luminance of a scene and not the contrast between the glare source and the non-glare source part of a scene. Nevertheless, the overall illuminance of the scene (E_v) contributes differently in the contrast and adaptation parts of the equation.

For optimizing the $c1$ to $c4$ parameters, the authors used a random optimisation algorithm, where thousands of different parameter settings were tested against the glare votes. The highest correlation with the subjective glare rating was found for the following parameter settings:

$$DGP = 5.87 \cdot 10^{-5} \cdot E_v + 9.18 \cdot 10^{-2} \cdot \log_{10} \left(1 + \sum_{i=1}^n \frac{L_{s,i}^2 \cdot \omega_{s,i}}{E_v^{1.87} \cdot P_i^2} \right) + 0.16 \quad \text{EQ 11}$$

with this equation producing an extremely good correlation with the subjective glare evaluation (Wienold, 2010).

The DGP is considered a metric that is based on both the contrast and saturation effects (Wienold et al., 2019), with these two effects combined in an additive manner. It measures the probability of people disturbed by discomfort glare, expressed as a percentage. For example, a calculated DGP value of 0.7 indicates a probability that 70% of occupants of a space would be disturbed by discomfort glare.

Due to the conditions of the study, the base DGP equation is valid for a range between 0.2 and 0.8, although due to later validation studies, the authors state that values above 0.8 can be trusted to some extent. A correction of the equation using an 's-curve' was introduced by (Wienold, 2012) to extend its applicability to values below 0.2. This correction, called low-light correction, is applied to the base equation, when the E_v ranges between 0 and 300 lux.

$$DGP_{\text{lowlight}} = DGP \cdot \frac{e^{0.024 \cdot E_v - 4}}{1 + e^{0.024 \cdot E_v - 4}} \quad \text{EQ 12}$$

DGP is the metric adopted in the recently published European daylight standard for the analysis of daylight glare (Comité Européen de Normalisation, 2018).

Recent validation studies (Wienold et al., 2017) (Wienold et al., 2019), have shown that DGP is the most accurate and robust of a wide range of metrics at predicting discomfort glare, passing all six statistical tests that were performed, for all the seven tested datasets in that study. However, along with several of the glare indexes presented above, DGP was found to perform rather poorly or moderately in a range of field studies that were carried out in the recent years (Konis, 2014) (Hirning et al., 2014) (Van Den Wymelenberg and Inanici, 2014) (Mahić et al., 2017) (Yamin Garretón et al., 2018).

2.2.11 Unified Glare Probability (UGP)

Hirning et al. (2014) conducted a visual comfort survey in 5 green office buildings in Brisbane under clear-sky conditions during a 9-month period, for a total of 419 subjective glare evaluations. The investigation revealed that all tested glare indices (DGI, DGP, CGI, UGR and VCP) tended to underestimate reported discomfort. In that study, DGP showed a lower correlation than DGI, UGR and CGI, with VCP performing the worst. Although all glare indices showed some correlation to discomfort, the authors state that there was no significant difference in the correlations of the best performing indices - DGI, UGR and CGI. The authors also tested a wide range of glare source identification multipliers to find that the best performing indices produced their highest correlations with multipliers between five and seven, with almost identical correlation values for the three indices.

Based on their results, the authors defined a new glare index, UGP, which is based on a linear transformation of UGR, to express the probability (as a percentage) of persons disturbed by glare.

$$\text{UGP} = 0.26 \cdot \log_{10} \left(\frac{0.25}{L_b} \cdot \sum_{i=1}^n \frac{L_{s,i}^2 \cdot \omega_{s,i}}{P_i^2} \right) \quad \text{EQ 13}$$

The correlations obtained for the UGP were high and somewhat above than what was obtained for the best performing glare index (CGI).

The authors note that very low vertical illuminance measurements were recorded at the subject's workspaces. The average illuminance was 445 lux, with the maximum illuminance recorded being 2,354 lux. This is in contrast to the DGP investigation, where recorded illuminances reached 10,000 lux. The authors note that in open plan buildings, occupants seated next to windows are usually not facing them directly, but sit adjacent to them. In these situations glare comes not necessarily from the adjacent window, but from windows that are further away but directly in the field of view.

Like UGR, UGP is considered a contrast-based only metric. In (Wienold et al., 2019), the two metrics were found to perform rather poorly.

2.2.12 Perceived Glare Level (PGL)

Stating inaccuracy of existing glare indices and complexity of the glare metric equations and calculation procedures, Suk et al. (2016) developed a new metric called Perceived Glare Level (PGL).

The development of PGL is based on an experiment involving 53 test sessions in a cellular office type of space (2.9 m x 3.5 m), with each session including 3 task conditions (no task, typing task and writing on paper task) and 3 shading conditions (no blinds, roller blinds and venetian blinds), for a total of 450 data points. The experiment was carried out in south-California, in a period from February to June, under daylight only and mostly clear-sky conditions. The number of subjects is not provided but it is said to be small to keep a focus on the number of tested conditions. The subjects sat in a workstation facing the window light source directly, having also another window to their side.

The PGL equation is based on the idea of combining what the authors call the 'absolute glare factor' and the 'relative glare factor'. The absolute glare factor concerns the maximum luminance in the visual field and the relative glare factor concerns a measure of contrast involving the glare source.

They compared the identification of glare sources by the subjects in a map of their visual fields with their glare ratings to find that the glare sources detected by the luminance threshold of 5,000 cd/m² matched the visual maps better than when detected with a multiplier of 5.

For the measure of contrast they tested the ratio of the mean luminance of the background to the mean luminance of the glare source, L_b/L_s and the ratio between the mean luminance of glare source to the mean luminance of the task area, L_s/L_t . They found a weak correlation between the first ratio and the categories of glare. As they were only able to find a strong correlation between the L_s/L_t and the glare categories for the typing task, the PGL metric is applicable to the conditions of a typing task only. The PGL equation was defined using regression and is based on the summation of the glare source luminance and the contrast between the glare source and task luminance. The new formula, presented below, produced a reasonably good correlation to reported glare.

$$\text{PGL} = 0.206 + 0.00016 \cdot L_s + 0.00337 \cdot R_t$$

with

$$R_t = \frac{L_s}{L_t}$$

EQ 14

It is important to note that the authors found that the glare ratio had no or minimal influence on perceived discomfort glare levels, which they attributed to the strong daylight conditions of their experiment. Although the authors seem to accept that the contrast effect is important in the perception of glare, their experimental set-up does not seem to cover conditions that lead to high levels of contrast, which might be the reason why no significant correlations for the ratio metrics were found.

According to (Wienold et al., 2019), PGL is an equation based on the contrast effect and absolute thresholds, that does not consider the size of the glare source nor the saturation effect and uses the contrast effect in a linear way. In that study, the equation was found to have a relatively poor performance, failing all six statistical tests that were performed in three of the seven datasets.

2.2.13 Glare Sensation Vote (GSV)

Claiming that existing discomfort glare metrics are usually tested in controlled environments and have certain limitations when predicting glare in extremely bright conditions, Yamin Garretón et al. (2018) conducted a study on real working spaces with the presence of direct sunlight in the bright sunny climate of Mendoza, Argentina. The 26 participants were evaluated in their actual office spaces, under two lighting conditions, for a total of 52 data points. Each office (of the same typology) was 4.62 m × 2.32 m with a window of 1.56 m × 1.8 m. The subjects' view direction is presumed parallel to the window. The subjects evaluated a preferred lighting condition, where blinds were adjusted to their preferences and an unfavorable lighting condition, where the blinds were adjusted to achieve the highest level of glare.

The authors studied the adequacy of several metrics ranging from simple luminance and illuminance metrics, luminance ratios, luminance distribution and DGP. The investigation was conducted along the same lines as the investigation by Suk et al. (2016), where the metrics were subdivided into an 'absolute glare factor' group and a 'relative glare factor' group.

In the 'absolute glare factor' group, they found the best correlations for the percentage of the central (30°) and near (60°) regions of the field-of-view with a luminance greater than 2,000 cd/m² (named $L_{s\%2000C}$) and for the minimum luminance of the glare source (L_{s_min}). For the 'relative glare factor' group they found the best correlation for the ratio between the mean luminance of the glare source and the mean luminance of the task (L_{s_mean}/L_{t_mean}).

Testing two multiple regression models with these variables, the model including $L_s\%2000C$ and L_{s_mean}/L_{t_mean} provided the best correlation with glare. Based on that, the following equation was derived:

$$GSV = 1.61 + 0.152 \cdot L_{s\%2000C} + 0.019 \cdot \frac{L_s}{L_t} \quad \text{EQ 15}$$

Where $L_{s\%2000c}$ is the area of pixels larger or equal to 2,000 cd/m² within the central and near field of view.

GSV is specifically recommended for situations when direct sunlight is present in the work area. In Wienold et al. (2019), GSV is classified as an equation based on the contrast effect and absolute thresholds that uses the contrast in a linear way. In that study, GSV was one of the worst performing metrics, a result that the authors attribute to the linear approach to contrast and to the absence of luminance information in the absolute threshold term. The dataset in Wienold et al. (2019) does however include cases with and without sun incident on the work area.

2.2.14 Daylight Glare Probability Modified (DGPmod)

After studying the effects of daylight glare for cases with the sun in the field of view seen through windows with roller shades, Konstantzos and Tzempelikos (2017) proposed a new equation based on a modification of the DGP to account for discomfort glare in those specific conditions.

The authors collected subjective glare assessments from 41 subjects while performing specific office activities in a series of mock cellular office spaces. The spaces were equipped with 14 shading devices of different openness factors and visible transmittance installed on the windows, for a total of 355 data points. Although a higher correlation was found for UGR in comparison to the other studied metrics (E_{dir} , E_v/DGP_s , L_{avg} , DGP, DGI and UGR), the authors have chosen to develop an alternative form of the DGP, allegedly due to the generalizability of the metric. Using a similar method to the one used for the development of the DGP, the authors performed an optimisation of the parameters of the DGP equation. The analysis showed that DGP could indeed be modified in order to predict the reported discomfort glare better than any of the investigated glare indices, achieving a very high correlation, for an equation of the following form:

$$\text{DGP}_{\text{mod}} = 8.40 \cdot 10^{-5} \cdot E_v + 11.97 \cdot 10^{-2} \cdot \log_{10} \left(1 + \sum_{i=1}^n \frac{L_{s,i}^2 \cdot \omega_{s,i}}{E_v^{2.12} \cdot P_i^2} \right) + 0.16 \quad \text{EQ 16}$$

The metric is said to apply to the specific conditions of windows with sun seen through fabrics and has not been validated by other studies or for other conditions.

2.3 Simple luminance metrics

Simple luminance metrics and luminance photometric quantities are also used for the analysis of discomfort glare. The origins of these metrics and their applicability to discomfort glare prediction is not very clear. Nevertheless, they have been studied in the context of discomfort glare and shown to sometimes have better predictive ability than the glare indices (Van Den Wymelenberg et al., 2010) (Konis, 2014) (Mahić et al., 2017). Due to the characteristics of the used questionnaires, it is likely that those studies pertain to the problem of visual discomfort in its general sense and not necessarily to the specific problem of discomfort glare.

2.3.1 Contrast ratios

Luminance contrast ratios fit into the classification of metrics that depict the contrast effect only but contrary to the glare indices they usually represent contrast in a linear way. The size and position of the glare source as well as variables that account for the adaptation level are excluded in these metrics. They also pertain not to the general contrast within a scene but to the contrast between regions of interest in a scene.

2.3.1.1 Window-based contrast ratios

The contrast ratio between the mean luminance of the window and the mean luminance of the task ($L_{win_mean}/L_{task_mean}$) is a metric proposed for the analysis of discomfort from daylight in the IES Lighting Handbook (Dilaura et al., 2011), with a borderline between comfort and discomfort set at 20/1. Van Den Wymelenberg and Inanici (2015) propose a revised threshold for this metric of 22/1. In a study carried out by Konis (2014) in the core zones of an open-plan office building, the author found that the contrast ratio between the maximum luminance of the window to the mean luminance of the task ($L_{win_max}/L_{task_mean}$) was one of the most successful from the fifteen analysed metrics, predicting 77.4% of the measured subjective assessments of visual discomfort correctly. In the study carried out by Mahić et al. (2017), which was run in a range of rooms and sitting positions the authors found that the ratio between the 98% luminance percentile and the mean luminance of the lower part of the window was among the best performing metrics.

2.3.1.2 Glare source-based contrast ratios

Although in the case of daylight illumination the glare source will likely correspond to the window light source, some authors propose metrics that refer to the glare source in a general way. In fact, a glary spot can occur in areas outside the window area for instance when sun is being reflected off from surfaces within a room. This is in some cases called 'reflected glare' and later in this thesis as 'secondary glare sources'. This highlights one of the problems of considering specific regions such as the window area as the sole source of glare in the prediction of discomfort glare - there can be other parts of the visual field producing similar levels of discomfort.

Suk et al. (2016) suggest a maximum contrast ratio between the mean luminance of the glare source and the mean luminance of the task (L_g/L_t) of 22/1, with values above 39/1 corresponding to disturbing glare situations. Their proposed ratio is however only applicable to situations where subjects are engaged on typing tasks.

2.3.2 Region-based metrics

Region-based metrics fit into the classification of equations that use neither the saturation nor the contrast effect or metrics that use the saturation effect only.

2.3.2.1 Window-based metrics

The mean luminance of the entire window (L_{win_mean}) is one of the metrics proposed by Van Den Wymelenberg and Inanici (2015), with a proposed borderline between comfort and discomfort between 2,000 and 2,500 cd/m^2 , with values above 2,500 cd/m^2 indicating discomfort.

The standard deviation of the window luminance (L_{win_std}) is also one of the three metrics proposed by Van Den Wymelenberg and Inanici (2015). They propose a borderline between comfort and discomfort for a luminance range between 2,500 and 4,000 cd/m^2 , with values above 4,000 cd/m^2 indicating discomfort.

The metrics above fit into the classification of equations that use neither the saturation nor the contrast effect. In the study carried by Wienold et al. (2019), L_{win_mean} failed three of the six statistical tests, while L_{win_std} performed worse than L_{win_mean} , failing four tests.

2.3.2.2 The 40° horizontal band

The mean luminance of the region within the 40° horizontal band of the visual field along the central horizontal axis ($L_{40^\circ_mean}$) is another of the metrics proposed by Van Den Wymelenberg and Inanici (2015), with a borderline between comfort and discomfort of 500 to 700 cd/m^2 , where values above 700 cd/m^2 indicate discomfort. In the study carried out by Wienold et al. (2019), $L_{40^\circ_mean}$ performed rather poorly. The authors note that important sources of glare can easily fall outside the 40° horizontal band and this might cause a poor performance of the metric.

Mahić et al. (2017), found that the coefficient of variation (COV) of the luminance of the 40° horizontal band ($L_{40^\circ_COV}$), defined as the standard deviation divided by the mean, showed a good correlation and stability in predicting several visual discomfort indicators. A high likelihood of subjective discomfort was found for a $COV > 3.25$.

2.3.2.3 Combined regions

In the study carried out by Van Den Wymelenberg and Inanici (2015), where 2,000 luminance-based metrics and several possible semantic differential subjective ratings were analysed, the authors found the strongest correlation for a model built upon three variables: the standard deviation of window luminance, the 50th percentile luminance value from the lower part of the window and the mean luminance of the 40° horizontal band.

2.3.2.4 Luminance of the visual field

The average luminance (L_{avg}) is considered a metric that is based on the saturation effect only, as it produces a measure of the total amount of light in the visual field. It is one of the metrics proposed by Van Den Wymelenberg and Inanici (2014) and it was found to perform reasonably well in (Wienold et al., 2019), failing only one of the six statistical tests performed in that study. The L_{avg} is defined by (Wienold et al., 2019) as:

$$L_{\text{avg}} = \frac{1}{2\pi} \cdot \sum_{i=1}^n L_i \cdot \omega_i \quad \text{EQ 17}$$

Some researchers have looked into the possibility of defining an upper limit for the luminance of the visual field, contrasting with the typical approach based on the definition of the luminance ratio between the source and the background for the prediction of glare. Dubois (2001) refers to a maximum luminance of 2,000 cd/m² in any point of the visual field and admits these can be doubled in case of daylighting.

Wienold and Christoffersen (2006) propose detailed thresholds of 2,000, 4,000 and 6,000 cd/m² for ‘acceptable’, ‘just uncomfortable’ and ‘intolerable glare’, respectively. Shin et al. (2012) propose significantly higher values for the same three categories – 3,200, 5,600 and 10,000 cd/m².

Suk et al. (2016) propose new thresholds of 5,000 cd/m² for situations when subjects are engaged with a typing or writing task and of 7,000 cd/m² for situations where subjects are not engaged on a task.

2.4 Vertical eye illuminance (E_v)

The vertical illuminance at eye level (E_v) is not a proposed discomfort glare metric by itself but it has been studied and used as such, given the high correlation that was found between E_v and subjective glare evaluations by Velds (1999) and by Wienold (2010) for this metric. In (Wienold et al., 2019), E_v is considered a metric that is based on the saturation effect only and it was found to be one of the best performing metrics among the metrics of that kind. Vertical eye illuminance was also found to outperform all the luminance and illuminance-based metrics and glare indices studied by Van Den Wymelenberg and Inanici (2014). The experimental set-ups of the above-mentioned studies are similar in many respects (cellular-office), which might explain the success of the metric in all of the three studies. The metric was however found to perform rather poorly in (Hirning et al., 2014) and in (Konstantzos and Tzempelikos, 2017).

2.5 Illuminance of the glare source (E_{dir})

Even though the illuminance of the glare source E_{dir} is not a proposed discomfort glare metric by itself, it has been studied as such by Wienold et al. (2019). In that study, E_{dir} it is considered a metric that is based on the saturation effect only and from all the metrics of that kind it was the one that performed the worst. The authors state that this results from the fact that the metric only considers the glare source and omits the contribution of the background luminance.

2.6 Daylight Glare Probability simplified (DGPs)

After finding that the vertical eye illuminance (E_v) had a reasonably good correlation with reported glare perception, Wienold (2007) derived a simplified version of DGP that is based on the E_v only, called the Daylight Glare Probability simplified (DGPs).

$$\text{DGPs} = 6.22 \cdot 10^{-5} \cdot E_v + 0.184$$

EQ 18

DGPs neglects the influence of individual glare sources and since it is based on the vertical eye illuminance only it is easily calculated using a single point calculation, greatly reducing the computation time involved in the calculation of discomfort glare metrics based on luminance. The DGPs is only applicable if no direct sun or specular reflection of it hits the eye of the observer, which reduces its application to situations where the sun is not visible in the visual field. As the equation only takes the total amount of light in the eye into consideration, DGPs can be classified as a saturation glare metric.

An improvement of DGPs was tested by Wienold (2009) in the form of the enhanced Daylight Glare Probability simplified (eDGPs). The basic idea behind the eDGPs is to add the contrast part of the calculation of DGP to DGPs, via a simplification of the luminance simulation. This is done by the calculation of the direct lighting component of a luminance simulation only, i.e. the luminance of the glare sources, leaving the indirect light contribution, i.e. light reflected from a rooms' surfaces, out of the simulation. Although a rendered image of the visual field is still required, a significant reduction of the computation time for the glare simulation is achieved in this way.

The accuracy of DGPs and eDGPs was evaluated in (Wienold, 2009) in comparison to a hour-by-hour calculation of DGP for a window with a range of shading devices and without a shading device, producing relatively good results. The eDGPs is said to be applicable to all window types other than those with scattering or re-directing properties, where the indirect calculation might be necessary and the metric is currently implemented in several software tools for the evaluation of annual discomfort glare.

2.7 Glare_{EV}

After proposing a modification of the DGP equation (DGPmod) to account for cases of glare with the sun in the field of view seen through roller shades and arguing that DGPs is not applicable in those cases, Konstantzos and Tzempelikos (2017) looked at developing a simplified metric that would apply to the prediction of discomfort glare in those conditions. The proposed metric, Glare_{EV}, combines a term to describe the effect of the sun and another term that captures the overall sensation of brightness or adaptation, the total vertical illuminance on the eye or E_v. The metric applies to cases where there is sun in the visual field, excluding cases where the observer is looking directly at it. The authors have chosen two variables to base the development of the equation on, the direct vertical illuminance of the sun and the fraction of the total vertical illuminance to the direct vertical illuminance of the sun. Following the same procedure that was used for the development of DGPmod, the authors found a relatively high fit for the equation:

$$\text{Glare}_{\text{EV}} = 0.13 \cdot E_{v,\text{dir}(\text{sun})}^{0.27} + 0.04 \cdot \left(\frac{E_v}{E_{v,\text{dir}(\text{sun})}} \right)^{0.84} - 0.48 \quad \text{EQ 19}$$

Where E_{v,dir(sun)} is the direct illuminance on the eye from the sun.

The authors state that other combinations of direct and total vertical eye illuminance were tested without satisfactory results. The Glare_{EV} was found to be much more effective than E_v or DGPs in predicting discomfort glare in the conditions of the study.

2.8 Useful Daylight Illuminance (UDI)

Firstly proposed in (Nabil and Mardaljevic, 2005) and (Nabil and Mardaljevic, 2006), the UDI pertains to the range of horizontal illuminances, generally measured at desk level, that are neither too low to produce an insufficient illumination condition nor too high to cause visual discomfort. After a review of the existing literature regarding occupant's response to daylight levels, the authors in Nabil and Mardaljevic (2006) state that daylight illuminances in the range of 100 to 500 lux are considered effective either as the sole source of illumination or in conjunction with artificial lighting, that daylight illuminances in the range of 500 to 2,000 lux are often perceived either as desirable or at least tolerable and that daylight illuminances higher than 2,000 lux are likely to produce visual and/or thermal discomfort. The upper threshold of the metric indicates the propensity for discomfort glare due to high levels of illumination, and in that sense UDI can be considered a metric based on the saturation effect only, where the eye adaptation level is equivalent to the illuminance of the desk surface.

New UDI ranges are proposed in (Mardaljevic et al., 2012), for an upper threshold, or borderline between comfort and discomfort of 3,000 lux. The authors explain that the newly proposed thresholds are based on surveys carried out in office buildings where daylight glare on visual display devices is a common problem. They add that those surveys were carried out before liquid-crystal display screen technology, much less prone to glare than cathode-ray tube screens. Given the simplicity of its calculation, UDI was investigated as an alternative metric to DGP for the simulation of discomfort glare by Mardaljevic et al. (2012), where the different ranges of the UDI have shown a good agreement with the corresponding DGPs classes.

In a review of existing visual comfort metrics, Carlucci et al. (2015) refer to a range of studies that establish an upper bound for UDI varying between 2,000 lux and 8,000 lux.

Although horizontal desk illuminance was not found to be significantly correlated to visual discomfort in the study carried out by Van Den Wymelenberg and Inanici (2015), based on their results the authors propose a revised upper comfort threshold between 2,000 and 4,300 lux for the metric.

There seems therefore to exist some uncertainty regarding what the upper threshold for UDI should be. On the other hand, as UDI pertains to the light conditions of the horizontal task area, one might ponder about the applicability of the metric to the

situation of a vertical task like the board-based tasks in a classroom. The UDI is nevertheless widely used due to its simplicity and ease of computation and for that reason it has been recently integrated in codes such as the daylighting design guide for schools in the UK (Education Funding Agency, 2014).

2.9 Annual sunlight hours (ASH)

Following the results of the daylight metrics validation project PIER (Heschong, 2012) in the US, the Annual Sunlight Hours (ASH), measured by means of illuminance at the task level, has been proposed as a glare assessment method in the LM-83-12 standard (IESNA, 2012). It is important to note that luminance-based metrics were not covered in the PIER project due to the aforementioned difficulties imposed by the luminance calculation, requiring field-of-view luminance capture or rendered views of the visual field. The ASH was simply found to be the easiest metric to calculate that provided the best correlation with the subjective assessments of glare, although that correlation wasn't found to be particularly strong. The metric has nevertheless been adopted as the visual discomfort and glare assessment method in WELL (USGBC, 2019) and in LEED (USGBC, 2013). In these certification systems, it is specified that no more than 10% of the area of a regularly occupied space should receive more than 1,000 lux for 250 hours of one year. As an annual-based metric, the focus is on the reduction of the period of discomfort rather than on the reduction of discomfort at a given point in time.

2.10 Cross-validation of existing glare metrics

The cross-validation study carried out by Wienold et al. (2019) was cited in several occasions in this review due to its comprehensive nature and relevance. The authors studied the accuracy and robustness of 22 existing and newly proposed metrics using data from seven independent studies carried out in office-like test rooms in different parts of the world, for a total of 420 subjects and over 1,000 data points. The accuracy of the glare metrics was analysed based on a range of statistical tests

and the robustness of the metrics was analysed based on the number of passed tests in each of the seven datasets. The exercise resulted in the most comprehensive validation study of discomfort glare metrics to date.

The conclusion of that study is that the six highest ranked metrics for both the performance and the robustness evaluation were the metrics that consider the saturation effect as a main effect in the glare equation, with DGP performing better than any of the other metrics. Metrics based only on contrast or regions of the field of view, as well as equations based on one single variable, did not perform as well and were found to be less robust. This outcome is however said to be valid for what the authors call daylight-dominated workplaces and that those results might not be fully transferrable to scenarios which differ significantly from the conditions of those studies. All the studies of that investigation were carried out in test rooms of relatively small dimensions and mostly under high vertical eye illuminance.

The authors suggest that future research should aim at optimising the combination of contrast-driven and saturation-driven terms in the metrics' equations, for the equations that already include those terms.

2.11 Physiological response to discomfort glare

In the search for an objective way of measuring discomfort glare, there have been several attempts to identify and study physiological responses to discomfort glare that could be used to measure it, with studies on this subject being carried out as early as 1956 (Hopkinson, 1956). It is believed that such response can partially resolve the problem of large variation that is found regarding the self-reported perception of discomfort glare by different subjects. Hamedani et al. (2019) made a cross-examination of existing literature on this subject, providing a list of fourteen articles written on the matter so far. The focus of the study is on the characteristics and scientific reliability of these studies. The authors make a list of the physiological indicators of discomfort that have been studied: pupil size, eye movement, gaze direction, degree of eye-opening and blink rate and conclude that there is still limited scientific evidence regarding the link between lighting conditions and any of these potential physical responses to discomfort glare.

2.12 Discussion

The review presented above traced the evolution of the discomfort glare metrics' and their formulation and explored how different studies in working spaces have contributed to their understanding and definition through time.

The review presents both luminance and illuminance-based metrics. The luminance metrics include the discomfort glare indices and simple luminance metrics such as contrast ratios and absolute luminance thresholds.

One of the aspects that has been often exposed as a limitation of the early glare indices (BGI, UGR, CGI, VCP) is the fact that these were developed based on experiments with artificial light sources of general small size. These equations express discomfort glare primarily as a problem of luminance contrast between a light source and its background. In daylight scenes, where the window source can occupy a large portion of the visual field this contrast effect is diminished and the eye is generally adapted to higher luminance.

Several metrics have since been developed or improved based on experiments with either simulated (DGI, PGSV) or real windows (DGP, UGP, DGI_{mod}, UGR_{exp}) and in many cases with the intention of addressing the problem of the lack of an adaptation term.

This adaptation term, that in some cases is also referred to as the 'absolute factor group' came to be introduced with some metrics in the form of the average luminance on the visual field (UGR_{exp}, DGI_{mod}, DGI_N), of the total illuminance reaching the eye of the observer (DGP, DGP_{mod}) and in some cases in the form of the task luminance (PGSV). The term is intended to represent the portion of the visual field that is responsible or mostly responsible for the level of light that the eye is adapted to, as it came to be accepted that in daylight scenes, the background luminance (L_b) or any other single region of the visual field might not be adequate to represent it. In some cases, this added adaptation term replaces the background luminance (L_b) in the equations; in other cases, it is used in combination with the background luminance.

However, the average luminance (L_{avg}) or the total illuminance (E_v) are only considered representative of adaptation when used additively in the glare index equations (UGR_{exp}, DGP) or explicitly in the definition of adaptation (PGSV).

When average luminance (L_{avg}) or the total illuminance (E_v) are introduced in the equations, it is also understood that the saturation effect of glare is adequately represented, as it is expected saturation to be driven by the total amount of light reaching the eye. The designation of 'contrast and saturation-based' equation serves to distinguish equations that have this additional or explicit term from the equations that only have a contrast term as per the original glare sensation formula.

A range of simple luminance- and illuminance-based metrics mentioned in the literature has also been presented. Simple luminance metrics are generally proposed or studied in the context of visual discomfort in general. However, as methods of visual discomfort prediction there seems to be an interest in finding to what extent these simple metrics are applicable to the prediction of discomfort glare. The calculation and simulation of discomfort glare is simplified and faster via the use of illuminance-based metrics, however in most cases these metrics do not show particularly good correlations with reported discomfort glare and there is high uncertainty to what the discomfort glare threshold for these metrics should be.

While there is an interest in using simple metrics and faster discomfort glare calculation methods, the formulations of these metrics do often lack either a contrast or an adaptation term indicating that they might not be fully capable of depicting the discomfort glare problem in its different manifestations of saturation and contrast. On the other hand, the problem of calculation time has been largely overcome in recent years, after developments on the computation of luminance front (Jones and Reinhart, 2017).

Some concluding remarks can be made based on the above review:

- Existing metrics have tended to be developed or validated in conditions prone to saturation glare. The glare indices, and in particular the saturation-based metrics, perform generally better under these conditions than contrast-based or simple luminance-based metrics.
- In most field studies (real work environments), metrics that are based on the contrast-effect seem to perform better than other metrics. This can be attributed to the lower overall luminance levels and therefore higher luminance contrast of window to background that can be found in these deeper spaces.
- Most of the existing studies on discomfort glare have been carried out in the context of offices and in mock-up spaces of small dimensions.
- Metrics have been developed based on experiments involving desk-based visual tasks (personal computer or paper-based work). The existing metrics have not been developed or tested for the conditions of a 'vertical' or 'distant' task like a board-based task of a classroom.

- Most metrics have not been tested in contexts other than the ones that they have been developed for. In some cases, metrics have been developed in conditions that are too specific and therefore possibly not generalizable to other contexts.
- Many of the existing glare metrics have been developed for situations where subjects are either looking at the glare source directly or are asked to look at the source before doing their glare assessments.

It is observed that a wide range of metrics were developed at high proximity from a window in many cases for a subject facing directly or almost directly the window light source. This situation is rarely found in real-life situations and is even less likely to occur in a classroom, where subjects near a window tend to look inwards and subjects away from a window will have a reduced view of the window light source. Any discomfort glare situation in a classroom is more likely to be caused by contrast than by saturation in the positions away from the window and it might be of saturation or contrast near the window light source, depending on view direction. In a classroom, a situation of saturation glare near a window will also likely be of a smaller effect than in an office space (where the line of sight is usually parallel to the window) since the window light source will at times be quite peripheral in the visual field of the observer (with a line of sight directed to the board in the centre of the room). This indicates that contrast-based metrics or metrics that consider the contrast effect might be able to predict a wider range of glare situations in a classroom environment but are probably not enough to depict glare in all situations.

A summary of the presented metrics and of the conditions in which they have been developed, including the position of the subject in space and view direction, is provided in Table 2.1. Metrics are classified as 'contrast', 'saturation' or 'contrast and saturation' depending on whether their definition is only contrast-based, only saturation-based or have terms to account for both effects of glare. Within the contrast definition, 'contrast simple' is used to identify metrics that do not include terms for the characteristics of the glare source (i.e., size and position) in their definitions.

TABLE 2.1 Summary of presented metrics, their characterization, and conditions of their development.

Metric	Date	Type of metric	Source type	Source size [steradians]	Distance to window [m]	View direction ^(a)
BGI	1950	Contrast	-	Point sources up to $2.7 \cdot 10^{-2}$	-	-
VCP	1963	Contrast	Artificial lighting	-	-	-
DGI	1972	Contrast	Artificial window	-	-	-
CGI	1979	Contrast	Multiple glare sources	-	-	-
UGR	1995	Contrast	Artificial lighting	Between $3 \cdot 10^{-4}$ and 10^{-1}	-	-
PGSV	1990	Contrast and saturation	Artificial window	(Window of 2 m width)	0.75, 1.5, 3	Parallel and perpendicular
DGI _N	2000	Contrast	Simulated window	-	-	-
DGI _{mod}	2003	Contrast	Real window	-	3	Perpendicular
UGR _{exp}	2003	Contrast and saturation	Real window	-	3	Perpendicular
DGP	2006	Contrast and saturation	Real window	Cellular-office type of window	1.5	Diagonal towards the window + parallel to window
UGP	2014	Contrast	Real window	Open-plan office windows	-	-
PGL	2016	Contrast simple ^(b)	Real window	Cellular-office type of window	Close proximity to window	Perpendicular
GSV	2018	Contrast simple ^(b)	Real window	(Window of 1.56 m × 1.8 m)	-	Parallel
DGP _{mod}	2017	Contrast and saturation	Real window	Cellular-office type of window	Close proximity to window	Perpendicular
$L_{win_mean} / L_{task_mean}$	2011	Contrast simple	Real window	-	-	-
L_s / L_t	2016	Contrast simple	Real window	-	-	-
$L_{win_mean} L_{win_std} / L_{40^\circ_mean}$	2015	Neither contrast nor saturation	Real window	Cellular-office type of window	Close proximity to window	Parallel
$L_{40^\circ_COV}$	2017	Neither contrast nor saturation	Real window	Classroom and office type of window	Variable	Variable
L_{avg}	2014	Saturation	Real window	-	Close proximity to window	Parallel
E_v	1999, 2010	Saturation	Real window	-	Close proximity to window	Diagonal and parallel
E_{dir}	2019	Neither contrast nor saturation ^(d)	-	-	-	-
DGPs	2007	Saturation	Real window (DGP)	-	1.5	Diagonal towards the window + parallel to window

>>>

TABLE 2.1 Summary of presented metrics, their characterization, and conditions of their development.

Metric	Date	Type of metric	Source type	Source size [steradians]	Distance to window [m]	View direction ^(a)
Glare _{Ev}	2017	Saturation	Real window	-	Close proximity to window	Perpendicular
UDI	2005, 2012	Saturation ^(c)	Real window (2005) Simulated window (2012)	-	-	-
ASH	2012	Saturation ^(c)	Real window	-	Variable	Variable

^(a) View direction in relation to the window: perpendicular = looking directly at the window, parallel = looking in the direction parallel to window, diagonal = looking at an angle towards the window.

^(b) Includes an absolute threshold in their definition.

^(c) Eye is considered adapted to the task illuminance level.

^(d) Considered a 'saturation' metric in (Wienold et al., 2019).

2.13 Conclusion

The investigation in this thesis will primarily focus on the metrics that have been developed for the analysis of discomfort glare from daylight and on metrics that can in principle be generalizable to the wider range of glare conditions that are expected to occur in classrooms. In positions near a window of a classroom it is expected discomfort glare to occur mostly due to saturation, particularly in sunny sky conditions, whereas in positions in the inner room, it is expected glare to occur mostly due to contrast. Metrics that contain terms that describe both saturation and contrast (e.g., DGP, UGR_{exp} and PGSV) might therefore be more capable to identify glare in the wider range of visual conditions that can be found in these spaces. On the other hand, there is interest in investigating if the success of metrics that have been developed or proposed in the context of studies in deep spaces (e.g., UGP, L_{40°_COV}) extends to the visual conditions of the classroom.

It is also considered relevant to study the applicability of the metrics that have been adopted in current lighting standards and codes (e.g., DGP, ASH and $L_{win_mean}/L_{task_mean}$), particularly as these are familiar to the architect and to the lighting designer and are therefore widely in use. In terms of standard metrics, it is also considered relevant to investigate to what extent UGR, the metric that is most commonly in use for the purpose of quantifying discomfort glare from artificial lighting is applicable to the conditions of daylight glare, particularly given that the metric has shown a good performance in studies in deep spaces with daylight.

Simple luminance- and illuminance-based metrics that have in some cases been found to outperform the glare indices, such as E_v , L_{win_mean} , L_{win_std} and $L_{40^\circ_mean}$ will also be investigated in this dissertation.

Metrics that have been developed in the context of very specific conditions and are therefore limited in their applicability (e.g., DGPmod, GSV, PGL, DGPs) are considered secondary and will therefore not be part of this investigation.

3 Measurement of discomfort glare

3.1 Introduction

The way the human eye processes light is a phenomenon that is measured via the photometric quantities of luminance or illuminance. The discomfort glare prediction models are originally formulated based on luminance, making it the primary quantity of interest when it comes to measuring glare. In the past, luminance was either measured using luminance measuring set-ups specifically built for laboratory experiments (Figure 3.1) or inferred from field-of-view illuminance measurements using illuminance meters (Figure 3.2). Although measured on a point, the illuminance measurement can cover or almost cover the measurement of light from a 180° view angle, using cosine-corrected illuminance instruments.



FIG. 3.1 A modern version of the discomfort glare measuring set-up used by Luckiesh and Guth in 1949 for the development of the glare sensation formula, showing the dome used for measuring the background luminance and the movable glare source. Source: (Kim and Kim, 2010).

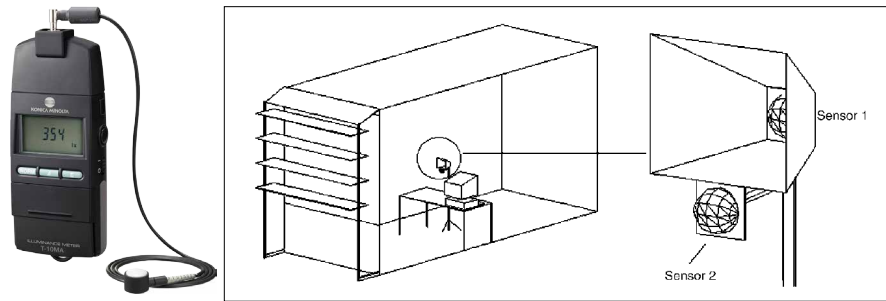


FIG. 3.2 A cosine-corrected illuminance meter (source: (Konica Minolta Sensing Americas, Inc, 2020) and field-of-view luminance measurement set-up using unshielded and shielded illuminance metres. Source: (Fisekis et al., 2003).

Deriving the luminance of particular areas of the visual field for the calculation of discomfort glare metrics using illuminance meters, does generally require the use of shields (Figure 3.2).

Image-based measurement of luminance however came to transform the way glare is measured and predicted, as it conveniently allows the measurement of the luminance distribution within the totality of the human visual field¹, in one single image (Figure 3.3).

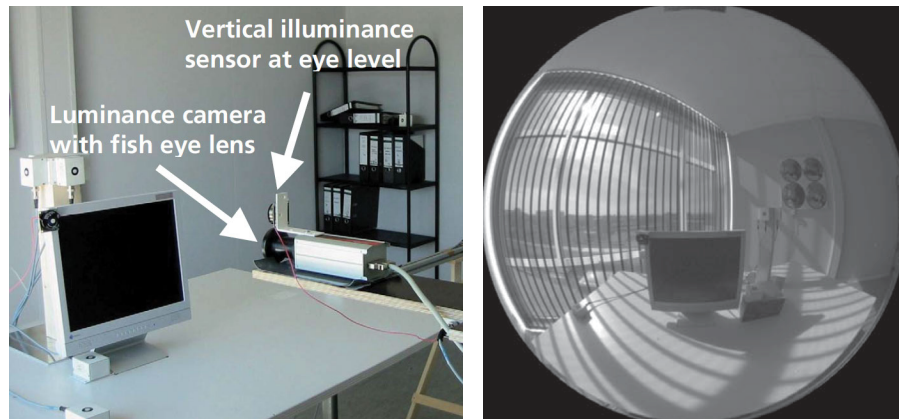


FIG. 3.3 A field-of-view measurement of discomfort glare set-up using image-based luminance capture (Wienold, 2010).

¹ In this work, the expression “visual field” pertains to the extension of the field of human vision or part of it, whereas the expression ‘field-of-view’ is used in relation to a measurement, i.e. the area of the visual field that is captured by an illuminance or luminance measurement.

This chapter describes the use of the image-based luminance measurement technique and how discomfort glare is computed based on this measurement.

3.2 Image-based luminance measurement

As the name indicates, an image-based luminance measurement is based on an image. The technique has been in use in lighting simulation since the first digital image file format capable of accurately reproducing visible light was created by Gred Ward (Ward, 1991) (Ward, 1994). Advances in photo-camera technology and manufacture, and in particular in what regards sensor technology, first by the use of CCD and more recently by the use of CMOS sensors, made it possible to extend luminance capture to real world scenes using digital technology. The technique came into practice in the late 1990s, in the fields of computer graphics and cinematography via the work of Paul Debevec who developed an algorithm for the calibration and processing of real world luminance data from photographs (Debevec and Malik, 2008) (Debevec, 1998).

The technique started to be used in building lighting research in the early 2000s by researchers that created their own systems (Coutelier and Dumortier, 2002) or via the use of calibrated image-based photometers, manufactured by specialist light metrology firms (Velds, 2002) (Wienold and Christoffersen, 2006).

Given the very high price of calibrated photometers and based on the knowledge gained from the advances in the field of computer graphics, Jacobs (Jacobs, 2007) and Inanici (Inanici, 2006) studied the calibration of commercial DSLR photo cameras as luminance acquisition systems for building lighting research. Inanici (Inanici, 2006) showed that image-based luminance capture using regular cameras had an average accuracy of 10% for a wide range of light sources and conditions and the technique has since been in use for the study of visual discomfort and glare (Fan et al., 2009) (Jakubiec and Reinhart, 2013) (Konis, 2014) (Hirning et al., 2014) (Van Den Wymelenberg and Inanici, 2014) (Rodriguez et al., 2017) (Konstantzos and Tzempelikos, 2017).

3.3 High dynamic range imaging

Visible light in the real world covers a very wide dynamic range. The human visual system is capable of simultaneously perceiving light over 4 orders of magnitude, a dynamic range corresponding to 1:10,000 and can adapt its sensitivity up and down to at least another 6 orders of magnitude, 1:1,000,000 (Jacobs, 2007) (Inanici, 2006). This is in extreme contrast with the luminance range that a single photo can hold, which can be as low as 1:100 (Reinhard et al., 2010).

To overcome this problem, image-based luminance measurements rely on what is called high dynamic range imaging (HDRI) a technique that extends the otherwise very low luminance range of a conventional photo. The HDRI is based on the capture of a sequence of photographs with different exposures, called low dynamic range images (LDR) and their combination into a single high dynamic range image (HDR) (Figure 3.4).



FIG. 3.4 Sequence of low dynamic range photographs captured with different exposures (aperture fixed at F2.6, ISO 100, shutter speed range 1/60" - 15") and the resulting high dynamic range image. Source: (Jacobs, 2007).

Using the HDRI technique, image-based luminance measurements can capture the very wide range of luminances that can be perceived by the human eye.

3.4 Image-based luminance measuring devices

Humans can perceive light in the wavelength range of 380 to 740 nanometers approximately, with the spectral sensitivity of the human visual system standardized as the CIE photopic luminous efficiency curve by the Commission Internationale de l'Eclairage, known as the $V(\lambda)$ curve (Figure 3.5). This curve forms the basis of photometry, the science of measuring light as perceived by the human eye.

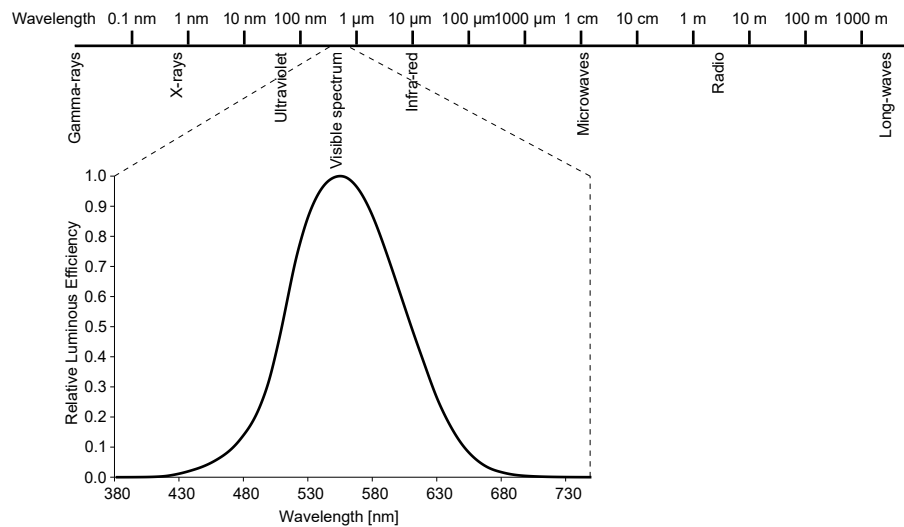


FIG. 3.5 The CIE photopic luminous efficiency curve, data source: (Stockman, 2020) plotted against the electromagnetic spectrum, data source: (Zwinkels, 2016).

Image-based luminance measuring devices differ in their spectral matching to the $V(\lambda)$ curve with the so called luminance photometers (or luminance cameras) offering the lowest $V(\lambda)$ spectrum mismatch or higher-measuring accuracy, with uncertainties as low as 3-4% reported by manufactures (Technoteam, 2019).

These high precision instruments use advanced RGB glass filter technology and can be custom-built to the particular purpose that they serve. The $V(\lambda)$ spectral matching of systems based on regular DSLR consumer cameras is based on a simple numerical transformation of the RGB sensor data (no special filters used) and therefore produce a higher spectral mismatch.

Nevertheless, absolute-calibrated DSLR cameras for luminance photography can offer high levels of accuracy (8% uncertainty) (Technoteam, 2016). Figure 3.6 shows the spectral mismatch for an absolute-calibrated system. The green line represents the spectral response of the human eye $V(\lambda)$ and the red line shows the spectral response of the DSLR camera. The difference between the two lines, called the integral spectrum mismatch would be zero for a perfect light-measuring instrument.

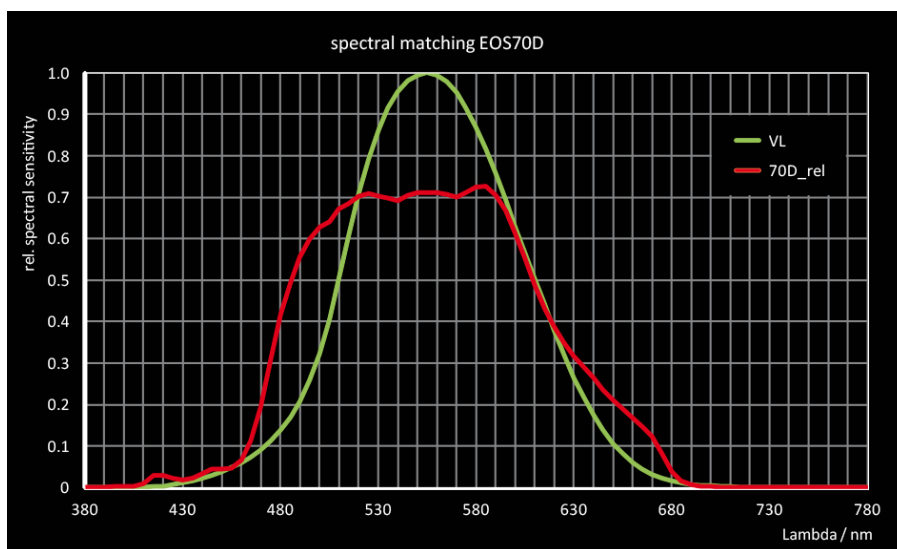


FIG. 3.6 Spectral mismatch of an absolute-calibrated Canon EOS700 DSLR camera, based on the $V(\lambda)$ curve of the CIE 1931 2° standard modified photopic observer. Source: (Technoteam, 2016).

The reported uncertainties for user-calibrated systems is generally higher than absolute-calibrated systems, with error maxima reaching values of 20% (Inanici, 2006) (Hansen et al., 2017).

The calibration of DSLR cameras for luminance capture is a three-step process that includes a radiometric calibration, a uniformity calibration and a photometric calibration (Inanici, 2006) (Porsch and Schmidt, 2010).

The radiometric calibration refers to the estimation of the camera opto-electronic conversion function (OECF), or the relationship between the irradiation reaching the camera sensor and the corresponding RGB sensor data and output pixel colour value.

The uniformity calibration refers to the error estimation and correction of the vignetting effect displayed by images captured with fisheye lenses, with higher differences between real and output luminance occurring in the edges of the image. This error needs to be identified and corrected for each camera aperture, or F-number (Figure 3.7).

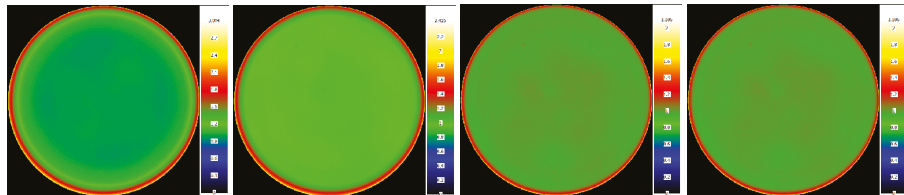


FIG. 3.7 Estimated vignetting effect for apertures F4, F5, F8 and F11 (left to right) for an LMK mobile air system. Source: Technoteam.

The photometric calibration involves the extraction of calibration-factors for the different camera settings (e.g., aperture and ISO sensitivity of sensor) corresponding to the ratio between an externally measured luminance and the luminance measured by a particular luminance acquisition system. In the case of absolute-calibrated systems, this ratio is calculated based on the output of standard illuminant, generally the CIE standard illuminant A, while user-based calibration procedures generally involve a luminance-meter point-based measurement of a reference point in a scene with known reflection properties, such as a reference grey card or a Munsell colour chart.

3.5 Measuring the luminance of the visual-field

The central or binocular visual field of humans does typically extend to an angle of 120° on the horizontal and to a slightly wider angle of around 124° on the vertical, with the individual eye extending that range by 30° on each side (Figure 3.8).

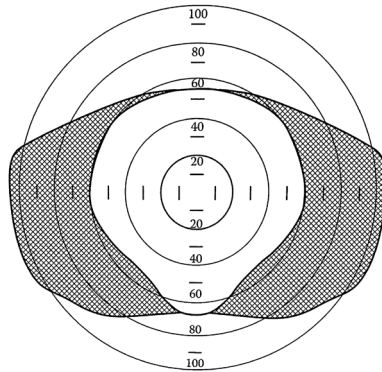


FIG. 3.8 The human binocular visual field, or area that is seen by both eyes simultaneously (in white) and the monocular visual field (in grey). Source: (Boyce, 2014).

To collect the luminance information in the very wide human visual field, image-based luminance capture does generally resort to the use of cameras equipped with fisheye lenses. Fisheye lenses capture a hemispherical view of the visual field that to be represented in the form of a 2-dimensional planar image requires the use of a particular geometrical distortion mapping technique. Every lens has its own distortion that should match one of the hemispherical projection equations presented in Table 3.1. Representations of these projections can be found in Figure 3.9.

TABLE 3.1 The equations for different fisheye image projection methods (Bettonvil, 2005).

Projection	Equation
Equi-solid angle	$r(\theta) = 2 f \sin(\theta/2)$
Equi-angle (or equidistant)	$r(\theta) = f \theta$
Stereographic	$r(\theta) = 2 f \tan(\theta/2)$
Orthographic	$r(\theta) = f \sin(\theta)$
Rectilinear (no distortion)	$r(\theta) = f \tan(\theta)$

θ is the entrance angle, measured from the optical axis, f is the lens' focal length and r is the distance at the image plane measured from the optical axis.

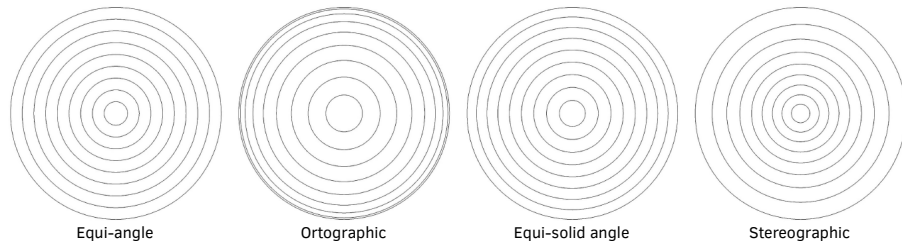


FIG. 3.9 The four commonly used methods for projecting fisheye images, showing the curves for theta angles, θ , from 10° to 90° . Source: (Wagdy et al., 2019).

Most fisheye lenses on the market have an equi-angle or an equi-solid angle projection. The equi-angle lenses produce images with angular distances of equal size across the image view while the equi-solid angle lenses (also called Lambert azimuthal equal-area) produce images with equal area across the image view. There are other hemispherical projection methods such as the orthographic and the stereographic projections, the first one being also used by fisheye lenses.

Different equations are used to compute the pixel-based luminance from fisheye images, depending on the type of projection used. To ensure that measured luminance is independent of the view type, pixels are weighed by their solid angle, which is calculated differently depending on the projection of the fish-eye image. For an equi-angle projection, for example, the solid angle (Ω_e) subtended by an arbitrary area of pixels in an image is expressed as:

$$\Omega_e = \frac{\pi^2}{4 \cdot r_0^2} \cdot \sum_k \frac{\sin \theta_k}{\theta_k} \quad \text{EQ 20}$$

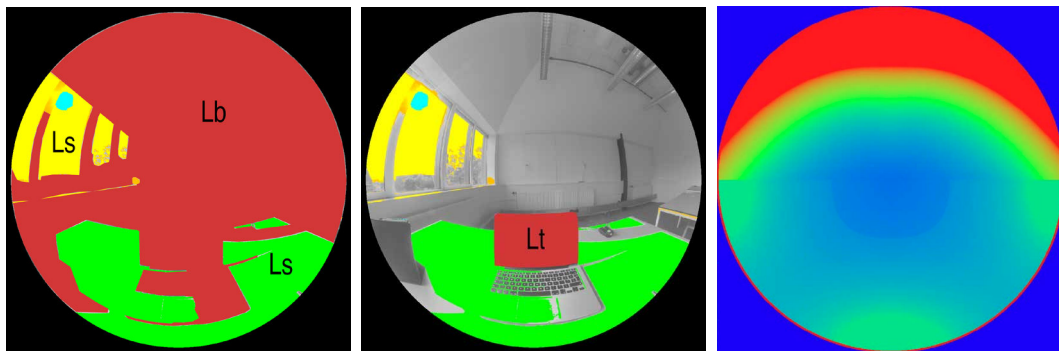
Where k is the number of image indices to compute dependent on the specified image area, r_0 is the fisheye image radius in pixels and θ is the angle between the pixel and the optical axis of the camera, in radians.

The luminance for an arbitrary portion of an image with an equi-angle projection (L_e) being defined as:

$$L_e = \frac{\sum_k L_k \cdot \frac{\sin(\theta_k)}{\theta_k}}{\sum_k \frac{\sin(\theta_k)}{\theta_k}} \quad \text{EQ 21}$$

The computation of discomfort glare metrics from fisheye luminance images involves the use of specific image-processing software such as Radiance's *findglare* (Ward, 2018) or *evalglare* (Wienold, 2012). These tools are able to compute a range of glare metrics based on the HDR luminance image input. The *evalglare* does pixel-by-pixel calculations, where each pixel has a luminance value L , a theta angle θ (angular distance to the optic axis), a position index P , and a solid angle ω , associated with it, and is from the two tools, the most comprehensive in terms of the amount of glare metrics and calculations that it can produce.

Figure 3.10 shows how different areas of a luminance image are computed for the purpose of calculating the discomfort glare indices and other metrics, using *evalglare*.



Region of a luminance image corresponding to the background (L_b) is identified in red. The coloured regions represent three different glare sources (L_s).

The image shows one of the specific features of *evalglare* - the extraction of peak values within a larger glare source into a separate glare source (the light blue area, corresponding to the solar disc). What is considered a glare source for the purpose of glare analysis is matter of discussion. For Radiance's *findglare*, every pixel larger than x -times the mean luminance of the image is treated as glare source (default = 7) whereas in *evalglare* three different methods for the detection of glare source are provided.

Region of the luminance image corresponding to the task (L_t). This area is either explicitly defined using a mask (in red) or calculated based on a given circular area defined by the coordinates of the centre and radius of the task.

A false-colour map representation of the position index (P) (Wienold and Christoffersen, 2006), following the work from Guth (Luckiesh and Guth, 1949) and Iwata (Iwata and Tokura, 1997). Higher values of the position index (in red) indicate a higher displacement from the line of sight. The index accounts for the fact that a light source located directly in the line of sight produces a higher glare sensation than a light source located at the periphery.

FIG. 3.10 Region definitions in a fisheye luminance image for the purpose of calculating discomfort glare metrics with *evalglare*.

3.6 Conclusion

HDRI photography offers the opportunity to produce luminance maps of the full human visual field with a known degree of precision. The technique has been in use since the early 2000's for the evaluation of visual comfort and discomfort glare in buildings, either via de use of user-calibrated or absolute-calibrated luminance measuring systems.

HDRI luminance measurement comes hand-in-hand with developments in the field of computation, making it possible to process the images produced with this technique with a range of purposely developed software tools with two of these, Radiance's *findglare* and *evalglare*, being in use for the specific purpose of assessing glare in buildings.

The work that is carried out in this thesis will use the HDRI luminance capture technique in combination with *evalglare* HDR image processing software for the computation of luminance and of the discomfort glare metrics.

4 Experimental method

4.1 Introduction

This chapter describes the methods that were used for the collection, processing and analysis of the empirical data collected in this thesis.

The data was collected in two experimental studies, Study I and Study II that were performed in a mock classroom space and for a range of representative classroom visual conditions. In Study I, the reported glare was investigated for four sitting positions in the space with the test subjects engaged on a task running on a screen centrally located in the front of the room. In Study II, the reported glare was investigated for a range of different room layouts for both a desk task condition and a screen task condition.

The glare evaluation information was collected using a questionnaire, where subjects reported their perceived level of glare using a glare sensation ordinal scale. The luminance measurements were collected via image-based luminance measurements performed with a LMK mobile air luminance-acquisition system, with task surface illuminance and vertical eye illuminance measurements also being collected. The image-based luminance measurements were used to calculate a range of discomfort glare metrics that were then compared to the subjective glare evaluations via statistical analysis. The data processing, calculation and statistical analysis methods that were used are described next.

4.2 Experiment set-up

Discomfort glare metrics are calculated based on field-of-view luminance or illuminance measurements that require data to be collected in the position of the subject's eye. In real-world situations, it is not possible to collect measurements and subjective glare evaluations simultaneously, as the measuring instrument needs to be in the location of the eye. To overcome this problem some researchers have used a twin-room approach (a test room next to a measurement room) (Velds, 1999) (Wienold, 2010) (Van Den Wymelenberg, 2012), a set-up that proved difficult to arrange in the context of this experiment. Even in the very few cases where similar sized classrooms were found next to each other at the TU Delft campus, the also larger window area of these spaces meant that differences regarding sky exposure due to overshadowing asymmetries between the two rooms were impossible to avoid. A two-classroom set-up outside campus was also considered, but none was found within the experiment preparation timeframe where that problem could be avoided.

A single-room set up on the campus with adjustments in relation to the luminance measurement was then considered to be the most practical option.

In terms of the room itself, given the intention of investigating the effect of position in space on the perception of glare it was important that the area of the visible window would not change from one position to the next other than due to the actual changes due to a varying distance / view direction from a particular sitting position. A room with a full-length window was therefore preferred to a room with punch-windows or irregularly distributed windows.

It was a consideration that the room would not be too big or have a very specific arrangement like for instance a lecture hall, but be representative of a general primary or secondary school type of classroom, usually with areas around 50m² and a width between 5.5 and 6.5 meters.

A classroom with acceptable characteristics was found at the Faculty of Architecture and the Built Environment, TU Delft. The room, with an area of 49m² (7.6m x 6.45m) and floor-to-ceiling height of 3.36m is situated on a corner on the top floor of the Faculty building and is originally daylit from two sides. For the experiments one of the windows was occluded with white cardboard. The final set-up is of a room that is daylit from only one side, through a full-length window (7.6m x 1.4m) to the Southwest.

The interior of the room is mostly made of diffuse surfaces: white plastered walls, red-coloured carpet and grey vinyl floor and a combination of white plastered and chipboard ceiling with exposed ductwork. The desks of the classroom had a very untypical and somewhat specular black colour and were covered with white print paper in Study I and with grey cardboard in Study II. These covers were used to mark the position of the different objects on the desks, so their location would not change much from one session to the next.

TABLE 4.1 Light properties of the room's surfaces. Reflectance measured with one illuminance and luminance meter. Transmittance measured with two illuminance meters.

Room surface	Reflectance
Walls	87%; 85% (paneling, in parts)
Floor	8% (carpet); 43% (vinyl, in part)
Ceiling	60% aprox.
Window frames	90%
Radiators	80%
Chairs	27%
Desk tops	89% (Study I); 74% (Study II)
Window	Transmission
Glass	63%

Even though the room is located on the top floor of the building, some trees and buildings produced some obstruction of the view to the sky. The orientation of the desks in the room in relation to the board was reversed so a higher portion of sky would be seen from the sitting positions in the room.

The experiments for the two studies occurred over a range of specific time frames from 2016 to 2019, depending on a combination of factors such as room availability, subject availability and sky conditions.



FIG. 4.1 Experiment room in four photographs.

4.3 Experiment design

The main objective of the two experiments performed in this research was to analyse the perception of glare for a range of representative visual conditions in the classroom.

The experiment consisted of collecting subjective glare evaluations for a range of sitting positions and view directions and corresponding luminance measurements.

In Study I, the effect of position was analysed for a single view direction, the view towards the board (in this case a projecting screen) in the centre of the front wall of the room. The study was run for the four extreme positions in the room, corresponding to positions 1, 2, 3 and 4, in Figure 4.2. The positions and visual target result in four distinct visual conditions (Figure 4.3).

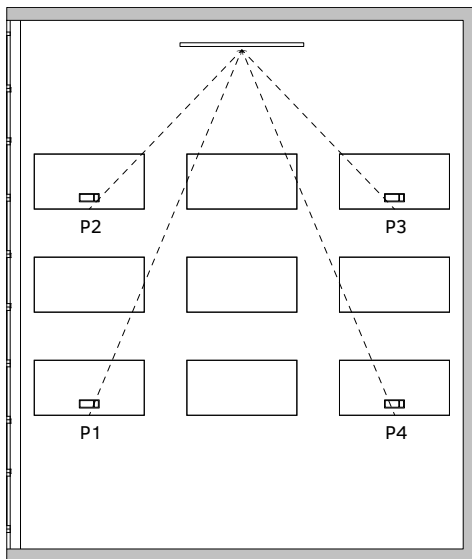


FIG. 4.2 Plan view of the room in Study I, with view direction from each position.

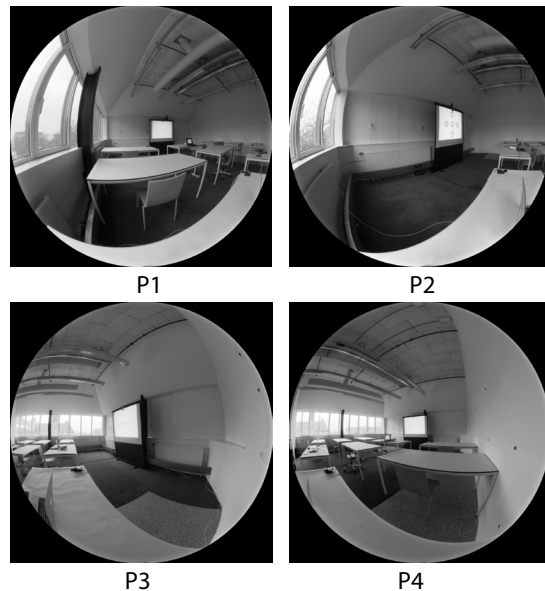


FIG. 4.3 The four visual conditions of Study I.

For positions 1 and 2 the subjects sit at a 1 m distance from the window. For positions 3 and 4 the subjects sit at approximately 5.5m from the window. In positions 1 and 2 the subjects look towards the inside of the room and in positions 3 and 4 the subjects look towards the outside of the room.

The Study II experiment was run for a range of room layouts and for a desk and board task. The desk arrangement recreates three common classroom layouts that can be found in primary, secondary and higher education schools: a 'U' layout, where desks are parallel to the window, a regular layout where desks are laid perpendicular to the window and a diagonal layout where desks are at an angle of approximately 40° to the window (Figure 4.4). For the board task, the desk layout is not relevant, as the body or head naturally rotates in the direction of the visual target, and the desks were simply rotated to the angle that allowed subjects to face the board directly (40° to the window, in the front row and of 22° to the window, in the back row).

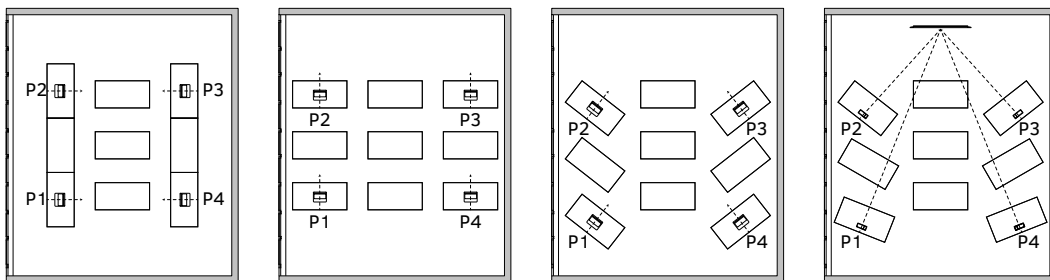


FIG. 4.4 Four room layouts for two different visual tasks. From left to right: 'U' layout (desk task), regular layout (desk task), diagonal layout (desk task) and the layout used for the board task.

These layouts and view directions resulted in sixteen different visual field conditions (Figure 4.5) and in a wider variety of window apparent sizes in the field-of view in comparison to Study I.

The experiment was run in a total of 32 sessions, corresponding to 8 board-based task sessions and 24 desk-based task sessions.

The Study II had the objective of investigating if the results obtained in Study I would be confirmed for a wider range of visual conditions in the classroom and for predominantly bright sky conditions. In that process, several improvements to the data collection method were also introduced that are described in the next sections.

'U' layout



P1



P2



P3



P4

Regular layout



P1



P2



P3



P4

Diagonal layout



P1



P2



P3



P4

Board task layout



P1



P2



P3



P4

FIG. 4.5 The sixteen visual conditions of Study II (images with adjusted exposure).

4.4 Measurements

4.4.1 Luminance measurement

The luminance measurement is of central importance to this research as all metrics are calculated based on it. The luminance data was collected using the image-based measurement technique that was described in the previous chapter. The luminance-acquisition system that was used in the research, the additional actions that were taken to adjust the system to the capture of daylight, and other details regarding the use of the system in the experiments are described next.

4.4.2 The LMK luminance-acquisition system

The luminance measurements in this research were performed with a LMK mobile air (hereby, called LMK), a luminance-calibrated photo camera manufactured by Technoteam Bildverarbeitung GmbH (Technoteam, 2016). The system is based on a Canon EOS70D and is equipped with a Sigma 4.5mm/2.8 EX DC circular fisheye lens.

The calibration of the system follows the general steps of the luminance calibration of photo-cameras, consisting of a radiometric calibration, a uniformity calibration and a photometric calibration. The photometric calibration of the LMK is an absolute calibration made according to the DIN 5032-6 (DIN, 1995). The original calibration of the system is done for Apertures F4 to F11, for ISO settings 100 to 1600 and for shutter speed in the range 0.001 to 2.5 seconds. The resulting uncertainty of the system for these settings was determined as $\pm 4.7\%$ to which other uncertainties relating to the calibration procedure are added. The final uncertainty of the system corresponds to the summation of those uncertainties and is less than $\pm 8\%$ (see Appendix A, section 3).

The LMK comes with its own set of calibration files and its own luminance image processing software called Labsoft (Technoteam, 2017). The software reads the system's calibration information to transform a sequence of LDR images, in this case a set of Canon RAW CR2 image files, into one single HDR luminance-calibrated image, called the PF file.

The default operation of the LMK is based on the capture of an auto-bracketed (multiple exposure shooting) sequence of 3 photographs that can be spaced up to $\pm 3\text{EV}$, with an estimated dynamic range of 1:32,000 (Figure 4.6).

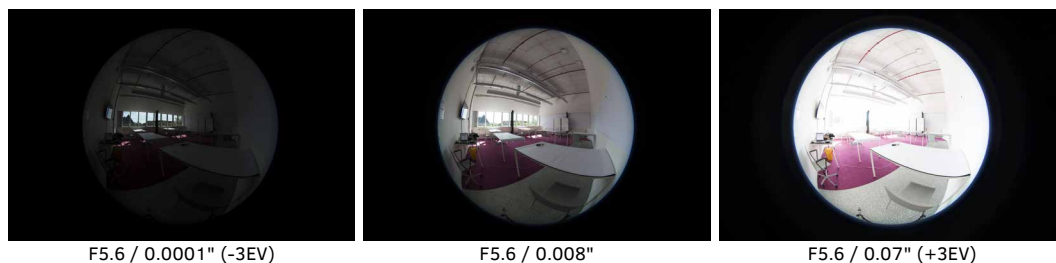


FIG. 4.6 A typical LMK $\pm 3\text{EV}$ sequence.

Scenes in the human visual environment can have dynamic ranges well in excess of 1:100,000 (Jacobs, 2007) and although a typical artificially lit indoor environment can have a dynamic range as low as 1:100 (Reinhard et al., 2010) an indoor daylight scene can have a dynamic range as high as 10^9 when the sun is in the field of view (Jakubiec et al., 2016).

The capture of daylight scenes and in particular of sunlight requires a wider dynamic range and lower exposure settings than those offered by the standard calibration of the LMK and as it can also be seen by the comparison presented in Figure 4.7.

An extension of the calibrated range of exposures of the LMK system was therefore performed. This extension could have either been done by the calibration for lower shutter speeds or for smaller Apertures (higher F-numbers), with the LMK manufacturers recommending a calibration based on Aperture.

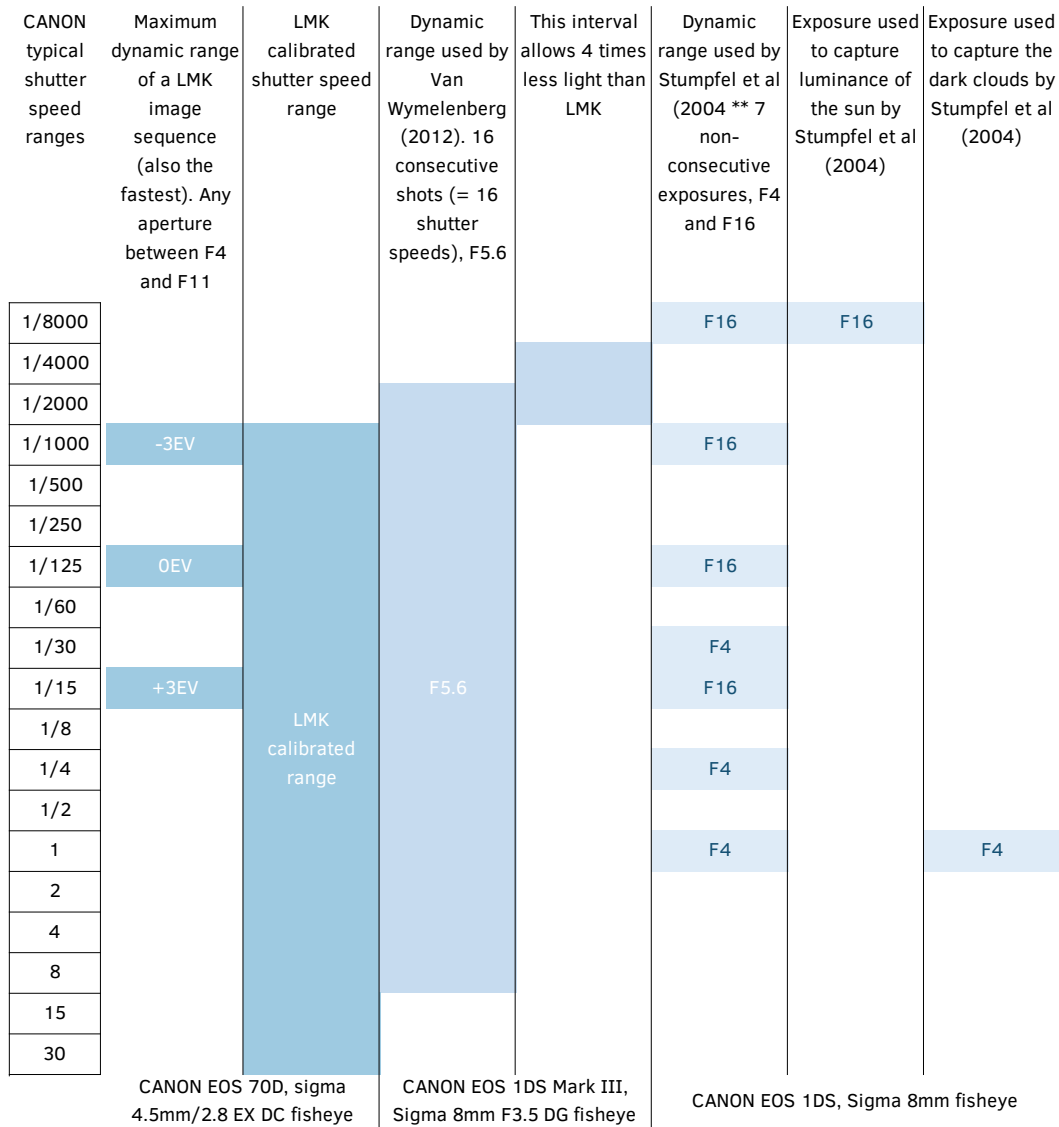


FIG. 4.7 Comparison of the LMK calibrated shutter speed and aperture range with the ranges used in other two studies using Canon DSLR cameras and fisheye lenses (Stumpfel et al., 2004) (Van Den Wymelenberg, 2012) for the measurement of daylight. Stumpfel et al. captured the luminance of the sun with an aperture of F16, shutter speed of 0.00013" and an additional neutral density filter. Van Den Wymelenberg captured a daylight scene over 90 days in a cellular office space with aperture F5.6 and a shutter speed as low as 0.00025".

4.4.2.1 Extended calibration of the LMK for daylight glare measurements

F-number

The calibration of the LMK for additional exposure settings depends solely on the photometric calibration, i.e. on the determination of calibration factors for the new F-numbers to calibrate the system for. This photometric calibration was carried out at TU Delft by the author with the use of an integrating sphere calibration standard provided by Spectra Partners (Spectra Partners, 2021). The standard is a stabilized light source that offers constant and uniform intensity of light.

The calibration was carried out for Apertures F16, F20 and F22 and the calibration procedure is explained in section 4 of the Appendix A. The result of this calibration is a set of correction factors that are loaded into Labsoft whenever one of these Apertures is used.

For a calibrated LMK system equipped with a particular lens, the variation of the measured uncertainty for different exposure settings depends solely on the repeatability of the photometric calibration. The repeatability of the measurement, for apertures F16, F20 and F22 was found to deviate by less than 1.1% which is within the range of the original system calibration deviation (0.5% to 2%) and therefore the measured uncertainty for the system with the newly calibrated apertures is assumed to be the same as the highest uncertainty found for the original LMK calibrated range ($\pm 6\%$, for F11).

Although it was possible to increase the dynamic range of the system significantly by the use of higher F-numbers, tests carried out in the room of the experiment showed that it was not possible to avoid luminance overflow at all times. Luminance overflow, also called pixel saturation, occurs when the dynamic range of the system is not enough to capture the higher luminance of a scene. Figure 4.8 shows the brightest scenes that were possible to capture in the room of the experiment in the summer of 2016. The images were captured with the lowest exposure settings of the camera (aperture F22 and shutter speed range between 0.001" and 0.062"). In the first scene, luminance overflow occurs in the area of the sun, which in this case is somewhat occluded by dark clouds. Higher luminance was to be expected on clear sky days or days with sun and brighter clouds scattering the solar rays. In the second scene, luminance overflow occurs due to solar reflections in several parts of the scene (Figure 4.9).

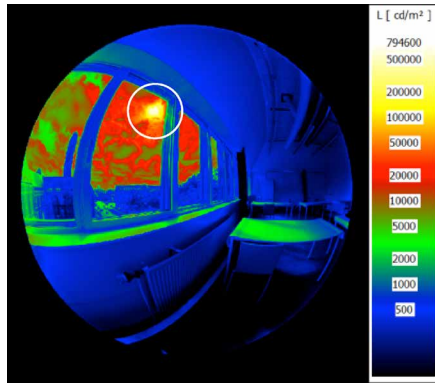


FIG. 4.8 Luminance capture with luminance overflow in the indicated area (F22, shutter speed 0.001" to 0.062").

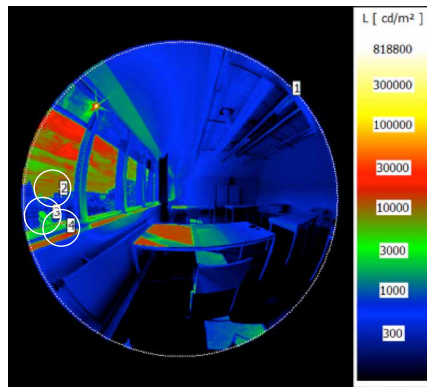


FIG. 4.9 Luminance capture with luminance overflow in the indicated areas (F22, shutter speed 0.001" to 0.062").

After an extensive study analysing the accuracy of luminance measurements of daylit scenes using luminance-calibrated cameras, (Jakubiec et al., 2016) found significant deviations for the value of the UGR and DGP discomfort glare indices depending on the dynamic range of the captured luminance. By comparing measurements done with and without a neutral density filter, the authors show that in the case of DGP, the value of the metric could often move from the “noticeable” to the “disturbing” glare range depending on an increase of the luminance range allowed by the use of a filter.

Given the impact that a dynamic range could have on the results of the glare metrics calculation, it was found appropriate to extend the calibrated dynamic range of the LMK further for a system equipped with a neutral density filter.

Neutral density filter

The calibration of the LMK with a neutral density filter was carried out by the system manufacturers, Technoteam. The filter, a Kodak Wratten ND2.0 with a 1% transmittance, is a gelatin film filter that is placed in the back of the fisheye lens. According to the filter manufacturer, the neutral density filter is expected to have a constant transmittance across its surface. However, the calibration showed that the transmittance of the filter varies depending on the angle of incident light and the system's original uniformity calibration was corrected accordingly. The resulting uncertainty of the LMK equipped with the ND2.0 filter was determined as $\pm 5.7\%$.

After calibration with the filter, the highest luminance that was measured in the research room setting with the LMK and without luminance overflow was $2,183,000 \text{ cd/m}^2$, a measurement done with aperture F22 and shutter speed in the range $0.001''$ to $0.067''$. Although the use of a lower transmission filter could have increased the captured luminance range further, a lack of knowledge relating to the impact that such a filter could have in the capture of the lower luminance areas of the experiment room discouraged any further modifications of the system.

The use of the ND2.0 filter improved the luminance capture particularly in reducing the size and the number of regions of an image with luminance overflow. For the system equipped with the film filter, overflow is restricted to either the solar disc or to a reflection of the solar disk, in which conditions it is possible to perform a correction of the image as explained in section 4.11.2.

4.4.2.2 Fish-eye lens projection estimation

Commercial fisheye lenses are not generally produced for scientific purposes and even less so for the purpose of measuring glare. The total field-of-view and type of projection of these lenses are normally not readily available and needs to be estimated so glare metrics can be calculated with accuracy.

The Sigma 4.5mm F2.8 EX DC HSM circular fisheye lens is fabricated by Sigma and according to its specifications has an equi-solid angle projection and total field of view of 180° . However, the information received from the LMK manufacturers was that the system had a total field-of-view of 179° and an equi-angle projection. The difference in the centre and in the border of an image for the two projections is around 20%, which means that a glare source can be either over or underestimated by that amount if the wrong type of projection is used. In addition, it was found by

other researchers that the total field-of-view angle of Sigma fisheye lenses can be larger than 180° (Jacobs, 2012) (Hansen et al., 2017).

The characteristics of the Sigma 4.5mm F2.8 EX DC HSM used in this research were measured by the author, using the method explained in the section 5 of the Appendix A. The measurements showed that the lens has an equi-solid angle projection and a total field-of-view of approximately 185°.

4.4.3 **Luminance capture in the experiments**

For stability of the luminance measurement and for flexibility regarding the selection of the exposure settings, the LMK camera was remotely operated using qDslrdashboard v3.5.3 (DslrDashboard, 2017). The camera was connected to a laptop running the software via USB connection in session 1 of Study I and via a locally created Wi-Fi network connection in all other sessions. The Wi-Fi connection allowed easier movement of the camera from one position to the next and greatly simplified the experiment's workflow.

The qDslrdashboard allows for custom bracketing (the selection of multiple exposure shooting settings) and collection of a wide range of exposures.

The approach in this research was to collect a wide range of LDR photographs from which a useful range could be selected from at HDR image processing stage, if required.

In the Study I experiment, the collected luminance data consisted of fourteen LDR photographs with shutter speeds between 0.001" and 8". From that sequence, a minimum of eight LDR images were selected to compose the HDR luminance image, mostly from the range of higher exposures as many of the lower exposures did not provide any extra luminance information.

Different apertures were used depending on the general luminance conditions in each session. In session 1, the camera was not equipped with the neutral density filter yet. The captures were done with aperture F22 in order to reduce the chances of pixel saturation. In session 2, the camera was already equipped with the neutral density filter. The captures were done with aperture F11 in sunny conditions and F5.6 in overcast conditions. In session 3, the camera was equipped with the neutral density filter and the captures were done with aperture F8 in the near-window positions and F5.6 in the near-wall positions. F16 was occasionally used in the situations when the sun was visible through the window.

In the Study I experiment, it was verified that little or no information was collected for a number of exposures. For that reason, in the Study II experiment, only 7 LDR images were collected. These images were collected with different EV intervals, so the dynamic range was kept as wide as possible.

In the Study II experiment, the shutter speed range varied between 0.001" and 15" and an aperture of F5.6 was used for all measurements.

4.4.4 Pairing luminance measurement and evaluation of glare

In the case of a single-room set-up, the luminance measurement needs to either be collected before or after the subjective evaluation or at a distance from the subject's sitting position. None of the approaches is without undesirable consequences. For a time lag, between the subjective evaluation and the measurement there is a risk of variation of the field-of-view luminance due to changes in the sky. For a position offset between the subject's eye and the camera, there is the risk of a variation of the field-of-view luminance due to differences between the camera view and the subject's view.

Measurements done in the experiment room showed that the variation of light within the time frame of each experimental instance (planned for a minimum of 3 minutes) even in a mostly clear sky day could be significant (Figure 4.10) and for this reason the first experimental study (Study I), was carried out for a camera positioned at a distance from the subject's sitting position.

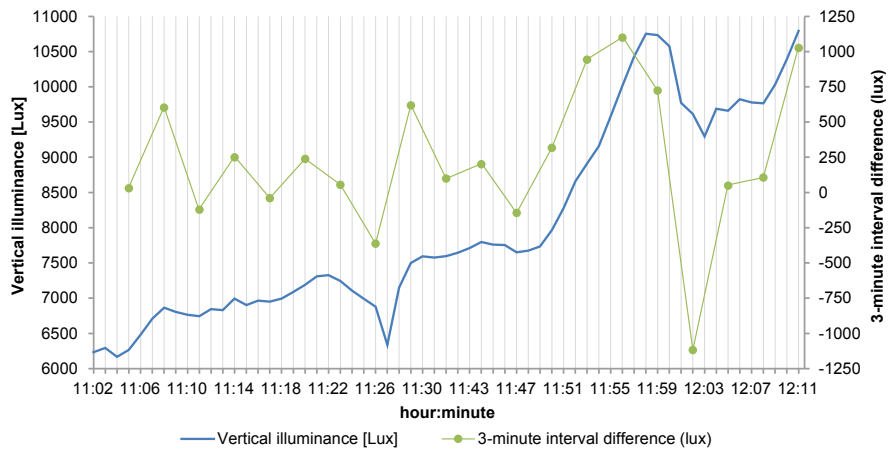


FIG. 4.10 Figure 1-minute vertical eye illuminance measured at eye level near the window in the experiment room for an hour, in a clear sky day in June with a few scattered clouds and a light breeze.

In a study carried out by (Fan et al., 2009), luminance differences for a camera placed at a distance from the sitting position (23 to 118 cm) was found to be of 20% on average. That study was performed under overcast sky conditions only and for a relatively high and narrow window centrally located in the subject's field-of-view. The authors advise that these differences are strongly scenario dependent and that in situations with sun the differences might be bigger.

A test done in the experiment room showed that a camera positioned at a distance of 75cm from the subject would in general guarantee that the subject is not visible in the luminance image, which could otherwise obstruct part of the window view that in reality is "seen" by the subject, particularly in the positions near the wall, positions 3 and 4. A 75cm distance was then considered to be the suitable distance to use in the experiment.

A simulation was done to estimate what type of error could be expected from this approach (see section 9 of Appendix A for image results). The field-of-view luminance for an image from a 75cm distance to the subject and from an image from the sitting position of the subject was simulated for two extreme sitting positions in the room, position 1, near the window and position 3, near the wall (Figure 4.11). Position 1 is from all positions in the room the one that "sees" more window surface and position 3 contains a relatively small window but centrally located in the field-of-view. The luminance differences were analysed for a sky with and without a visible sun through the window. In the case of position 1, an additional condition for a sun located more peripherally in the field-of-view was also tested. Table 4.2 shows the results of the test in terms of the overall luminance and for three different glare indices.

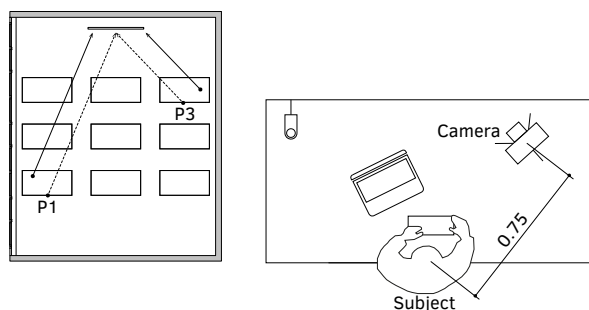


FIG. 4.11 Camera location and view direction in the two positions.

TABLE 4.2 Simulated field-of-view luminance, L (cd/m²), and glare indices DGP, DGI and UGR, in the subject's position and in a position of 75 cm from the subject, in sitting positions 1 and 3.

	Day, time, sun	Statistic	Subject view	Camera-view	% Difference	% Change
Position 3	13 Aug	L_min	0.9	2.1	76	123
	10:45	L_max	6,923	6,859	1	-1
	sun: is not visible through the window view or inside the room	L_mean	270	259	4	-4
		L_median	141	140	1	-1
		L_std	820	776	6	-5
		DGP	0.25	0.24	3	-3
		DGI	18	17	3	-3
		UGR	24	23	3	-3
	21 Dec	L_min	9.9	11.5	15	16
	15:00	L_max	429,829,408	427,936,224	0	0
	sun: is visible through the window view and inside the room	L_mean	6,432	7,016	9	9
		L_median	619	654	5	6
		L_std	1,128,468	1,220,495	8	8
		DGP	1.00	1.00	0	0
		DGI	29	29	0	0
UGR		44	44	1	-1	
Position 1	13 Aug	L_min	3.1	3.5	10	11
	10:45	L_max	5,689	5,657	1	-1
	sun: is not visible through the window view or inside the room	L_mean	688	801	15	16
		L_median	245	280	13	14
		L_std	1227	1318	7	7
		DGP	0.26	0.27	2	2
		DGI	13	13	3	4
		UGR	18	19	3	3
	21 Mar	L_min	11	8	27	-24
	17:00	L_max	666,272,768	693,600,832	4	4
	sun: is visible through the window view and inside the room (sun is peripheral)	L_mean	10989	10525	4	-4
		L_median	742	760	2	3
		L_std	1,920,010	1,822,444	5	-5
		DGP	0.53	0.46	14	-13
		DGI	10	13	20	22
UGR		17	19	10	10	
21 Jun	L_min	7.8	11.0	34	41	
18:00	L_max	657,126,144	728,202,560	10	11	
sun: is visible through the window view and inside the room (sun is more central)	L_mean	9,939	12,015	19	21	
	L_median	758	803	6	6	
	L_std	1,700,130	2,042,254	18	20	
	DGP	1.00	1.00	0	0	
	DGI	32	32	2	2	
	UGR	55	57	3	3	

Based on the simulation study, the difference for the mean field-of-view luminance is found to be as high as 19%, when the sun is in the field-of-view. This however did not produce a significant difference in the value of the glare indices, except in the situation when due to the camera offset the view of the sun through the window changed considerably (21 March, in position 1), in which case errors of 10% to 20% can be verified for the glare indices.

In Study II, for the desk task, placing the camera at a distance from the subject's sitting position would result in a significantly different view of the room, of the window and of the task in relation to the actual subject's view. For a 75cm distance, the task surface would fall outside the field-of-view of the camera and a reduction of this distance would cause the obstruction of the field-of-view of the camera by the subject. For this reason, in Study II, the measurement is carried out at the subject's sitting position, before and after the subject's glare evaluation, and the glare metrics were analysed based on those two measurements.

4.4.5 **Illuminance measurements**

4.4.5.1 **Task surface illuminance**

The task illuminance was measured using a multi-point set-up of five Konica Minolta CL-200A chromameters, one in each of the four desks and one at the board.

The meters were laid on the desks in a way to avoid being shaded by the subject. The board task illuminance was measured at a point right above the electronic display or projecting screen. These measurements were collected at a 5-second interval with the purpose of monitoring illuminance at task surface level and to possibly evaluate the performance of illuminance-based glare metrics. However, it was observed that there could be a significant difference between the illuminance of the desk in the position of the subject compared to the illuminance of the desk in the point of measurement, invalidating a wide range of measurements for the purpose of assessing the performance of any illuminance-based glare metrics. This problem was often due to the shadow cast of the window mullions or other window elements on the desk (Figure 4.12).



FIG. 4.12 Variation of light between the sitting position and the point of illuminance measurement. Illuminance meter is circled in red.

4.4.5.2 Vertical eye illuminance

Vertical eye illuminance (E_v) is a quantity of interest in glare research for several reasons. Beyond being a commonly used metric itself, an E_v measurement is also used to check the integrity of the luminance image and for correcting any pixel saturation of the luminance image. In this research, the E_v measurement was also used to monitor the light variation between the start and the end of the subjective glare assessment (Study II).

As a measure of the amount of the overall light reaching a subject's eye, the E_v is generally measured at a point right above the camera lens.

In Study I, the E_v measurement was collected with a T10M Konica Minolta illuminance meter adapted to the camera's flash mount. The small head of the T10M meter makes it an ideal type of meter for this purpose. The camera-meter adapter was improved throughout the experimental process (Figure 4.13) in an attempt to get an externally measured measurement as close as possible to the luminance image-derived E_v measurement, when differences higher than expected were found between these two. In session 1, the meter was at around 15cm from the lens centre. An improved adapter was used from session 3 onwards, which set the meter in the same plane of the lens, at a distance of 7 cm from its centre.



FIG. 4.13 Vertical eye illuminance measurement set-ups used: a) and b) adapters in Study I and c) adapter in Study II.

As the T10 meter does not have data storage capacity, the measurements were collected visually. There were 4 E_v measurements taken during each luminance capture in general.

In Study II, the vertical eye illuminance was collected using a Konica Minolta CL-200A chromameter that allowed for data to be recorded in real-time rather than collected visually. In Study II, the E_v measurements were collected at a 5-second interval.

4.4.6 Other measurements

4.4.6.1 Degree of eye opening

In Study II it was attempted to include a degree of eye opening (DEO) measurement (Yamin Garretón et al., 2015) (Hamedani et al., 2019) in the experiment, by making a movie recording of the eye in each condition of the study and for a reference comfort condition, a condition that was created by closing the room's blinds and by switching on the electric light. The movie recording of the eye was made using a mini-spy camera adapted to a headset and remotely operated from a mobile phone application. The subjects gave their signed consent to the movie recording of their eye and faces.

Several attempts were made to process this information using human motion capture and measuring software (Charmant, 2019) for tracking and measuring distances between fixed points of an image. The definition of these points is quite challenging as the changing light conditions around the eye (highlights, shadows) create colour differences in the image that make it difficult the fixation of the measuring points. Several eye markers were tested none of them guaranteeing a comfortable condition for the subject nor consistent and reliable outcomes by the software. The data was nevertheless collected (no markers used) with the ambition of finding an adequate data processing and analysis workflow in the future. It is expected that as software and algorithms for eye movement recognition get improved, it might be possible to overcome the complexities inherent to the analysis and interpretation of this type of data.

4.4.6.2 Room temperature

In Study I the classroom environment was free-running in the summer season and centrally heated in the other seasons.

In Study II, that occurred during summertime only, the room temperature was monitored at a 5-minute interval using a HOBO U12-012 data logger placed in one of the walls in the middle of the room.

4.5 Questionnaire

There are no validated questionnaires for visual discomfort and glare research and for this reason researchers tend to develop their own, sometimes basing their questions on the questionnaires from other researchers. The questionnaire used in this research is a three-part questionnaire, created by the author after consultation of several literature resources from research in the field of visual discomfort and glare. The first part includes demographic questions, a self-assessment of the sensitivity to bright light and a self-assessment of the importance of a view out in the work place. The second part relates to the evaluation of the visual discomfort and glare. The third part is related to the general comfort in the room, which for simplicity and to shorten the questionnaire duration, was excluded for the experiment of Study II.

For the purpose of the Study I and Study II analysis, only the part of the questionnaire concerning the visual discomfort and glare evaluation was analysed.

The questionnaire was created using the Qualtrics XM platform and was ran online. It uses a range of Likert scales with 5, 6 and 7 categorical values depending on the question, with the exception of the question on discomfort glare, which is based on a unipolar 4-value ordinal scale. This 4-value scale was proposed by (Osterhaus and Bailey, 1992), adopted by (Wienold and Christoffersen, 2006) and by several other researchers. It provides the means to categorise the level of perceived glare as 'imperceptible', 'noticeable', 'disturbing' or 'intolerable'. It is the scale adopted for the rating of the DGP glare index and a categorisation of various other glare indices according to this scale has also been proposed by (Hirning et al., 2014).

In Study I, the discomfort glare question was formulated as: "When doing the test in this position, which degree of glare from the window have you experienced?"

In order to make sure that there was a common understanding of the scale categories, the question was formulated using the descriptors provided in (Osterhaus and Bailey, 1992):

- Imperceptible: I do not feel any discomfort
- Noticeable: This is a very slight discomfort that I can tolerate for approximately one day if I was placed in a desk under these conditions
- Disturbing: I can tolerate this discomfort for 15 to 30 minutes, but I would require a change in lighting conditions for any longer period
- Intolerable: I cannot tolerate these lighting conditions

Critical considerations regarding questionnaires for discomfort glare research based on subjective evaluations are provided in (Fotios, 2015) and in (Fotios, 2018). Some of the recommendations provided in (Fotios, 2015) have been introduced in the questionnaire, by the use of clear descriptors to the ordinal values of the scale.

To address the problem of the semantics and possible scale range bias mentioned in (Fotios, 2018), some means of validation of the discomfort glare question were introduced in the questionnaire of Study II. This consisted of asking the discomfort glare question in three different ways, in order to verify if the evaluation of a particular lighting situation is consistent or not depending on the way the question is formulated.

The three questions and their scales are provided below:

- 1 Please grade the level of glare (discomfort due to the brightness of the room surfaces, brightness of the window, light contrast) that you have experienced, if any, during the time you spent doing the visual task.
 - Imperceptible: I did not feel any discomfort, I could work under these conditions for any period of time.
 - Noticeable: I could work for approximately one day under these conditions, but it would bother me to work under these conditions every day.
 - Disturbing: I could tolerate these conditions for 15 to 30 minutes, but I would require a change in the conditions for any longer period of time.
 - Intolerable: I could not tolerate working in these conditions.

- 2 Please state how did the brightness or contrast of the room surfaces and window contributed to your feeling of visual (dis)comfort while performing the visual task?
 - I felt extremely comfortable
 - I felt very comfortable
 - I felt just comfortable
 - I felt somewhat uncomfortable
 - I felt very uncomfortable
 - I felt extremely uncomfortable

- 3 If you had to perform this task for a longer period under the conditions you have experienced, would you want to put the window blinds down?
 - No
 - Yes

Question (1) and (2), which are the most similar of the three questions, were asked with a different question in-between, so the subject would not notice that he/she was being asked the same question. In question (2) the subject is asked to assess discomfort glare without mentioning the word glare and instead using the designation of (dis)comfort. A 6-point bipolar scale is used in this case with the same number of values in the negative and positive sides, to remove ambiguities relating to the middle value of the scale. In question (3), the glare question is asked more indirectly, without the use of the words (dis)comfort or glare. The wish to put the window blinds down is expected to be an indicator of discomfort glare.

The questionnaire used in Study II, was also improved in two other aspects:

- a Introduction of a more effective way of decoupling the reporting of discomfort glare from the reporting of veiling reflections;
- b A more effective way of decoupling reported discomfort due to sunlight (visual) from possible discomfort due to radiant heat (thermal).

The situation described in a) arises if subjects are not be able to dissociate discomfort due to the brightness of the window, room surfaces or other visible elements (discomfort glare) from a situation of discomfort due to a brightness condition that impairs them from seeing their task in a clear way (veiling reflections).

For that reason the subject was asked to state what exactly was the source of glare after responding to question (1) above, in the following way:

- 4 Please state what was the source of glare:
 - The window
 - The walls
 - The desk
 - The screen
 - Objects visible through the window
 - Other

The situation described in b) arises if subjects are not able to dissociate discomfort due to the brightness that is generated by the sun around him, particularly due to incident sunlight on the desk and room surfaces, from feeling too hot due to incident solar radiation. To assess if the reason for the reported discomfort was one or the other, the following questions were asked:

- 5 While doing the visual task in this desk have you been bothered by the sun?
 - No
 - Yes

When responding 'Yes', the subject was asked:

- 6 Please state in which way did the sun bothered you:
- I could see the sun through the window
 - The heat from the sun
 - The sunlight on my desk
 - The sunlight on the walls, floor or other room surfaces
 - The sunlight reaching my body
 - Other

The questionnaire of Study II does additionally measure other aspects such as satisfaction with the level of light (light sufficiency) and level of visual distraction.

4.6 Visual activity

The main objective of the visual activity was to have the subjects focus on a task with their views directed to defined visual target, either the board in the centre of the room or to the screens on their desks. A visual search task was used as a visual activity in Study I and a character search task and was used in Study II.

The visual search task of Study I was created by the author using the OpenSesame environment (Mathôt, 2016), a software for building graphic experiments for the social sciences (Mathôt et al., 2012). The task is based on visual tests used in the context of other experimental studies on visual discomfort and glare (Van Den Wymelenberg, 2012).

The task consisted of asking the subjects to analyse a field of Landolt 'C' rings to find rings with gaps facing in a specified direction. A field of rings consists of a group of five rings that was presented for 2 seconds to the participant (Figure 4.14). The participant was asked to select the ring (from the four surrounding rings) with the gap facing in the same direction as the reference ring (the central ring), using the keyboard arrow keys (up, down, right, left). The speed (time in seconds) that it took to select a ring and the accuracy of the answer (correct or incorrect) were measured and recorded.

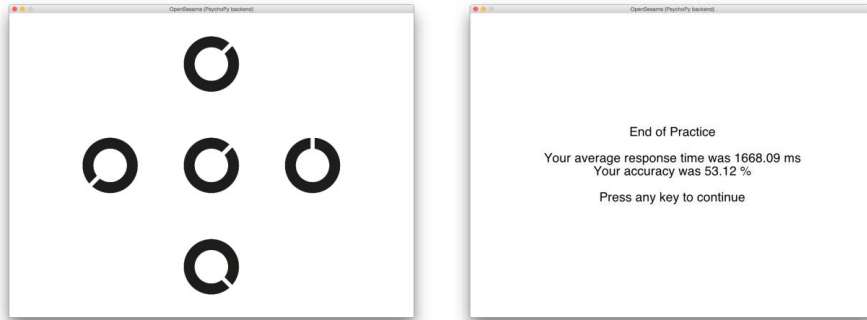


FIG. 4.14 Visual activity from Study I.

The order of appearance of the rings was random within each session and from one session to the next. The subjects were introduced to the test before starting the experiment and they did two sessions of the test in each position, a practice session and the actual test session. The practice session served as an adaptation stage to the conditions in each desk. The practice session had a duration of 1 minute and the actual task was performed over 2 minutes.

Several aspects were observed regarding the performance in this task:

- Subjects tended to rarely fail the test in their 3rd or 4th test / sitting position, with keying in speed increasing considerably as subjects got acquainted with the task and the hardware and with the subjects themselves reporting that they felt they improved their performance over time.
- Some subjects reported that even though they understood the explanation (visual and oral) that they were given in the beginning, they would often confuse the gap position in the circle with the direction where the gap was pointing to as the right answer.
- Subjects reported a response delay (lag) of the wireless keyboard in some cases, for which a reason wasn't clearly identified.

The character search task (CST) of Study II was created by the author in PowerPoint with the main intention of eliminating the use of the wireless keyboard. The task has a positive polarity (black letters on a white background) and was done in two versions: a board version and a desk version, with character sizes appropriate to each situation (Type = Calibri, Bold, 28 for board task and Calibri, Bold, 15 for desk task).

The text of the CST was randomly generated and consists of groups of words with 5 characters. To adapt to the conditions in each desk, the subject would start by reading a text extract for around 2 minutes and then proceed to carry out the CST, with had a duration of 4 minutes. The sequence of characters was the same but the letter to identify was a different one in each desk.

The author did not validate these tasks as actual tests to measure subject's performance. Drawing relationships between task performance and glare is therefore not attempted in this research.

4.7 General equipment

For the study I experiment, the task area or viewpoint of the subjects was a screen in the centre of the room, from where a visual task was performed by the subjects via a keyboard, wirelessly connected to the laptop where the test ran from. The online questionnaire ran on a laptop, on the participant's desk.

In the experiment of Study I, a regular classroom portable pull-up projecting screen that was used to project the visual task using a Panasonic PT-LB20EA mobile projector, with 2000 lumens, Daylight View and 400:1 contrast. The questionnaire was run from a MacBook Air that the subject would take with himself from desk to desk.

In the experiment of Study II, a 55' Samsung ME55C Edge Lit LED, with a resolution of 1920 x 1080 (HD), a brightness of 450cd/m² and a contrast ratio of 5,000:1 electronic screen was used for the board task. For the desk task, a 13'' MacBook Pro Retina (2015) laptop was used, equipped with a MyGadget M0225 matte anti-glare film protector to reduce veiling reflections. The laptop has a resolution of 2560 x 1600, a contrast ratio of 900:1 and a brightness of 300 cd/m².

Both the electronic screen and the laptop were run at their maximum contrast settings and the task was displayed in positive polarity in both board and desk tasks. The questionnaire was run from a MacBook Air in case of Study I and from an iPad in case of Study II, that the subject would take with himself from desk to desk.

Jupiter is the fifth planet from the Sun and the largest in the Solar System. It is a giant planet with a mass one-thousandth that of the Sun, but two-and-a-half times that of all the other planets in the Solar System combined. Astronomers have known Jupiter since antiquity. It is named after the Roman god Jupiter. When viewed from Earth, Jupiter can reach an apparent magnitude of -2.94 , bright enough for its reflected light to cast shadows and making it on average the third-brightest natural object in the night sky after the Moon and Venus.

Jupiter is primarily composed of hydrogen with a quarter of its mass being helium, though helium comprises only about a tenth of the number of its molecules. Like the other giant planets, Jupiter lacks a well-defined solid surface. Because of its rapid rotation, the planet's shape is that of an oblate spheroid (it has a slight but noticeable bulge around the equator). The outer atmosphere is visibly segregated into several bands at different latitudes, resulting in turbulence and storms along their interacting boundaries. A prominent result is the Great Red Spot, a giant storm that is known to have existed since at least the 17th century when it was first seen by telescope. Surrounding Jupiter is a faint planetary ring system and a powerful magnetosphere.

Jupiter has 79 known moons. Ganymede, the largest of these, has a diameter greater than that of the planet Mercury.

Jupiter has a faint planetary ring system composed of three main segments: an inner torus of particles known as the halo, a relatively bright main ring, and an outer gossamer ring. These rings appear to be made of dust, rather than ice as with Saturn's rings.

Jupiter receives the most frequent comet impacts of the Solar System's planets. It experiences about 200 times more asteroid and comet impacts than Earth. It was thought that the planet served to partially shield the inner system from cometary bombardment. However, recent computer simulations suggest that Jupiter does not cause a net decrease in the number of comets that pass through the inner Solar System, as its gravity perturbs their orbits inward roughly as often as it accretes or ejects them.

zhoaz sbxnn vfwfn akklm kswdt mipsz nwlvu anwod bsnqs dhlel ssodt xyxut lumdi onvub hrpic kufwo mnggt hxssd gsof lundc msgxr nsmgb wpaec jnkcm eztyy uqtlq vienu lltzh dupth gsgag fwbjtj uwjsb grpjg kaldw jilte iyikz gyhxc wcnvm julkd jpmhq guymx hvngx grdnb jwlpq owyzh wvokf mouxd fgmsb wrirg wxert laibk qoxoc vioxy bmsut bmhca bcvup duwil ktty bncwl mgmtv jjsae rgrtr lizir mntij nszz ufogo mrmve adgcm pbgzy shybd zadjw lpwwq kjkid oitqn mkjkm nolxr hryyh hylcl muwpy ewpvj flmnh hghea wxzsw ismzy mvzon zkowe btaiv pavnq smjjz zftfx ksdwh duqmq vysxh touot gslol eftxk mufsx yfykl jwely lczly qgqln ztmcj ceobo qqsdg krmho nofbt zyiwy nasxn hisiq vwxhq vyzui rbkpw zpogv eohlt qbfpt lmayd saubx caabs sqezp rpiso ppciy dllyz gpykj rotrk awrfq ujlly ctsvv qqjhj bjzjm cftsb ccksi xdzaz uvswm qvwot dkiaf qbydk nlfua yfzfr tuyfh qnjz dwrcv hkffd plgtr bgzae moqph tlaug yqpcw uamkf vatyl zeuge aarzb bkkjd vzlzu axiph emghj aawst yuane zfued rjdhl aectr gorvk razbm xwasz fapcg moevh iqnvq gouma wwbzt thtmg nhdiv jjesb qtcex txrds hhuox kastp tgnxw ovtun prnuu eoezb phsxb xxaqq ycfxm pfzaj cmhew xsok kntex xcrce ycsjt osgnj epsoc uriyy xdjpz nrdeg tnfhj esbgb cneeq ctlbw gdymm lgerj sqkss hqckp idnqg xnuew rpnxt yixss gmare upnib ebaoz gepyd tpdma tcark suifj amzzi njsmu ydqle xsyy ukfzw shoya vcdmz eraaj xlzqn ypdwe msonz xfwbs idrww wcbzf zvodm uzkyj xjuho cruhs nrauh jggys ldrsd jookr eujsj gvluq anorq cuptl mxwzw yjoxq ocewk xmlms wvjzf rseaz zkap siteu xsknq cwuis aunbc pojgp osonw ssmz devff ptkgq gjlgu bajzf ietgf hanov cvthm vxcdx selex micnx lfydq tkogu fyzoo metkl nhwpr vfvwr kdwhl lkrvo hvcdn lfwsz xjrvi whqjc bxdpb lqdcx dvthh arpzi xsmxy tnkqr kvyoq grcjl sphok nelva qkweh ahfjk lmjsa ukmtx klqgf odldc qhwpk ohunm ogase bezdw golrh zvhei oplzi zpsdw trcfw pmdth xihzy gcdwg degwp ehgab htwwr dgzkm rlvtot uyxdl xcpfv sixbu morqy znfpo rwtbj decdq warwr kmihb qenld lrcmx ykcut ihyeq kngnn fwjvx csohm dkhkg desij cdryl ojpt jdziw xxdur ievmg ynoqs rmxax kctwu doodl ltlai tkjfh obhhy ockfp zqjf vxayy mitij ewkid tejfv fikgd unoyu sldqt hztak fuigs osgyq lpzbq yhlde fjmki sfffh rjef yqama

FIG. 4.15 Visual activity for Study II (desk task). An adaptation stage text (top) and the character search task (bottom).

4.8 Experiments workflow

In Study I, the desks were marked with the position of the instruments, so these were kept as constant as possible from one session to the next. The angle between the camera's viewing direction and the window plane was approximately $+42^\circ$ in position 1, -42° in position 2, $+22^\circ$ in position 3 and -22° in position 4.

The researcher set the visual task running and the remote shooting of the camera, each time the participant changed position. The assistant moved the camera to the different desks and recorded the vertical illuminance being measured on the top of the camera. The luminance measurement was collected when the subject was doing the second round of the visual activity and just before starting to fill in the questionnaire.

The participants spend 3.5 to 4 minutes in each sitting position, spending around 30 minutes in the room. The sitting order was changed from one participant to the next to avoid a bias of the responses due to the order of sitting. Table 4.3 shows the workflow for the experiment of Study I.

In Study I, each subject sat in the four sitting positions in the room (P1, P2, P3 and P4) each time he or she attended the experiment, but in this case for a varying number of view directions. The sitting order in the four positions was random from subject to subject. The experiment workflow is very similar to that of Study II, but in this case the luminance measurement was collected immediately before and after the subject performed the visual activity.

The subjects spent 8.5 to 10 minutes in each position carrying out the visual task and responding to the questionnaire and around 1 hour in the room.

The experiment of Study II was designed as a within-subject experiment (where all subjects would evaluate all the room layouts) however due to subject availability and weather conditions (periods of strong wind where the blinds of the room had to be closed for security) it was instead run as a between-subject experiment, with most subjects assessing two different room layouts.

TABLE 4.3 Experiment workflow for the Study I experiment.

Step #	Subject	Researcher and assistant	Duration (mn)
1	Receives explanation about the experiment, about the workflow and about the visual task		4
2	Sits in indicated desk (desk #1)	Sets equipment	1
3	Fills in the 1 st part of the questionnaire: demographic questions	Move to their positions in the room	2
4	Starts the visual task using the wireless keyboard		0.5
5	Reads the on-screen visual task instructions		0.5
6	Performs the adaptation stage of the visual task		1.3
7	Performs the visual task	Make the luminance measurement and take the vertical eye illuminance measurements	1.3
8	Fills in the 2 nd part of questionnaire relating to the visual comfort and glare		1
9	Moves to the indicated desk (desk #2)	Move camera to desk #2 and set-up a new visual task	0.5
10	Starts the visual task using the keyboard	Move to their positions in the room	0.5
11	Performs the adaptation stage of the visual task		1.3
12	Performs the visual task	Make the luminance measurement and take the vertical eye illuminance measurements	1.3
13	Fills in the 2 nd part of questionnaire relating to the visual comfort and glare		1
14	Repeat steps 9-13 in a new desk (desk #3)	Repeat steps 9-10 for desk #3	5.1
15	Repeat steps 9-13 in a new desk (desk #4)	Repeat steps 9-10 for desk #4	5.1
16	Fills in the 3 rd part of the questionnaire: general comfort in the room		3
17	Is greeted and leaves		

Duration = approximate duration of each step, in minutes (decimal).

TABLE 4.4 Experiment workflow for the Study II experiment.

Step #	Subject	Researcher	Duration (mn)
1	Receives explanation about the experiment, about the workflow experiment, about the movie-recording headset and about the visual task. Signs consent for movie recording.		5
2	Is equipped with eye-movie recording headset	Fits eye-movie recording headset to subject	2
3	Sits in the indicated desk (desk #1)		0.5
4	Fills in the 1 st part of the questionnaire: demographic questions	Starts face- and eye-movie recording session	2
5	Opens the first screen for the visual task	Makes the first luminance measurement in desk #1	1
6	Performs the adaptation stage of the visual task	Moves to her position	1.5
7	Performs the visual task and writes result on slip of paper		4
8	Fills in the 2 nd part of questionnaire relating to the visual comfort and glare		2
9	Stays sitting behind the camera, while measurement is taken	Makes the second luminance measurement in desk #1	1
10	Moves to the indicated desk (desk #2)	Moves camera to desk #2	0.5
11	Sets the screen for the visual task	Makes the first luminance measurement in desk #2	1
12	Performs the adaptation stage of the visual task	Moves to her position	1.5
13	Performs the visual task and writes result on slip of paper		4
14	Fills in the 2 nd part of questionnaire relating to the visual comfort and glare		2
15	Stays sitting behind the camera, while measurement is taken	Makes the second luminance measurement in desk #2	1
16	Repeats steps 10-14 in a new desk (desk #3)	Repeats steps 10-15 for desk #3	9
17	Repeats steps 10-14 in a new desk (desk #4)	Repeats steps 10-15 for desk #4	9
18	Moves to the reference desk in the centre of the room	Moves camera to reference desk	1.5
19	Sets the screen for the visual task	Makes the first luminance measurement in reference desk	1
20	Performs the adaptation stage of the visual task		1.5
21	Performs the visual task and writes result on slip of paper		4
22		Makes second luminance measurement in reference desk	1
23		Stops face- and eye-movie recording session	1
24	Removes headset, is greeted and leaves		

Duration = approximate duration of each step, in minutes (decimal).

4.9 Experiment population



FIG. 4.16 Participants in the experiment of Study I.



FIG. 4.17 Room set-up for the screen task and participant performing a desk task, in the experiment Study II.

The subjects that took part in the experiments were all higher education students from TU Delft of Asian, Middle-Eastern, European and South American origin (16 nationalities) with an average age of 30 years old. The population in both studies is to be considered a 'convenience sample'. The subjects were recruited via email within the AE+T department of the Faculty of Architecture and the Built Environment and via poster and/or flyers distributed in several parts of the TU Delft campus.

The email, poster or flyer explained the objective of the experiment and upon confirmation of interest from a subject more information regarding the experiment was provided (e.g. location, time). The subjects that attended the experiment of Study I received a 6 Euro compensation or a book voucher of the same value and subjects that attended the experiment of Study II received a 7 Euro/hour compensation.

There were no particular criteria in the selection of subjects other than being students between the ages of 18 and 40. The objective was not to study a particular student population but to rather make use of an accessible student population resource to assess the problem of glare in the classroom space. Setting a minimum age of 18 years ensured that subjects could attend the experiment on their own and a maximum age of 40 years ensured a certain degree control over the 'eye aging' characteristics of the population.

The experiment of Study I was attended by 50 subjects ($N = 50$) and the experiment of Study II was attended by 17 subjects ($N = 17$).

4.10 Sky conditions

All the experimental work occurred under naturally occurring sky conditions, between the hours of 10:00 and 18:00. The blinds of the room were kept open in all sessions and the electric lighting was switched off.

The Study I experiment, occurred over three distinct time periods (here called sessions) between 2016 and 2018, in autumn and summer. The first session occurred over 6 days in October and November 2016, the second session over 5 days in August 2017 and the third session over 6 days in July 2018, for a wide range of sky conditions: clear skies on the first session, overcast and cloudy skies on the second session and mostly clear skies on the third session. The Study II experiment ran for two weeks in the end of August 2019 for mostly clear sky conditions.

4.11 Data processing

4.11.1 Matching luminance and illuminance measurement

Matching the luminance and illuminance measurements was required to extract the measured vertical eye illuminance for each luminance capture. The date and time of all the CR2 image files used to compose each HDR luminance image was extracted using Exiftool-11.80 (Harvey, 2019), including the exact time of each picture to the millisecond. The first image file of each luminance sequence was used to match with the readings of the illuminance meter to the second. The three illuminance values corresponding to the duration of each luminance capture were extracted and the average of those values was taken as the vertical eye illuminance of the observation.

4.11.2 Luminance image pixel saturation correction

During the conversion of the LDR sequence into the HDR luminance image, Labsoft gives a warning in case of pixel saturation (i.e. if areas of unreadable luminance are found) and allows for that area to be identified.

Pixel saturation correction can be performed in *evalglare*, based on an externally measured vertical eye illuminance value. *Evalglare* calculates E_v by integrating the luminance values over the luminance image, using the cosine of the angle between the centre and the position of a pixel in the image. The luminance of the saturated area is derived based on that calculation. The implemented algorithm will only work for one single region of saturation, which was the case for all the images where saturation was verified for the collected data.

4.11.3 Comparison of measured and image-derived illuminance

The vertical eye illuminance derived by *Evalglare* for all the images was compared with the external vertical eye illuminance measured on the top of the camera, a step that is often used to verify the integrity of the luminance image (Wienold and Christoffersen, 2006) (Hirning, 2014) (Karlsen et al., 2015) (Konstantzos and Tzempelikos, 2017) (Wienold *et al.*, 2019). It was expected that the difference between the two measurements to be within the range of the combined LMK and illuminance meter uncertainties ($\pm 8\%$ and $\pm 5\%$, respectively) but this was found not to be the case, with much higher differences being found for the data collected in Study I, where differences of up to 54% were found.

Further checks done to the photometric calibration of the illuminance meter (Appendix A, section 8) and of the LMK camera (Appendix A, section 7) showed that this deviation could not be exclusively attributed to inaccuracies of calibration. It is also the case that the photometric calibration of the Konica Minolta illuminance meter and of the LMK is based on the same type of light source (the CIE, illuminant A). An estimation of the error due to spectral differences between the light source used for the calibration of the LMK (tungsten halogen lamp) and the daylight light source was performed by the author (Appendix A, section 6). The test compares the luminance output from the LMK camera with the luminance derived from a spectrophotometer measurement, under daylight. The difference between the two measurements was found to reach 7.6%, which indicates there can be an additional uncertainty due to the spectrum of the daylight light source.

As the illuminance measurement was collected visually, the possibility of human error cannot be excluded as a cause for the higher deviations that were found in Study I. For that reason a different illuminance meter with data recording capabilities was used in the experiment of Study II, for a better agreement between the measured and derived illuminance (maximum error of 27%). The cases with a high deviation in Study I could then have been caused by a faulty collection of the data. But there could be other reasons for the high deviation. Although the two instruments do not show any apparent problems regarding their photometric calibrations, these are still very different pieces of hardware with possibly different characteristics regarding the resolution at which they are capable of measuring the light over the visual field.

4.11.4 Metrics calculation

All the luminance-based metrics that were analysed in this thesis were calculated using *evalglare* (Wienold, 2017a) (Wienold, 2019) or derived from an *evalglare* calculation output. The *evalglare* is a command-line image-processing software for the analysis of luminance images and calculation of glare metrics, that reads the Radiance's PIC file format (Larson and Shakespeare, 1998) a digital HDR file format in its origin. The programme is the most comprehensive tool for the calculation of glare metrics currently available, offering the possibility of calculating the wider range of existing glare indices and most of the newly proposed ones.

As explained previously, the HDR luminance images were produced in Labsoft (PF file), where they were checked for pixel saturation and cropped to the actual fisheye image boundary. The images were then converted to the Radiance's PIC image file format using *pftopic*, a convertor for LMK images developed at the Fraunhofer Institut (Wienold, 2017b).

As a Radiance-based tool, *Evalglare* will only take fish-eye images with either hemispherical or equi-angle projection. The luminance images had therefore to be re-projected from their original equi-solid angle projection to one of these supported formats, in this case an equi-angle projection, using Radiance's *pcomb* tool (Ward, 2018).

For the *evalglare* calculation it is also recommended that the luminance image resolution does not exceed 1500 pixels. The luminance image was therefore reduced to 1200x1200 pixels using *pfilt* (Ward, 2018).

Evalglare reads the information stored in the PIC file header regarding the image resolution, view size and projection that results from this process, so the calculation of the metrics are done according to those image settings. A small artefact resulting from the preparation of the PIC file was found regarding an extra space at the view description in the header of the PIC file, causing *evalglare* to produce an error when reading the file. The header of the images had to be corrected with the removal of that space.

As the *evalglare* calculation is based on the luminance of a 180° luminance image, the original 185° LMK image is clipped to that size by the programme prior to the calculation.

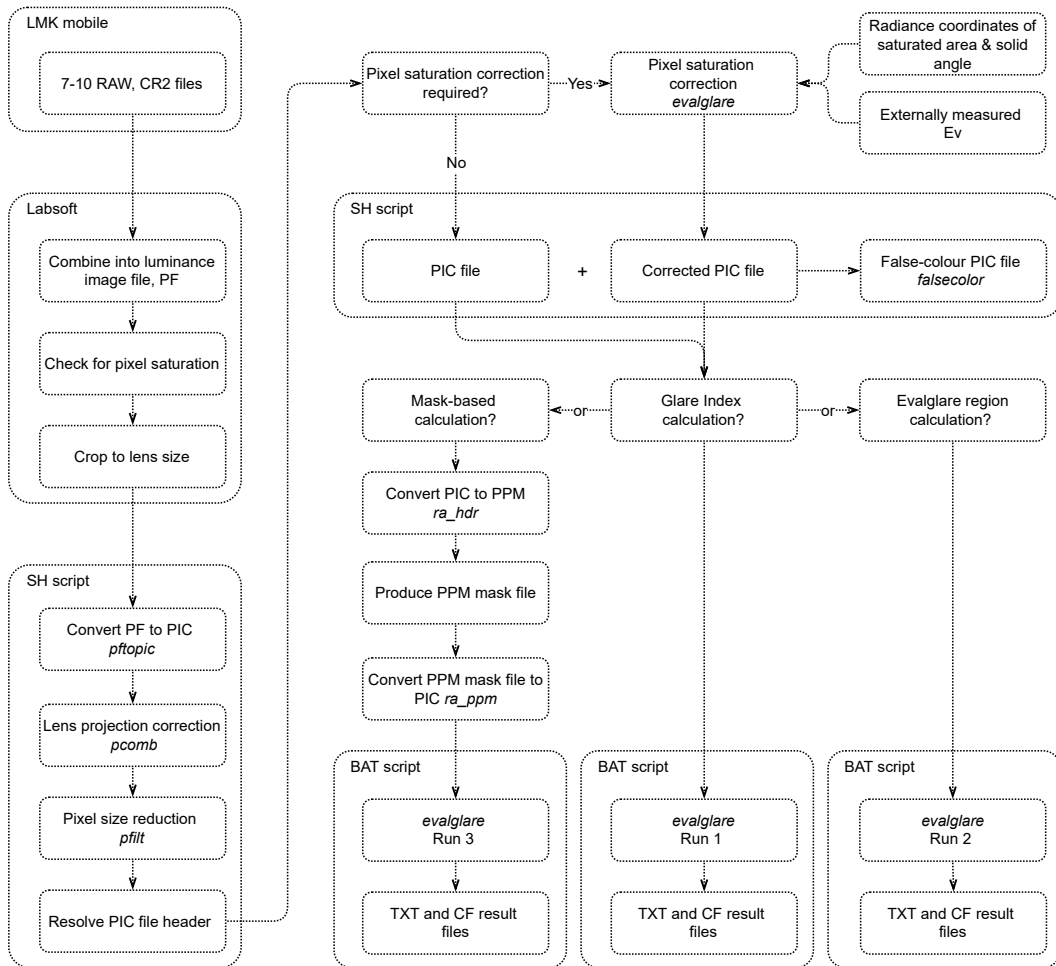
After the PIC files were produced, any images with pixel saturation were individually corrected based on the externally measured E_v value using *evalglare* and then processed into false-colour luminance images, for visualisation.

The PIC files were then either further processed for the purpose of calculating mask based glare metrics, or other types of glare metrics (indices, regions).

For a mask-based metric, mask files were produced in Photoshop which are basically black and white images where the white area corresponds to the region to be calculated. Again, as *evalglare* will only read a Radiance file format, the mask files need to be converted into the PIC file format using image-processing Radiance tools.

Three runs of *evalglare* were done depending on the type of metrics to calculate, so the calculation would not be affected by the specific operations that have to be done to the images for each of them.

The workflow for the calculation of the glare metrics described above was automated where possible using *bash* scripting, with one script for the batch preparation of the PIC file, a script to post-process the images for visualisation and a script to run the actual *evalglare* calculation and output its results in batch mode (Appendix G). The diagram in Figure 4.18 summarizes the workflow described above.



LMK mobile (Technoteam, 2016); Labsoft (Technoteam, 2017); *evalglare*, *ptopic* (Wienold, J. 2010); *pcomb*, *pfilt*, *falsecolor*, *ra_hdr*, *ra_ppm* (Ward, G. 2019)

FIG. 4.18 Luminance data processing workflow, from luminance capture to the calculation of the glare metrics.

4.12 Statistical analysis method

The objective of the experimental studies, Study I and Study II, was to collect data to conduct an assessment of the predictive power of the discomfort glare metrics. This assessment was carried out by statistical analysis that compare the calculated discomfort glare metrics with the subjects' glare evaluations. The sources of data were combined in Excel and the statistical analysis was performed with SPSS v24 (IBM Corporation, 2016), with JMP 14 (SAS Institute Inc., 2019) also being used for data exploration and visualisation.

The dependent variable of the analysis is the subjects' evaluation of their perception of glare for the different visual conditions in each experiment. The independent variable of the analysis is a group of selected glare metrics. The analysis was based on common statistical methods of correlation and classification and in some aspects, on the methodology proposed in (Wienold et al., 2017) for the analysis of discomfort glare metrics. It consists of using a combination of statistical tests to find 1) the ability of a metric to describe the full glare scale, i.e., how well does a metric correlate with reported glare and 2) the accuracy of a metric, i.e., how well does a metric distinguish a 'glare' vote from a 'no glare' vote.

4.12.1 Ability of a metric to describe the full glare scale

Since the dependent variable of the study is of ordinal level, the ability of a metric to describe the full glare scale was analysed via a Spearman rank correlation. The Spearman rank correlation is a non-parametric test that is particularly suitable in the cases where there is violation of one or more assumptions of a parametric test such as the Pearson correlation. As the name indicates, the Spearman rank correlation is based on a transformation of the data into ranks and for that reason it is neither affected by a non-normal distribution of the data nor by any potential outliers. The Spearman rank correlation algorithm implemented in SPSS, uses the Siegel's definition (Siegel, 1956) for the calculation of the correlation coefficient.

For each variable X and Y separately, the observations are sorted into ascending order and replaced by their ranks. For each of the N observations, the difference between the rank of X and the rank of Y is computed as:

$$d_i = R(X_i) - R(Y_i)$$

The Spearman's rho (ρ) is calculated as:

$$\rho = \frac{T_x + T_y - \sum_{i=1}^N d_i^2}{2\sqrt{T_x \cdot T_y}}$$

Where N is the number of observations, $T_x = \frac{N^3 - N - ST_x}{12}$ and $T_y = \frac{N^3 - N - ST_y}{12}$.

If T_x or T_y is 0, the statistic is not computed. In situations where t observations are tied, the average ranked is assigned. Each time $t > 1$, the quantity $t^3 - t$ is calculated and summed separately for each variable, with these sums being designated as ST_x and ST_y in the equations above.

4.12.2 Accuracy of a metric

The accuracy or predictive ability of a metric was analysed via a Receiver Operating Characteristic (ROC) curve statistic, a classification type of statistic that is very popular in diagnostic medical research. To perform a ROC curve analysis, the independent variable (reported glare) needs to be transformed into a dichotomous variable, where one of the values represents the positive condition ('glare') and the other value represents the negative condition ('no glare'). For the performed analysis, the 'no glare' value includes the 'imperceptible' and 'noticeable' glare votes and the 'glare' value includes the 'disturbing' and 'intolerable' glare votes.

The output of a ROC statistical test is a plot of points corresponding to the values of the independent variable (metric), whose positions are defined by the number of correct 'no glare' and correct 'glare' predictions that are made based on each value of the independent variable. Figure 4.19 illustrates the process of plotting a ROC curve.

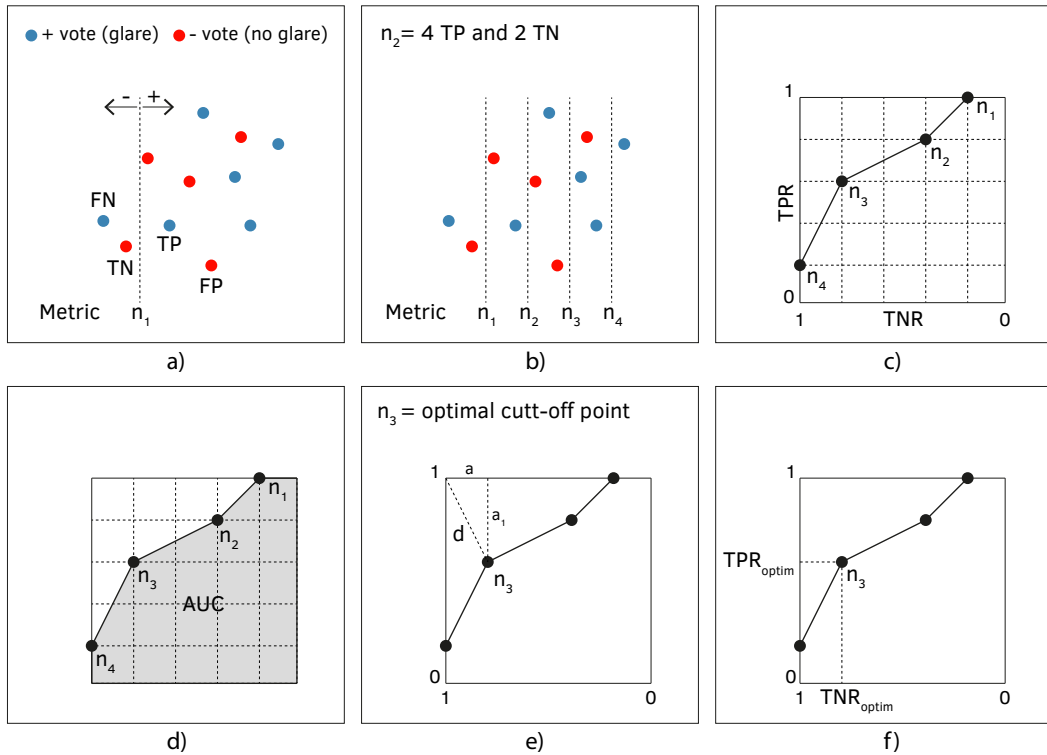


FIG. 4.19 ROC curve definition. Source: by the author.

- a) The dots show the glare evaluations coded as 'glare' (positives) and 'no glare' (negatives). For each value of the metric (n) there are correct positive predictions, called true positives (TP) (the blue dots on the right side of the dotted line) and correct negative predictions, called true negatives (TN) (the red dots on the left side of the dotted line). A blue dot on the left side of the dotted line is a false negative (FN) and a red dot on the right side of the line is a false positive (FP).
- b) To each value of the metric there will be a corresponding number of TP, TN, FP and FN observations. The ROC curve is a plot of the TP versus the TN observations for all values of a metric.

- c) The Y-axis of a ROC curve shows the true positive rate (TPR) and the X-axis, the true negative rate (TNR). The TPR stands for the correct prediction of reported 'glare' and the TNR stands for the correct prediction of 'no glare'. The TPR and TNR rates are defined as:

$$\text{TPR} = \frac{\text{Number of TP}}{\text{Number of TP} + \text{Number of FN}}$$

$$\text{TNR} = \frac{\text{Number of TN}}{\text{Number of TN} + \text{Number of FP}}$$

- d) The Area Under the Curve (AUC) of a ROC plot is a measure of the accuracy of the model. The higher the AUC is the more accurate a model is. The AUC provides a measure of how well a glare metric can distinguish between the two groups, the 'glare' group and the 'no glare' group.
- e) The point corresponding to the shortest distance of the curve to the top left corner of the plot (d) is called the optimal cut-off point of the curve or optimal decision threshold and it is calculated as:

$$d = \sqrt{a^2 + a_1^2}$$

- f) The optimal cut-off point of the curve is the value of a metric for which a better prediction is made. This point corresponds to the point where the combined true positive rate (TPR) and true negative rate (TNR) of the metric is at its highest.

The metrics are compared based on their AUC, on their TPR and TNR at the optimal cut-off point and on their shortest distance. The AUC algorithm implemented in SPSS, uses the non-parametric definition from DeLong et al. (1988), described below.

When x_+ denotes values for cases with positive actual states and x_- denotes values with negative actual states, the 'true' area under the curve (Θ) is:

$$\Theta = \Pr(x_+ > x_-)$$

with the non-parametric approximation of Θ being defined as

$$W = \frac{1}{n_+ n_-} \sum_{\text{all possible combinations of } (x_+, x_-)} s(x_+, x_-)$$

Where n_+ is the sample size of the actual positive group and n_- is the sample size of the actual negative group, and

$$s(x_+, x_-) = \begin{cases} 1 & \text{if } x_+ > x_- \\ \frac{1}{2} & \text{if } x_+ = x_- \\ 2 & \text{if } x_+ < x_- \end{cases}$$

W corresponds to the observed area under the ROC curve, which connects successive points by a straight line (trapezoidal rule).

The next chapters, Chapters V and VI, present the results and statistical analysis of the data collected in the experimental studies I and II.

5 Experimental study I

5.1 Introduction

The objective of Study I is to investigate how well existing and newly proposed visual discomfort from glare metrics predict reported discomfort in a classroom environment and how good that prediction is across the classroom space.

The experiment in the basis of the study occurred in the classroom setting of the research (described in Chapter IV) over three sessions, in summer and autumn periods, between the hours of 10:00 and 18:00, under naturally occurring sky conditions. A range of metrics of three different types - glare indices, simple luminance-based metrics and luminance contrast ratios, were selected and are analysed for their performance.

Aspects relating to the luminance data preparation and to the metrics calculation method are firstly discussed, followed by the analysis of the results of the questionnaire and by the analysis of the performance of the metrics.

5.2 Population

The population of the study consisted of 50 subjects, 21 females and 29 males of Asian, South American, African, Middle-Eastern and European origin. From the 50 subjects, 28 needed corrective eyewear (contact lenses = 6, glasses = 22) and all subjects were wearing their eyewear at the time of the experiment. 39 of

the subjects were right-handed and 11 were left-handed. Subjects were all higher education students with ages between 20 and 40 years old and an average age of 28. No eye-colour information was collected in this study.

Most subjects reported being 'moderately' (41%) to 'very' (29%) sensitive to bright light (Figure 5.1). A high percentage of the subjects reported that having a window view in the workplace was 'very' (39%) to 'extremely' (35%) important for them (Figure 5.2).

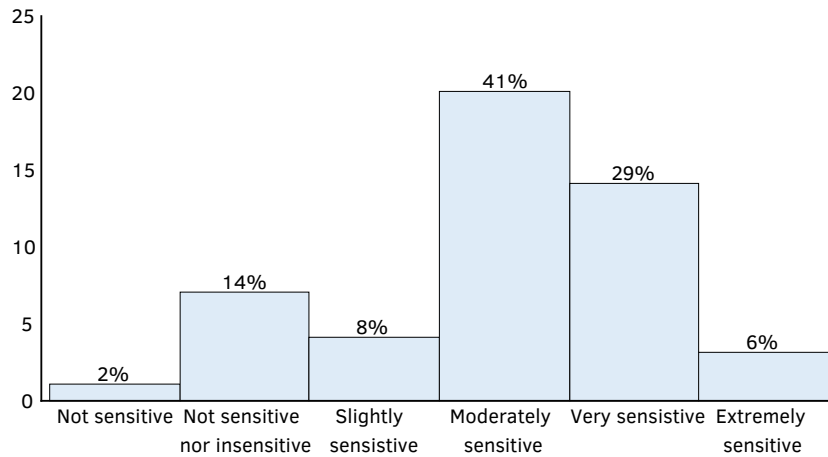


FIG. 5.1 Counts of the self-reported 'sensitivity to bright light'.

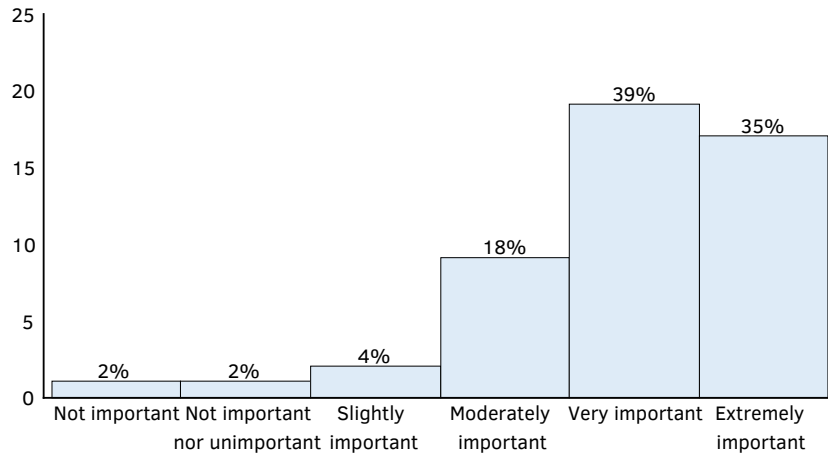


FIG. 5.2 Counts of the 'importance of a view out in the workplace'.

5.3 Metrics

The glare metrics investigated in the study include a selection of relevant glare indices (DGP, DGI, DGI_{mod}, UGR and UGP), a range of recently proposed luminance-based metrics (Van Den Wymelenberg and Inanici, 2015), the luminance contrast ratio proposed in the IES Lighting Handbook (Dilaura et al., 2011) and the vertical illuminance at eye level (Wienold and Christoffersen, 2006). It was also found appropriate to include the metrics that have shown high correlation in the studies by Konis (2014) and by Mahić et al. (2017). In the study by Konis (2014), glare was evaluated in sitting positions of 6 to 9 meters from the façade and in the study by Mahić et al. (2017) glare was evaluated in variable positions in space (see Chapter II for more information on these metrics).

The thirteen investigated metrics, their borderline between comfort and discomfort (BCD) threshold, when provided, and the labels used to identify them in the study are listed in Table 5.1.

TABLE 5.1 Metrics, their borderline between comfort and discomfort (BCD) threshold and label used in the study.

#	Metric	BCD	Label
1	Daylight Glare Probability [1]	0.35 - 0.40	DGP
2	Vertical illuminance at eye level [2]	2,600** [Lux]	E_v
3	Daylight Glare Index [3]	18 - 24	DGI
4	Modified Daylight Glare Index [4]	-	DGI _{mod}
5	Unified Glare Rating [5]	13 - 22	UGR
6	Unified Glare Probability [6]	-	UGP
7	Mean luminance in the 180° field-of-view [6]	-	$L_{180^\circ_mean}$
8	Mean luminance within a 40° central band [7]	500 - 700 [cd/m ²]	$L_{40^\circ_mean}$
9	Coefficient of variation of the luminance within the 40° central band [8]	3.5	$L_{40^\circ_COV}$
10	Window mean luminance [7]	2,000 - 2,500 [cd/m ²]	L_{win_mean}
11	Window standard deviation [7]	2,500 - 4,000 [cd/m ²]	L_{win_std}
12	Window mean luminance to task mean luminance contrast ratio [7] [9]	1:20, 1:22*	L_{win_mean}/L_{t_mean}
13	Window maximum luminance to task mean luminance contrast ratio [10]	-	L_{win_max}/L_{t_mean}

[1] (Wienold and Christoffersen, 2006) [2] (Wienold, 2009) [3] (Hopkinson, 1972) [4] (Fisekis et al., 2003) [5] (CIE, 1995) [6] (Hirning et al., 2014) [7] (Van Den Wymelenberg and Inanici, 2015) [8] (Mahić et al., 2017) [9] (Dilaura et al., 2011) [10] (Konis, 2014). (*) - threshold proposed in (Van Den Wymelenberg and Inanici, 2014). (**) threshold derived from DGPs.

5.4 Data processing

5.4.1 Luminance overflow correction

From the collected 199 luminance measurements, there were nine images with luminance overflow. Session 1 produced six HDR images with luminance overflow, independently of the range and number of LDR photos used. Session 2 produced one HDR image with luminance overflow when nine LDR photos were used but not when the full fourteen set of LDR images was used. Session 3 produced three HDR images with luminance overflow. In the case of session 3, overflow occurred always in the area of the visible sun and in captures done in position 1. Different combinations of LDR photos could not remedy this.

Seven of the nine HDR images with luminance overflow that resulted from the three sessions were corrected in *evalglare* using the externally measured mean vertical eye illuminance. It was not possible to correct two of the images because the externally measured illuminance was lower than luminance image-derived illuminance. In one of these cases this is possibly due to the fact that the illuminance meter was at a 15 cm distance from the centre of the lens and was therefore not able to capture the luminance of the sun disc, which was visible in the image in this case. The other image corresponded to a measurement with the sun in the very edge of the image, a zone of higher error for the two types of measurement. These two images were excluded from the dataset.

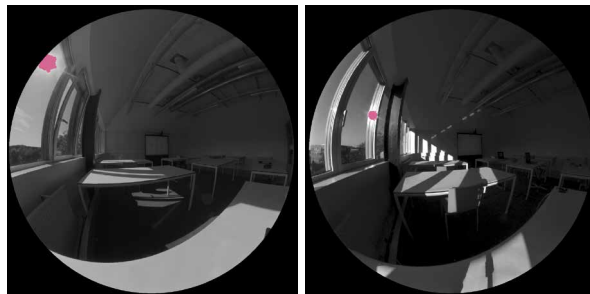


FIG. 5.3 Examples of images with luminance overflow (in pink).

5.4.2 Measurement selection

From the 199 measurements (4 x 50 – 1 technical problem), fourteen measurements were excluded from the analysis sample: two where there was accidental movement of a person (either researcher or subject) in front of the camera, two images with luminance overflow that could not be corrected, four cases where the sun reached the task area (screen), five cases where the sun reached the task area and the subjects reported having had problems seeing the projected image and a case that was very unique within the dataset, corresponding to the highest measured luminance in the study and reported ‘imperceptible’ glare by the subject.

From the 50 subjects that attended the experiment only 49 subjects are included in the study as all measurements for one of the subjects (4) were excluded as a result of the image selection process.

This resulted in a data sample comprising of 185 cases: 44 cases in position 1, 46 cases in position 2, 46 cases in position 3 and 48 cases in position 4.



FIG. 5.4 Some of the eliminated measurements: a) movement in front of camera, b) sun in the edge of a window, c) sun incident on task, d) sun on the task area.

5.4.3 Comparison of measured and image-derived illuminance

The error between the measured and image-derived vertical illuminance (E_v) was estimated for the original dataset of 199 measurements and for the dataset after elimination of the images with problems (185 measurements).

For the original dataset, the externally measured versus the luminance-image derived E_v showed a bias of 33 Lux, a normalised bias of 3%, a root mean square error (RMSE) of 207 Lux and a normalised root mean square error (NRMSE) of 11%.

After the exclusion of the 14 images with problems and overflow correction, there is a bias of 19 Lux, a normalised bias of 2%, a root mean square error (RMSE) of 169 Lux and a normalised root mean square error (NRMSE) of 11%, between the two measurements. Figure 5.5 shows the scatter plots for the two datasets.

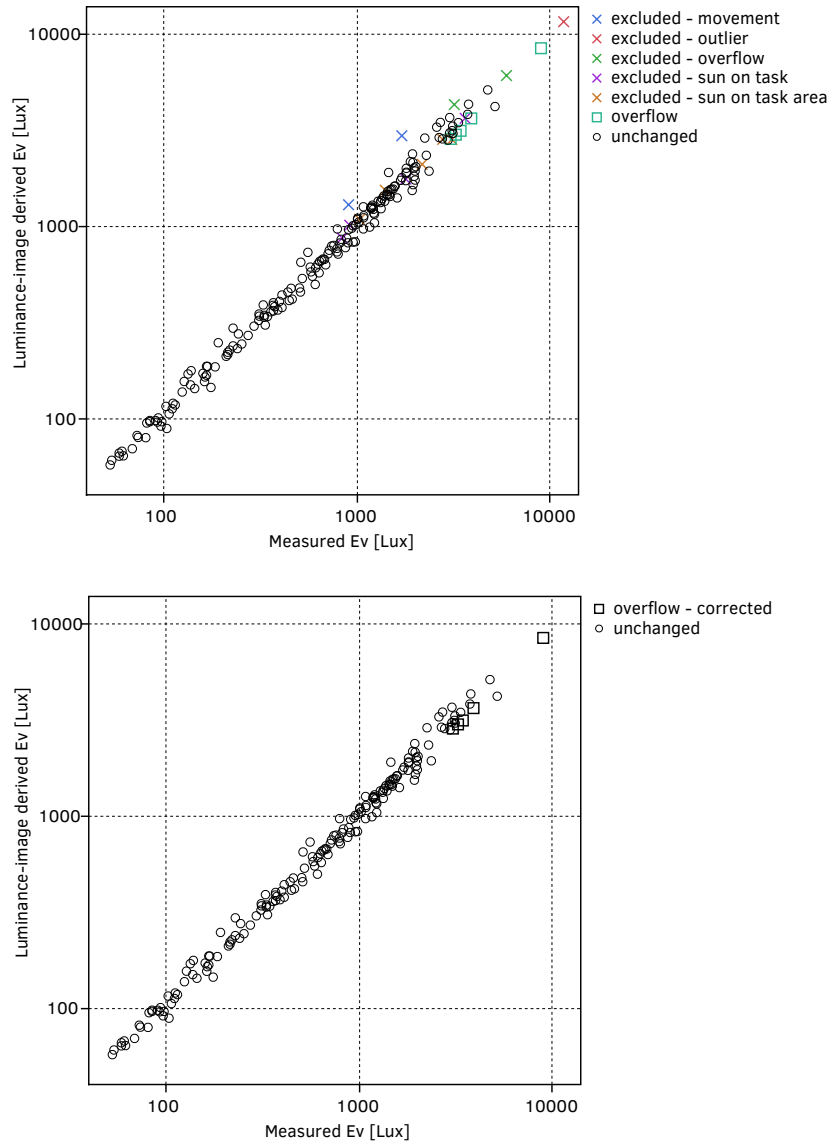


FIG. 5.5 Luminance-derived versus externally measured vertical illuminance (Ev) for the initial sample of 199 cases (top) and for the study sample of 185 cases (bottom).

5.5 Metrics calculation

5.5.1 Glare source detection method in DGP

The image-based luminance measurement technique enables a more detailed visualisation of the luminance distribution in the human visual field and with it a question regarding what should be considered a source of glare in the particularly complex daylight glare conditions emerges.

For the DGP definition, a sensitivity study was carried out by Wienold (2010) comparing several glare source detection methods that the author calls the factor method, the task method and the threshold method. For the factor method, an area of an image is considered a glare source if its luminance exceeds the average luminance of the image by a given factor. For the threshold method, any area of an image above a given fixed value is counted as a glare source. For the task method, any area of an image is considered a glare source if its luminance exceeds the luminance of the task area by a given factor. The author found the task method to be the most reliable of the three methods and although implemented in *evalglare*, the use of the factor method is not recommended (Wienold, 2016). It has been recommended until very recently, to use the task method with a factor of 4 or 5 (Wienold and Christoffersen, 2006) (Wienold, 2014). However, recent research suggests that the choice of a method should be made on the basis of the luminance characteristics of a scene (Pierson et al., 2018), particularly in the case of situations of either saturation or contrast glare. The use of the threshold method instead of the task method greatly reduces the time that needs to be spend on preparing the data for the DGP calculation in that a task position and size can vary from image to image requiring the sorting of images based on those characteristics and the need to run separate calculations based on that.

A study was done to find how the two recommended glare source detection methods – task and threshold – compare with the subjective glare evaluations collected in the experiment, where a higher correlation between metric calculated with a particular method and the subjects' evaluation of glare would indicate the superiority of a method in relation to another.

The task method was tested for two factors:

- Factor of 4 (DGP_{f4})
- Factor of 5 (DGP_{f5})

The threshold method was tested for two thresholds:

- 1000 cd/m² (DGP_{1000})
- 2000 cd/m² (DGP_{2000})

A mixed task and threshold method was also tested, where the threshold method with a threshold of 2000 cd·m⁻² was used for what were defined as saturation scenes and the task method with a factor of 5 was used for the other scenes ($DGP_{f5,2000}$).

A saturation scene is defined as a scene with either a high illuminance at eye level (E_v) or a scene where a large amount of incident sunlight could be observed in the room surfaces.

For the case of high illuminance at eye level, two E_v thresholds were used to identify the saturation scenes:

- 2000 cd/m² ($DGP_{f5,2000}$)
- 3000 cd/m² ($DGP_{f5,2000}$).

For the case of high sunlight incidence, the scenes were separated into those where large patches of sunlight were visible in the scene and those where weren't. The definition based on the visibility of sunlight within the room corresponds to:

- Sunlight, $DGP_{f5,sun}$.

A Spearman correlation was chosen, given that the dependent variable of the test is of ordinal level. The correlations were carried out for the full dataset and for the dataset separated into sets of measurements: the measurements collected at the window positions (position 1 and position 2) and the measurements collected in the wall positions (position 3 and position 4). The results of the correlations are presented in Table 5.2.

The threshold method with factor 2,000 cd/m² (DGP_{2000}) showed a somewhat better correlation for all the tested samples and the method used to identify the glare source for the calculation of DGP was then the threshold method with a threshold of 2,000 cd/m².

As a task-independent method, the threshold method significantly simplifies the analysis and evaluation of discomfort glare of spaces based on DGP, being its benefit in relation to the classroom space possibly even bigger than for any other type of working space, considering that in a classroom there could be as many sizes and positions of a task area as the number of sitting positions in that space and as the wider range of points towards which gaze is directed to (board task, desk task, teacher).

The use of the threshold method is particularly convenient in the context of this investigation given that small deviations regarding the position of the desks, screen and camera from one session to the next meant that a compromise solution needed to be found regarding the location and size of the task so images could be processed in batches of 4 (1 per position) rather than individually when calculating DGP.

TABLE 5.2 Spearman correlation coefficient (ρ) and significance for different DGP calculation methods for the full, window positions and wall positions samples.

Source detection method		Full room		P1, P2		P3, P4	
		ρ	p-value	ρ	p-value	ρ	p-value
Task	DGP _{fs}	0.342	< 0.001	0.418	< 0.001	0.200	0.05329
	DGP _{f4}	0.332	< 0.001	0.414	< 0.001	0.192	0.06373
Threshold	DGP ₁₀₀₀	0.334	< 0.001	0.412	< 0.001	0.189	0.06772
	DGP₂₀₀₀	0.343	< 0.001	0.421	< 0.001	0.202	0.05120
Task + Threshold	DGP _{fs,2000}	0.341	< 0.001	0.412	< 0.001	0.201	0.05190
	DGP _{fs,3000}	0.341	< 0.001	0.414	< 0.001	0.200	0.05329
	DGP _{fs,sun}	0.340	< 0.001	0.419	< 0.001	0.189	0.06866

The same type of inconvenience relating to the task-based calculation method of the DGP extends to the calculation of mask-based metrics like the window-based metrics, where one mask per type and sitting position needs to be created and calculated more or less individually depending on the number of groups that is possible to define. This makes this type of metrics rather more difficult to calculate and requires the development of specific calculation methods in order for them to be of practical use in the context of an actual design process.

5.5.2 Region and mask-based calculation

Evalglare provides the possibility to calculate the luminance statistics for some pre-defined regions (e.g., 40° band) or for any other region specified by a mask file. The task and window mask files for the four positions were created and provided as inputs for the calculation of the luminance in these regions (Figure 5.6).

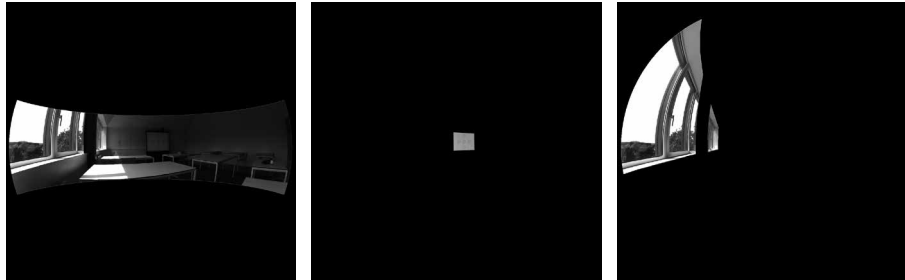


FIG. 5.6 Region and masks used in the study (position 1). From left to right: 40° band region, task and window masks.

5.6 Results

5.6.1 Reported visual comfort and glare

A series of questions was asked in relation to the visual comfort in each position: how well was the screen seen by the subject, if the subject felt any discomfort due to sunlight, if the subject was bothered by reflections on the screen or by a screen washed out, how the subject would rate the overall comfort of the lighting condition and finally how the subject would rate the level of glare.

In 80% of the cases, subjects reported that they could see the screen well, with positions 2 and 3 being the positions where the visibility of the screen was rated the worst (Figure 5.7).

In 82% of the cases the subjects reported that they were not bothered or felt neutral to the sunlight. Less discomfort due to sunlight was reported for the positions 3 and 4, which is to be expected given that these are farther from the window (Figure 5.8).

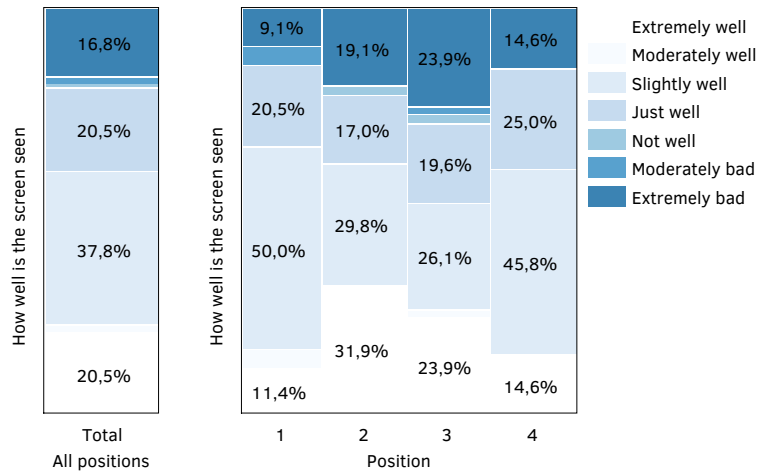


FIG. 5.7 Distribution of the 'how well is screen seen' responses.

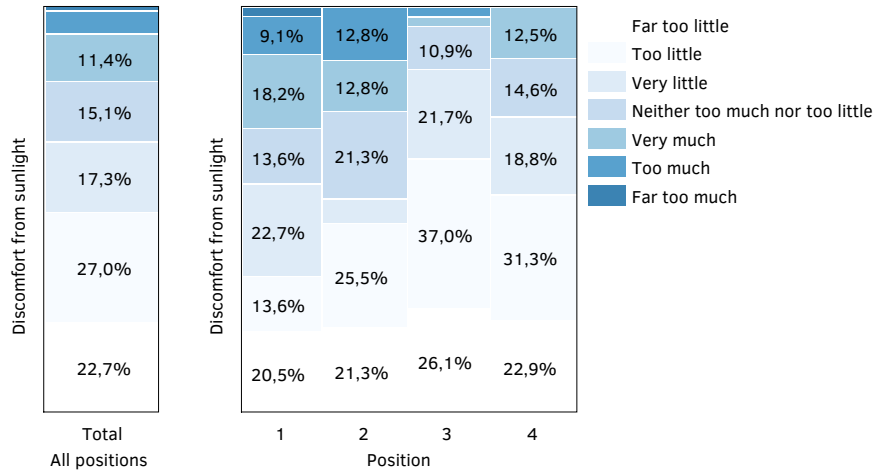


FIG. 5.8 Distribution of the 'discomfort due to sunlight' responses.

In 76% of the cases, subjects reported that they were not bothered by or were neutral to reflections on the screen or screen washed out by light. Position 3 was the position where more discomfort due to the visual conditions of the screen was reported followed by position 2 (Figure 5.9).

In only 66% of the cases the subjects indicated that they considered the lighting situation comfortable. More discomfort was reported for position 3 and position 1 and less discomfort was reported for position 4 (Figure 5.10).

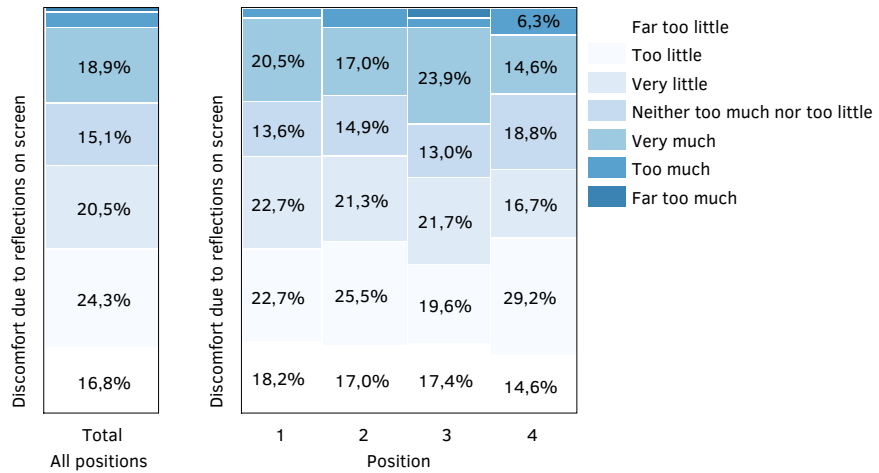


FIG. 5.9 Distribution of the 'discomfort due to reflections on screen / screen washed out' responses.

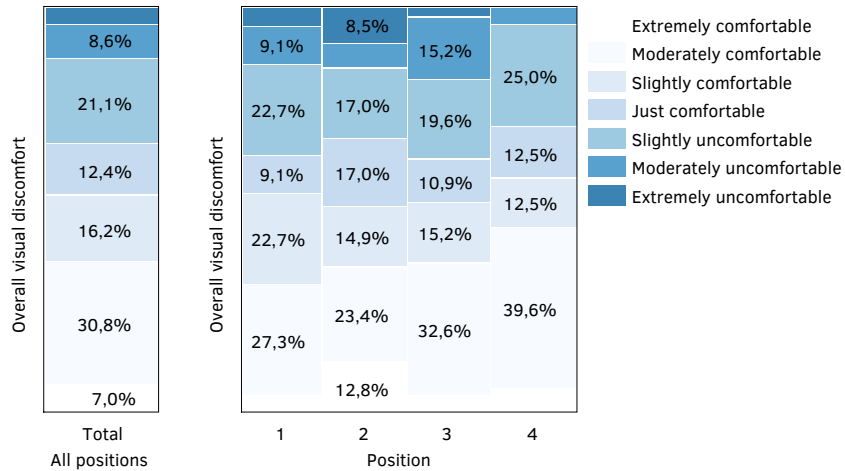


FIG. 5.10 Distribution of the 'overall visual discomfort' responses.

Noticeable to intolerable glare was reported in 66% of the cases. Disturbing to intolerable glare was reported in 22% of the cases. Most subjects reported noticeable (44%) or imperceptible (34%) levels of glare. In total there were more cases of glare (noticeable to disturbing) reported in position 3 followed by position 4 and overall, there were less cases of glare reported for position 2. In positions 1, 3 and 4 glare was mostly noticeable while in position 2 glare was mostly imperceptible. Intolerable glare was only reported in position 2 and in position 3 (Figure 5.11).

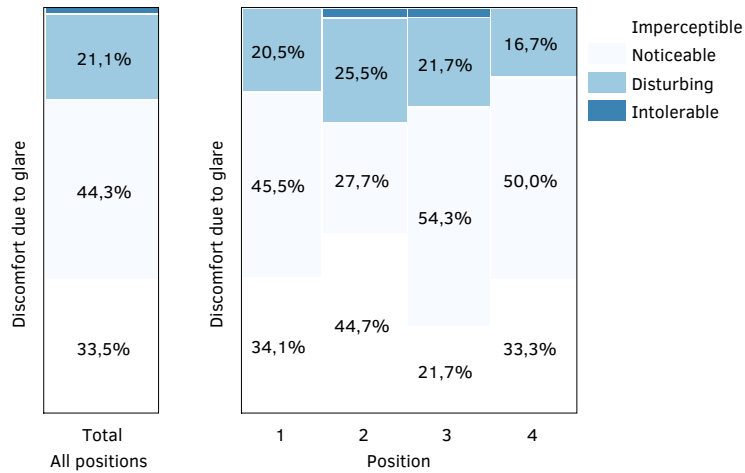


FIG. 5.11 Distribution of the 'discomfort due to glare' responses

5.6.2 Glare metrics

The results of the metrics show that most metrics have their higher values in position 1, but for some metrics, particularly for the window-based luminance metrics the values in position 3 and 4 are (almost) as high as in position 1. Position 2 showed the lowest values for all metrics. It stands out that based on the metrics' BCD thresholds, the results of the metrics indicate a low risk of glare in some or even all the positions (Figure 5.12).

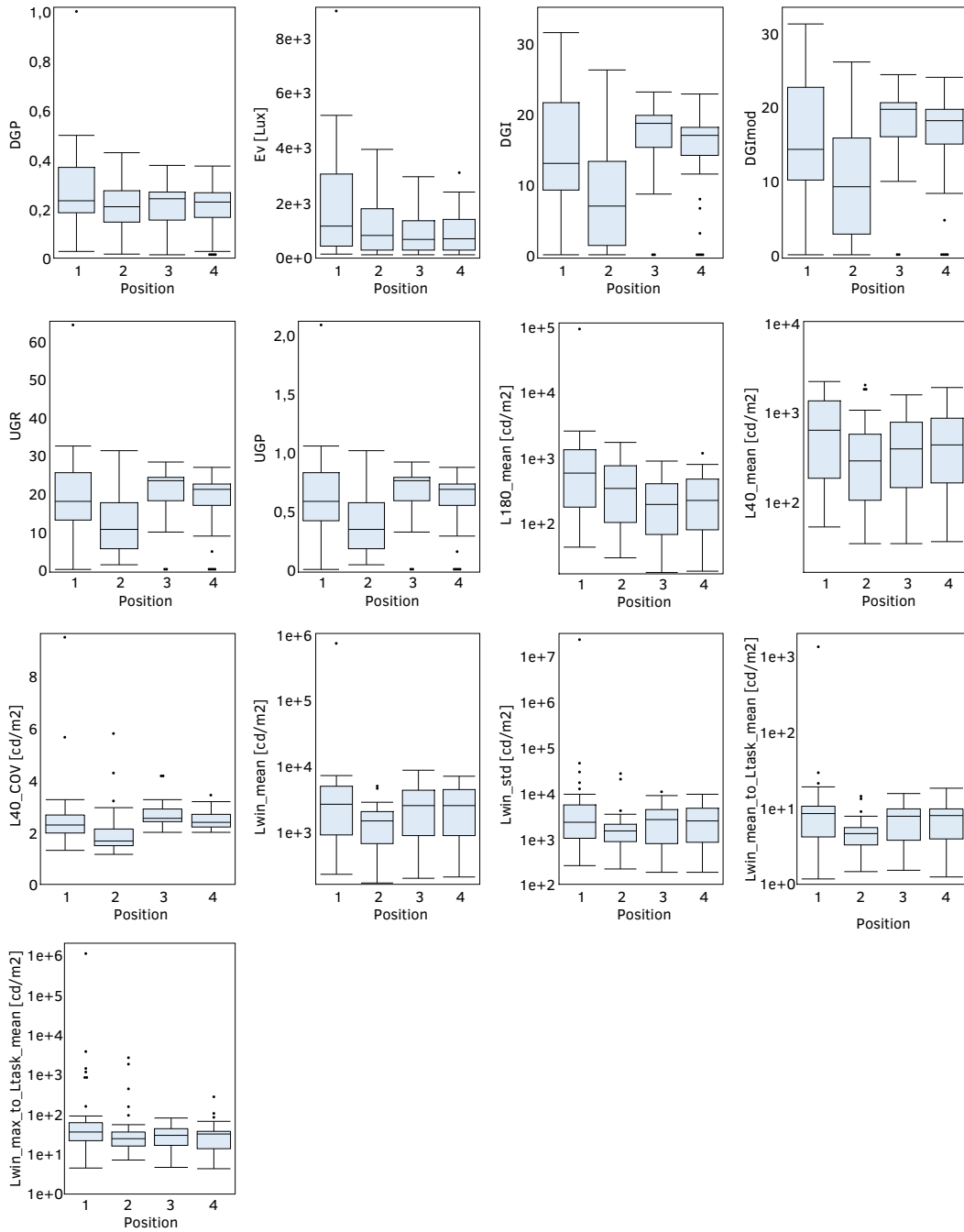


FIG. 5.12 Distributions for the glare metrics, by position.

5.7 Analysis

5.7.1 Analysis criteria

As mentioned in Chapter IV, the analysis of the predictive power of the metrics is based on two statistical tests, a Spearman rank correlation test and on a Receiver Operating Characteristic (ROC) curve test. The Spearman correlation indicates the ability of a metric to describe the full glare scale and the ROC curve statistic shows the accuracy of the glare prediction in terms of the ability to distinguish a glare vote from a no-glare vote.

Several aspects of the statistical tests are considered, namely their effect sizes, their significance and the 95% confidence intervals of their correlation coefficients, following recommendations in (Cumming, 2014).

According to (Cohen, 1988), the Spearman correlation shows a medium effect size for a correlation coefficient ρ between 0.3 and 0.5 and large effect size for $\rho > 0.5$.

The ROC curve analysis includes the calculation of the area under the curve (AUC) as well as the accuracy of each metric in terms of the number of correct predictions that it makes based on the true positive rate (TPR) and true negative rate (TNR). For this analysis, the variable's value 'not disturbed by glare' includes the 'imperceptible' and 'noticeable' glare responses and the variable's value 'disturbed by glare' includes the 'disturbing' and 'intolerable' glare responses. The analysis includes the calculation of the cut-off point of the curve, or the metric's BCD based on this calculation.

The higher the AUC, the better the performance of the metric, with an AUC > 0.7 being considered good and an AUC > 0.8 being considered very good (Šimundić, 2009). Similarly, the higher the TPR and TNR of a metric the better is its performance, with a value lower than 0.5 (or 50%) indicating no discriminatory power of the two conditions – 'glare' and 'no-glare'.

The significance of the Spearman correlation coefficient and of the ROC's AUC statistics are also considered, for a typical alpha value of 0.05. The effect size is therefore considered significant when $p < 0.05$.

The analysis of the 95% confidence interval of the Spearman correlation coefficient and of the ROC's AUC is also analysed. As the intervals were found to be very similar for the different metrics within each test, the analysis is based on the interval and on the lower bound value of the interval. A smaller interval corresponds to a lower error of the statistic and the closer the lower bound of the interval is to zero the higher the chance of no correlation. The best performance therefore occurs for the narrowest 95% confidence interval and for the higher lower bound of an interval of a metric.

As a rank type of statistic, the 95% confidence intervals of the Spearman correlation are only possible to calculate after bootstrapping the dataset and bootstrapping is done for 2,000 samples.

The performance of the metrics is rated based on their higher or lower performance in all these tests, a final score being provided for each metric based on the ranked performance in these tests and on the number of tests where the minimum criteria was met (passed tests).

5.7.2 Two-zone approach

To respond to the questions of this study the dataset was subdivided in two-zones, a near-window zone and a near-wall zone. Although an analysis based on each position would allow a more detailed understanding regarding the effect of position in space on discomfort glare, a more granular approach is preferred in return of higher statistical power (more cases per visual condition). A subdivision based on the front and back of the room zones was also considered. However, there are more similarities regarding the visual conditions for the two positions to aggregate in the window/wall subdivision compared with the front/back subdivision. The results of the metrics as previously analysed tend to show more similarities for the window/wall pairs than for the front/back pairs. In this two-zone approach, each zone corresponds to an orientation of the subject in relation to the window and room. In the window zone, the subjects face the inside of the room and in the wall zone the subjects face the outside of the room, each zone encapsulating one variation in terms of the size of the window in the field-of-view and distance to the task. The two zones are also distinct in terms of their overall luminance conditions, with the window zone corresponding to the higher lit area of the room and the wall zone to the dimmer lit area of the room.

The analysis is performed based on the full room dataset comprising the 185 cases, the near-window zone sample that includes the cases for positions 1 and 2 (91 cases) and a near-wall zone sample that includes the cases for positions 2 and 3 (94 cases).

5.7.3 Glare metrics and evaluations reported by zone

It is observed that what is considered imperceptible, noticeable and disturbing glare by the subjects can correspond to very similar values of a metric (Figure 5.13). Within the same level of glare, there is some difference regarding the metric range of values in the window and wall zones, indicating that what is considered a particular level of glare can correspond to different values of a metric depending on the zone. The median values for the different levels of glare are higher in the wall zone than in the window zone for all glare indices and for most of the other metrics, with the exception of E_v and $L_{180^\circ_mean}$. In the case of some metrics like DGI and DGImod this is quite accentuated. In the case of DGP this difference is much smaller.

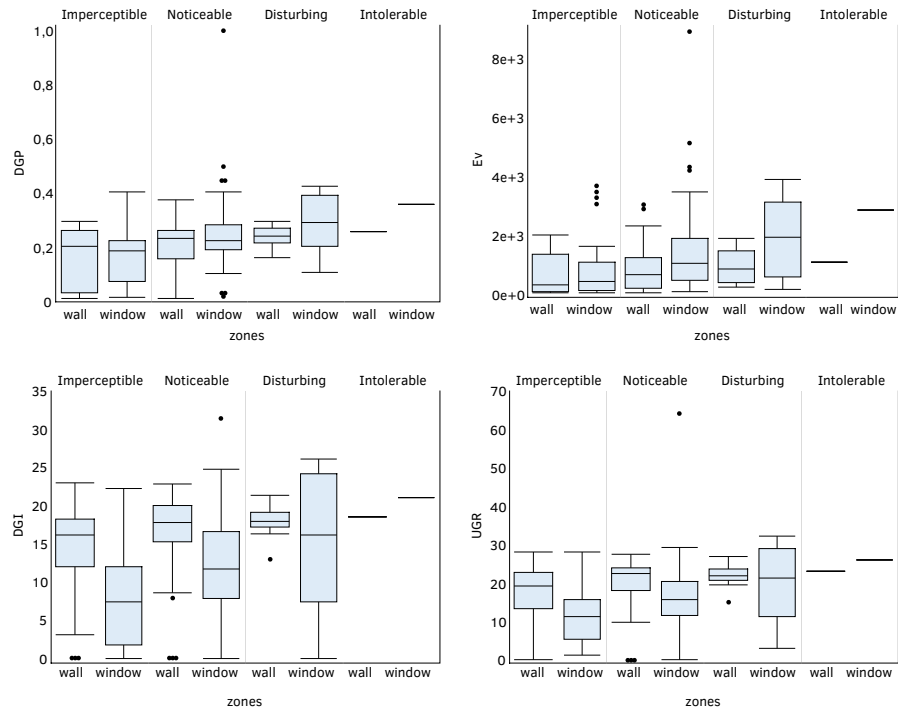


FIG. 5.13 Distributions of DGP, E_v , DGI and UGR, per glare level and per zone. Boxplots for all other metrics can be found in the Appendix B, section3.

5.7.4 Spearman correlation analysis

The results of the Spearman correlation can be seen in Tables 5.3 to 5.5. The metrics are firstly ranked based on their lower to higher performance in each test and receive a score for each test based on their order in the rank. The scores of a metric in all the tests are summed up and a final position in a rank is found depending on that sum, with a metric higher in the rank performing better than a metric lower in the rank.

The cells of the tables are shaded according to the defined performance criteria (Table 5.3), the dark blue and the greyed out value indicating a failed test.

TABLE 5.3 Performance criteria (Spearman).

	Fail	Pass	Good	Very Good
ρ	< 0.3	> 0.3	> 0.5	> 0.7
Significance	> 0.05	< 0.05		
Lower 95% CI	< 0.2	> 0.2		

Note: the lower 95% CI is the lower bound of the 95% confidence of ρ .

For the full dataset (Table 5.4) most metrics show significant correlations, with only $L_{40^\circ_COV}$ failing the test. DGP, UGR and UGP show the highest effect sizes ($\rho = 0.34$), while four of the metrics fail the effect size test ($\rho < 0.3$). DGP, UGR and UGP are also the only metrics that show a lower 95% CI above 0.2. DGP ranks higher in the tests due to marginal differences in relation to UGR and UGP, in terms of the effect size, significance and confidence intervals.

For the window zone (Table 5.5), most metrics show a significant correlation. It can be seen that L_{win_std} shows the highest correlation ($\rho = 0.44$) followed by DGP and L_{win_max}/L_{t_mean} ($\rho = 0.42$) with only one metric failing the effect size test ($L_{40^\circ_COV}$). The L_{win_std} metric followed by the DGP rank the highest in the wall zone.

TABLE 5.4 Spearman correlation results and ranks for the full dataset.

#	Metric	ρ	sig.	95% CI		ρ	sig.	low CI	CI	Total
				Lower	Upper					
1	DGP	0.34	0.000	0.21	0.46	1	1	1	1	1
2	E_v	0.31	0.000	0.17	0.44	9	9	9	11	9
3	DGI	0.33	0.000	0.20	0.45	4	5	4	7	4
4	DGI _{mod}	0.33	0.000	0.20	0.46	5	4	5	9	6
5	UGR	0.34	0.000	0.21	0.46	2	2	2	2	2
6	UGP	0.34	0.000	0.21	0.46	3	3	3	3	3
7	$L_{180^\circ_mean}$	0.28	0.000	0.14	0.41	12	12	12	10	12
8	$L_{40^\circ_mean}$	0.29	0.000	0.16	0.41	10	10	10	8	10
9	$L_{40^\circ_COV}$	0.05	0.480	-0.09	0.20	13	13	13	13	13
10	L_{win_mean}	0.31	0.000	0.18	0.43	8	8	8	5	8
11	L_{win_std}	0.33	0.000	0.20	0.45	6	6	6	4	5
12	L_{win_mean}/L_{t_mean}	0.29	0.000	0.15	0.42	11	11	11	12	11
13	L_{win_max}/L_{t_mean}	0.33	0.000	0.19	0.44	7	7	7	6	7

TABLE 5.5 Spearman correlation results and ranks for the window zone.

#	Metric	ρ	sig.	95% CI		ρ	sig.	low CI	CI	Total
				Lower	Upper					
1	DGP	0.42	0.000	0.24	0.58	3	3	2	1	2
2	E_v	0.41	0.000	0.23	0.57	4	5	4	3	4
3	DGI	0.36	0.001	0.15	0.53	11	11	13	12	13
4	DGI _{mod}	0.37	0.000	0.17	0.54	10	10	11	9	10
5	UGR	0.37	0.000	0.18	0.55	9	9	10	11	9
6	UGP	0.38	0.000	0.18	0.55	8	8	9	10	8
7	$L_{180^\circ_mean}$	0.39	0.000	0.21	0.56	6	6	7	6	6
8	$L_{40^\circ_mean}$	0.38	0.000	0.19	0.54	7	7	8	5	7
9	$L_{40^\circ_COV}$	-0.01	0.966	-0.23	0.22	13	13	6	13	12
10	L_{win_mean}	0.41	0.000	0.22	0.57	5	4	5	4	5
11	L_{win_std}	0.44	0.000	0.26	0.60	1	1	1	2	1
12	L_{win_mean}/L_{t_mean}	0.35	0.001	0.16	0.52	12	12	12	8	11
13	L_{win_max}/L_{t_mean}	0.42	0.000	0.23	0.59	2	2	3	7	3

All metrics fail the effect size test in the wall zone (Table 5.6) and show either very poor significance and/or large errors, with negative lower confidence intervals in some cases.

TABLE 5.6 Spearman correlation results and ranks for the wall zone.

#	Metric	ρ	sig.	95% CI		ρ	sig.	low CI	CI	Total
				Lower	Upper					
1	DGP	0.20	0.051	0.00	0.38	6	7	12	7	6
2	E_v	0.20	0.051	0.00	0.38	7	6	13	6	7
3	DGI	0.25	0.014	0.06	0.42	1	1	2	1	1
4	DGI _{mod}	0.24	0.022	0.04	0.41	2	2	4	2	2
5	UGR	0.22	0.033	0.02	0.40	3	3	8	4	3
6	UGP	0.22	0.033	0.02	0.40	4	4	9	5	4
7	$L_{180^\circ_mean}$	0.19	0.070	-0.02	0.37	8	8	11	9	10
8	$L_{40^\circ_mean}$	0.18	0.079	-0.02	0.37	9	9	7	10	8
9	$L_{40^\circ_COV}$	-0.03	0.785	-0.24	0.18	13	13	1	13	13
10	L_{win_mean}	0.18	0.089	-0.03	0.36	10	10	6	11	11
11	L_{win_std}	0.16	0.118	-0.04	0.35	11	11	5	8	9
12	L_{win_mean}/L_{t_mean}	0.16	0.136	-0.06	0.35	12	12	3	12	12
13	L_{win_max}/L_{t_mean}	0.22	0.036	0.02	0.39	5	5	10	3	5

5.7.5 ROC curve analysis

The ROC curves for the different metrics for the three samples, full window and wall zone are presented in Figures 5.14, 5.15 and 5.16.

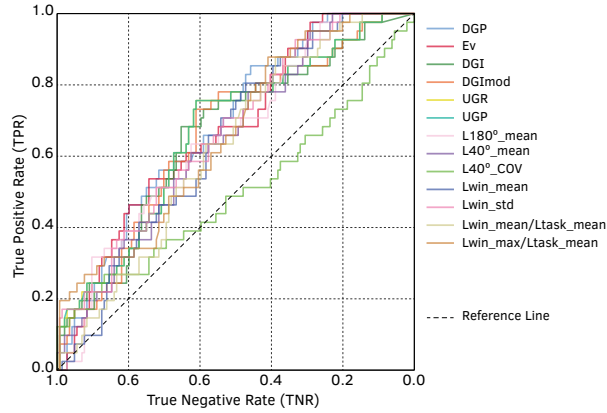


FIG. 5.14 ROC curve of the metrics for the full room dataset.

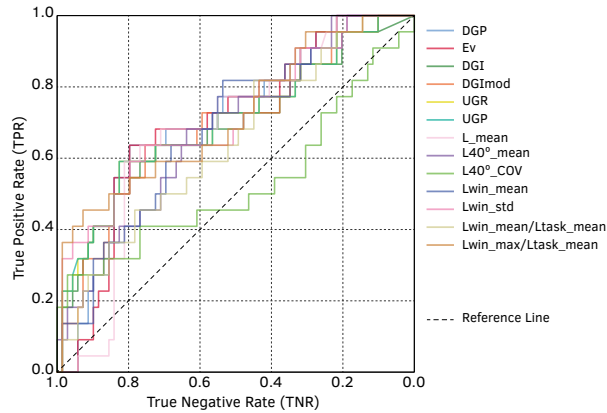


FIG. 5.15 ROC curve of the metrics for the window zone.

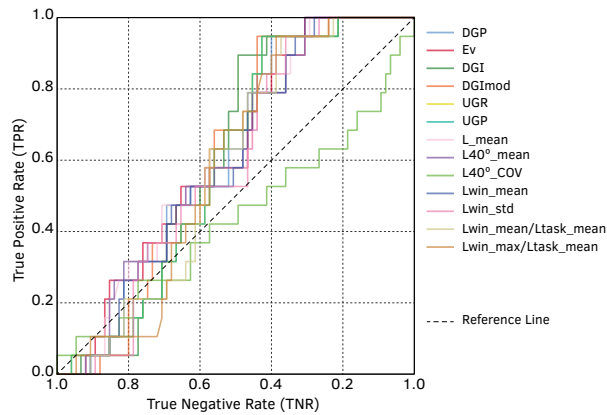


FIG. 5.16 ROC curve of the metrics for the wall zone.

The results of the AUC and of the TPR and TNR tests are presented in Tables 5.8 to 5.13. The cells of the tables are shaded according to the defined performance criteria (Table 5.7), the dark blue and the greyed out value indicating a failed test.

TABLE 5.7 Performance criteria (ROC).

	Fail	Pass	Good	Very Good
AUC	< 0.6	> 0.6	> 0.7	> 0.8
Significance	> 0.05	< 0.05		
Lower 95% CI	< 0.5	> 0.5		
TPR, TNR	< 0.5	> 0.5		

Note: lower 95% CI is the lower bound of the 95% confidence interval of the AUC.

For the full dataset (Table 5.8), most metrics achieve a significant level of correlation however all metrics have AUC values lower than 0.7 showing just fair discriminatory power. DGP reaches a high level of significance and the lowest error.

For the window zone (Table 5.9), DGP, E_v , UGR, UGP, L_{win_std} and L_{win_max}/L_{t_mean} achieve good AUC values and significant correlations. However, all these metrics fail the significance test and the lower 95% CI test in the wall zone (Table 5.10).

TABLE 5.8 AUC test results and ranks for the full room.

#	Metric	AUC	sig.	95% CI		AUC	sig.	low CI	CI	Total
				Lower	Upper	rank	rank	rank	rank	rank
1	DGP	0.69	0.000	0.60	0.77	1	1	1	1	1
2	E_v	0.67	0.001	0.59	0.76	2	2	2	3	2
3	DGI	0.66	0.002	0.57	0.75	7	7	9	12	9
4	DGI _{mod}	0.66	0.002	0.57	0.75	6	6	6	9	6
5	UGR	0.67	0.001	0.58	0.76	3	3	4	10	4
6	UGP	0.67	0.001	0.58	0.76	4	4	5	11	5
7	$L_{180^\circ_mean}$	0.66	0.002	0.57	0.75	9	9	8	7	8
8	$L_{40^\circ_mean}$	0.65	0.004	0.56	0.74	10	10	10	5	10
9	$L_{40^\circ_COV}$	0.50	0.971	0.39	0.61	13	13	13	13	13
10	L_{win_mean}	0.64	0.005	0.56	0.73	11	11	11	2	11
11	L_{win_std}	0.67	0.001	0.58	0.76	5	5	3	6	3
12	L_{win_mean}/L_{t_mean}	0.63	0.014	0.54	0.71	12	12	12	4	12
13	L_{win_max}/L_{t_mean}	0.66	0.002	0.57	0.75	8	8	7	8	7

TABLE 5.9 AUC test results and ranks for the window zone.

#	Metric	AUC	sig.	95% CI		AUC	sig.	low CI	CI	Total
				Lower	Upper	rank	rank	rank	rank	rank
1	DGP	0.71	0.003	0.59	0.83	3	3	1	2	1
2	E_v	0.70	0.004	0.58	0.82	4	4	4	3	4
3	DGI	0.69	0.009	0.55	0.82	8	8	11	12	11
4	DGImod	0.69	0.007	0.56	0.82	7	7	9	9	9
5	UGR	0.70	0.005	0.57	0.84	6	6	6	10	6
6	UGP	0.70	0.004	0.57	0.84	5	5	5	11	5
7	$L_{180^\circ_mean}$	0.68	0.011	0.56	0.80	10	10	8	1	7
8	$L_{40^\circ_mean}$	0.68	0.012	0.55	0.80	11	11	10	5	10
9	$L_{40^\circ_COV}$	0.53	0.690	0.37	0.69	13	13	13	13	13
10	L_{win_mean}	0.69	0.009	0.56	0.81	9	9	7	4	8
11	L_{win_std}	0.71	0.003	0.59	0.84	2	2	3	6	3
12	L_{win_mean}/L_{t_mean}	0.64	0.042	0.51	0.77	12	12	12	8	12
13	L_{win_max}/L_{t_mean}	0.72	0.002	0.59	0.85	1	1	2	7	2

TABLE 5.10 AUC test results and ranks for the wall zone.

#	Metric	AUC	sig.	95% CI		AUC	sig.	low CI	CI	Total
				Lower	Upper	rank	rank	rank	rank	rank
1	DGP	0.61	0.124	0.50	0.73	2	2	1	6	1
2	E_v	0.62	0.111	0.50	0.74	1	1	2	10	2
3	DGI	0.61	0.146	0.49	0.72	5	5	3	1	3
4	DGImod	0.61	0.156	0.49	0.72	6	6	4	2	4
5	UGR	0.60	0.192	0.48	0.71	8	8	8	3	7
6	UGP	0.60	0.192	0.48	0.71	10	10	10	4	9
7	$L_{180^\circ_mean}$	0.61	0.139	0.49	0.73	3	3	6	12	5
8	$L_{40^\circ_mean}$	0.61	0.143	0.49	0.73	4	4	5	11	6
9	$L_{40^\circ_COV}$	0.44	0.405	0.28	0.59	13	13	13	13	13
10	L_{win_mean}	0.60	0.174	0.48	0.72	7	7	7	9	8
11	L_{win_std}	0.59	0.241	0.47	0.71	11	11	11	8	11
12	L_{win_mean}/L_{t_mean}	0.58	0.261	0.47	0.70	12	12	12	7	12
13	L_{win_max}/L_{t_mean}	0.59	0.230	0.47	0.71	10	10	10	5	10

A wide range of metrics pass the TPR and TNR tests (Tables 5.11, 5.12, 5.13). For the full room sample, UGR, DGImod and DGI are the metrics that achieve the highest scores. In the window zone, the DGP, E_v and UGR achieve the highest total score, whereas in the wall zone, the E_v , DGI and DGImod achieve the highest total score.

However, DGI fails the TNR in this zone. The $L_{40^\circ_COV}$ fails the accuracy test for all the three samples.

TABLE 5.11 TPR and TNR test results and ranks for the full room.

#	Metric	cut-off	TPR	TNR	TPR	TNR	TPR / TNR
					rank	rank	rank
1	DGP	0.26	0.56	0.72	11	2	6
2	E_v	1281	0.54	0.74	12	1	7
3	DGI	17	0.68	0.65	6	3	2
4	DGI _{mod}	18	0.73	0.61	3	6	3
5	UGR	20	0.76	0.61	1	7	1
6	UGP	0.64	0.76	0.61	2	8	4
7	$L_{180^\circ_mean}$	349	0.63	0.63	7	4	5
8	$L_{40^\circ_mean}$	509	0.61	0.63	9	5	8
9	$L_{40^\circ_COV}$	2.4	0.49	0.53	13	13	13
10	L_{win_mean}	1850	0.71	0.54	4	11	9
11	L_{win_std}	1853	0.71	0.53	5	12	10
12	L_{win_mean}/L_{t_mean}	7.4	0.63	0.58	8	9	11
13	L_{win_max}/L_{t_mean}	32	0.61	0.57	10	10	12

TABLE 5.12 TPR and TNR test results and ranks for the window zone.

#	Metric	cut-off	TPR	TNR	TPR	TNR	TPR/TNR
					rank	rank	rank
1	DGP	0.27	0.64	0.80	3	3	1
2	E_v	1741	0.64	0.80	4	4	2
3	DGI	13	0.64	0.72	5	8	7
4	DGI _{mod}	16	0.64	0.75	6	6	5
5	UGR	20	0.59	0.83	9	1	3
6	UGP	0.64	0.59	0.83	10	2	6
7	$L_{180^\circ_mean}$	540	0.68	0.71	1	10	4
8	$L_{40^\circ_mean}$	509	0.68	0.64	2	12	8
9	$L_{40^\circ_COV}$	2.4	0.41	0.77	13	5	10
10	L_{win_mean}	2001	0.64	0.68	7	11	11
11	L_{win_std}	2392	0.64	0.75	8	7	9
12	L_{win_mean}/L_{t_mean}	5.5	0.59	0.59	11	13	13
13	L_{win_max}/L_{t_mean}	38	0.59	0.72	12	9	12

TABLE 5.13 TPR and TNR test results and ranks for the wall zone.

#	Metric	cut-off	TPR	TNR	TPR	TNR	TPR/TNR
					rank	rank	rank
1	DGP	0.22	0.84	0.44	2	12	5
2	E_v	996	0.53	0.65	11	1	3
3	DGI	17	0.89	0.49	1	9	1
4	DGI _{mod}	19	0.68	0.56	6	5	2
5	UGR	21	0.68	0.53	7	6	4
6	UGP	0.69	0.68	0.53	8	7	10
7	$L_{180^\circ_mean}$	291	0.53	0.64	12	2	6
8	$L_{40^\circ_mean}$	273	0.79	0.45	3	11	7
9	$L_{40^\circ_COV}$	2.5	0.42	0.58	13	3	11
10	L_{win_mean}	1848	0.79	0.47	4	10	8
11	L_{win_std}	1788	0.79	0.44	5	13	13
12	L_{win_mean}/L_{t_mean}	8.1	0.63	0.57	10	4	9
13	L_{win_max}/L_{t_mean}	30	0.68	0.53	9	8	12

5.7.6 Borderline between comfort and discomfort (BCD)

The TPR and TNR tables (Tables 5.11, 5.12, 5.13) include the optimum cut-off value of the metric, which corresponds to the point of the ROC curve where the TPR and TNR are the highest and effectively, the BCD threshold for a metric resulting from the calculation. It can be seen that these values are different for the three samples. For most metrics, the BCD thresholds that resulted from this calculation are lower than the metrics' actual BCD thresholds. The biggest difference occurs for DGP with a calculated BCD ranging from 0.22 (wall zone) to 0.27 (window zone), comparing to the metric's BCD range of 0.35-0.40.

Interestingly, from the glare indices, only DGP shows a higher BCD in the window zone in comparison to the BCD of the wall zones, all other indices showing an opposite tendency.

UGR shows a quite stable BCD of 20 to 21, independently of the zone, a range that is within the metrics' actual BCD range of 13-22. In this study, this corresponds to a probability of people that report glare (as depicted by the UGP) ranging from 0.64 to 0.69.

The DGI shows lower BCD thresholds (13-17) than DGImod (16-18) and somewhat lower than the metric's actual BCD range of 18-24.

It is to note that the BCD thresholds found for the L_{win_mean}/L_{t_mean} contrast ratio (5.5 to 8.1) is much lower than the defined as metric threshold (20 to 22).

5.7.7 Performance analysis

The results of the performance of the metrics based on the number of passed and failed tests for each metric are analysed next. The Tables 5.14 to 5.16 show the number of passed tests for the three samples, with the greyed-out cells (0) indicating a failed test.

It can be seen that for the full dataset, DGP alongside UGR and UGP perform the best in the full room sample. In the window zone, DGP, E_v , $L_{180^\circ_mean}$, L_{win_mean} , L_{win_std} and L_{win_max}/L_{t_mean} pass all the tests. In the wall zone, there is a poor performance of the metrics with none passing all the tests.

TABLE 5.14 Passed statistical tests for the full room sample.

#	Metric	Spearman			ROC					All
		sig.	ρ	low CI	sig.	AUC	low CI	TPR	TNR	rank
1	DGP	1	1	1	1	1	1	1	1	1
2	E_v	1	1	0	1	1	1	1	1	2
3	DGI	1	1	0	1	1	1	1	1	2
4	DGImod	1	1	0	1	1	1	1	1	2
5	UGR	1	1	1	1	1	1	1	1	1
6	UGP	1	1	1	1	1	1	1	1	1
7	$L_{180^\circ_mean}$	1	0	0	1	1	1	1	1	3
8	$L_{40^\circ_mean}$	1	0	0	1	1	1	1	1	3
9	$L_{40^\circ_COV}$	0	0	0	0	0	0	0	1	4
10	L_{win_mean}	1	1	0	1	1	1	1	1	2
11	L_{win_std}	1	1	0	1	1	1	1	1	2
12	L_{win_mean}/L_{t_mean}	1	0	0	1	1	1	1	1	3
13	L_{win_max}/L_{t_mean}	1	1	0	1	1	1	1	1	2

TABLE 5.15 Passed statistical tests for the window zone sample.

#	Metric	Spearman			ROC					All
		sig.	ρ	low CI	sig.	AUC	low CI	TPR	TNR	rank
1	DGP	1	1	1	1	1	1	1	1	1
2	E_v	1	1	1	1	1	1	1	1	1
3	DGI	1	1	0	1	1	1	1	1	2
4	DGI _{mod}	1	1	0	1	1	1	1	1	2
5	UGR	1	1	0	1	1	1	1	1	2
6	UGP	1	1	0	1	1	1	1	1	2
7	$L_{180^\circ_mean}$	1	1	1	1	1	1	1	1	1
8	$L_{40^\circ_mean}$	1	1	0	1	1	1	1	1	2
9	$L_{40^\circ_COV}$	0	0	1	0	0	0	0	1	3
10	L_{win_mean}	1	1	1	1	1	1	1	1	1
11	L_{win_std}	1	1	1	1	1	1	1	1	1
12	L_{win_mean}/L_{t_mean}	1	1	0	1	1	1	1	1	2
13	L_{win_max}/L_{t_mean}	1	1	1	1	1	1	1	1	1

TABLE 5.16 Passed statistical tests for the wall zone sample.

#	Metric	Spearman			ROC					All
		sig.	ρ	low CI	sig.	AUC	low CI	TPR	TNR	rank
1	DGP	0	0	0	0	1	0	1	0	3
2	E_v	0	0	0	0	1	0	1	1	2
3	DGI	1	0	0	0	1	0	1	0	2
4	DGI _{mod}	1	0	0	0	1	0	1	1	1
5	UGR	1	0	0	0	0	0	1	1	2
6	UGP	1	0	0	0	0	0	1	1	2
7	$L_{180^\circ_mean}$	0	0	0	0	1	0	1	1	2
8	$L_{40^\circ_mean}$	0	0	0	0	1	0	1	0	3
9	$L_{40^\circ_COV}$	0	0	0	0	0	0	0	1	4
10	L_{win_mean}	0	0	0	0	1	0	1	0	3
11	L_{win_std}	0	0	0	0	0	0	1	0	4
12	L_{win_mean}/L_{t_mean}	0	0	0	0	0	0	1	1	3
13	L_{win_max}/L_{t_mean}	1	0	0	0	0	0	1	1	2

Overall, and considering the performance of the metrics in the three samples, DGP, E_v , DGI_{mod}, UGR, UGP and L_{win_max}/L_{t_mean} are the metrics that offer the best performance. It is observed that from these, only DGP passes all the tests for the full room and for the window zone.

5.8 Conclusion

The objective of this study was to investigate how well a group of metrics predict reported visual discomfort from daylight glare in a classroom environment.

Several questions were asked to the subjects regarding the visual comfort conditions in the four positions of the classroom, with varying degrees of discomfort being reported. It is verified that visual discomfort in the classroom can result from a number of reasons other than discomfort glare. It is found that position 3 in the room is the position where more problems of veiling reflections, poor visibility of the task surface and overall visual discomfort were reported. This is also the position where more discomfort glare is reported in the study. This indicates that in the conditions of the classroom, the problem of discomfort glare can be as critical if not more critical in the inner parts of a room. On the one hand, this could be expected given that the window is more centrally located in the visual field for a subject sitting in position 3. On the other hand, is generally expected most problems of discomfort glare occur in the vicinity of a window, where the light levels are generally the highest. Detection of daylight glare problems and deployment of mitigation measures do also generally occur based on the lighting conditions in the window zone, in which case any discomfort glare in the inner parts of a room will tend to go unnoticed.

The analysis of the performance of the metrics was based on the results of a Spearman rank correlation and on the AUC, TPR and TNR of a ROC curve, with the metrics being compared based on the number of passed statistical tests.

The analysis shows that for the full dataset, DGP, UGR and UGP were the most successful metrics. In the window zone, there are a range of metrics - DGP, E_v , $L_{180^\circ_mean}$, L_{win_mean} , L_{win_std} and L_{win_max}/L_{t_mean} - that perform well, having passed all the statistical tests. In the wall zone all metrics show a poor performance, consistently failing most of the statistical tests. Based on these results, it can be said that the studied metrics show poor predictability of discomfort glare across the classroom space.

It was observed that discomfort glare can be reported for low light conditions, a result that is in line with findings from other studies in non-cellular office spaces and in particular in field-studies (Hirning et al., 2014) (Mahić et al., 2017). The discomfort glare BCD values that resulted from the study reflect that fact, being in most cases lower than the metrics' actual BCD thresholds.

From all metrics, the biggest difference occurs for DGP with a calculated BCD ranging from 0.22 (wall zone) to 0.27 (window zone), comparing to the metric's BCD range of 0.35-40. This should be related to the fact that DGP was developed in conditions of much higher field-of-view luminance than the conditions of this study. The higher field-of-view luminance of the DGP research is not only motivated by the fact that skies were possibly brighter but also by the fact that the subjects were facing a window at close proximity. This indicates that the range of conditions for which DGP and possibly other discomfort glare metrics have been developed might limit their applicability to the visual conditions of classrooms.

The present study was limited to a range of tested conditions and is extended to a wider range of visual conditions, in the next chapter.

6 Experimental study II

6.1 Introduction

The previous study, Study I, showed that the metrics were not successful enough to predict the glare in the spatial conditions that were covered by that study. Study I carried out for one view direction only – the view towards the board. The aim of Study II was to investigate if the results obtained in the Study I withstand when the direction that the subjects look in is extended to a wider range of view directions in the classroom.

The problem under investigation is the same as in the previous study: how well do existing glare metrics predict reported visual discomfort from glare in the classroom environment and how good is that prediction done across space? The results of the questionnaire relating to the general visual comfort evaluation and discomfort glare are first presented and analysed, followed by an analysis of the performance of the metrics.

6.2 Population

The population of the study consisted of 17 subjects, 11 males and 6 females, of Asian, Middle-Eastern and European origin. The subjects had ages between 24 and 40 and an average age of 28 years. They had mostly brown eyes and a few had blue eyes. Only 3 of the subjects didn't need any sort of visual correction, with 11 of them wearing distance glasses and 3 of them wearing contact lenses.

Subjects reported a degree of sensitivity to bright light in 89% of the cases, with most reporting being 'somewhat sensitive' (65%) (Figure 6.1). All subjects reported that having a window view in the workplace was important for them, with 59% declaring it to be 'very important' and 29% declaring it to be 'extremely important' (Figure 6.2).

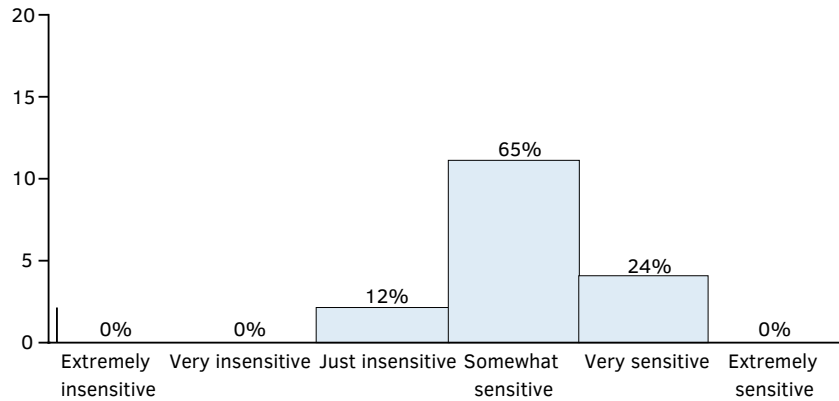


FIG. 6.1 Counts of the self-reported 'sensitivity to bright light'.

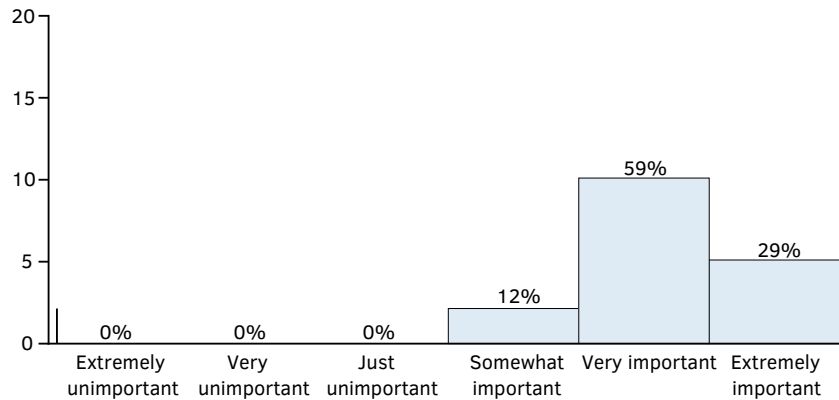


FIG. 6.2 Counts of the 'importance of a view out in the workplace'.

6.3 Metrics

The glare metrics investigated in the study correspond to a wider selection of glare indices (DGP, DGI, DGI_{mod}, UGR, UGP, UGR_{exp}, VCP, CGI and PGSV), a range of recently proposed luminance-based metrics (Van Den Wymelenberg and Inanici, 2015), the luminance contrast ratio proposed in the IES Lighting Handbook (Dilaura et al., 2011), the metric that showed a high correlation in the study by (Konis, 2014) and the vertical illuminance at eye level (Wienold and Christoffersen, 2006). The metric proposed by (Mahić et al., 2017) showed an extremely poor correlation in the previous study ($L_{40^\circ_COV}$) and was dropped. As a result, four new metrics are included in this study - UGR_{exp}, VCP, CGI and PGSV. The sixteen investigated metrics, their borderline between comfort and discomfort (BCD) threshold (when provided) and the labels used to identify the metrics in the study are listed in Table 6.1.

TABLE 6.1 Metrics, their borderline between comfort and discomfort (BCD) threshold and label used in the study.

#	Metric	BCD	Label
1	Daylight Glare Probability [1]	0.35-0.40	DGP
2	Vertical illuminance at eye level [2]	2600** [Lux]	E_v
3	Daylight Glare Index [3]	18-24	DGI
4	Modified Daylight Glare Index [4]	-	DGI _{mod}
5	Unified Glare Rating [5]	13-22	UGR
6	Unified Glare Probability [6]	-	UGP
7	Experimental Unified Glare Rating [4]	-	UGR _{exp}
8	Visual Comfort Probability [7]	60-80	VCP
9	CIE Glare Index [8]	13-22	CGI
10	Predicted Glare Sensation Vote [9]	2***	PGSV
11	Mean luminance in the 180° field-of-view [6]	-	$L_{180^\circ_mean}$
12	Mean luminance within a 40° central band [10]	500-700 [cd/m ²]	$L_{40^\circ_mean}$
13	Window mean luminance [10]	2,000-2,500 [cd/m ²]	L_{win_mean}
14	Window standard deviation [10]	2,500-4,000 [cd/m ²]	L_{win_std}
15	Window mean luminance to task mean luminance contrast ratio [11]	1:20, 1:22*	L_{win_mean}/L_{T_mean}
16	Window maximum luminance to task mean luminance contrast ratio [12]	-	L_{win_max}/L_{T_mean}

[1] (Wienold and Christoffersen, 2006) [2] (Wienold, 2009) [3] (Hopkinson, 1972) [4] (Fisekis et al., 2003) [5] (CIE, 1995) [6] (Hirning et al., 2014) [7] (IESNA, 2000) [8] (CIE, 1995) [9] (Wienold et al., 2019) [10] (Van Den Wymelenberg and Inanici, 2015) [11] (Dilaura et al., 2011) [12] (Konis, 2014). (*) - threshold proposed in (Van Den Wymelenberg and Inanici, 2014) for this metric. (**) - as derived from DGPs. (***) (Boyce, 2014) provides information on the scale of PGSV as: 0=just perceptible glare, 1= just acceptable glare, 2 = just uncomfortable glare and 3 = just intolerable glare.

6.4 Data processing

6.4.1 Evaluation of the validity of the glare question

An evaluation of the validity of the 'glare question' was performed by analysing how the results obtained from the different ways of asking the question correlate to each other, a high correlation providing some means of validation of the performed evaluation.

To check the internal validity of questionnaires and the correlation of questions measuring the same factors, Collingridge (2014) proposes the use of the Cronbach's Alpha statistical method. The Cronbach Alpha is a correlational type of test with a result ranging from 0 to 1. According to Field (2009), there is correlation for a minimum Cronbach's Alpha value of $\alpha = 0.7$, with a value of $\alpha = 0.8$ showing a good correlation.

Correlations between the results of the 'level of glare' question and of the 'discomfort due to glare' question and between the 'level of glare' question and the 'would you want to put the window blinds down' question were performed (see Chapter V for more details on these questions). The first test resulted in a Cronbach's $\alpha = 0.86$ and the second test resulted in a Cronbach's $\alpha = 0.69$.

For the 'would you want to put the window blinds down' question, it was found that subjects would have wanted to put the window blinds down even when glare was reported as imperceptible (8 cases) or simply noticeable (21 cases). The reason for wanting to put the window blinds down in these cases might then have other reasons, for instance to reduce any veiling reflections or simply improve the visibility of the visual task. In any case it is shown that subjects might want to put the window blinds down even for reasons other than feeling discomfort glare. This question therefore is deemed not to be a valid way of evaluating discomfort glare.

The high Cronbach's α value for the 'level of glare' and the 'discomfort due to glare' questions indicates that independently of the way the question is asked and of the scale that is used, there is agreement of the result. For the purpose of the analysis carried out in this chapter it was chosen to use the 'level of glare' question.

6.4.2 Light variation during glare assessment

The vertical illuminance at camera level (E_v) was measured to monitor the variation of light between the measurement done at start and at the end of the subjective assessment. Figure 6.3 shows the vertical illuminance difference between these two measurements. It can be seen that the variation can be very significant even though the skies were mostly clear or sunny during the experiment. This is possibly due to moving clouds on days with some wind.

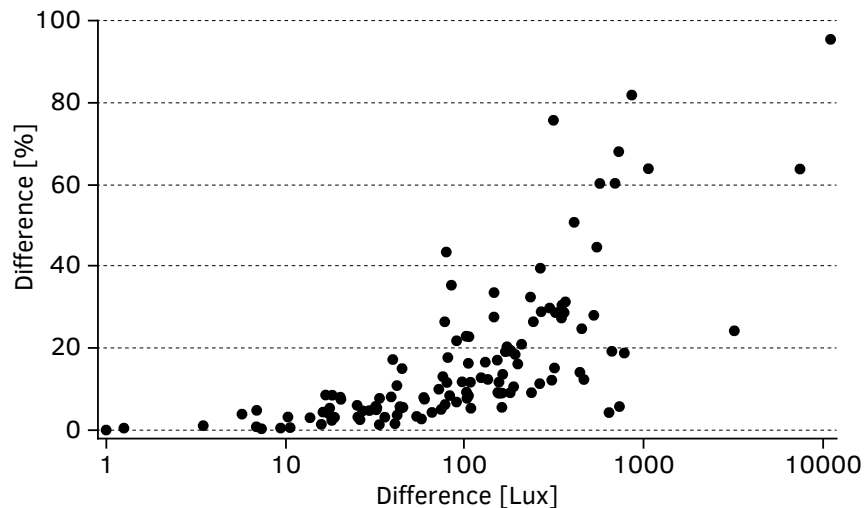


FIG. 6.3 Percentage difference (%) and illuminance difference (Lux) of the measured E_v between the start and end measurements.

The analysis is therefore performed based on two measurements, the measurement done at the start of the session, hereby designated as the 'start measurement' and the mean of the start and end measurement designated as the 'mean measurement'. The 'start measurement' represents the conditions that the subject found when he/she started the experiment. The 'mean measurement' is an approximation of the conditions that the subject found during the experiment. As the questions were asked in relation to the situation that the subjects found while performing the task, the 'mean measurement' is considered more representative than the 'end measurement', which was taken after the subject filled in the questionnaire. It is expected the two measurements, the 'start' and the 'mean', to show similar correlational trends. While none of the measurements correspond to the exact condition of the evaluation, agreement in their results is taken as indicative of a trend.

6.4.3 Luminance overflow correction

There were 12 luminance images with pixel overflow. All images were corrected apart from two where the vertical illuminance was lower than the image-derived vertical illuminance. Images that were corrected for luminance overflow can be found in the section 2 of Appendix C.

6.4.4 Comparison of measured and image-derived illuminance

For Study II a better agreement between the measured illuminance and the derived illuminance of the sample was verified, with differences of more than 15% occurring in only 3% of the data. A data point with a difference above 25% was excluded from the dataset.

Figure 6.4 shows the comparison between the externally measured illuminance and the luminance image derived illuminance for the collected 256 measurements.

It can be seen that there is a good agreement between the measured illuminance and luminance image-derived illuminance of the sample, with a normalised bias of 66 Lux, root mean square error (RMSE) of 106 Lux, normalised bias of 4% and normalised root mean square error (NRMSE) of 4%.

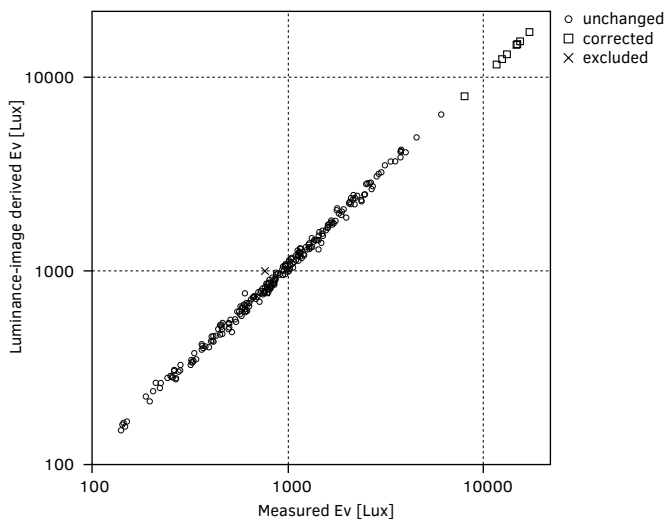


FIG. 6.4 Luminance-derived versus externally measured E_v for the 256 measurements (2 measurements per case, measurement at the start and at the end of the evaluation). 'Corrected' refers to the images that were corrected for luminance overflow, 'excluded' refers to images that showed a difference above 25% (1 case) and 'unchanged' relates to all other data points.

6.5 Metrics calculation

The method used to identify the glare source for the DGP calculation was the threshold method with a threshold of $2,000 \text{ cd/m}^2$, as this was the method that was found to offer the best correlation with the subjective assessments of discomfort in the previous study (Chapter V).

Window-based metrics and window-based glare indices like PGSV cannot be calculated for the conditions where the subjects have their backs facing the window (positions 1 and 2 in the 'U' layout,).

As explained in Chapter V (Experimental study I), several regions and masks need to be defined for the calculation of the metrics. These regions are identified in Figure 6.5, for this study.

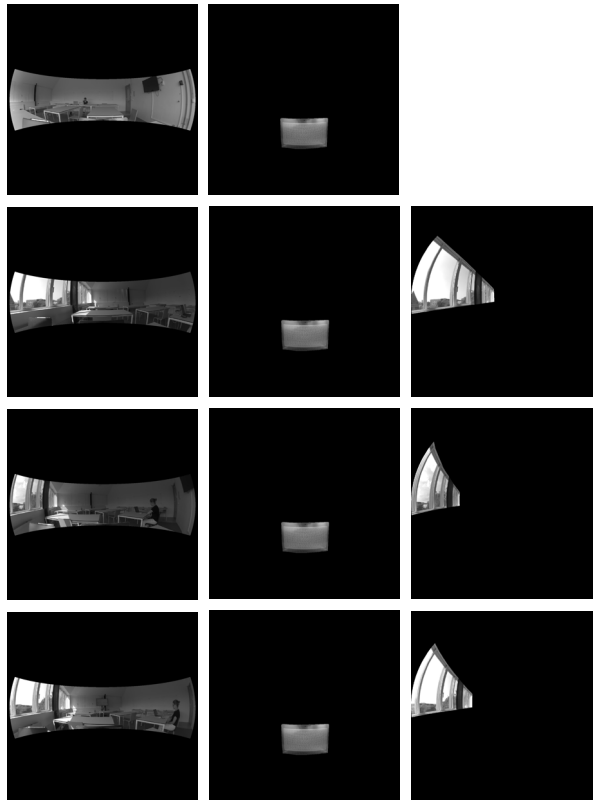


FIG. 6.5 Region and masks used in the study for the four studied layouts and position 1. From top to bottom: 'U' layout, 'regular' layout, 'diagonal' layout and 'board-task' layout; From left to right: 40° band region, task mask and window mask mask.

6.6 Results

6.6.1 Reported visual comfort and glare

A series of questions was asked to the subjects in relation to the visual comfort in each position: satisfaction with visual conditions, visual discomfort due to glare, level of glare, what was the source of glare when the subject reported that there was glare, if the subject would have wanted to put the window blinds down, if the subject felt discomfort due to reflections on the screen or screen washed out, if the subject felt discomfort due to sun, and in the case where discomfort due to sun was reported, what was the cause of discomfort.

The level of satisfaction with the visual conditions question is a way of identifying the level of overall visual comfort of the subject, without directly using the word 'comfort'. It is expected that a subject that is satisfied with a visual condition to feel comfortable with that visual condition.

The 'visual discomfort due to glare', 'level of glare' and the 'would have wanted to put the window blinds down' questions correspond to two different ways of formulating the discomfort glare question. The results of these three evaluations are provided below. However, for the purpose of responding to the research question of Study II, the 'level of glare' evaluation will be chosen, as it is the same type of question that was used in Study I.

Subjects reported being satisfied with the visual conditions in 66% of the cases and unsatisfied in 34% of the cases. More dissatisfaction was reported in position 1 followed by position 2. Subjects only reported to be extremely dissatisfied ('extremely unsatisfied') in positions 1 and 2. In positions 3 and 4, subjects reported being mostly 'just satisfied' or 'very satisfied' (Figure 6.6).

Visual discomfort due to glare - 'somewhat uncomfortable' to 'extremely uncomfortable' evaluations, was reported in 33% of the cases. Visual discomfort due to glare was higher in position 1 (50%) followed by position 2 (44%). Position 4 and 3 are the positions where less discomfort was reported (19%). Extreme discomfort glare was only reported in position 1 (Figure 6.7).

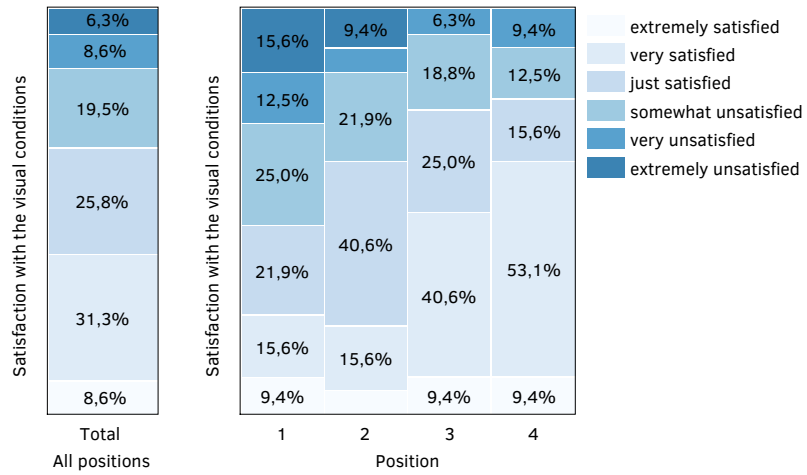


FIG. 6.6 Distribution of '(in)satisfaction with visual conditions' responses.



FIG. 6.7 Distribution of '(dis)comfort due to glare' responses.

The reported level of glare was 'imperceptible' (no glare) in 48% of the cases and 'noticeable' (low level of glare) in 27% of the cases. Glare - 'disturbing' and 'intolerable' levels of glare - was only reported in 26% of the cases. Position 1 was the position where more glare was reported (41%) followed by position 2 (34%). Position 4 is the position where less glare was reported (9%) followed by position 3 (19%). Intolerable glare was only reported in positions 1 and 2 (Figure 6.8).

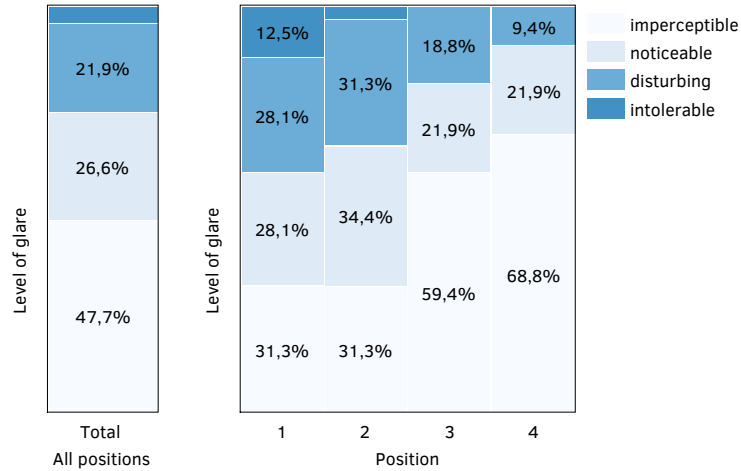


FIG. 6.8 Distribution of 'level of glare' responses.

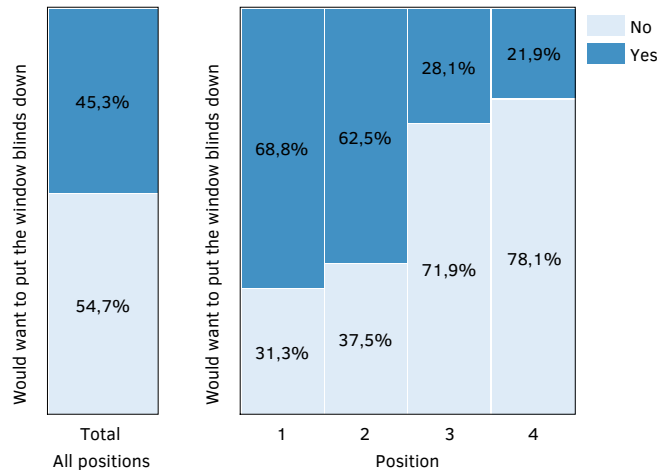


FIG. 6.9 Distribution of 'would have wanted to put the window blinds down' responses.

When the level of glare was reported as 'noticeable' to 'intolerable', the subject was asked to specify what was the source of glare from a list of possibilities. The objective of this question was to disassociate the problem of veiling reflections of the task surface from the problem of discomfort glare. In most cases (84) the subjects reported that the source of glare was the window, walls, desk, objects seen through the window and other. In these cases it is expected that the reported glare problem is discomfort glare. For 34 cases the screen was considered a source of glare and in 13 of these cases the screen was considered the only source of glare. From these 13 cases, the level of glare was considered 'disturbing' or 'intolerable' in 3 cases and 'noticeable' in 10 cases. In these cases it is expected that the problem of glare that the subjects are reporting is veiling reflections. There was one case where the subject reported that the source of discomfort was the screen and reflections in his glasses, therefore also excluding the possibility of discomfort glare.

The subjects reported that they would have wanted to put the window blinds down in 45% of the cases. Subjects would have wanted to lower the blinds the most in position 1 (69% of the cases, in this position) and the least in position 4 (22% of the cases, in this position).

For 29 of the cases where the subjects reported having wanted to lower the window blinds, the reported level of glare was either 'imperceptible' or just 'noticeable'. The reason for wanting to lower the blinds is therefore not related to discomfort glare in those cases. This indicates that the subjects wanted to lower the blinds for low levels of discomfort glare. Reasons other than discomfort glare could then be on the basis of their responses, e.g. improve visibility of the screen or keep a view to the outside.

TABLE 6.2 Counts of votes for the 'would you want to put the blinds down' question, by level of glare.

Would want to put the window blinds down?	Level of glare			
	imperceptible	noticeable	disturbing	intolerable
No	53	13	4	0
Yes	8	21	24	5

In 32% of the cases the subjects reported to have felt uncomfortable due to reflections on the screen or a screen washed out. Discomfort due to that was mostly reported in position 1 (44% of the cases in this position) and the least reported in position 4 (13% of the cases in this position).

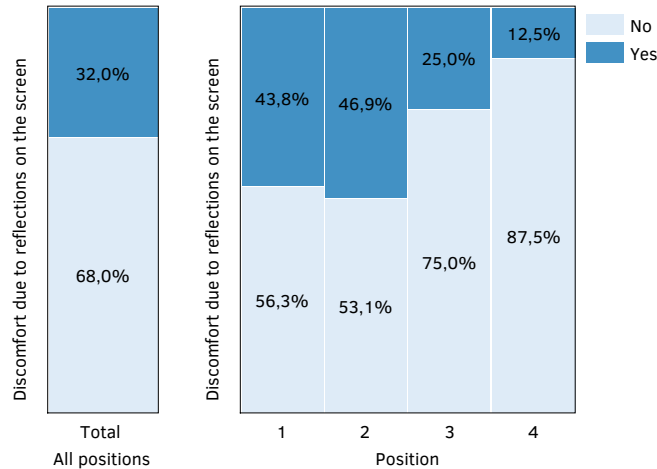


FIG. 6.10 Distribution of 'reflections on screen / screen washed out' responses.

There were 41 cases where reflections on the screen caused discomfort. In 20 of these cases the reported level of glare was reported from 'noticeable' to 'intolerable'. Twelve (12) of these 20 cases, correspond to situations where the reported source of glare (level of glare question) was the screen only. It is concluded that in 8 cases the subjects have experienced both discomfort glare and veiling reflections.

TABLE 6.3 Counts of votes for the 'discomfort due to reflections on the screen' question, by level of glare.

Discomfort due to reflections on the screen?	Level of glare			
	imperceptible	noticeable	disturbing	intolerable
No	57	17	11	2
Yes	4	17	17	3

In 26% of the cases the subjects reported to have felt uncomfortable because of the sun. Sun was mostly reported as uncomfortable in position 1 (53% of the case in this position) and the least uncomfortable in position 4 (6% of the cases in this position).

When the subjects reported having felt uncomfortable with the sun, which occurred in 33 cases, they were also asked to specify in which way the sun was uncomfortable, from a list of possibilities.

In 23 of these cases the subjects provided a range of reasons for their discomfort caused by the sun, indicating co-existence of thermal discomfort, veiling reflections and discomfort glare problems.

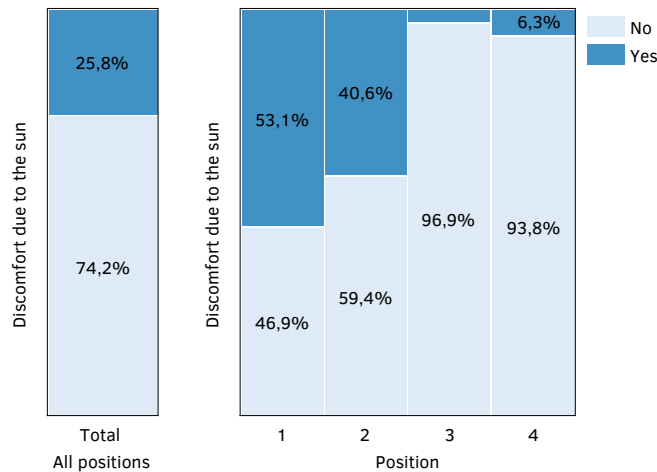


FIG. 6.11 Distribution of 'discomfort due to sun' responses.

There were 10 cases where reasons other than the intensity and contrast of the sunlight in the room (discomfort glare) was the source of discomfort. In 6 of these cases the source of discomfort was the heat from the sun or the sunlight reaching the body. In the other 4 cases, the reason for the discomfort was related to reflections on the screen. In these 4 cases, the subjects have reported 'noticeable' to 'intolerable' discomfort glare (level of glare question), suggesting that subjects might have experienced both veiling reflections and discomfort glare.

6.6.2 Glare metrics

The metrics results are presented for the 'mean' measurement by position in Figure 6.12. The results for the window-based metrics refer to 112 cases (N=112), as there are 16 cases where there isn't a view of the window (positions 1 and 2 – 'U' layout).

The box plots show many values outside the quartile ranges. These correspond exclusively to situations of either very high or very low overall luminance. Cases of very high luminance were measured when the sun was directly shining through the window. Cases of very low luminance were measured in the morning period, when the room was not exposed to sun.

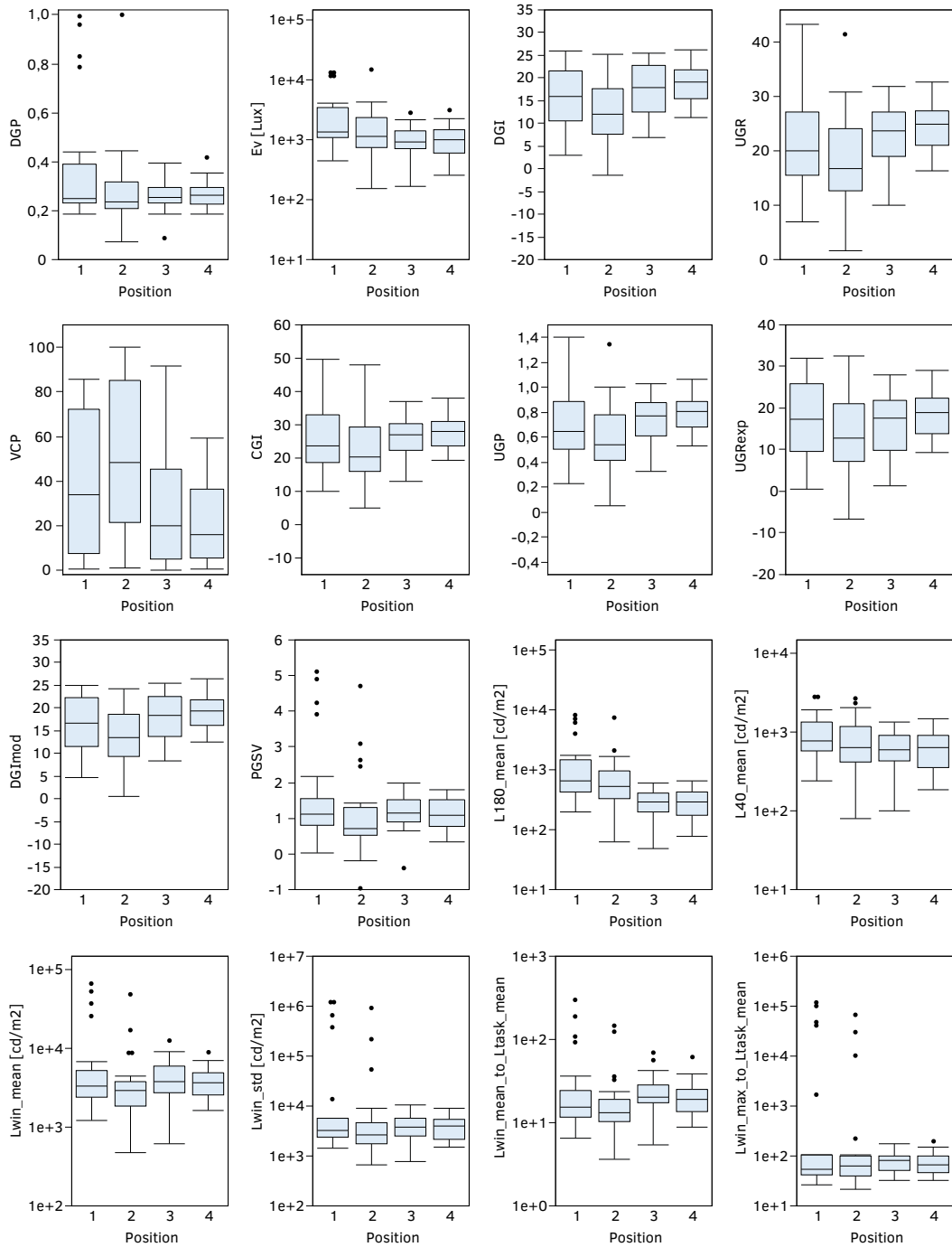


FIG. 6.12 Distributions of the metrics based on the 'mean' measurement, by position.

6.7 Analysis

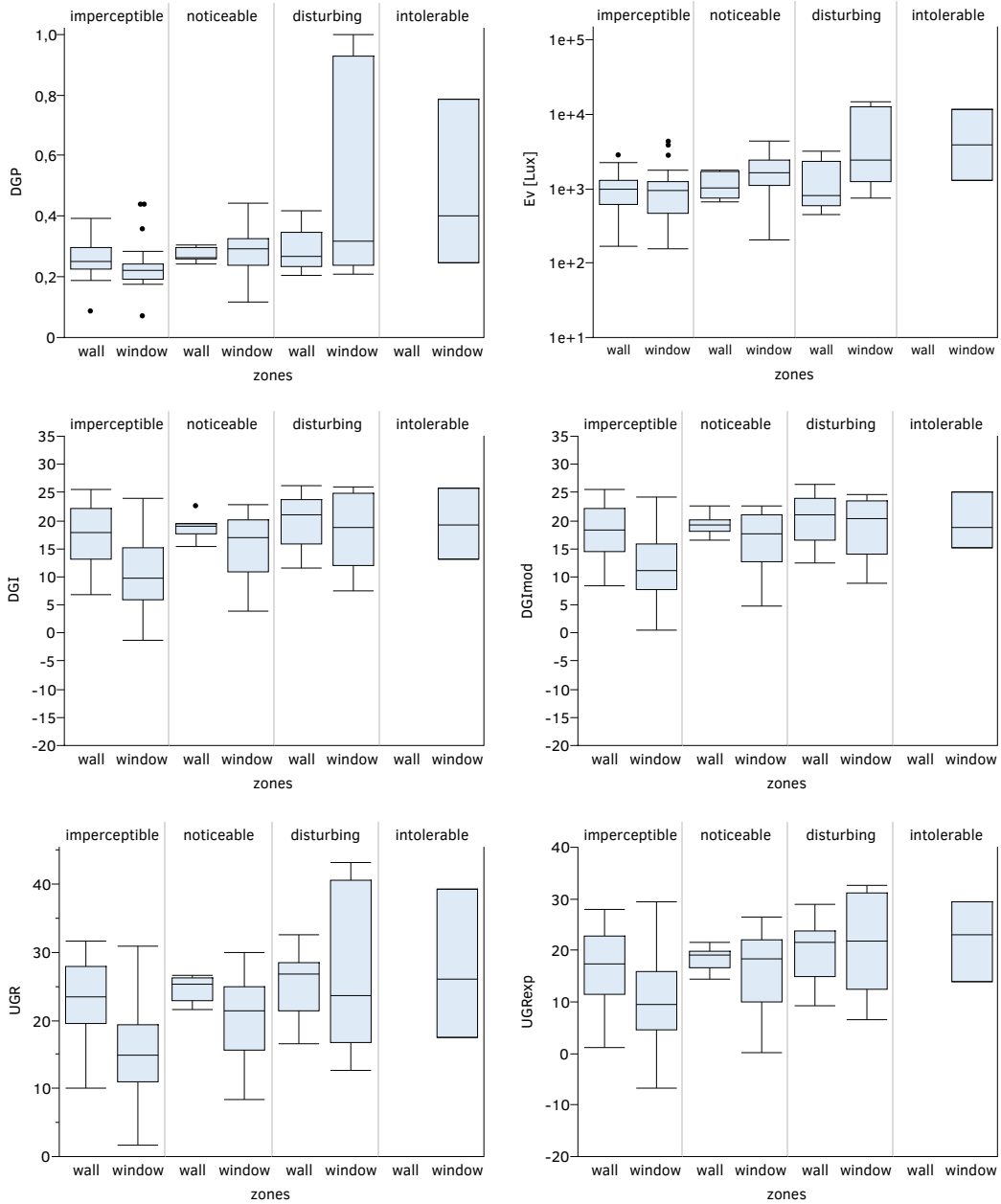
6.7.1 Analysis sample

From the 128 cases, the 13 cases where subjects reported that the source of glare was the screen only ('level of glare' question) were excluded. This includes the cases identified as cases of potential veiling reflections based on the responses to the 'discomfort due to sun' and 'discomfort due to reflections on the screen / screen washed out' questions. An additional case where the subject reported that the sources of discomfort were the screen and reflections in his glasses was also removed. For the 'U' layout, the subjects sit with their backs to the window in position 1 and 2 (16 cases), which means that they don't have a view of the window. In these cases it is not possible to calculate window-based metrics like some of the contrast ratios and PGSV. Although glare might occur due to sunlight incident or reflected from the desk surface, these cases were excluded so the metrics are compared based on the same number of cases. Ten of these cases are also cases where the reported source of glare was the screen and therefore only 6 cases are effectively excluded for this reason. This means that the sample is reduced to 101 cases, all metrics being analysed based on the same number of cases.

Similarly to study I, the analysis is done based on the full room dataset, comprising the 101 cases, a near-window zone sample that includes the cases for positions 1 and 2 (47 cases) and a near-wall zone sample that includes the cases for positions 3 and 4 (54 cases).

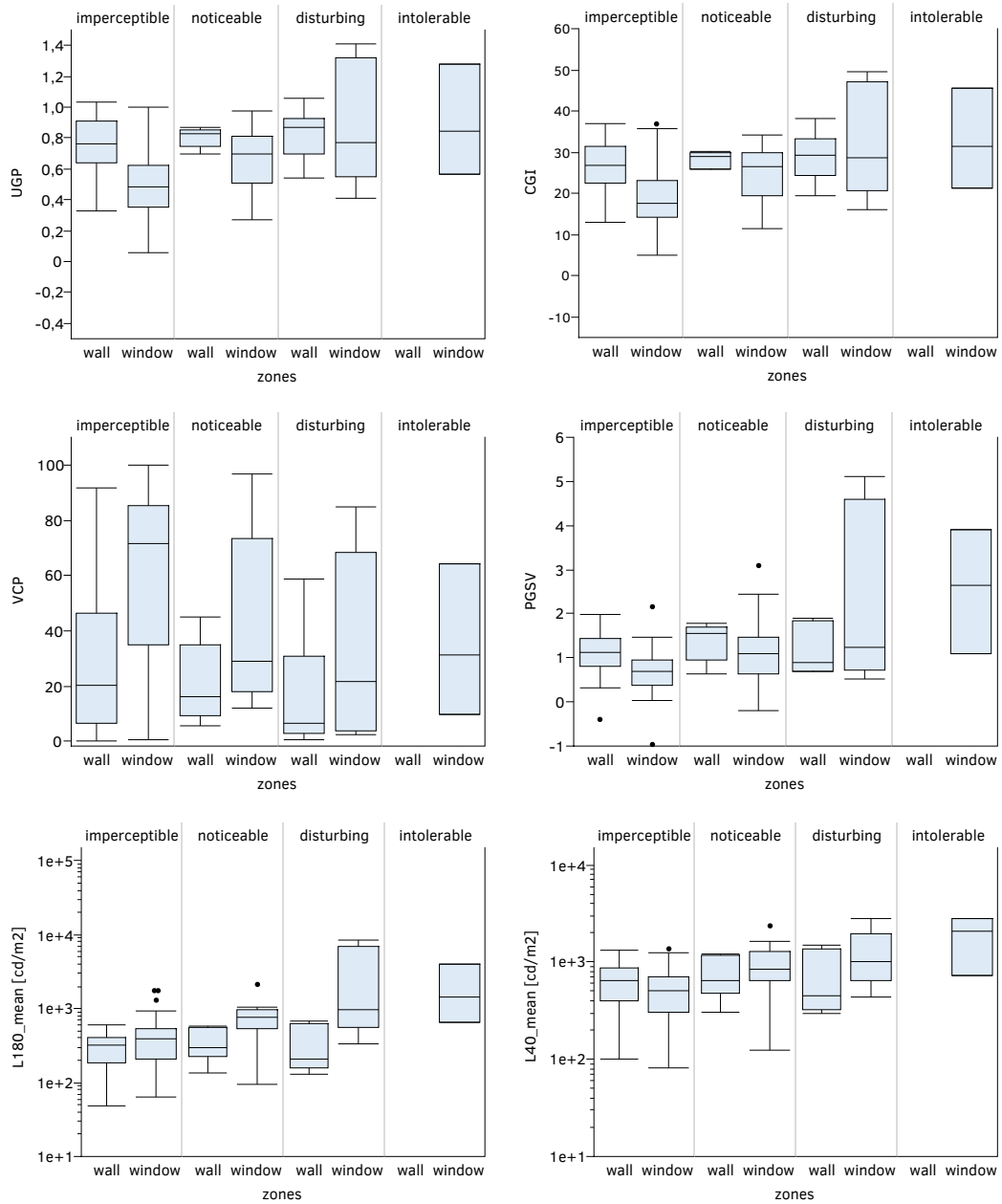
6.7.2 Glare metrics and evaluations reported by zone

The box plots below show the distributions for the metrics, calculated based on the 'mean' measurement, for the window zone and for the wall zone separately.



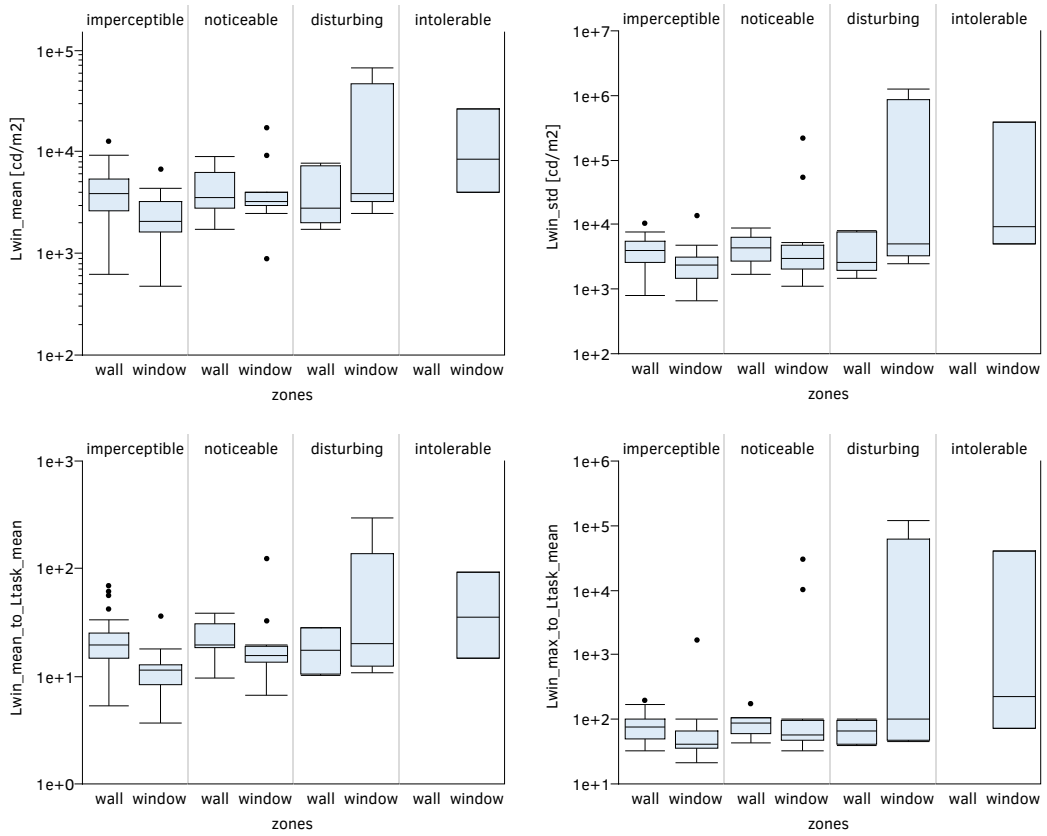
a

FIG. 6.13 Distributions of the metrics for the 'mean' measurement, by zone.



b

FIG. 6.13 Distributions of the metrics for the 'mean' measurement, by zone.



c

FIG. 6.13 Distributions of the metrics for the 'mean' measurement, by zone.

6.7.3 Spearman correlation analysis

The results of the Spearman correlation can be seen in Tables 6.4 to 6.6. The metrics are first ranked based on their lower to higher performance in each test and receive a score for each test based on their order in the rank. The scores of a metric in all the tests are summed up and a final position in a rank is found depending on that sum, with a metric higher in the rank performing better than a metric lower in the rank.

The cells of the tables are shaded according to the defined performance criteria (Table 6.4), the dark blue and the greyed-out value indicating a failed test.

The analysis is done for the 'start measurement' and for the 'mean measurement'. The tables for the 'start measurement' are presented in the section 4 of the Appendix C, for readability, and only the information regarding how the two datasets compare to each other is provided below.

TABLE 6.4 Performance criteria (Spearman).

	Fail	Pass	Good	Very Good
ρ	< 0.3	> 0.3	> 0.5	> 0.7
Significance	> 0.05	< 0.05		
Lower 95% CI	< 0.2	> 0.2		

Note: the lower 95% CI is the lower bound of the 95% confidence of ρ .

Given the definition of the VCP, it is expected the metric to produce negative correlations. Consequently, the analysis of the lower bound of the 95% confidence interval is reversed in the case of that metric, i.e., it fails when the upper CI is < 0.2.

The analysis shows, that for the full dataset (Table 6.5), a wide range of metrics show significant correlations, however just a few pass the effect size test.

The $L_{180^\circ_mean}$ shows the best performance ($\rho = 0.47$, $p < 0.001$).

For the window dataset (Table 6.6), all metrics show significant correlations. Most metrics have a good performance, with window-based metrics showing the highest effect sizes and L_{win_mean} topping the rank ($\rho = 0.62$, $p < 0.001$).

TABLE 6.5 Spearman correlation and ranks for the full room dataset (mean measurement).

#	Metric	ρ	sig.	95% CI		ρ	sig.	low CI	CI	Total
				Lower	Upper					
1	DGP	0.37	0.000	0.19	0.536	4	4	3	1	3
2	E_v	0.39	0.000	0.20	0.551	2	2	2	2	2
3	DGI	0.22	0.027	0.03	0.408	11	11	12	8	11
4	UGR	0.21	0.036	0.01	0.405	13	13	14	14	14
5	VCP	-0.11	0.277	-0.31	0.088	16	16	5	16	13
6	CGI	0.24	0.015	0.04	0.430	7	7	8	12	8
7	UGP	0.21	0.036	0.01	0.405	14	14	15	15	16
8	UGRexp	0.28	0.005	0.09	0.458	5	5	6	6	5
9	DGImod	0.22	0.031	0.03	0.397	12	12	11	4	9
10	PGSV	0.24	0.018	0.03	0.425	9	9	13	13	12
11	$L_{40^\circ_mean}$	0.37	0.000	0.18	0.551	3	3	4	5	4
12	$L_{180^\circ_mean}$	0.47	0.000	0.28	0.639	1	1	1	3	1
13	L_{win_mean}	0.24	0.016	0.04	0.417	8	8	9	7	7
14	L_{win_std}	0.26	0.009	0.06	0.441	6	6	7	10	6
15	L_{win_mean}/L_{t_mean}	0.18	0.066	-0.01	0.365	15	15	16	9	15
16	L_{win_max}/L_{t_mean}	0.23	0.021	0.03	0.416	10	10	10	11	10

TABLE 6.6 Spearman correlation and ranks for the window dataset (mean measurement).

#	Metric	ρ	sig.	95% CI		ρ	sig.	low CI	CI	Total
				Lower	Upper					
1	DGP	0.55	0.000	0.31	0.74	6	6	6	7	6
2	E_v	0.54	0.000	0.30	0.727	7	7	8	6	8
3	DGI	0.50	0.000	0.25	0.699	11	11	10	9	9
4	UGR	0.48	0.001	0.24	0.687	13	13	13	12	13
5	VCP	-0.37	0.011	-0.61	-0.108	16	16	16	16	16
6	CGI	0.49	0.000	0.25	0.699	12	12	11	14	12
7	UGP	0.48	0.001	0.24	0.687	14	14	14	13	14
8	UGRexp	0.48	0.001	0.24	0.683	15	15	15	10	15
9	DGImod	0.50	0.000	0.25	0.707	9	9	9	15	10
10	PGSV	0.50	0.000	0.24	0.690	10	10	12	11	11
11	$L_{40^\circ_mean}$	0.56	0.000	0.32	0.746	5	5	4	5	4
12	$L_{180^\circ_mean}$	0.56	0.000	0.32	0.756	4	4	5	8	5
13	L_{win_mean}	0.62	0.000	0.40	0.780	1	1	1	2	1
14	L_{win_std}	0.60	0.000	0.40	0.754	2	2	2	1	2
15	L_{win_mean}/L_{t_mean}	0.57	0.000	0.34	0.759	3	3	3	4	3
16	L_{win_max}/L_{t_mean}	0.54	0.000	0.31	0.722	8	8	7	3	7

In the wall zone (Table 6.7), all metrics show correlations with very low effect sizes and non-significant. The error of the statistic, as depicted by its 95% confidence intervals can be quite significant, with some metrics showing an inverse relationship (negative lower 95% confidence interval) between the reported glare and the metric.

TABLE 6.7 Spearman correlation and ranks for the wall dataset (mean measurement).

#	Metric	ρ	sig.	95% CI		ρ	sig.	low CI	CI	Total
				Lower	Upper					
1	DGP	0.17	0.229	-0.10	0.404	1	1	3	7	2
2	E_v	0.06	0.661	-0.22	0.336	11	11	9	11	9
3	DGI	0.16	0.250	-0.10	0.391	2	2	2	3	1
4	UGR	0.15	0.267	-0.11	0.392	3	3	5	5	4
5	VCP	-0.12	0.378	-0.37	0.145	8	8	1	8	7
6	CGI	0.15	0.296	-0.11	0.378	6	6	7	2	6
7	UGP	0.15	0.267	-0.11	0.392	4	4	6	6	5
8	UGRexp	0.15	0.289	-0.11	0.381	5	5	4	1	3
9	DGI _{mod}	0.14	0.312	-0.12	0.374	7	7	8	4	8
10	PGSV	0.08	0.579	-0.25	0.404	9	9	11	16	11
11	$L_{40^\circ_mean}$	0.08	0.582	-0.23	0.384	10	10	10	14	10
12	$L_{180^\circ_mean}$	0.05	0.722	-0.26	0.358	13	13	12	15	14
13	L_{win_mean}	-0.06	0.690	-0.33	0.246	12	12	16	12	13
14	L_{win_std}	0.00	0.987	-0.29	0.303	16	16	15	13	16
15	L_{win_mean}/L_{t_mean}	-0.03	0.840	-0.28	0.239	14	14	14	9	12
16	L_{win_max}/L_{t_mean}	0.00	0.981	-0.27	0.276	15	15	13	10	15

Tables for the 'start' measurement can be found in Appendix C. There is a small difference between the 'mean' and of the 'start' measurement regarding the effect size of the metrics for the 'full' and the 'window' datasets. However, the top-4 ranked metrics of the full dataset and the top-3 ranked metrics of the window dataset are the same for the two measurements. For the wall dataset both measurements produce the same behaviour of no correlation. The two measurements – 'mean' and 'start', can therefore be said to show the same correlation trends.

6.7.4 ROC curve analysis

6.7.4.1 ROC's AUC

The ROC curves for the different metrics for the three samples, full window and wall zone are presented in Figures 6.14 to 6.16.

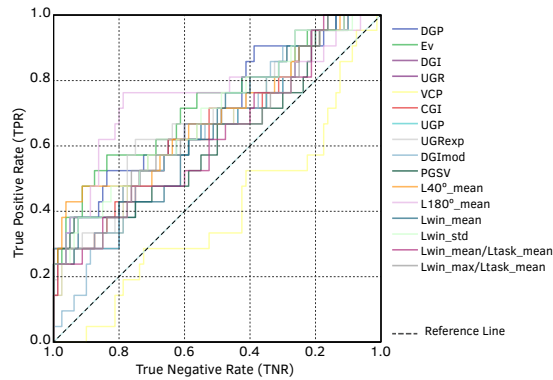


FIG. 6.14 ROC curve for the full room (mean measurement).

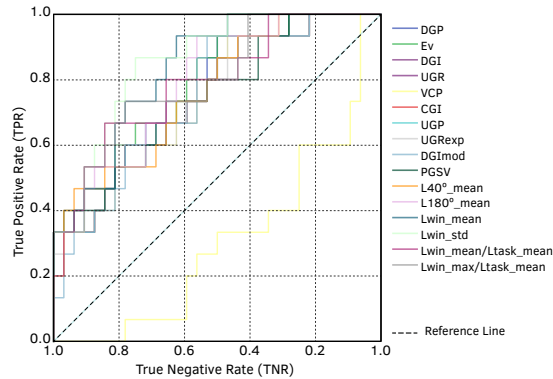


FIG. 6.15 ROC curve for the window zone (mean measurement).

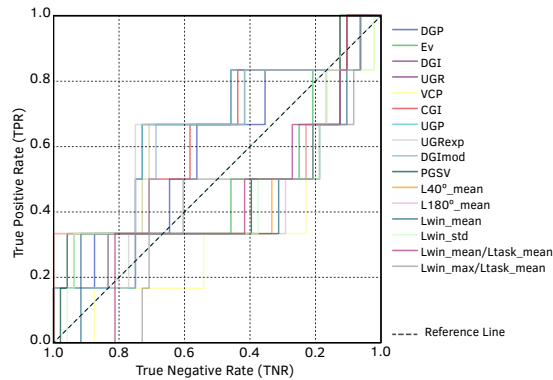


FIG. 6.16 ROC curve for the wall zone (mean measurement).

The results of the AUC test are presented in Tables 6.9 to 6.11. The cells of the tables are shaded according to the defined performance criteria (Table 6.8), the dark blue and the greyed-out value indicating a failed test.

TABLE 6.8 Performance criteria (ROC).

	Fail	Pass	Good	Very Good
AUC	< 0.6	> 0.6	> 0.7	> 0.8
Significance	> 0.05	< 0.05		
Lower 95% CI	< 0.5	> 0.5		
TPR, TNR	< 0.5	> 0.5		
Shortest dist.	> 0.5	< 0.5		

For the full dataset (Table 6.9), most metrics pass the AUC test and show a significant AUC. The DGP, Ev and $L_{180^\circ_mean}$ have a good effect size, with $L_{180^\circ_mean}$ showing the highest effect size (AUC = 0.75, $p < 0.001$).

For the window dataset (Table 6.10), most metrics show a significant AUC and 'good' to 'very good' effect sizes. The L_{win_mean} and L_{win_std} have the highest effect sizes, with L_{win_std} showing the highest correlation (AUC = 0.86, $p < 0.001$).

TABLE 6.9 AUC test and ranks for the full room (mean measurement).

#	Metric	AUC	sig.	95% CI		AUC	sig.	low CI	CI	Total
				Lower	Upper	rank	rank	rank	rank	rank
1	DGP	0.71	0.004	0.58	0.84	3	3	3	2	1
2	E_v	0.72	0.002	0.59	0.86	2	2	2	5	2
3	DGI	0.66	0.029	0.52	0.79	9	9	9	7	9
4	UGR	0.65	0.036	0.51	0.79	11	11	12	11	12
5	VCP	0.39	0.139	0.26	0.53	16	16	16	8	14
6	CGI	0.66	0.024	0.52	0.80	7	7	8	9	7
7	UGP	0.65	0.036	0.51	0.79	12	12	13	12	13
8	UGRexp	0.69	0.008	0.56	0.82	5	5	5	3	5
9	DGImod	0.64	0.042	0.52	0.77	13	13	10	1	10
10	PGSV	0.63	0.075	0.48	0.77	14	14	15	16	16
11	$L_{40^\circ_mean}$	0.69	0.008	0.55	0.83	6	6	6	15	8
12	$L_{180^\circ_mean}$	0.75	0.000	0.61	0.89	1	1	1	10	3
13	L_{win_mean}	0.66	0.024	0.53	0.80	8	8	7	6	6
14	L_{win_std}	0.69	0.007	0.56	0.82	4	4	4	4	4
15	L_{win_mean}/L_{t_mean}	0.63	0.079	0.48	0.77	15	15	14	14	15
16	L_{win_max}/L_{t_mean}	0.65	0.034	0.51	0.79	10	10	11	13	11

TABLE 6.10 AUC test and ranks for the window zone (mean measurement).

#	Metric	AUC	sig.	95% CI		AUC	sig.	low CI	CI	Total
				Lower	Upper	rank	rank	rank	rank	rank
1	DGP	0.77	0.003	0.63	0.91	7	7	7	7	7
2	E_v	0.79	0.002	0.65	0.92	6	6	5	5	5
3	DGI	0.75	0.007	0.60	0.90	15	15	15	14	15
4	UGR	0.75	0.006	0.60	0.90	10	10	11	11	10
5	VCP	0.30	0.032	0.15	0.46	16	16	16	16	16
6	CGI	0.75	0.006	0.60	0.90	11	11	12	12	11
7	UGP	0.75	0.006	0.60	0.90	12	12	13	13	12
8	UGRexp	0.76	0.005	0.61	0.90	9	9	9	10	9
9	DGImod	0.75	0.006	0.61	0.89	17	14	10	9	13
10	PGSV	0.75	0.006	0.60	0.90	14	13	14	15	14
11	$L_{40^\circ_mean}$	0.76	0.004	0.62	0.91	8	8	8	8	8
12	$L_{180^\circ_mean}$	0.79	0.001	0.66	0.92	4	4	4	3	4
13	L_{win_mean}	0.83	0.000	0.72	0.95	2	2	2	2	2
14	L_{win_std}	0.86	0.000	0.75	0.96	1	1	1	1	1
15	L_{win_mean}/L_{t_mean}	0.79	0.002	0.65	0.93	5	5	6	6	6
16	L_{win_max}/L_{t_mean}	0.80	0.001	0.66	0.93	3	3	3	4	3

For the wall dataset (Table 6.11), although some of the metrics have AUC values above 0.6, none of the metrics produced a significant correlation. A trend for the glare indices to perform better than the simple luminance metrics can be observed, suggesting that luminance contrast might have an effect in the perception of glare in this zone.

TABLE 6.11 AUC test and ranks for the wall zone (mean measurement).

#	Metric	AUC	sig.	95% CI		AUC	sig.	low CI	CI	Total
				Lower	Upper	rank	rank	rank	rank	rank
1	DGP	0.58	0.509	0.32	0.85	7	9	7	10	7
2	E_v	0.49	0.956	0.20	0.79	8	16	8	11	11
3	DGI	0.64	0.283	0.39	0.88	1	2	2	5	1
4	UGR	0.63	0.296	0.39	0.87	3	4	3	2	3
5	VCP	0.34	0.205	0.10	0.58	16	1	16	1	8
6	CGI	0.61	0.378	0.37	0.86	6	7	6	6	6
7	UGP	0.63	0.296	0.39	0.87	4	5	4	3	4
8	UGRexp	0.64	0.283	0.39	0.88	2	3	1	4	2
9	DGI _{mod}	0.63	0.322	0.38	0.87	5	6	5	8	5
10	PGSV	0.46	0.762	0.16	0.77	10	14	11	13	12
11	$L_{40^\circ_mean}$	0.47	0.826	0.16	0.78	9	15	10	15	13
12	$L_{180^\circ_mean}$	0.46	0.741	0.14	0.78	11	13	13	16	16
13	L_{win_mean}	0.42	0.527	0.12	0.72	14	10	15	12	14
14	L_{win_std}	0.44	0.640	0.14	0.75	12	12	14	14	15
15	L_{win_mean}/L_{t_mean}	0.42	0.545	0.17	0.67	13	11	9	9	9
16	L_{win_max}/L_{t_mean}	0.40	0.425	0.15	0.65	15	8	12	7	10

There is a minimal difference between the 'mean' and the 'start' measurement regarding the effect size of the AUC for the top-ranked metrics of the 'full' and of the 'window' zones. However, at least the top-6 ranked metrics are the same for the 'mean' and the 'start' measurements, for the full room and window zone datasets.

For the wall dataset both measurements produce the same behaviour of a non-significant AUC. The two measurements can therefore be said to show the same AUC trend.

6.7.4.2 ROC's TPR, TNR and 'shortest distance'

For the full room, most metrics pass the TPR and TNR tests with the $L_{180^\circ_mean}$ achieving the highest score, followed by E_v , DGP and UGRexp (Table 6.12).

TABLE 6.12 TPR and TNR test and ranks for full room (mean measurement).

Full (mean meas.)		shorter				dist.	TPR	TNR	Total
#	Metric	dist.	cut-off	TPR	TNR	rank	rank	rank	rank
1	DGP	0.50	0.31	0.52	0.84	4	12	1	4
2	E_v	0.46	1884	0.57	0.84	3	9	2	3
3	DGI	0.52	19	0.57	0.71	5	10	8	6
4	UGR	0.54	26	0.52	0.74	11	13	6	11
5	VCP	0.76	21	0.52	0.41	16	14	16	16
6	CGI	0.52	27	0.62	0.65	7	4	10	5
7	UGP	0.54	0.84	0.52	0.74	12	15	7	13
8	UGRexp	0.46	21	0.62	0.75	2	5	5	2
9	DGI _{mod}	0.53	19	0.62	0.63	10	6	12	10
10	PGSV	0.60	1	0.67	0.50	15	2	15	12
11	$L_{40^\circ_mean}$	0.53	720	0.62	0.64	9	7	11	9
12	$L_{180^\circ_mean}$	0.32	535	0.76	0.79	1	1	3	1
13	L_{win_mean}	0.56	3560	0.62	0.59	13	8	14	15
14	L_{win_std}	0.52	4616	0.57	0.71	6	11	9	8
15	L_{win_mean}/L_{t_mean}	0.58	23	0.48	0.76	14	16	4	14
16	L_{win_max}/L_{t_mean}	0.52	71	0.67	0.60	8	3	13	7

For the window zone, most metrics pass the TPR and TNR tests with L_{win_std} achieving the highest score, followed by L_{win_mean} (Table 6.13).

In the wall zone, UGR and UGRexp achieve the highest scores, followed by DGI and UGP (Table 6.14).

TABLE 6.13 TPR and TNR test and ranks for window zone (mean measurement).

Window (mean meas.)		shorter				dist.	TPR	TNR	Total
#	Metric	dist.	cut-off	TPR	TNR	rank	rank	rank	rank
1	DGP	0.44	0.29	0.67	0.72	8	7	11	9
2	E_v	0.42	1884	0.67	0.75	5	8	9	5
3	DGI	0.46	17	0.60	0.78	10	11	2	6
4	UGR	0.46	23	0.60	0.78	11	12	3	10
5	VCP	0.83	56	0.33	0.50	16	16	16	16
6	CGI	0.46	27	0.60	0.78	12	13	4	11
7	UGP	0.46	0.74	0.60	0.78	13	14	5	13
8	UGRexp	0.44	18	0.67	0.72	9	9	12	12
9	DGI _{mod}	0.46	19	0.60	0.78	14	15	6	15
10	PGSV	0.44	1	0.73	0.66	7	3	13	7
11	$L_{40^\circ_mean}$	0.46	720	0.73	0.63	15	4	14	14
12	$L_{180^\circ_mean}$	0.43	555	0.80	0.63	6	2	15	8
13	L_{win_mean}	0.34	3560	0.73	0.78	2	5	7	2
14	L_{win_std}	0.28	3260	0.87	0.75	1	1	10	1
15	L_{win_mean}/L_{t_mean}	0.37	17	0.67	0.84	4	10	1	3
16	L_{win_max}/L_{t_mean}	0.34	70	0.73	0.78	3	6	8	4

TABLE 6.14 TPR and TNR test and ranks for wall zone (mean measurement).

Wall (mean meas.)		shorter				dist.	TPR	TNR	Total
#	Metric	dist.	cut-off	TPR	TNR	rank	rank	rank	rank
1	DGP	0.55	0.26	0.67	0.56	7	1	15	6
2	E_v	0.67	2073	0.33	0.94	12	9	4	9
3	DGI	0.44	21	0.67	0.71	4	2	11	3
4	UGR	0.43	27	0.67	0.73	2	3	9	1
5	VCP	0.81	21	0.33	0.54	16	10	16	16
6	CGI	0.53	28	0.67	0.58	6	4	14	7
7	UGP	0.43	0.86	0.67	0.73	3	5	10	4
8	UGRexp	0.42	22	0.67	0.75	1	6	8	2
9	DGI _{mod}	0.46	21	0.67	0.69	5	7	12	8
10	PGSV	0.67	2	0.33	0.96	11	11	3	10
11	$L_{40^\circ_mean}$	0.67	1328	0.33	1.00	9	12	1	5
12	$L_{180^\circ_mean}$	0.67	608	0.33	1.00	10	13	2	11
13	L_{win_mean}	0.67	7023	0.33	0.92	14	14	6	14
14	L_{win_std}	0.67	7276	0.33	0.94	13	15	5	13
15	L_{win_mean}/L_{t_mean}	0.69	28	0.33	0.81	15	16	7	15
16	L_{win_max}/L_{t_mean}	0.64	82	0.50	0.60	8	8	13	12

There is good agreement between the 'start' and the 'mean' measurement ranks, with at least the top-4 ranked metrics being the same for the 'full' dataset. There is some difference between the 'start' and the 'mean' measurement ranks for the 'window' dataset. However, the same two metrics - L_{win_mean} and L_{win_std} - are within the top three metrics in both measurements. There is little difference between the 'start' and the 'mean' measurement ranks for the 'wall' dataset, with no variation regarding the top-4 ranked metrics. The two measurements can therefore be said to show similar trends.

The TPR and TNR tables also include the optimum cut-off value of the metric, which corresponds to the point of the ROC curve where the TPR and TNR are the highest, i.e. the BCD threshold resulting from the ROC curve analysis. These thresholds are analysed next.

6.7.4.3 Borderline between comfort and discomfort (BCD)

Similarly to Study I, in this study it is observed that the BCD thresholds are different for the three samples - full, window and wall zone. The BCD thresholds in Study II tend to be either within or higher than the metrics' actual BCD thresholds, depending on the sample. This is in contrast with Study I, where the thresholds were mostly lower than the metrics' actual BCD threshold. The exception to this is DGP and E_v that present thresholds below the metrics' actual thresholds. Some fluctuation of the BCD thresholds for those metrics depending on the measurement - 'start' or 'mean' - for the full room and window zone is observed. In the wall zone, DGP has a BCD threshold of 0.26 in both measurements and E_v ranges between 2,073 and 2,088 cd/m².

The thresholds for window-based metrics in the wall zone are much higher than in Study I and than the metrics' actual thresholds (above 7,000 cd/m² for both L_{win_mean} and L_{win_std} metrics). The same happens for the two window-to-task contrast ratios, L_{win_mean}/L_{t_mean} and L_{win_max}/L_{t_mean} , with threshold values ranging between 26 and 28 and between 79 and 82, respectively.

6.7.5 Performance analysis

The results of the performance of the metrics based on the number of passed and failed tests for each metric are analysed next. Tables 6.15 to 6.17 show the number of passed tests for the three samples, with the greyed-out cells (0) indicating a failed test.

The results show that for the full room, E_v and $L_{180^\circ_mean}$ have the best performance, having passed all the tests. For the window zone, all metrics pass the tests with the exception of VCP that has consistently underperformed in all tests.

For the wall zone, none of the metrics pass all the tests. It can be observed that the glare indices – DGI, UGR, UGP, UGRexp and DGImod, pass more tests than the other metrics.

There is agreement between the ‘start’ and the ‘mean’ measurements for the full, window and wall zone datasets regarding the final performance of the metrics.

TABLE 6.15 Passed statistical tests for the full room sample, ‘mean measurement’.

Full (mean meas.)		Spearman			ROC						All
#	Metric	sig.	ρ	low CI	sig.	AUC	low CI	dist.	TPR	TNR	rank
1	DGP	1	1	0	1	1	1	0	1	1	2
2	E_v	1	1	1	1	1	1	1	1	1	1
3	DGI	1	0	0	1	1	1	0	1	1	3
4	UGR	1	0	0	1	1	1	0	1	1	3
5	VCP	0	0	0	0	0	0	0	1	0	6
6	CGI	1	0	0	1	1	1	0	1	1	3
7	UGP	1	0	0	1	1	1	0	1	1	3
8	UGRexp	1	0	0	1	1	1	1	1	1	2
9	DGImod	1	0	0	1	1	1	0	1	1	3
10	PGSV	1	0	0	0	1	0	0	1	1	4
11	$L_{40^\circ_mean}$	1	1	0	1	1	1	0	1	1	2
12	$L_{180^\circ_mean}$	1	1	1	1	1	1	1	1	1	1
13	L_{win_mean}	1	0	0	1	1	1	0	1	1	3
14	L_{win_std}	1	0	0	1	1	1	0	1	1	3
15	L_{win_mean}/L_{t_mean}	0	0	0	0	1	0	0	0	1	5
16	L_{win_max}/L_{t_mean}	1	0	0	1	1	1	0	1	1	3

TABLE 6.16 Passed statistical tests for the window sample, 'mean measurement'.

Window (mean meas.)		Spearman			ROC						All
#	Metric	sig.	ρ	low CI	sig.	AUC	low CI	dist.	TPR	TNR	rank
1	DGP	1	1	1	1	1	1	1	1	1	1
2	E_v	1	1	1	1	1	1	1	1	1	1
3	DGI	1	1	1	1	1	1	1	1	1	1
4	UGR	1	1	1	1	1	1	1	1	1	1
5	VCP	1	1	0	1	0	0	0	0	1	2
6	CGI	1	1	1	1	1	1	1	1	1	1
7	UGP	1	1	1	1	1	1	1	1	1	1
8	UGRexp	1	1	1	1	1	1	1	1	1	1
9	DGImod	1	1	1	1	1	1	1	1	1	1
10	PGSV	1	1	1	1	1	1	1	1	1	1
11	$L_{40^\circ_mean}$	1	1	1	1	1	1	1	1	1	1
12	$L_{180^\circ_mean}$	1	1	1	1	1	1	1	1	1	1
13	L_{win_mean}	1	1	1	1	1	1	1	1	1	1
14	L_{win_std}	1	1	1	1	1	1	1	1	1	1
15	L_{win_mean}/L_{t_mean}	1	1	1	1	1	1	1	1	1	1
16	L_{win_max}/L_{t_mean}	1	1	1	1	1	1	1	1	1	1

TABLE 6.17 Passed statistical tests for the wall sample, 'mean measurement'.

Wall (mean meas.)		Spearman			ROC						All
#	Metric	sig.	ρ	low CI	sig.	AUC	low CI	dist.	TPR	TNR	rank
1	DGP	0	0	0	0	0	0	0	1	1	3
2	E_v	0	0	1	0	0	0	0	0	1	3
3	DGI	0	0	0	0	1	0	1	1	1	1
4	UGR	0	0	0	0	1	0	1	1	1	1
5	VCP	0	0	0	0	0	0	0	0	1	4
6	CGI	0	0	0	0	1	0	0	1	1	2
7	UGP	0	0	0	0	1	0	1	1	1	1
8	UGRexp	0	0	0	0	1	0	1	1	1	1
9	DGImod	0	0	0	0	1	0	1	1	1	1
10	PGSV	0	0	1	0	0	0	0	0	1	3
11	$L_{40^\circ_mean}$	0	0	1	0	0	0	0	0	1	3
12	$L_{180^\circ_mean}$	0	0	1	0	0	0	0	0	1	3
13	L_{win_mean}	0	0	1	0	0	0	0	0	1	3
14	L_{win_std}	0	0	1	0	0	0	0	0	1	3
15	L_{win_mean}/L_{t_mean}	0	0	1	0	0	0	0	0	1	3

6.8 Discussion

The objective of this study was to investigate how well a group of metrics predict reported visual discomfort from daylight glare in a classroom environment.

Several questions were asked relating to the visual comfort conditions in the four sitting positions, with varying degrees of discomfort being reported by the subjects. As expected, visual discomfort in the classroom resulted from a number of reasons other than discomfort glare and particularly from veiling reflections.

More general visual discomfort (dissatisfaction with visual conditions), more discomfort glare, more risk of veiling reflections and more discomfort due to sun are reported for positions 1 and 2. This is in contrast with Study I, where more visual discomfort, veiling reflections and discomfort glare were reported for position 3. This likely results from the sky conditions under which the experiment of Study II was carried out and of the different room layout conditions that were tested in the study. It was observed that due to the higher solar angle, any sunlight entering the room was concentrated in the window zone, producing strong sun patches of light only in position 1 and 2. The higher overall luminance conditions of the room should have also contributed to a general reduction of luminance contrast, particularly the contrast between the window and window surrounding surfaces, as perceived from the positions near the wall (positions 3 and 4). Figure 6.17 shows the differences regarding the vertical illuminance distribution of the two studies, showing considerably higher illuminance in all areas of the room in Study II.

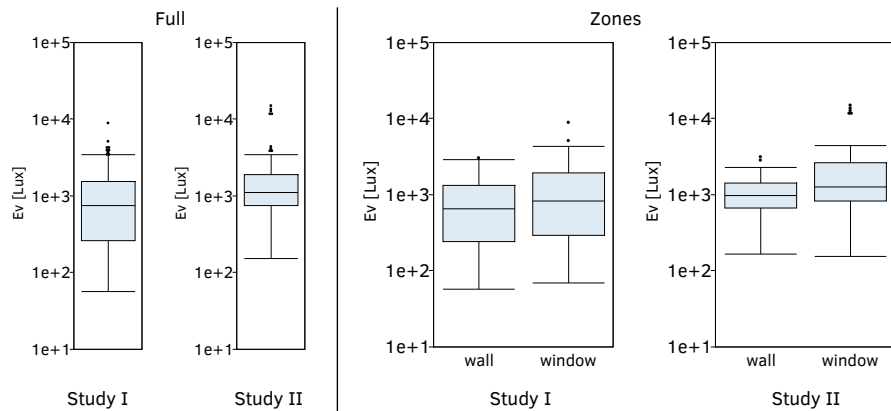


FIG. 6.17 Vertical illuminance (E_v) distribution in Study I and in Study II (Log scale).

In terms of the room layout, in Study II, the apparent size of the window in the visual field increased in the window zone and got reduced in the wall zone as a result of the 'regular layout'. This has potentially increased glare in the positions 1 and 2 and when combined with a higher overall luminance, has reduced the potential of glare in positions 3 and 4.

It appears that in a summer situation, the critical positions in a classroom from a visual discomfort and discomfort glare viewpoint are the positions near the window, whereas for an extended period of the year, the positions near the wall and in particular the position in front of the classroom near the wall, are the more critical ones.

For the analysis of the performance of the discomfort glare metrics, the data that was identified as referring solely to the problem of veiling reflections was eliminated as well as the conditions in which there wasn't a view of the window – position 1 and 2 for the 'U' layout, so metrics would be compared based on the same number of cases.

Due to the luminance differences between the two luminance measurements collected, the measurement at the 'start' and the measurement at the 'end' of the glare evaluation, the analysis was performed based on the 'start' measurement and on a 'mean' luminance measurement. For the majority of the tests, there was a good agreement regarding the correlation and classification trends for the two measurements, indicating that the results of the analysis acceptably represent the conditions in which the subjects made their evaluations.

The results show that for the full room dataset, the $L_{180^\circ_mean}$ and E_v are the best performing metrics, passing all tests, with DGP also showing a good performance. This is in some contrast with the results of Study I, where DGP alongside UGR and UGP performed the best. In study II, the total luminance in the visual field, depicted by $L_{180^\circ_mean}$ and E_v , showed a better performance perhaps because of the relatively higher luminance conditions of this experiment and a resulting less contrasting luminance environment overall.

For the window zone dataset, there is a good performance of most metrics, with the window-based metrics, particularly L_{win_mean} and L_{win_std} , scoring generally higher than the other metrics in the tests. These metrics were also among the best performing metrics in Study I. For the wall zone dataset, there is a very poor performance of the metrics, with none passing all the tests. However, a small trend to a better performance can be observed for some of the glare indices, particularly DGI and UGR. These results can be attributed to the distinct luminance characteristics

of the two classroom zones in this study- a window zone more prone to saturation glare and a wall zone more prone to contrast glare. In these conditions it could be expected that metrics that are more suitable to depict contrast glare like the glare indices to perform better in the wall zone.

Figure 6.18 shows an example of the luminance distribution in position 1 and position 4 for the same session, where the saturation- and the contrast-prone effects in these positions can be observed.

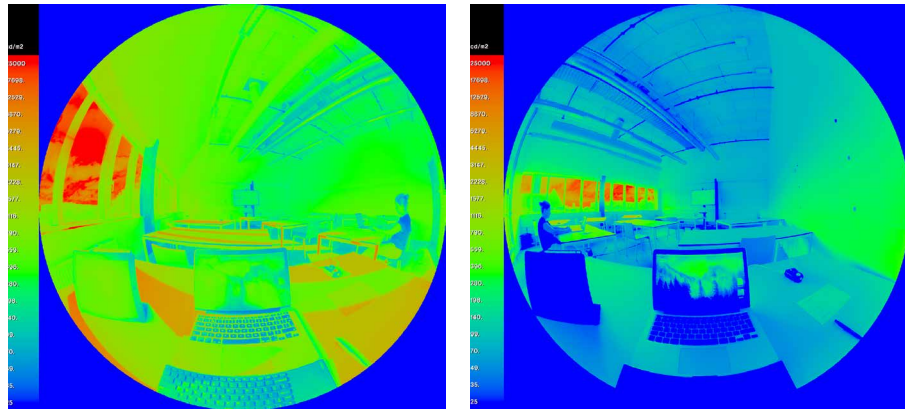


FIG. 6.18 Luminance distribution in position 1 (left) and in position 4 (right), in the same session and for a clear sky.

Interestingly, the metric that passes more tests considering the performance in all samples and the 'start' and 'mean' measurements is UGR_{exp}, resulting from the fact that the metric has a relatively better performance in the wall zone than DGP and passes more tests in the full room sample than the other glare indices. Similarly to DGP, UGR_{exp} is a metric with both 'adaptation' and 'contrast' terms however, contrary to DGP, the metric uses a logarithmic form of 'adaptation'.

6.9 Conclusion

In study II, the range of classroom conditions to study was extended to include a desk-based task and different desk layouts. This results in a wider range of spatial and field-of view conditions in comparison to the previous study.

The results of this study corroborate the results of the previous study in that no correlation was found between the metrics and the reported discomfort glare in the wall zone.

In this study the metrics that showed the best performance in the window zone were the window luminance-based metrics, particularly the L_{win_mean} and the L_{win_std} .

Based on the analysis of the full room data, $L_{180^\circ_mean}$ and E_v show the best performance but when all the dataset combinations tested are considered, UGR_{exp} does emerge as the best performing metric. Like other glare indices, the UGR_{exp} formulation does contain a 'contrast' and an 'adaptation' term, arguably providing for a more adequate identification of both saturation- and contrast-prone discomfort glare effects.

The results of this study are representative of a high solar angle condition in a classroom and for a situation of a continuously bright sky. Although the study included many visual conditions, the resulting subject and statistical analysis sample is small. More results would be required to employ more robust statistical analysis methods. In addition, the analysis based on the 'mean' measurement should be considered as the best possible approximation to the actual luminance conditions under which the subjects performed their evaluations.

The study does nevertheless support the findings of Study I in that discomfort glare metrics have been found to correlate very poorly with the glare evaluations in the inner part of the classroom, an aspect that requires further investigation.

In the next chapters, the metrics are examined in more detail with the intention of finding if a more adequate discomfort glare model can be developed for the classroom space.

7 Identifying successful glare parameters

7.1 Introduction

The results of the previous studies have shown that none of the existing discomfort glare metrics are successful enough to predict glare across the classroom space. In this chapter an analysis of the parameters that form these metrics is done. The objective of the analysis is to identify if there is a range of parameters that are better predictors than others. A range of successful parameters can in principle be used to develop a model of discomfort glare that would produce a better fit to the conditions of the classroom space.

These parameters are called glare parameters in this chapter and they correspond to the variables that make up the different glare metrics' equations.

The metrics, as presented in the literature review (Chapter II), are generally based on a selection of the following parameters:

	Luminance parameter	Illuminance parameter
Adaptation parameter	Average luminance (L_{avg})	Vertical illuminance (E_v)
	Luminance of the task (L_t)	
Glare source parameter	Luminance of the glare source (L_s)	Illuminance of the glare source (E_{dir})
	Position index (P)	
	Solid angle of the glare source (ω_s)	
Background parameter	Background luminance (L_b)	Illuminance of the background (E_{ind})

The L_s and E_{dir} describe the contribution of the glare source, respectively measured by either its luminance or illuminance at the eye level. The L_b and E_{ind} describe the contribution of the background, respectively measured by either its luminance or illuminance at the eye level.

The L_{avg} and E_v are generally associated with the adaptation term of the glare equations, when they have one. When an equation has a contrast term, the L_{avg} , E_v , L_t and L_b appear in the denominator of that part of the equation (Figure 7.1).

The P and ω_s only appear in the contrast part of the equations, associated with the individual glare sources in each scene.

The diagram shows two equations with terms circled in red. The top equation is $UGR_{exp} = 8 \cdot \log L_{avg} + 3 \cdot \log \sum_{i=1}^n \frac{L_{s,i} \cdot \omega_{s,i}}{L_b \cdot P_i^2}$. The bottom equation is $DGP = 5.87 \cdot 10^{-5} \cdot E_v + 9.18 \cdot 10^{-2} \cdot \log(1 + \sum_{i=1}^n \frac{L_{s,i}^2 \cdot \omega_{s,i}}{E_v^{1.87} \cdot P_i^2}) + 0.16$. Red lines connect the labels 'Adaptation' and 'Contrast' to the circled terms in both equations.

FIG. 7.1 Adaptation and contrast terms in two equations. Note that in UGR_{exp} , L_{avg} is replaced by L_b in the contrast part of the equation.

These parameters are analysed in their basic form and in a range of different combinations corresponding to alternative definitions of adaptation and contrast indicators.

The general question of the study, is: are there parameters that have more predictive power than others and in that way are more appropriate for the definition of a new model of discomfort glare for the classroom?

In the context of this question, there are three aspects that are considered relevant to investigate:

- 1 The comparative performance of parameters representing the light contribution from the same area of a scene, specifically those corresponding to the glare source and those corresponding to the adaptation term;
- 2 The success of the luminance of the background and of the task area in the description of alternative forms of adaptation;
- 3 The comparative performance of different definitions of contrast;

The analysis is based on the data from the experimental Study I, since it corresponds to a larger data sample compared to the sample of Study II. A combination of the two datasets creates a wide variability in terms of the number of assessments per subject and per study condition, which is undesirable for most statistical tests and for the purpose of model development. Study I corresponds to a subject sample of 49 persons, which is comparable to other laboratory studies on daylight glare metrics (Van Den Wymelenberg and Inanici, 2014) (Konstantzos and Tzempelikos, 2017) in terms of population size. The study also occurred over a period of time that included summer and autumn conditions and a variety of sky types (clear, clear with clouds and overcast). For the analysis in this Chapter, a data point that is somewhat out of range (corresponding to the highest illuminance in the dataset) has been removed and the analysis is therefore based on 184 cases.

7.2 Glare parameters in the study

7.2.1 Basic parameters

As seen in the literature review, there can be several glare sources in one scene, each with a different luminance, size and position within that scene. In this study, a definition of the glare-source related parameters L_s , P and ω_s , is used that aggregates the individual glare source values of each scene into one indicator of the performance of those parameters.

For L_s , one of the indicators is the mean, referred to as L_{s_mean} , which as the name indicates corresponds to the mean luminance of all glare sources in a scene. In addition, the mean of the solid angle-weighted luminance of the glare sources L_{s_w} is also considered. This last indicator does in principle describe the luminance of the glare source parameter in a better way, as it takes the size of the individual glare sources into account. A comparison between these two will show how beneficial the inclusion of the size of the source in the definition of the glare source is.

As E_{dir} corresponds to the contribution of the source measured at the eye level, only the mean of the direct vertical illuminance of the glare sources is considered.

The size of the glare source, corresponding to the source solid angle, is looked specifically at from the perspective of the sum of the solid angles of all the glare sources in a scene (ω_{s_total}).

In terms of the position index, the chosen definition is the minimum P in a scene, $P_{_min}$. As lower values of P correspond to positions of a glare source near the central field of vision, a negative correlation between $P_{_min}$ and the reported glare is expected.

The higher the correlation between the above indicators and the glare votes, the better the performance of the indicator.

The considered parameters and indicators of the parameters are therefore:

- L_{avg} [cd/m^2]
- E_v [lux]
- L_b [cd/m^2]
- L_t [cd/m^2]
- L_{s_w} [cd/m^2]
- L_{s_mean} [cd/m^2]
- ω_{s_total} [steradians]
- $P_{_min}$ [-]
- E_{dir} [lux]
- E_{ind} [lux]

These are referred to as the basic parameters.

7.2.2 Adaptation ratio parameters

It is hypothesized that in the spatial conditions of a classroom, the luminance of the background L_b might influence adaptation, since L_b occupies a larger area within the field of view in comparison to the typical setting of the existing metrics' development whereby subjects sit near the window looking either parallel or towards it. Further away from the window, the size of the background in the field of view increases significantly for a reduction in the size of the window and generally of the glare source in comparison to that setting.

On the other hand, as subjects are focused on a task and generally under lower daylight levels in the larger space of a classroom, it is hypothesized that the luminance of the task might influence adaptation too.

To investigate this, new parameters E_v/L_t and E_v/L_b are analysed to find if they have greater predictive power than E_v alone. This analysis focuses on E_v instead of L_{avg} , as that parameter provided a slightly better result than L_{avg} in the previous analysis.

The new parameters are:

- E_v/L_b [lux.m²/cd]
- E_v/L_t [lux.m²/cd]

7.2.3 Contrast parameters

The contrast description in the glare indices does generally correspond to a ratio between the luminance of the glare source L_s and either E_v , L_{avg} , L_b or L_t .

These different definitions are tested in the study to find if there is one that has better predictive power than the other. The contrast parameters that are considered in the analysis are:

- L_{s_mean}/E_v [lux.cd/m²], general definition of contrast in DGP
- L_{s_mean}/L_{avg} [-], general definition of contrast in DGImod
- L_{s_mean}/L_t [-], general definition of contrast in metrics such as PGL and GSV

L_{s_mean} is also compared to the ratios to find how contrast is relevant in each condition, whereby a stronger correlation between L_{s_mean} and the reported glare would indicate that contrast is not as strong as a predictor as the mean luminance of the glare source by itself.

The results and analysis are presented in relation to three aspects:

- A1: comparison of L_{s_mean} to E_{dir} and comparison of E_v , L_{avg} , L_b and L_t
- A2: comparison of E_v/L_b and E_v/L_t to each other, and to E_v
- A3: comparison of L_{s_mean}/E_v , L_{s_mean}/L_{avg} and L_{s_mean}/L_t to each other, and to L_{s_mean}

The analysis also includes DGP, to provide some perspective on how the parameters compare to one of the glare indices.

7.3 Method

As mentioned in Chapter IV, the luminance images are processed in *evalglare* for the calculation of the metrics. The parameters of the present analysis are either directly extracted or calculated based on the output of the *evalglare* calculation.

The statistical analysis of the parameters and parameter indicators, described simply as parameters hereafter, is based on the analysis of the ROC curve and of the Spearman correlations of each parameter.

As explained previously, the ROC curve is a binomial classification method that involves the subdivision of the dependent variable, the glare votes, into two categories broadly defined as the 'glare' and 'no-glare' groups. For the analysis in this chapter, the curve is calculated for two binomial classifications: one whereby the cut-off point for glare perception is established at the 'any glare' level and the other where the cut-off point is established at the 'disturbing glare' level (Table 7.1). The first definition is called the 'any glare' definition and 'glare' group includes the 'noticeable', 'disturbing' and 'intolerable' glare votes (votes 2 to 4). The second definition is called the 'disturbing glare' definition and the 'glare' group includes the 'disturbing' and 'intolerable' glare votes (votes 3 and 4).

TABLE 7.1 Glare classifications used in the ROC curve definition.

Glare definition	No Glare	Glare
Any glare	imperceptible	noticeable
		disturbing
		intolerable
Disturbing glare	imperceptible	disturbing
	noticeable	intolerable

It is worth mentioning that the 'disturbing glare' definition is the definition that has been used in other studies concerning validation of glare metrics using ROC curve analysis (Wienold et al., 2017) (Wienold et al., 2019).

The parameters are compared based on the results of these three statistical tests: the 'any glare' ROC curve, the 'disturbing glare' ROC curve and the Spearman correlation. The first test expresses how good the prediction of low levels of glare is, the second test expresses how good the prediction of disturbing levels of glare and the third test expresses how good a parameter is in describing the full glare scale.

The statistical performance criteria used in the analysis are as previously defined in Chapter IV and used in Chapters V and VI. The analysis was done for the complete dataset (referred to as 'full') and for eight subsamples of the dataset, corresponding to the data for positions 1, 2, 3 and 4 and to four zones within the room - the window, the wall, the front and the back zone (Figure 7.2). An analysis based on different subdivisions of the dataset provide the possibility of understanding the performance of the glare parameters in the different positions of the room and of identifying any patterns of performance that might exist in different zones of the room.

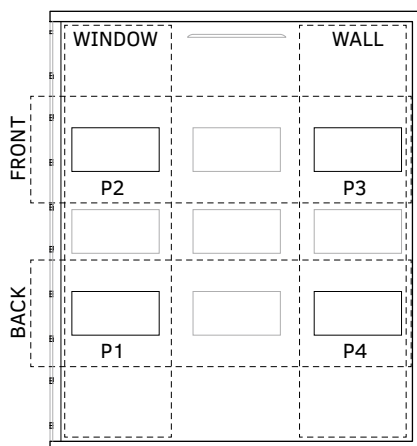


FIG. 7.2 Areas corresponding to the dataset subsamples: position 1 (P1), position 2 (P2), position 3 (P3), position 4 (P4), window zone (window), wall zone (wall), front zone (front) and back zone (back).

As the output of *evalglare* is an unstructured data file, the analysis required the use of scripting to read, calculate the new variables and parse the data for the different analysis and combinations of datasets. The process of preparing the data and performing the statistical analysis was carried out using the R programming language for statistical computing (R Core Team, 2020) and the RStudio development environment (RStudio Team, 2020).

7.4 Results

This section starts with the descriptive statistics of the glare parameters grouped into basic parameters, adaptation ratio parameters and contrast parameters. It then shows the results of the two ROC curves and of the Spearman correlation analysis.

7.4.1 Descriptive statistics

The distributions of the parameters for the full dataset are presented in Figures 7.3 to 7.5.

It can be observed that there is a tendency for a non-normal distribution for most of the parameters. Some plots also show a range of points that can be interpreted as potential outliers, here identified as values that are at a distance of more than 1.5 times the interquartile range from the median of the plot. Both the ROC curve and the Spearman correlation are non-parametric statistical methods that are based on ranked data and therefore the non-normality and the presence of these potential outliers is not considered a problem.

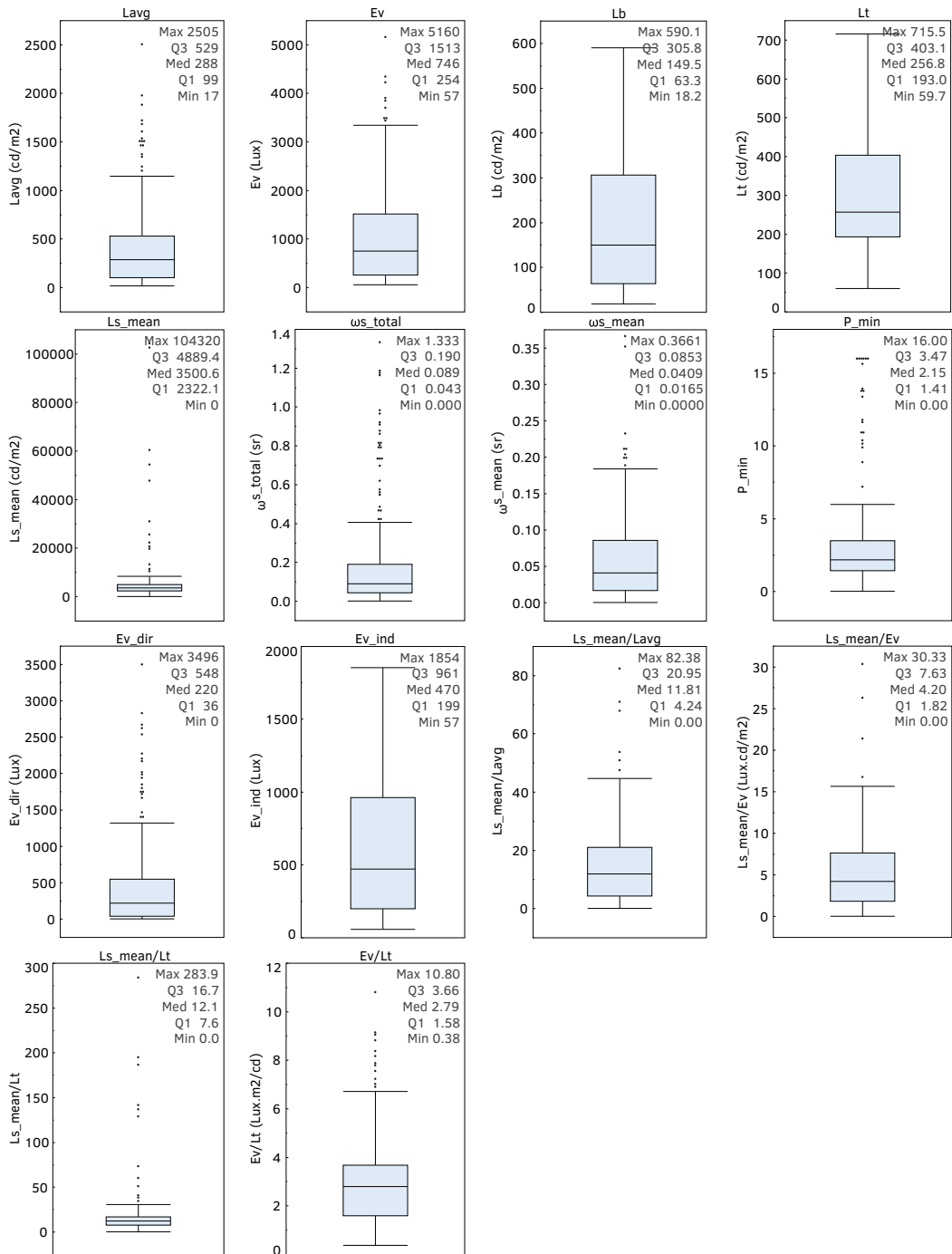


FIG. 7.3 Box plots for the basic parameters (complete dataset).

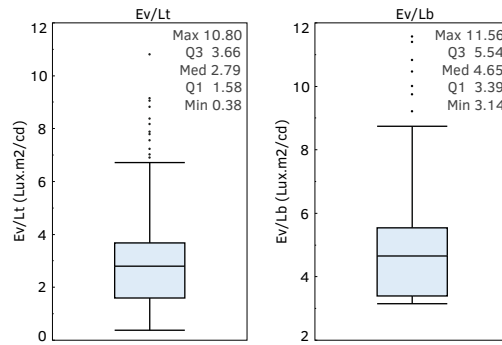


FIG. 7.4 Box plots of the adaptation ratios E_v/L_b and E_v/L_t (complete dataset).

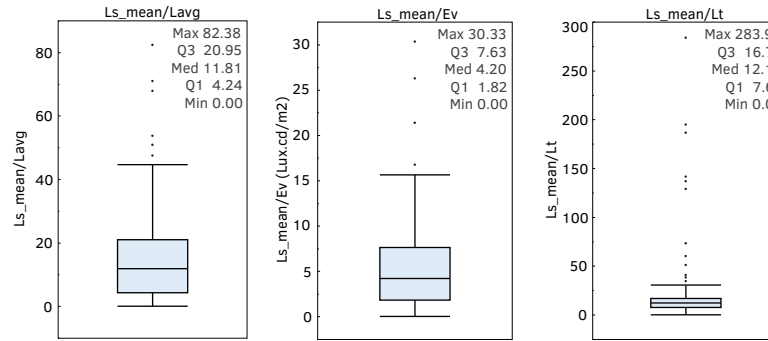


FIG. 7.5 Box plots of $L_{s,mean}/E_v$, $L_{s,mean}/L_{avg}$ and $L_{s,mean}/L_t$ (complete dataset).

7.4.2 ROC curve and Spearman correlation

The results for the statistics are presented in a series of tables, for the full dataset and for the zone subsamples, followed by an analysis of the results. There are three tables for each sample, the two ROC curve tables for the 'any glare' and 'disturbing glare' definitions and the Spearman correlation table.

The statistical performance criteria used in the analysis is as described in previous chapters and provided below (Tables 7.2 and 7.3).

The parameters are ranked from higher to lower AUC in the ROC tables and from higher to lower rho (ρ) in the Spearman table.

The analysis of aspects A1, A2 and A3 is presented after each statistical test. The results of DGP are plotted alongside the results of the glare parameters, for some perspective regarding their performance, increasing the number of the parameters in the tables to 17. The ROC curves' charts as well as the calculation of the parameters' cut-off values for the 'any glare' and 'disturbing glare' definitions can be found in the Appendix D.

TABLE 7.2 Performance criteria (Spearman).

	Fail	Pass	Good	Very Good
Spearman ρ	< 0.3	> 0.3	> 0.5	> 0.7
Significance	> 0.05	< 0.05		
Lower 95% CI	< 0.2	> 0.2		

TABLE 7.3 Performance criteria (ROC).

	Fail	Pass	Good	Very Good
AUC	< 0.6	> 0.6	> 0.7	> 0.8
Significance	> 0.05	< 0.05		
Lower 95% CI	< 0.5	> 0.5		
TPR, TNR	< 0.5	> 0.5		

7.4.2.1 Full room

TABLE 7.4 ρ -ranked Spearman correlation for the full room.

sample	#	parameter	ρ	sig.	95% lower	95% upper
					bound CI	bound CI
full	12	DGP	0.34	0.000	0.22	0.47
full	17	E_v/L_b	0.34	0.000	0.20	0.46
full	10	E_{dir}	0.32	0.000	0.19	0.45
full	6	L_{s_mean}	0.32	0.000	0.18	0.45
full	2	E_v	0.31	0.000	0.17	0.44
full	1	L_{avg}	0.28	0.000	0.14	0.40
full	16	E_v/L_t	0.27	0.000	0.13	0.41
full	5	L_{s_w}	0.27	0.000	0.14	0.41
full	4	L_t	0.26	0.000	0.12	0.39
full	7	ω_{s_total}	0.26	0.000	0.12	0.39
full	3	L_b	0.26	0.000	0.13	0.39
full	11	E_{ind}	0.26	0.000	0.13	0.39
full	15	L_{s_mean}/L_t	0.25	0.001	0.11	0.39
full	13	L_{s_mean}/L_{avg}	0.23	0.002	0.08	0.37
full	14	L_{s_mean}/E_v	0.20	0.005	0.05	0.34
full	8	ω_{s_mean}	0.18	0.015	0.03	0.32
full	9	P_{min}	0.01	0.878	-0.14	0.16

None of the parameters have a good performance.

A1 – parameters depicting same aspect of glare:

- L_{s_mean} same as E_{dir}
- E_v better than L_{avg} and better than L_b and L_t

A2 – adaptation ratio parameters:

- E_v/L_b performs better than E_v and than E_v/L_t

A3 – contrast parameters:

- None of the contrast parameters pass the test
- None of the contrast parameters perform better than L_{s_mean}

TABLE 7.5 AUC-ranked ROC curve results for any glare for the full room

sample	#	parameter	AUC	sig.	95% lower	95% upper	TPR	TNR
					bound CI	bound CI		
full	17	E_v/L_b	0.68	0.000	0.61	0.76	0.66	0.68
full	12	DGP	0.68	0.000	0.60	0.76	0.75	0.61
full	10	E_{dir}	0.67	0.000	0.59	0.75	0.75	0.60
full	6	L_{s_mean}	0.66	0.000	0.58	0.74	0.66	0.61
full	2	E_v	0.66	0.000	0.58	0.74	0.68	0.55
full	5	L_{s_w}	0.65	0.001	0.56	0.73	0.70	0.60
full	4	L_t	0.64	0.001	0.56	0.72	0.57	0.68
full	16	E_v/L_t	0.64	0.001	0.56	0.72	0.60	0.63
full	7	ω_{s_total}	0.64	0.001	0.56	0.72	0.70	0.55
full	1	L_{avg}	0.64	0.001	0.56	0.72	0.57	0.65
full	3	L_b	0.63	0.002	0.55	0.72	0.70	0.52
full	11	E_{ind}	0.63	0.002	0.55	0.72	0.70	0.52
full	15	L_{s_mean}/L_t	0.62	0.004	0.53	0.70	0.52	0.65
full	13	L_{s_mean}/L_{avg}	0.60	0.015	0.51	0.68	0.54	0.58
full	8	ω_{s_mean}	0.58	0.030	0.50	0.67	0.77	0.42
full	14	L_{s_mean}/E_v	0.58	0.042	0.49	0.66	0.58	0.52
full	9	P_{min}	0.49	0.584	0.40	0.58	0.58	0.50

A wide range of parameters passes the test. None of the parameters have a good performance.

A1 – parameters depicting same aspect of glare:

- L_{s_mean} similar to E_{dir}
- E_v is better than L_{avg} and better than L_b and L_t

A2 – adaptation ratio parameters:

- E_v/L_b performs better than E_v and somewhat better than E_v/L_t

A3 – contrast parameters:

- L_{s_mean}/L_t performs better than L_{s_mean}/L_{avg} and than L_{s_mean}/E_v
- None of the contrast parameters performs better than L_{s_mean}

TABLE 7.6 AUC-ranked ROC curve for disturbing glare for the full room

sample	#	parameter	AUC	sig.	95% lower	95% upper	TPR	TNR
					bound CI	bound CI		
full	12	DGP	0.69	0.000	0.59	0.79	0.56	0.72
full	6	L_{s_mean}	0.69	0.000	0.59	0.79	0.59	0.69
full	2	E_v	0.68	0.000	0.58	0.78	0.54	0.75
full	10	E_{dir}	0.67	0.000	0.58	0.77	0.54	0.72
full	17	E_v/L_b	0.67	0.000	0.57	0.77	0.76	0.52
full	13	L_{s_mean}/L_{avg}	0.67	0.001	0.57	0.77	0.61	0.59
full	15	L_{s_mean}/L_t	0.67	0.001	0.57	0.77	0.56	0.71
full	14	L_{s_mean}/E_v	0.66	0.001	0.56	0.76	0.51	0.76
full	1	L_{avg}	0.66	0.001	0.56	0.76	0.63	0.63
full	16	E_v/L_t	0.66	0.001	0.56	0.76	0.63	0.57
full	3	L_b	0.64	0.003	0.54	0.74	0.59	0.66
full	11	E_{ind}	0.64	0.003	0.54	0.74	0.59	0.66
full	5	L_{s_w}	0.64	0.004	0.54	0.74	0.71	0.55
full	7	ω_{s_total}	0.64	0.004	0.54	0.74	0.61	0.59
full	4	L_t	0.63	0.005	0.53	0.73	0.56	0.68
full	8	ω_{s_mean}	0.61	0.015	0.51	0.71	0.51	0.64
full	9	P_{min}	0.53	0.266	0.43	0.63	0.61	0.46

A wide range of parameters passes the test. None of the parameters have a good performance.

A1 – parameters depicting same aspect of glare:

- L_{s_mean} marginally better than E_{dir}
- E_v better than L_{avg} and better than L_b and L_t

A2 – adaptation ratio parameters:

- E_v marginally better than E_v/L_b and than E_v/L_t

A3 – contrast parameters:

- Contrast parameters perform similarly
- None of the contrast parameters performs better than L_{s_mean}

7.4.2.2 Position 1

TABLE 7.7 ρ -ranked Spearman correlation for position 1

sample	#	parameter	ρ	sig.	95% lower	95% upper
					bound CI	bound CI
P1	17	E_v/L_b	0.60	0.000	0.36	0.79
P1	6	L_{s_mean}	0.53	0.000	0.27	0.76
P1	10	E_{dir}	0.49	0.001	0.24	0.71
P1	16	E_v/L_t	0.48	0.001	0.22	0.70
P1	12	DGP	0.48	0.001	0.22	0.69
P1	2	E_v	0.47	0.002	0.20	0.67
P1	7	ω_{s_total}	0.44	0.003	0.13	0.66
P1	1	L_{avg}	0.43	0.004	0.16	0.64
P1	15	L_{s_mean}/L_t	0.42	0.005	0.11	0.68
P1	5	L_{s_w}	0.39	0.009	0.10	0.62
P1	4	L_t	0.37	0.014	0.08	0.61
P1	3	L_b	0.34	0.026	0.05	0.55
P1	11	E_{ind}	0.34	0.026	0.07	0.56
P1	8	ω_{s_mean}	0.31	0.043	-0.01	0.59
P1	14	L_{s_mean}/E_v	0.22	0.157	-0.15	0.53
P1	13	L_{s_mean}/L_{avg}	0.20	0.195	-0.14	0.51
P1	9	P_{min}	-0.10	0.544	-0.41	0.23

A wide range of parameters have good performance. E_v/L_b and L_{s_mean} have very good performance.

A1 – parameters depicting same aspect of glare:

- L_{s_mean} has better performance than E_{dir}
- E_v has better performance than L_{avg} and better performance than L_b and L_t

A2 – adaptation ratio parameters:

- E_v/L_b has a better performance than E_v/L_t and than E_v

A3 - contrast parameters:

- L_{s_mean}/L_t performs better than L_{s_mean}/L_{avg} and than L_{s_mean}/E_v
- None of the contrast parameters performs better than L_{s_mean}

TABLE 7.8 AUC-ranked ROC curve results for any glare for position 1

sample	#	parameter	AUC	sig.	95% lower	95% upper	TPR	TNR
					bound CI	bound CI		
P1	17	E_v/L_b	0.82	0.000	0.70	0.95	0.75	0.80
P1	10	E_{dir}	0.78	0.001	0.65	0.92	0.79	0.67
P1	12	DGP	0.78	0.002	0.64	0.92	0.61	0.87
P1	2	E_v	0.78	0.002	0.64	0.91	0.61	0.87
P1	6	L_{s_mean}	0.78	0.002	0.64	0.91	0.71	0.73
P1	16	E_v/L_t	0.77	0.002	0.63	0.91	0.79	0.67
P1	1	L_{avg}	0.76	0.003	0.62	0.91	0.57	0.93
P1	5	L_{s_w}	0.76	0.003	0.61	0.90	0.71	0.73
P1	7	ω_{s_total}	0.76	0.003	0.61	0.90	0.75	0.67
P1	3	L_b	0.73	0.007	0.58	0.88	0.79	0.60
P1	4	L_t	0.73	0.007	0.58	0.88	0.61	0.80
P1	11	E_{ind}	0.73	0.007	0.58	0.88	0.79	0.60
P1	8	ω_{s_mean}	0.70	0.016	0.54	0.86	0.79	0.60
P1	15	L_{s_mean}/L_t	0.69	0.022	0.53	0.85	0.61	0.87
P1	14	L_{s_mean}/E_v	0.56	0.270	0.38	0.74	0.43	0.67
P1	13	L_{s_mean}/L_{avg}	0.55	0.305	0.37	0.73	0.43	0.67
P1	9	P_{min}	0.50	0.515	0.31	0.68	0.71	0.47

A wide range of parameters have good performance. E_v/L_b has very good performance.

A1 – parameters depicting same aspect of glare:

- L_{s_mean} has similar performance to E_{dir}
- E_v has marginally better performance than L_{avg} , and better than L_b and L_t

A2 – adaptation ratio parameters:

- E_v/L_b has a better performance than E_v/L_t and than E_v

A3 – contrast parameters:

- L_{s_mean}/L_t performs better than L_{s_mean}/L_{avg} and than L_{s_mean}/E_v

TABLE 7.9 AUC-ranked ROC curve for disturbing glare for position 1

sample	#	parameter	AUC	sig.	95% lower	95% upper	TPR	TNR
					bound CI	bound CI		
P1	17	E_v/L_b	0.82	0.002	0.64	1.00	0.78	0.85
P1	6	L_{s_mean}	0.81	0.003	0.62	0.99	0.78	0.82
P1	15	L_{s_mean}/L_t	0.78	0.005	0.59	0.97	0.78	0.76
P1	16	E_v/L_t	0.75	0.013	0.55	0.94	0.78	0.76
P1	10	E_{dir}	0.73	0.017	0.53	0.94	0.78	0.79
P1	12	DGP	0.72	0.022	0.52	0.93	0.78	0.74
P1	14	L_{s_mean}/E_v	0.72	0.024	0.51	0.92	0.56	1.00
P1	2	E_v	0.71	0.027	0.51	0.92	0.78	0.74
P1	13	L_{s_mean}/L_{avg}	0.71	0.030	0.50	0.91	0.56	0.94
P1	7	ω_{s_total}	0.70	0.034	0.49	0.91	0.67	0.82
P1	1	L_{avg}	0.68	0.055	0.47	0.89	0.78	0.74
P1	4	L_t	0.65	0.087	0.44	0.86	0.67	0.65
P1	5	L_{s_w}	0.64	0.110	0.42	0.85	0.78	0.59
P1	8	ω_{s_mean}	0.61	0.162	0.39	0.83	0.78	0.50
P1	3	L_b	0.60	0.173	0.39	0.82	0.67	0.62
P1	11	E_{ind}	0.60	0.173	0.39	0.82	0.67	0.62
P1	9	P_{min}	0.37	0.890	0.17	0.56	0.56	0.35

A wide range of parameters have good performance. E_v/L_b and L_{s_mean} have a very good performance.

A1 – parameters depicting same aspect of glare:

- L_{s_mean} has better performance than E_{dir}
- E_v has better performance than L_{avg} , L_b and L_t

A2 – adaptation ratio parameters:

- E_v/L_b has a better performance than E_v/L_t and than E_v

A3 – contrast parameters:

- L_{s_mean}/L_t performs better than L_{s_mean}/L_{avg} and than L_{s_mean}/E_v
- L_{s_mean}/L_t does not perform better than L_{s_mean}

7.4.2.3 Position 2

TABLE 7.10 ρ -ranked Spearman correlation for position 2

sample	#	parameter	ρ	sig.	95% lower	95% upper
					bound CI	bound CI
P2	6	L_{s_mean}	0.41	0.004	0.11	0.64
P2	2	E_v	0.40	0.005	0.13	0.65
P2	12	DGP	0.39	0.006	0.10	0.65
P2	10	E_{dir}	0.38	0.008	0.10	0.63
P2	16	E_v/L_t	0.38	0.009	0.12	0.61
P2	1	L_{avg}	0.38	0.009	0.10	0.64
P2	3	L_b	0.37	0.010	0.11	0.63
P2	11	E_{ind}	0.37	0.010	0.10	0.62
P2	5	L_{s_w}	0.36	0.014	0.08	0.61
P2	17	E_v/L_b	0.35	0.016	0.05	0.59
P2	4	L_t	0.34	0.019	0.04	0.59
P2	7	ω_{s_total}	0.30	0.040	0.01	0.55
P2	15	L_{s_mean}/L_t	0.29	0.048	-0.02	0.52
P2	8	ω_{s_mean}	0.22	0.141	-0.07	0.48
P2	13	L_{s_mean}/L_{avg}	0.18	0.223	-0.12	0.47
P2	14	L_{s_mean}/E_v	0.17	0.244	-0.12	0.47
P2	9	P_{min}	-0.03	0.846	-0.33	0.28

A wide range of parameters pass the test. L_{s_mean} and E_v have a good performance.

A1 – parameters depicting same aspect of glare:

- L_{s_mean} performs better than E_{dir}
- E_v has better performance than L_{avg} , L_b and L_t

A2 – adaptation ratio parameters:

- E_v has better performance than E_v/L_t and E_v/L_b

A3 – contrast parameters:

- L_{s_mean}/L_t , L_{s_mean}/L_{avg} and L_{s_mean}/E_v perform poorly
- L_{s_mean} performs better than any of the contrast parameters

TABLE 7.11 AUC-ranked ROC curve results for any glare for position 2

sample	#	parameter	AUC	sig.	95% lower	95% upper	TPR	TNR
					bound CI	bound CI		
P2	2	E_v	0.69	0.011	0.54	0.84	0.69	0.76
P2	3	L_b	0.69	0.013	0.54	0.84	0.69	0.76
P2	11	E_{ind}	0.69	0.013	0.54	0.84	0.69	0.76
P2	12	DGP	0.69	0.013	0.54	0.84	0.69	0.76
P2	1	L_{avg}	0.68	0.016	0.53	0.83	0.69	0.71
P2	4	L_t	0.68	0.019	0.52	0.83	0.65	0.76
P2	16	E_v/L_t	0.68	0.019	0.52	0.83	0.69	0.76
P2	10	E_{dir}	0.67	0.023	0.52	0.82	0.65	0.71
P2	6	L_{s_mean}	0.66	0.031	0.50	0.82	0.73	0.52
P2	5	L_{s_w}	0.66	0.033	0.50	0.81	0.62	0.71
P2	17	E_v/L_b	0.63	0.061	0.47	0.79	0.73	0.57
P2	7	ω_{s_total}	0.63	0.072	0.47	0.79	0.50	0.76
P2	15	L_{s_mean}/L_t	0.58	0.167	0.42	0.75	0.77	0.48
P2	8	ω_{s_mean}	0.55	0.274	0.39	0.72	0.77	0.43
P2	13	L_{s_mean}/L_{avg}	0.53	0.374	0.36	0.70	0.88	0.38
P2	14	L_{s_mean}/E_v	0.53	0.374	0.36	0.70	0.88	0.38
P2	9	P_{min}	0.43	0.805	0.26	0.59	0.85	0.38

A wide range of parameters passes the test with the top parameters showing very similar performance. None of the parameters have a good performance.

A1 – parameters depicting same aspect of glare:

- L_{s_mean} and E_{dir} have similar performance
- E_v , L_{avg} , L_b and L_t have similar performance

A2 – adaptation ratio parameters:

- E_v perform similarly to E_v/L_t and better than E_v/L_b

A3 – contrast parameters:

- L_{s_mean}/L_t , L_{s_mean}/L_{avg} and L_{s_mean}/E_v perform poorly
- L_{s_mean} performs better than any of the contrast parameters

TABLE 7.12 AUC-ranked ROC curve for disturbing glare for position 2

sample	#	parameter	AUC	sig.	95% lower	95% upper	TPR	TNR
					bound CI	bound CI		
P2	6	L_{s_mean}	0.81	0.001	0.66	0.97	0.69	0.94
P2	15	L_{s_mean}/L_t	0.79	0.001	0.63	0.95	0.69	0.79
P2	17	E_v/L_b	0.77	0.002	0.60	0.93	0.69	0.68
P2	10	E_{dir}	0.75	0.004	0.58	0.92	0.77	0.65
P2	2	E_v	0.74	0.005	0.57	0.91	0.62	0.85
P2	12	DGP	0.74	0.006	0.57	0.91	0.62	0.79
P2	16	E_v/L_t	0.74	0.006	0.56	0.91	0.62	0.82
P2	5	L_{s_w}	0.73	0.008	0.56	0.90	0.69	0.76
P2	13	L_{s_mean}/L_{avg}	0.73	0.008	0.56	0.90	0.69	0.71
P2	1	L_{avg}	0.72	0.010	0.55	0.90	0.62	0.85
P2	14	L_{s_mean}/E_v	0.72	0.011	0.54	0.89	0.69	0.68
P2	8	ω_{s_mean}	0.71	0.013	0.54	0.89	0.85	0.53
P2	7	ω_{s_total}	0.71	0.015	0.53	0.88	0.62	0.74
P2	3	L_b	0.71	0.015	0.53	0.88	0.69	0.68
P2	11	E_{ind}	0.71	0.015	0.53	0.88	0.69	0.68
P2	4	L_t	0.68	0.031	0.50	0.86	0.62	0.71
P2	9	P_{min}	0.58	0.189	0.40	0.77	0.92	0.44

A wide range of parameters have good performance. L_{s_mean} has a very good performance.

A1 – parameters depicting same aspect of glare:

- L_{s_mean} has a better performance than E_{dir}
- E_v is better than L_{avg} and better than L_b and L_t

A2 – adaptation ratio parameters:

- E_v/L_b has a somewhat better performance than E_v and than E_v/L_t

A3 – contrast parameters:

- L_{s_mean}/L_t has better performance than L_{s_mean}/L_{avg} and than L_{s_mean}/E_v
- L_{s_mean} performs better than any of the contrast parameters

7.4.2.4 Position 3

TABLE 7.13 ρ -ranked Spearman correlation for position 3

sample	#	parameter	ρ	sig.	95% lower	95% upper
					bound CI	bound CI
P3	13	L_{s_mean}/L_{avg}	0.33	0.025	0.05	0.56
P3	14	L_{s_mean}/E_v	0.31	0.037	0.01	0.55
P3	15	L_{s_mean}/L_t	0.24	0.108	-0.04	0.50
P3	7	ω_{s_total}	0.23	0.131	-0.08	0.46
P3	17	E_v/L_b	0.21	0.160	-0.09	0.51
P3	2	E_v	0.21	0.166	-0.08	0.45
P3	1	L_{avg}	0.20	0.186	-0.07	0.44
P3	10	E_{dir}	0.19	0.211	-0.11	0.46
P3	3	L_b	0.18	0.229	-0.10	0.44
P3	11	E_{ind}	0.18	0.229	-0.12	0.43
P3	12	DGP	0.18	0.235	-0.11	0.45
P3	8	ω_{s_mean}	0.17	0.256	-0.15	0.45
P3	9	P_{min}	0.16	0.282	-0.17	0.47
P3	4	L_t	0.16	0.293	-0.14	0.39
P3	5	L_{s_w}	0.15	0.316	-0.17	0.42
P3	16	E_v/L_t	0.14	0.363	-0.17	0.42
P3	6	L_{s_mean}	0.13	0.397	-0.19	0.41

L_{s_mean}/L_{avg} and L_{s_mean}/E_v pass the test, but none of the parameters show a good performance. No conclusions can be taken regarding the relative performance of the parameters as most have non-significant correlations.

TABLE 7.14 AUC-ranked ROC curve results for any glare for position 3

sample	#	parameter	AUC	sig.	95% lower	95% upper	TPR	TNR
					bound CI	bound CI		
P3	13	L_{s_mean}/L_{avg}	0.71	0.023	0.54	0.88	0.72	0.60
P3	7	ω_{s_total}	0.70	0.026	0.53	0.87	0.75	0.60
P3	14	L_{s_mean}/E_v	0.70	0.030	0.53	0.87	0.72	0.60
P3	2	E_v	0.68	0.046	0.50	0.85	0.69	0.60
P3	15	L_{s_mean}/L_t	0.68	0.045	0.50	0.85	0.67	0.70
P3	1	L_{avg}	0.68	0.048	0.50	0.85	0.89	0.50
P3	3	L_b	0.66	0.064	0.48	0.84	0.64	0.60
P3	10	E_{dir}	0.66	0.062	0.48	0.84	0.78	0.60
P3	11	E_{ind}	0.66	0.064	0.48	0.84	0.64	0.60
P3	12	DGP	0.66	0.064	0.48	0.84	0.78	0.60
P3	17	E_v/L_b	0.64	0.086	0.46	0.83	0.81	0.60
P3	4	L_t	0.64	0.091	0.46	0.83	0.83	0.50
P3	9	P_{min}	0.63	0.102	0.45	0.82	0.83	0.60
P3	16	E_v/L_t	0.63	0.110	0.44	0.82	0.83	0.60
P3	5	L_{s_w}	0.63	0.117	0.44	0.81	0.72	0.60
P3	6	L_{s_mean}	0.63	0.117	0.44	0.81	0.89	0.50
P3	8	ω_{s_mean}	0.62	0.134	0.43	0.81	0.89	0.50

A range of parameters passes the AUC and the p tests. L_{s_mean}/L_{avg} and ω_{s_total} show a good performance.

A1 – parameters depicting same aspect of glare:

- E_{dir} and L_{s_mean} have a non-significant AUC
- E_v has a similar performance to L_{avg} ; L_b and L_t have a non-significant AUC

A2 – adaptation ratio parameters:

- E_v performs better than the adaptation ratios, all of which have a non-significant AUC

A3 – contrast parameters:

- L_{s_mean}/L_{avg} performs marginally better than L_{s_mean}/E_v and than L_{s_mean}/L_t
- The contrast parameters have better performance than L_{s_mean}

TABLE 7.15 AUC-ranked ROC curve for disturbing glare for position 3

sample	#	parameter	AUC	sig.	95% lower	95% upper	TPR	TNR
					bound CI	bound CI		
P3	13	L_{s_mean}/L_{avg}	0.66	0.052	0.47	0.86	0.55	0.80
P3	14	L_{s_mean}/E_v	0.65	0.067	0.46	0.85	0.55	0.80
P3	17	E_v/L_b	0.59	0.180	0.40	0.79	0.82	0.43
P3	15	L_{s_mean}/L_t	0.59	0.183	0.39	0.79	0.73	0.57
P3	8	ω_{s_mean}	0.56	0.268	0.36	0.76	0.64	0.51
P3	9	P_{min}	0.56	0.272	0.36	0.76	0.73	0.49
P3	2	E_v	0.55	0.306	0.35	0.75	0.45	0.66
P3	7	ω_{s_total}	0.55	0.321	0.35	0.75	0.82	0.37
P3	10	E_{dir}	0.55	0.321	0.35	0.75	0.91	0.37
P3	1	L_{avg}	0.55	0.333	0.35	0.75	0.45	0.66
P3	5	L_{s_w}	0.54	0.349	0.34	0.74	0.73	0.43
P3	3	L_b	0.54	0.361	0.34	0.74	0.91	0.37
P3	11	E_{ind}	0.54	0.361	0.34	0.74	0.91	0.37
P3	12	DGP	0.54	0.361	0.34	0.74	0.91	0.37
P3	4	L_t	0.53	0.380	0.33	0.73	0.73	0.40
P3	16	E_v/L_t	0.52	0.420	0.32	0.72	0.45	0.66
P3	6	L_{s_mean}	0.51	0.459	0.31	0.71	0.91	0.34

All parameters have a non-significant AUC and their differences of performance are too small to warrant any conclusions regarding their relative performance.

7.4.2.5 Position 4

TABLE 7.16 ρ -ranked Spearman correlation for position 4

sample	#	parameter	ρ	sig.	95% lower	95% upper
					bound CI	bound CI
P4	7	ω_{s_total}	0.22	0.129	-0.04	0.46
P4	3	L_b	0.21	0.159	-0.08	0.46
P4	11	E_{ind}	0.21	0.159	-0.07	0.48
P4	2	E_v	0.20	0.176	-0.11	0.45
P4	1	L_{avg}	0.19	0.185	-0.11	0.46
P4	12	DGP	0.19	0.187	-0.09	0.46
P4	17	E_v/L_b	0.19	0.202	-0.09	0.43
P4	4	L_t	0.18	0.211	-0.10	0.44
P4	10	E_{dir}	0.18	0.222	-0.10	0.43
P4	5	L_{s_w}	0.15	0.314	-0.14	0.42
P4	16	E_v/L_t	0.13	0.379	-0.17	0.42
P4	15	L_{s_mean}/L_t	0.11	0.472	-0.19	0.38
P4	6	L_{s_mean}	0.10	0.484	-0.16	0.36
P4	8	ω_{s_mean}	0.09	0.549	-0.19	0.36
P4	9	P_{min}	0.04	0.789	-0.26	0.32
P4	13	L_{s_mean}/L_{avg}	0.04	0.802	-0.26	0.32
P4	14	L_{s_mean}/E_v	0.03	0.824	-0.27	0.33

All parameters fail the correlation test and have a non-significant correlation to glare.

TABLE 7.17 AUC-ranked ROC curve results for any glare for position 4

sample	#	parameter	AUC	sig.	95% lower	95% upper	TPR	TNR
					bound CI	bound CI		
P4	17	E_v/L_b	0.63	0.077	0.47	0.79	0.75	0.63
P4	15	L_{s_mean}/L_t	0.59	0.154	0.42	0.76	0.63	0.63
P4	7	ω_{s_total}	0.58	0.181	0.41	0.75	0.72	0.50
P4	10	E_{dir}	0.56	0.245	0.39	0.73	0.72	0.50
P4	12	DGP	0.56	0.254	0.39	0.73	0.69	0.50
P4	2	E_v	0.56	0.261	0.39	0.73	0.75	0.50
P4	3	L_b	0.56	0.261	0.39	0.73	0.72	0.50
P4	11	E_{ind}	0.56	0.261	0.39	0.73	0.72	0.50
P4	1	L_{avg}	0.56	0.269	0.39	0.73	0.75	0.50
P4	6	L_{s_mean}	0.56	0.266	0.39	0.73	0.63	0.56
P4	13	L_{s_mean}/L_{avg}	0.54	0.319	0.37	0.72	0.69	0.50
P4	14	L_{s_mean}/E_v	0.54	0.326	0.37	0.71	0.47	0.69
P4	16	E_v/L_t	0.54	0.329	0.37	0.71	0.81	0.50
P4	4	L_t	0.54	0.344	0.36	0.71	0.53	0.56
P4	8	ω_{s_mean}	0.54	0.350	0.36	0.71	0.66	0.44
P4	5	L_{s_w}	0.53	0.375	0.36	0.70	0.81	0.44
P4	9	P_{min}	0.52	0.409	0.35	0.70	0.69	0.44

Most parameters fail the AUC test and have non-significant discriminatory power.

TABLE 7.18 AUC-ranked ROC curve for disturbing glare for position 4

sample	#	parameter	AUC	sig.	95% lower	95% upper	TPR	TNR
					bound CI	bound CI		
P4	4	L_t	0.73	0.022	0.52	0.94	0.75	0.70
P4	3	L_b	0.72	0.025	0.51	0.94	0.75	0.65
P4	11	E_{ind}	0.72	0.025	0.51	0.94	0.75	0.65
P4	2	E_v	0.71	0.033	0.49	0.92	0.75	0.60
P4	1	L_{avg}	0.71	0.035	0.49	0.92	0.63	0.73
P4	7	ω_{s_total}	0.70	0.039	0.48	0.92	0.63	0.70
P4	12	DGP	0.70	0.042	0.48	0.91	0.88	0.53
P4	5	L_{s_w}	0.68	0.052	0.47	0.90	0.63	0.68
P4	10	E_{dir}	0.67	0.069	0.45	0.89	1.00	0.50
P4	16	E_v/L_t	0.63	0.128	0.41	0.86	0.63	0.63
P4	8	ω_{s_mean}	0.58	0.257	0.35	0.80	0.75	0.43
P4	6	L_{s_mean}	0.56	0.314	0.33	0.78	0.88	0.43
P4	17	E_v/L_b	0.55	0.337	0.33	0.77	1.00	0.45
P4	9	P_{min}	0.52	0.428	0.30	0.75	1.00	0.33
P4	15	L_{s_mean}/L_t	0.49	0.539	0.27	0.71	0.38	0.83
P4	13	L_{s_mean}/L_{avg}	0.48	0.593	0.26	0.69	0.38	0.65
P4	14	L_{s_mean}/E_v	0.47	0.604	0.25	0.69	0.38	0.65

A range of parameters pass the AUC test. L_t , L_b and E_{ind} have a good performance and very similar performance.

A1 – parameters depicting same aspect of glare:

- Neither L_{s_mean} nor E_{dir} show a significant AUC
- E_v and L_{avg} have similar performance, but not better than L_b and L_t

A2 – adaptation ratio parameters:

- E_v is better than any of the adaptation ratios, E_v/L_t and E_v/L_b

A3 – contrast parameters:

- Contrast parameters perform rather poorly, as well as L_{s_mean}

7.4.2.6 Window zone

TABLE 7.19 ρ -ranked Spearman correlation for the window zone

sample	#	parameter	ρ	sig.	95% lower	95% upper
					bound CI	bound CI
window	6	L_{s_mean}	0.47	0.000	0.28	0.63
window	12	DGP	0.42	0.000	0.25	0.59
window	16	E_v/L_t	0.42	0.000	0.24	0.58
window	2	E_v	0.41	0.000	0.23	0.58
window	17	E_v/L_b	0.40	0.000	0.22	0.56
window	10	E_{dir}	0.40	0.000	0.21	0.58
window	1	L_{avg}	0.39	0.000	0.20	0.56
window	5	L_{s_w}	0.37	0.000	0.18	0.54
window	7	ω_{s_total}	0.35	0.001	0.15	0.52
window	3	L_b	0.35	0.001	0.16	0.52
window	11	E_{ind}	0.35	0.001	0.16	0.52
window	4	L_t	0.35	0.001	0.15	0.53
window	15	L_{s_mean}/L_t	0.33	0.001	0.11	0.52
window	8	ω_{s_mean}	0.27	0.011	0.08	0.45
window	13	L_{s_mean}/L_{avg}	0.21	0.043	-0.02	0.41
window	14	L_{s_mean}/E_v	0.21	0.046	-0.03	0.42
window	9	P_{min}	-0.06	0.579	-0.28	0.15

A wide range of parameters pass the test. L_{s_mean} , E_v/L_t , E_v , E_v/L_b and E_{dir} have good performance.

A1 – parameters depicting same aspect of glare:

- L_{s_mean} better than E_{dir}
- E_v is better than L_{avg} and better than L_b and L_t

A2 – adaptation ratio parameters:

- E_v/L_t marginally better than E_v and E_v/L_b

A3 – contrast parameters:

- L_{s_mean}/L_t better than L_{s_mean}/L_{avg} and L_{s_mean}/E_v , but does not perform better than L_{s_mean}

TABLE 7.20 AUC-ranked ROC curve results for any glare for the window zone

sample	#	parameter	AUC	sig.	95% lower	95% upper	TPR	TNR
					bound CI	bound CI		
window	12	DGP	0.73	0.000	0.63	0.83	0.74	0.69
window	2	E_v	0.72	0.000	0.62	0.83	0.70	0.69
window	16	E_v/L_t	0.72	0.000	0.62	0.83	0.74	0.69
window	1	L_{s_avg}	0.72	0.000	0.61	0.82	0.72	0.67
window	10	E_{dir}	0.72	0.000	0.61	0.82	0.70	0.67
window	6	L_{s_mean}	0.72	0.000	0.61	0.82	0.65	0.67
window	17	E_v/L_b	0.71	0.000	0.61	0.82	0.74	0.58
window	5	L_{s_w}	0.70	0.001	0.60	0.81	0.69	0.69
window	3	L_b	0.70	0.001	0.60	0.81	0.63	0.75
window	11	E_{ind}	0.70	0.001	0.60	0.81	0.63	0.75
window	4	L_t	0.70	0.001	0.59	0.81	0.63	0.78
window	7	ω_{s_total}	0.70	0.001	0.59	0.80	0.61	0.75
window	8	ω_{s_mean}	0.65	0.007	0.54	0.77	0.56	0.69
window	15	L_{s_mean}/L_t	0.62	0.024	0.51	0.74	0.52	0.72
window	14	L_{s_mean}/E_v	0.55	0.225	0.43	0.67	0.81	0.36
window	13	L_{s_mean}/L_{avg}	0.55	0.235	0.42	0.67	0.83	0.36
window	9	P_{min}	0.45	0.805	0.32	0.57	0.59	0.44

A wide range of parameters have a good performance, but they tend to perform rather similarly (very similar AUC and confidence intervals).

A1 – parameters depicting same aspect of glare:

- E_{dir} and L_{s_mean} have similar performance
- E_v and L_{s_avg} perform similarly and slightly better than L_b and L_t

A2 – adaptation ratio parameters:

- E_v , E_v/L_t and E_v/L_b have similar performance

A3 – contrast parameters:

- L_{s_mean}/L_t is the only of the contrast parameters that passes the test
- L_{s_mean} has a better performance than L_{s_mean}/L_t

TABLE 7.21 AUC-ranked ROC curve for disturbing glare for the window zone

sample	#	parameter	AUC	sig.	95% lower	95% upper	TPR	TNR
					bound CI	bound CI		
window	6	L_{s_mean}	0.80	0.000	0.68	0.92	0.73	0.88
window	15	L_{s_mean}/L_t	0.78	0.000	0.66	0.90	0.73	0.76
window	13	L_{s_mean}/L_{avg}	0.74	0.000	0.61	0.87	0.59	0.84
window	14	L_{s_mean}/E_v	0.73	0.001	0.60	0.86	0.73	0.63
window	16	E_v/L_t	0.73	0.001	0.59	0.86	0.73	0.69
window	17	E_v/L_b	0.72	0.001	0.59	0.85	0.59	0.75
window	12	DGP	0.72	0.001	0.59	0.85	0.64	0.81
window	2	E_v	0.71	0.001	0.58	0.85	0.64	0.81
window	10	E_{dir}	0.71	0.002	0.57	0.84	0.59	0.76
window	1	L_{avg}	0.69	0.004	0.56	0.83	0.68	0.72
window	5	L_{s_w}	0.68	0.005	0.55	0.82	0.73	0.68
window	7	ω_{s_total}	0.67	0.009	0.53	0.81	0.64	0.65
window	4	L_t	0.66	0.014	0.52	0.80	0.59	0.71
window	3	L_b	0.66	0.014	0.52	0.79	0.68	0.65
window	11	E_{ind}	0.66	0.014	0.52	0.79	0.68	0.65
window	8	ω_{s_mean}	0.62	0.041	0.48	0.76	0.64	0.57
window	9	P_{min}	0.50	0.479	0.36	0.64	0.64	0.50

A wide range of parameters have a good performance and L_{s_mean} has very good performance.

A1 – parameters depicting same aspect of glare:

- Parameters describing the luminance of the source:
- L_{s_mean} better than E_{dir}

A2 – adaptation ratio parameters:

- E_v/L_t , E_v/L_b and E_v perform rather similarly

A3 – contrast parameters:

- L_{s_mean}/L_t performs somewhat better than L_{s_mean}/L_{avg} and L_{s_mean}/E_v
- L_{s_mean} performs better than the contrast parameters

7.4.2.7 Wall zone

TABLE 7.22 ρ -ranked Spearman correlation for the wall zone

sample	#	parameter	ρ	sig.	95% lower	95% upper
					bound CI	bound CI
wall	17	E_v/L_b	0.23	0.026	0.03	0.41
wall	7	ω_{s_total}	0.22	0.034	0.04	0.40
wall	2	E_v	0.20	0.051	0.00	0.37
wall	12	DGP	0.20	0.051	0.00	0.38
wall	10	E_{dir}	0.20	0.058	0.00	0.38
wall	3	L_b	0.19	0.067	-0.03	0.37
wall	11	E_{ind}	0.19	0.067	-0.02	0.37
wall	1	L_{avg}	0.19	0.070	-0.01	0.38
wall	13	L_{s_mean}/L_{avg}	0.19	0.070	-0.01	0.38
wall	4	L_t	0.17	0.097	-0.02	0.35
wall	14	L_{s_mean}/E_v	0.17	0.108	-0.04	0.36
wall	15	L_{s_mean}/L_t	0.16	0.116	-0.03	0.34
wall	5	L_{s_w}	0.16	0.116	-0.06	0.36
wall	16	E_v/L_t	0.14	0.192	-0.08	0.33
wall	6	L_{s_mean}	0.11	0.281	-0.10	0.30
wall	8	ω_{s_mean}	0.11	0.290	-0.10	0.31
wall	9	P_{min}	0.08	0.428	-0.13	0.30

None of the parameters pass the test. As most parameters have either a low effect size or a non-significant correlation, no conclusions can be drawn regarding their relative performance.

TABLE 7.23 AUC-ranked ROC curve results for any glare for the wall zone

sample	#	parameter	AUC	sig.	95% lower	95% upper	TPR	TNR
					bound CI	bound CI		
wall	17	E_v/L_b	0.65	0.014	0.53	0.77	0.72	0.65
wall	7	ω_{s_total}	0.63	0.028	0.51	0.75	0.76	0.50
wall	15	L_{s_mean}/L_t	0.62	0.035	0.50	0.74	0.63	0.62
wall	13	L_{s_mean}/L_{avg}	0.62	0.042	0.49	0.74	0.68	0.54
wall	10	E_{dir}	0.61	0.054	0.48	0.73	0.79	0.50
wall	12	DGP	0.61	0.056	0.48	0.73	0.78	0.50
wall	14	L_{s_mean}/E_v	0.61	0.056	0.48	0.73	0.63	0.54
wall	2	E_v	0.60	0.060	0.48	0.73	0.72	0.54
wall	1	L_{avg}	0.60	0.075	0.47	0.72	0.71	0.54
wall	3	L_b	0.60	0.077	0.47	0.72	0.66	0.54
wall	11	E_{ind}	0.60	0.077	0.47	0.72	0.66	0.54
wall	6	L_{s_mean}	0.58	0.118	0.45	0.71	0.81	0.46
wall	4	L_t	0.58	0.124	0.45	0.70	0.71	0.46
wall	16	E_v/L_t	0.58	0.126	0.45	0.70	0.78	0.54
wall	5	L_{s_w}	0.57	0.135	0.45	0.70	0.74	0.50
wall	8	ω_{s_mean}	0.56	0.182	0.43	0.69	0.85	0.38
wall	9	P_{min}	0.55	0.215	0.42	0.68	0.69	0.50

A range of parameters pass the test. E_v/L_b followed by ω_{s_total} have the best performance. None of the parameters shows a good performance.

A1 – parameters depicting same aspect of glare:

- Both E_{dir} and L_{s_mean} have a non-significant AUC
- E_v , L_{avg} , L_b and L_t have a non-significant AUC

A2 – adaptation ratio parameters:

- E_v/L_b is the only that has a significant AUC, E_v and E_v/L_t fail the test

A3 – contrast parameters:

- L_{s_mean}/L_t and L_{s_mean}/L_{avg} perform similarly and better than L_{s_mean}/E_v

TABLE 7.24 AUC-ranked ROC curve for disturbing glare for the wall zone

sample	#	parameter	AUC	sig.	95% lower	95% upper	TPR	TNR
					bound CI	bound CI		
wall	2	E_v	0.62	0.056	0.47	0.77	0.53	0.65
wall	4	L_t	0.62	0.060	0.47	0.76	0.58	0.61
wall	12	DGP	0.61	0.062	0.47	0.76	0.84	0.44
wall	3	L_b	0.61	0.064	0.47	0.76	0.53	0.65
wall	11	E_{ind}	0.61	0.064	0.47	0.76	0.53	0.65
wall	1	L_{avg}	0.61	0.070	0.46	0.76	0.53	0.64
wall	5	L_{s_w}	0.61	0.073	0.46	0.76	0.84	0.45
wall	7	ω_{s_total}	0.61	0.074	0.46	0.76	0.47	0.71
wall	10	E_{dir}	0.60	0.080	0.46	0.75	0.74	0.48
wall	17	E_v/L_b	0.60	0.099	0.45	0.74	0.95	0.41
wall	13	L_{s_mean}/L_{avg}	0.59	0.123	0.44	0.73	0.47	0.71
wall	14	L_{s_mean}/E_v	0.57	0.163	0.43	0.72	0.47	0.71
wall	16	E_v/L_t	0.57	0.176	0.42	0.72	0.53	0.63
wall	8	ω_{s_mean}	0.56	0.225	0.41	0.70	0.68	0.44
wall	15	L_{s_mean}/L_t	0.55	0.266	0.40	0.69	0.58	0.49
wall	9	P_{min}	0.54	0.293	0.39	0.69	0.89	0.36
wall	6	L_{s_mean}	0.53	0.332	0.39	0.68	0.89	0.36

Although some parameters pass the test, all have non-significant AUC, and therefore no conclusions can be drawn regarding their relative performance.

7.4.2.8 Front zone

TABLE 7.25 ρ -ranked Spearman correlation for the front zone

sample	#	parameter	ρ	sig.	95% lower	95% upper
					bound CI	bound CI
front	12	DGP	0.35	0.001	0.16	0.53
front	17	E_v/L_b	0.34	0.001	0.15	0.52
front	10	E_{dir}	0.34	0.001	0.13	0.52
front	6	L_{s_mean}	0.32	0.002	0.13	0.49
front	2	E_v	0.31	0.003	0.10	0.49
front	13	L_{s_mean}/L_{avg}	0.28	0.007	0.08	0.46
front	7	ω_{s_total}	0.27	0.008	0.06	0.47
front	5	L_{s_w}	0.27	0.008	0.07	0.45
front	1	L_{avg}	0.27	0.008	0.07	0.46
front	4	L_t	0.27	0.009	0.07	0.45
front	15	L_{s_mean}/L_t	0.26	0.011	0.06	0.45
front	3	L_b	0.26	0.012	0.06	0.44
front	11	E_{ind}	0.26	0.012	0.07	0.46
front	16	E_v/L_t	0.26	0.012	0.07	0.46
front	14	L_{s_mean}/E_v	0.24	0.020	0.03	0.43
front	8	ω_{s_mean}	0.18	0.093	-0.05	0.37
front	9	P_{min}	0.05	0.645	-0.19	0.29

A range of parameters pass the test. None have a good performance.

A1 – parameters depicting same aspect of glare:

- L_{s_mean} and E_{dir} have similar performance
- E_v is better than L_{avg} , L_b and L_t

A2 – adaptation ratio parameters:

- E_v/L_b is somewhat better than E_v and better than E_v/L_t

A3 - contrast parameters:

- None of L_{s_mean}/L_{avg} , L_{s_mean}/E_v and L_{s_mean}/L_t pass the test, while L_{s_mean} does.

TABLE 7.26 AUC-ranked ROC curve results for any glare for the front zone

sample	#	parameter	AUC	sig.	95% lower	95% upper	TPR	TNR
					bound CI	bound CI		
front	12	DGP	0.69	0.002	0.58	0.80	0.74	0.71
front	10	E_{dir}	0.68	0.002	0.57	0.79	0.69	0.71
front	17	E_v/L_b	0.68	0.003	0.57	0.79	0.73	0.65
front	4	L_t	0.66	0.005	0.55	0.78	0.66	0.61
front	2	E_v	0.66	0.006	0.55	0.77	0.53	0.74
front	5	L_{s_w}	0.66	0.007	0.54	0.77	0.69	0.65
front	6	L_{s_mean}	0.66	0.008	0.54	0.77	0.61	0.61
front	1	L_{avg}	0.64	0.014	0.53	0.76	0.52	0.74
front	3	L_b	0.64	0.014	0.52	0.76	0.50	0.77
front	11	E_{ind}	0.64	0.014	0.52	0.76	0.50	0.77
front	7	ω_{s_total}	0.64	0.015	0.52	0.75	0.61	0.65
front	16	E_v/L_t	0.63	0.022	0.51	0.75	0.56	0.68
front	13	L_{s_mean}/L_{avg}	0.62	0.028	0.51	0.74	0.81	0.45
front	15	L_{s_mean}/L_t	0.60	0.055	0.48	0.72	0.73	0.52
front	14	L_{s_mean}/E_v	0.59	0.079	0.47	0.71	0.89	0.42
front	8	ω_{s_mean}	0.54	0.247	0.42	0.67	0.74	0.45
front	9	P_{min}	0.48	0.651	0.35	0.60	0.69	0.48

A wide range of parameters pass the test. None has a good performance.

A1 – parameters depicting same aspect of glare:

- E_{dir} is slightly better than L_{s_mean}
- E_v has similar performance to L_t and is somewhat better than L_{avg} and L_b

A2 – adaptation ratio parameters:

- E_v/L_b somewhat better than E_v and better than E_v/L_t

A3 – contrast parameters:

- Only L_{s_mean}/L_{avg} passes the test. L_{s_mean}/E_v and L_{s_mean}/L_t have non-significant AUC
- L_{s_mean} passes the test

TABLE 7.27 AUC-ranked ROC curve for disturbing glare for the front zone

sample	#	parameter	AUC	sig.	95% lower	95% upper	TPR	TNR
					bound CI	bound CI		
front	15	L_{s_mean}/L_t	0.70	0.002	0.57	0.83	0.71	0.64
front	13	L_{s_mean}/L_{avg}	0.69	0.002	0.56	0.82	0.71	0.59
front	14	L_{s_mean}/E_v	0.69	0.003	0.56	0.82	0.79	0.54
front	17	E_v/L_b	0.69	0.003	0.56	0.82	0.71	0.62
front	6	L_{s_mean}	0.69	0.003	0.56	0.82	0.58	0.72
front	10	E_{dir}	0.68	0.005	0.55	0.81	0.79	0.54
front	12	DGP	0.68	0.005	0.54	0.81	0.79	0.51
front	2	E_v	0.66	0.010	0.53	0.79	0.58	0.65
front	8	ω_{s_mean}	0.65	0.015	0.52	0.78	0.75	0.51
front	7	ω_{s_total}	0.65	0.015	0.52	0.78	0.50	0.70
front	1	L_{avg}	0.65	0.017	0.51	0.78	0.54	0.65
front	16	E_v/L_t	0.64	0.018	0.51	0.78	0.58	0.61
front	3	L_b	0.63	0.029	0.50	0.77	0.54	0.67
front	11	E_{ind}	0.63	0.029	0.50	0.77	0.54	0.67
front	5	L_{s_w}	0.62	0.037	0.49	0.76	0.54	0.68
front	4	L_t	0.61	0.060	0.47	0.74	0.46	0.77
front	9	P_{min}	0.60	0.075	0.46	0.73	0.71	0.49

A wide range of parameters pass the test. L_{s_mean}/L_t has good performance, but is not significantly better than the other metrics on the top of the rank.

A1 – parameters depicting same aspect of glare:

- L_{s_mean} and E_{dir} have same performance
- E_v has a similar performance to L_{avg} , somewhat better than L_b and better than L_t

A2 – adaptation ratio parameters:

- E_v/L_b better than E_v and better than E_v/L_t

A3 – contrast parameters:

- There is no significant difference between L_{s_mean}/L_{avg} , L_{s_mean}/E_v and L_{s_mean}/L_t
- The contrast parameters have similar performance to L_{s_mean}

7.4.2.9 Back zone

TABLE 7.28 ρ -ranked Spearman correlation for the back zone

sample	#	parameter	ρ	sig.	95% lower	95% upper
					bound CI	bound CI
back	17	E_v/L_b	0.37	0.000	0.18	0.54
back	12	DGP	0.35	0.001	0.18	0.52
back	10	E_{dir}	0.35	0.001	0.16	0.51
back	2	E_v	0.33	0.001	0.16	0.52
back	6	L_{s_mean}	0.33	0.001	0.12	0.52
back	16	E_v/L_t	0.31	0.003	0.11	0.46
back	1	L_{avg}	0.30	0.004	0.11	0.46
back	7	ω_{s_total}	0.28	0.007	0.09	0.46
back	5	L_{s_w}	0.27	0.009	0.07	0.46
back	3	L_b	0.27	0.011	0.05	0.44
back	11	E_{ind}	0.27	0.011	0.08	0.42
back	4	L_t	0.26	0.013	0.06	0.44
back	15	L_{s_mean}/L_t	0.26	0.015	0.03	0.46
back	8	ω_{s_mean}	0.22	0.038	0.01	0.40
back	13	L_{s_mean}/L_{avg}	0.16	0.140	-0.07	0.36
back	14	L_{s_mean}/E_v	0.15	0.161	-0.07	0.37
back	9	P_{min}	-0.05	0.668	-0.25	0.17

A range of parameters pass the test: E_v/L_b , E_{dir} , E_v , L_{s_mean} , E_v/L_t and L_{avg} . None of the parameters has good performance.

A1 – parameters depicting same aspect of glare:

- E_{dir} marginally better than L_{s_mean}
- E_v somewhat better than L_{avg} and better than L_b and L_t

A2 – adaptation ratio parameters:

- E_v/L_b is better than E_v and than E_v/L_t

A3 - contrast parameters:

- All contrast parameters fail the test

TABLE 7.29 AUC-ranked ROC curve results for any glare for the back zone

sample	#	parameter	AUC	sig.	95% lower	95% upper	TPR	TNR
					bound CI	bound CI		
back	17	E_v/L_b	0.71	0.001	0.60	0.82	0.72	0.65
back	10	E_{dir}	0.68	0.003	0.57	0.79	0.75	0.55
back	12	DGP	0.67	0.004	0.56	0.78	0.80	0.52
back	6	L_{s_mean}	0.66	0.005	0.55	0.78	0.67	0.65
back	2	E_v	0.66	0.006	0.55	0.77	0.72	0.55
back	16	E_v/L_t	0.66	0.007	0.54	0.77	0.80	0.52
back	7	ω_{s_total}	0.65	0.010	0.53	0.76	0.55	0.68
back	1	L_{avg}	0.65	0.011	0.53	0.76	0.68	0.58
back	5	L_{s_w}	0.64	0.015	0.52	0.76	0.67	0.61
back	15	L_{s_mean}/L_t	0.64	0.015	0.52	0.76	0.53	0.77
back	3	L_b	0.63	0.021	0.51	0.75	0.65	0.58
back	11	E_{ind}	0.63	0.021	0.51	0.75	0.65	0.58
back	8	ω_{s_mean}	0.63	0.026	0.51	0.74	0.57	0.68
back	4	L_t	0.62	0.031	0.50	0.74	0.55	0.71
back	13	L_{s_mean}/L_{avg}	0.56	0.163	0.44	0.69	0.52	0.58
back	14	L_{s_mean}/E_v	0.56	0.178	0.44	0.68	0.53	0.58
back	9	P_{min}	0.50	0.525	0.37	0.62	0.75	0.35

A wide range of parameters pass the test. E_v/L_b has a good performance.

A1 – parameters depicting same aspect of glare:

- E_{dir} is somewhat better than L_{s_mean}
- E_v is marginally better than L_{avg} and is better than L_b and L_t

A2 – adaptation ratio parameters:

- E_v/L_b is better than E_v and than E_v/L_t

A3 – contrast parameters:

- L_{s_mean}/L_t is better than the other contrast ratios; L_{s_mean} is better than L_{s_mean}/L_t .

TABLE 7.30 AUC-ranked ROC curve for disturbing glare in the back zone

sample	#	parameter	AUC	sig.	95% lower	95% upper	TPR	TNR
					bound CI	bound CI		
back	12	DGP	0.73	0.002	0.58	0.87	0.65	0.73
back	2	E_v	0.72	0.003	0.57	0.86	0.65	0.70
back	6	L_{s_mean}	0.70	0.005	0.55	0.85	0.53	0.76
back	10	E_{dir}	0.70	0.005	0.55	0.85	0.65	0.66
back	1	L_{avg}	0.69	0.007	0.54	0.84	0.76	0.61
back	16	E_v/L_t	0.68	0.009	0.53	0.84	0.71	0.55
back	4	L_t	0.68	0.011	0.53	0.83	0.65	0.69
back	17	E_v/L_b	0.68	0.011	0.53	0.83	0.59	0.62
back	3	L_b	0.67	0.015	0.52	0.82	0.76	0.58
back	11	E_{ind}	0.67	0.015	0.52	0.82	0.76	0.58
back	5	$L_{s_ω}$	0.66	0.019	0.51	0.81	0.82	0.53
back	7	$ω_{s_total}$	0.66	0.023	0.50	0.81	0.71	0.54
back	15	L_{s_mean}/L_t	0.64	0.041	0.48	0.79	0.59	0.70
back	13	L_{s_mean}/L_{avg}	0.62	0.057	0.47	0.78	0.47	0.78
back	14	L_{s_mean}/E_v	0.62	0.065	0.46	0.77	0.47	0.74
back	8	$ω_{s_mean}$	0.60	0.090	0.45	0.76	0.59	0.64
back	9	P_{min}	0.44	0.791	0.29	0.58	0.76	0.31

Most parameters pass the test. E_v , L_{s_mean} and E_{dir} have good performance, but none of these parameters has significantly different performance.

A1 – parameters depicting same aspect of glare:

- L_{s_mean} same performance as E_{dir}
- E_v better than L_{avg} , L_t and L_b

A2 – adaptation ratio parameters:

- E_v better than the adaptation ratios

A3 – contrast parameters:

- No significant difference regarding the performance of the ratios, with some showing a non-significant AUC. The L_{s_mean} is significantly better than the ratios.

7.5 Analysis

The analysis that is done in this chapter tries to identify how successful a range of individual and combined glare parameters are at predicting the reported discomfort glare, and how these parameters compare to each other. The analysis is done for the full room dataset and for a series of subsamples of the room dataset, the four individual positions and four zones – window, wall, front and back zones.

For the full room dataset, L_{s_mean} , E_v/L_b , E_{dir} and E_v pass the three statistical tests – the Spearman correlation and the AUC for the ‘any glare’ and ‘disturbing glare’ definitions. However, none of these parameters show a good performance.

The analysis of the individual positions shows that a wide range of parameters show a good performance in position 1, with E_v/L_b and L_{s_mean} performing either very well or well. In position 2, a wide range of parameters shows good prediction of ‘disturbing glare’, with L_{s_mean}/L_t and L_{s_mean} at the top of the ranks. However, none performs satisfactorily regarding the prediction of ‘any glare’.

All the parameters tend to perform poorly in position 3 particularly regarding the prediction of ‘disturbing glare’.

In position 4, the parameters tend to perform also rather poorly particularly regarding the prediction of ‘any glare’. L_t , L_b and E_{ind} show a good performance regarding the prediction of ‘disturbing glare’ but similarly to position 2, the parameters at the top of the ranks for position 4 tend to be quite different for the three tests.

It can be observed that there is high variability in terms of what the successful parameters are in each position. It is however possible to extract a range of parameters that tend to either perform well in most positions or are distinctively better than the others in the same position. These are E_v/L_b , L_{s_mean} , L_{s_mean}/L_{avg} , L_{s_mean}/E_v and E_v .

In the analysis based on the room zones, the parameters show the same tendency observed for the metrics, i.e. acceptable to good performance in the window zone and poor performance in the wall zone. Generally, a good performance of the parameters can be obtained in the window zone, in a combination of source-related (L_{s_mean} , and eventually E_{dir}) and adaptation-related parameters (either E_v , E_v/L_b or E_v/L_t).

In the wall zone, it is not possible to determine any good parameters, but there are some parameters that have relative success in that zone, namely E_v/L_b and ω_{s_total} .

The performance of the parameters in the front of the room is generally not good, although not as poor as in the wall zone. In this zone, E_v/L_b and E_{dir} show some relative success.

Generally, a good performance of the parameters can be obtained in the back zone, in a combination of the source-related parameters L_{s_mean} or E_{dir} , with the adaptation-related parameters E_v or E_v/L_b .

The E_v/L_b is the only parameter that shows some relative success in all zones, suggesting that in a zone-based approach to discomfort glare the inclusion of the background luminance in the definition of adaptation might be beneficial. The relative success of this metric indicates that the luminance of the background can have an influence on the definition of the adaptation level in the classroom space. The region defined as the background does indeed fill a higher proportion of the field-of-view in all positions of the classroom space in comparison to the field-of-view in a cellular office type of space. The borderline between comfort and discomfort (BCD) thresholds that was found for the E_v/L_b ranges between 3.6 and 5.3 ($\text{lux}\cdot\text{m}^2/\text{cd}$) depending on the zone of the classroom, window or wall (see Appendix D).

In addition to the findings above, it is observed that L_{s_mean} tends to have a better performance than L_{s_w} , which is particularly clear for the 'disturbing glare' definition. This seems to indicate that the size of the glare source does not provide additional predictive power in relation to the luminance of the glare source itself.

It is also observed that, L_{avg} and L_t tend to perform better as the denominators in the definition of contrast than E_v , which is the denominator in the definition of contrast of DGP.

The statistics for all parameters for the 'any glare' definition in position 3 were all non-significant as well as the statistics for the 'disturbing glare' definition in position 4, indicating poor potential of the individual parameters in these positions.

A classification of the performance of the metrics can be found in Tables 7.31 and 7.32. A good performance in the table indicates a potentially good glare predictor.

It can be seen that the parameters are generally different within the position and zones' subdivisions, indicating that a model based on either of the approaches would possibly require a different set of parameters depending on position or zone.

TABLE 7.31 Classification of the parameters' performance for the full dataset and for the positions' subsamples.

Performance	Rank	Full	Position 1	Position 2	Position 3	Position 4
Very good	1	-	E_v/L_b	-	-	-
Good	1	-	L_{s_mean}	-	-	-
	2		E_{dir}			
	3		E_v			
	4		E_v/L_t			
	5		ω_{s_total}			
Partially good	1	-	L_{s_mean}/L_t	L_{s_mean}	-	-
	2			E_{dir}		
	3			E_v		
	4			E_v/L_t		
	5			L_{s_w}		
	6			L_{avg}		
	7			L_b		
	8			E_{ind}		
Some potential	1	-	E_v/L_b	L_{s_mean}	L_{s_mean}/L_{avg}	L_t
	2		L_{s_mean}	L_{s_mean}/L_t	ω_{s_total}	L_b
	3		E_{dir}	E_v/L_b		E_{ind}
	4		L_{s_mean}/L_t	E_{dir}		E_v
	5		E_v	E_v		L_{avg}
	6		E_v/L_t	E_v/L_t		ω_{s_total}
	7		L_{avg}	L_{s_w}		
	8		L_{s_w}	L_{s_mean}/L_{avg}		
	9		ω_{s_total}	L_{avg}		
	10		L_b	L_{s_mean}/E_v		
	11		L_t	ω_{s_mean}		
	12		E_{ind}	ω_{s_total}		
	13		L_{s_mean}/E_v	L_b		
Best score	1	E_v/L_b				
	2	E_{dir}				
	3	L_{s_mean}				

Very good = parameters that are very good in at least two tests; Good = parameters that are good in at least two tests; Partially good = parameters that are good in at least one test and pass at least one of the other two tests; Some potential = parameters that are good in just one test; Best score = from the 3 top-ranked parameters in each test, the parameters that pass at least two of the tests. Note that tests need to produce a significant result ($p > 0.05$) for all the mentioned classifications.

TABLE 7.32 Classification of the parameters' performance for the zones' subsamples.

Performance	Rank	Window	Wall	Front	Back
Very good	1	-	-	-	-
Good	1	L_{s_mean}	-	-	-
	2	E_v/L_t			
	3	E_v			
	4	E_v/L_b			
	5	E_{dir}			
Partially good	1	L_{s_mean}/L_t	-	-	E_v
	2	L_{avg}			E_v/L_b
	3	L_{s_w}			E_{ind}
	4	L_b			L_{s_mean}
	5	E_{ind}			
	6	L_t			
Some potential	1	L_{s_mean}	-	-	E_{dir}
	2	L_{s_mean}/L_t			
	3	L_{s_mean}/L_{avg}			
	4	L_{s_mean}/E_v			
	5	E_v/L_t			
	6	E_v			
	7	E_v/L_b			
	8	L_{avg}			
	9	E_{dir}			
	10	L_{s_w}			
	11	L_b			
	12	E_{ind}			
	13	L_t			
Best score	1		E_v/L_b	E_v/L_b	
	2		ω_{s_total}	E_{dir}	

Very good = parameters that are very good in at least two tests; Good = parameters that are good in at least two tests; Partially good = parameters that are good in at least one test and pass at least one of the other two tests; Some potential = parameters that are good in just one test; Best score = from the 3 top-ranked parameters in each test, the parameters that pass at least two of the tests. Note that tests need to produce a significant result ($p > 0.05$) for all the mentioned classifications.

7.6 Conclusion

In this chapter, an analysis of a range of glare parameters was carried out to find suitable candidates for the development of a model of discomfort glare for the classroom space. The data was tested for different subsamples of the dataset and for two definitions of glare, 'any glare' and 'disturbing glare'. The 'any glare' definition corresponds to the glare votes 'noticeable', 'disturbing' and 'intolerable', while the 'disturbing glare' definition corresponds to the votes 'disturbing' and 'intolerable'. None of the parameters produced a good performance for the full sample, which indicates that none of the parameters is by itself a good predictor of glare at room level. This indicates that models based on a range of parameters are required to describe discomfort glare for an analysis based on the full space of a classroom. This was also the case for positions 3 and 4, for the wall and for the front zones. Contrary to that, a range of good predictors could be found for position 1 and for the window zone.

It is verified that for the four positions in the room or for the zones of the room, there is a high variability in terms of what the most successful or best parameters are. A parameter or a combination of parameters that would significantly perform better than other(s) for the data sample or for the different tested subsamples was not found.

8 A metric-based discomfort glare equation

8.1 Introduction

In the previous chapter it was found that although several glare parameters showed some good predictive power in the window zone and in positions 1 and 2 of the room, none has shown good predictive power in the wall zone or in positions 3 and 4. That analysis also suggests that a range of parameters is required to produce a more successful model of discomfort glare for classrooms. In this chapter, it is investigated if models that already combine a range of parameters, such as the glare indices, can be adapted to better predict discomfort glare in the classroom. This study in this chapter looks at the possibility of establishing a successful relationship between one of the glare indices and the reported discomfort glare, in the form of a new glare equation.

The DGP provided an overall better performance than most other metrics in Study I. In addition, as the metric adopted in Europe for the general evaluation of discomfort glare from daylight (Comité Européen de Normalisation, 2018), it is considered relevant to investigate if it can be adapted to the conditions of the classroom space.

The UGP also performed relatively well in Study I. The metric has been developed under conditions of low luminance and of arguably higher luminance contrast and from that perspective, it is relevant to further investigate in the context of this research. It is also interesting to find how UGP, which is a metric that only contains a contrast term compares to DGP, which is a metric that contains both a contrast and an adaptation term.

As shown in Chapter II, several existing glare metrics have either a logarithmic form or a logarithmic definition of adaptation. From the glare indices, DGP and the metrics derived from DGP are the only metrics where the logarithm of the adaptation term was dropped in favour of a linear adaptation term. As explained before, the reason for this was the fact that in the DGP investigation a better correlation was found for a linear rather than a logarithmic form of the vertical eye illuminance (E_v) (Wienold, 2010). This result was however met with surprise as, as it is explained in the same study, in the field of psychophysics the magnitude of perception is thought to be logarithmic towards the magnitude of the physical stimulus (Weber-Fechner law) (Fechner, 1860).

Hirning (Hirning et al., 2014) also attributes the lower correlation that was found in his study between DGP and the reported discomfort to the very strong linear dependence that the DGP equation has on E_v . In that study, the logarithm of the vertical eye illuminance provided a higher correlation to discomfort than its linear counterpart.

Based on the above, it is considered relevant to test DGP, UGP and a logarithmic definition of E_v as part of the DGP equation, where $DGPlog(E_v)$ designates the DGP with the logarithmic form of E_v .

As explained in Chapter II, DGP was originally validated for values higher than 0.2 and later adapted to provide an estimated DGP in situations where the overall light measured via E_v is between 0 and 300 Lux. The analysis in this chapter includes both the low light-corrected and -non corrected versions of DGP, extending that definition also to $DGPlog(E_v)$. The DGP and UGP metrics (presented in Chapter II as equations 11 and 13, respectively), the low-light correction definition (equation 12) and the new $DGPlog(E_v)$ definition are provided below:

$$DGP = 5.87 \cdot 10^{-5} \cdot E_v + 9.18 \cdot 10^{-2} \cdot \log_{10} \left(1 + \sum_{i=1}^n \frac{L_{s,i}^2 \cdot \omega_{s,i}}{E_v^{1.87} \cdot P_i^2} \right) + 0.16 \quad \text{EQ 11}$$

$$DGPlog(E_v) = 5.87 \cdot 10^{-5} \cdot \log_{10}(E_v) + 9.18 \cdot 10^{-2} \cdot \log_{10} \left(1 + \sum_{i=1}^n \frac{L_{s,i}^2 \cdot \omega_{s,i}}{E_v^{1.87} \cdot P_i^2} \right) + 0.16 \quad \text{EQ 22}$$

With the low light correction being:

$$\text{DGP}_{\text{lowlight}} = \text{DGP} \cdot \frac{e^{0.024 \cdot E_v - 4}}{1 + e^{0.024 \cdot E_v - 4}} \quad \text{EQ 12}$$

$$\text{UGP} = 0.26 \cdot \log_{10} \left(\frac{0.25}{L_b} \cdot \sum_{i=1}^n \frac{L_{s,i}^2 \cdot \omega_{s,i}}{P_i^2} \right) \quad \text{EQ 13}$$

The DGP, DGPl_{og}(E_v) and UGP metrics were calculated based on the E_v, L_b, L_s, ω_s and P outputs of *evalglare*.

8.2 Method

8.2.1 Equation definition

The study pertains the definition of an equation that represents a successful relationship between the metric and the reported glare, using statistical regression. The choice of a regression modelling method is generally defined based on the level of measurement of the dependent and independent variables of the study.

As the dependent variable of the study has ordinal level of measurement, one option is the use of multinomial or binomial logistic regression. However, tests done using these two modelling approaches showed that none was appropriate. Multinomial regression produced a large number of zero frequency cells, a problem that does generally occur when like in this case, the independent variable - DGP, UGP and DGPl_{og}(E_v) - is continuous (Field, 2009). Binomial logistic regression produced standardised residuals outside the recommended range for most of the tested conditions suggesting that this approach results in poorly fitted models.

Linear regression becomes a possibility if the dependent variable is transformed into a continuous variable, a procedure that was also adopted by others within this research field (Wienold, 2010) (Hirning et al., 2014) (Karlsen et al., 2015) (Konstantzos and Tzempelikos, 2017). This transformation involves grouping

the glare metric into a given number of groups and calculating the percentage of subjects affected by glare in each of these groups. This grouping, however, reduces the data sample to a lower number of data points. Several authors suggest that an optimal solution can be found for a number of groups equalling the number of observations in each group (Hirning et al., 2014) (Konstantzos and Tzempelikos, 2017). In the case of the Study I dataset, this corresponds to 7 groups (or 7 data points) for an analysis of the data by position and to 10 groups for an analysis by zone. Since as a rule-of-thumb, there should be at least 10 data points per predictor to produce a linear model (Field, 2009), a zone-based modelling approach is taken for the purpose of this analysis.

A zones approach based on the window and wall zones conveniently aligns with the identified problem of the metrics and glare parameters in the classroom - their general poor performance in positions 3 and 4. The window and the wall zones also correspond to two distinct light conditions in terms of the overall light levels in the classroom – a high illumination zone near the window and a dimmer zone near the wall.

8.2.2 Linear regression

The linear regression expresses the linear relationship between a dependent variable Y and one or more independent variables X , as

$$Y_i = (b_0 + b_1 \cdot X_i)$$

where b_0 is the constant and b_1 is the regression coefficient of the model.

The model that is being investigated in this study thus has the form:

$$\text{Glare} = (b_0 + b_1 \cdot \text{Metric})$$

The fitness of a linear model is generally measured via the coefficient of determination r^2 . The r^2 shows the percentage of variance of the dependent variable (reported discomfort glare) that is explained by a predictor (in this case, a metric), i.e., an r^2 of 0.8 for a particular metric indicates that 80% of the variance on the reported discomfort glare is explained by that metric. The r^2 expresses the size of the effect of the relationship between the dependent and independent variables. In this study it is assumed that the effect is significant when there is a chance of less than 5% ($p < 0.05$) that the null hypothesis is true, i.e., that there is no relationship between reported glare and the metric.

8.2.3 Transformation of the variables

The process of converting the ordinal dependent variable (glare votes) into a continuous variable (percentage of reported glare) involves the calculation of the percentage of subjects that declare being affected by glare in each group of the independent variable. The groups of the independent variable are created after ranking the independent variable from its lower to its higher value, by dividing the values into a number of groups and by calculating the mean value of the metric in each group. Thus, the independent variable of the regression model becomes the mean of the metric in each group.

To calculate the percentage of reported glare for each group, a threshold value of 'glare' for the dependent variable needs again to be defined. The definition of this threshold follows the same definition presented in the previous chapter for the binomial classification of the ROC curve. The regressions are therefore performed for an 'any glare' definition, where the percentage of persons that report glare in each group includes the 'noticeable', 'disturbing' and 'intolerable' glare votes and for a 'disturbing glare' definition, where the percentage of persons that report glare includes the 'disturbing' and 'intolerable' glare votes.

8.2.4 The analysis models

Based on the analysis conditions presented above a total of twenty linear regressions are performed, as presented in Table 8.1.

TABLE 8.1 Regression models in the analysis.

#	Zone	Metric	Glare definition	Regression model
1	wall	DGP	any_glare	wall_DGP_any_glare
2		DGPlog(E_v)		wall_DGPlog(E_v)_any_glare
3		UGP		wall_UGP_any_glare
4		DGP _{lowlight}		wall_DGP_lowlight-any_glare
5		DGPlog(E_v) _{lowlight}		wall_DGPlog(E_v)_lowlight-any_glare
6	wall	DGP	disturbing	wall_DGP_disturbing
7		DGPlog(E_v)		wall_DGPlog(E_v)_disturbing
8		UGP		wall_UGP_disturbing
9		DGP _{lowlight}		wall_DGP_lowlight-disturbing
10		DGPlog(E_v) _{lowlight}		wall_DGPlog(E_v)_lowlight-disturbing
11	window	DGP	any_glare	window_DGP_any_glare
12		DGPlog(E_v)		window_DGPlog(E_v)_any_glare
13		UGP		window_UGP_any_glare
14		DGP _{lowlight}		window_DGP_lowlight-any_glare
15		DGPlog(E_v) _{lowlight}		window_DGPlog(E_v)_lowlight-any_glare
16	window	DGP	disturbing	window_DGP_disturbing
17		DGPlog(E_v)		window_DGPlog(E_v)_disturbing
18		UGP		window_UGP_disturbing
19		DGP _{lowlight}		window_DGP_lowlight-disturbing
20		DGPlog(E_v) _{lowlight}		window_DGPlog(E_v)_lowlight-disturbing

any glare = noticeable, disturbing and intolerable votes; disturbing glare = disturbing and intolerable votes.

8.2.5 Grouping the variables

It was noted previously that the coefficients of determination r^2 can vary depending on the number of groups that is used to subdivide the data, a fact that has been reported by others that used the same statistical modelling strategy of grouped variables (Wienold, 2010) (Hirning et al., 2014) (Karlsen et al., 2015) (Konstantzos and Tzempelikos, 2017).

Hirning (Hirning et al., 2014) states that if the number of observations in each group is exceeded by the number of groups the system is under-determined, while for a number of observations in each group exceeding the number of groups the system is over-determined, leading to higher coefficients of determination. To avoid an overly optimistic or pessimistic r^2 , the best option is therefore to avoid a higher or lower number of points in the groups than the number of groups.

A test was done that shows that there is indeed a downward tendency for the r^2 as the number of observations per group decreases in relation to the number of groups for this dataset (Table 8.2). The tests compare a 7-group approach with 14 to 13 cases per group, a 10-group approach with 9 to 10 cases per group and a 13-group approach with 7 to 8 cases per group. The 10-group approach thus then corresponds to the best approximation to a number of groups equalling the number of points in the groups, for this dataset. The maximum standard deviations for each of the groups of the metrics and for the 3 grouping approaches (7-group, 10-group and 13-group) were also calculated and are provided in Table 8.2. The best performance is of course obtained when the standard deviations are the lowest, i.e. when the individual values of the metric within each group are the closest to the mean value of the metric in that group. It can be seen that the 10-group and the 13-group approaches perform similarly and better than the 7-group approach.

The 10-group approach, which corresponds to the theoretical best solution for the r^2 in terms of number of groups vs. number of observations, does also produce a comparatively good performance in terms of the maximum standard deviation of the groups.

Maximum standard deviation values are colour-coded from lighter to darker blue (best to worst). Values for the standard deviations of the metrics do not change between 'any glare' and the 'disturbing glare' definitions as the only change for those models occurs at the dependent variable level only (reported glare).

TABLE 8.2 Coefficient of determination r^2 and maximum standard deviation for the different grouping approaches.

Regression model	Coefficient of determination (r^2)			Maximum standard deviation		
	7-group	10-group	13-group	7-group	10-group	13-group
wall_DGP_any_glare	0.33	0.32	0.24	0.0320	0.0314	0.0316
wall_DGPlog(E_v)_any_glare	0.61	0.62	0.40	0.0087	0.0090	0.0094
wall_UGP_any_glare	0.68	0.58	0.54	0.2273	0.1336	0.1636
wall_DGP_lowlight-any_glare	0.47	0.50	0.32	0.0531	0.0399	0.0316
wall_DGPlog(E_v)_lowlight-any_glare	0.71	0.71	0.40	0.0472	0.0343	0.0207
wall_DGP_disturbing	0.26	0.18	0.19	0.0320	0.0314	0.0316
wall_DGPlog(E_v)_disturbing	0.45	0.13	0.27	0.0087	0.0090	0.0094
wall_UGP_disturbing	0.31	0.28	0.24	0.2273	0.1336	0.1636
wall_DGP_lowlight-disturbing	0.42	0.36	0.32	0.0531	0.0399	0.0316
wall_DGPlog(E_v)_lowlight-disturbing	0.62	0.73	0.33	0.0472	0.0343	0.0207
window_DGP_any_glare	0.48	0.51	0.39	0.0378	0.0315	0.0326
window_DGPlog(E_v)_any_glare	0.63	0.60	0.38	0.0093	0.0089	0.0091
window_UGP_any_glare	0.80	0.68	0.70	0.0900	0.0868	0.0965
window_DGP_lowlight-any_glare	0.56	0.64	0.49	0.0378	0.0315	0.0326
window_DGPlog(E_v)_lowlight-any_glare	0.81	0.64	0.39	0.0259	0.0255	0.0184
window_DGP_disturbing	0.69	0.47	0.46	0.0378	0.0315	0.0326
window_DGPlog(E_v)_disturbing	0.75	0.57	0.56	0.0093	0.0089	0.0091
window_UGP_disturbing	0.58	0.56	0.49	0.0900	0.0868	0.0965
window_DGP_lowlight-disturbing	0.72	0.49	0.48	0.0378	0.0315	0.0326
window_DGPlog(E_v)_lowlight-disturbing	0.52	0.40	0.40	0.0259	0.0255	0.0184

8.2.6 Assumptions of linear regression

As any other type of regression modelling, there are several assumptions behind the production of a linear model that need to be verified. In the case of linear regression there are four assumptions that require particular attention: a) sample size, b) independence of the dependent variable, c) normality of the dependent variable and d) absence of outliers.

The required sample size for linear regression depends on the expected power of the model, expected effect size and its number of predictors, with the required sample increasing when any of those variables increase. As there is only one predictor in the model and at least 10 data points per predictor are required to produce a linear model (Field, 2009), the 7-group approach to the grouping strategy (7 data points) does not comply with the sample size assumption.

The assumption of independence of the dependent variables does not apply to within-subject designs, as in that case each subject evaluates a number of specified conditions as in that case any 'dependence' is equally distributed across the dataset. However, although Study I has a within-subject design there was a need to eliminate some of the observations at data pre-processing stage. In the case of the data used for this analysis, there are 7 subjects that did not make a complete number of observations, corresponding to 13% of the data. There is therefore a degree of non-independence to the data.

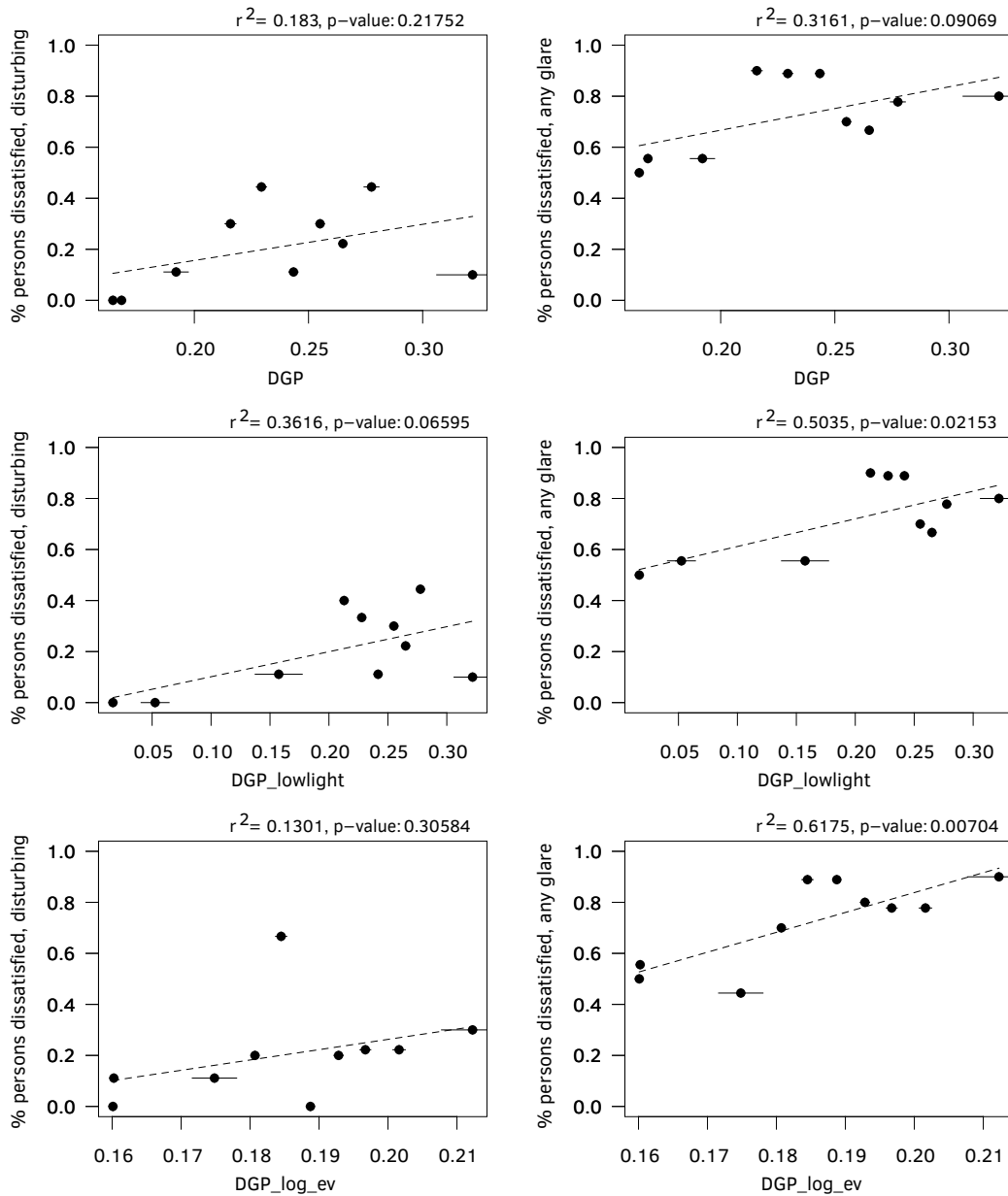
The Kolmogorov–Smirnov test of the dependent variable produced a $p > 0.05$ for all models, showing that the dependent variable is normally distributed in all cases. More information regarding the test of the normality can be found in the Appendix E, section 1.

In regards to the outliers, a Cook's distance outlier detection statistic (Cook and Weisberg, 1982) was run for the different models and it was found that distances were less than 1 for all models except for the *wall_dgp_disturbing* model, which contains one data point with a distance of 1.55. This model does therefore fail the assumption of absence of outliers and that should be considered in the final analysis.

8.3 Results and analysis

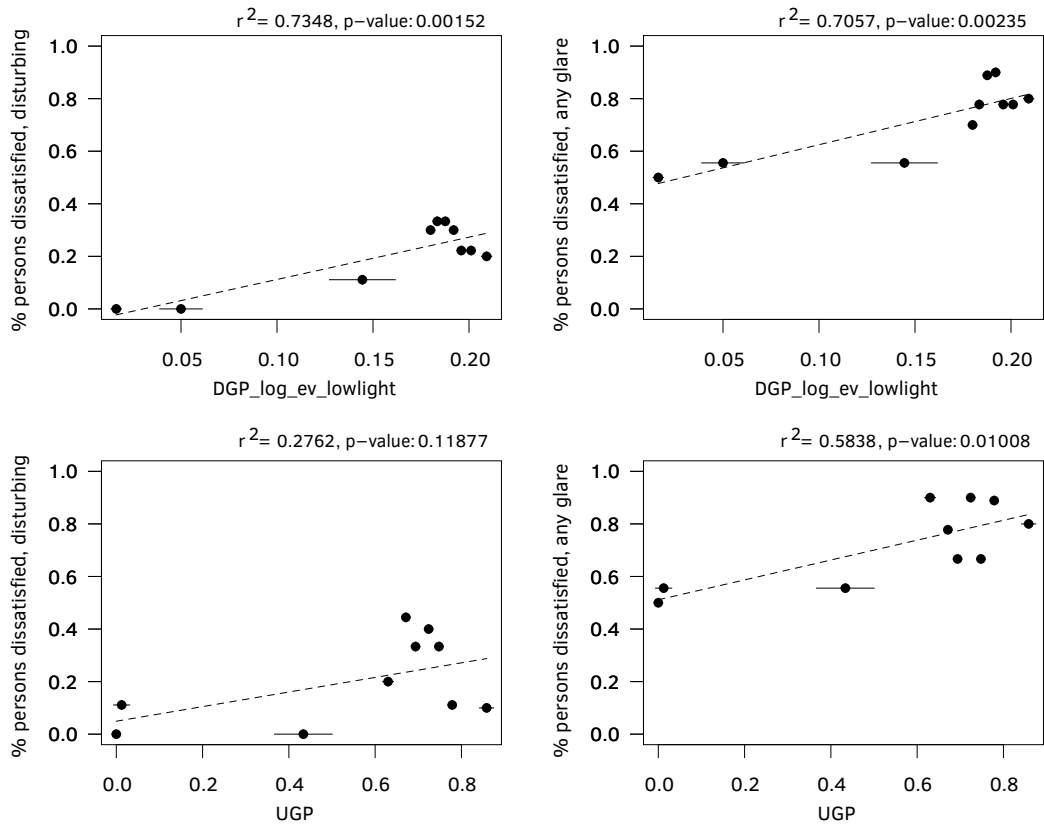
The regressions for the twenty models were performed for all the grouping approaches – the 7-group, 10-group and 13-group and full results for these are provided in Appendix E, section 2.

The 7-group approach is the least favourable in terms of the variation of the coefficient of determination, of the standard deviation of the groups and of the sample size, as seen above. A comparison of the models produced with the 10-group and 13-group approaches showed that the models produced with one or the other approaches have very similar levels of accuracy. The analysis therefore focuses on the 10-group approach and only these results will be discussed below. The scatter plots for the regressions are provided in Figure 8.1 and Figure 8.2.



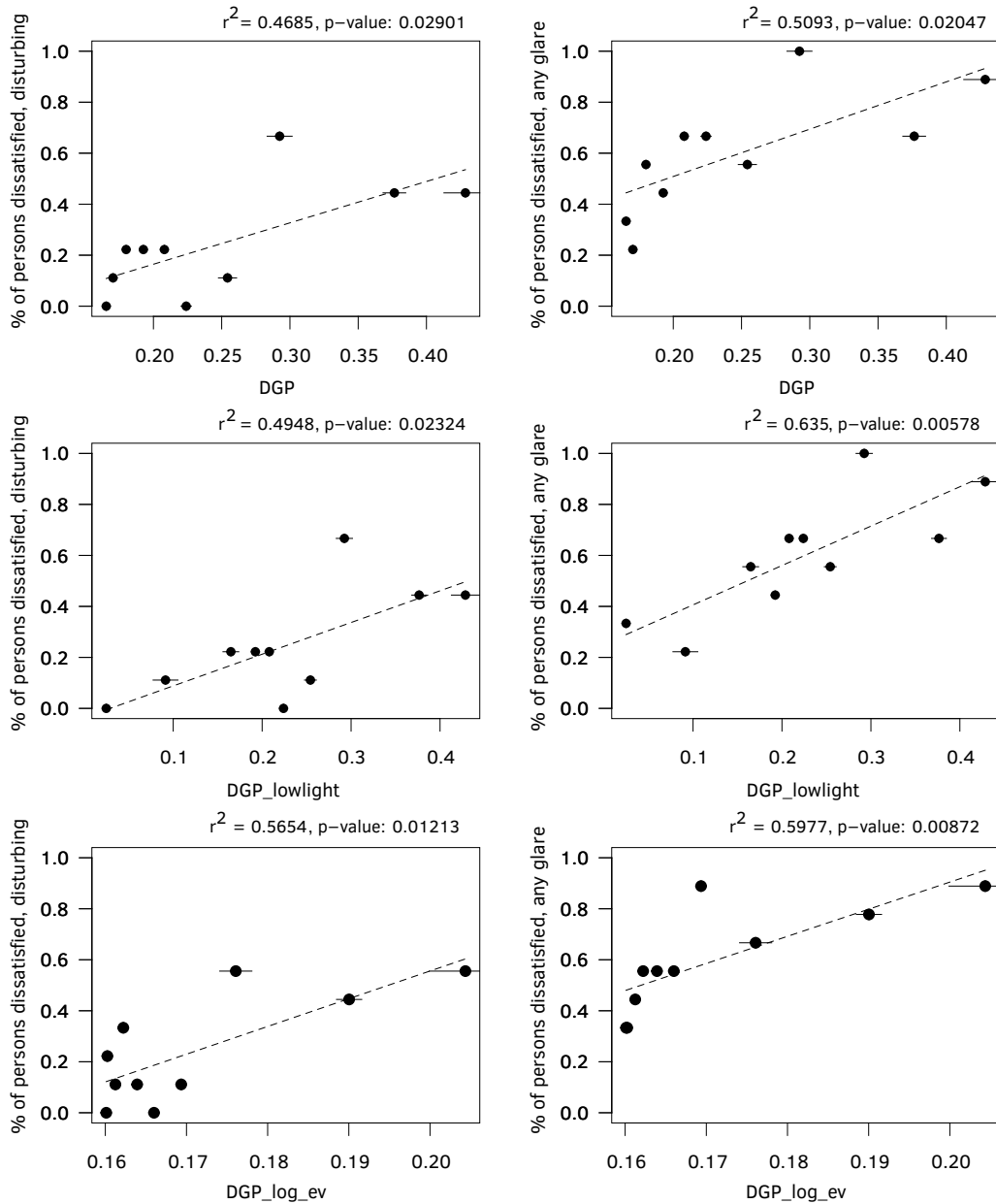
a

FIG. 8.1 Scatter plots of the linear regressions for DGP and DGLog(E_v) with and without low light correction and for UGP, in the window zone; 'disturbing glare' regressions on the left and 'any glare' regressions on the right.



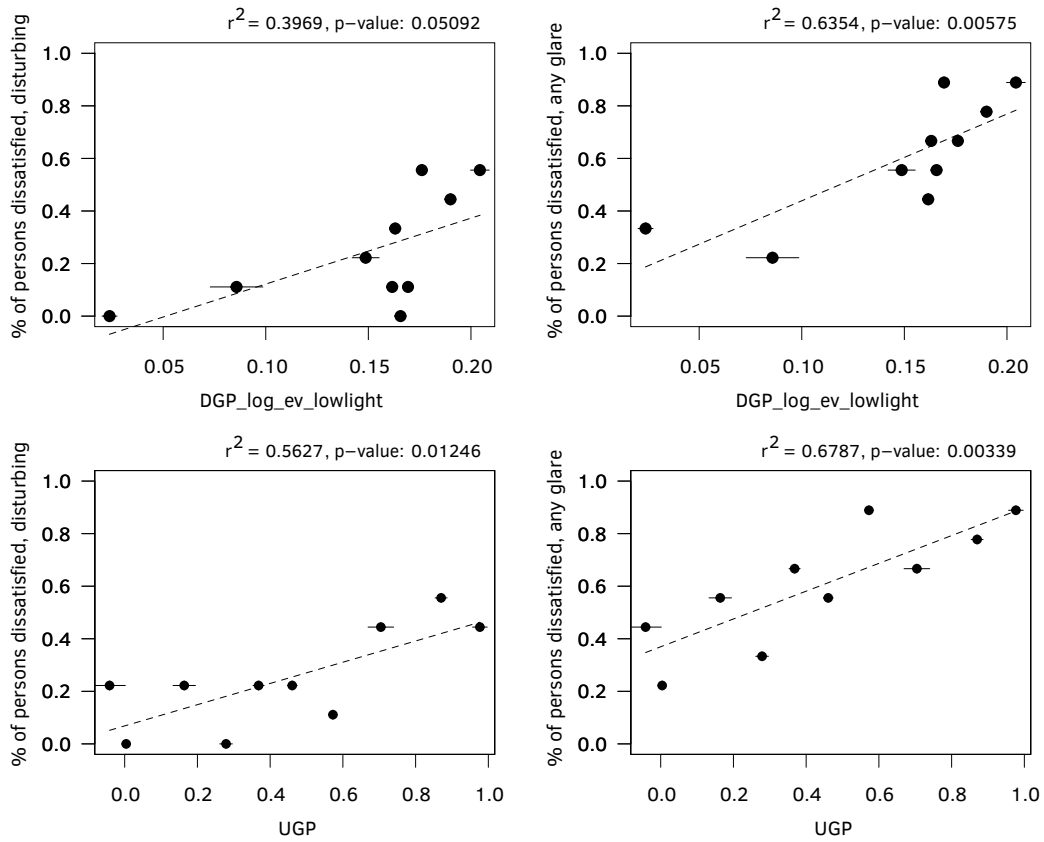
b

FIG. 8.1 Scatter plots of the linear regressions for DGP and DGLog(E_v) with and without low light correction and for UGP, in the window zone; 'disturbing glare' regressions on the left and 'any glare' regressions on the right.



a

FIG. 8.2 Scatter plots of the linear regressions for DGP and DGPlow(Ev) with and without low light correction and for UGP, in the wall zone; 'disturbing glare' regressions on the left and 'any glare' regressions on the right.



b

FIG. 8.2 Scatter plots of the linear regressions for DGP and DGPlot(Ev) with and without low light correction and for UGP, in the wall zone; 'disturbing glare' regressions on the left and 'any glare' regressions on the right.

The full results of the linear regressions are provided in Table 8.3. The fitness of the models is determined by their effect size, or coefficient of determination r^2 and by the significance of the statistic, with significance set at $p < 0.05$. Attention is also given to the standard error of b_1 and to the bounds of the 95% confidence interval of b_1 . If these values show an opposite tendency in terms of the direction of the slope, e.g., if they are negative when the slope is positive, they are signalled in grey. The effect size column (r^2) is colour-coded from best to worst (brighter to darker blue).

The results show that in the window zone, UGP produces the best coefficients of determination for the ‘any glare’ definition ($r^2 = 0.68$ $p = 0.003$) and a similar coefficient of determination to DGPl $og(E_v)$ for the ‘disturbing glare’ definition ($r^2 = 0.56$ $p = 0.012$ and $r^2 = 0.57$ $p = 0.012$, respectively). The standard error of b_1 is also very similar for the UGP and DGPl $og(E_v)$, for the ‘disturbing glare’ definition.

TABLE 8.3 Linear regression results for the 20 models.

Zone	Metric	Glare	r^2	p	b_0		b_1		b_1	
						SE		SE	lower	upper
									95% CI	95% CI
wall	DGP	any_glare	0.32	0.091	0.33	0.21	1.70	0.88	-0.03	3.43
wall	DGPl $og(E_v)$	any_glare	0.62	0.007	-0.72	0.40	7.79	2.17	3.54	12.04
wall	UGP	any_glare	0.58	0.010	0.51	0.07	0.38	0.11	0.16	0.60
wall	DGP _{lowlight}	any_glare	0.50	0.022	0.50	0.08	1.08	0.38	0.34	1.83
wall	DGPl $og(E_v)$ _{lowlight}	any_glare	0.71	0.002	0.45	0.07	1.76	0.40	0.97	2.55
wall	DGP	disturbing	0.18	0.218	-0.13	0.25	1.42	1.06	-0.66	3.49
wall	DGPl $og(E_v)$	disturbing	0.13	0.306	-0.55	0.69	4.04	3.69	-3.20	11.28
wall	UGP	disturbing	0.28	0.119	0.05	0.10	0.28	0.16	-0.03	0.59
wall	DGP _{lowlight}	disturbing	0.36	0.066	0.00	0.10	0.98	0.46	0.08	1.88
wall	DGPl $og(E_v)$ _{lowlight}	disturbing	0.73	0.002	-0.05	0.06	1.61	0.34	0.94	2.28
window	DGP	any_glare	0.51	0.020	0.14	0.17	1.86	0.64	0.59	3.12
window	DGPl $og(E_v)$	any_glare	0.60	0.009	-1.22	0.53	10.63	3.08	4.59	16.68
window	UGP	any_glare	0.68	0.003	0.37	0.07	0.53	0.13	0.28	0.78
window	DGP _{lowlight}	any_glare	0.64	0.006	0.25	0.10	1.54	0.41	0.73	2.36
window	DGPl $og(E_v)$ _{lowlight}	any_glare	0.64	0.006	0.11	0.14	3.30	0.88	1.57	5.04
window	DGP	disturbing	0.47	0.029	-0.16	0.16	1.62	0.61	0.42	2.82
window	DGPl $og(E_v)$	disturbing	0.57	0.012	-1.62	0.58	10.87	3.37	4.27	17.48
window	UGP	disturbing	0.56	0.012	0.07	0.07	0.40	0.13	0.16	0.65
window	DGP _{lowlight}	disturbing	0.49	0.023	-0.04	0.11	1.24	0.44	0.37	2.11
window	DGPl $og(E_v)$ _{lowlight}	disturbing	0.40	0.051	-0.13	0.17	2.51	1.09	0.37	4.65

Effect size (r^2) is colour-coded from lighter to darker blue (best to worst). A greyed-out cell indicates a value with poor performance. SE stands for standard error. And CI stands for confidence interval.

In the wall zone, all the metrics produce a non-significant correlation for ‘disturbing glare’, except the DGPl $og(E_v)$ with low light correction, DGPl $og(E_v)$ _{lowlight}. In the wall zone, a model based on the DGPl $og(E_v)$ _{lowlight} provides the best results, with r^2 values of 0.71 ($p = 0.002$) for the ‘any glare’ definition and of 0.73 ($p = 0.002$) for the ‘disturbing glare’ definition. This represents a significant improvement over the non-corrected version of the metric for the prediction of ‘disturbing glare’, in particular.

Understandably, extending the range of values of the DGP and $DGPlog(E_v)$ metrics to include values lower than 0.2, seems to improve the correlations. This improvement does mostly occur in the wall zone, where lower light levels and therefore a lower E_v , is verified. The standard error of b_1 is also considerably reduced when the metric is calculated with low light correction. As it can be seen in the scatter plots, the low light correction provides more definition in the lower range of the DGP and $DGPlog(E_v)$. Including these lower values in the regressions produces a better correlation with the reported glare.

Overall, the results of the study show that an adapted UGP provides a reasonably good model in the window zone but provides a poor model in the wall zone, particularly for the 'disturbing glare' definition. The adaptation of the $DGPlog(E_v)$ metric with low light correction, $DGPlog(E_v)_{lowlight}$, provides models with good predictive power in the wall zone but with poor to reasonable predictive power in the window zone.

The best obtained model in the study is therefore one based on two metrics, with UGP-based equations for the window zone and with $DGPlog(E_v)_{lowlight}$ -based equations for the wall zone. These equations, including the standard errors of b_0 and b_1 , are

Wall zone, disturbing glare:

$$\text{Glare} = -0.05(\pm 0.06) + 1.61(\pm 0.34) \cdot DGPlog(E_v)_{lowlight} \quad \text{EQ 23}$$

Wall zone, any glare:

$$\text{Glare} = 0.45(\pm 0.07) + 1.76(\pm 0.40) \cdot DGPlog(E_v)_{lowlight} \quad \text{EQ 24}$$

Window zone, disturbing glare:

$$\text{Glare} = 0.07(\pm 0.07) + 0.4(\pm 0.13) \cdot UGP \quad \text{EQ 25}$$

Window zone, any glare:

$$\text{Glare} = 0.37(\pm 0.07) + 0.53(\pm 0.13) \cdot UGP \quad \text{EQ 26}$$

It is observed that the slopes (b_1) of the two pairs of models don't change considerably within the same zone, indicating that the relationship between the percentage of persons that report discomfort glare as defined by $DGPlog(E_v)_{lowlight}$ and by UGP tends to be similar, independently of the definition of glare that one chooses to look at (any or disturbing).

When the standard errors of the constant and of the coefficient of the equations are taken into consideration, 'disturbing glare' should equal zero when the $DGPlog(E_v)_{lowlight}$ and the UGP are zero, whereas 'any glare' does not seem to be preventable at a $DGPlog(E_v)_{lowlight}$ and UGP of zero, with approximately 40% of the people still experiencing some form of glare.

8.4 Conclusion

The study that was here presented shows that it is possible to produce a discomfort glare equation based on the $DGPlog(E_v)$ and UGP metrics that provide reasonable predictions of discomfort glare for the conditions of this study.

In the window zone, a UGP-based equation produces the best coefficients of determination for the 'any glare' definition ($r^2 = 0.68$, $p = 0.003$) and a similar coefficient of determination to the $DGPlog(E_v)$ -based equation for the 'disturbing glare' definition ($r^2 = 0.56$ $p = 0.012$ and $r^2 = 0.57$ $p = 0.012$, respectively). In the wall zone, an equation based on the $DGPlog(E_v)_{lowlight}$ provides the best results, with r^2 values of 0.71 ($p = 0.002$) for the 'any glare' definition and of 0.73 ($p = 0.002$) for the 'disturbing glare' definition.

It can be observed that the UGP-based equations perform better than DGP-based equations in the window zone. This result indicates that the glare condition in the window zone might tend to be of contrast glare as UGP is a contrast-only type of metric. In the window zone, as the subjects look inwards and their visual fields are almost totally filled by the darker walls of the room, the contrast of the peripheral window glare source with those walls can be contributing towards a mostly contrast glare situation.

It was expected that the much smaller apparent size of the window glare source against the background as seen from the positions in the wall zone would produce a higher luminance contrast situation and as a result, the UGP-based equations would perform better than they did in that zone. However, the overall luminance also increases when looking in the direction of the window, which could explain why an equation that is based on a metric that includes an adaptation term in its definition, such as the $DGPlog(E_v)_{lowlight}$, tends to perform better than the equation based on UGP.

It is verified that the DGP-based equations (with or without low light correction) are the least successful from the three options of equations at predicting discomfort glare in the study. As explained earlier, DGP has been developed and validated for conditions where subjects were facing directly or almost directly the window glare source, a situation that is very different from the field-of-view conditions of this study.

The fact that the $DGPlog(E_v)$ -based equations tend to perform better than the DGP-based equations, indicate that the logarithmic form of the adaptation term E_v has benefits over its linear form.

9 Developing a discomfort glare model based on a modified metric

9.1 Introduction

This chapter follows the previous two chapters on the investigation of a new model of discomfort glare for the classroom space. The improvement of the predictive power that was verified in the previous two chapters, either based on an analysis of a range of glare parameters (Chapter VI) or on an equation based of the current definition of the DGP and UGP metrics (Chapter VII), did not show satisfactory results. In this chapter, it is investigated if a modified version of the DGP and of the UGP metrics provides a better predictive model than the previous attempts and if a successful index based on an alternative form of these equations can be defined.

Since neither DGP nor UGP performed clearly well in all the cases that were analysed in the previous chapter, this study is based on both metrics. A transformed version of DGP, $DGP_{log}(E_v)$, is also included since in the previous study, the use of the logarithm of E_v in the adaptation term of DGP produced better results than its linear form. The modification of the glare indices that is here investigated corresponds to an adjustment of the value of a range of components of the equations, such as its coefficients, exponents and constants (Figure 9.1).

$$DGP = 5.87 \cdot 10^{-5} \cdot E_v + 9.18 \cdot 10^{-2} \cdot \log\left(1 + \sum_{i=1}^n \frac{L_{s,i}^2 \cdot \omega_{s,i}}{E_v^{1.87} \cdot P_i^2}\right) + 0.16$$

FIG. 9.1 Components of the DGP equation.

The objective of the study is to find if new values for these components can produce equations with a better correlation to the reported discomfort glare.

The method used to find these values is based on a computational optimisation approach, similar to the method that has been used in the development of the DGP (Wienold, 2010) and in the development of DGPmod (Konstantzos and Tzempelikos, 2017).

The data used in this investigation is the data from Study I (N = 184) divided into two samples, the window zone sample (N=90) and the wall zone sample (N=94). The reasons for the use of the Study I dataset are explained in Chapter VII.

9.2 Metrics and their components

The DGP and UGP are two different glare indices that are based on a range of parameters and on a range of coefficients and exponents to those parameters. Both metrics inherit the basic form of the glare sensation formula (Chapter II) with some modifications in terms of their variables and of their specific set of coefficients, exponents and constants. The modification of these components was defined based on empirical studies, conducted with the specific purpose of developing better discomfort glare metrics. These components are also the object of this investigation and are explained next.

The DGP contains two coefficients applied to its variables, the coefficient of the adaptation term, c1, and the coefficient of the contrast term, c2, and one additional constant, c4. The equation also has three exponents applied to the luminance of the source (L_s), to the position index (P) and to the vertical illuminance (E_v), in the contrast part of the equation.

The present study focuses on the components of the equations that have gone through previous modifications, namely its coefficients, its constant and the exponent of the vertical illuminance (E_v). The exponents of the luminance of the source (L_s) and of the position index (P) are kept at their original value of 2. The components of the DGP that are optimised in the study are represented as $c1$, $c2$, $c3$ and $c4$ in the equation below.

$$\text{DGP} = c1 \cdot 10^{-5} \cdot E_v + c2 \cdot 10^{-2} \cdot \log_{10} \left(1 + \sum_{i=1}^n \frac{L_{s,i}^2 \cdot \omega_{s,i}}{E_v^{c3} \cdot P_i^2} \right) + c4$$

Since the use of the logarithmic form of E_v in the adaptation term of DGP was found to produce an improved correlation with reported discomfort glare (Chapter VIII), a definition of DGP with this formulation, $\text{DGPlg}(E_v)$, is also included in the study. The $\text{DGPlg}(E_v)$ optimization is based on the same components as the DGP optimisation, $c1$, $c2$, $c3$ and $c4$.

$$\text{DGPlg}(E_v) = c1 \cdot 10^{-5} \cdot \log_{10}(E_v) + c2 \cdot 10^{-2} \cdot \log_{10} \left(1 + \sum_{i=1}^n \frac{L_{s,i}^2 \cdot \omega_{s,i}}{E_v^{c3} \cdot P_i^2} \right) + c4$$

The UGP is a contrast-based metric that contains a contrast term only. This contrast term contains two coefficients, $c1$ and $c2$ and exponents to the luminance of the source (L_s) and to the position index (P) variables. Similarly to the DGP, the UGP contains a fixed exponent of 2 for L_s and P . The metric evolved from UGR by the transformation of one of its coefficients. In this study, the two UGP coefficients, represented as $c1$ and $c2$ in the equation below are optimised.

$$\text{UGP} = c1 \cdot \log_{10} \left(\frac{c2}{L_b} \cdot \sum_{i=1}^n \frac{L_{s,i}^2 \cdot \omega_{s,i}}{P_i^2} \right)$$

9.3 Method

9.3.1 Optimisation goal

In order to find a form of the DGP and UGP equations with a higher predictive power, an optimisation of the equations exercise is carried out in this study. The optimal form of the metric's equations is obtained for the combination of c1, c2, c3 and c4 components that deliver the highest predictive power. The optimisation that is performed is based on statistical linear regression. As explained in the previous Chapter, the option for linear regression fits this dataset better than other forms of regression. On the other hand, the transformation of the dependent variable into a 'percentage of persons that report glare' required for linear regression (see Chapter VIII) is a convenient one as it allows the development of a model that reports glare in the original DGP and UGP scales (see 9.3.2).

The predictive power of the optimised equations is measured by the effect size of the linear regression, or coefficient of determination r^2 , with the objective of the optimisation being the maximisation of the r^2 . The r^2 corresponds to the quotient between the variance of the fitted values and the variance of the observed values of the dependent variable Y.

$$r^2 = 1 - \frac{\sum_i^n (y_i - \hat{y}_i)^2}{\sum_i^n (y_i - \bar{y}_i)^2}$$

Where, \hat{y} is the fitted value for the observation i , \bar{y} is the mean value of Y, $Y = b_0 + b_1 \cdot X$, where X is the independent variable, and b_0 and b_1 are the constant and the coefficient of the fitted regression line, respectively.

The r^2 therefore represents the fraction of variance of an event that is explained by a particular model, in this case, the variance of the 'percentage of persons that report glare' that is explained by the improved metric.

9.3.2 Model development approach

By calculating the r^2 value of the linear regression $Y = b_0 + b_1 \cdot X$, it is assumed that there is a linear relationship between the percentage of disturbed people, Y , and the modified metrics DPG, $DGP_{\log}(E_v)$ and UGP, or X . As the scale of the DPG and UGP metrics directly corresponds to the 'percentage of persons that report glare', the new metric should result in a relationship of $Y = X$. This relationship is obtained when the linear regression equation is combined with the optimised metric as demonstrated below.

For DGP:

$$DGP_{\text{new}} = b_0 + b_1 \cdot DGP_{\text{optimised}}$$

$$DGP_{\text{new}} = b_0 + b_1 \cdot \left(c1 \cdot 10^{-5} \cdot E_v \cdot c2 \cdot 10^{-2} \cdot \log_{10} \left(1 + \sum_{i=1}^n \frac{L_{s,i}^2 \cdot \omega_{s,i}}{E_v^{c3} \cdot P_i^2} \right) + c4 \right)$$

$$DGP_{\text{new}} = b_1 \cdot c1 \cdot 10^{-5} \cdot E_v + b_1 \cdot c2 \cdot 10^{-2} \cdot \log_{10} \left(1 + \sum_{i=1}^n \frac{L_{s,i}^2 \cdot \omega_{s,i}}{E_v^{c3} \cdot P_i^2} \right) + b_0 + b_1 \cdot c4$$

where b_0 and b_1 are the constant and coefficient of the linear regression. New $c1$ to $c4$ components can now be defined as

$$c1_{\text{new}} = b_1 \cdot c1; c2_{\text{new}} = b_1 \cdot c2; c3_{\text{new}} = c3; c4_{\text{new}} = b_0 + b_1 \cdot c4$$

so that the new improved DGP metric is defined as

$$DGP_{\text{new}} = c1_{\text{new}} \cdot 10^{-5} \cdot E_v + c2_{\text{new}} \cdot 10^{-2} \cdot \log_{10} \left(1 + \sum_{i=1}^n \frac{L_{s,i}^2 \cdot \omega_{s,i}}{E_v^{c3_{\text{new}}} \cdot P_i^2} \right) + c4_{\text{new}}$$

Similarly, for DGPl_{og}(Ev):

$$\text{DGPl}_{og}(\text{Ev})_{new} = c1_{new} \cdot 10^{-5} \cdot \log_{10} E_v + c2_{new} \cdot 10^{-2} \cdot \log_{10} \left(1 + \sum_{i=1}^n \frac{L_{s,i}^2 \cdot \omega_{s,i}}{E_v c3_{new} \cdot P_i^2} \right) + c4_{new}$$

where b_0 and b_1 are the constant and coefficient of the linear regression and new $c1$ to $c4$ components defined as

$$c1_{new} = b_1 \cdot c1; c2_{new} = b_1 \cdot c2; c3_{new} = c3; c4_{new} = b_0 + b_1 \cdot c4$$

For UGP:

$$\text{UGP}_{new} = c1_{new} \cdot \log_{10} \left(\frac{c2_{new}}{L_b} \cdot \sum_{i=1}^n \frac{L_{s,i}^2 \cdot \omega_{s,i}}{P_i^2} \right) + b_0$$

where b_0 and b_1 are the constant and coefficient of a linear regression and new $c1$ and $c2$ components, and b_0 are defined as

$$c1_{new} = b_1 \cdot c1; c2_{new} = c2 \text{ and } b_0 = 0$$

The demonstration that the r^2 does not change with this operation is provided in Appendix F, section 1.

9.3.3 Optimisation approach

The search for a new set of components c_1 , c_2 , c_3 and c_4 that is performed in this study uses a genetic algorithm optimisation approach. The optimisation was performed using the R programming language for statistical computing (R Core Team, 2020), the RStudio development environment (RStudio Team, 2020) and the 'GA' package for R (Scrucca, 2013a). The 'GA' package for R is a collection of general-purpose functions for optimisation using genetic algorithms. The optimisation in this study uses a floating-point representation of the decision variables c_1 , c_2 , c_3 and c_4 , designated as a the "real-valued" type within the 'GA' package (Scrucca, 2013b). The description of the functions and arguments of the 'GA' package are provided in (Scrucca, 2013b).

The genetic algorithm is a computational optimisation technique that uses operation mechanisms that mimic the process of natural selection, to produce an optimal solution to a problem in a faster and more efficient way than a sequential computational approach. A flow chart representing this optimisation process can be found in Figure 9.2.

The process starts with a random generation of a group of individuals, which form the initial population and for each iteration, a generation. The fitness of these individuals is assessed according to user-defined fitness criteria (Fitness evaluation) and the fittest of these individuals are selected for reproduction (Selection). The amount of individuals selected from each generation can vary for different implementations of a genetic algorithm. During reproduction (Crossover), pairs of these fittest individuals are combined producing offspring, by exchange of the parents' genes, until a predefined crossover point is reached. Some of these offspring go through a process of mutation of their genes (Mutation), according to a predefined and usually low probability rate. The population that results from these operations forms the new generation of the next iteration. The algorithm terminates after a predefined number of generations (or iterations) is reached or when a predefined number of generations have been produced without any improvement in the best fitness value. In this case it is said that the algorithm has converged and a solution to the problem has been reached (GA output).

In this study some of the parameters of the optimisation were kept as variables so these could be tested in the process. These are the population size, the maximum number of iterations, the convergence criteria (the number of consecutive generations without any improvement in the best fitness value) and the seed. The seed is a random number used to generate the initial population, which is mainly used to replicate the results of a genetic algorithm search.

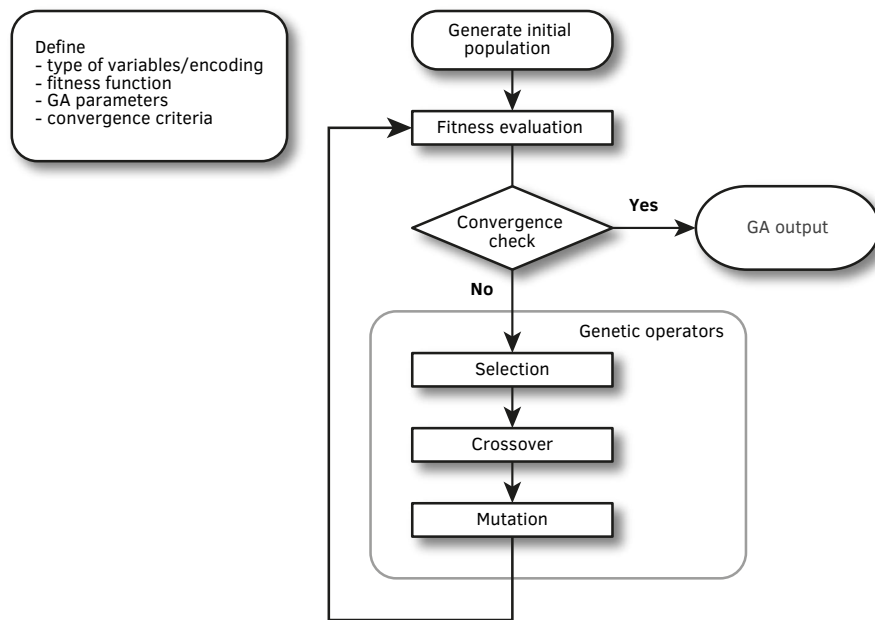


FIG. 9.2 Flow chart of the genetic algorithm search process (Scrucca, 2013b).

In the case of the ‘GA’ package for R, 5% of the fittest individuals are selected for reproduction. The probability of crossover was set to 0.8, which means that there is 80% probability of crossover between individuals (or pairs of components). The probability of mutation of the offspring is set to 0.1, which means that there is 10% chance of mutation. The suggested matrix of c_1 , c_2 , c_3 and c_4 to be included in the initial population were set to the metrics’ original components. The optimisation returns the best fitness value (r^2) found and the solutions for the decision variables c_1 , c_2 , c_3 and c_4 .

The use of a linear regression-based fitness function like the r^2 requires some particular attention in the search for a solution. On the one hand, the use of the r^2 implies that an optimal solution can be produced based on a negative correlation, which would be an invalid result. For this reason, the Pearson correlation value r is firstly checked and if $r < 0$, the candidate solution is excluded. On the other hand, as the data needs to be grouped for the linear regression to be performed and this grouping process needs to be repeated every time a new candidate solution (equation) is tested, there is no guarantee that there are no outliers in the newly created datasets, unless some form of control is implemented. A Cook’s distance function was then integrated to check for outliers every time a new grouping is produced. If the Cook’s distance is higher than 1, the r^2 of that candidate solution is set to zero, which means that solution does not pass on to the next generation.

To address the above-mentioned aspects, a specific fitness algorithm was designed, as presented in Figure 9.3.

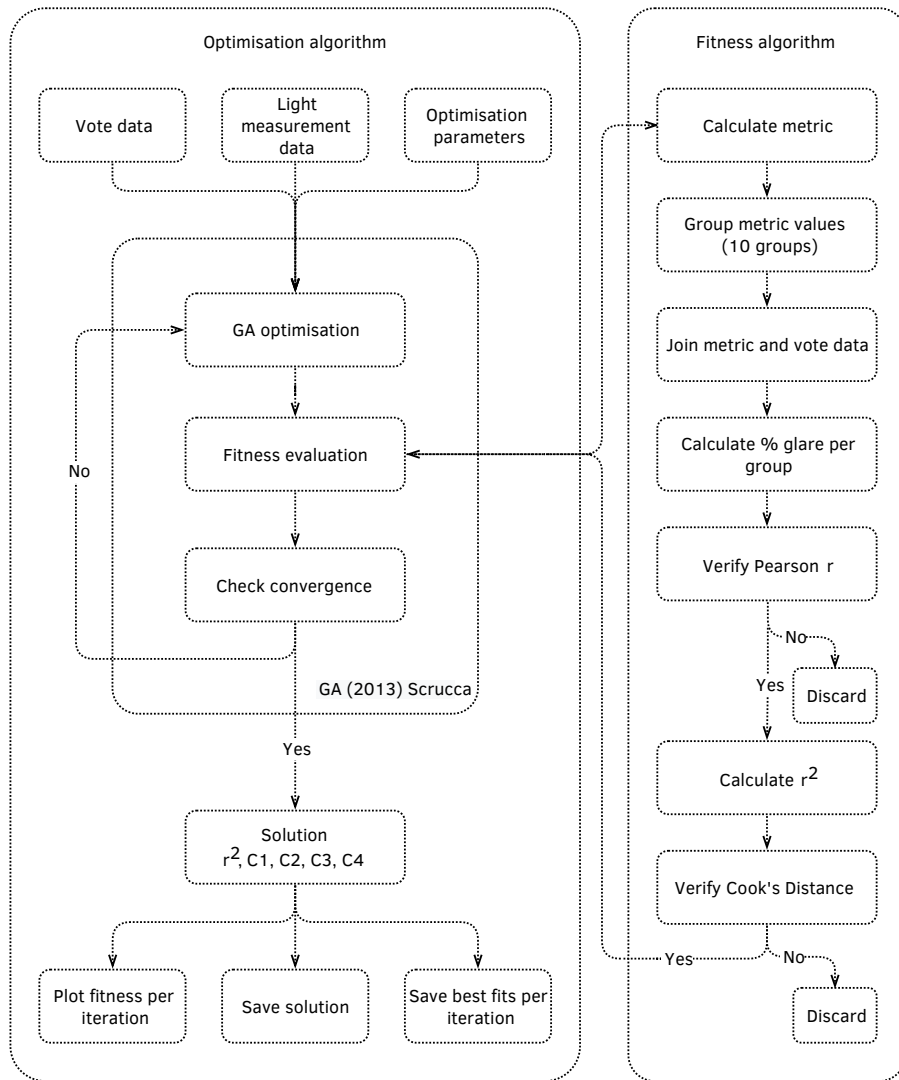


FIG. 9.3 Flow chart of the optimisation and fitness algorithms.

The optimisation process will show if there is potential for improvement of the glare indices based on a modification of their components c1, c2, c3 and c4.

9.3.4 Analysis models

As the study is based on a statistical linear regression, it follows the same approach that was used in Chapter VIII, where the dataset of Study I is divided into two zones, the window zone with $N = 90$ observations and the wall zone with $N = 94$ observations. These observations are grouped into 10 groups, as explained in Chapter VIII, for the purpose of transforming the dependent variable into a ‘percentage of people that report glare’.

The optimisation is run for the two zones (window and wall), for the two definitions of glare (‘any glare’ and ‘disturbing’ glare) and the three metrics, resulting in twelve different analysis models (Table 9.1).

TABLE 9.1 Analysis models.

#	Zone	Metric	Glare	Sample
1	wall	DGP	disturbing	N = 10
2		DGPlog(Ev)		
3		UGP		
4		DGP	any glare	
5		DGPlog(Ev)		
6		UGP		
7	window	DGP	disturbing	N = 10
8		DGPlog(Ev)		
9		UGP		
10		DGP	any glare	
11		DGPlog(Ev)		
12		UGP		

As a reminder, the reason for an analysis based on two definitions of glare emerges from the transformation of the original ordinal scale of the dependent variable into a continuous variable (percentage discomfort). For the ‘any glare’ definition the cut-off point is set to a level of glare perception rated by the subjects as ‘disturbing’ or ‘intolerable’ (votes 3 and 4) and for the ‘any glare’ definition the cut-off point is set to a level of glare perception rated by the subjects from ‘noticeable’ to ‘intolerable’ (votes 2 to 4).

It is worth mentioning that the ‘disturbing’ glare definition is the definition that has more commonly been used in the development of glare models based on a similar statistical approach (Wienold, 2010) (Konstantzos and Tzempelikos, 2017).

As the model is developed based on a linear regression, the optimisation of the DGP and of the $DGPlog(E_v)$ metrics is performed for the metrics without low light correction, as the low light correction introduces a non-linear behaviour to the DGP equation (Wienold, 2012, pag. 19), making the equation development operation described in 9.3.2 not a viable one.

9.3.5 Statistical power analysis

A question arises regarding the statistical power of models based on a sample of 10 points. Statistical power is a concept proposed by Cohen (1988) to measure the probability that an effect of a particular statistical model or test will be revealed when a true effect really exists. Typically, the minimum recommended power of a test is set to 0.8 (Field, 2009). The size of the sample required to achieve a particular power depends on the expected effect size (r^2), a given significance and on the number of predictors of a model with the expected effect size generally obtained from published literature in the field (Field, 2009).

A power analysis was done to determine if the 10-point sample of this study would deliver the required statistical power of 0.8, using the 'pwr' package (Champely et al., 2020) for R. The analysis uses the 'pwr.f2.test' function to estimate the sample size for the general linear model, from the following inputs: effect size = 0.84; significance = 0.01, number of predictors = 3 and power = 0.8. The effect size of 0.84 corresponds to the average effect sizes from the studies of Wienold (2010), Hirning et al. (2014), Karlsen et al. (2015) and Konstantzos and Tzempelikos (2017), which use the same statistical approach of grouped variables as this study. The number of predictors is defined as the number of coefficients in the model, minus the intercept, which in the case of the DGP is 3. The minimum required sample size for these conditions was estimated as $N = 9$. The models produced based on the 10-point sample have therefore adequate statistical power.

9.4 Results

9.4.1 Testing the parameters of the optimisation

The parameters of the genetic algorithm optimisation were firstly tested to find how sensitive the solution was to these and establish a range of suitable values for the final optimisation. A description, the inputs and outputs of these tests are provided in the Appendix F, section 2. Tables 9.2 and 9.3 provide a summary of the parameters and results of the tests.

As a summary, it was found that a reduction of the upper bounds of the components (limiting the solution space) and an increase of the number of iterations (from 1,000 to 10,000) produced an improvement of the r^2 . Changes to the other parameters of the optimisation did not provide any significant improvements to the results of the optimisation.

TABLE 9.2 Tests to the parameters of the genetic algorithm optimisation, 1 to 5.

Run	1		2		3/4/5		
Test	initial		adjusted bounds		adjusted bounds - UGP		
Metric	DGP &	UGP	DGP &	UGP	UGP	UGP	UGP
	DGPlog(Ev)		DGPlog(Ev)				
c1	0 - 20	0 - 20	0 - 15	0 - 15	0 - 1	0 - 0.2	0 - 0.26
c2	0 - 20	0 - 20	0 - 20	0 - 1	0 - 1	0 - 0.2	0 - 0.15
c3	0 - 20		0 - 5				
c4	0 - 20		0 - 0.16				
Population	50		50		50		
Iterations	1000		1000		1000		
Convergence setting	100		100		100		
Seed	12345		12345		12345		
Result			same or improved r^2		minor improvement of r^2		

TABLE 9.3 Tests to the parameters of the genetic algorithm optimisation, 6 to 13.

Run:	6/7		8/9		10/11/12		13	
Test	adjusted bounds - DGP		population size		different seed		increased iterations	
Metric	DGP &	DGP &	DGP &	UGP	DGP &	UGP	DGP &	UGP
	DGPlog(Ev)	DGPlog(Ev)	DGPlog(Ev)		DGPlog(Ev)		DGPlog(Ev)	
c1	0 - 15	0 - 15	0 - 15	0 - 1	0 - 15	0 - 1	0 - 15	0 - 0.26
c2	0 - 20	0 - 20	0 - 20	0 - 1	0 - 20	0 - 1	0 - 20	0 - 0.15
c3	2 - 2	0 - 4	0 - 5		0 - 5		0 - 5	
c4	0 - 0.16	0 - 0.16	0 - 0.16		0 - 0.16		0 - 0.16	
Population:	50		25/100		50		50	
Iterations	1000		1000		1000		10000	
Convergence setting	100		100		100		none	
Seed	12345		12345		31254/24153/52134		12345	
Result	no improvement of r^2		no clear benefit		no significant difference		improvement of r^2	

9.5 Optimisation

The optimisation was run with the parameter values that showed to provide the best r^2 results in the tests that were performed previously. The parameters used in the optimisation are, therefore, the parameters of run number 13, presented in Table 9.3 above. The results of the optimisation can be found in Table 9.4.

TABLE 9.4 Results of the first optimisation run: r^2 and resulting components c1, c2, c3, c4.

Zone	Metric	Glare	r^2	c1	c2	c3	c4
wall	DGP	disturbing	0.44	6.94	3.54	0.01	0.12
wall	DGPlog(E _v)	disturbing	0.86	6.12	11.50	3.09	0.13
wall	UGP	disturbing	0.29	0.21	0.09		
wall	DGP	any glare	0.84	1.02	18.06	1.49	0.04
wall	DGPlog(E _v)	any glare	0.83	5.59	0.11	2.17	0.14
wall	UGP	any glare	0.65	0.09	0.05		
window	DGP	disturbing	0.62	0.23	12.59	1.83	0.07
window	DGPlog(E _v)	disturbing	0.72	8.91	15.07	2.48	0.15
window	UGP	disturbing	0.66	0.08	0.05		
window	DGP	any glare	0.93	0.06	19.19	0.78	0.13
window	DGPlog(E _v)	any glare	0.93	14.08	0.49	0.80	0.12
window	UGP	any glare	0.81	0.08	0.002		

The evolution of the optimisation was monitored in two ways, via the convergence plots of the r^2 and by plotting the components that were produced for the iterations that resulted on an improved r^2 . These last plots, are hereby called the components plots.

The convergence plots showed that the r^2 value evolved up until iteration number 7,200, which means that all cases were properly converged at iteration number 10,000. The components plots however, showed a somewhat surprising result. Figure 9.4 shows two of these plots. It is observed that the value of c4 of the DGP and of the DGPlog(E_v) and the value of c1 of the UGP varies significantly after the r^2 stabilises to its best result. For this reason, the final optimisation was run with fixed values for these components. The UGP's c1 is fixed at 0.26, the metric's original c1 value. This effectively means that for UGP, the optimisation is performed for c2 only. For DGP and DGPlog(E_v) two optimisations were run with fixed c4 values of 0.16 (the metric's original c4 value) and of 0. The parameters of the final optimisation runs are presented in Table 9.5.

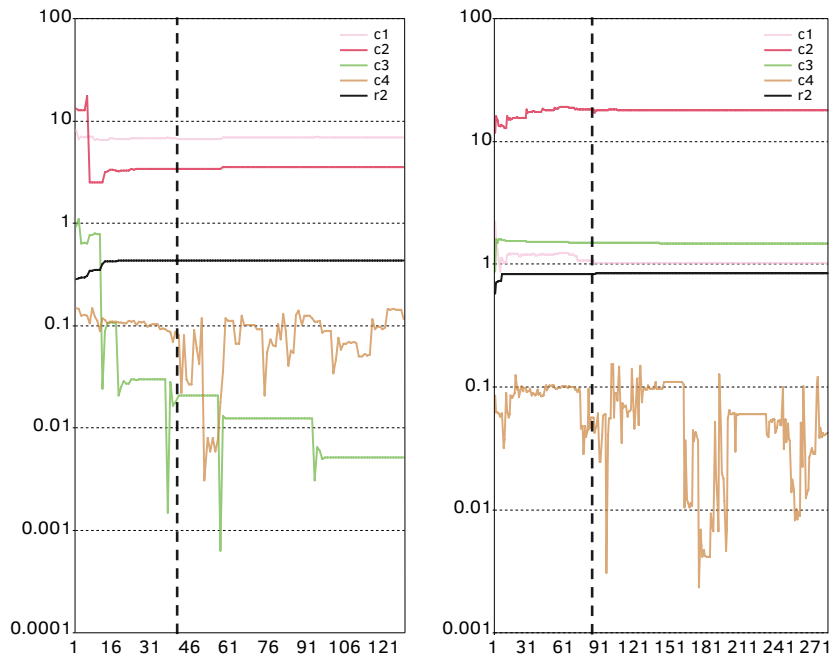


FIG. 9.4 Components' plots for DGP, in the wall zone: 'disturbing glare' (left) and 'any glare' (right). The vertical black line shows the iteration from which the r^2 does not change. The plots show the components obtained for every improvement of the r^2 . As an improved r^2 is not always found for all the iterations, the number of data points in these plots (x-axis) is much smaller than the total number of iterations.

TABLE 9.5 Parameters of the final optimisation runs.

Optimization run:	optimisation 1		optimisation 2
Metric	DGP & DGPlog(Ev)	UGP	DGP & DGPlog(Ev)
c1	0 - 15	0.26 - 0.26	0 - 15
c2	0 - 20	0.15	0 - 20
c3	0 - 5		0 - 5
c4	0.16 - 0.16		0 - 0
Population	50		50
Iterations	10000		10000
Convergence setting	none		none
Seed	12345		12345

9.5.1 Optimisation results

The resulting coefficient of determination r^2_{optim} and components c1, c2, c3 and c4, for the 12 different analysis models and for the two optimisations, are presented in Tables 9.6 and 9.7. The coefficients of determination that were obtained for the three metrics before the optimisation r^2_{before} and the coefficients of determination that are obtained for DGPl_{og}(E_v) and DGP calculated with low light correction $r^2_{\text{before}^*}$ are also provided for reference.

TABLE 9.6 Results of the optimisation 1: r^2_{optim} and components c1, c2, c3 and c4 in comparison with the coefficient of determination obtained before optimisation, $r^2_{\text{before}^*}$.

Zone	Glare	Metric	r^2_{before}	$r^2_{\text{before}^*}$	r^2_{optim}	c1	c2	c3	c4
Wall	Disturbing	DGP	0.18	0.36	0.44	7.142	3.648	0.004	0.16
Wall	Disturbing	DGPl _{og} (Ev)	0.13	0.62	0.86	5.290	9.945	3.091	0.16
Wall	Disturbing	UGP	0.28		0.29	0.260	0.093		
Wall	Any glare	DGP	0.32	0.51	0.84	1.046	18.517	1.487	0.16
Wall	Any glare	DGP log(Ev)	0.62	0.74	0.81	6.639	13.411	3.099	0.16
Wall	Any glare	UGP	0.58		0.65	0.260	0.045		
Window	Disturbing	DGP	0.47	0.49	0.62	0.247	13.760	1.823	0.16
Window	Disturbing	DGPl _{og} (Ev)	0.57	0.37	0.72	7.859	13.288	2.475	0.16
Window	Disturbing	UGP	0.56		0.66	0.260	0.045		
Window	Any glare	DGP	0.51	0.63	0.93	0.047	19.236	0.776	0.16
Window	Any glare	DGPl _{og} (Ev)	0.60	0.67	0.93	11.759	0.396	0.801	0.16
Window	Any glare	UGP	0.68		0.81	0.260	0.002		

r^2_{optim} is r^2 after optimisation, r^2_{before} is r^2 before the optimisation, $r^2_{\text{before}^*}$ is r^2 before the optimisation, for the metric calculated with low light correction.

TABLE 9.7 Results of the optimisation 2: r^2_{optim} and components c1, c2, c3 and c4 in comparison with the coefficient of determination obtained before optimisation, $r^2_{\text{before}^*}$.

Zone	Glare	Metric	r^2_{before}	$r^2_{\text{before}^*}$	r^2_{optim}	c1	c2	c3	c4
Wall	Disturbing	DGP	0.18	0.36	0.44	6.595	3.369	0.004	0
Wall	Disturbing	DGPl _{og} (Ev)	0.13	0.62	0.86	5.368	10.092	3.091	0
Wall	Any glare	DGP	0.32	0.51	0.84	0.958	16.982	1.486	0
Wall	Any glare	DGPl _{og} (Ev)	0.62	0.74	0.82	7.126	2.343	2.754	0
Window	Disturbing	DGP	0.47	0.49	0.57	2.953	12.918	1.557	0
Window	Disturbing	DGPl _{og} (Ev)	0.57	0.37	0.72	7.736	13.080	2.475	0
Window	Any glare	DGP	0.51	0.63	0.93	0.078	17.699	0.780	0
Window	Any glare	DGPl _{og} (Ev)	0.60	0.67	0.93	12.766	0.429	0.801	0

r^2_{optim} is r^2 after optimisation, r^2_{before} is r^2 before the optimisation, $r^2_{\text{before}^*}$ is r^2 before the optimisation, for the metric calculated with low light correction.

As expected, the optimisation 1 and optimisation 2 deliver similar r^2 results. For DGPl_{og}(E_v), the r^2 is the same for a c4 of 0.16 or 0, with only one very small difference verified for the wall zone / 'any glare' model. There is a small improvement of the DGP model for the for the window zone / 'disturbing glare' model when c4 is fixed at 0.16, with the other models showing the same r^2 for a c4 of 0.16 or 0.

9.6 Analysis

9.6.1 Magnitude of the improvement

The best r^2 results are obtained for DGPl_{og}(E_v) and for DGP. Although improvement of the r^2 is verified for all the UGP models, this improvement is much smaller than the verified for the DGP and DGPl_{og}(E_v).

The improvement is quite significant for the prediction of 'any glare', particularly in the window zone where it reaches a r^2 of 0.93. In the wall zone, where all the studied metrics including DGP and UGP showed a poor performance before, there is a significant improvement, with the r^2 reaching 0.84 for 'any glare' (DGP) and 0.86 for 'disturbing glare' (DGPl_{og}(E_v)). The improvement in the wall and window zones is therefore significant.

From the three optimised metrics, the DGPl_{og}(E_v) shows the best performance for the 'disturbing glare' definition and the same performance as DGP for the 'any glare' definition in the window zone. DGP shows the best performance for the definition of 'any glare' in the wall zone. As DGPl_{og}(E_v) still provides for a good model in the wall zone / 'any glare' condition, it can be said that overall DGPl_{og}(E_v) performs better than the other two metrics. Depending on the definition of glare, the optimised DGPl_{og}(E_v) metric accounts for 81% to 86% of the variance on the percentage of persons that report glare in the wall zone and for 72% to 93% on the variance on the percentage of persons that report glare in the window zone.

9.6.2 Fitness of the optimised models

The fitness of the produced models is examined based on the detailed results of the linear regressions, provided in Tables 9.8 and 9.9.

TABLE 9.8 Detailed results of the linear regressions for optimisation 1.

Zone	Glare	Metric	r^2	adj. r^2	p-value	RMSE	b_0	b_1	SE b_0	SE b_1
Wall	Disturbing	DGP	0.44	0.37	0.0374	0.101	-0.08	0.75	0.12	0.30
Wall	Disturbing	DGP log(Ev)	0.86	0.84	0.0001	0.045	-518	3232	75	470
Wall	Disturbing	UGP	0.29	0.20	0.1103	0.132	0.05	0.33	0.10	0.18
Wall	Any glare	DGP	0.84	0.82	0.0002	0.051	0.33	1.14	0.06	0.18
Wall	Any glare	DGP log(Ev)	0.81	0.79	0.0004	0.059	-457	2855	77	483
Wall	Any glare	UGP	0.65	0.61	0.0046	0.090	0.50	0.55	0.06	0.14
Window	Disturbing	DGP	0.62	0.58	0.0067	0.121	-0.74	5.34	0.27	1.47
Window	Disturbing	DGP log(Ev)	0.72	0.69	0.0019	0.098	-84	527	19	116
Window	Disturbing	UGP	0.66	0.62	0.0042	0.099	0.12	0.47	0.05	0.12
Window	Any glare	DGP	0.93	0.92	0.0000	0.047	0.21	0.67	0.04	0.06
Window	Any glare	DGP log(Ev)	0.93	0.92	0.0000	0.047	-4.97	33.01	0.54	3.17
Window	Any glare	UGP	0.81	0.79	0.0004	0.065	0.62	0.50	0.02	0.08

SE is standard error, root mean standard error is $RMSE = \sqrt{\sum_{i=1}^n (x_i - \bar{x}_i)^2}$, adj.r2 is adjusted r2. A greyed-out value indicates a poor performance.

TABLE 9.9 Detailed results of the linear regressions for DGP for optimisation 2.

Zone	Glare	Metric	r^2	adj. r^2	p-value	RMSE	b_0	b_1	SE b_0	SE b_1
Wall	Disturbing	DGP	0.44	0.37	0.0374	0.101	0.04	0.82	0.08	0.33
Wall	Disturbing	DGPlog(Ev)	0.86	0.84	0.0001	0.045	-0.32	3185	0.08	463
Wall	Any glare	DGP	0.84	0.82	0.0002	0.051	0.51	1.24	0.04	0.19
Wall	Any glare	DGPlog(Ev)	0.82	0.80	0.0003	0.060	0.16	2476	0.10	406
Window	Disturbing	DGP	0.57	0.51	0.0118	0.117	0.11	1.38	0.06	0.43
Window	Disturbing	DGPlog(Ev)	0.72	0.69	0.0019	0.098	0.00	535	0.06	118
Window	Any glare	DGP	0.93	0.92	0.0000	0.047	0.32	0.73	0.03	0.07
Window	Any glare	DGPlog(Ev)	0.93	0.92	0.0000	0.047	0.31	30.46	0.03	2.92

SE is standard error, root mean standard error is $RMSE = \sqrt{\sum_{i=1}^n (x_i - \bar{x}_i)^2}$, adj.r2 is adjusted r2. A greyed-out value indicates a poor performance.

The results of the regressions show that the coefficients of determination are generally significant for all cases ($p < 0.05$) apart from the UGP for the 'disturbing glare' definition in the wall zone, where a non-significant coefficient of determination was found ($p = 0.11$).

The $DGPlog(E_v)$ generally achieves the highest levels of significance, with p-values between 0.0000 and 0.0019.

The scatter plots of the results of the DGP, $DGPlog(E_v)$ and UGP before and after optimisation (optimisation 1) are shown in Figures 9.5 to 9.7, for the wall zone and in Figures 9.8 to 9.10, for the window zone.

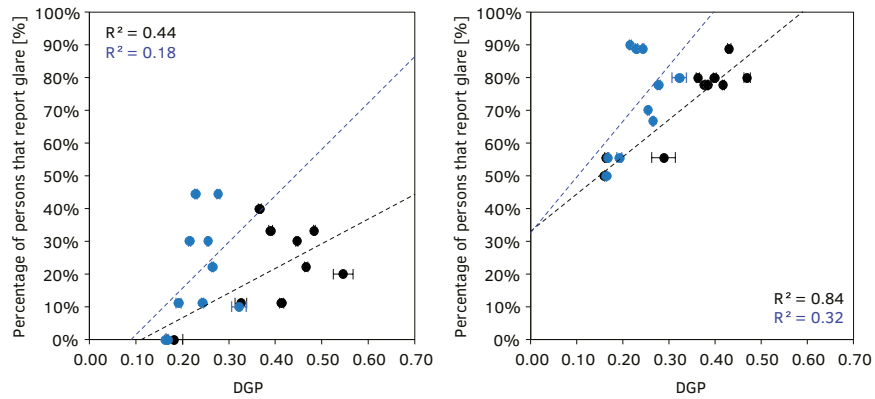


FIG. 9.5 DGP optimised in comparison to the DGP non-optimised (before) versus the percentage of persons that report glare, for the wall zone. Left: 'disturbing' glare definition; right: 'any glare' definition. Before optimisation (in blue) and after optimisation (in black).

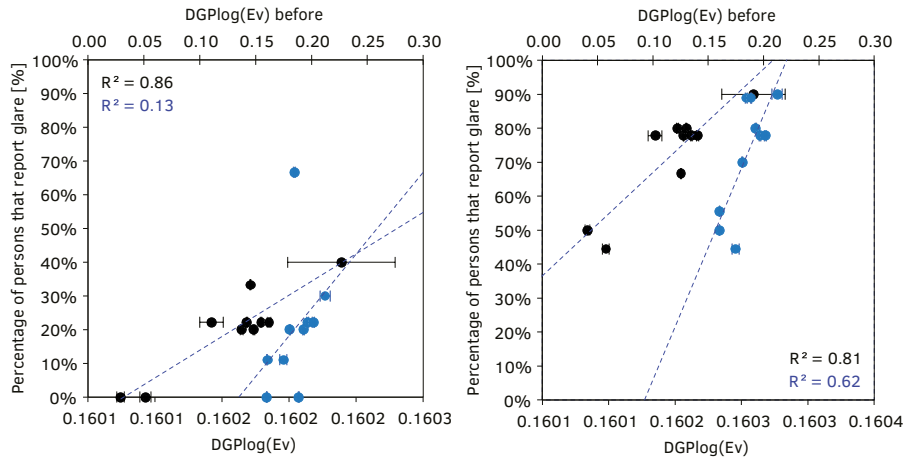


FIG. 9.6 $DGPlog(E_v)$ optimised in comparison to the $DGPlog(E_v)$ non-optimised (before) versus the percentage of persons that report glare, for the wall zone. Left: 'disturbing' glare definition; right: 'any glare' definition. Before optimisation (in blue) and after optimisation (in black).

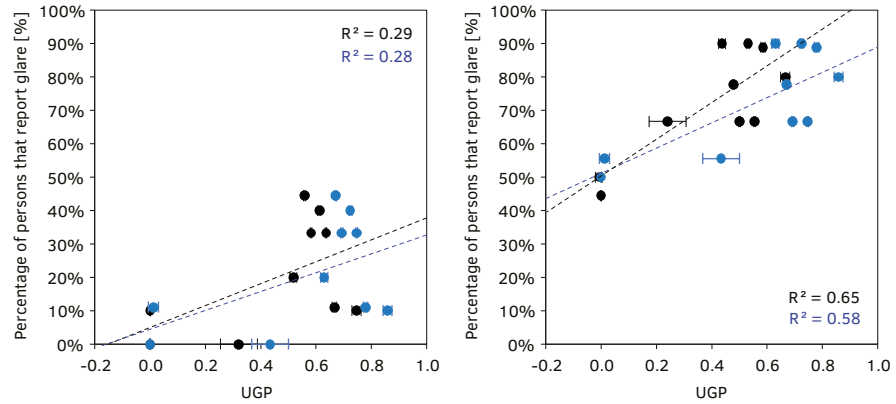


FIG. 9.7 UGP optimised in comparison to the UGP non-optimised (before) versus the percentage of persons that report glare, for the wall zone. Left: 'disturbing' glare definition; right: 'any glare' definition. Before optimisation (in blue) and after optimisation (in black).

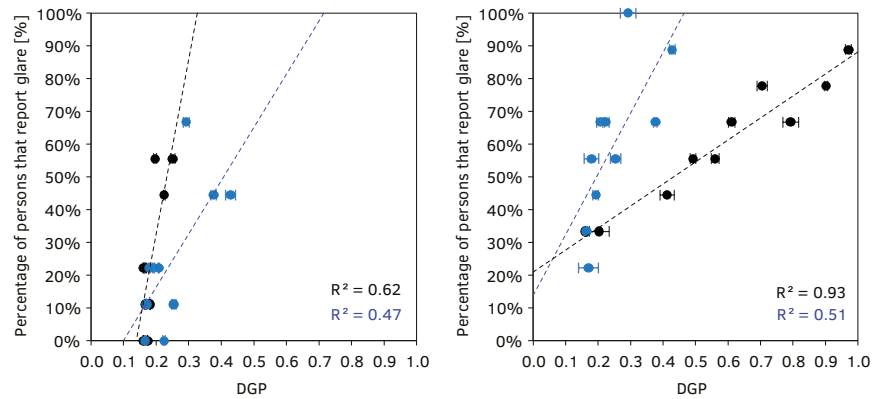


FIG. 9.8 DGP optimised in comparison to the DGP non-optimised (before) versus the percentage of persons that report glare, for the window zone. Left: 'disturbing' glare definition; right: 'any glare' definition. Before optimisation (in blue) and after optimisation (in black).

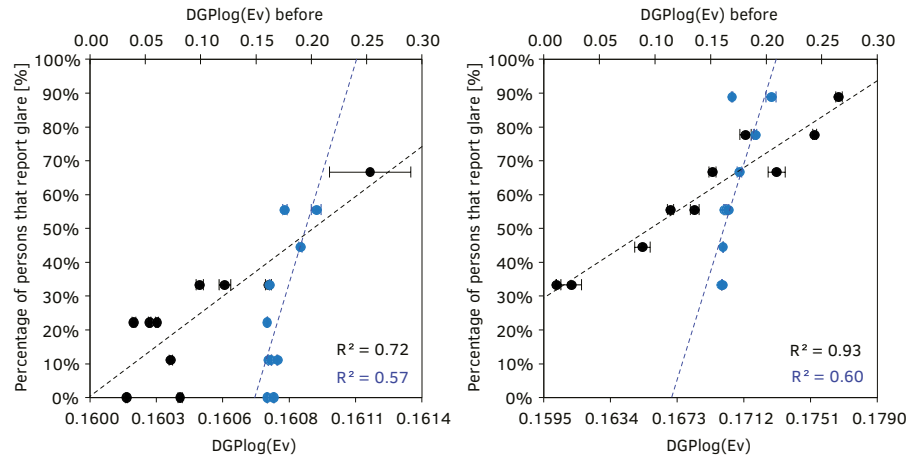


FIG. 9.9 DGplog(E_v) optimised in comparison to the DGplog(E_v) non-optimised (before) versus the percentage of persons that report glare, for the window zone. Left: 'disturbing' glare definition; right: 'any glare' definition. Before optimisation (in blue) and after optimisation (in black).

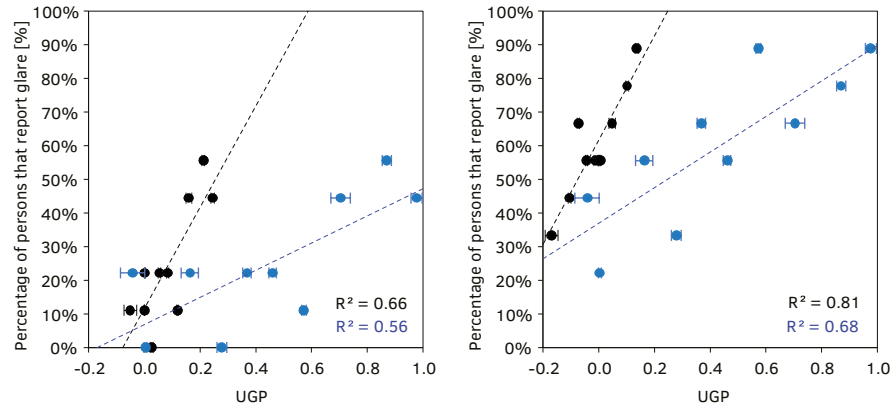


FIG. 9.10 UGP optimised in comparison to the UGP non-optimised (before) versus the percentage of persons that report glare, for the window zone. Left: 'disturbing' glare definition; right: 'any glare' definition. Before optimisation (in blue) and after optimisation (in black).

9.6.3 Deriving the equations

As the optimisation simply provides a set of optimal values, the scale of the newly created equations is adjusted to the actual percentage of people that report glare using the procedure described in section 9.3.2.

9.6.3.1 $DGPlog(E_v)_{new}$

The process of deriving the new equations is described in detail below for $DGPlog(E_v)$ after calculating the new components $c1_{new}$ to $c4_{new}$ based on the results of the obtained optimised $c1$ to $c4$ (Tables 9.6 and 9.7) and of the regression coefficients from Tables 9.8 and 9.9.

The components used for the development of the $DGPlog(E_v)$ equations are based on the optimisation 1 ($c4 = 0$). A $c4$ of 0 allows the equations to assume a form that results in values of the metric that are lower than 0.16, effectively extending the range of values that it can cover.

$$DGPlog(E_v)_{new} = b_1 \cdot c_1 \cdot 10^{-5} \cdot \log_{10}(E_v) + b_1 \cdot c_2 \cdot 10^{-2} \cdot \log_{10} \left(1 + \sum_{i=1}^n \frac{L_{s,i}^2 \cdot \omega_{s,i}}{E_v^{c_3} \cdot P_i^2} \right) + b_0 + b_1 \cdot c_4$$

For the wall zone and 'disturbing glare':

$$DGPlog(E_v)_{new} = 3185 \cdot 5.37 \cdot 10^{-5} \cdot \log_{10}(E_v) + 3185 \cdot 10.09 \cdot 10^{-2} \cdot \log_{10} \left(1 + \sum_{i=1}^n \frac{L_{s,i}^2 \cdot \omega_{s,i}}{E_v^{3.09} \cdot P_i^2} \right) - 0.32 + 3185 \cdot 0$$

$$DGPlog(E_v)_{new} = 17099 \cdot 10^{-5} \cdot \log_{10}(E_v) + 32144 \cdot 10^{-2} \cdot \log_{10} \left(1 + \sum_{i=1}^n \frac{L_{s,i}^2 \cdot \omega_{s,i}}{E_v^{3.09} \cdot P_i^2} \right) - 0.32$$

For the wall zone and 'any glare':

$$DGPlog(E_v)_{new} = 2476 \cdot 7.13 \cdot 10^{-5} \cdot \log_{10}(E_v) + 2476 \cdot 2.34 \cdot 10^{-2} \cdot \log_{10} \left(1 + \sum_{i=1}^n \frac{L_{s,i}^2 \cdot \omega_{s,i}}{E_v^{2.75} \cdot P_i^2} \right) + 0.16 + 2476 \cdot 0$$

$$DGPlog(E_v)_{new} = 17645 \cdot 10^{-5} \cdot \log_{10}(E_v) + 5802 \cdot 10^{-2} \cdot \log_{10} \left(1 + \sum_{i=1}^n \frac{L_{s,i}^2 \cdot \omega_{s,i}}{E_v^{2.75} \cdot P_i^2} \right) + 0.16$$

For the window zone and 'disturbing glare':

$$\text{DGPlg}(E_v)_{\text{new}} = 535 \cdot 7.74 \cdot 10^{-5} \cdot \log_{10}(E_v) + 535 \cdot 13.08 \cdot 10^{-2} \cdot \log_{10} \left(1 + \sum_{i=1}^n \frac{L_{s,i}^2 \cdot \omega_{s,i}}{E_v^{2.48} \cdot P_i^2} \right) + 0 + 535 \cdot 0$$

$$\text{DGPlg}(E_v)_{\text{new}} = 4142 \cdot 10^{-5} \cdot \log_{10}(E_v) + 7004 \cdot 10^{-2} \cdot \log_{10} \left(1 + \sum_{i=1}^n \frac{L_{s,i}^2 \cdot \omega_{s,i}}{E_v^{2.48} \cdot P_i^2} \right) + 0$$

For the window zone and 'any glare':

$$\text{DGPlg}(E_v)_{\text{new}} = 30 \cdot 12.77 \cdot 10^{-5} \cdot \log_{10}(E_v) + 30 \cdot 0.43 \cdot 10^{-2} \cdot \log_{10} \left(1 + \sum_{i=1}^n \frac{L_{s,i}^2 \cdot \omega_{s,i}}{E_v^{0.80} \cdot P_i^2} \right) + 0.31 + 30 \cdot 0$$

$$\text{DGPlg}(E_v)_{\text{new}} = 389 \cdot 10^{-5} \cdot \log_{10}(E_v) + 13 \cdot 10^{-2} \cdot \log_{10} \left(1 + \sum_{i=1}^n \frac{L_{s,i}^2 \cdot \omega_{s,i}}{E_v^{0.80} \cdot P_i^2} \right) + 0.31$$

The resulting DGPlg(E_v) equations, $\text{DGPlg}(E_v)_{\text{new}}$, including the standard errors for the new components, are

Wall, 'disturbing glare':

$$\text{DGPlg}(E_v)_{\text{new}} = (0.17 \pm 0.02) \cdot \log_{10}(E_v) + (321 \pm 47) \cdot \log_{10} \left(1 + \sum_{i=1}^n \frac{L_{s,i}^2 \cdot \omega_{s,i}}{E_v^{3.09} \cdot P_i^2} \right) - (0.32 \pm 0.05) \quad \text{EQ 27}$$

Wall, 'any glare':

$$\text{DGPlg}(E_v)_{\text{new}} = (0.18 \pm 0.03) \cdot \log_{10}(E_v) + (58 \pm 10) \cdot \log_{10} \left(1 + \sum_{i=1}^n \frac{L_{s,i}^2 \cdot \omega_{s,i}}{E_v^{2.75} \cdot P_i^2} \right) + (0.16 \pm 0.03) \quad \text{EQ 28}$$

Window, 'disturbing glare':

$$\text{DGPlg}(E_v)_{\text{new}} = (0.04 \pm 0.009) \cdot \log_{10}(E_v) + (70 \pm 15) \cdot \log_{10} \left(1 + \sum_{i=1}^n \frac{L_{s,i}^2 \cdot \omega_{s,i}}{E_v^{2.48} \cdot P_i^2} \right) + (0 \pm 0) \quad \text{EQ 29}$$

Window, 'any glare':

$$\text{DGPlg}(E_v)_{\text{new}} = (0.004 \pm 0.0004) \cdot \log_{10}(E_v) + (0.13 \pm 0.012) \cdot \log_{10} \left(1 + \sum_{i=1}^n \frac{L_{s,i}^2 \cdot \omega_{s,i}}{E_v^{0.8} \cdot P_i^2} \right) + (0.31 \pm 0.03) \quad \text{EQ 30}$$

For the defined equations, the probability of glare becomes directly proportional to the percentage of persons that report glare, as it can be seen in the scatter plots presented in Figure 9.11.

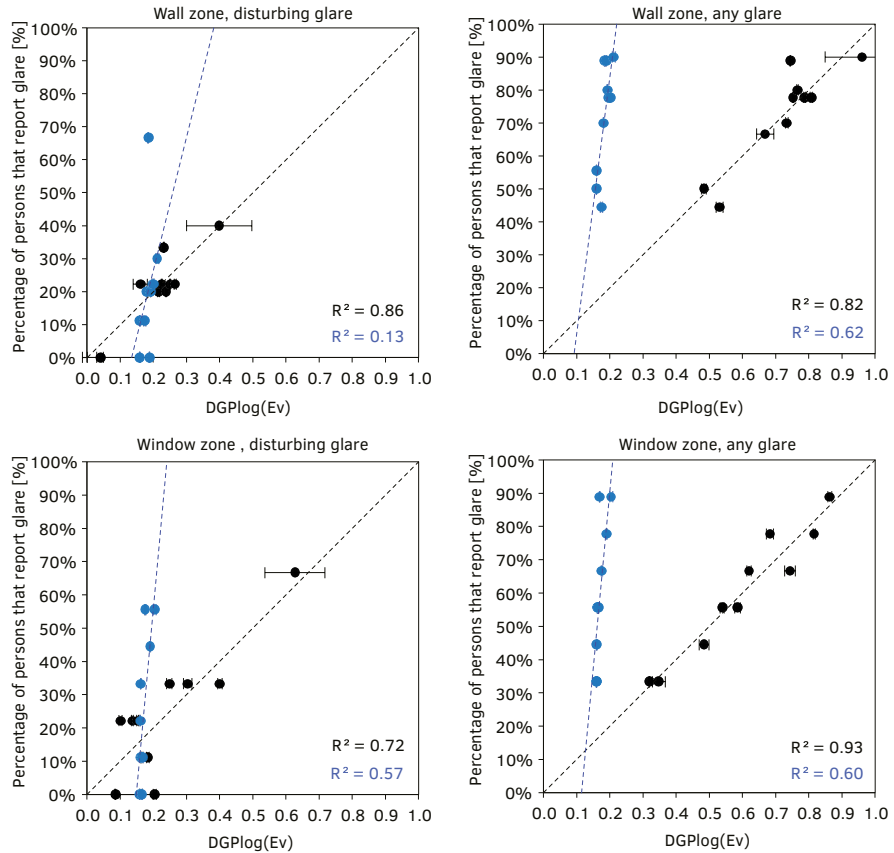


FIG. 9.11 Scatter plots of the new DGPIog(E_v) model. Results before optimisation (in blue) and results for the DGPIog(E_v)_{new} model (in black).

The components that are used for the development of the DGP equations are based on the optimisation 1 and 2 ($c_4 = 0$ and $c_4 = 0.16$), as there is a better performance of the metric for the optimisation 2 for one of the analysed DGP models.

Following the procedure that was described before, the resulting DGP equations, DGP_{new}, based on the optimisation 2, including the standard errors of the new components, are

Wall, 'disturbing glare':

$$DGP_{\text{new}} = (5.4 \pm 2) \cdot 10^{-5} \cdot E_v + (0.03 \pm 0.01) \cdot \log_{10} \left(1 + \sum_{i=1}^n \frac{L_{s,i}^2 \cdot \omega_{s,i}}{E_v^{0.004} \cdot P_i^2} \right) + (0.04 \pm 0.02) \quad \text{EQ 31}$$

Wall, 'any glare':

$$DGP_{\text{new}} = (1.2 \pm 0) \cdot 10^{-5} \cdot E_v + (0.21 \pm 0.03) \cdot \log_{10} \left(1 + \sum_{i=1}^n \frac{L_{s,i}^2 \cdot \omega_{s,i}}{E_v^{1.49} \cdot P_i^2} \right) + (0.51 \pm 0.08) \quad \text{EQ 32}$$

Window, 'disturbing glare':

$$DGP_{\text{new}} = (4.1 \pm 1) \cdot 10^{-5} \cdot E_v + (0.18 \pm 0.06) \cdot \log_{10} \left(1 + \sum_{i=1}^n \frac{L_{s,i}^2 \cdot \omega_{s,i}}{E_v^{1.56} \cdot P_i^2} \right) + (0.11 \pm 0.03) \quad \text{EQ 33}$$

Window, 'any glare':

$$DGP_{\text{new}} = (0.1 \pm 0) \cdot 10^{-5} \cdot E_v + (0.13 \pm 0.01) \cdot \log_{10} \left(1 + \sum_{i=1}^n \frac{L_{s,i}^2 \cdot \omega_{s,i}}{E_v^{0.78} \cdot P_i^2} \right) + (0.32 \pm 0.03) \quad \text{EQ 34}$$

9.6.3.2 DGP_{new}

The resulting DGP equations, DGP_{new} , based on the optimisation 1, including the standard errors of the new components, are:

Wall, 'disturbing glare':

$$DGP_{\text{new}} = (5.4 \pm 2) \cdot 10^{-5} \cdot E_v + (0.03 \pm 0.01) \cdot \log_{10} \left(1 + \sum_{i=1}^n \frac{L_{s,i}^2 \cdot \omega_{s,i}}{E_v^{0.004} \cdot P_i^2} \right) + (0.04 \pm 0.02) \quad \text{EQ 35}$$

Wall, 'any glare':

$$DGP_{\text{new}} = (1.2 \pm 0) \cdot 10^{-5} \cdot E_v + (0.21 \pm 0.03) \cdot \log_{10} \left(1 + \sum_{i=1}^n \frac{L_{s,i}^2 \cdot \omega_{s,i}}{E_v^{1.49} \cdot P_i^2} \right) + (0.51 \pm 0.08) \quad \text{EQ 36}$$

Window, 'disturbing glare':

$$DGP_{\text{new}} = (1.3 \pm 0) \cdot 10^{-5} \cdot E_v + (0.73 \pm 0.2) \cdot \log_{10} \left(1 + \sum_{i=1}^n \frac{L_{s,i}^2 \cdot \omega_{s,i}}{E_v^{1.82} \cdot P_i^2} \right) + (0.11 \pm 0.03) \quad \text{EQ 37}$$

Window, 'any glare':

$$DGP_{\text{new}} = (0.03 \pm 0) \cdot 10^{-5} \cdot E_v + (0.13 \pm 0.01) \cdot \log_{10} \left(1 + \sum_{i=1}^n \frac{L_{s,i}^2 \cdot \omega_{s,i}}{E_v^{0.78} \cdot P_i^2} \right) + (0.32 \pm 0.03) \quad \text{EQ 38}$$

For the defined equations, the probability of glare becomes directly proportional to the percentage of persons that report glare, as it can be seen in the scatter plots presented in Figure 9.12.

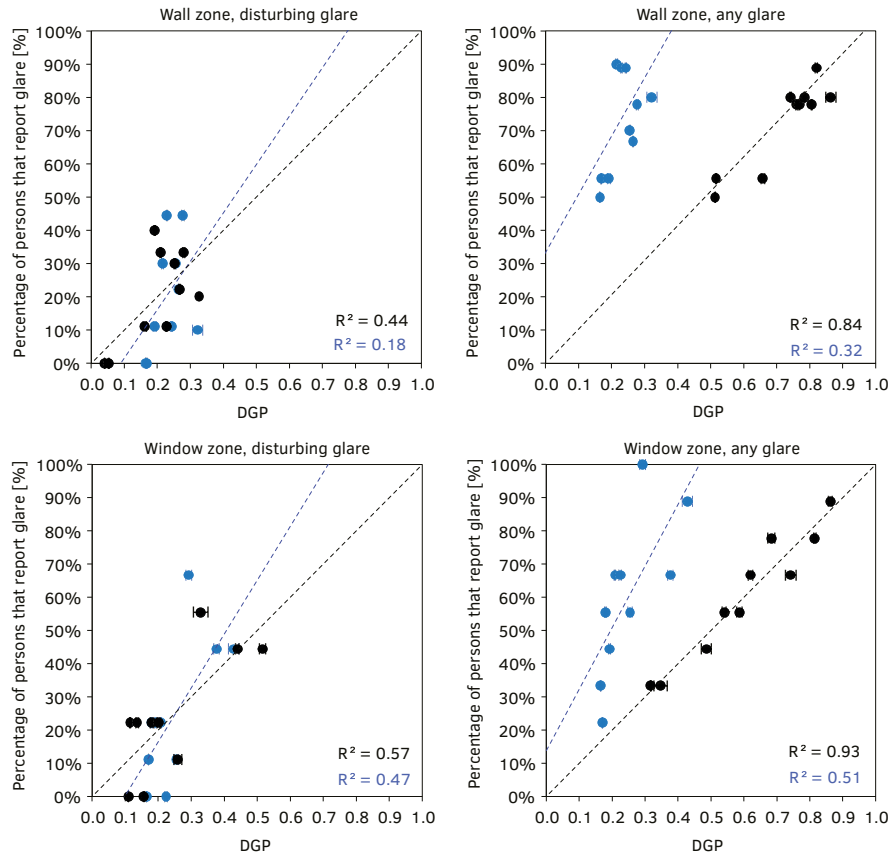


FIG. 9.12 Scatter plots of the new DGP model. Results before the optimisation (in blue) and results for the DGP_{new} (in black).

9.6.3.3 UGP_{new}

Following the same procedure described for the other two metrics, the resulting optimised UGP equations, UGP_{new} , including the standard errors of the new components are:

Wall, 'disturbing glare':

$$UGP_{new} = (0.09 \pm 0.047) \cdot \log_{10} \left(\frac{0.03}{L_b} \cdot \sum_{i=1}^n \frac{L_{s,i}^2 \cdot \omega_{s,i}}{P_i^2} \right) \quad \text{EQ 39}$$

Wall, 'any glare':

$$UGP_{new} = (0.14 \pm 0.036) \cdot \log_{10} \left(\frac{0.02}{L_b} \cdot \sum_{i=1}^n \frac{L_{s,i}^2 \cdot \omega_{s,i}}{P_i^2} \right) \quad \text{EQ 40}$$

Window, 'disturbing glare':

$$UGP_{new} = (0.12 \pm 0.031) \cdot \log_{10} \left(\frac{0.02}{L_b} \cdot \sum_{i=1}^n \frac{L_{s,i}^2 \cdot \omega_{s,i}}{P_i^2} \right) \quad \text{EQ 41}$$

Window, 'any glare':

$$UGP_{new} = (0.13 \pm 0.02) \cdot \log_{10} \left(\frac{0.0009}{L_b} \cdot \sum_{i=1}^n \frac{L_{s,i}^2 \cdot \omega_{s,i}}{P_i^2} \right) \quad \text{EQ 42}$$

For the defined equations, the probability of glare becomes directly proportional to the percentage of persons that report glare, as it can be seen in the scatter plots presented in Figure 9.13.

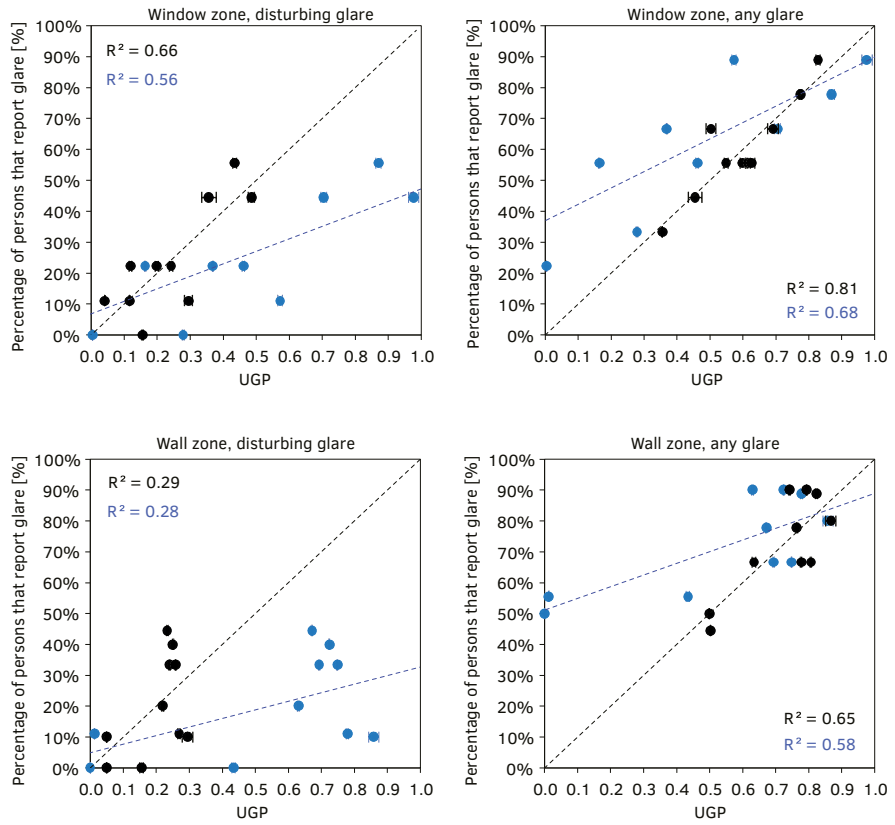


FIG. 9.13 Scatter plots of the new UGP model. Results before the optimisation (in blue) and results for the UGP_{new} (in black).

9.7 Discussion

The optimisation of the DGP, $DGP_{log}(E_v)$ and UGP metrics that was performed in the study shows that these metrics can indeed be improved to better fit the reported discomfort glare, with $DGP_{log}(E_v)$ generally producing the best results. As verified in the previous Chapter (VII) there are benefits in using the logarithm of E_v in the adaptation term of the DGP equation. Other researchers have also reported better results for that form of E_v , particularly when glare was studied in the context of deeper spaces (Hirning et al., 2014) (Konis, 2014). Like in those studies, the range of light levels in the present study is lower than the range of light levels of the DGP development investigation. The linear form of DGP might be more appropriate to the conditions of saturation glare whereas a logarithmic form might be more appropriate to the conditions of contrast glare. What exactly constitutes one or the other and to what extent is one or the other more prevalent in the actual built space needs further focused research.

9.7.1 DGP_{new} in comparison to DGP

It is observed that for the cases where the optimisation of the DGP is successful, the equations present a much higher c_2 and a much lower c_1 in relation to the original DGP equation. This indicates that a better prediction of the reported glare occurs when the contribution of the contrast term of the DGP equation is increased and the contribution of the adaptation term is reduced. The contrast part of the newly created DGP_{new} equation has a much higher influence on the final value of the metric than the DGP currently accounts for. This is verified for both window and the wall zone equations, seconding the previous observation that even in the window zone, the reported glare seems to result from a contrast effect rather than from a saturation effect. It is worth mentioning that the DGP investigation was carried out in purposely-selected unobstructed sites (rooftop or isolated structures) when in fact most buildings in the characteristically overshadowed urban environment are composed of spaces with very limited views of the sky and of the sun. In these conditions, discomfort glare due to saturation-effects might tend to be less frequent than due to contrast-effects.

Figure 9.14 shows the contribution of the contrast and adaptation terms of DGP_{new} to the overall value of the metric in comparison to the original DGP equation, based on the data of Study I.

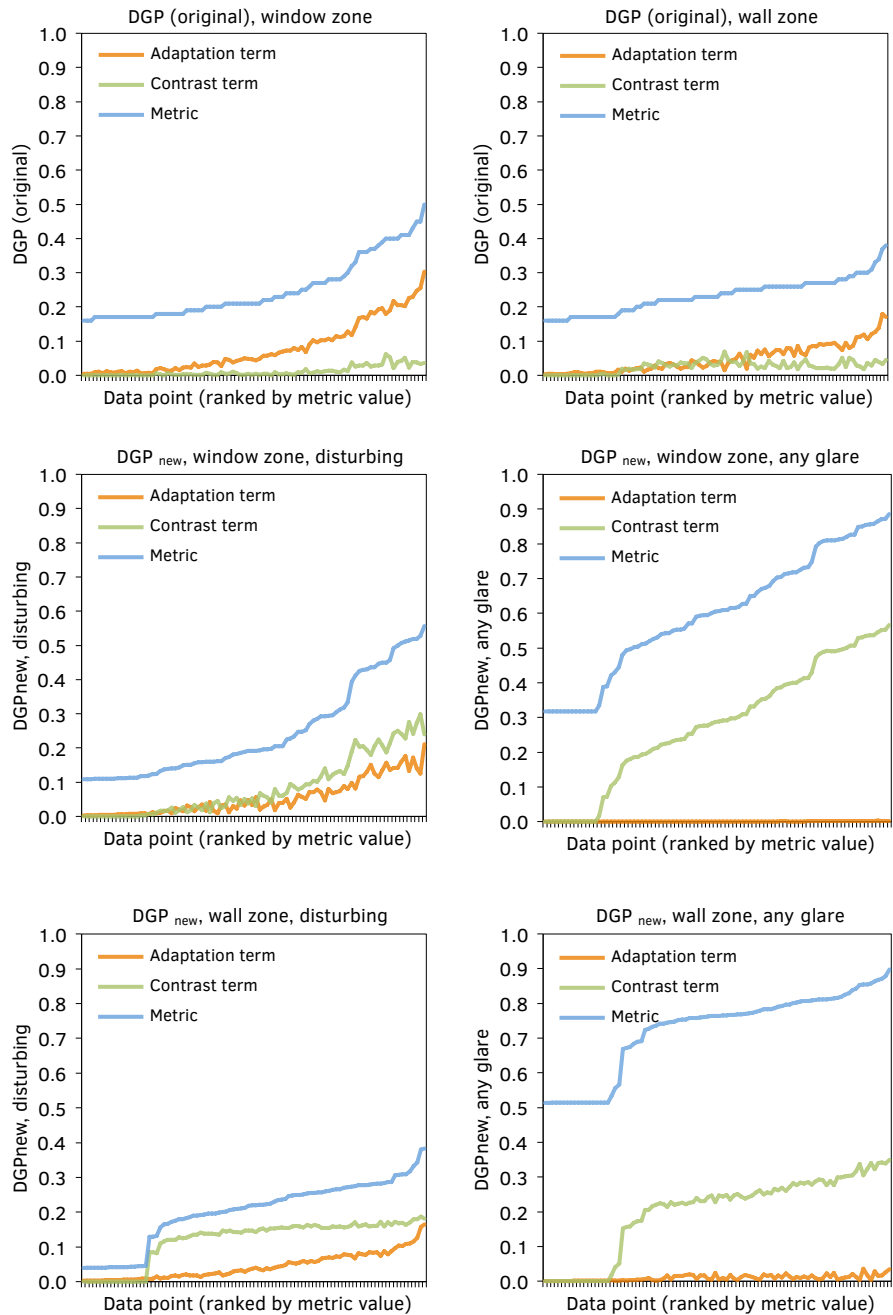


FIG. 9.14 Calculated contrast and adaptation terms of DGP_{new} and of DGP, based on the Study I data.

9.7.2 DGPlot(E_v)_{new} in comparison to DGP

The DGPlot(E_v)_{new} equations were used to compute the data from Study I. Table 9.10 shows the descriptive statistics for the DGPlot(E_v)_{new} resulting from the 4 equations and Figure 9.15 shows the distributions for the DGPlot(E_v)_{new}, by zone.

TABLE 9.10 Descriptive statistics for DGPlot(E_v)_{new}, for the two zones and the two definitions of glare.

Zone	Glare	N	Range	Min	Max	Mean	Std. Dev.	Median	SE (mean)	95% CI of mean	
										Lower	Upper
Wall	Disturbing	94	0.89	-0.02	0.87	0.20	0.13	0.23	0.01	0.18	0.23
Wall	Any glare	94	1.01	0.47	1.47	0.72	0.15	0.75	0.02	0.70	0.76
Window	Disturbing	90	0.94	0.08	1.02	0.24	0.17	0.19	0.02	0.21	0.28
Window	Any glare	90	0.57	0.32	0.89	0.60	0.18	0.60	0.02	0.56	0.64

A 95% CI with lower and upper bounds of 0.70 and 0.76 for a mean of 0.72, indicates that there is 95% chance that the mean varies between 0.70 and 0.76.

It is observed that for the 'any glare' definition the values of the metric are higher than for the 'disturbing' definition, corresponding to a higher percentage of persons that report glare. In that case, the threshold to what is considered glare is set to a relatively low value (it is stricter), raising the percentage of persons that report glare. The opposite happens for the 'disturbing glare' definition, where the threshold to what is considered to be glare is set to a higher level (is less strict), reducing the percentage of persons that report glare.

Interestingly, DGPlot(E_v)_{new} is on average higher in the wall zone than in the window zone (higher median value) particularly for the 'any glare' definition. This is in line with the reported glare percentages in Study I, where more cases of glare were reported in the wall zone than in the window zone.

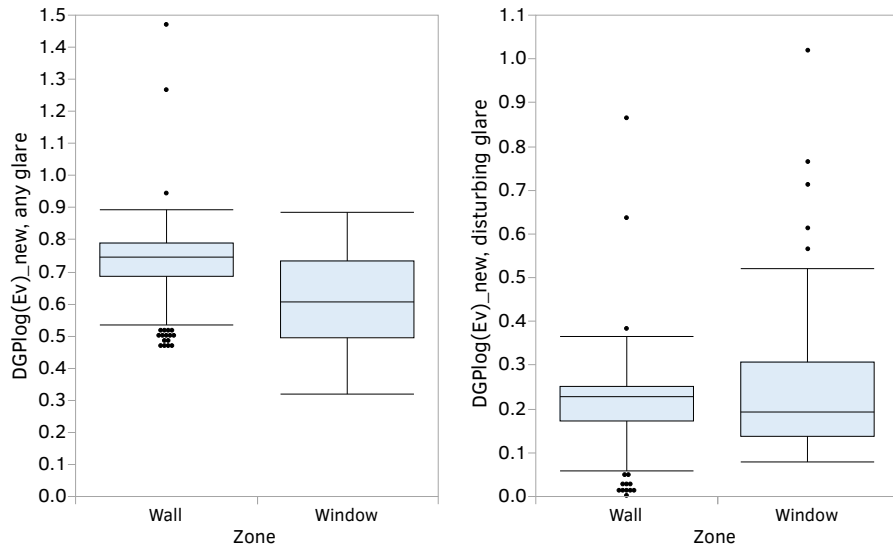


FIG. 9.15 Distributions of $DGPlg(E_v)_{new}$ for the 'any glare' definition (left) and for the 'disturbing glare' definition (right), per zone.

The contrast and adaptation terms of the $DGPlg(E_v)_{new}$ based on the data of Study are presented in Figure 9.16.

Contrary to the original DGP, where the risk of glare linearly increases with saturation and the adaptation term dominates the equation, there is a marked influence of the contrast term in the $DGPlg(E_v)_{new}$ equations. For the original DGP a reduction of the overall luminance of the visual field (saturation) directly corresponds to a reduction of the risk of glare, with contrast having a relatively lower impact on the final result of the metric. For the $DGPlg(E_v)_{new}$ equations, the contrast effect will tend to dominate the reported glare as the risk of glare increases, independently of the adopted glare definition ('any glare' or 'disturbing glare') and of sitting zone.

In the sitting positions in the window zone, a reduction of the contrast in the visual field immediately produces a reduction of the risk of glare. In the sitting positions in the wall zone, the contrast effect becomes the driving term of the equation for the higher levels of glare. Independently of the adopted glare definition ('any glare' or 'disturbing glare'), the overall light in the scene (adaptation) dominates the level of glare in the sitting positions in the wall zone for the lower levels of glare. For the higher levels of glare, the contrast term tends to dominate the value of the metric.

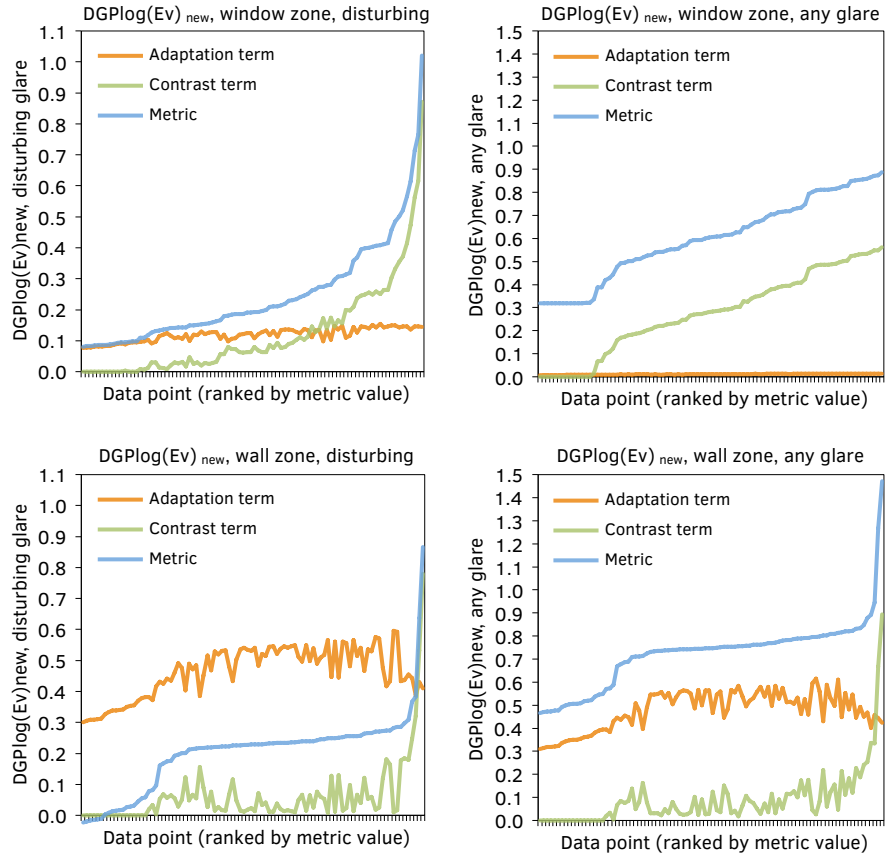


FIG. 9.16 Calculated contrast and adaptation terms of $DGPllog(E_v)_{new}$, based on Study I data.

It is observed that the newly created $DGPllog(E_v)_{new}$ model produces equations with a logarithmic form, of the type:

$$DGPllog(E_v)_{new} = c1_{new} \cdot 10^{-5} \cdot \log_{10}(E_v) + c2_{new} \cdot 10^{-2} \cdot \log_{10} \left(1 + \sum_{i=1}^n \frac{L_{s,i}^2 \cdot \omega_{s,i}}{E_v^{c3_{new}} \cdot P_i^2} \right) + c4_{new}$$

Assuming that the equation is solved for a situation where a glare source is identified and therefore the entity 1 can be dropped in the contrast term of the equation, and that there is only one source of glare identified (), the equation can be derived as:

$$\text{DGPl}_{\text{og}}(E_v)_{\text{new}} \approx c1_{\text{new}} \cdot 10^{-5} \cdot \log_{10}(E_v) + c2_{\text{new}} \cdot 10^{-2} \cdot \log_{10}\left(\frac{L_s^2 \cdot \omega_s}{E_v^{c3_{\text{new}}} \cdot P^2}\right) + c4_{\text{new}}$$

$$\text{DGPl}_{\text{og}}(E_v)_{\text{new}} \approx \log_{10} E_v^{c1_{\text{new}} \cdot 10^{-5}} + \log_{10}\left(\frac{L_s^{2 \cdot c2_{\text{new}} \cdot 10^{-2}} \cdot \omega_s^{c2_{\text{new}} \cdot 10^{-2}}}{E_v^{c3_{\text{new}} \cdot c2_{\text{new}} \cdot 10^{-2}} \cdot P^{2 \cdot c2_{\text{new}} \cdot 10^{-2}}}\right) + c4_{\text{new}}$$

$$\text{DGPl}_{\text{og}}(E_v)_{\text{new}} \approx \log_{10}\left(\frac{E_v^{c1_{\text{new}} \cdot 10^{-5}} \cdot L_s^{2 \cdot c2_{\text{new}} \cdot 10^{-2}} \cdot \omega_s^{c2_{\text{new}} \cdot 10^{-2}}}{E_v^{c3_{\text{new}} \cdot c2_{\text{new}} \cdot 10^{-2}} \cdot P^{2 \cdot c2_{\text{new}} \cdot 10^{-2}}}\right) + c4_{\text{new}}$$

$$\text{DGPl}_{\text{og}}(E_v)_{\text{new}} \approx \log_{10}\left(\frac{L_s^{2 \cdot c2_{\text{new}} \cdot 10^{-2}} \cdot \omega_s^{c2_{\text{new}} \cdot 10^{-2}}}{E_v^{c3_{\text{new}} \cdot c2_{\text{new}} / c1_{\text{new}} \cdot 10^3} \cdot P^{2 \cdot c2_{\text{new}} \cdot 10^{-2}}}\right) + c4_{\text{new}}$$

$$\text{DGPl}_{\text{og}}(E_v)_{\text{new}} \approx \log_{10}\left(\frac{L_s^{2 \cdot a} \cdot \omega_s^a}{E_v^b \cdot P^{2 \cdot a}}\right) + c4_{\text{new}}$$

where

$$a = c2_{\text{new}} \cdot 10^{-2}$$

$$b = c3_{\text{new}} \cdot c2_{\text{new}} / c1_{\text{new}} \cdot 10^3$$

The above derivation demonstrates that the $\text{DGPl}_{\text{og}}(E_v)_{\text{new}}$ model is in its basic form a ‘contrast’ formulation, as per the definition adopted to classify the different glare equations earlier. The $\text{DGPl}_{\text{og}}(E_v)_{\text{new}}$ model implies that a reduction of the percentage of persons that report glare is achieved by a reduction of the luminance of the glare source L_s , a reduction of the size of the glare source ω , an increase of the position index P and an increase of the overall vertical eye illuminance, E_v . However, an increase of E_v should not represent an increase of the vertical eye illuminance for the area of the visual field corresponding to the glare sources, as this would in turn contribute to the increase of the value of the metric.

If we consider that $E_v = E_{\text{dir}} + E_{\text{ind}}$, where E_{dir} is a measure of the light contribution of the glare source and E_{ind} is a measure of the light contribution from the background, then the strategy to reduce discomfort glare from light contrast should be to increase the indirect component of E_v , E_{ind} , only.

9.7.3 UGP_{new} in comparison to UGP

For UGP_{new}, it is observed that there is a reduction of the value of the component c_2 in all the equations, which results in a reduction of the contribution of the background luminance in relation to the original UGP equation. As the metric only contains a contrast term, the results of the optimisation of the UGP suggest that an adjustment of UGP is still beneficial for a better prediction of contrast glare.

9.8 Conclusion

In this chapter, it is investigated if the prediction of reported discomfort glare from daylight in the classroom space could be improved based on a modification of the DGP and UGP equations. The investigation is based on a search for an equation solution that produces a better fit to the glare reported by subjects in four sitting positions of a classroom space.

The performed optimisation of the DGP, DGPl $\log(E_v)$ and UGP equations shows that the metrics can indeed be improved to better fit the data of this dataset. For the newly produced DGP-based models the fitness is very high. For the UGP-based models, the fitness is acceptable in most cases but they present lower effect sizes and lower significance in relation to the models based on the other metrics. The fitness of the DGPl $\log(E_v)$ equations is generally the highest, with r^2 values ranging from 0.81 to 0.93 and p -values from 0.0000 to 0.0002. This confirms that the use of the logarithm form of E_v over the linear form of E_v is beneficial. It is verified that for the 'any glare' definition, the optimised DGP metric shows a fit of $r^2 = 0.84$, $p = 0.0001$ for the wall zone and $r^2 = 0.93$, $p < 0.0001$ for the window zone. This indicates that the benefit of the logarithm of E_v is more obvious for the equations of the 'disturbing glare' definition.

A set of four equations, for two different definitions of glare - 'disturbing glare' and 'any glare' - and two defined classroom zones (window zone and wall zone) were defined, based on the best performing metric, the DGPl $\log(E_v)$. The optimised DGPl $\log(E_v)$, DGPl $\log(E_v)_{new}$, is therefore presented as a tentative model of discomfort glare from daylight for classrooms. It is important to stress that any optimisation process produces a solution that is optimised to the particular range of conditions that it is based on and further testing and validation studies are required

until a model can be called a generalisable one. The study does, nevertheless, demonstrate that improved models of discomfort glare, better than the existing ones, can be created for the conditions of the classroom space. This confirms that there is indeed a need to develop more appropriate discomfort glare models for this type of space. The results of the study also indicate that the problem of glare in the studied classroom space and possibly other classrooms is one of contrast glare rather than one of excess light or saturation glare, as hypothesized in the beginning of this thesis. It is worth mentioning that that the space that was used in this investigation is one that produces limited contrast overall (empty walls and light-coloured surfaces). A more noticeable contrast-effect can be expected in the situation of a real classroom where walls are in many cases covered with all sorts of media and are not necessarily of a light colour, as in the room of this study.

In the next chapter a number of possibilities for reducing luminance contrast and therefore prevent discomfort glare in classrooms are discussed.

10 Design strategies for a discomfort glare free classroom

10.1 Introduction

In this chapter, architectural design advice towards minimising discomfort glare from daylight in classrooms is provided based on the results from this investigation and in particular on the predictive discomfort glare model developed in Chapter IX, the $DGPlog(Ev)_{new}$. Based on the $DGPlog(Ev)_{new}$ model, to prevent glare in the classroom it is necessary to reduce the luminance contrast effect. The contrast effect can be reduced by a reduction of the luminance of the glare source, a reduction of the size of the glare source, a reduction of the area of the glare source in the central part of the visual field and an increase of the illuminance contribution of the surfaces of the rooms other than the glare source (i.e. the background). These requirements are listed in Table 10.1, in relation to the $DGPlog(Ev)_{new}$ equations presented below, with the different items of the table colour-coded in relation to the parameter of the equations that they relate to.

TABLE 10.1 Requirements to reduce the contrast effect in relation to the DGPllog(Ev)new.

[1]	Reduce the luminance of the glare source
[2]	Reduce the size of the glare source
[3]	Reduce the area of the glare source in the central part of the visual field
[4]	Increase the illuminance contribution of the background surfaces other than the glare source

Equation for wall zone, 'disturbing glare':

$$\text{DGPllog}(E_v)_{\text{new}} = (0.17 \pm 0.02) \cdot \log_{10}(E_v) + (321 \pm 47) \cdot \log_{10} \left(1 + \sum_{i=1}^n \frac{L_{s,i}^2 \cdot \omega_{s,i}}{E_v^{3.09} \cdot P_i^2} \right) - (0.32 \pm 0.05) \quad \text{EQ 27}$$

Equation for wall zone, 'any glare':

$$\text{DGPllog}(E_v)_{\text{new}} = (0.18 \pm 0.03) \cdot \log_{10}(E_v) + (58 \pm 10) \cdot \log_{10} \left(1 + \sum_{i=1}^n \frac{L_{s,i}^2 \cdot \omega_{s,i}}{E_v^{2.75} \cdot P_i^2} \right) + (0.16 \pm 0.03) \quad \text{EQ 28}$$

Equation for window zone, 'disturbing glare':

$$\text{DGPllog}(E_v)_{\text{new}} = (0.04 \pm 0.009) \cdot \log_{10}(E_v) + (70 \pm 15) \cdot \log_{10} \left(1 + \sum_{i=1}^n \frac{L_{s,i}^2 \cdot \omega_{s,i}}{E_v^{2.48} \cdot P_i^2} \right) + (0 \pm 0) \quad \text{EQ 29}$$

Equation for window zone, 'any glare':

$$\text{DGPllog}(E_v)_{\text{new}} = (0.004 \pm 0.0004) \cdot \log_{10}(E_v) + (0.13 \pm 0.012) \cdot \log_{10} \left(1 + \sum_{i=1}^n \frac{L_{s,i}^2 \cdot \omega_{s,i}}{E_v^{0.8} \cdot P_i^2} \right) + (0.31 \pm 0.03) \quad \text{EQ 30}$$

The listed requirements can be broadly divided into the requirements that relate to the glare source and the requirements that relate to the room walls. There are two types of potential glare sources in the daylit space, the window light source and surfaces or portions of the surfaces of the room that have a similar brightness to the window light source. These surfaces are hereby called secondary glare sources. A range of strategies to address each of these three requirements is provided in Table 10.2.

TABLE 10.2 Discomfort glare strategies.

Windows	[1]	Reduce the window luminance
	[2]	Avoid a view of the window
	[3]	Avoid a view of the window within the central visual field
Walls	[4]	Increase the reflectance of the walls
	[4]	Increase the illuminance of the walls
Secondary glare sources	[1]	Reduce the luminance of the desks
	[2] [3]	Reduce the area of desk exposed to direct solar radiation

10.2 Design strategies

Design strategies relating to the design of windows will have the highest impact on the classroom daylight levels. For this reason, the focus should be on the improvement of the situation regarding the classroom walls first and then make modifications to the classroom windows if necessary. Figure 10.1 shows a typical side-lit classroom for an occupancy of 30 people that is based on the classroom setting of this research. As the $DGPlog(Ev)_{new}$ model was developed under the conditions of a typical classroom layout of lined desks, the guidance is provided with reference to this condition.

In the typical side-lit classroom space, the window wall (W2) will have the highest luminance, with the adjacent walls (W1 and W3) being partially illuminated by the windows and the wall opposite to the window wall (W4) being the darkest or the least illuminated wall. The objective in terms of reducing glare due to light contrast in a side-lit classroom should then be to bring the luminance of the 'inner' wall, W4, as close as possible to the luminance of the window and window wall, W2, or to reduce the luminance of the window and window wall, W2, to a level as close as possible to the luminance of W4, with the other walls providing a luminance gradient between those two.

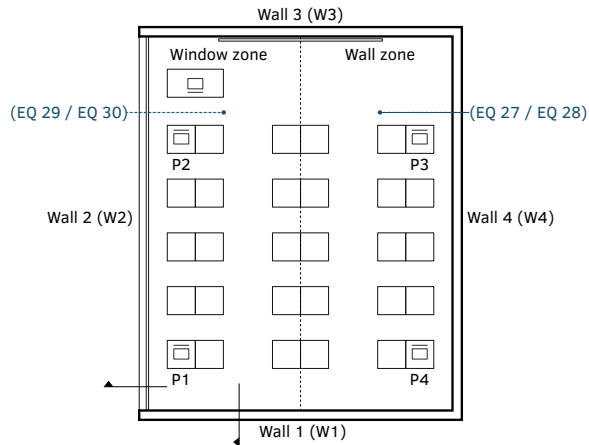


FIG. 10.1 A typical classroom² setting with walls and four critical sitting positions – P1, P2, P3 and P4 and zones, studied in this research.

Figure 10.2 illustrates a luminance distribution condition in the side-lit classroom corresponding to a situation when discomfort glare is reported.

Figure 10.3 shows the sightlines for the critical positions in the classrooms space. It can be seen that all walls of the room are seen by all sitting positions, with the wall in the back of the room, W1, generally seen only by the teacher, who for most of the time faces in the opposite direction to the students.

As the great majority of the occupants of the classroom are the students that look in the opposite direction to the teacher, it is appropriate to focus on the visual environment of the students primarily and then provide adjustments for the teacher situation if required.

The design strategies relating to the classroom walls, windows and to address the problem of secondary glare sources in classrooms are presented next.

² The represented room has a floor area of 52 m² (6.5 x 8 m²), a string window of 10m² (8 x 1.25 m²) and a ceiling height of 2.7 m. It is equipped with a large board of 3.5 x 1.2 m and the desks are equipped with a personal visual display unit of 13".

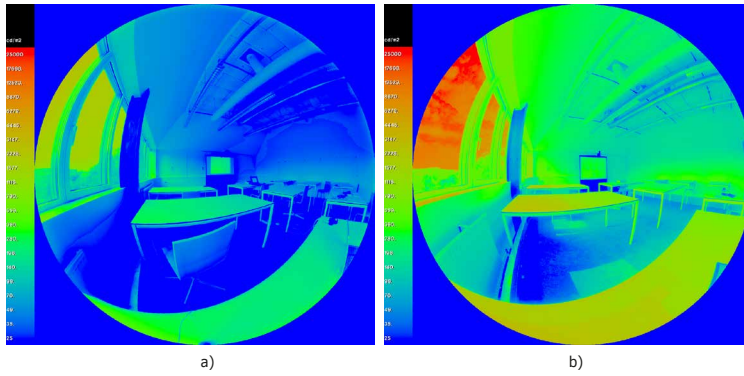


FIG. 10.2 Luminance distribution in the side-lit classroom of this research for a situation where discomfort glare is reported on (a) an overcast day and (b) on a sunny day. The images refer to the situation where the walls of the room are very visible to the observer (position 1 / board task).

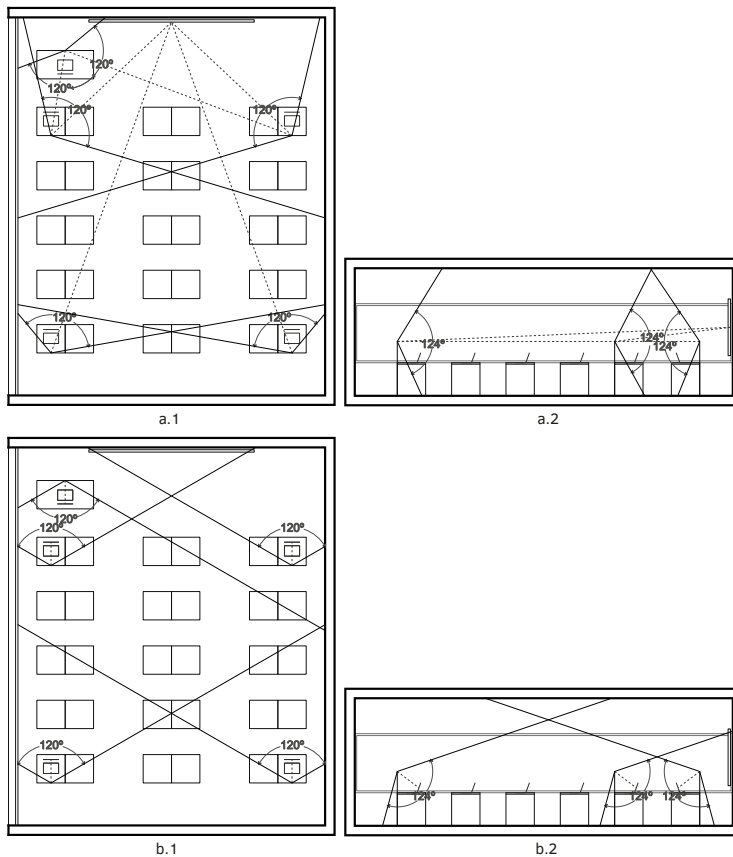


FIG. 10.3 Sightlines and respective binocular visual field for the four critical positions of the classroom P1, P2, P3 and P4, for students engaged on a board task and for a teacher looking at critical student positions (P2 and P3): Plan and longitudinal section for (a) board task and (b) desk task.

10.3 Classroom walls

The classroom walls corresponding to the background area of the visual field, should be designed for an increased illuminance. The first step towards this goal is to increase the wall reflectance, or its luminance. The second step is to provide direct illumination to these surfaces. An increase of the illuminance of the classroom walls is especially important for the reduction of the risk of glare in the sitting positions near the window.

10.3.1 Increasing the reflectance of the walls

The luminance of the classroom walls will increase as a function of their capacity to reflect light, which depends on the wall material properties and to a great extent on the wall colour. Increasing the classroom walls reflectance using lighter colours should be considered as the first step towards the improvement of wall luminance. A lighter colour not only provides for an increase of the luminance of a particular wall but also for an increase of the luminance of all other walls in the room by inter-reflection. The room reflectance for the classroom setting used in this research was 87% for walls (white paint, with wear), ~40% for the ceiling (white paint, chipboard and aluminium) and 0.08% for floor (carpet). It can be seen that the reflectance is low for ceiling and floor according to the standards (Table 10.3), therefore contributing to an increase of the light contrast in the room.

TABLE 10.3 Reflectance requirements for classrooms. Source: (The Society of Light and Lighting, 2011).

Room surface	Reflectance range	Illuminance
Ceiling	0.7 - 0.9	30-90% of task illuminance or $E_h \text{ min} > 50 \text{ lux}$; $U_0 > 0.1$
Walls	0.5 - 0.8	50-90% of task illuminance or $E_h \text{ min} > 50 \text{ lux}$; $U_0 > 0.1$
Task area	0.2 - 0.6	According to task requirement
Floor	0.2 - 0.4	Maintained value of 30 - 50 lux

In this case, the first step would be to increase the surface reflectance of ceiling and floor by the specification of lighter colours for these surfaces.

TABLE 10.4 Typical reflectance of a range of reflective diffusive wall finishes. Source: (IESNA, 2000).

Material	% Reflectance
White plaster	90-92
White paint	75-90
White terra-cotta	65-80
Limestone	35-65

A totally white space would of course offer the highest reflectance conditions but might not satisfy other design requirements. In order to add colour to the classroom walls, it is advisable to use a colour with a high value within a particular chroma and hue (see Figure 10.4).

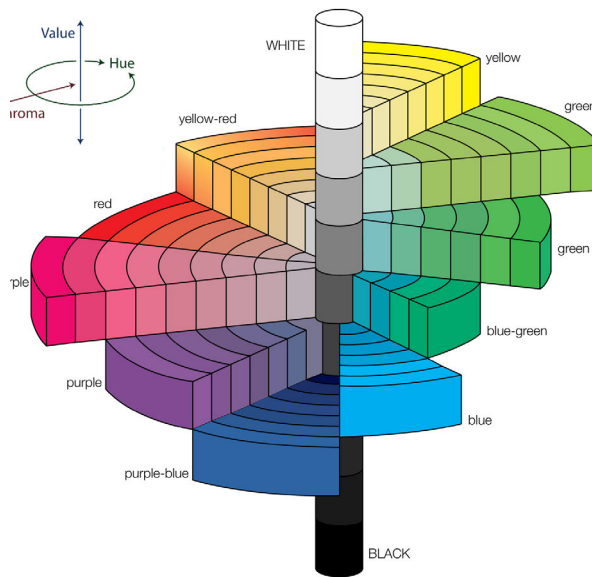


FIG. 10.4 A colour wheel, showing hue, chroma and value. Source: based on <https://www.britannica.com/science/Munsell-color-system>.

For simple reflectance based on colour, the designer can refer to a CIBSE colour chart or to a RAL colour fan, by matching a particular sample to colour in these charts and looking up its reflectance value.

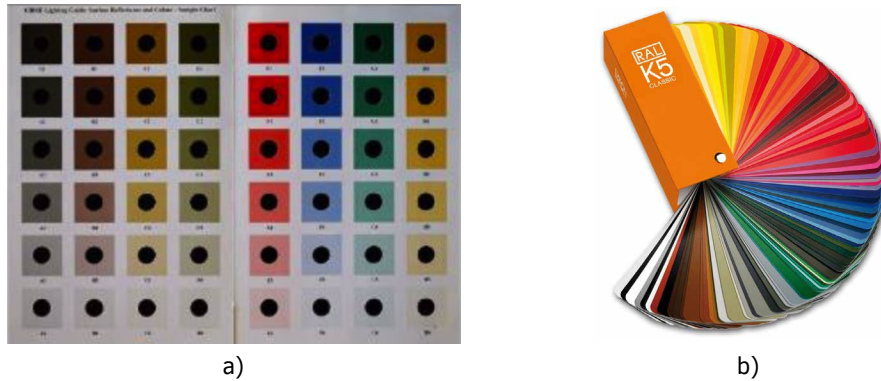


FIG. 10.5 CIBSE colour chart (a), source: (Society of Light and Lighting, 2001); RAL colour fan (b), source: https://en.wikipedia.org/wiki/RAL_colour_standard.

Surface reflectance will almost directly increase, as a function of colour value as far as the surface is what in lighting is called a diffusive surface, or a surface that reflects light evenly in all directions.

The luminance of a material will also depend on the way it scatters light, defined by its specularity and roughness. A material with a high roughness has a degree of 'self-shading' and therefore produces a reduced luminance. This is quite a relevant point as it is often the case that for the purpose of reducing the need for maintenance, rough materials such as bare brick or concrete-based products are used as finished walls of classrooms.

The characterization of the reflectance properties of rough materials can only be obtained with specialised laboratory equipment and for that reason is most of the times not readily available. After a recent effort to create a physically accurate materials library for lighting simulation (Jakubiec, 2016), a source for this type of information can be found in the database provided in (Design for Climate & Comfort Lab, 2021).

It should be considered that in classrooms and particularly in primary school, walls are often covered with all sorts of media and this can significantly reduce the benefit produced by an increase of their luminance based on light-coloured walls. If this media is in high quantity and of such colour properties that could contribute to a decrease of the wall surface luminance, it is suggested to place such media in the areas that are situated visually peripheral to the visual field of the occupants. The back of the room W1 is the least visible wall in the classroom as well as small portions of wall W2 and wall W4. Media of darker colours can be placed in these areas of the room (Figure 10.6).

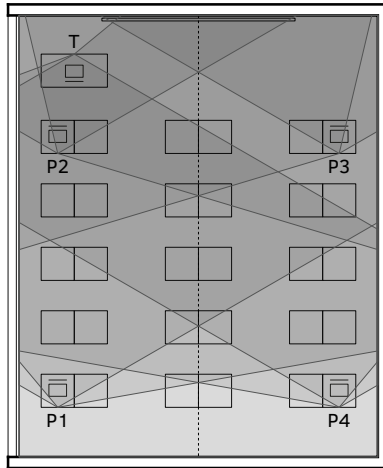


FIG. 10.6 Wall visibility from the four critical positions and from the teacher sitting position. Lighter grey represents the less visible part of the room.

10.3.2 Increasing the illuminance of the walls

10.3.2.1 Room lighting

Most classrooms today would be equipped with room lighting systems with zone-based switching and/or dimming operation modes for the purposes of energy saving. Under zonal lighting, when the window is very bright, lighting near the window will be switched off or dimmed and lighting in the inner part of the room switched on or increased. This type of operation does provide more uniform and adequate illuminance to the horizontal work plane and will also contribute to a higher luminance to the otherwise darker walls of the room. Some problems of discomfort glare might be avoided by the simple use of the room general illumination, particularly in cases where the glare source luminance is not critically high but the overall illumination of the room from daylight is low. Figure 10.7 shows an example scene where high level of glare is reported even though the glare source luminance is just over the threshold of $2,000 \text{ cd/m}^2$ ($2,500 \text{ cd/m}^2$) but the average background illuminance is quite low (132 Lux).

The artificial lighting is likely to be switched on when levels of daylight are low. What is important to note is that room illumination can also have a role in reducing glare and should also be operated for that purpose.

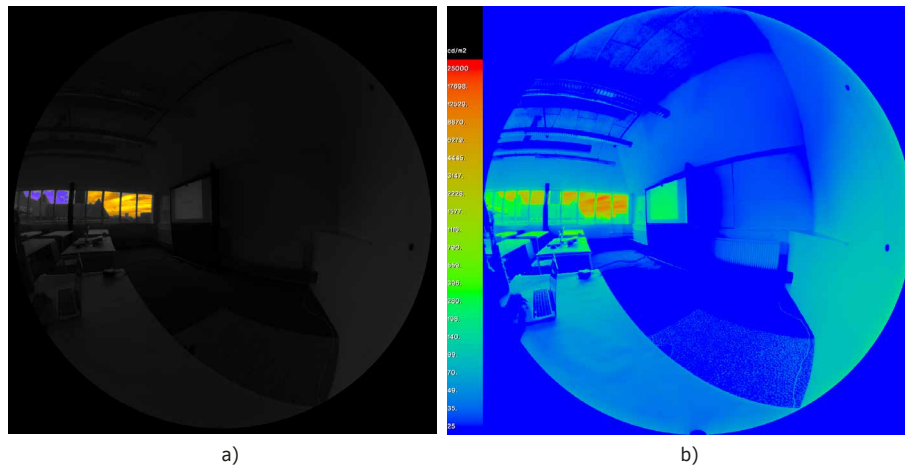


FIG. 10.7 Example of a scene where glare is reported for a low illuminance: (a) the identified glare sources in colour (image exposure reduced to -5.5) and (b) the luminance distribution of the scene.

10.3.2.2 Illuminated walls

The concept of an illuminated wall might sound a bit strange in the context of a lighting design practice that is still dominated by the provision of adequate levels of illumination to the horizontal workplane. Neither a common feature nor a requirement in classroom lighting design, it does however become a relevant concept in the context of preventing discomfort glare in these spaces and possibly other spaces.

Direct illumination of the walls would be appropriate to reduce the contrast between the window and the walls of the room, particularly of the darker wall (W4), and can also be considered for the walls 'in-between' (W3, W1), for an overall balanced light distribution.

Wall illumination can be provided by wall- or by additional ceiling-mounted artificial lighting fixtures (Figure 10.8). Several lighting fixtures can be found for this purpose, in some cases providing for down- and up-lighting, offering flexibility in terms of their vertical position on the wall. Wall lighting is frequently used in hospital ward lighting design, in this case with the objective of illuminating the task (patient), in the lighting of architectural offices where walls are task areas themselves or in museum lighting, in all these spaces for the same reason of providing adequate illumination to

particular objects on or objects in the vicinity of the wall. Examples of such fixtures might be found in those contexts. In most cases these fixtures will be equipped with light-diffusing devices but it should be considered that additional shielding might still be required in case the light source might become visible to the classroom occupants and cause discomfort glare itself.

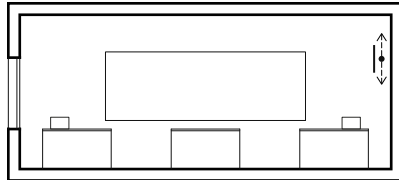


FIG. 10.8 Increasing illuminance of W4 with artificial lighting.

A 'self-illuminated' W4 via the inclusion of a window can be considered (Figure 10.9), which would effectively produce a double sided-lit classroom. This strategy has some similarities to what in classroom design is called a secondary window, using 'borrowed' light from an illuminated adjacent corridor or space, which can produce a benefit in terms of glare if the level of illumination of the adjacent space is high and constant. However, it is important to note that this strategy would not necessarily provide for a brighter W4 than a blank white wall unless the window has the same level of un-obstruction as the room's primary window (not shaded by external obstructions).

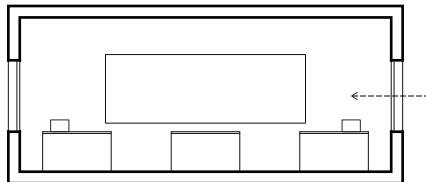


FIG. 10.9 Increasing illuminance of W4 with additional window.

Wall illumination can also be provided by daylight. There are several possibilities for the illumination of W4 using daylight when top-lighting is an option, by either the use of a dedicated skylight, by a monitor window or by a light well, as illustrated in Figure 10.10.

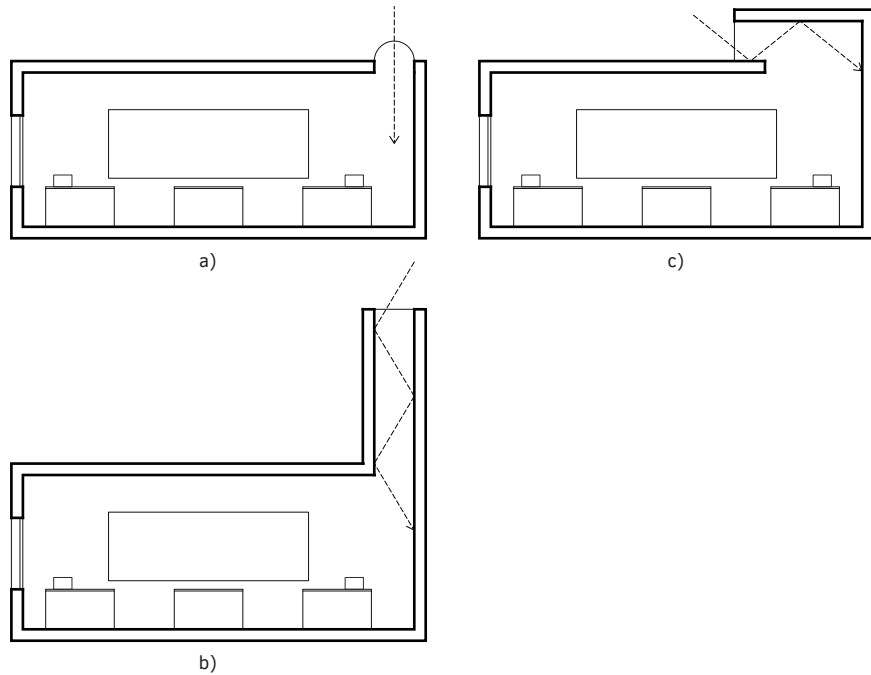


FIG. 10.10 Increasing W4 illuminance using daylight with (a) a sky-light, (b) a light-well and (c) a monitor window.

Illumination of walls using daylight can be combined with artificial lighting, so one system can compensate for the other if needed.

Orientation aspects could be considered regarding the monitor window. Shading of the skylight can be provided towards a required orientation or using internal baffles.

It should be noticed that one of the walls (either W3 or W1) is the board wall and that an increase of its illuminance needs to be considered in relation to the interaction with the board. In general, the smaller the luminance or illuminance contrast between the board and the adjacent wall the better, and therefore any strategies to increase its luminance will not tend to conflict with visibility requirements of the board, if veiling reflections can be avoided.

10.4 Classroom windows

Windows should be firstly designed to provide adequate levels of daylight for visibility of the visual task in a classroom, for which design criteria can be found in the lighting codes (Dilaura et al., 2011) (Society of Light and Lighting, 2018) or in daylighting design resources such as (Baker and Steemers, 2002), for example. Health and well-being aspects can also be considered in determining window size and location (International WELL Building Institute, 2015) as well as the quality of the view out (USGBC, 2013) (CEN, 2108). As a reduction of the window luminance will have a direct impact on the daylight levels, the first strategy to reduce discomfort glare should be to focus on the reduction of the apparent size of the window light source in the visual field.

10.4.1 Avoiding a view of the window

10.4.1.1 Roof-lights with occluded windows

Applicable if a top-lit room is an option, this solution would be the best in reducing discomfort glare from daylight as a view of the window is excluded. Occlusion of the window is provided if the widest vertical view angle for a sitting position, in this case 63° (view angle in P2 and P3, for board task), is used to define the inclination of the window glass surface, providing a shaded view for all other sitting positions (Figure 10.11). A few internal baffles can be provided to occlude the view of the window from the teacher's sitting position. The aperture size and number of the roof-lights should be defined based on workplane illuminance requirements, as defined in (Baker and Steemers, 2002) for example.

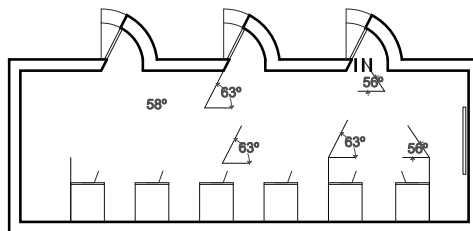


FIG. 10.11 Roof-lights with 'view-shaded' windows.

This solution has the obvious disadvantage of cancelling a view to the outside. As it might be difficult to reconcile the need for a view out and the necessity of avoiding discomfort glare, the duplication of strategies might be required, whereby occlusion of view windows can be activated in periods of a lower risk of glare (overcast skies) or for activities that are more visually demanding. Similarly, problems of veiling glare on the board or personal visual displays might be avoided with light redirecting or diffusing elements placed internally at the base of the roof-lights.

The roof-lights should ideally face North to maximise daylight and minimise the risk of overheating.

10.4.1.2 Side-windows with occluding baffles

Internal baffles, which can be part of a blinds system or an addition to a blinds system, can provide full occlusion of side windows. To totally 'view-shade' the window from the sitting positions, the baffles should be designed based on the defined angles of the central visual field, which in the case of the defined classroom is 85° in the sitting positions of the window zone and 50° in the sitting positions in the wall zone (see 10.4.2). This results in four different arrangements of baffles depending on the view angles from sitting positions 1, 3 and 4. As this arrangement is based in the extreme positions of the room, occlusion of the window is provided for all other sitting positions in-between. The baffles are more or less spaced depending on the view angles from the four extreme positions. The spacing is defined by the view angle from each of the four positions, resulting in different levels of occlusion of the window, or zones. In the case of the defined classroom, this produces a baffle with a spacing of 0.04 m in zone 1, 0.12 m in zone 2, 0.15 m in zone 3 and no-baffles in zone 4, for a baffle width of 33 cm (Figure 10.12). With this baffle arrangement, the view of the teacher is also occluded. Other baffle spacing arrangements would result for a different baffle depth.

This strategy has the disadvantage of considerably reducing the direct view out for the sitting positions, a situation that again can be improved if the baffles are designed to be operable and disengaged in periods of low risk of glare. Simple sheets of fabric-like materials as in common vertical blinds systems could be used for flexibility. These baffles should also be operable for the purpose of maintenance.

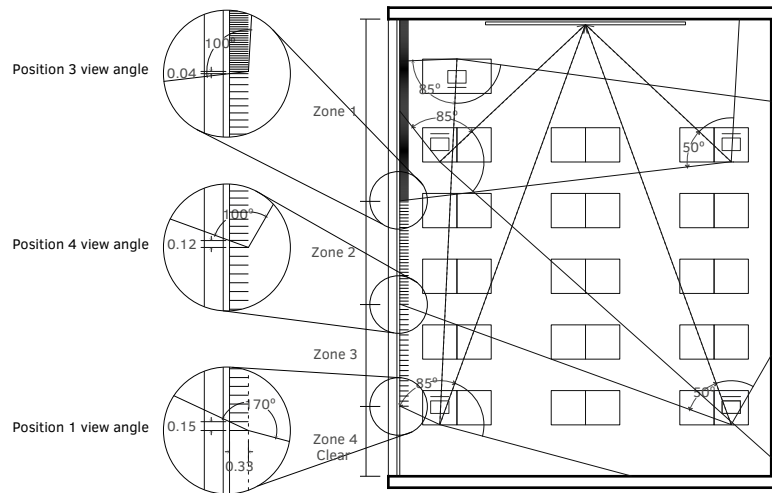


FIG. 10.12 A baffle system that offers a fully shaded view of the window in the central part of the visual field for all the sitting positions. The zones correspond to four different baffle arrangements.

10.4.1.3 Repositioning of the visual task

Repositioning the board can reduce the apparent size of the window in the field of view by shifting the point of observation from the centre, where the board is generally located, to a zone as far as possible from the window light source (Figure 10.13).

The improvement is mostly obtained for the sitting positions in the wall zone (where more glare was found to be reported). Some improvement is also verified for position 2 whereas additional glare protection to position 1 still needs to be provided, when required.

In the cases where the classroom is to be equipped with a range of devices (e.g. blackboard, smartboard, whiteboard, projecting screen) it would be an option to position these as layers in the inner part of the room or to provide units with mobility, so different devices can be positioned in that location when needed. This strategy will also likely have a positive effect in the reduction of veiling glare problems on the board, particularly for the sitting positions 3 and 4.

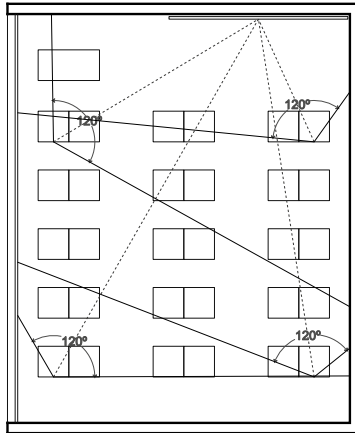


FIG. 10.13 Repositioning the board.

There is generally some flexibility regarding the repositioning of the individual visual display units and other task surfaces on the desks, which should be encouraged in order to reduce both discomfort and veiling glare problems.

10.4.1.4 Teacher situation

The risk of glare for the teacher can be greatly reduced for a sitting location in the window zone and that should be the preferred location for the teacher's desk (Figure 10.14). Similarly to the other room positions, a reduction of the window luminance might still be required (see 10.4.3).

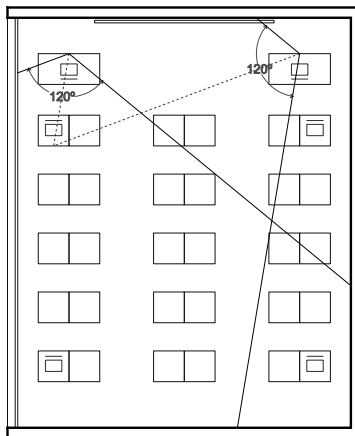


FIG. 10.14 Sightlines and central visual field of the teacher, for the critical point of observation (looking at P2) when sitting in the window zone and when sitting in the wall zone.

10.4.2 Avoiding a view of the window within the central visual field

Avoiding a view of the window in the central part of the visual field would be a way of significantly minimising the risk of glare, given the influence that the position of the glare source has on glare perception. This is especially important for the sitting positions in the wall zone, for which the window is more centrally located in the visual field. But what should be considered the central visual field? In this study, when glare was reported (glare source luminance $> 2,000 \text{ cd/m}^2$), the average Position Index of the glare source was 2.6 in the wall zone and 7.7 in the window zone (see Appendix G).

Figure 10.15 shows a Position Index diagram and Figure 10.16 shows the average Position Index value for a glare source in the two zones, plotted on that diagram.

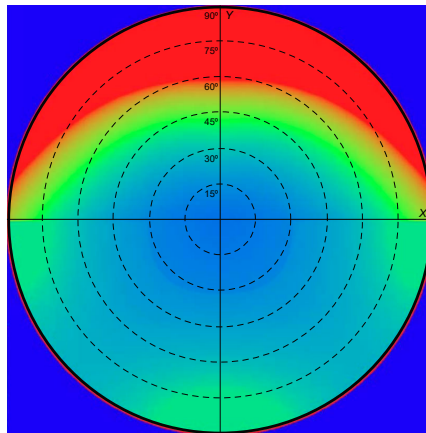


FIG. 10.15 Position Index (1-15) overlaid on view angles 15° to 90°.

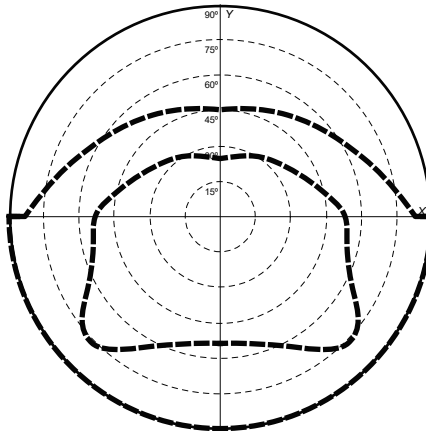


FIG. 10.16 Curves for a Position Index of 7.7 and of 2.6.

Based on the average position index for a glare source in the sitting positions of the wall zone, glare can be minimised if the window glare source is placed outside an area approximately defined by a 50° angle on the horizontal and a 25° angle on the positive direction of the vertical. Based on the average Position Index for a glare source in the sitting positions of the window zone, glare can only be minimised if the window glare source is placed outside an area defined by a 85° angle on the horizontal and by a 45° angle on the positive vertical direction.

As the window glare source is generally positioned in the upper half of the visual field, a window placed vertically outside the 45° central visual field cone should be considered in order to minimise the risk of glare (Figures 10.17 and 10.18).

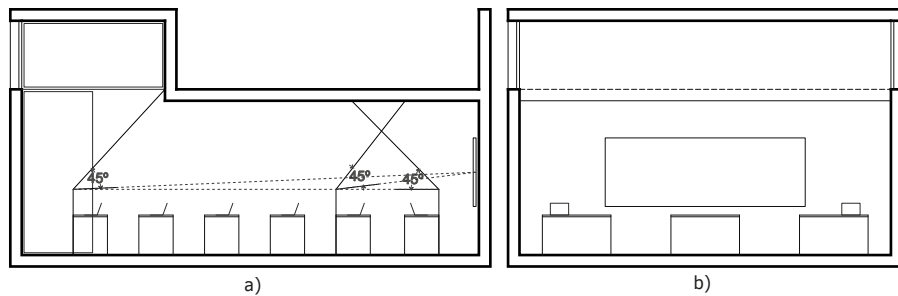


FIG. 10.17 High window totally located outside the 45° central view cone, combined with a semi-raised ceiling: (a) longitudinal and (b) cross-section. The high window can be extended to the back of room wall (W1) and to the 'inner' wall (W4), as shown in (b).

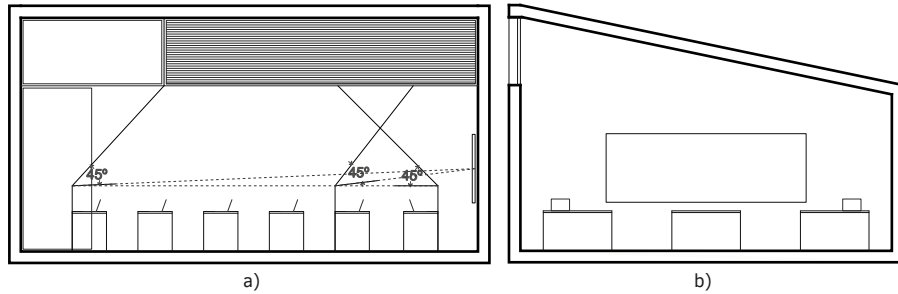


FIG. 10.18 High window partially located outside the 45° central view cone, with a raised slanted ceiling: (a) longitudinal and (b) cross-section. The visible part of the window will require a reduction of window luminance (see 10.4.2).

The strategies proposed above provide for a degree of visual contact with the exterior as a localised side window can be provided in the back of the room and views of the sky are also partially provided. However, direct views to the outside from the sitting positions are not provided. Lower view windows with shading can be provided and used when the risk of glare is low. The height of the ceiling should be defined based on the required amount of window area to satisfy the workplane illuminance level requirement. However, both strategies have the disadvantage of reducing the uniformity of daylight distribution across the room. The raised slanted ceiling solution will likely provide for a more uniform daylight distribution in the room in comparison to the semi-raised ceiling, as it offers redirection of the daylight to the workplane.

10.4.3 Reducing the window luminance

The window luminance or its brightness is a function of its light transmittance, where the higher the window glass transmittance the higher its luminance, with mullions and other window elements contributing to a reduction or an increase of the overall window luminance, depending on their colour and material properties.

The first aspect to consider is that any situation where the sun is visible from any sitting position in the classroom, i.e., as seen through the window, will cause severe discomfort glare. In these situations, full occlusion of at least the area of the window from where the sun can be seen needs to be provided.

This occlusion should be done by the external solar shading system primarily. If the solar shading system does not allow for full occlusion, for instance in cases where it does not provide for low sun angle protection, a secondary strategy needs to be adopted, like the use of the classroom's blinds system, which for that effect should offer a black-out mode or a high degree of protection to light transmission.

In order to reduce the window luminance when the sun is not visible and the window is still too bright ($> 2,000 \text{ cd/m}^2$) a reduction of its luminance needs to be provided.

In this study, for the situations where the sun was not visible through the window and glare was still reported by the subjects, the average glare source luminance reached $7,569 \text{ cd/m}^2$ for the sitting positions in window zone and $7,152 \text{ cd/m}^2$ for the sitting positions in the wall zone (see Appendix G), indicating that independently of the sitting position, the need to reduce window luminance might be as high as 70%.

The reduction of the window luminance can be done using either a blinds system or by reducing the light transmittance of the window glass. Dynamic blind systems, such as operable venetian blinds, should be used for control of the light transmittance at different times and ensure that a view out is partially provided. To ensure that window luminance can be adequately reduced but daylight levels are the least compromised and a view out is maintained at all times, the use of a shading system with light redirecting properties and view permeability might be a good option (Figure 10.19).

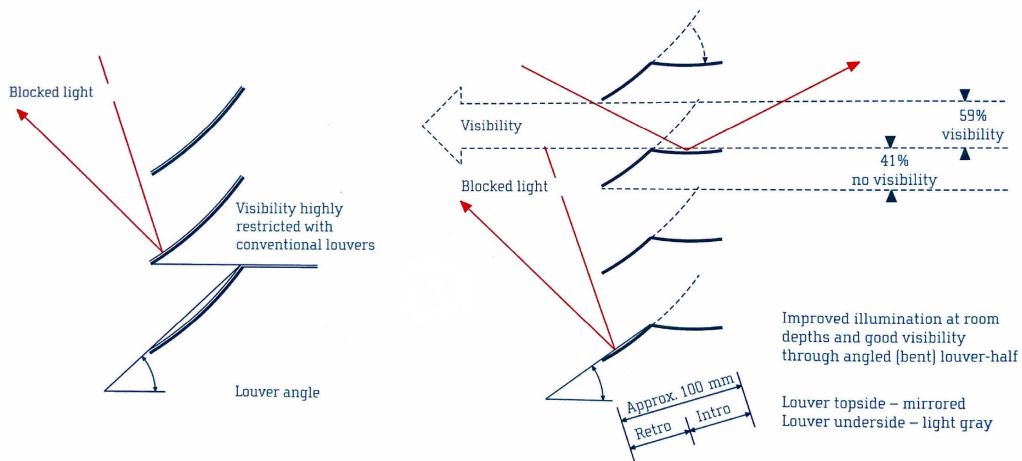


FIG. 10.19 Light redirection with Retrolux window shading technology. Source: (Köster, 2004).

A reduction of the window glass luminance, either via the use of a dynamic system (e.g., phase-change material, electrochromic glass) or by the simple reduction of the glass light transmission factor could be considered as an alternative to the use of blinds. However, a reduction of the window glass luminance in this way will likely not provide for the same level of occlusion that a blinds system can provide.

It should also be considered that even though north-facing windows do not necessarily offer reduced window luminance all the time, they certainly eliminate the possibility of an increased luminance due to the visibility of the sun and could therefore contribute to an overall reduced window luminance, when a north orientation for the classroom is a possibility.

10.5 Avoiding secondary glare sources

Even though window light sources are generally located in the upper half of the visual field, glare sources from reflections from direct solar exposure can also occur in the bottom half of the visual field, affecting large areas of the desks and of the lower part of the classroom walls (Figure 10.20). For the sitting positions in the window zone, this situation occurs in summer and in the mid-seasons and for the sitting positions near the wall in the late afternoon, early morning and wintertime (Northern Europe).

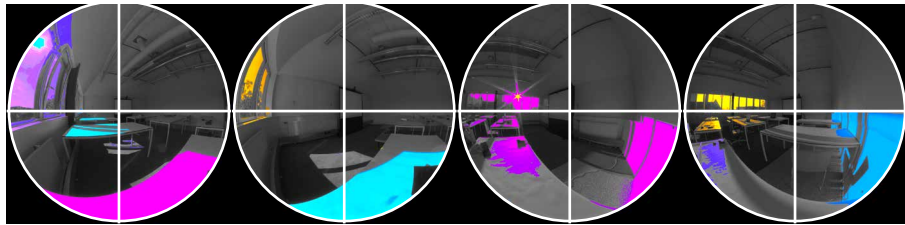


FIG. 10.20 Identified glare sources in positions P1 and P2 (a) and for positions P3 and P4 (b), showing the window glare source mostly situated in the upper half of the visual field and other large glare source areas in the bottom half of the visual field. (Image exposure set to -5.5).

A specific approach to this problem is required as the risk of glare from sources located in the bottom half of the visual field can be higher than in the periphery and in the upper half of the visual field.

One solution could be the reduction of the luminance of the affected surfaces by the use of a darker colour and therefore lower reflectance surfaces. Although this should be considered as an option it is quite at odds with visibility requirements of the desk task, which requires low contrast between task media and its immediate surroundings.

On the other hand, the problem is hardly completely solved with a reduction of the desks reflectance only, as in this study secondary glare sources affecting large areas of the desks were found to occur for both a desk reflectance of 89% (Study I) and of 48% (Study II).

In any case, a lower reflectance for the classroom desks tops should be considered as good visibility of the task was found for those conditions and a high reflectance will quite possibly aggravate the problem. It can be observed that the problem of secondary glare sources does not extend to the floor surface for example, which in this study had a very low reflectance (0.08%). Considering the recommended reflectance range of 20%-70% for classroom furniture (The Society of Light and Lighting, 2011), it would be appropriate to investigate what the reflectance is that in the range of 20% to 48% provides for the required task visibility and minimises the secondary glare source problem.

The specularity of the room surfaces was not measured in this research. In some cases, it is possible to anticipate that the specularity was likely to be low (desks covered with a very matte cardboard in Study II). However, it is fair to say that specularity would aggravate the problem of secondary glare sources and therefore finishes with zero or near-zero specularity should be selected for desk tops and for the lower part of the room surfaces.

If windows can be located in the upper part of the visual field (high window) as indicated previously, the problem can be solved to a certain extent, particularly if the window is combined with a light-shelf (Figure 10.21). For the low sun angles the reflections will be shifted to the upper part of the visual field where they are less of a problem and for the high sun angles reflections will be shifted to the ceiling or top of the visual field. Shading of the window will still need to be provided on sunny days in the mid-season.

A northern orientation of the window light source would eliminate the problem of secondary glare sources altogether and should always be considered if a north orientation is a possibility for the classroom. Note that protection from late afternoon sun of a north-facing window might still be required in Northern Europe.

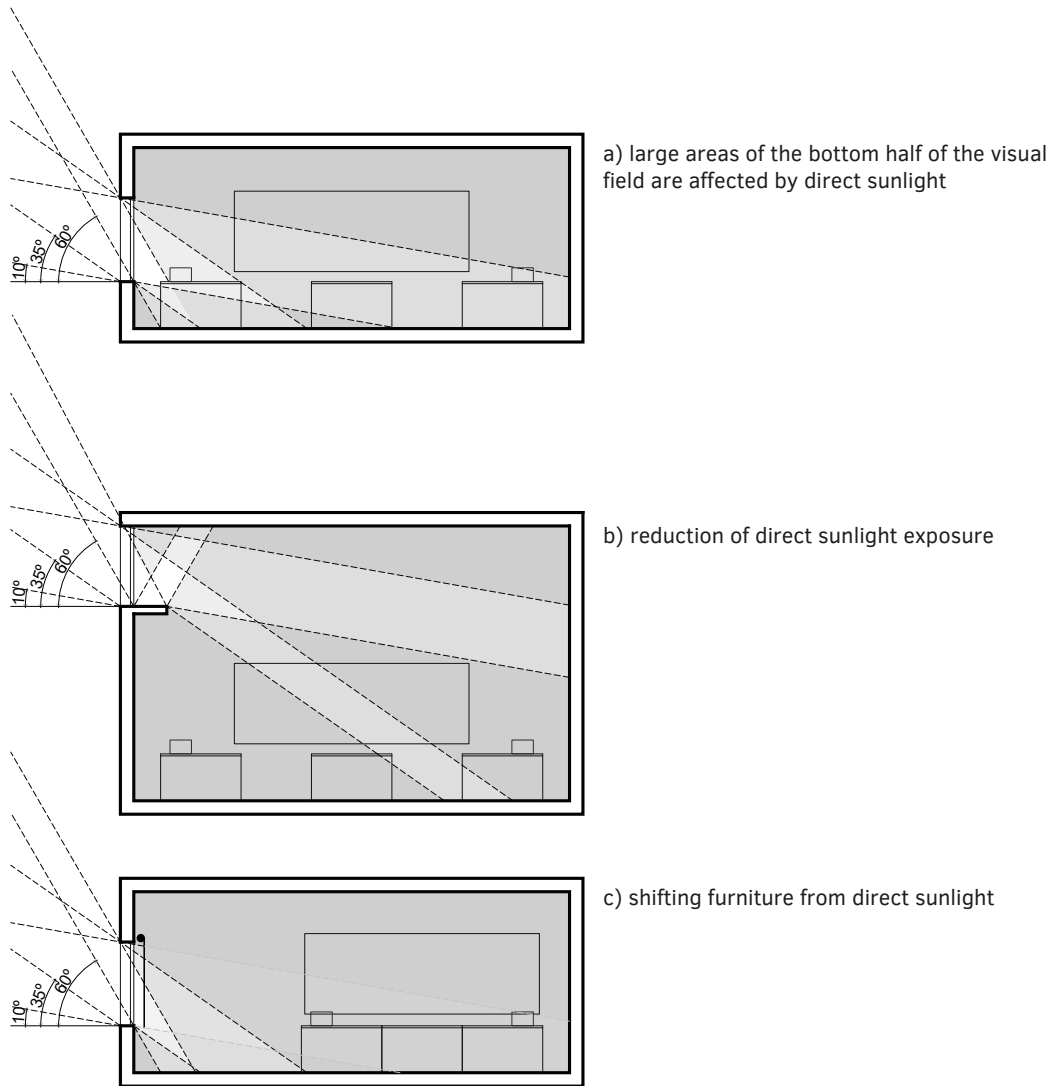


FIG. 10.21 Avoiding secondary glare sources: interaction of the room with typical solar angles for a Northern Europe location and (a) a window of normal height, with (b) a high window and a light-shelf and with (c) a “in-use” solution for a window of normal height, by changing position of desks and using window blinds when required. In the images, a darker shading of grey indicates an area that is less affected by solar reflections all year around.

10.6 Summary

In order to minimise discomfort glare in classrooms, the architect and lighting designer should then consider the solutions that are summarised in the flow chart provided in Figure 10.22, in combination with the equations 27, 28, 29 and 30 to evaluate the discomfort glare performance of the classroom. The equations provide a percentage discomfort in the classroom and it is left to the architect and lighting designer to decide what is the level of discomfort to accept.

The DGPl_{og}(E_v) model is applicable to classrooms with a depth of up to 6.5 meters. The evaluation of discomfort glare in the classroom should be made based on the four extreme sitting positions in the room, corresponding to the positions P1, P2, P3 and P4, in Figure 10.1. For the sitting positions corresponding to P1 and P2, equations 29 and 30 should be used and for the sitting positions corresponding to P3 and P4, equations 27 and 28 should be used.

The architect and the lighting designer will have to decide which specific equation definition – ‘any glare’ or ‘disturbing glare’ - to use, depending on the duration of the occupancy. For short-stay classrooms (around one hour) the equations for the ‘disturbing glare’ definition can be used. For long-stay classrooms, as for example primary school classrooms, the equations for the ‘any glare’ definition should be used.

The provided equations apply to situations of classrooms illuminated by side-windows. When daylight is provided by rooflights with occluded windows, the levels of discomfort glare can be considered negligible.

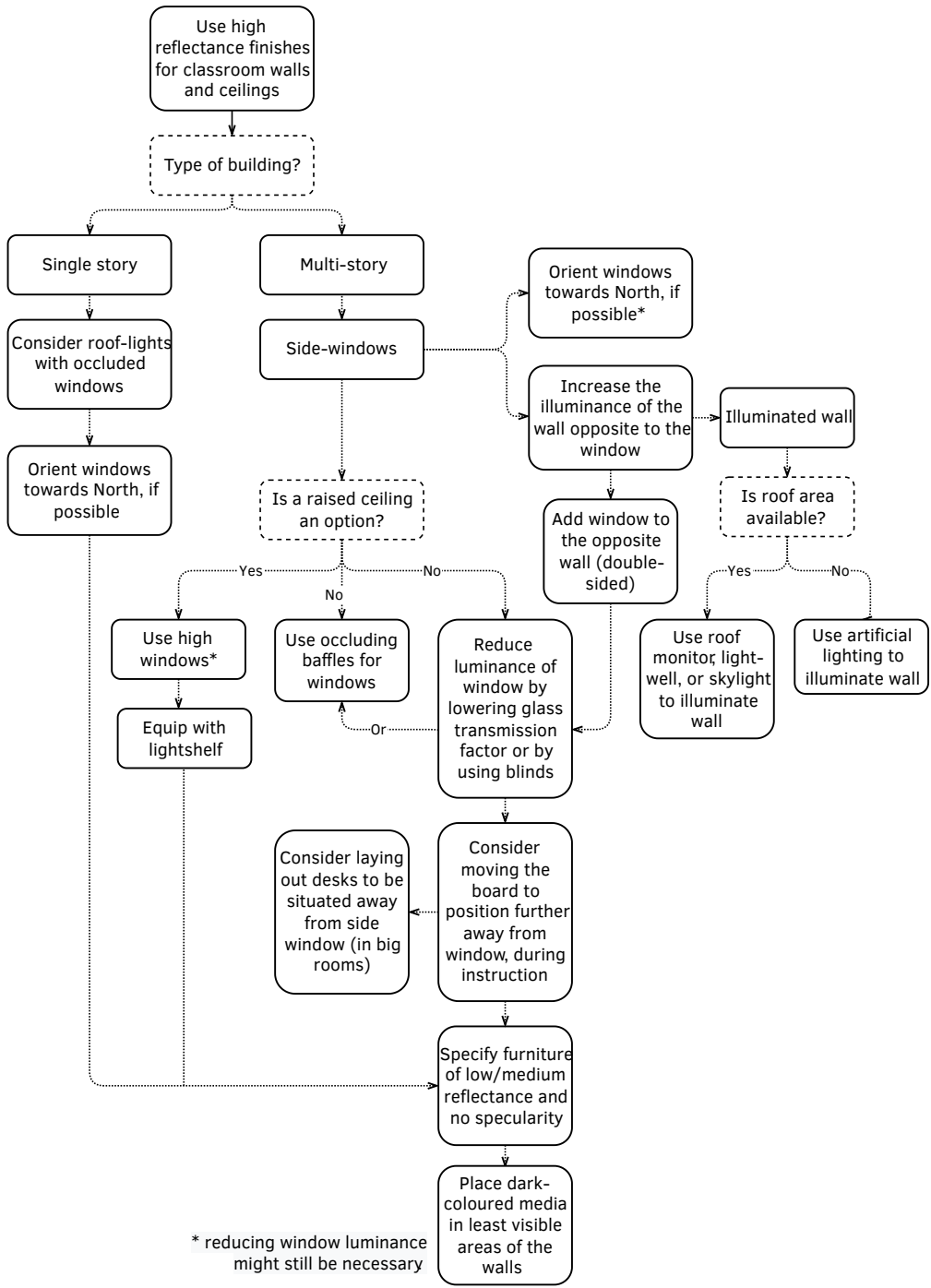


FIG. 10.22 Design workflow to minimise discomfort glare.

10.7 Conclusion

The design strategies that are presented in this chapter to address the problem of discomfort glare in the classroom are grouped into strategies that relate to the window, walls and to the secondary glare sources. These design strategies are listed in Table 10.5 in reference to the discomfort glare requirements that were defined earlier.

TABLE 10.5 Design strategies to prevent discomfort glare in the classroom.

Windows	[1]	Reduce the window luminance	Provide blinds with light-redirecting properties Reduce window glass transmittance
	[2]	Avoid a view of the window	Provide roof-lights with occluded windows Provide roof-lights with occluding baffles
	[3]	Avoid a view of the window within the central visual field	Provide high windows with raised ceilings
Walls	[4]	Increase the reflectance of the walls	Use high reflectance wall finishes
		Increase the illuminance of the walls	Use the room lighting to illuminate the darker walls Provide direct illumination to the darker walls using additional lighting fixtures, skylights, a light-well or roof monitors
Secondary glare sources	[1]	Reduce the luminance of the desks	Use low reflectance finishes for desks
	[2]	Reduce the area of the desk exposed to direct solar radiation	Provide high windows with light shelves
	[3]		Consider repositioning the desks

Strategies relating to repositioning of furniture and equipment, together with the use of particular finishes to walls and room furniture, will have the lowest impact on building capital costs and on building design and should be introduced first. It is appropriate to plan for movable and modular furniture and equipment for 'in-use' adaptation and flexibility.

Strategies that involve the creation of particular façade or roof elements will significantly affect the design of a school building and need to be considered as part of its overall conceptual design, as these require particular building and site conditions. This is the case of strategies involving the use of roof-assemblies or of slanted ceilings that will primarily apply to the low-rise school building.

Strategies that involve the windows affect the primary source of daylight illumination of a classroom and of the view out and should be implemented in consideration to those aspects. The provision of daylight illumination to the classroom will particularly be affected when using baffles or blinds, even when light redirecting systems are employed. In these cases it might be necessary to increase the window area so the required amount of lumens can be delivered to the room. Strategies involving high windows or roof-windows have the disadvantage of partially or totally reducing the view out of the room. These strategies can be complemented by low side-windows for views that would need to be occluded in the periods where there is a risk of glare.

Strategies related to the increase of the brightness of the classroom walls will on the other hand have the lowest impact on daylight illumination and views out. It was verified in this study that even a room with walls with a high overall reflectance has a low brightness at times and would benefit from direct illumination of its walls for the reduction of light contrast in the room. To the illumination requirement of the horizontal surfaces of the classroom space for light sufficiency and task visibility, there is a need to consider the illumination of the vertical surfaces of the classroom space for a reduction of discomfort glare. Wall illumination provided by daylight systems will have the additional benefit of increasing the daylight levels in the classroom and the light uniformity across the classroom space.

It has been pointed out that there is a benefit in choosing a northern orientation to windows and roof-lights when possible, a strategy that eliminates discomfort glare due to the presence of the sun in the field of view and due to secondary glare sources, with the additional benefit of reducing the risk of overheating.

Finally, it should be said that the presented strategies are not mutually exclusive and should ideally be combined for the best performance regarding the elimination of discomfort glare in classrooms.

11 Discussion

The applicability of existing metrics to the prediction of discomfort glare in the classroom, the improvement of the existing metrics and the provision of design guidance towards a discomfort–glare free classroom have been studied and discussed in the previous chapters.

In this chapter, a final reflection regarding several aspects of this investigation is made, focusing on its most relevant aspects.

11.1 Luminance measurement

The field-of-view luminance measurement, on which most of the discomfort glare metrics are based, presents a significant limitation to glare research: the impossibility of obtaining a measurement at the exact location of the subject's eye or at the exact time of the subject's glare evaluation. In Study I this has been resolved by placing the camera at a distance from the subject. In Study II, the measurements were collected before and after the subject's glare evaluation. Both options have disadvantages and introduce a degree of error to the luminance measurement. In the case of a displacement of the camera, the error is particularly high when the sun is in the field-of-view and in such a position that it can be visible to the camera and not visible to the subject, or the other way around. In the case of Study II, the use of the measurement at the start of the evaluation and of the mean measurement between the start and end measurement should be considered as the best possible approximation to the actual luminance conditions under which the subjects performed their evaluations.

The difficulty on pairing field-of-view luminance measurements and subject's glare evaluations not only poses a problem to discomfort glare research but also to building post-occupancy evaluation. Alternative methods for the study and verification of performance of discomfort glare to overcome this problem need to be investigated. This could resort to the use of calibrated simulation models

for luminance measurement, fitted/wearable luminance measuring devices or the investigation of reliable alternatives to field-of-view luminance measurement.

It was observed in this thesis that the errors associated with real-world luminance measurement using HDRI luminance capture can be in the same order of magnitude as simulated luminance using physically accurate light rendering techniques, making the use of subjective evaluations coupled with luminance measurements via high quality simulations a valid option for the investigation and validation of discomfort glare performance of buildings.

It was also found that the accuracy of the HDR luminance measurement wasn't as high as it was expected, an aspect that could be related to the camera settings, the length of the luminance capture and/or to the resolution of the produced image.

11.2 Data range

The experiments in this thesis were designed to obtain a sample 'in space' exclusively and not 'in time'. The focus was on obtaining responses from the maximum number of subjects for different sitting positions and view directions in a space. Ideally the same subjects

would have also evaluated different sky conditions, in different times of the year, extending the evaluations to a wider range of sky luminance conditions. The nature of the study also meant that the sky luminance was not a controlled variable within each evaluation session and throughout the experiment. The variability of a real sky remains one of the most challenging aspects of conducting discomfort glare research, with long periods of data collection being required to obtain data for a variety and/or for particular sky luminance conditions.

Although Study I covered a wide range of sky types that are representative of the summer and mid-season conditions generally, the investigation would have also benefited from data collected for the low-sun angles of wintertime, particularly considering that classrooms are largely occupied in that period of the year.

It should be noted that the fact that some data needs to be eliminated at pre-processing stage not only reduces the size of the analysis sample but also creates

imbalanced datasets from a statistical analysis standpoint. Longer periods of data collection and possible repetition of experiments need to be considered in future research, possibly requiring commissioned subjects.

The collected data is also limited in terms of the population age-group. Even if not proven within the young and working-age population, it is possible that glare perception could be affected by age and ideally subjects from other age-groups would have been involved in this investigation, with age possibly constituting a new variable of the study.

In terms of the subjective evaluation, care was taken regarding the full adaptation of the subjects' visual systems to each visual condition that was tested, however it should be noted that subjects were asked to provide a glare evaluation with reference to a duration but they weren't effectively providing an evaluation for the duration of a classroom task or lesson.

11.3 Evaluation of discomfort glare

Future discomfort glare research would benefit from the creation of validated questionnaires for investigations that like the present one rely on self-reported discomfort glare. Some means of auto-validation of the discomfort glare question were introduced in this thesis but more work is needed in this area possibly contributing to the definition of a more universal and standard method of evaluation. The development of standard methods for the subjective evaluation of glare would greatly increase the reliability and quality of discomfort glare research.

Research should nevertheless continue regarding the identification of physical response indicators that could be used to measure discomfort glare in an objective rather than in a subjective way, an investigation that should be done in articulation with the medical sciences and human vision science. This investigation could also be extended to the identification of particular behaviours that are associated with discomfort glare, in articulation with psychology and other behavioural sciences.

11.4 Tested metrics

This work was focused on field-of-view luminance metrics including a range of 'contrast', 'saturation' and 'contrast and saturation' types and with a particular attention to DGP, as this is the metric that has been adopted in Europe. Absent from this investigation is the performance of task-area based illuminance metrics, such as UDI and ASH, two metrics that are widely in use. As explained early in the thesis, there is much uncertainty regarding the thresholds for these metrics and their applicability to the conditions of the vertical task (board) is also unknown. The one-point approach to illuminance measurement of the task area used in this work was insufficient to conduct a meaningful analysis of the performance of these metrics. Several points of measurement are required as the illuminance distribution of a desk can be quite variable. This aspect should be considered in future studies investigating task-based illuminance metrics.

The relevance of these metrics to the future of discomfort glare prediction will not lie on the fastness of their computing, as there has been great improvements regarding the computation of luminance in recent years. It will mainly lie on the possibility of developing alternatives to field-of-view metrics for building performance verification and to the reduction of the large volume of information that a full field-of-view discomfort glare assessment of a real space can still generate.

11.5 Contrast glare in the window zone

It was surprising to find in Chapter VIII that a UGP-based metric can outperform a DGP-based metric in the window zone. It was expected that a metric that contains terms for both saturation and contrast glare such as the DGP and that was developed in the conditions of close proximity to the window, to perform better in this zone. However, the fact that in a classroom subjects look inwards when sitting by the window when engaged in board-based work and not outwards, as it has been investigated in the development of DGP and most of the other existing glare indices, might be the reason leading to this result. In the case of Study I, the overall quantity of light that the subjects were exposed to is in general low, and therefore their conditions could be more similar to the conditions in which UGP has been developed.

When looking inwards, the subjects are possibly more exposed to contrast than to saturation glare, as a large portion of the visual field is filled by the darker walls of a room rather than by a large bright window. The window in this case is also much more peripheral in the field-of-view than in previous studies, a situation that might be more conducive to contrast glare.

11.6 Variability of gaze

To reduce the complexity of the glare evaluation and measurement, the experimental studies in this thesis were carried out for fixed view directions. A choice was made in this work to control the variability of gaze variable in order to study the impact of the variability in space. However, depending on the type of activity, gaze can be more or less variable in a classroom. In primary school for instance, students tend to be involved in one task at a time, either looking at the board for board-based instruction or at the desk, for desk-based work. In secondary school, students might have a more variable gaze, as they take notes while a lesson is being delivered. This variability of gaze creates a tri-dimensional field-of-view that can only be captured with tri-dimensional luminance measuring devices. Spherical luminance measurements, lower resolution representations of those such as a cubic illuminance measurement or the use of panoramic photocameras, offer the opportunity to capture this tri-dimensional luminance field, a possibility that should be explored in future research.

11.7 Produced model and future developments

In terms of the model of discomfort glare for classrooms that was developed in this thesis it should be considered that the required process of transformation of the data into groups for linear regression entails a smoothing of the individual differences regarding the perception of discomfort glare. The used grouping strategy for the

statistical analysis implies that the developed model corresponds to an averaged subjective response to discomfort glare. For this reason, this model is not one that is expected to capture the individual differences regarding reported discomfort glare but the general tendency towards discomfort glare perception.

The use of a two-zone approach for the analysis and model development work that is carried out in the thesis does also result in a smoothing of the differences regarding the perception of glare that may exist in different positions in the room. It should be noted that evaluation of discomfort glare in the positions in the middle of the room was not part of the study and therefore the developed model can be said to be applicable to the extreme spatial and visual conditions of a classroom. The perception of daylight glare in the middle of the room and the extent to which the produced model applies to that area of the room is therefore not known. It is however expected that glare perception in this area of the room to be somewhere in-between the two studied conditions.

As the model was developed based on the data of Study I it primarily applies to the assessment of glare when subjects are engaged in a board task in the classroom. This corresponds to the visual conditions where there is less opportunity for adaptation. However, as individual adjustments regarding the positioning of a task are possible to a certain degree when subjects are engaged on a desk task, the produced model can be said to apply to the most critical discomfort glare conditions in the classroom.

As a reminder, the analysis that was done for the Study II dataset has revealed that in addition to the variable position in space, the existing metrics also don't perform satisfactorily when a range of typical classroom view directions are considered. This means that the applicability of the model to the wider range of field-of-view conditions in classrooms that were identified early in this thesis remains to be identified. An optimisation exercise similar to the one that was performed but for the visual conditions defined in Study II should show how applicable the developed equations are to these other field-of-view conditions. If the resulting equations are again different from the ones that are obtained for the conditions of a board task, then a model of discomfort glare for classrooms that includes view direction variables alongside position in the room variables might need to be considered.

It is also observed that the discomfort glare model resulting from this research is a 'contrast' type of model indicating that similarly to other studies investigating glare 'in space', the discomfort glare conditions in this study were mainly a result from contrast glare. It would be interesting to find if this is always the case in

the classroom environment by conducting an investigation for a wider range of classroom types (e.g. floor and surface area, different reflectance properties, window sizes and types) and a wider range of sky luminance conditions.

Finally, the proposed discomfort glare model was developed based on a small subject and data sample. It explains a considerably high percentage of the variation on the reported discomfort glare in this study but due to the size of the data sample on which it is based, it cannot be said to be representative of the wider student or classroom population. The small size of the sample also means that more robust analysis methods based on the use of 'train and test split' data samples, which are becoming the state-of-the-art in the field of predictive model development, could not be used in this investigation. Such an approach provides the possibility to test the model in the process of its own development, prevent an overfitted solution and provide a test of its possible generalizability.

In terms of the testing and validation of the discomfort glare model produced in this thesis, there is therefore the need to extend the present dataset in terms of the data sample, particularly in the range of the spatial conditions defined in Study II (room layout/view direction) including the middle-room positions, extend this investigation to other student groups (primary and secondary school students) and to the variety of their typical classroom spaces.

11.8 Design guidelines

Lastly, the architectural design guidance provided in this thesis towards a discomfort glare-free classroom needs to be evaluated in relation to its impacts on other visual requirements of classrooms, namely light sufficiency, visual legibility, visual interest, veiling reflections, views out and well-being as well as in relation to its impacts on thermal comfort, an investigation that needs to be done in the context of the classroom's annual lighting, heating and cooling performance. This investigation will be crucial for the identification of the actual period of the year when daylighting can be successfully provided to classrooms and its comfort, well-being and energy benefits be enjoyed by all.

12 Conclusion

Several metrics have been proposed in recent years for the prediction of discomfort glare from daylight. None was previously validated for the field-of-view conditions in the classroom space. Most of the existing and newly proposed metrics have been developed in cellular offices for subjects sitting at close proximity to the window and in many cases facing directly the window light source. This seating arrangement is quite an extreme scenario that not always occurs in the real working environment and certainly does not occur in a classroom type of space.

The first research question of this investigation, RQ1, therefore was: “To what extent are existing metrics appropriate to capture the problem of discomfort glare in the visual conditions of classrooms?” Two other questions were also asked: “How can better predictive models of discomfort glare be defined?” (RQ2) and “What aspects of the architectural design and what design strategies should be considered in order to reduce the risk of discomfort glare in classrooms?” (RQ3).

12.1 Experimental conditions

To respond to RQ1, two experimental studies were conducted. The objective of these studies was to collect paired field-of-view luminance measurements and subjective glare evaluations for a range of representative visual conditions in the classroom.

The two studies occurred in the same space, an adapted classroom at the Faculty of Architecture and the Built Environment at TU Delft, in The Netherlands. The room, with a typical size of primary and secondary school classroom (7.6m x 6.45m) was side-lit by a full-length window (7.6m x 1.4m) to the Southwest. The experiment occurred in different times of the year between 2016 and 2019, covering summer and autumn periods and a range of sky types including sunny, clear and overcast sky conditions. Although the studies were conducted with a specific student population (higher-education students) care was taken for this population to be as young as possible (average age of 30) so their visual systems were at least at a very similar

state of degeneration to that of the average general student population. The subjects that attended the experiment, 21 females and 29 males (N = 50), were of Asian, South American, African, Middle-Eastern and European origin.

The luminance data was collected using HDRI capture and required tuning of the used luminance acquisition system in order to increase its dynamic range. Further characterization of the system was also required in order to process the luminance images with *evalglare* in order to calculate the glare metrics. The subjective evaluations of glare were collected via an online questionnaire that was built based on other existing questionnaires available in the literature of discomfort glare research. Subjects performed a screen-based visual task, after which the subjective glare evaluations and luminance measurements were collected.

The experimental study I (Study I) consisted of collecting subjective glare evaluations in four positions of the room (two positions near the window and two positions near the wall) for subjects engaged in a board-task activity. The experimental study II (Study II) consisted of collecting subjective glare evaluations in the same four positions in the room but for a board and a desk task, corresponding to three different desk layouts (or subject's view directions). Study II therefore extends the range of field-of-view luminance conditions that were tested.

12.2 Performance of existing discomfort glare metrics (RQ1)

The analysis of the data collected in the two experimental studies was based on a two-zone approach - a window zone and a wall zone. A zone-based approach instead of a position-based approach was adopted in order to obtain a higher number of data points for statistical analysis. The performance of the discomfort glare metrics was analysed using statistical correlation and classification methods. The selected metrics included the most relevant glare indices, some of the recently proposed luminance-based metrics, the vertical eye illuminance and a range of metrics that showed a good correlation with reported glare in other studies in deep spaces. The selection included 'contrast-based', 'saturation-based' and 'contrast- and saturation-based' types of metrics.

The results showed that contrary to what could be expected, more cases of discomfort glare were reported in the sitting positions in the wall zone (72% of the votes in that zone) than in the sitting positions in the window zone (60% of the votes in that zone). In Study II, more cases of discomfort glare were reported in the window zone (57% of the votes in that zone) than in the wall zone. This result supports the hypothesis that discomfort glare from daylight in the inner part of the classroom space is at least as critical if not more critical than in the positions near the window. In the inner part of the room, the levels of illumination were relatively lower than in the window zone, which indicates that the discomfort glare that occurs in that part of the classroom is mostly motivated by luminance contrast.

The results showed that a range of metrics, namely DGP, E_v , $L_{180^\circ\text{-mean}}$, $L_{\text{win-mean}}$, $L_{\text{win-std}}$ and $L_{\text{win-max}}/L_{\text{t-mean}}$ are appropriate metrics for the assessment of situations of discomfort glare near a window in Study I. In Study II, DGP passed all statistical tests in the window zone but $L_{\text{win-mean}}$ and the $L_{\text{win-std}}$ showed a somewhat better performance in the individual statistical tests that were performed. A much lower borderline between comfort and discomfort (BCD) threshold for the metric in that zone (0.27) than its current value (0.35) was however found. In Study II, a lower BCD threshold for the DGP in that zone (0.29) was also found.

The results of Study I and II showed that while a wide range of metrics have a good performance regarding the prediction of reported discomfort glare in the window zone, none of the metrics showed an acceptable performance in the wall zone.

12.3 Development of a new discomfort glare metric (RQ2)

As the existing discomfort glare metrics were not successful at capturing the reported glare across the classroom space, an investigation was conducted on the definition of a more adequate discomfort glare model for classrooms.

Three methods were successively applied. The first method was an analysis of the predictive power of the individual parameters or variables of the glare equations and a range of other possible combinations of parameters. The second method was the development of a metric based on a linear equation that included the current

definition of the DGP and UGP metrics as variables of that equation and the final method was the development of a metric based on a modified version of the DGP and UGP equations.

The development of the discomfort glare model is based on the data from the experimental Study I (N=184). Study I has a larger data sample compared to Study II (N=101) and the combination of the two datasets would create a wide variability in terms of the number of assessments per subject and per study condition, which is undesirable for the purpose of most statistical analyses. As Study I occurred in summer and autumn periods it provides a wider and more representative range of classroom daylight illumination conditions than Study II. The possibility of testing or validating any produced models with the data from Study II was considered. However, when grouped according to the statistical analysis strategy used for metric development, Study II resulted in a dataset with an insufficient number of data points.

The model development is based on two definitions of glare – ‘any glare’ and ‘disturbing glare’. ‘Disturbing glare’ is defined as a glare situation that is found to be difficult to endure for more than 15/30 minutes. ‘Any glare’ is defined as a situation that is found to be difficult to endure for more than one day, or would become annoying if occurring repeatedly. The use of these two definitions results from the need to establish a ‘glare/no glare’ cut-off point for some of the performed statistical analyses, which were either based on binomial classification methods or on linear regression. For the ‘any glare’ definition, ‘glare’ corresponds to the ‘imperceptible’, ‘disturbing’ and ‘intolerable’ glare votes, whereas for the ‘disturbing glare’ definition, only the ‘disturbing’ and ‘intolerable’ glare votes are included in the definition of ‘glare’.

12.3.1 Method 1: predictive power of individual glare parameters

The objective of the analysis of the individual glare parameters was to find if there was one or a group of variables that are more successful as predictors of discomfort glare than others. Several variables of the glare equations (L_{avg} , E_v , L_b , L_t , L_{s_w} , L_{s_mean} , ω_{s_total} , P_{min} , E_{dir} , E_{ind}), new definitions of the adaptation term (E_v/L_b and E_v/L_t) and a range of different definitions of contrast (L_{s_mean}/E_v , L_{s_mean}/L_{avg} , L_{s_mean}/L_t) were tested. These parameters were analysed for the full room and for the division of the dataset into the four positions and zones. The analysis showed the same tendency observed for the analysis of the performance of the metrics, i.e. acceptable to good performance in the window zone and a poor performance in the wall zone. Interestingly for the full room analysis, none of the parameters showed a

good performance indicating that a single variable equation might not be adequate for the prediction of glare in the classroom as a whole. The analysis showed that when successful parameters were found, these tended to be different for different subdivisions of the dataset, indicating that different equations might be needed for different parts of the room.

12.3.2 Method 2: metric based on the current DGP and UGP

The second method consisted of developing a model based on the DGP and UGP metric definitions. DGP provided the best performance from all glare indices in Study I and the UGP is a metric that has been specifically developed for deep spaces and for situations of contrast-glare. The analysis uses statistical linear regression to find if a successful relationship between reported glare and the DGP and UGP metric definitions could be established. The analysis is based on the window zone and wall zone and resorts to the transformation of the data into groups so the dependent variable of the study, the 'reported glare', could be converted into a continuous variable, in this case a 'percentage of people that report glare'. This operation involves the definition of a 'glare/no-glare' cut-off point and for that reason the model is developed for the two definitions of glare that were mentioned before - 'any glare' and 'disturbing glare'.

A transformed version of the DGP, $DGPlog(E_v)$, where the linear form of the adaptation term of the DGP equation (E_v) is replaced by a logarithmic form, was also tested. The reason for this test emerges from the fact that in previous studies carried out in conditions of low-illumination and contrast-glare, the lack of success of the DGP has been attributed to the use of the linear form of the E_v in the DGP equation. It is also noted that DGP and the metrics derived from DGP are the only glare indices that do not have a logarithmic formulation.

The results of the study showed that the model based on the UGP produced the best correlation with the reported glare in the window zone, with a $r^2 = 0.56$ ($p = 0.01$) for the 'disturbing glare' definition and a $r^2 = 0.68$ ($p = 0.003$) for the 'any glare' definition. In the window zone, $DGPlog(E_v)$ produced the best correlation with the reported glare with a $r^2 = 0.71$ ($p = 0.001$) for the 'any glare' definition and a $r^2 = 0.73$ ($p = 0.001$) for the 'disturbing glare' definition.

The results of the study indicate that the replacement of the linear form of E_v in the DGP by its logarithmic form produces an improved model of discomfort glare based on the DGP in the wall zone of a classroom. It was also noted that, in the window

zone, discomfort glare can also be caused by luminance contrast. In that zone, a model based on the UGP, a 'contrast' metric, outperforms a model based on the DGP, a 'contrast and saturation' metric.

12.3.3 Method 3: metric based on a modified DGP or UGP

The third method corresponds to the development of a new metric based on a modified version of the DGP and UGP equations. The coefficients, exponents and constants of the DGP, DGPl_{og}(E_v) and UGP equations, identified as c1, c2, c3 and c4 in the equations below, were optimised using a genetic algorithm and the coefficient of determination of the linear regression r² as the fitting function.

$$\text{DGP} = c1 \cdot 10^{-5} \cdot E_v + c2 \cdot 10^{-2} \cdot \log_{10} \left(1 + \sum_{i=1}^n \frac{L_{s,i}^2 \cdot \omega_{s,i}}{E_v^{c3} \cdot P_i^2} \right) + c4$$

$$\text{DGPl}_{og}(E_v) = c1 \cdot 10^{-5} \cdot \log_{10}(E_v) + c2 \cdot 10^{-2} \cdot \log_{10} \left(1 + \sum_{i=1}^n \frac{L_{s,i}^2 \cdot \omega_{s,i}}{E_v^{c3} \cdot P_i^2} \right) + c4$$

$$\text{UGP} = c1 \cdot \log_{10} \left(\frac{c2}{L_b} \cdot \sum_{i=1}^n \frac{L_{s,i}^2 \cdot \omega_{s,i}}{P_i^2} \right)$$

The results show that there is a significant improvement of the predictive power of all the three metrics, DGP, DGPl_{og}(E_v) and UGP, when the components of the equations are modified. The resulting optimised DGP equations, DGP_{new}, indicate that a better prediction of the reported glare occurs when the contribution of the contrast term of the DGP is increased and the contribution of the adaptation term is reduced in relation to the original DGP equation. This is verified for both the window and the wall zone equations, supporting the idea that the reported discomfort glare, in this study, is more a consequence from contrast glare than from saturation glare.

The model based on the new DGPl_{og}(E_v) equations provided the highest correlation with the ‘percentage of persons that report glare’. In the window zone, the DGPl_{og}(E_v) produced a r^2 of 0.72 ($p = 0.0019$) for the ‘disturbing glare’ definition and a r^2 of 0.93 ($p < 0.0001$) for the ‘any glare’ definition. In the wall zone, the metric produced a r^2 of 0.81 ($p = 0.0004$) for the ‘any glare’ definition and a r^2 of 0.86 ($p = 0.0001$) for the ‘disturbing glare’ definition.

Following these results, a set of four DGPl_{og}(E_v) equations, DGPl_{og}(E_v)_{new}, were identified as the best solution of a model of discomfort glare for classrooms resulting from the investigation. The produced equations relate to the two definitions of glare and to the two zones on which the analysis was based.

Wall zone, ‘disturbing glare’:

$$\text{DGPl}_{\text{og}}(\text{Ev})_{\text{new}} = (0.17 \pm 0.02) \cdot \log_{10}(E_v) + (321 \pm 47) \cdot \log_{10}\left(1 + \sum_{i=1}^n \frac{L_{s,i}^2 \cdot \omega_{s,i}}{E_v^{3.09} \cdot P_i^2}\right) - (0.32 \pm 0.05) \quad \text{EQ 27}$$

Wall zone, ‘any glare’:

$$\text{DGPl}_{\text{og}}(\text{Ev})_{\text{new}} = (0.18 \pm 0.03) \cdot \log_{10}(E_v) + (58 \pm 10) \cdot \log_{10}\left(1 + \sum_{i=1}^n \frac{L_{s,i}^2 \cdot \omega_{s,i}}{E_v^{2.75} \cdot P_i^2}\right) + (0.16 \pm 0.03) \quad \text{EQ 28}$$

Window zone, ‘disturbing glare’:

$$\text{DGPl}_{\text{og}}(\text{Ev})_{\text{new}} = (0.04 \pm 0.009) \cdot \log_{10}(E_v) + (70 \pm 15) \cdot \log_{10}\left(1 + \sum_{i=1}^n \frac{L_{s,i}^2 \cdot \omega_{s,i}}{E_v^{2.48} \cdot P_i^2}\right) + (0 \pm 0) \quad \text{EQ 29}$$

Window zone, ‘any glare’:

$$\text{DGPl}_{\text{og}}(\text{Ev})_{\text{new}} = (0.004 \pm 0.0004) \cdot \log_{10}(E_v) + (0.13 \pm 0.012) \cdot \log_{10}\left(1 + \sum_{i=1}^n \frac{L_{s,i}^2 \cdot \omega_{s,i}}{E_v^{0.8} \cdot P_i^2}\right) + (0.31 \pm 0.03) \quad \text{EQ 30}$$

The use of one or the other set of equations would depend on the definition of glare that is found to be most appropriate. The ‘any glare’ equations represent a stricter approach to glare, the ‘disturbing glare’ equations a less strict approach. The ‘disturbing glare’ definition might be the most applicable generally. However, in situations as for example in the case of a primary school classroom, occupied by the same group of students over long periods of time, and where students by virtue of being young might not easily express their discomfort, it could be appropriate to prevent all glare, in which case the ‘any glare’ equations would apply.

The $DGPlog(E_v)_{new}$ model has a logarithmic relationship with the adaptation and with the contrast terms of the DGP equation. The linear form of adaptation, as it is currently defined in the DGP equation, might be the most appropriate for the conditions of saturation glare but not for the conditions of contrast glare that were verified in this study. It is also observed that for the same definition of glare, the produced $DGPlog(E_v)_{new}$ model equations differ significantly between the window and the wall zone. This suggests that an improved model of discomfort glare for the classroom is better defined based on a range of equations for different sitting positions or that new variables that account for the sitting position need to be included in the equations.

12.4 Architectural design guidelines (RQ3)

The final chapter of this thesis provides guidance on how the developed $DGPlog(E_v)_{new}$ model can be translated into a set of architectural design strategies for the prevention of discomfort glare in classrooms. The $DGPlog(E_v)_{new}$ is in its basic form a 'contrast' metric, as per the definition adopted to classify the different glare equations in this study. The design strategy for a discomfort glare-free classroom based on this model does therefore call for a reduction of the light contrast in the classroom space. To achieve this goal, several design strategies have been proposed involving the increase of the brightness of the classroom walls, the reduction of the window luminance, the reduction of the visibility of the window light source to the classroom occupants and the prevention of what has been described as secondary glare sources. Table 12.1 provides a summary of the proposed strategies.

Most of these strategies are not new to design. However, in the context of the current daylighting design literature these are generally presented as strategies to address the problem of light sufficiency of the workplane (desk) and adequate visibility of a task.

In this work, it has been discussed how these can be implemented to prevent discomfort glare in the daylit classroom. It is of particular relevance that in the context of designing a daylit classroom that is free from discomfort glare, the illumination of the classroom's vertical surfaces or walls might become as critical as the illumination of the horizontal task surface, or desks.

TABLE 12.1 Design strategies to prevent discomfort glare in the classroom.

Windows	[1]	Reduce the window luminance	Provide blinds with light-redirecting properties Reduce window glass transmittance
	[2]	Avoid a view of the window	Provide roof-lights with occluded windows Provide roof-lights with occluding baffles
	[3]	Avoid a view of the window within the central visual field	Provide high windows with raised ceilings
Walls	[4]	Increase the reflectance of the walls	Use high reflectance wall finishes
		Increase the illuminance of the walls	Use the room lighting to illuminate the darker walls Provide direct illumination to the darker walls using additional lighting fixtures, skylights, a light-well or roof monitors
Secondary glare sources	[1]	Reduce the luminance of the desks	Use low reflectance finishes for desks
	[2]	Reduce the area of the desk exposed to direct solar radiation	Provide high windows with light shelves
	[3]		Consider repositioning the desks

12.5 Future research

The main objective of this work was to extend the existing knowledge of discomfort glare prediction, that has been mostly focused on the office space, to the classroom and by doing so, to advance the understanding of discomfort glare from daylight as a phenomenon that occurs not only in the vicinity of a window but ‘in space’ (Figure 12.1).

The development of adequate methods of discomfort glare prediction and of design guidance towards discomfort glare-free classrooms is expected to contribute to the creation of better classroom environments, better learning and teaching experiences and in this way to higher levels of satisfaction and productivity in these spaces. Better estimation of the periods when classrooms can be comfortably daylight by the use of adequate discomfort glare metrics does also provide the possibility of performing more realistic assessments of the actual lighting requirements and energy performance of school buildings. This work is a first step in this direction and research in this area should continue for a successful use of daylight in these buildings.

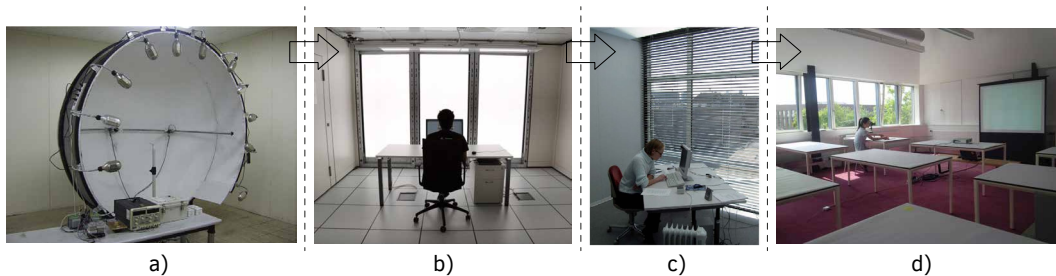


FIG. 12.1 Discomfort glare 'in space', experimental conditions of this research in comparison to other discomfort glare studies: a) modern version of the artificial light set-up used in the early glare index studies by Luckiesh and Guth in 1949 (Kim and Kim, 2010), b) an artificial window set-up used in laboratory glare research (Kent et al., 2019), c) the cellular office testing facility of the DGP investigation (Wienold, 2010) and d) the classroom set-up of this research.

Future research should look at how the produced discomfort glare model works in different conditions, particularly in terms of the subject's view direction and position in space. For this investigation it would be useful to extend the collection of data to wintertime or to a wider range of low sun-angle conditions. It would also be useful to extend the period of exposure of the subjects to each condition being tested to ideally the duration of an actual classroom lesson, so subjects are not only fully adapted to each condition but are also tested in a more realistic condition of work and focus. In this context, the variability of gaze in the classroom and ways of measuring it should also be investigated.

In terms of the experimental aspects of the research, digital alternatives to the field-of-view luminance measurement would help not only facilitating the study of discomfort glare but also verifying building actual performance (post-occupancy evaluation). The development of high accuracy simulation models, or of what is now defined as digital twins, is a very promising option. This would for instance allow the testing of several subjects at the same time, highly reducing the duration of future experimental studies in space. In addition, an investigation should be carried out regarding the accuracy of the HDRI luminance capturing technique, by testing the camera settings, duration of the capture and resolution of the luminance image. The development of a validated discomfort glare questionnaire that could be used with confidence by the lighting research community would also be a step forward towards the improvement of discomfort glare research.

Finally, there is a need to identify the impact that the design guidance to prevent discomfort glare in the classroom that is proposed in this study might have on the overall visual and thermal comfort performance of school buildings.

Appendices

Experimental method

A.1 Questionnaire 1

Introduction

Introduction

This questionnaire is part of a research about comfort in classrooms with daylight. You will be asked to perform a visual Test several times and to answer questions about the way you experience the lighting conditions in the room. Please be **frank and honest** in your answers.

Part 1: questions about yourself

Please provide a minimum 4-digit code that you will remember and that we can use to identify you in a future Test.

Part 1 Questions about yourself

How old are you?

What is your nationality?

Do you wear any corrective eye-ware?

- No
- Contact lenses
- Glasses

Are you wearing your corrective eye-ware now?

- Yes
- No

Are you female or male?

- Female
- Male

Are you left-handed or right-handed?

- Right-handed
- Left-handed

Do you consider yourself sensitive to bright light?

- Extremely sensitive
- Very sensitive
- Moderately sensitive
- Slightly sensitive
- Not sensitive nor insensitive
- Not sensitive

How important is it for you to have an exterior window view in your work place?

- Extremely important
- Very important
- Moderately important
- Slightly important
- Not important nor unimportant
- Not important

You will now be asked to perform a visual Test that will be projected on the screen that is in the centre of the room. Please put this questionnaire away for now and return to it only after finishing the Test.

Part 2: questions on your perception of comfort and glare

Part 2 Questions about your comfort with the lighting condition

Please enter below the number that is written on the desk where you are sitting.

- 1
- 2
- 3
- 4
- 5

- Disturbing**
I could tolerate this discomfort for 15 to 30 minutes, but I would require a change in the lighting conditions for any longer period.
- Intolerable**
I can't tolerate these lighting conditions.

Assume you have to perform this task daily in this space and in this position. How do you qualify the comfort of the lighting condition for that purpose?

- Extremely comfortable
- Moderately comfortable
- Slightly comfortable
- Just comfortable
- Slightly uncomfortable
- Moderately uncomfortable
- Extremely uncomfortable

You will now be asked to move to another desk in this room and repeat the Test you did before. Please put this questionnaire away for now and return to it only after finishing the Test.

Please enter below the number that is written on the desk where you are sitting.

- 1
- 2
- 3
- 4

Please look at the screen in the centre of the room for a few seconds and respond: how well can you see the screen?

- Extremely well
- Moderately well
- Slightly well
- Just well
- Not well
- Moderately bad
- Extremely bad

While doing the Test have you been bothered by:

	Far too little	Neither too much nor too little		Far too much			
	0	1	2	3	4	5	6
Sunlight incident on walls, on floor or on your desk	<input type="text"/>						
Reflections on the screen or screen washed out by light	<input type="text"/>						

When doing the Test in this position, which degree of glare from the window have you experienced?

- Imperceptible**
I did not feel any discomfort from the window.
- Noticeable**
A very slight discomfort that I could tolerate for approximately one day if I was placed in a desk carrying out this task under these conditions.

Is there any other reason?

Part 3: general comfort in the room

Part 4 General comfort in the room

For the last part of this questionnaire you will be asked some general questions about the room's overall comfort.

In general, how satisfied are you with the light level (amount of light) in the room to perform the task you were asked to?

- Extremely satisfied
- Moderately satisfied
- Slightly satisfied
- Neither satisfied nor dissatisfied
- Slightly dissatisfied
- Moderately dissatisfied
- Extremely dissatisfied

If you had to perform this task for a longer period under the conditions you have experienced during your stay in this room, would you want to turn the electric light on?

- Yes

- Maybe
- No

If you had to perform this task for a longer period under the conditions you have experienced during your stay in this room, would you want to put the window blinds down?

- Yes
- Maybe
- No

During your stay in this room, how comfortable did you feel regarding the following conditions?

	Extremely comfortable		Neither comfortable nor uncomfortable		Extremely uncomfortable		
	0	1	2	3	4	5	6
Air temperature	<input type="text"/>						
Incoming sun	<input type="text"/>						
Draft	<input type="text"/>						
Odour	<input type="text"/>						
Noise	<input type="text"/>						
Dust	<input type="text"/>						

Please add here any comments you may have regarding this survey.

A.2 Questionnaire 2

Introduction

Introduction

This questionnaire is part of a research about comfort in classrooms with daylight. You will be asked to perform a visual task several times and to answer questions about the way you experience the daylighting conditions in different sitting positions in the room. Please be **frank** and **honest** in your answers.

Part 1: questions about yourself

Please provide your identification code.

How old are you?

What is your nationality?

What is your eye colour?

- Brown
 Green

How (in)sensitive to bright light do you consider yourself to be?

- Extremely sensitive
 Very sensitive
 Somewhat sensitive
 Just insensitive
 Very insensitive
 Extremely insensitive

How (un)important is it for you to have an exterior window view from your work/study place?

- Extremely important
 Very important
 Somewhat important
 Just unimportant
 Very unimportant
 Extremely unimportant

You will now be asked to perform a visual task on the laptop that is in your desk. Please leave this questionnaire for now and return to it only after finishing the visual task.

Part 2: Desk 1

Please enter below the number that is written on the desk where you are sitting.

- Blue
 Hazel
 Other

What sort of visual correction do you normally require?

- I don't need visual correction
 Contact lenses
 Reading glasses
 Distance glasses
 Bi- or tri-focals
 Other

Are you wearing your corrective eye-ware today?

- Yes
 No
 I don't wear any corrective eye-ware

What is your gender?

- Female
 Male

Are you left-handed or right-handed?

- Right-handed
 Left-handed

- 1
 2
 3
 4

Please think about the conditions in which you just performed the visual task and respond to the following questions.

How satisfied were you with the visual conditions over the time you spent doing the visual task?

- Extremely unsatisfied
 Very unsatisfied
 Somewhat unsatisfied
 Just satisfied
 Very satisfied
 Extremely satisfied

Can you please state/explain the reason(s) for not being entirely satisfied with the visual conditions?

Please grade the level of glare (discomfort due to the brightness of the room surfaces, brightness of the window, light contrast) that you have experienced, if any, during the time you spent doing the visual task.

- Imperceptible
I did not feel any discomfort, I could work under these conditions for any period of

time.

Noticeable

I could work for approximately one day under these conditions, but it would bother me to work under these conditions every day.

Disturbing

I could tolerate these conditions for 15 to 30 minutes, but I would require a change in the conditions for any longer period of time.

Intolerable

I could not tolerate working in these conditions.

Please state what was the source of glare:

- The window
- The walls
- The desk
- The screen
- Objects visible through the window
- Other

Grade the level of visual distraction that you felt, if any, while performing the visual task.

Imperceptible

No distraction – conditions helped me focus.

Noticeable

I could feel some distraction but it did not really bother me.

Disturbing

The level of distraction was high and it could influence my ability to work after a while.

Intolerable

I experienced high distraction and could not focus on the work.

While doing the visual task in this desk have you been bothered by reflections on the screen or screen washed out by light?

- No
- Yes

While doing the visual task in this desk have you been bothered by the sun?

- No
- Yes

Please state in which way did the sun bother you:

- I could see the sun through the window
- The heat from the sun
- The sunlight on my desk
- The sunlight on the walls, floor or other room surfaces
- The sunlight reaching my body
- Other

You reached the end of the questionnaire in this desk. If you have any further comment in relation to your experience in this desk, please feel free to write it down here:

You will now be asked to move to another desk in this room and do another round of the visual task.

Please state how did the brightness or contrast of the room surfaces and window contributed to your feeling of visual (dis)comfort while performing the visual task?

- I felt extremely comfortable
- I felt very comfortable
- I felt just comfortable
- I felt somewhat uncomfortable
- I felt very uncomfortable
- I felt extremely uncomfortable

If you had to perform this task for a longer period under the conditions you have experienced, would you want to put the window blinds down?

- No
- Yes

Please explain in a few words why you wouldn't want to put the window blinds down:

If you had to perform this task for a longer period under the conditions you have experienced, would you want to turn the electric light on?

- No
- Yes

A.3 LMK standard calibration

A.3.1 Systems' total uncertainty

The mechanical uncertainty or repeatability of the luminance measurement (photometric calibration) is from 0.5% to 2%. The repeatability was estimated for all the combinations of aperture, ISO settings and shutter speed that the camera is calibrated for.

Uncertainty relating to laboratory conditions in which the calibration was carried out is estimated as 2.5%. After vignetting correction, the system does still display a uniformity uncertainty of +/-2%.

A.3.2 Elimination of black and white damaged pixels

One of the requirements of radiometric calibration is the need to identify and eliminate damaged pixels due to thermal inefficiencies of the camera sensor before producing the OECF (opto electronic conversion function) curve. The LMK calibration includes a dark signal pattern correction in the OECF that sets negative value pixels to zero, correcting the minimal signal-level of the OECF range in that way. On the other hand, as sensors can only handle a certain amount of light before becoming saturated, which results in images with damaged white pixels, the maximum accepted last significant bit (LSB) of the system is set to 12,500 at the luminance image conversion stage in Labsoft, a value that is lower than the original signal on the top of the OECF range ($2^{14} = 16,384$ LSB), with pixels above that range being neglected from being part of the luminance image.

A.3.3 LMK calibration certificate

The calibration certificate for the LMK system can be found next

WERKSKALIBRIERUNG (TechnoTeam)

Kalibrierung für optische Strahlungsmeßgrößen
Calibration for optical radiometry



0059
WK-K
2016-02

Kalibrierschein
Calibration Certificate

Kalibrierzeichen
Calibration mark

Gegenstand <i>Object</i>	Bildauffösendes Leuchtdichtemessgerät auf der Basis einer digitalen CMOS-Kamera mit verschiedenen Wechselobjektiven <i>Spatially resolved luminance measuring system based on a digital CMOS camera with different changeable lenses</i>	Dieser Kalibrierschein dokumentiert die Rückführung auf nationale und internationale Normale zur Darstellung der Einheiten in Übereinstimmung mit dem Internationalen Einheitensystem (SI). Für die Einhaltung einer angemessenen Frist zur Wiederholung der Kalibrierung ist der Benutzer verantwortlich. <i>The calibration certificate documents the traceability to national and international standards, which realize the units of measurement according to the International System of Units (SI).</i> <i>The user is obliged to have the object recalibrated at appropriate intervals.</i>
Hersteller <i>Manufacturer</i>	TechnoTeam Bildverarbeitung GmbH	
Typ <i>Type</i>	LMK mobile advanced	
Fabrikate/Serien-Nr. <i>Serial number</i>	163056007081	
Auftraggeber <i>Customer</i>	TU Delft	
Auftragsnummer <i>Order No.</i>	FM/70.171215.01	
Anzahl der Seiten des Kalibrierscheines <i>Number of pages of the certificate</i>	5	
Datum der Kalibrierung <i>Date of calibration</i>	29. Februar 2016 2016-02-29	

Dieser Kalibrierschein darf nur vollständig und unverändert weiterverarbeitet werden. Auszüge oder Änderungen bedürfen der Genehmigung der ausstellenden Kalibriereinrichtung. Kalibrierscheine ohne Unterschrift und Stempel haben keine Gültigkeit.

This calibration certificate may not be reproduced other than in full except with the permission of the issuing institution.
Calibration certificates without signature and seal are not valid.

Stempel <i>Seal</i>	Datum <i>Date</i>	Geschäftsführer <i>Manager</i>	Bearbeiter <i>Person in charge</i>
	29. Februar 2016 2016-02-29	Prof. Dr. -Ing. habil. F. Schmidt	Dr. -Ing. Udo Krüger

TechnoTeam Bildverarbeitung GmbH Werner-von-Siemens-Strasse 5 D-98693 Ilmenau Tel. +49 36 771 46 24 0 Fax. +49 36 771 46 24 10	Geschäftsführer: Prof. Dr.-Ing. habil. F. Schmidt Gesellschaftssitz: Ilmenau Handelsregister: Jena HRB 300912	Ust - Id Nr.: DE 150939174 Bankverbindung: Dresdner Bank Erfurt Kto.- Nr.: 0 802 362 100 BLZ: 820 400 00	Sparkasse Arnstadt/Ilmenau Kto.- Nr.: 1 113 010 661 BLZ: 840 510 10
--	---	--	---

Beschreibung des Kalibriergegenstandes

Description of the calibration-subject

Der Kalibriergegenstand ist eine bildauflösende Leuchtdichtemesskamera LMK mobile advanced auf der Basis einer digitalen CMOS-Kamera.

Die Sensordaten des Messgerätes werden durch eine numerischen Matrizierung an die Hellempfindungskurve $V(\lambda)$ angepasst. Durch eine Variation der Integrationszeit werden unterschiedliche Messbereiche realisiert. Die Messkamera kann mit verschiedenen Wechselobjektiven zur Vermessung unterschiedlicher Objektfelder und unterschiedlicher Messbereiche betrieben werden:

The calibration-subject is a spatially resolved luminance measuring camera LMK mobile advanced based on a digital CMOS camera. The sensor data of the measuring device are fitted onto the luminance-matching function $V(\lambda)$ by a numerical transformation. The luminance meter implements different measuring ranges by means of variation of the integration time. The luminance meter can be used with different changeable lenses to measure different subject fields and in different luminance ranges:

Kalibrierverfahren

Method of calibration

Die Kalibrierung erfolgte nach DIN 5032-6 „Lichtmessung, Teil 6: Photometer, Begriffe, Eigenschaften und deren Kennzeichnung“, Ausgabe 12/1995. Gemessen wird ein Kalibrierfaktor, der als das Verhältnis der Leuchtdichte des Kalibriernormales zur gemessenen Leuchtdichte definiert ist. Die Kalibrierung erfolgte für jede Kombination Leuchtdichtemessgerät und Wechselobjektiv.

The calibration was made according to DIN 5032-6 "Photometric measurement, part 6: Photometers, terms, qualities and their marking", edition 12/1995. A calibration-factor was measured that is defined as the ratio of the luminance of the calibration luminance standard to the measured luminance. The calibration occurred for every combination of luminance meter and changeable lens.

Messbedingungen

Measuring conditions

Messaufbau:

Die Kalibrierung wurde durch Vergleich mit einem Leuchtdichtenormal durchgeführt. Dabei wurde das Leuchtdichtenormal senkrecht zur Beobachtungsrichtung des Leuchtdichtemessers ausgerichtet. Als Messentfernung wurden die für die Wechselobjektive spezifizierten Entfernungen eingestellt. Bewertet wurde eine wesentlich kleinere als durch das Leuchtdichtenormal gegebene Fläche.

Measuring setup:

The calibration was carried out in comparison with a luminance standard. In this case the luminance standard was aligned vertically to the line of vision of the luminance meter. As measuring distance the distances specified for the changeable lenses were adjusted. The evaluation was made on a smaller surface than that was given by the luminance standard.

Leuchtdichtenormal

Luminance standard

Als Leuchtdichtenormal wurde das Modell LN3 S/N: 01B137 der Fa. LMT Lichtmesstechnik GmbH Berlin / Deutschland genutzt:

As luminance standard the model LN3 S/N: 01B137 of the Co. Lichtmesstechnik GmbH Berlin / Germany was used.

Das Leuchtdichtenormal wurde von der Physikalisch-Technischen Bundesanstalt auf ein nationales Normal (Kalibrierzeichen 40058 PTB 12 / Juni 2012) zurückgeführt.

The luminance standard is traceable to a national standard meter onto the Physical-Technical Federal Institution (Calibration mark 40058 PTB 12 / June 2012).

Umgebungsbedingungen

Ambient conditions

Die Messung wurde bei einer Umgebungstemperatur von $T_U = 25 \text{ °C} \pm 2 \text{ °C}$ durchgeführt. Das Kalibriernormal wurde vor der Messung bis zur Konstanz der lichttechnischen Werte eingebrannt.

The measurement was carried out with an ambient temperature of $T_U = 25 \text{ °C} \pm 2 \text{ °C}$. Before the measurement the calibration standard was burned in, until the photometric quantities remained constant

Bemerkungen

Remarks

Die in den Tabellen angegebenen Werte beinhalten nicht die mögliche Alterung durch die eine erneute Kalibrierung spätestens nach 2 Jahren erforderlich werden kann. Eine Abhängigkeit der Empfindlichkeit von anderen als den angegebenen Betriebsbedingungen oder Einflussgrößen ist nicht untersucht worden.

The given table values does not include an aging effect of the device which can make it necessary to do a new calibration after 2 years. A dependence of the sensitivity on other ones as the indicated operating conditions or influencing values was not examined.

Wechselobjektiv TT-14369367
Changeable lens TT-14369367

Objektiv-Nr. <i>lens no.</i>	Brennweite <i>focal length</i>	Messabstand *) <i>measuring distance*)</i>	Messfeld <i>measuring field</i>
TT-14369367	17 mm	> 280 mm	ca. 72,4° (diagonal)
	50 mm	> 280 mm	ca. 27,9° (diagonal)

*) Messabstand = Abstand von der Objektivfront zum Messobjekt

 *) *measuring distance = distance from the front of the lens to the measuring subject*
Nennleuchtdichte
Calibrated luminance

Die Kalibrierung erfolgt mit den Leuchtdichten des Kalibriernormales entsprechend den in den folgenden Tabellen aufgeführten Beträgen. Für die Kalibrierung des Leuchtdichtemessers in Kombination mit dem Wechselobjektiv **TT-14369367** wurden folgende Messergebnisse ermittelt und als Standardkalibrierung festgelegt:

The calibration with the luminance standard was made according to the luminance amounts that are listed in the following tables. For the calibration of the luminance meter in combination with the changeable lens TT-14369367 the results of measurement were determined as follows and assigned as standard calibration:

Messbereich <i>measuring range</i>			Nennleuchtdichte <i>nominal luminance</i>	Wert alt <i>value (old)</i>	Wert neu <i>value (new)</i>	Erweiterte Messunsicherheit *) <i>extended measurement uncertainty*)</i>
Brennweite <i>focal length</i>	Blende <i>aperture</i>	ISO				
18 mm	F4	100	L = 121,6cd/m ²		L = 121,6cd/m ²	5,7cd/m ²
18 mm	F4	100	L = 121,6cd/m ²		L = 121,6cd/m ²	5,7cd/m ²

*) Der Wert für den sich ergebenden Kalibrierfaktor wird häufig in der Form (100 ± 4,7)% ausgedrückt.

 *) *For the value of the resulting calibration factor, often the expression (100 ± 4.7)% will be used.*

Die Kalibrierung wurde mit den Leuchtdichten des Kalibriernormales für die Brennweiten 18mm; 25mm; 34mm; 50mm bei den Blendenzahlen F4; F5,6; F8; F11 und für die ISO - Verstärkungsstufen 100; 200; 400; 800; 1600 durchgeführt. Die angegebenen erweiterten Messunsicherheiten setzen sich zusammen aus den Messunsicherheiten des Kalibrierverfahrens und denen des Leuchtdichtemessers während der Kalibrierung. Angegeben ist die erweiterte Messunsicherheit, die sich aus der Standard-Messunsicherheit durch Multiplikation mit dem Erweiterungsfaktor k = 2 ergibt. Sie wurde gemäss DKD-3 ermittelt. Der Wert der Messgrösse liegt mit einer Wahrscheinlichkeit von 95% im zugeordneten Wertintervall.

The calibration with the luminance standard was done for focal lengths of 18mm; 25mm; 34mm; 50mm with the aperture values F4; F5.6; F8; F11 and ISO - settings of 100; 200; 400; 800; 1600. The indicated extended measurement uncertainties consist of the measurement uncertainties of the calibration procedure and those of the luminance meters during the calibration. It is indicated the extended measurement uncertainty, that results from the standard measurement uncertainty as a result of multiplication by the extension factor k = 2. It was determined in accordance with DKD-3. The index of the measuring value is in the assigned valuation interval with a probability of 95 %.

Beschreibung der spektralen Anpassung $s^*_{rel}(\lambda)$ an die $V(\lambda)$ - Funktion

Description of spectral match $s^*_{rel}(\lambda)$ on $V(\lambda)$

Kamera	LMK mobile advanced
Camera	SN: 163056007081
CMOS Empfänger	CMOS Canon APS-C
CMOS sensor	CMOS Canon APS-C
$V(\lambda)$- Filter:	Numerische Matrizierung der RGB – Sensordaten
$V(\lambda)$- filter	Numerical transformation of RGB – sensor data

Messbereichsendwerte

Typical accuracy rating

Blende <i>aperture</i>	ISO - Wert <i>ISO - setting</i>	Messbereich <i>measuring range</i>	Leuchtdichte <i>luminance</i>	Messbereich <i>measuring range</i>	Leuchtdichte <i>luminance</i>
F4	100	1 msec.	12664cd/m ²	3 sec.	4,2cd/m ²
			12664cd/m ²		4.2cd/m ²
	792cd/m ²		0,3cd/m ²		
	792cd/m ²				0.3cd/m ²
F11	100	1 msec.	95775cd/m ² 95775cd/m ²	3 sec.	31,9cd/m ² 31.9cd/m ²

Neutralgraufilter

Neutral density filter

Filter - Nr.	Transmission	Dichte <i>density</i>	Faktor <i>factor</i>
TTF 702-1	5,05%	1,30	19,82
TTF 702-2	0,96%	2,02	103,72
TTF 702-3	0,09%	3,07	1170,12

Wechselobjektiv TT-12505369
Changeable lens TT-12505369

Objektiv-Nr. <i>lens no.</i>	Brennweite <i>focal length</i>	Messabstand *) <i>measuring distance*)</i>	Messfeld <i>measuring field</i>
TT-12505369	4,5 mm	> 300 mm	ca. 180° (circular)

*) Messabstand = Abstand von der Objektivfront zum Messobjekt

 *) *measuring distance = distance from the front of the lens to the measuring subject*
Nennleuchtdichte
Calibrated luminance

Die Kalibrierung erfolgt mit den Leuchtdichten des Kalibriernormales entsprechend den in den folgenden Tabellen aufgeführten Beträgen. Für die Kalibrierung des Leuchtdichtemessers in Kombination mit dem Wechselobjektiv **TT-12505369** wurden folgende Messergebnisse ermittelt und als Standardkalibrierung festgelegt:

The calibration with the luminance standard was made according to the luminance amounts that are listed in the following tables. For the calibration of the luminance meter in combination with the changeable lens TT-12505369 the results of measurement were determined as follows and assigned as standard calibration:

Messbereich <i>measuring range</i>			Nennleuchtdichte <i>nominal luminance</i>	Wert alt <i>value (old)</i>	Wert neu <i>value (new)</i>	Erweiterte Messunsicherheit *) <i>extended measurement uncertainty*)</i>
Brennweite <i>focal length</i>	Blende <i>aperture</i>	ISO				
18 mm	F4	100	L = 119,9cd/m ²		L = 119,9cd/m ²	5,6cd/m ²
18 mm	F4	100	L = 119,9cd/m ²		L = 119,9cd/m ²	5,6cd/m ²

*) Der Wert für den sich ergebenden Kalibrierfaktor wird häufig in der Form (100 ± 4,7)% ausgedrückt.

 *) *For the value of the resulting calibration factor, often the expression (100 ± 4.7)% will be used.*

Die Kalibrierung wurde mit den Leuchtdichten des Kalibriernormales für die Brennweiten 18mm; 25mm; 34mm; 50mm bei den Blendenzahlen F4; F5,6; F8; F11 und für die ISO - Verstärkungsstufen 100; 200; 400; 800; 1600 durchgeführt. Die angegebenen erweiterten Messunsicherheiten setzen sich zusammen aus den Messunsicherheiten des Kalibrierverfahrens und denen des Leuchtdichtemessers während der Kalibrierung. Angegeben ist die erweiterte Messunsicherheit, die sich aus der Standard-Messunsicherheit durch Multiplikation mit dem Erweiterungsfaktor k = 2 ergibt. Sie wurde gemäss DKD-3 ermittelt. Der Wert der Messgröße liegt mit einer Wahrscheinlichkeit von 95% im zugeordneten Wertintervall.

The calibration with the luminance standard was done for focal lengths of 18mm; 25mm; 34mm; 50mm with the aperture values F4; F5.6; F8; F11 and ISO - settings of 100; 200; 400; 800; 1600. The indicated extended measurement uncertainties consist of the measurement uncertainties of the calibration procedure and those of the luminance meters during the calibration. It is indicated the extended measurement uncertainty, that results from the standard measurement uncertainty as a result of multiplication by the extension factor k = 2. It was determined in accordance with DKD-3. The index of the measuring value is in the assigned valuation interval with a probability of 95 %.

Beschreibung der spektralen Anpassung $s^*_{rel}(\lambda)$ an die $V(\lambda)$ - Funktion

Description of spectral match $s^*_{rel}(\lambda)$ on $V(\lambda)$

Kamera	LMK mobile advanced
Camera	SN: 163056007081
CCD Empfänger	CMOS Canon APS-C
CCD sensor	CMOS Canon APS-C
$V(\lambda)$ - Filter:	Numerische Matrizierung der RGB – Sensordaten
$V(\lambda)$ Filter	Numerical transformation of RGB – sensor data

Messbereichsendwerte

Typical accuracy rating

Blende aperture	ISO - Wert ISO - setting	Messbereich measuring range	Leuchtdichte luminance	Messbereich measuring range	Leuchtdichte luminance
F4	100	1 msec.	12531cd/m ²	3 sec.	4,2cd/m ²
			12531cd/m ²		4.2cd/m ²
	783cd/m ²		0,3cd/m ²		
	783cd/m ²		0.3cd/m ²		
F11	100	1 msec.	94769cd/m ² 94769cd/m ²	3 sec.	31,6cd/m ² 31.6cd/m ²

A.4 LMK extended calibration

A.4.1 F-number calibration



The calibration set-up.



Fish-eye image view of the source.

For the F-number extended calibration the camera was equipped with the fish-eye lens and fixed to a tripod directly facing and aligned with the integrating sphere light source. After setting the aperture manually, the room lighting was switched off and the camera was operated using a remote shooting trigger, so it would not move between shots. The room's window was fully covered with black cardboard prior to the measurements.

The data collection process consisted of taking a number of photographs of the light source for a calibrated aperture (F5.6) followed by a number of photographs for each of the three apertures to calibrate for. This process of repeated shots one right after the other is intended to deliberately create mechanical stress to the camera diaphragm which does not always open in the exact same way, even for the same aperture. This operation allows for the estimation of the repeatability of the measurement. There were 15 photographs taken for the calibrated aperture, F5.6, and 60 photographs taken of the aperture to calibrate for.

The correction factors are found as the ratio of the average luminance measured for the calibrated aperture (F5.6) to the average luminance measured for F16, F20 and F22 respectively. These correction factors are loaded into Labsoft, whenever one of these apertures is used.

Measured luminance for aperture F5.6 (15 photographs) and for the apertures F16, F20 and F22 (60 photographs) and respective correction factors are provided below.

F5.6		F16	
Avg. L (cd/m ²):	159.5063	Avg. L (cd/m ²):	156.8800
StdDev.:	1.0656	StdDev.:	1.7279
StdDev.(%):	0.67%	StdDev.(%):	1.10%
		Correc. Factor:	1.0167

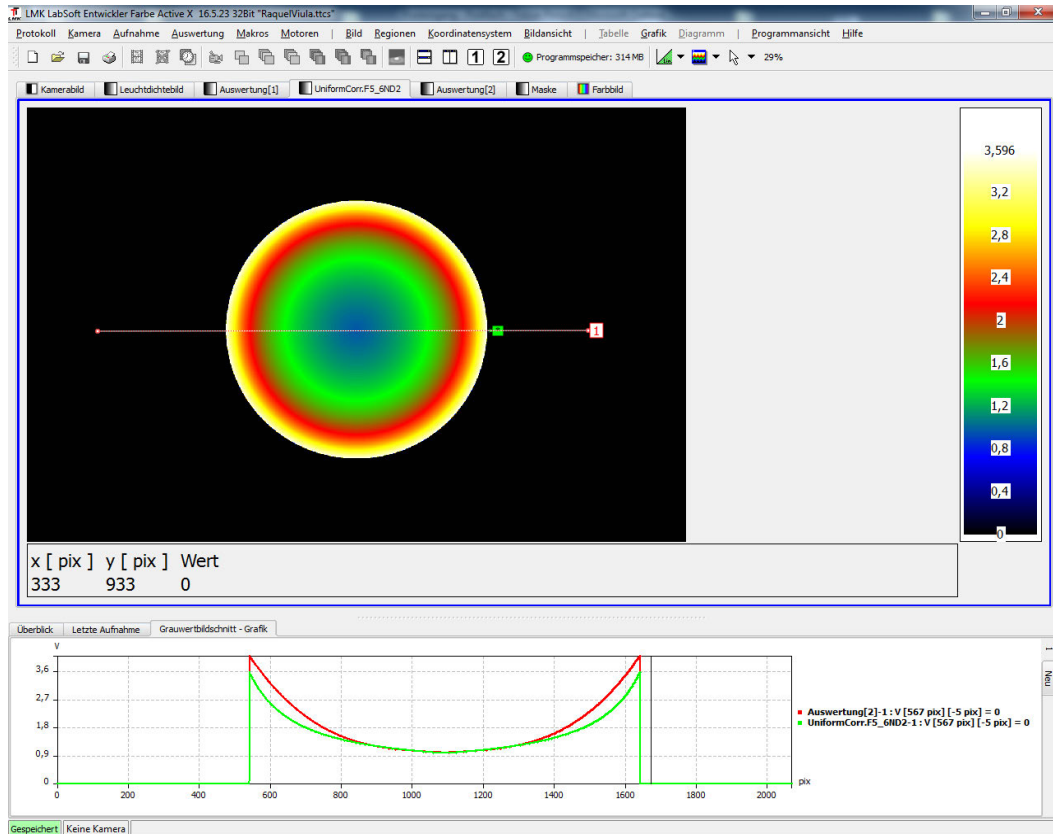
F5.6		F20	
Avg. L (cd/m ²):	160.1529	Avg. L (cd/m ²):	165.3867
StdDev.:	0.8712	StdDev.:	1.6619
StdDev.(%):	0.54%	StdDev.(%):	1.00%
		Correc. Factor:	0.9684

F5.6		F22	
Avg. L (cd/m ²):	159.8350	Avg. L (cd/m ²):	168.6393
StdDev.:	0.6901	StdDev.:	1.8516
StdDev.(%):	0.43%	StdDev.(%):	1.10%
		Correc. Factor:	0.9478

For a calibrated LMK system equipped with a particular lens, the variation of the measured uncertainty for different exposure settings depends solely on the repeatability of the photometric calibration.

The repeatability of the measurement (L_{avg} / L_{std}) for apertures F16, F20 and F22 was found of around 1.1% which is within the range of the repeatability of the original system calibration (0.5% to 2%) and therefore the measured uncertainty for the system with the newly calibrated apertures was assumed to be the same as the highest uncertainty found for the original LMK calibrated range ($\pm 6\%$, for F11).

A.4.2 Calibration with neutral density filter



The calibration of the system with a Kodak Wratten ND2.0 neutral density filter required a new uniformity calibration due to asymmetries of light transmission in the filter. This calibration was done using the same process described above for the photometric calibration, but measuring the light source standard for every rotation of the camera in steps of 10° .

The screenshot below shows the uniformity mask for the LMK system after loading the new uniformity factors file for the film filter calibration into Labsoft (top) and a graph of the uniformity curve (bottom). The red line of the graph shows the uniformity curve for the calibration of the original system and the green curve shows the uniformity curve for the system equipped with the ND2.0 film filter (image by Technoteam).

A.4.3 LMK/ND2.0 calibration certificate

The LMK calibration certificate after the ND.2.0 film filter calibration is provided next.

WERKSKALIBRIERUNG (TechnoTeam)

Kalibrierung für optische Strahlungsmeßgrößen
Calibration for optical radiometry



0230
WK-K
2017-08

Kalibrierschein
Calibration Certificate

Kalibrierzeichen
Calibration mark

Gegenstand <i>Object</i>	Bildauffösendes Leuchtdichtemessgerät auf der Basis einer digitalen CMOS-Kamera mit verschiedenen Wechselobjektiven <i>Spatially resolved luminance measuring system based on a digital CMOS camera with different changeable lenses</i>	Dieser Kalibrierschein dokumentiert die Rückführung auf nationale und internationale Normale zur Darstellung der Einheiten in Übereinstimmung mit dem Internationalen Einheitensystem (SI).
Hersteller <i>Manufacturer</i>	TechnoTeam Bildverarbeitung GmbH	Für die Einhaltung einer angemessenen Frist zur Wiederholung der Kalibrierung ist der Benutzer verantwortlich.
Typ <i>Type</i>	LMK mobile advanced	<i>The calibration certificate documents the traceability to national and international standards, which realize the units of measurement according to the International System of Units (SI).</i>
Fabrikate/Serien-Nr. <i>Serial number</i>	163056007081	<i>The user is obliged to have the object recalibrated at appropriate intervals.</i>
Auftraggeber <i>Customer</i>	TU Delft	

Auftragsnummer
Order No. **FM/70.171215.01**

Anzahl der Seiten des Kalibrierscheines
Number of pages of the certificate **4**

Datum der Kalibrierung
Date of calibration **3. August 2017**
 2017-08-03

Dieser Kalibrierschein darf nur vollständig und unverändert weiterverarbeitet werden. Auszüge oder Änderungen bedürfen der Genehmigung der ausstellenden Kalibriereinrichtung. Kalibrierscheine ohne Unterschrift und Stempel haben keine Gültigkeit.

This calibration certificate may not be reproduced other than in full except with the permission of the issuing institution.
Calibration certificates without signature and seal are not valid.

Stempel <i>Seal</i>	Datum <i>Date</i>	Geschäftsführer <i>Manager</i>	Bearbeiter <i>Person in charge</i>
	3. August 2017 2017-08-03	Dr. -Ing. Udo Krüger	Dr. -Ing. Benjamin Ruggaber

TechnoTeam Bildverarbeitung GmbH Werner-von-Siemens-Strasse 5 D-98693 Ilmenau Tel. +49 36 771 46 24 0 Fax. +49 36 771 46 24 10	Geschäftsführer/CEO: Frank Jugel; Dr.-Ing. Udo Krüger Gesellschaftsitz: Ilmenau Handelsregister: Jena HRB 300912	Ust - Id Nr.: DE 150939174 Bankverbindung: Dresdner Bank Erfurt Kto.- Nr.: 0 802 362 100 BLZ: 820 400 00	Sparkasse Arnstadt/Ilmenau Kto.- Nr.: 1 113 010 661 BLZ: 840 510 10
--	--	--	---

Beschreibung des Kalibriergegenstandes

Description of the calibration-subject

Der Kalibriergegenstand ist eine bildauflösende Leuchtdichtemesskamera LMK mobile advanced auf der Basis einer digitalen CMOS-Kamera.

Die Sensordaten des Messgerätes werden durch eine numerischen Matrizierung an die Hellempfindungskurve $V(\lambda)$ angepasst. Durch eine Variation der Integrationszeit werden unterschiedliche Messbereiche realisiert. Die Messkamera kann mit verschiedenen Wechselobjektiven zur Vermessung unterschiedlicher Objektfelder und unterschiedlicher Messbereiche betrieben werden:

The calibration-subject is a spatially resolved luminance measuring camera LMK mobile advanced based on a digital CMOS camera. The sensor data of the measuring device are fitted onto the luminance-matching function $V(\lambda)$ by a numerical transformation. The luminance meter implements different measuring ranges by means of variation of the integration time. The luminance meter can be used with different changeable lenses to measure different subject fields and in different luminance ranges:

Kalibrierverfahren

Methode of calibration

Die Leuchtdichtekalibrierung erfolgte in Anlehnung an ISO/CIE 19476:2014-06 „Characterization of the Performance of Illuminance Meters and Luminance Meters“. Gemäß diesem Dokument muss zur Kalibrierung eines Leuchtdichtemessers ein Leuchtdichtenormal mit einer homogenen leuchtenden Fläche verwendet werden, welche deutlich größer ist als das Messfeld des Leuchtdichtemessers. Die Leuchtdichteverteilung des Leuchtdichtenormals muss so homogen sein, dass jegliche Inhomogenität das Kalibrierergebnis nicht signifikant beeinflusst. Kann eine Beeinflussung nicht ausgeschlossen werden, so müssen Korrekturen erfolgen. Übertragen auf den Kalibriergegenstand wird die Forderung des Dokuments dadurch erfüllt, dass zur Auswertung der Messung eine deutlich kleinere Fläche (Pixelanzahl) verwendet wird, als sie vom Leuchtdichtenormal auf der Detektormatrix ausgefüllt wird. Gemessen wird die mittlere Leuchtdichte über eine Teilfläche des Leuchtdichtenormals. Die Farbkalibrierung erfolgte in Anlehnung an DIN 5033-8:1982-04 „Farbmessung; Meßbedingungen für Lichtquellen“.

The luminance calibration is based on ISO/CIE 19476:2014-06 „Characterization of the Performance of Illuminance Meters and Luminance Meters“. According to this document, a luminance meter shall be calibrated using a luminance standard whose uniform luminous surface is significantly larger than the measuring field of the luminance meter. The uniformity of the luminance standard shall be such that any non-uniformity does not significantly affect the calibration or is corrected for. Transferred to the device under test, the requirements of this document can be fulfilled if – for evaluating the measurement - an area is used (number of pixels) which is significantly smaller than the area which is filled by the luminance standard on the detector matrix. The result of the measurement is the averaged luminance of a subarea of the luminance standard. The colour calibration is based on DIN 5033-8:1982-04 „Farbmessung; Meßbedingungen für Lichtquellen“.

Messbedingungen

Measuring conditions

Die Entfernung zwischen dem Farb- und Leuchtdichtenormal (Normal) und dem Kalibriergegenstand wird so eingestellt, dass das Normal scharf auf die Detektormatrix abgebildet wird. Die Lichtaustrittsfläche des Normals wird senkrecht und mittig zur optischen Achse des Kalibriergegenstandes ausgerichtet. Ein jeweiliges Objektiv des Kalibriergegenstandes wurde für die Messung auf einen festen, im Abschnitt Messergebnisse angegebenen, Fokuszustand eingestellt. Die zur Auswertung der Messung verwendete kreisförmige Region wurde so gewählt, dass sie ca. den halben Durchmesser besitzt, wie das Bild des gesamten Normals auf der Detektormatrix. Sowohl das Normal als auch der Kalibriergegenstand wurden vor dem Beginn der Kalibrierung mindestens 30 min unter Messbedingungen betrieben.

The distance between the luminance and the colour standard (standard) and the device under test is set, such that the standard is sharply imaged onto the detector matrix. The standard is placed in the centre and orthogonally to the optical axis of the device under test. For the measurement, a particular lens was set to a fixed focus (cf. paragraph „Measurement results“). The circular area used for evaluating the measurement was chosen that it was half the diameter of the image of the complete standard on the detector matrix. Both the device under test and the standard had been operated under measurement conditions for about 30 min before calibration.

Leuchtdichtenormal

Luminance standard

Als Leuchtdichtenormal für die Rückführung wurde das Modell LN3 (S/N: 01B137) der Firma LMT Lichtmesstechnik GmbH Berlin verwendet. Das Leuchtdichtenormal wurde von der Physikalisch-Technischen Bundesanstalt auf ein nationales Normal (Kalibrierzeichen 40058 PTB 12/Juni 2014) zurückgeführt.

As luminance standard for the traceability the model LN3 (S/N: 01B137) manufactured by the Lichtmesstechnik GmbH Berlin company was used. The luminance standard was traced back to a national standard by the Physikalisch-Technischen Bundesanstalt (calibration mark 40058 PTB 12/June 2014).

Umgebungsbedingungen

Ambient conditions

Die Raumtemperatur lag bei der Messung bei $(25 \pm 2) ^\circ\text{C}$.

The measurement was carried out at an ambient temperature of $(25 \pm 2) ^\circ\text{C}$.

Bemerkungen

Remarks

Die in den Tabellen angegebenen Werte beinhalten nicht die mögliche Alterung durch die eine erneute Kalibrierung spätestens nach 2 Jahren erforderlich werden kann. Eine Abhängigkeit der Empfindlichkeit von anderen als den angegebenen Betriebsbedingungen oder Einflussgrößen ist nicht untersucht worden.

The given table values does not include an aging effect of the device which can make it necessary to do a new calibration after 2 years. A dependence of the sensitivity on other ones as the indicated operating conditions or influencing values was not examined.

Wechselobjektiv TT-12505369 (incl. Kodak ND2)
Changeable lens TT-12505369 (incl. Kodak ND2)

Objektiv-Nr. <i>lens no.</i>	Brennweite <i>focal length</i>	Messabstand *) <i>measuring distance</i> *)	Messfeld <i>measuring field</i>
TT-12505369 (incl. Kodak ND2)	4,5 mm	> 300 mm	ca. 180° (circular)

*) Messabstand = Abstand von der Objektivfront zum Messobjekt
 *) measuring distance = distance from the front of the lens to the measuring subject

Nennleuchtdichte
Calibrated luminance

Die Kalibrierung erfolgt mit den Leuchtdichten des Kalibriernormales entsprechend den in den folgenden Tabellen aufgeführten Beträgen. Für die Kalibrierung des Leuchtdichtemessers in Kombination mit dem Wechselobjektiv **TT-12505369 (incl. Kodak ND2)** wurden folgende Messergebnisse ermittelt und als Standardkalibrierung festgelegt:

The calibration with the luminance standard was made according to the luminance amounts that are listed in the following tables. For the calibration of the luminance meter in combination with the changeable lens TT-12505369 (incl. Kodak ND2) the results of measurement were determined as follows and assigned as standard calibration:

Messbereich <i>measuring range</i>			Nennleuchtdichte <i>nominal luminance</i>	Wert alt <i>value (old)</i>	Wert neu <i>value (new)</i>	Erweiterte Messunsicherheit *) <i>extended measurement uncertainty</i> *)
Brennweite <i>focal length</i>	Blende <i>aperture</i>	ISO				
4,5 mm	F4	100	L = 13888,5cd/m ²		L = 13888,5cd/m ²	652,8cd/m ²
4,5 mm	F4	100	L = 13888,5cd/m ²		L = 13888,5cd/m ²	652,8cd/m ²

*) Der Wert für den sich ergebenden Kalibrierfaktor wird häufig in der Form (100 ± 5,7)% ausgedrückt.
 *) For the value of the resulting calibration factor, often the expression (100 ± 5.7)% will be used.

Die Kalibrierung wurde mit den Leuchtdichten des Kalibriernormales für die Brennweiten 4,5mm bei den Blendenzahlen F4; F5,6; F8; F11 und für die ISO - Verstärkungsstufen 100; 200; 400; 800; 1600 durchgeführt. Die angegebenen erweiterten Messunsicherheiten setzen sich zusammen aus den Messunsicherheiten des Kalibrierverfahrens und denen des Leuchtdichtemessers während der Kalibrierung. Angegeben ist die erweiterte Messunsicherheit, die sich aus der Standard-Messunsicherheit durch Multiplikation mit dem Erweiterungsfaktor k = 2 ergibt. Sie wurde gemäss DKD-3 ermittelt. Der Wert der Messgrösse liegt mit einer Wahrscheinlichkeit von 95% im zugeordneten Wertintervall.

The calibration with the luminance standard was done for focal lengths of 4.5mm with the aperture values F4; F5.6; F8; F11 and ISO – settings of 100; 200; 400; 800; 1600. The indicated extended measurement uncertainties consist of the measurement uncertainties of the calibration procedure and those of the luminance meters during the calibration. It is indicated the extended measurement uncertainty, that results from the standard measurement uncertainty as a result of multiplication by the extension factor k = 2. It was determined in accordance with DKD-3. The index of the measuring value is in the assigned valuation interval with a probability of 95 %.

Beschreibung der spektralen Anpassung $s^*_{rel}(\lambda)$ an die $V(\lambda)$ - Funktion

Description of spectral match $s^*_{rel}(\lambda)$ on $V(\lambda)$

Kamera	LMK mobile air
Camera	SN: 163056007081
CCD Empfänger	CMOS Canon APS-C
CCD sensor	CMOS Canon APS-C
$V(\lambda)$ - Filter:	Numerische Matrizierung der RGB – Sensordaten
$V(\lambda)$ Filter	Numerical transformation of RGB – sensor data

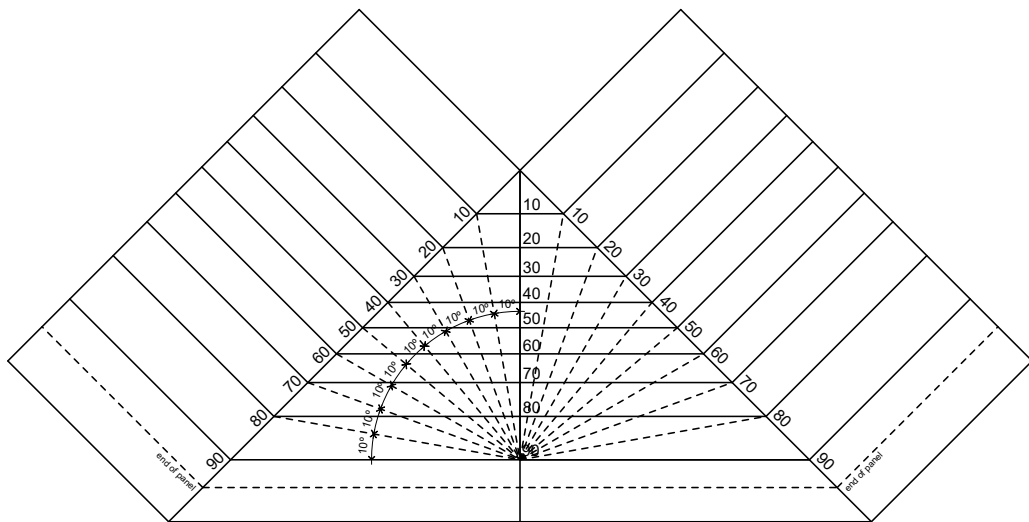
Messbereichsendwerte

Typical accuracy rating

Blende <i>aperture</i>	ISO - Wert <i>ISO - setting</i>	Messbereich <i>measuring range</i>	Leuchtdichte <i>luminance</i>	Messbereich <i>measuring range</i>	Leuchtdichte <i>luminance</i>
F4	100	1 msec.	1270327 cd/m ²	3 sec.	423 cd/m ²
	1600		79395 cd/m ²		27 cd/m ²
F11	100	1 msec.	9606848 cd/m ²	3 sec.	3202 cd/m ²

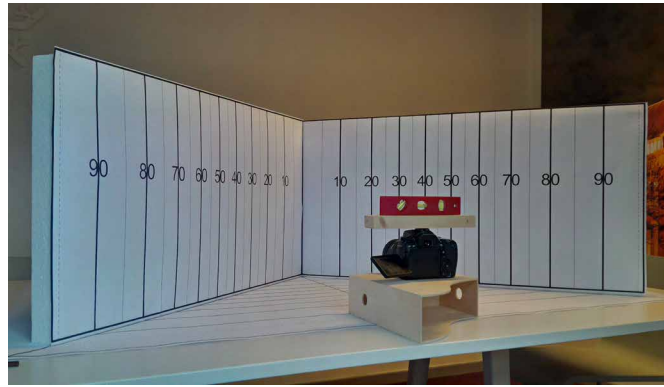
A.5 Sigma 4.5mm F2.8 fisheye projection and FOV estimation

The method used consists of projecting 10° interval marker lines onto a set-up of two vertical planes forming a right angle. This set-up is modelled in a CAD drawing as shown below. It contains a horizontal triangular base to facilitate the positioning of the camera in alignment with the centre of the model.



Planar view of the set-up:

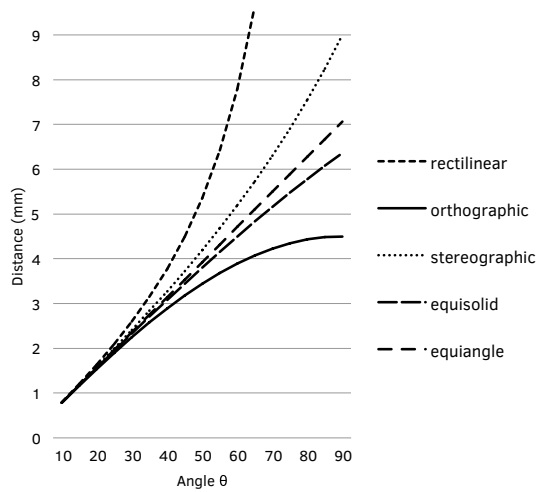
This drawing was printed and fixed onto two 1m-length polystyrene boards with enough thickness to support itself vertically and be mounted on a table. The camera was aligned with the 90° marker line and a photograph from that position was taken.



Physical set-up:

The second step consisted of finding the linear distances corresponding to the 10° interval curves for each projection method that one wants to test. The table below shows the linear distances 'r' from the centre of the image corresponding to angles θ 10° to 90° of a 4.5 mm lens and the figure below shows the distortion of each projection for that lens.

Linear distances 'r' (mm) for angle θ , for a 4,5 mm lens:					
Angle θ	Equi-solid angle	Equi-angle	Stereographic	Orthographic	Rectilinear
10	0,78	0,79	0,79	0,78	0,79
20	1,56	1,57	1,59	1,54	1,64
30	2,33	2,36	2,41	2,25	2,60
40	3,08	3,14	3,28	2,89	3,78
50	3,80	3,93	4,20	3,45	5,36
60	4,50	4,71	5,20	3,90	7,79
70	5,16	5,50	6,30	4,23	12,36
80	5,79	6,28	7,55	4,43	25,52
90	6,36	7,07	9,00	4,50	7,3E+16



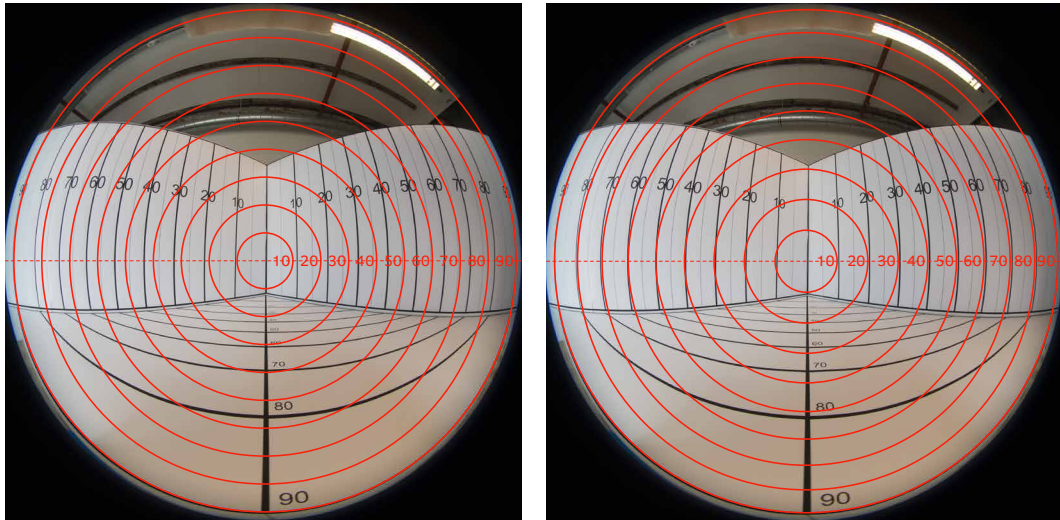
Distortion of the different fisheye projection methods, for a 4,5 mm lens:

The third step consisted of plotting in a CAD drawing the curves for the projections to test. In this case, only the equi-angle and equi-solid angle projections were considered.

The photographed image of the physical set-up is overlaid with these curves to find to which projection does it match, using common image processing software.

It can be seen that there is an almost exact match between the curves of the equi-solid angle projection and the corresponding markers of the physical set-up. The slight mismatch can be explained by a deviation between the centre of the image and the centre of the fisheye lens, an eccentricity that has also been found by Jacobs (Jacobs, 2012).

Based on this overlay, the linear distance between the centre and the periphery of the image is 6,5009 which corresponds to an angle of $92,494^\circ$ and a lens' total field-of-view of $184,988^\circ$.



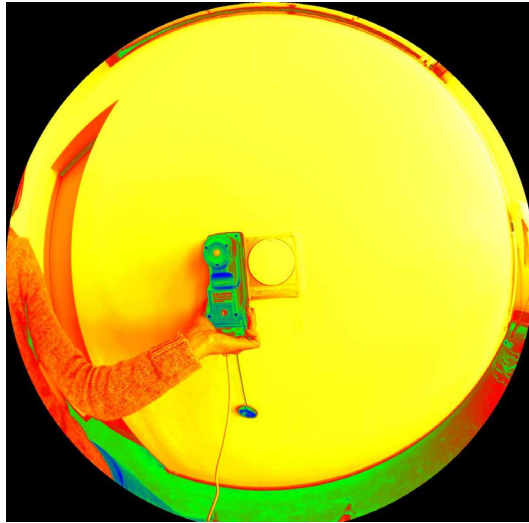
Overlay of the photograph of the set-up with the curves of an equi-angle (left) and of an equi-solid angle (right) projection:

A.6 Uncertainty due to the daylight light source

The calibration of the LMK is done against a luminance standard equipped with a tungsten halogen light source. Inaccuracies relating to differences of light spectrum and colour temperature of the particular light source that is used for calibration of the system and measurements carried out with different types of light source can be expected (Technoteam, 2016). A test was done to estimate what sort of uncertainty can be expected due to the daylight source. The test compares the luminance of the LMK luminance image with the luminance calculated from the illuminance measurement of a CL-500A spectrophotometer sitting next to a Hagner reflection reference disk of 95.2% reflectance ($\text{Luminance} = \text{reflectance} * \text{illuminance} / \text{Pi}$). The camera was placed directly in front of the reflection reference at a distance of about 50 cm. The test was carried out in a side-lit room of mostly white diffuse surfaces and redish-carpeted floor. The only light source in the room was daylight from the windows. It was a sunny day with clouds.

The LMK luminance capture was done using the system's original ABE range of +/- 3EV, with aperture F5.6, exposure time between 0.002" and 0.125" and ISO 100. The camera's white balance was set to default.

The average percentage difference between the LMK luminance and the calculated luminance from the spectrophotometer is 7.6%. Based on this test, an uncertainty of 7.6% of the luminance captured by the LMK can be attributed to the spectral characteristics of the daylight light source.



LMK luminance measurement:

Time of measurement	LMK luminance measurement (cd/m ²)	Spectrometer measurement (Lux)	Calculated luminance (cd/m ²)	% Difference
13:01:10	381.9	1305.3	395.5	3.5
13:01:18	386.4	1398.1	423.7	9.2
13:01:28	385.7	1397.2	423.4	9.3
13:01:36	380.7	1362.2	412.8	8.1
13:01:44	373	1335.1	405	8.1
			Average %	7.6

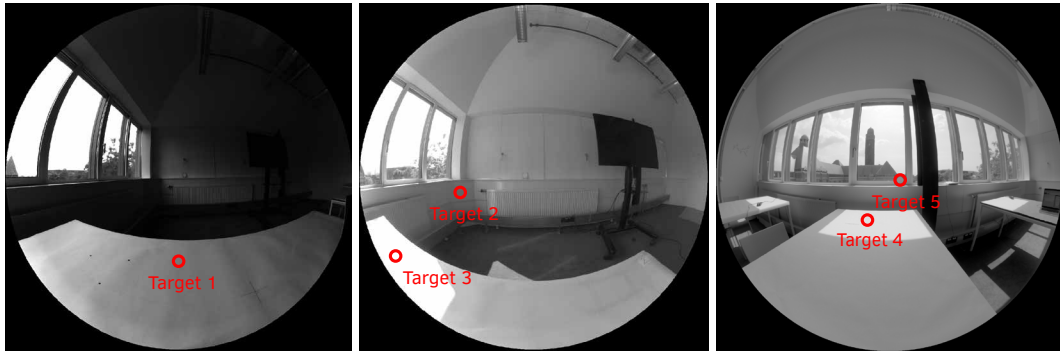
A.7 Testing the LMK against an external luminance measurement

The test was done to check the calibration of the LMK after ND2.0 film filter calibration and before conducting the experiment of Study II, after the large differences found between the measured and luminance-image derived vertical eye illuminance. The test consisted of collecting simultaneous measurements of luminance with the LMK and a Konica Minolta LS-150 luminance meter (point measurement) of a range of targets in the experiment room.

The LMK capture consisted of taking 7 low dynamic range images (CR2 picture files) in the speed range of 0.001' to 15' and aperture F5.6. Due to the use of the neutral density filter, an exposure as long as 15' was found to be required in order to have a properly overexposed picture for the creation of the high dynamic range luminance image. The camera was remotely operated using qDslrDashboard v3.5.3 (DslrDashboard, 2017) and using a locally created Wi-Fi network.

The targets are selected areas of the surfaces within the room and the conditions in which their luminance was captured was:

- Target 1 is centrally located on the desk and was photographed for a condition of low luminance (overcast sky)
- Target 2 is located in a zone of low illuminance, but in a condition of overall high luminance (sunny sky)
- Target 3 is located on a bright spot on the desk, in a condition of overall high luminance (sunny sky), but in a peripheral position within the field-of-view; this target is also located in an area of the image where the highest error is to be expected due to the lens' vignetting effect
- Target 4 is centrally located on a bright spot on the desk, in a condition of extreme high brightness (camera pointing to the outside in a sunny day)
- Target 5 is located in the window area, in a condition of extreme high brightness and in the most reflective surface within the room, the window mullions (camera pointing to the outside in a sunny day)



Location of the measuring targets in the three captured scenes.

There were three luminance measurements taken per target and the error of each measurement is presented in the next table.

	LMK	KM	% Difference
Target 1	276	290	-5
	288	301	-4
	297	304	-2
Target 2	801	816	-2
	820	810	1
	800	810	-1
Target 3	11222	11790	-5
	11513	11750	-2
	11136	11610	-4
Target 4	13445	13700	-2
	13078	13550	-4
	12892	13500	-5
Target 5	1818	1800	1
	1792	1860	-4
	1802	1880	-4

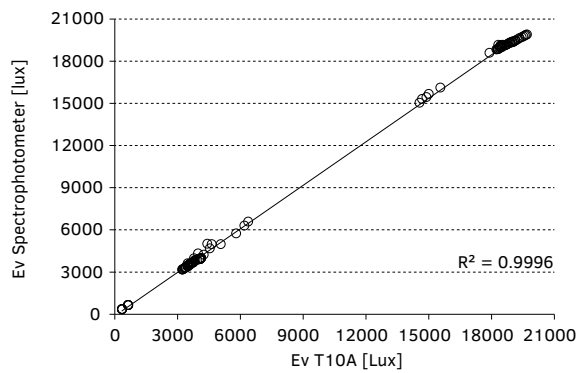
Luminance (L) of targets measured with LMK and with a Konica Minolta luminance meter (KN).

The test showed that for the conditions of this capture, the error of the LMK luminance system for daylight measurements is within the range of its calibration (-5%).

The settings of this luminance capture (Aperture, shutter speed and dynamic range) were the settings used for the luminance capture in Study II.

A.8 Testing T10M Konica Minolta measurement

Comparison of the illuminance measured with the T10M illuminance meter to the illuminance measured with a calibrated CL-500A spectrophotometer for 118 measurements ($N = 118$). Measurements were collected for a low and a high illuminance condition (overcast and sunny sky). Maximum percentage difference is 13% and average percentage difference is 2%.


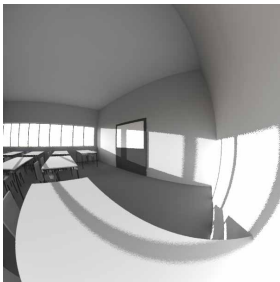
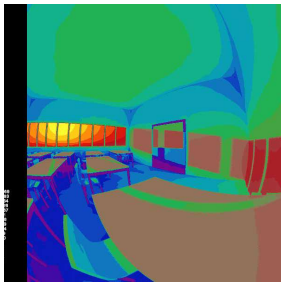
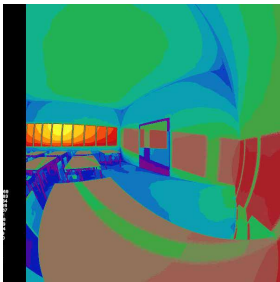




Illuminance measured with spectrophotometer versus illuminance measured with the used illuminance meter.

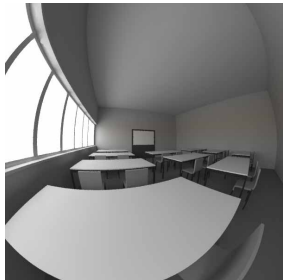
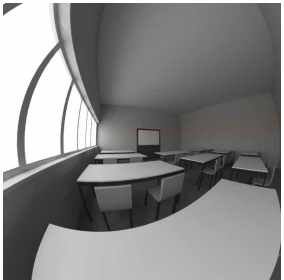
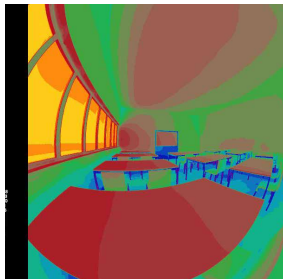
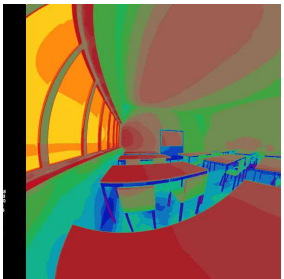
A.9 Simulation results from estimation of error due to camera offset



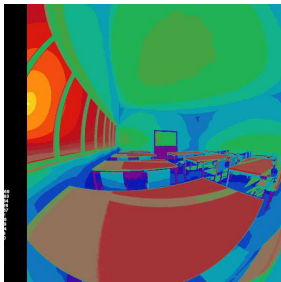
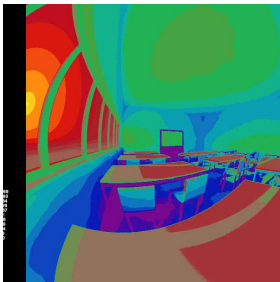


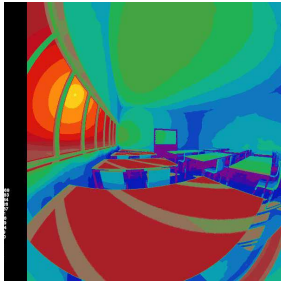
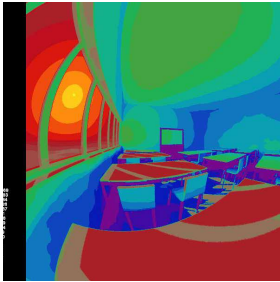
Image results from simulations comparing the field-of-view luminance in the subject's sitting position and of a camera positioned at 75 cm from the subject.

Position 3			
Day, Time, Sky		Subject-view	Camera-view
13/08/2017, 10:45 Perez sky (dir=893; diff=256) In this condition the sun is not visible through the window view or inside the room.	Luminance:		
	Luminance in false colour:		

Position 3			
Day, Time, Sky		Subject-view	Camera-view
21 Dec 15:00 Perez sky In this condition the sun is visible through the window view and inside the room.	Luminance:		
	Luminance in false colour:		
	Images with reduced exposure to see the sun position in the view:		

Position 1

Day, Time, Sky		Subject-view	Camera-view
<p>13/08/2017, 10:45</p> <p>Perez sky (dir=893; diff=256)</p> <p>In this condition the sun is not visible through the window view or inside the room.</p>	Luminance:		
	Luminance in false colour:		

Position 1			
Day, Time, Sky		Subject-view	Camera-view
21 Mar 17:00 Perez sky (dir=893; diff=256) In this condition the sun is visible through the window view and inside the room.	Luminance:		
	Luminance in false colour:		
21 Jun 18:00 Perez sky (dir=893; diff=256) In this condition the sun is visible through the window view and inside the room.	Luminance:		
	Luminance in false colour:		

A.10 Recruiting flyers / posters

Dear Colleague

Would you like to receive 6€ for 30 minutes of your time?

I'm looking for participants in an experiment for my PhD research, to take place at the Faculty of Architecture (TU Delft) during the period of the 22nd to the 31st of August.

What does the experiment consist of?

You will be asked to perform a visual task and to answer a questionnaire about the lighting conditions in the room.

If you would like to participate, please email Raquel Viula at r.j.a.v.viula@tudelft.nl

Thank you!

Dear Student

Would you like to receive 7 € for
1 hour of your time?

I'm looking for participants in an experiment for my PhD research, to take place in Room V at the Faculty of Architecture during the period **26 to 29 of August**.

What does the experiment consist of?

You will be asked to perform a simple task and to answer a questionnaire about the way you experience the lighting conditions in the room.

If you would like to participate, please email Raquel Viula at r.j.a.v.viula@tudelft.nl

Thank you!

I will need two and half hours of your time in separate days, making this possibly a nice little earner for you!

A.11 Eye-recording authorization

Delft, August 2019

I, _____ hereby confirm that I authorise that a movie recording of my face and eyes is collected during the experiment that will take place at the Faculty of Architecture (TU Delft) during the period 19th to 30th of August 2019, in the context of Raquel Viula's PhD research.

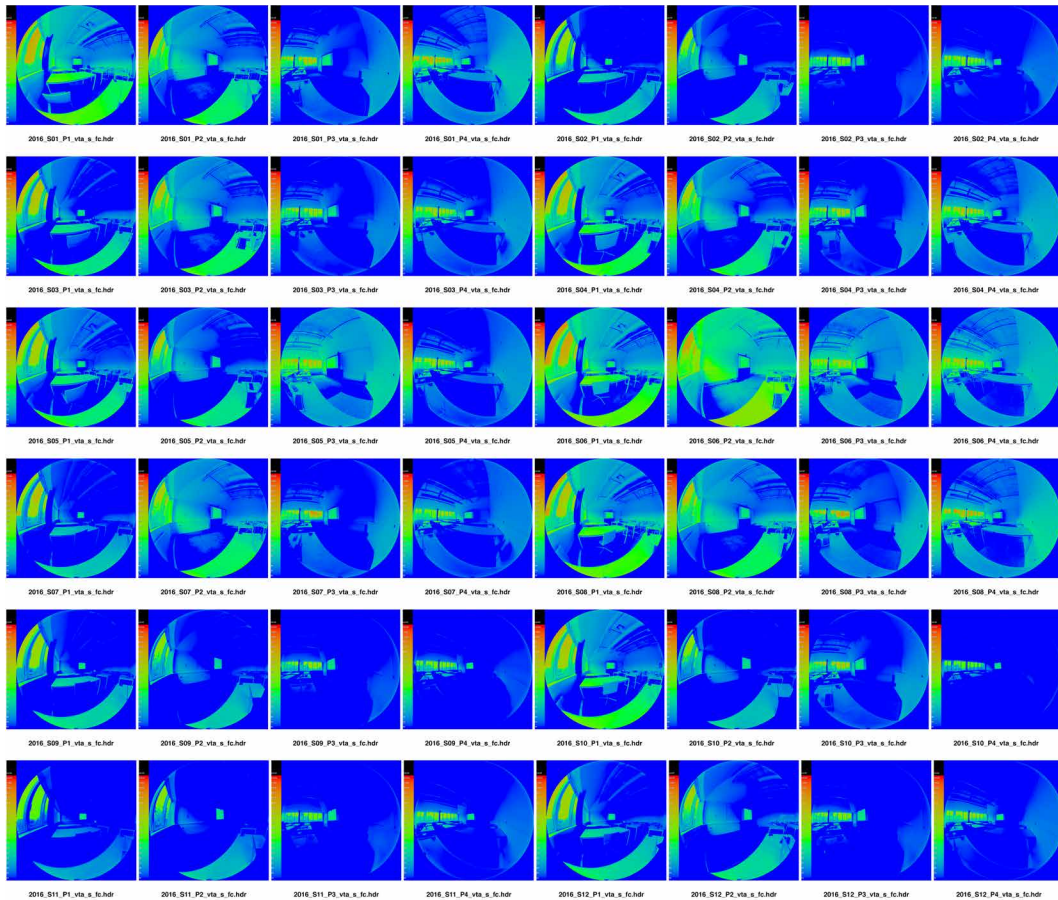
The data obtained will be used by the aforementioned PhD candidate for research purposes only and will remain totally confidential.

Date: _____

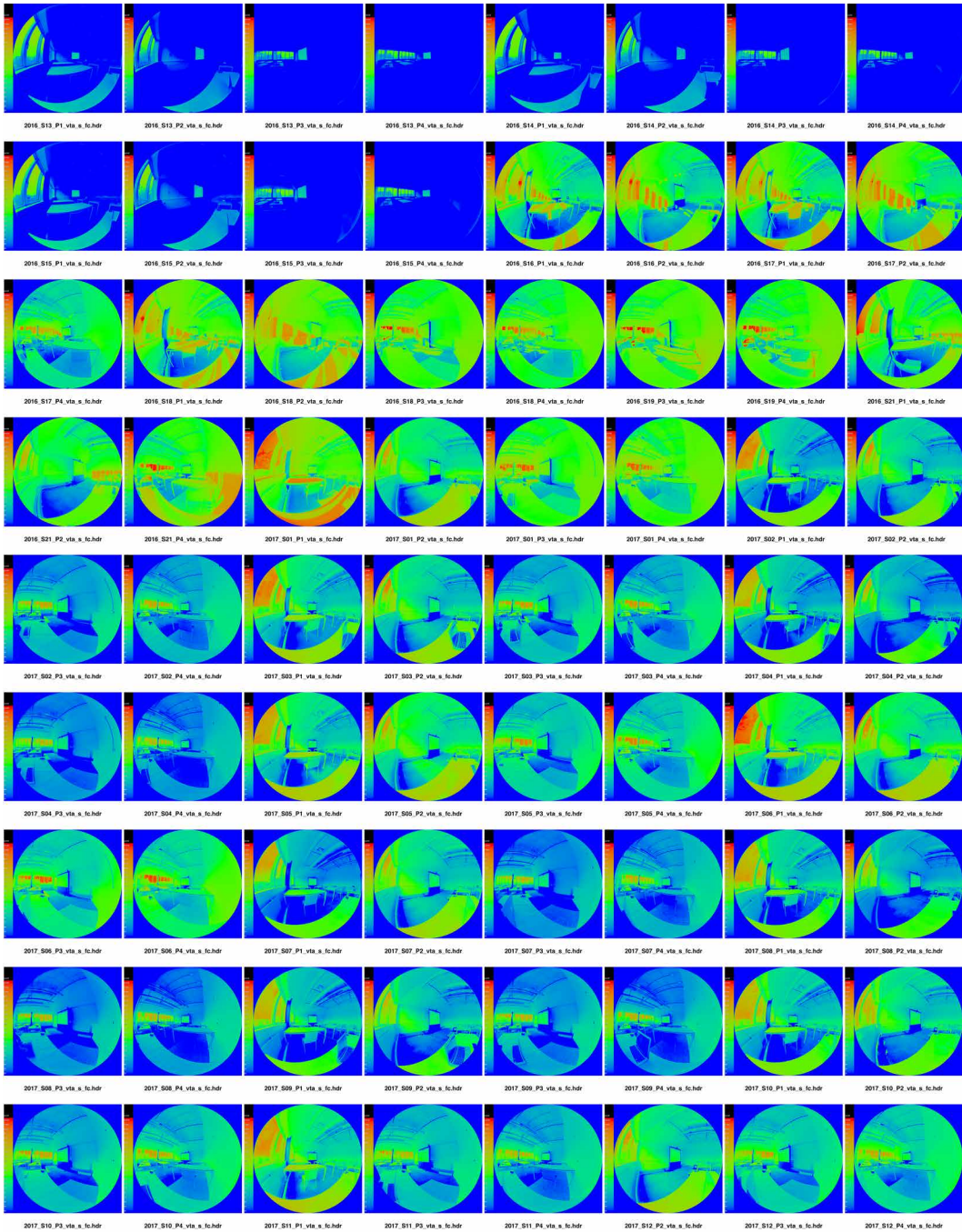
(Signature)

Experimental study I

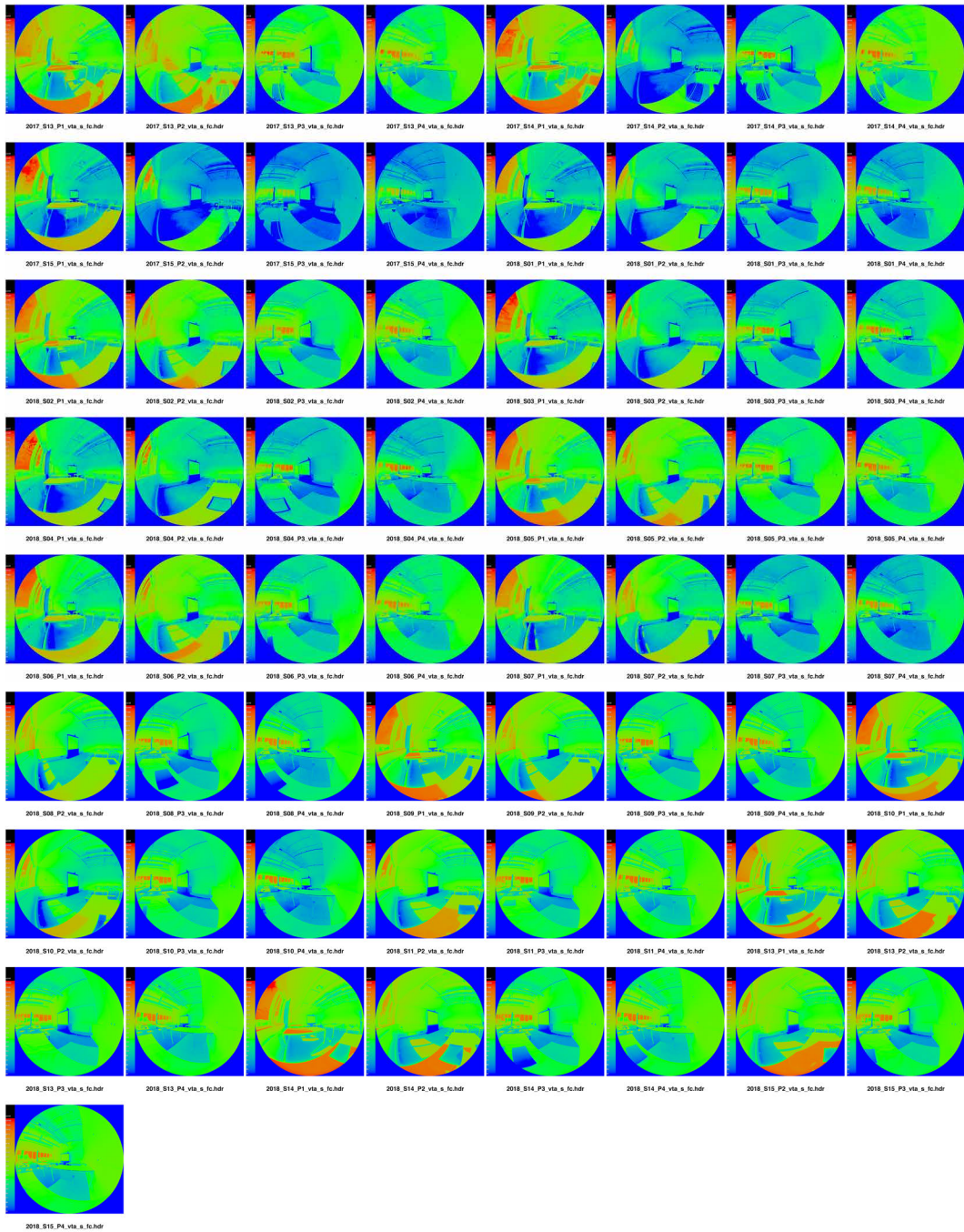
B.1 Luminance measurements



Luminance measurements in false colour. Images are ordered by position. Scale: 0 to 25,000 cd/m².

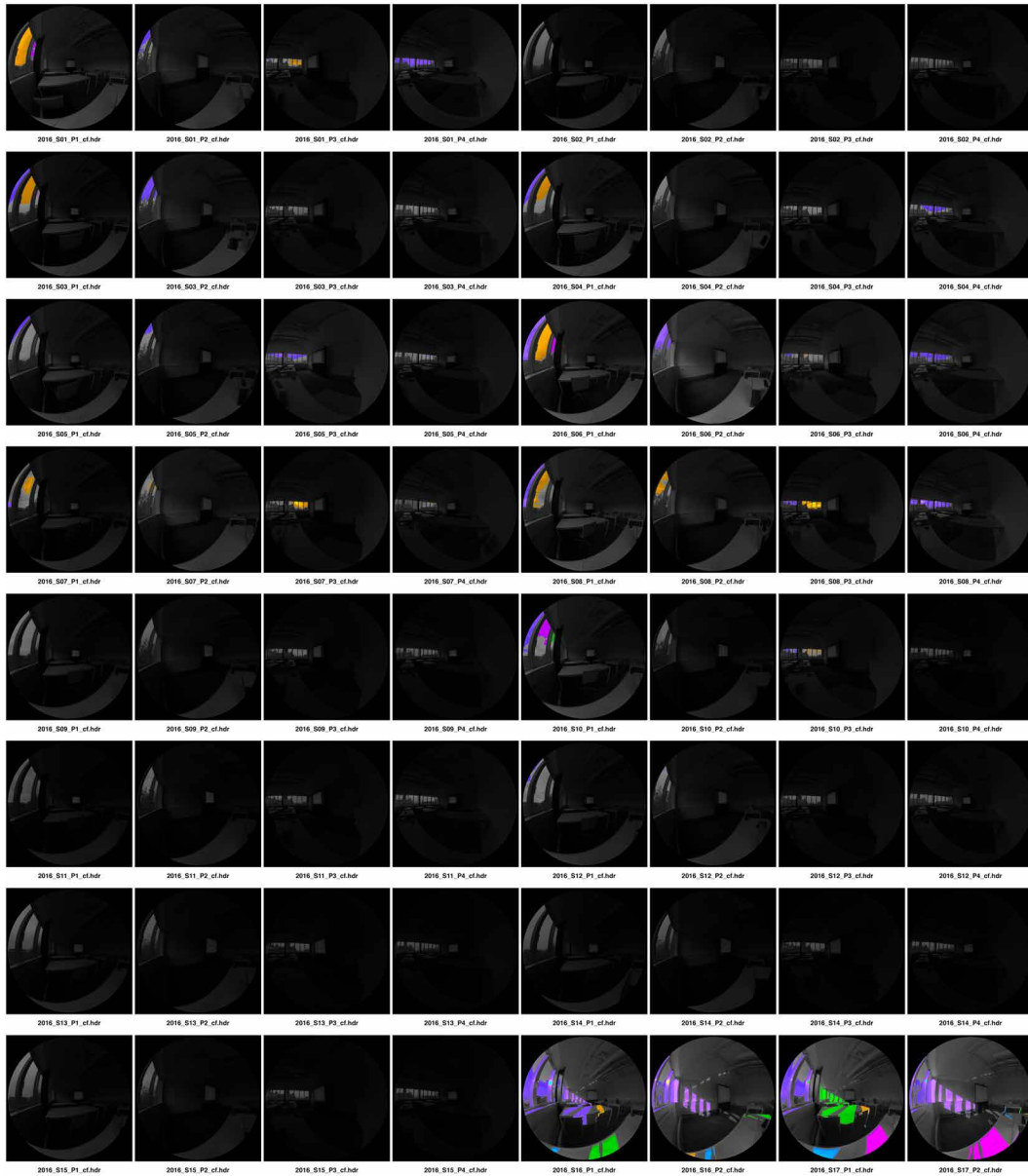


Luminance measurements in false colour. Images are ordered by position. Scale: 0 to 25,000 cd/m².

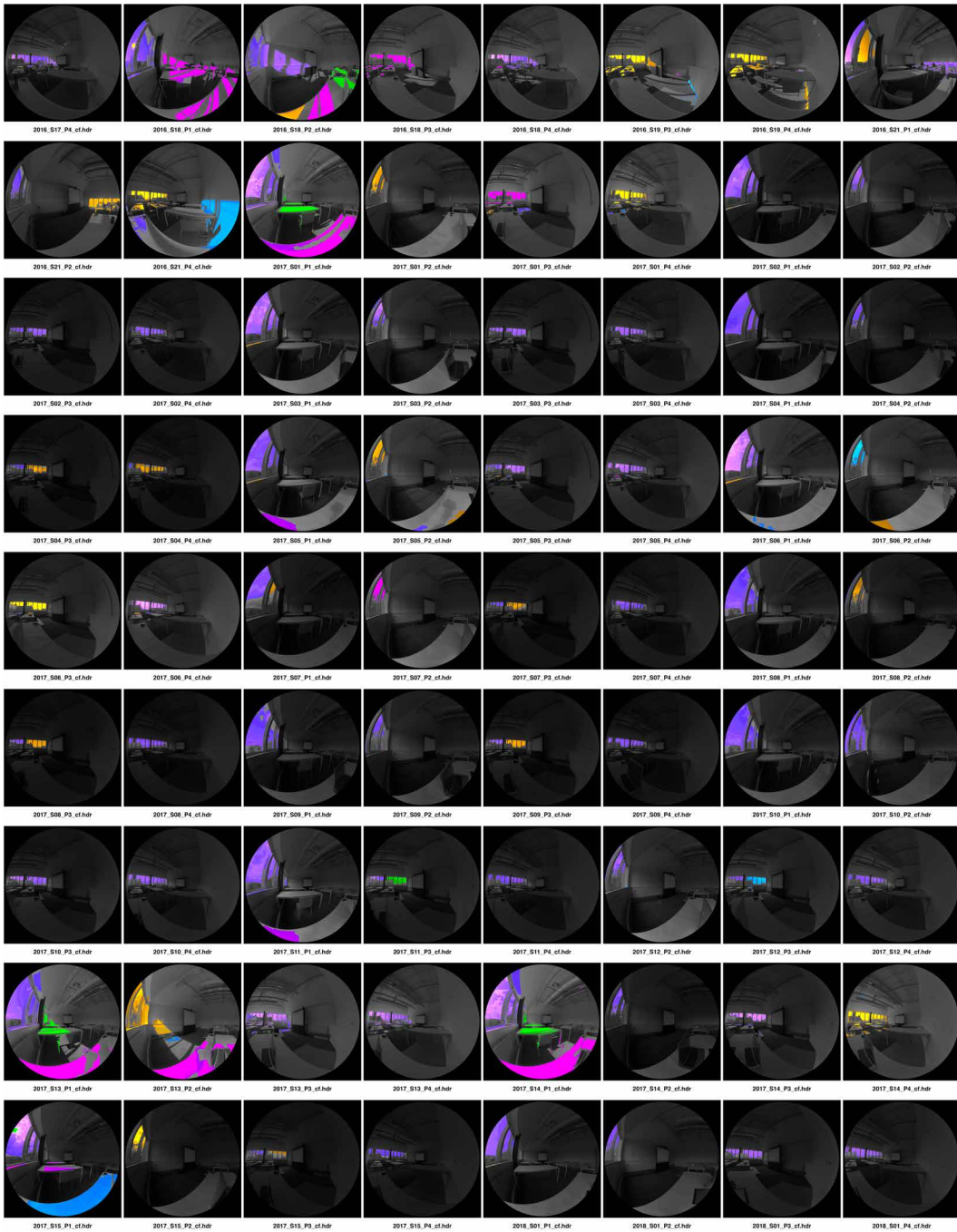


Luminance measurements in false colour. Images are ordered by position. Scale: 0 to 25,000 cd/m².

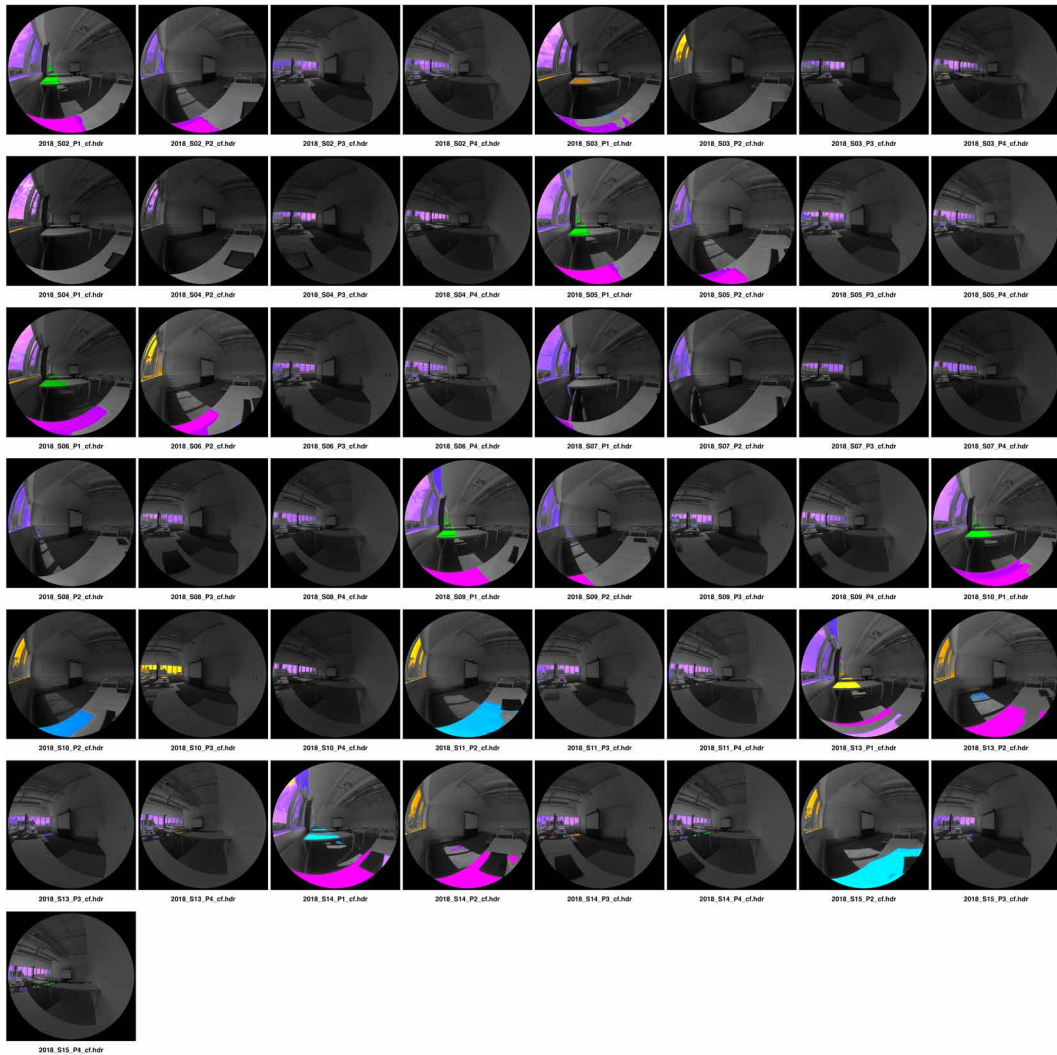
B.2 Evalglare calculation files



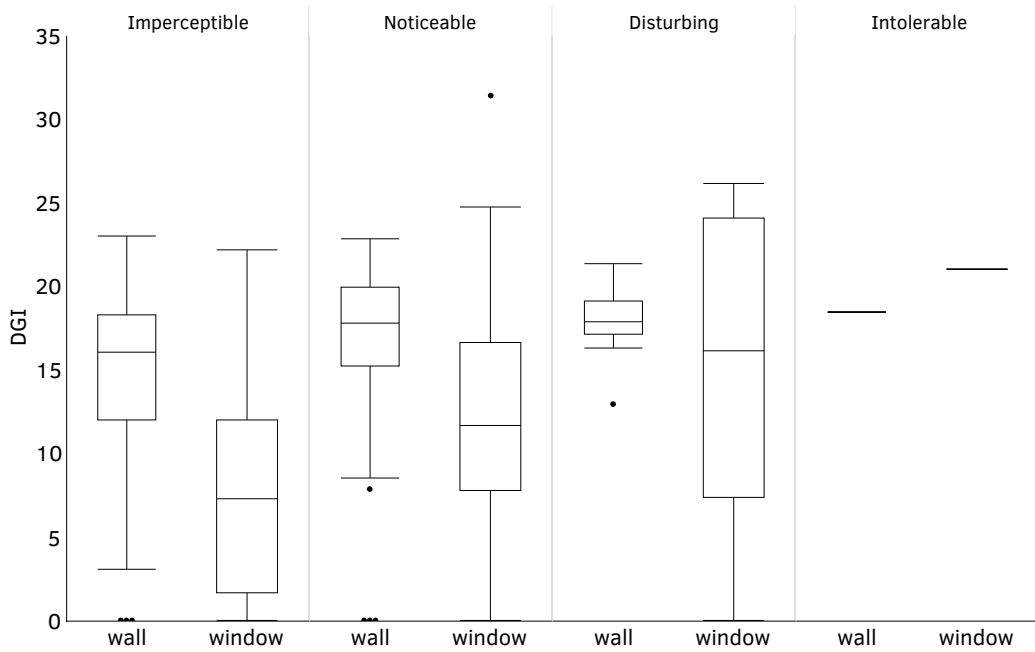
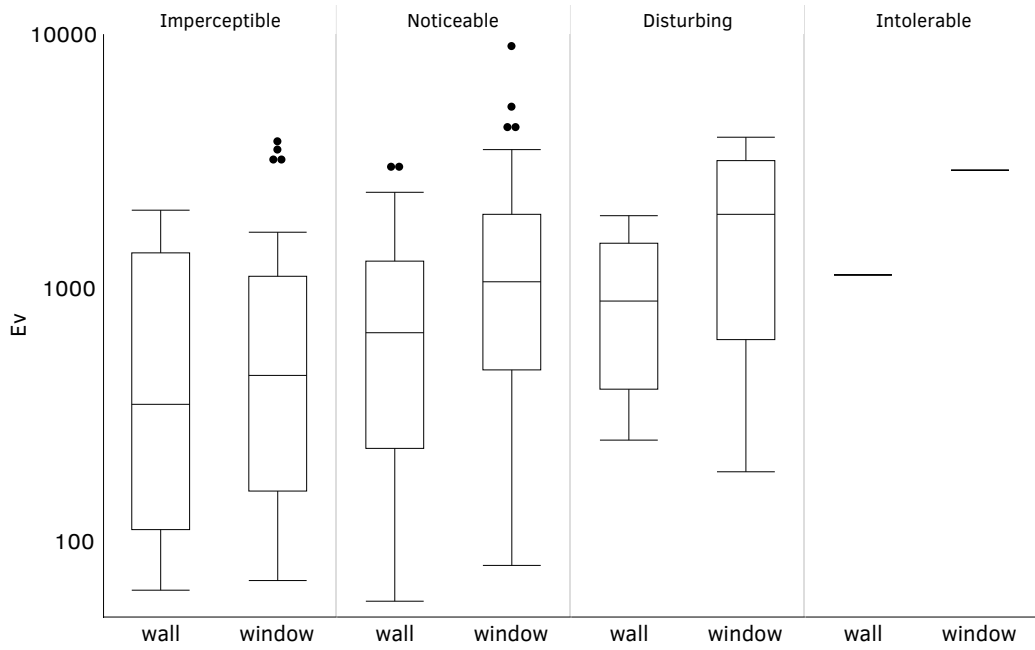
Evalglare check file images. Images have reduced exposure for visualisation of the glare sources (coloured regions).

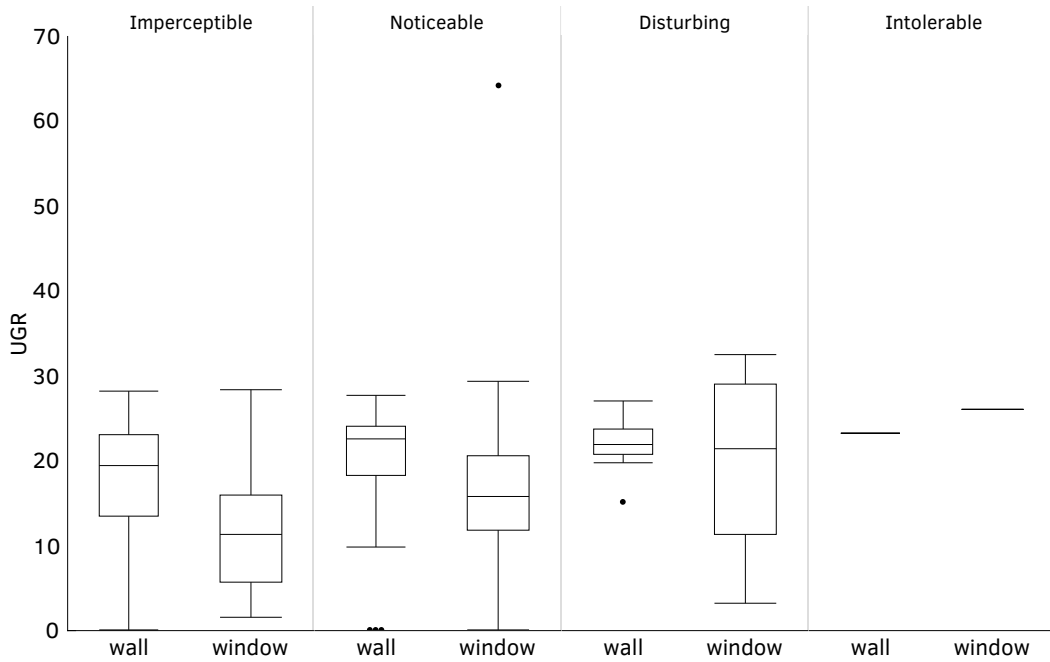
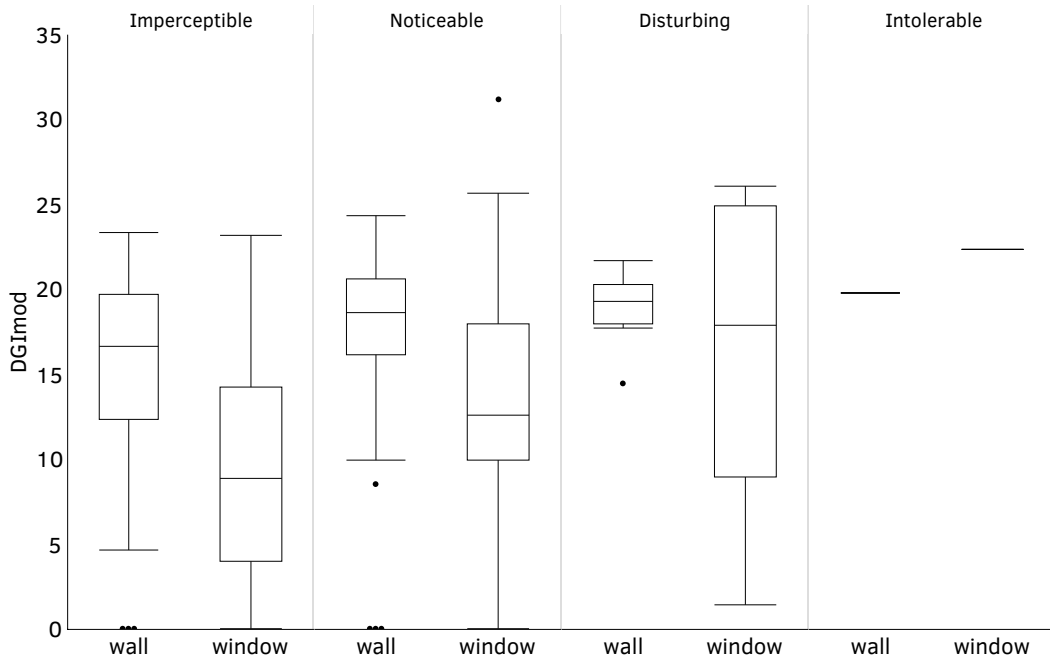


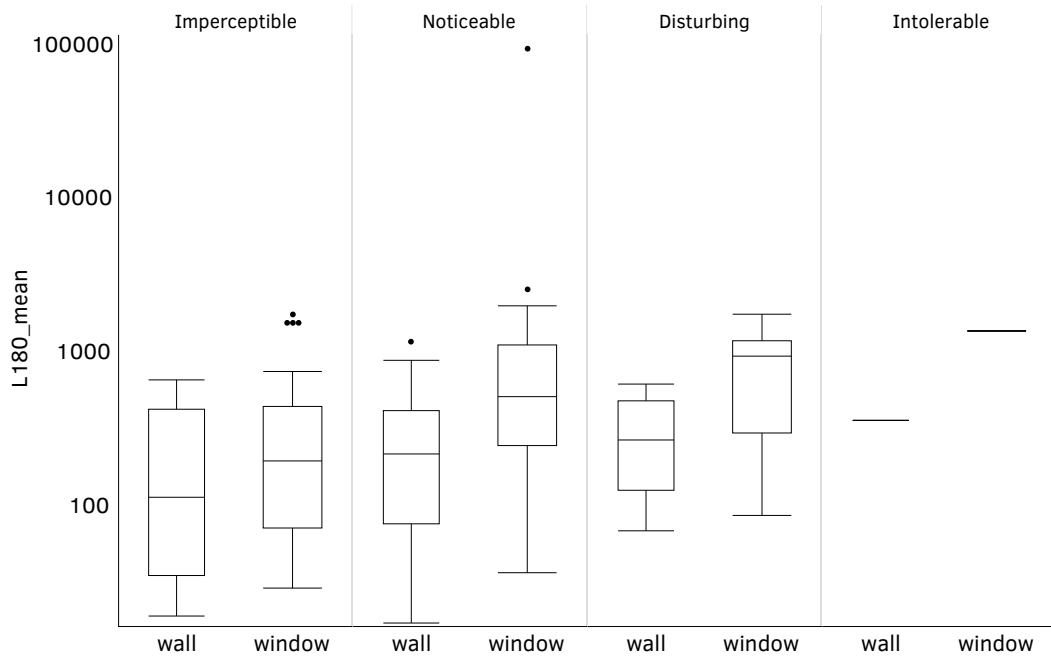
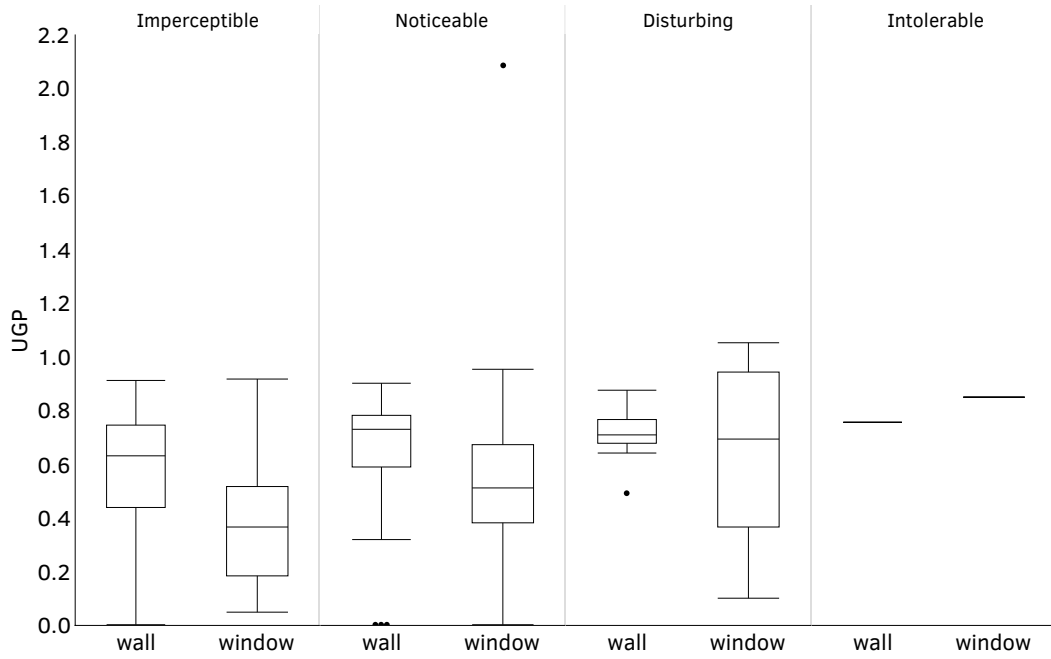
Evalglare check file images. Images have reduced exposure for visualisation of the glare sources (coloured regions).

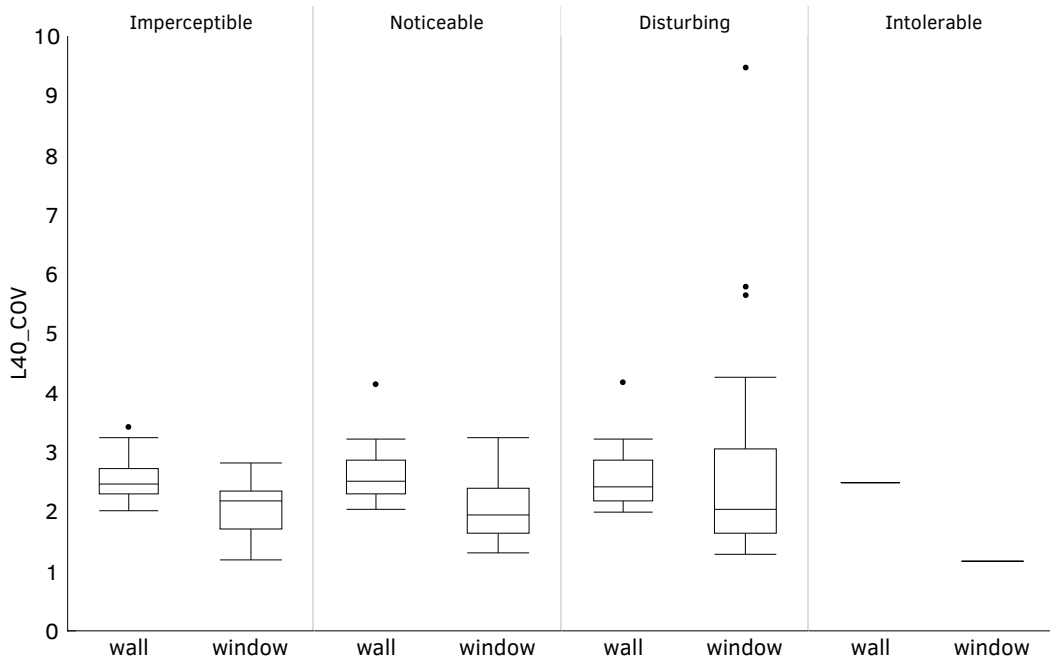
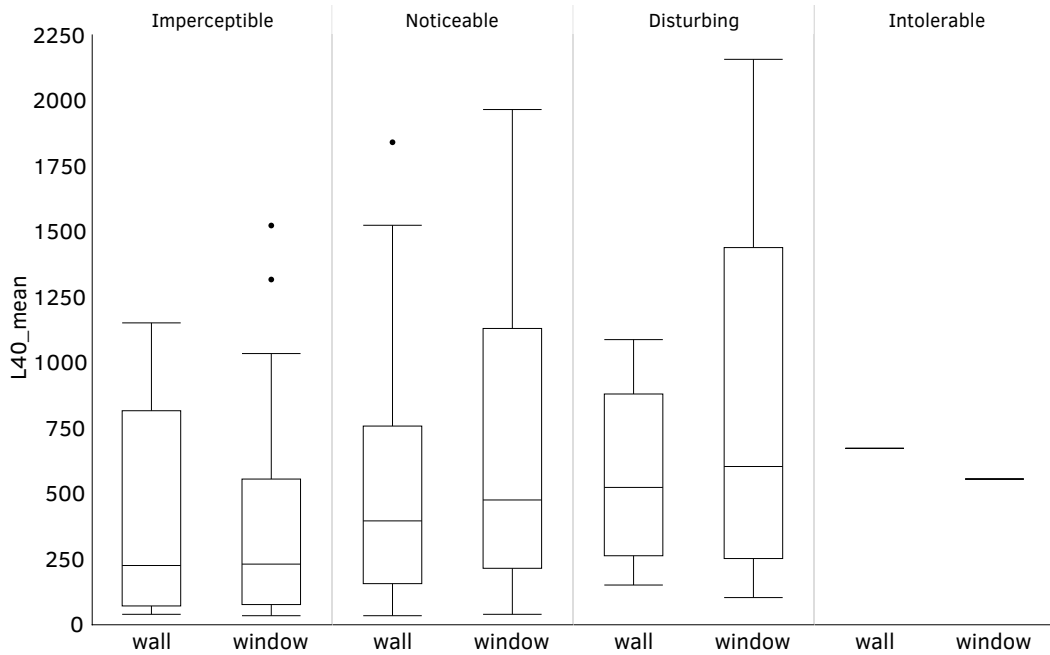


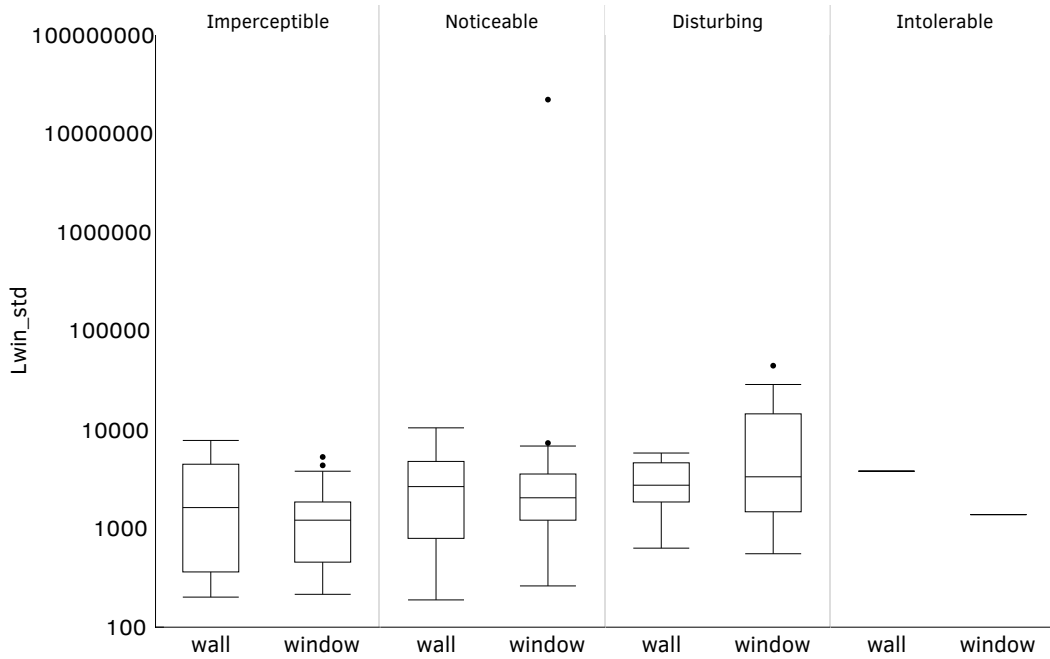
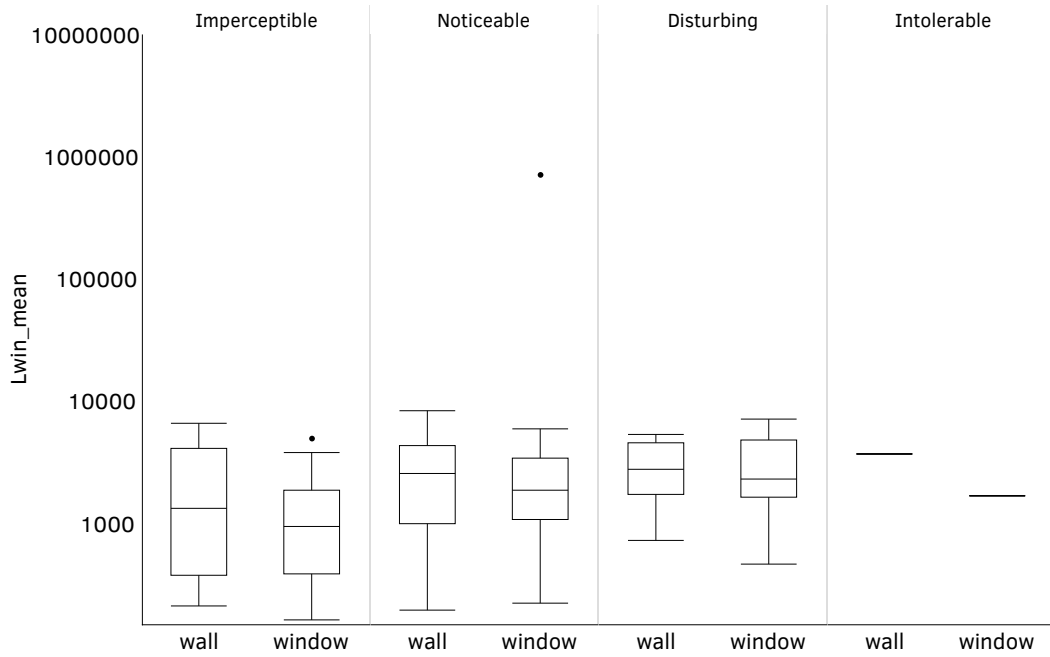
Evalglare check file images. Images have reduced exposure for visualisation of the glare sources (coloured regions).

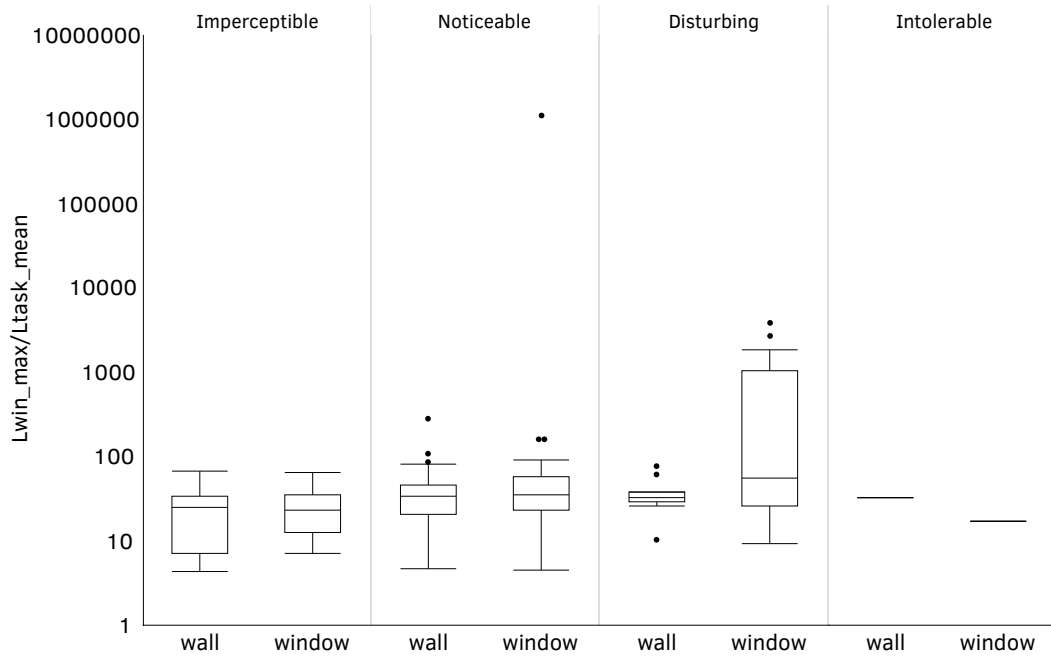
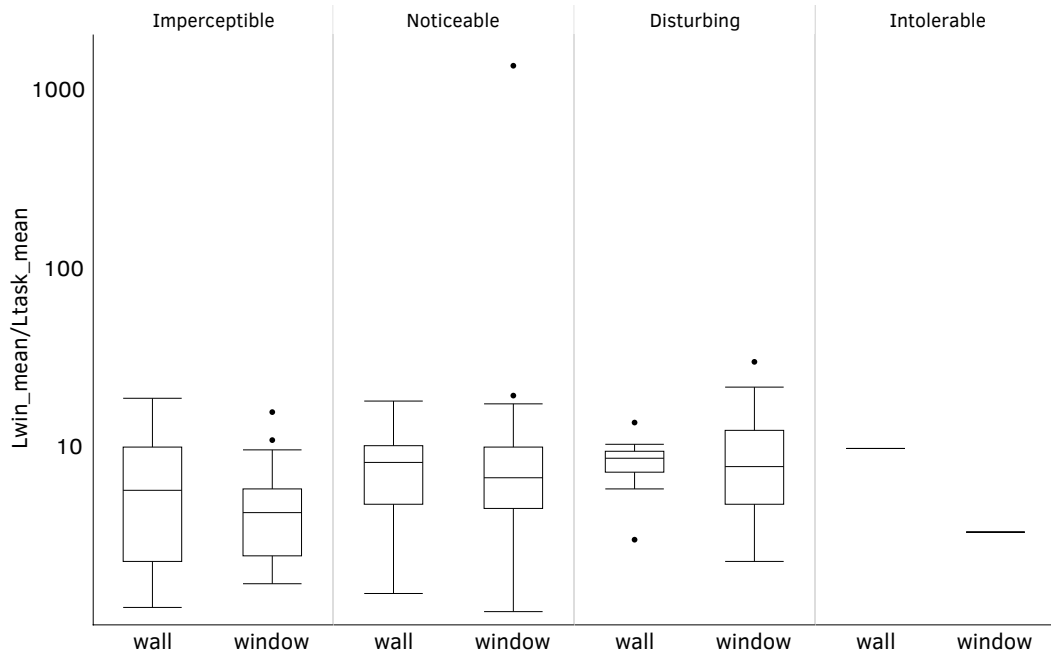








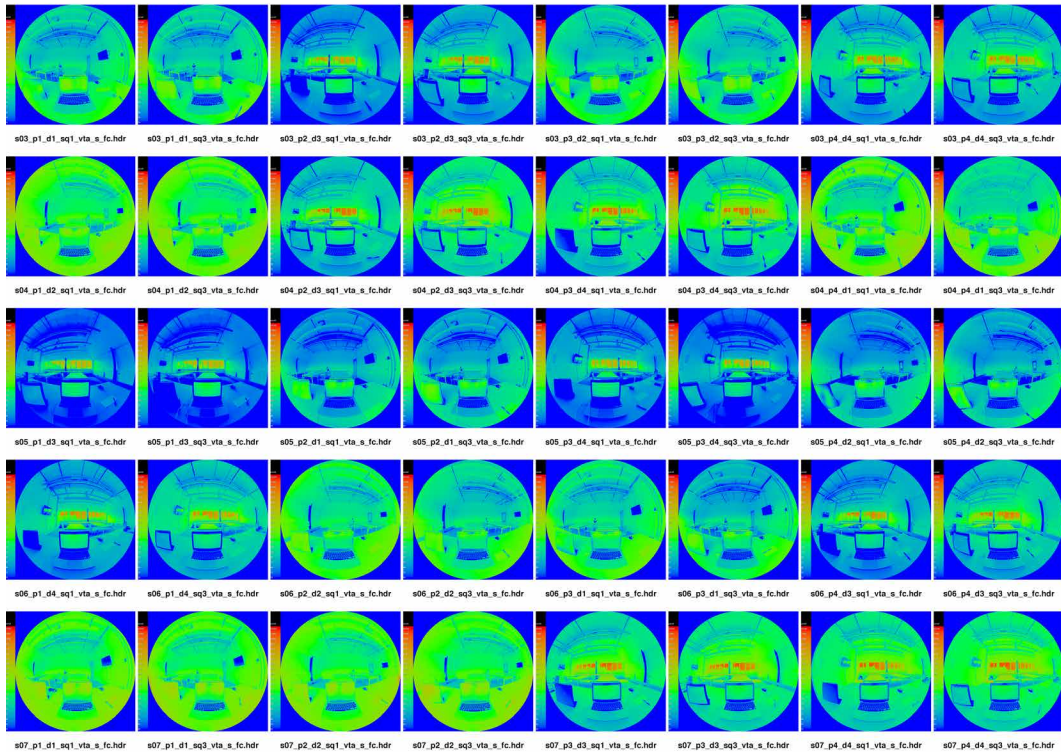




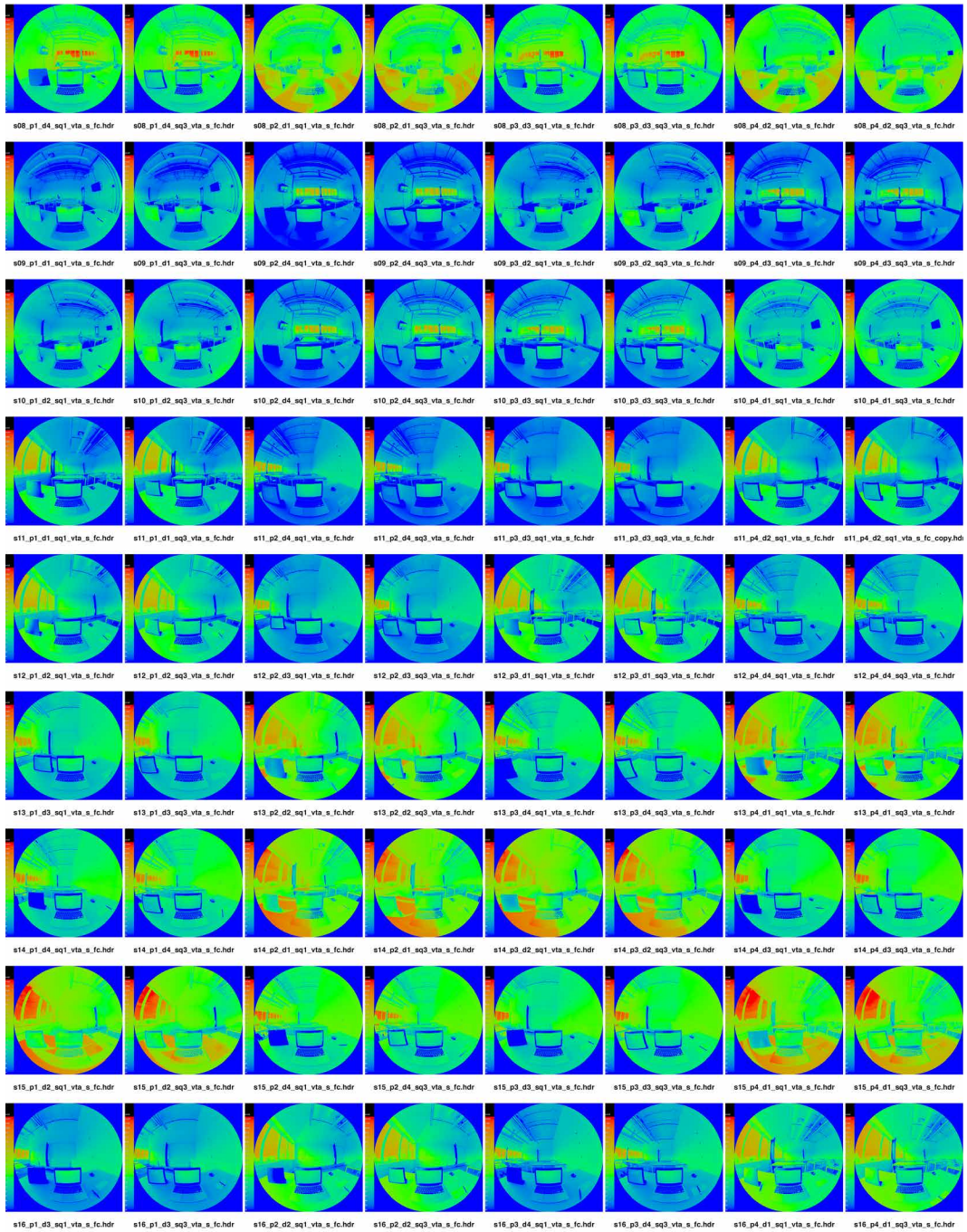
Experimental study II

C.1 Luminance measurements

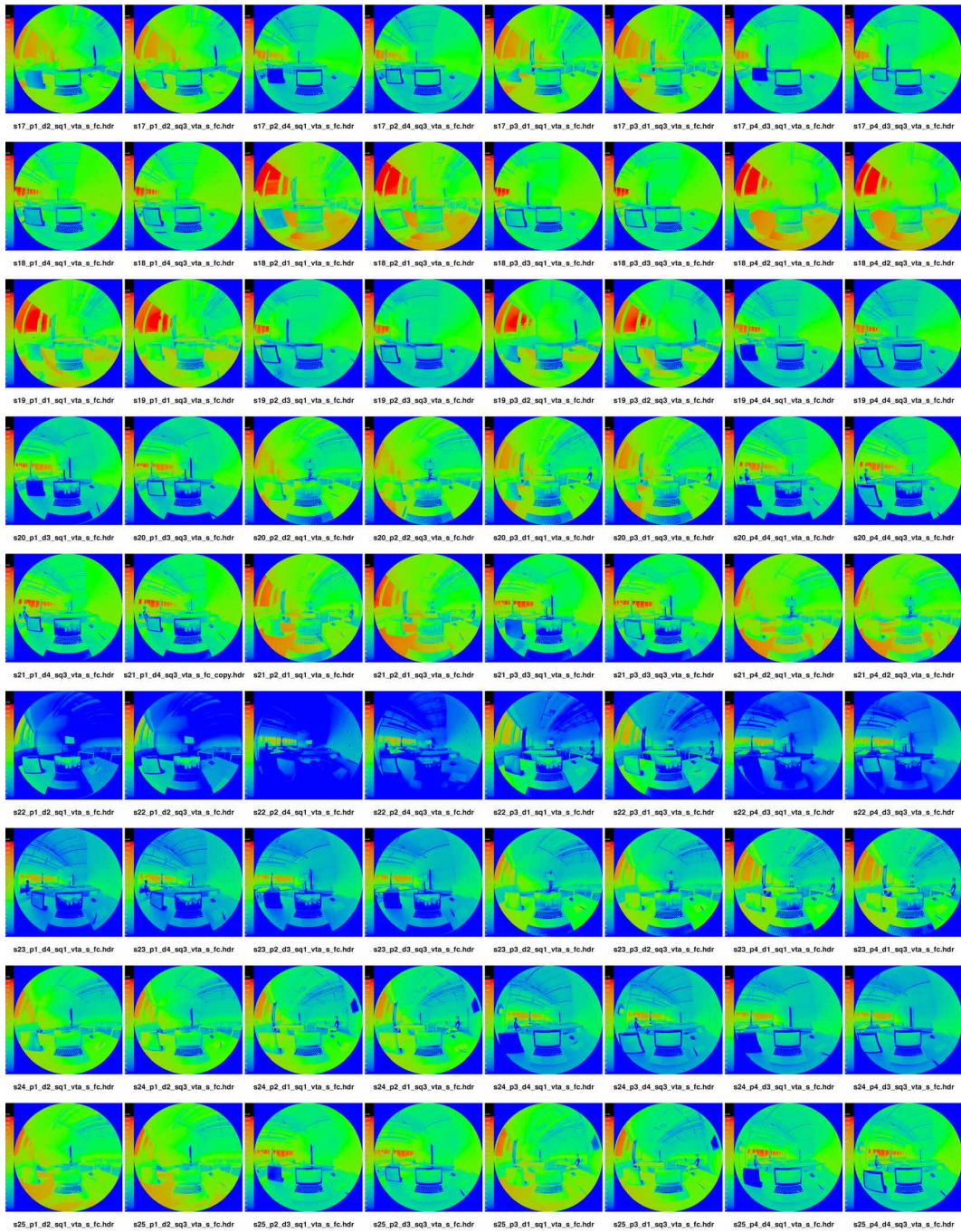
Luminance images in false colour, for the 'before' and 'end' measurement in each of the 4 positions. The order of the images corresponds to the order of sitting by the subjects. Scale: 0 - 25,000 cd/m².



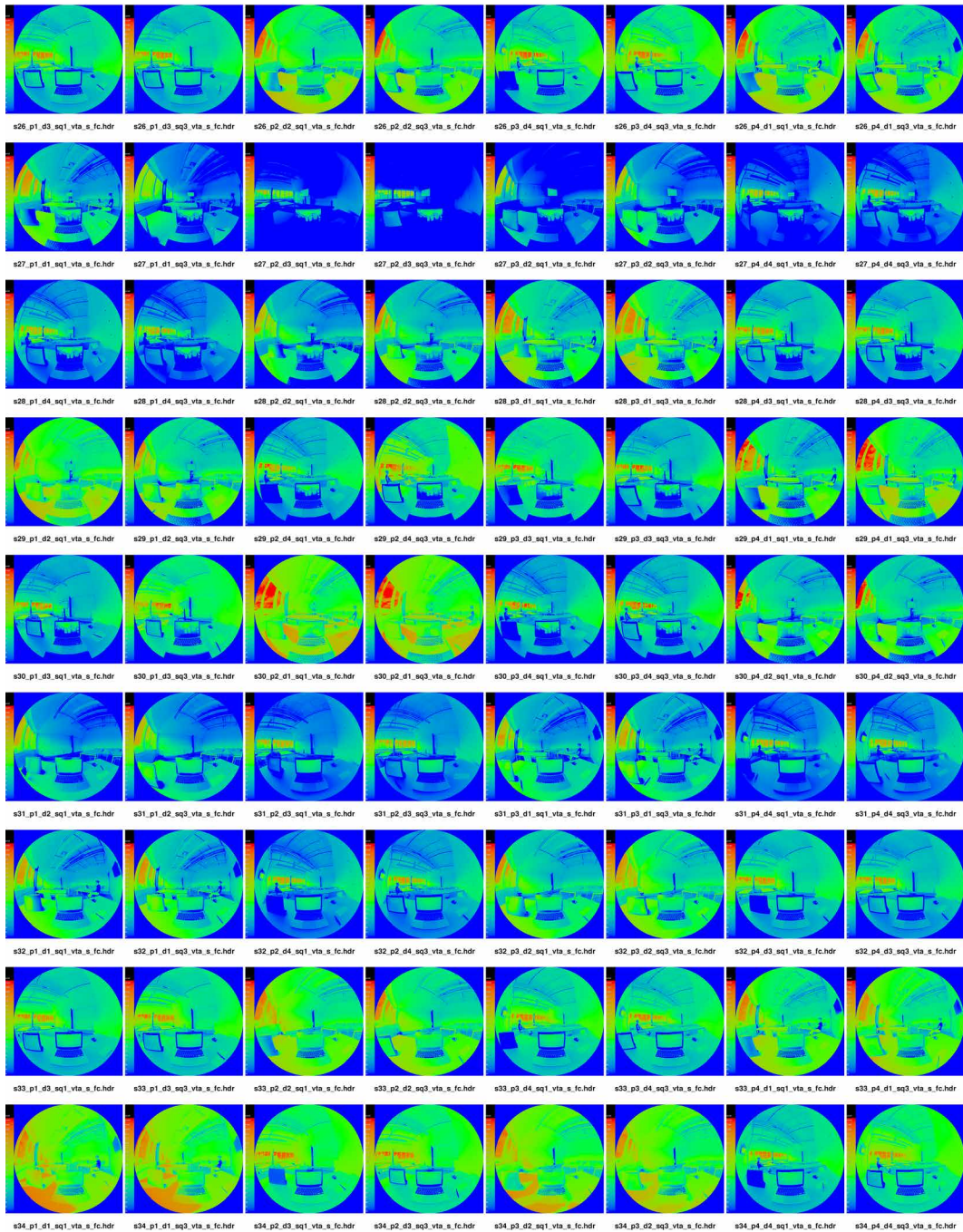
Luminance measurements in false colour. Images are ordered by position. Scale: 0 to 25,000 cd/m².



Luminance measurements in false colour. Images are ordered by position. Scale: 0 to 25,000 cd/m².



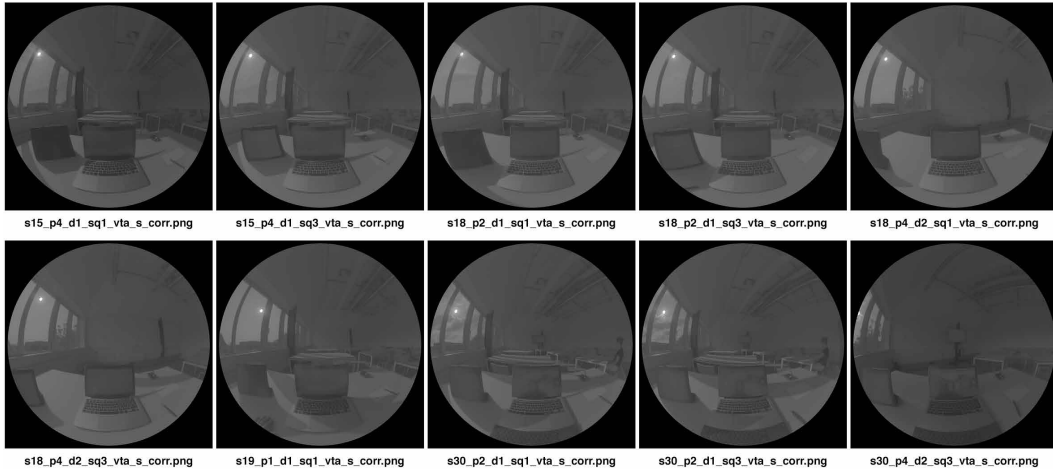
Luminance measurements in false colour. Images are ordered by position. Scale: 0 to 25,000 cd/m².



Luminance measurements in false colour. Images are ordered by position. Scale: 0 to 25,000 cd/m².

c.2 Pixel overflow correction

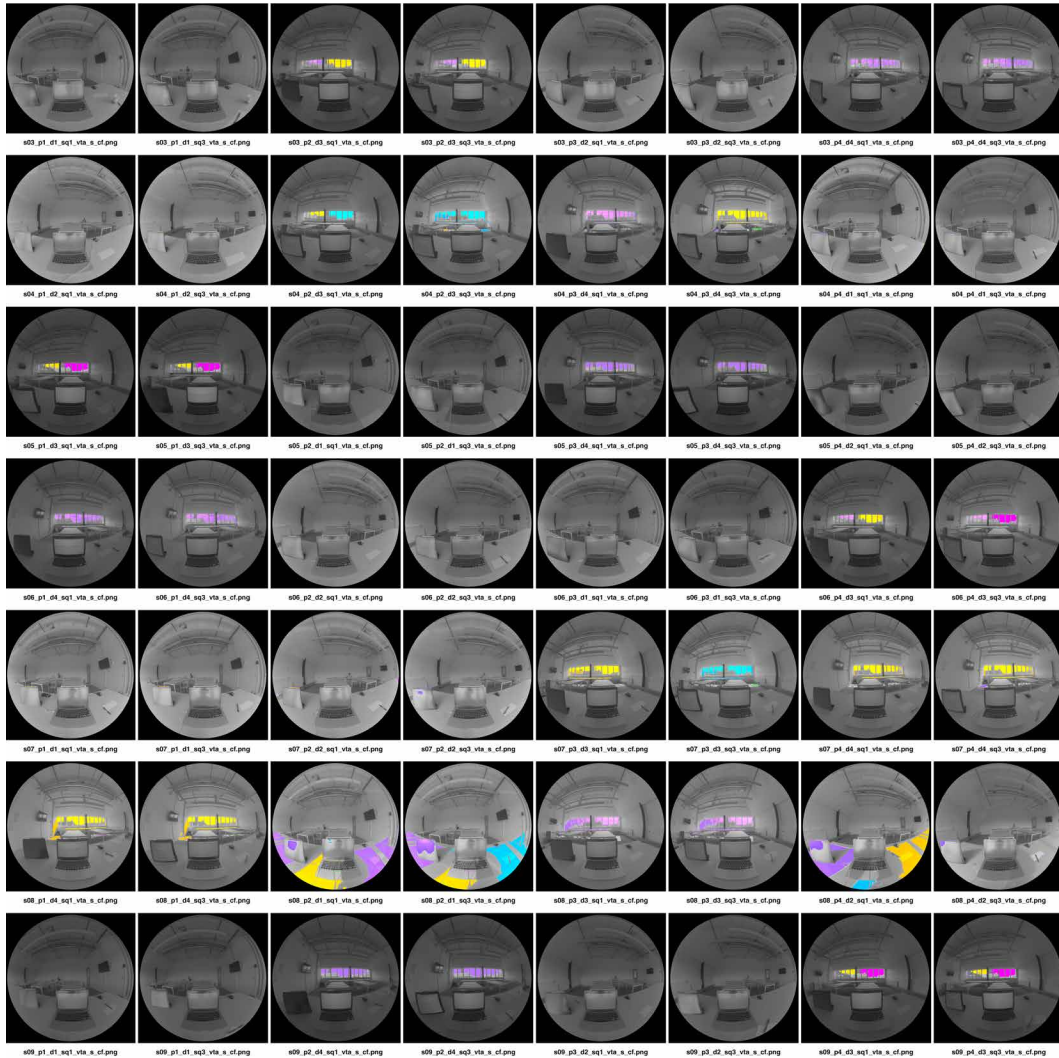
Images that were corrected for pixel saturation. The correction corresponds to the area of sun only. Images have reduced exposure for a better visualisation of the sun disk.



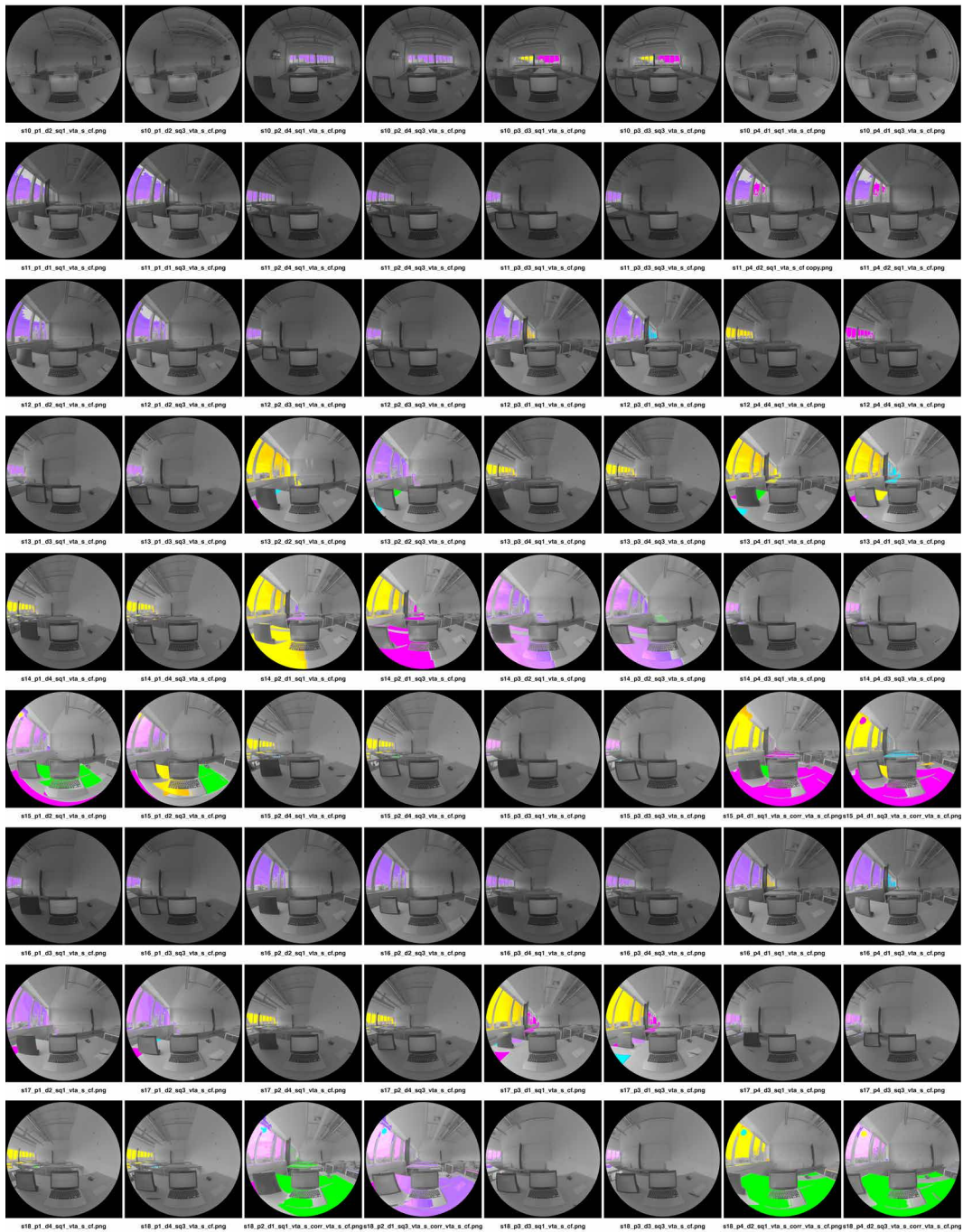
Corrected images.

c.3 Evalglare calculation files

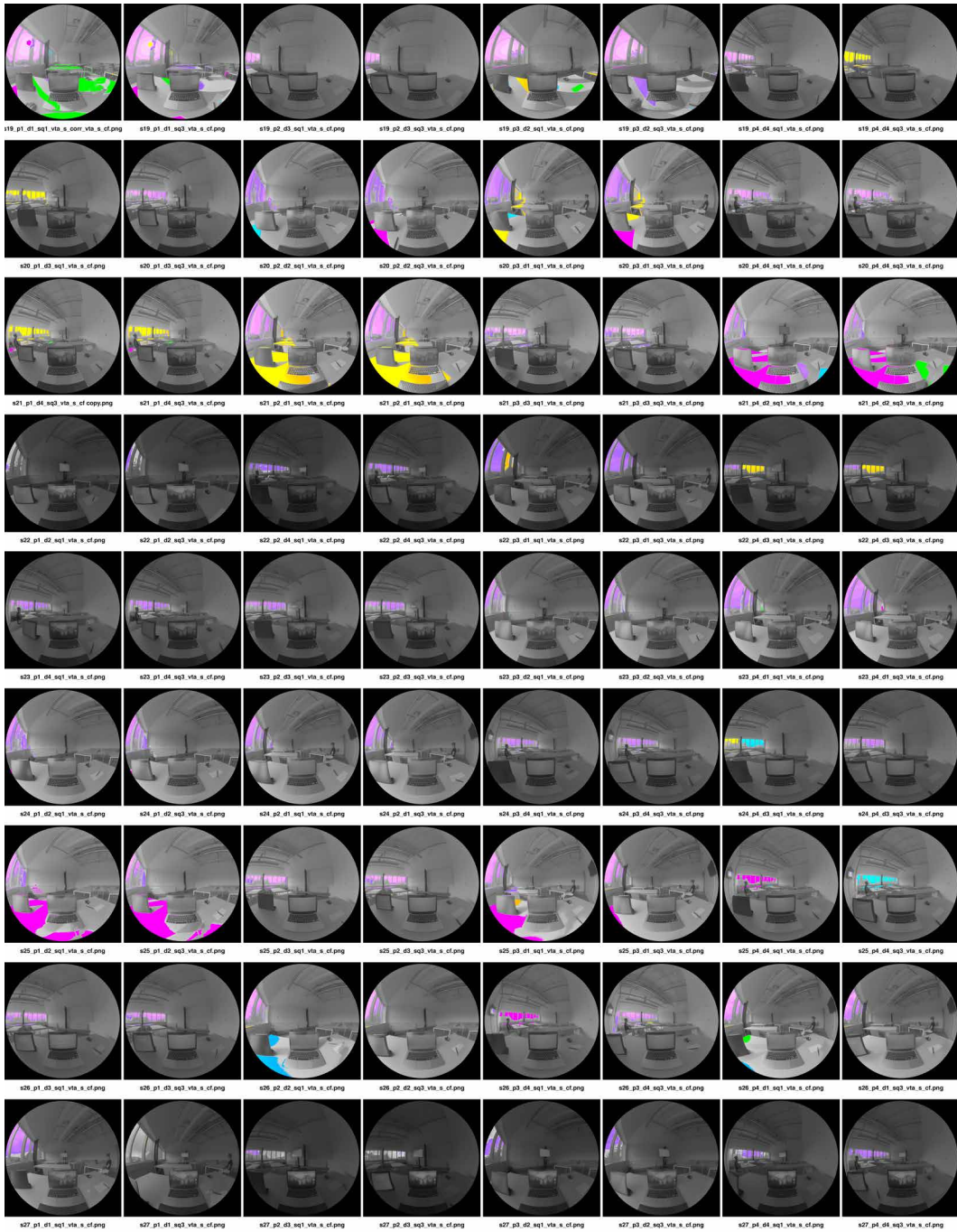
Evalglare's 'check files' images for the 'before' and 'end' measurements, in each of the 4 positions. The order of the images corresponds to the order of sitting by the subjects. The coloured areas correspond to the identified glare sources.



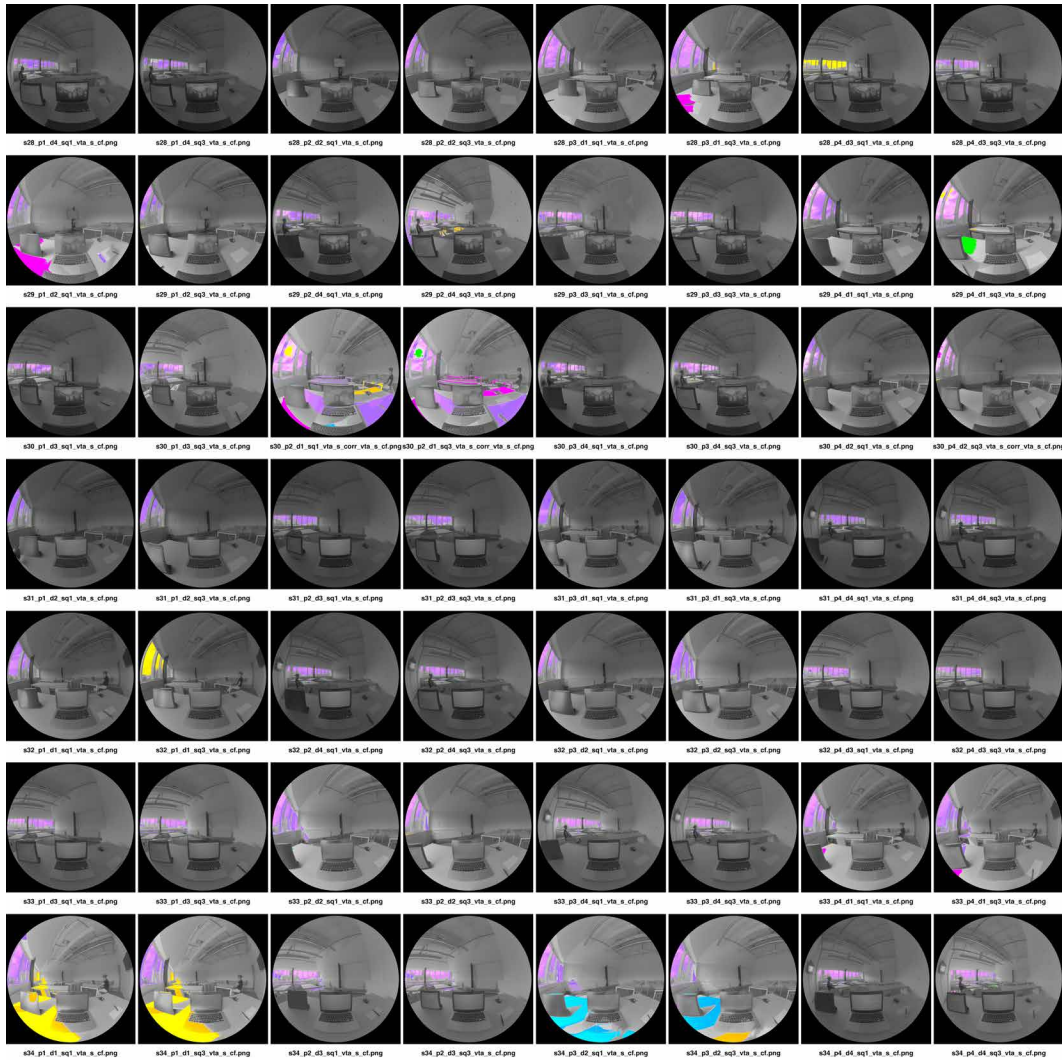
Evalglare's check files.



Evalglare 's check files.



Evalgre 's check files.



Evalglare 's check files.

C.4 Tables for the ‘start measurement’

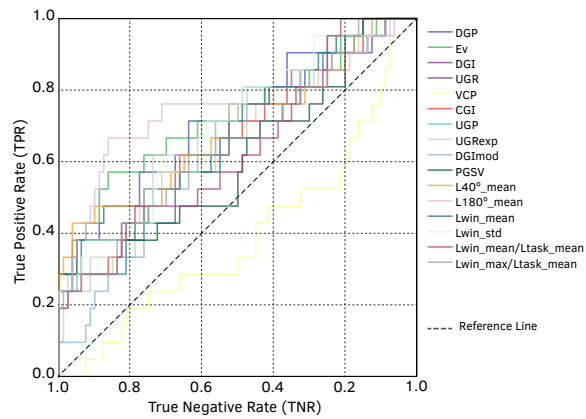
C.4.1 Spearman correlation analysis

Full (start measurement)			95% CI		ρ	sig.	low CI	CI	Total	
#	Metric	ρ	sig.	Lower	Upper	rank	rank	rank	rank	rank
1	DGP	0.38	0.000	0.19	0.544	4	4	4	1	4
2	EV	0.40	0.000	0.22	0.578	2	2	2	4	2
3	DGI	0.22	0.026	0.02	0.408	13	13	13	12	13
4	UGR	0.21	0.038	0.00	0.396	14	14	15	13	15
5	VCP	-0.12	0.233	-0.32	0.091	16	16	6	16	14
6	CGI	0.25	0.012	0.05	0.435	8	8	9	11	9
7	UGP	0.21	0.038	0.00	0.396	15	15	16	14	16
8	UGRexp	0.28	0.004	0.08	0.463	6	6	8	8	7
9	DGImod	0.23	0.022	0.02	0.410	11	11	12	9	10
10	PGSV	0.23	0.020	0.02	0.418	10	10	14	15	12
11	L40°mean	0.38	0.000	0.19	0.551	3	3	3	2	3
12	L180°mean	0.46	0.000	0.26	0.622	1	1	1	3	1
13	Lwinmean	0.27	0.006	0.08	0.448	7	7	7	6	6
14	Lwinstd	0.29	0.004	0.10	0.458	5	5	5	5	5
15	Lwinmean/Ltaskmean	0.22	0.025	0.02	0.410	12	12	11	10	11
16	Lwinmax/Ltaskmean	0.24	0.015	0.05	0.419	9	9	10	7	8

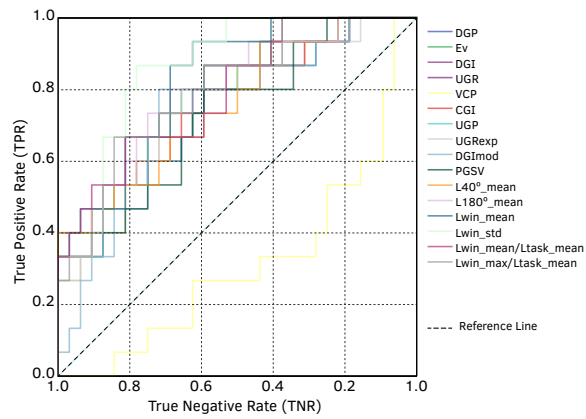
Window (start measurement)				95% CI		ρ	sig.	low CI	CI	Total
#	Metric	ρ	sig.	Lower	Upper	rank	rank	rank	rank	rank
1	DGP	0.56	0.000	0.31	0.760	6	6	6	6	5
2	EV	0.55	0.000	0.30	0.753	7	7	7	7	8
3	DGI	0.50	0.000	0.24	0.710	13	13	12	13	13
4	UGR	0.50	0.000	0.24	0.711	11	11	10	11	10
5	VCP	-0.36	0.012	-0.62	-0.089	16	16	16	16	16
6	CGI	0.52	0.000	0.27	0.730	9	9	9	9	9
7	UGP	0.50	0.000	0.24	0.711	12	12	11	12	11
8	UGRexp	0.48	0.001	0.23	0.707	14	15	14	14	15
9	DGI _{mod}	0.50	0.000	0.24	0.721	10	10	13	15	12
10	PGSV	0.48	0.001	0.23	0.693	15	14	15	10	14
11	L40° _{mean}	0.56	0.000	0.30	0.756	5	5	8	8	7
12	L180° _{mean}	0.57	0.000	0.33	0.759	4	4	4	5	4
13	Lwin _{mean}	0.63	0.000	0.42	0.786	1	1	1	2	1
14	Lwin _{std}	0.61	0.000	0.40	0.761	2	2	2	1	2
15	Lwin _{mean} /Ltask _{mean}	0.61	0.000	0.38	0.767	3	3	3	3	3
16	Lwin _{max} /Ltask _{mean}	0.54	0.000	0.32	0.725	8	8	5	4	6

Wall (start measurement)				95% CI		ρ	sig.	low CI	CI	Total
#	Metric	ρ	sig.	Lower	Upper	rank	rank	rank	rank	rank
1	DGP	0.17	0.232	-0.09	0.408	1	1	6	7	3
2	EV	0.06	0.673	-0.24	0.351	11	11	12	11	9
3	DGI	0.16	0.238	-0.08	0.409	2	2	2	6	2
4	UGR	0.16	0.254	-0.09	0.399	4	4	4	3	4
5	VCP	-0.13	0.359	-0.38	0.133	8	8	1	8	7
6	CGI	0.15	0.295	-0.09	0.384	6	6	7	1	6
7	UGP	0.16	0.254	-0.09	0.399	5	5	5	4	5
8	UGR _{exp}	0.14	0.304	-0.10	0.387	7	7	8	5	8
9	DGI _{mod}	0.16	0.247	-0.08	0.403	3	3	3	2	1
10	PGSV	0.06	0.661	-0.25	0.358	10	10	14	12	10
11	L40° _{mean}	0.07	0.631	-0.25	0.390	9	9	13	15	11
12	L180° _{mean}	0.04	0.751	-0.28	0.381	13	13	15	16	15
13	Lwin _{mean}	-0.02	0.911	-0.31	0.301	16	16	16	14	16
14	Lwin _{std}	0.05	0.705	-0.24	0.371	12	12	11	13	13
15	Lwin _{mean} /Ltask _{mean}	0.02	0.888	-0.24	0.293	15	15	10	9	14
16	Lwin _{max} /Ltask _{mean}	0.04	0.779	-0.23	0.321	14	14	9	10	12

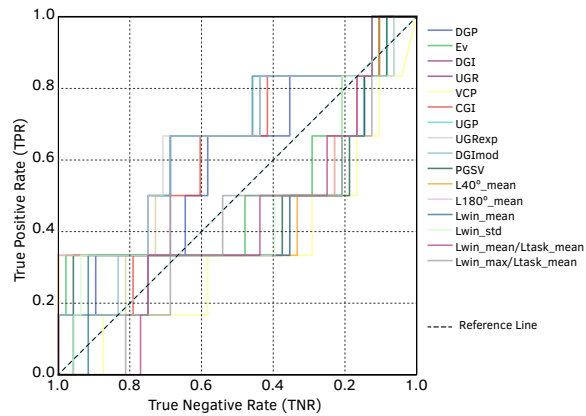
C.4.2 ROC curve analysis



ROC curve for full room
(start measurement).



ROC curve for the window zone
(start measurement).



ROC curve for wall zone
(start measurement).

Full				95% CI		AUC	sig.	low CI	CI	Total
#	Metric	AUC	sig.	Lower	Upper	rank	rank	rank	rank	rank
1	DGP	0.72	0.002	0.58	0.85	3	3	3	3	1
2	EV	0.73	0.001	0.59	0.86	2	2	2	6	2
3	DGI	0.65	0.034	0.52	0.79	10	10	10	7	9
4	UGR	0.65	0.036	0.51	0.79	11	11	12	12	12
5	VCP	0.39	0.130	0.25	0.53	16	16	16	14	16
6	CGI	0.66	0.020	0.53	0.80	8	8	8	10	8
7	UGP	0.65	0.036	0.51	0.79	12	12	13	13	13
8	UGRexp	0.69	0.007	0.56	0.83	5	5	5	4	5
9	DGImod	0.65	0.037	0.52	0.78	13	13	9	2	10
10	PGSV	0.62	0.094	0.47	0.77	15	15	15	16	15
11	L40°mean	0.69	0.007	0.55	0.83	6	6	6	15	7
12	L180°mean	0.75	0.000	0.61	0.89	1	1	1	11	4
13	Lwinmean	0.67	0.016	0.54	0.81	7	7	7	5	6
14	Lwinstd	0.70	0.005	0.57	0.83	4	4	4	1	3
15	Lwinmean/Ltaskmean	0.63	0.060	0.50	0.77	14	14	14	8	14
16	Lwinmax/Ltaskmean	0.65	0.033	0.51	0.79	9	9	11	9	11

Window				95% CI		AUC	sig.	low CI	CI	Total
#	Metric	AUC	sig.	Lower	Upper	rank	rank	rank	rank	rank
1	DGP	0.78	0.003	0.63	0.92	7	7	7	7	7
2	EV	0.78	0.002	0.63	0.92	6	6	6	6	6
3	DGI	0.75	0.007	0.59	0.90	13	13	14	12	14
4	UGR	0.75	0.006	0.60	0.90	11	11	11	13	11
5	VCP	0.31	0.040	0.15	0.48	16	16	16	16	16
6	CGI	0.76	0.004	0.62	0.91	8	8	8	9	8
7	UGP	0.75	0.006	0.60	0.90	12	12	12	14	13
8	UGRexp	0.76	0.004	0.61	0.91	9	9	9	10	9
9	DGImod	0.75	0.007	0.60	0.89	14	14	13	8	12
10	PGSV	0.74	0.010	0.58	0.89	15	15	15	15	15
11	L40°mean	0.76	0.005	0.61	0.91	10	10	10	11	10
12	L180°mean	0.80	0.001	0.66	0.93	4	4	4	4	4
13	Lwinmean	0.83	0.000	0.71	0.95	2	2	2	2	2
14	Lwinstd	0.86	0.000	0.76	0.97	1	1	1	1	1
15	Lwinmean/Ltaskmean	0.79	0.001	0.65	0.93	5	5	5	5	5
16	Lwinmax/Ltaskmean		0.001	0.67	0.93	3	3	3	3	3

Wall				95% CI		AUC	sig.	low CI	CI	Total
#	Metric	AUC	sig.	Lower	Upper	rank	rank	rank	rank	rank
1	DGP	0.59	0.474	0.33	0.86	7	8	7	10	7
2	EV	0.51	0.956	0.21	0.80	8	16	8	13	11
3	DGI	0.63	0.296	0.39	0.87	1	2	3	5	2
4	UGR	0.63	0.308	0.39	0.87	2	3	1	2	1
5	VCP	0.34	0.205	0.09	0.59	16	1	16	9	10
6	CGI	0.60	0.425	0.36	0.84	6	7	6	7	6
7	UGP	0.63	0.308	0.39	0.87	3	4	2	3	3
8	UGRexp	0.63	0.322	0.38	0.87	5	6	5	8	5
9	DGImod	0.63	0.308	0.39	0.87	4	5	4	6	4
10	PGSV	0.45	0.720	0.15	0.76	12	12	14	14	15
11	L40°mean	0.47	0.826	0.16	0.78	9	15	12	15	14
12	L180°mean	0.47	0.804	0.15	0.78	10	14	13	16	16
13	Lwinmean	0.44	0.620	0.15	0.73	13	11	15	11	13
14	Lwinstd	0.46	0.762	0.17	0.76	11	13	11	12	12
15	Lwinmean/Ltaskmean	0.42	0.509	0.19	0.65	15	9	9	1	8
16	Lwinmax/Ltaskmean	0.42	0.509	0.18	0.66	14	10	10	4	9

Full (start meas.)		shortest				dist.	TPR	TNR	Total
#	Metric	dist.	cut-off	TPR	TNR	rank	rank	rank	rank
1	DGP	0.46	0.26	0.71	0.64	3	1	12	3
2	EV	0.45	1306	0.67	0.70	2	4	8	2
3	DGI	0.52	19	0.57	0.71	7	10	7	7
4	UGR	0.53	26	0.52	0.76	11	12	4	9
5	VCP	0.79	19	0.48	0.41	16	14	16	16
6	CGI	0.51	27	0.62	0.66	6	6	9	5
7	UGP	0.53	0.84	0.52	0.76	12	13	5	11
8	UGRexp	0.46	21	0.62	0.74	4	7	6	4
9	DGImod	0.52	18	0.71	0.56	9	2	15	8
10	PGSV	0.62	2	0.38	0.95	15	16	1	12
11	L40°mean	0.52	723	0.62	0.65	8	8	11	10
12	L180°mean	0.36	607	0.67	0.86	1	5	2	1
13	Lwinmean	0.55	3982	0.57	0.66	13	11	10	15
14	Lwinstd	0.50	3446	0.71	0.59	5	3	14	6
15	Lwinmean/Ltaskmean	0.57	24	0.48	0.79	14	15	3	13
16	Lwinmax/Ltaskmean	0.53	73	0.62	0.64	10	9	13	14

Window (start meas.)		shortest				dist.	TPR	TNR	Total
#	Metric	dist.	cut-off	TPR	TNR	rank	rank	rank	rank
1	DGP	0.39	0.26	0.73	0.72	7	8	5	4
2	EV	0.39	1472	0.73	0.72	8	9	6	8
3	DGI	0.41	15	0.73	0.69	10	10	9	12
4	UGR	0.43	17	0.87	0.59	11	1	13	9
5	VCP	0.82	64	0.27	0.63	16	16	12	16
6	CGI	0.43	21	0.87	0.59	12	2	14	11
7	UGP	0.43	0.57	0.87	0.59	13	3	15	13
8	UGRexp	0.39	17	0.73	0.72	9	11	7	10
9	DGImod	0.35	16	0.80	0.72	3	6	8	2
10	PGSV	0.45	1	0.80	0.59	14	7	16	14
11	L40°mean	0.46	789	0.67	0.69	15	13	10	15
12	L180°mean	0.37	730	0.73	0.75	4	12	4	5
13	Lwinmean	0.34	3245	0.87	0.69	2	4	11	3
14	Lwinstd	0.26	3446	0.87	0.78	1	5	3	1
15	Lwinmean/Ltaskmean	0.38	16	0.67	0.81	6	14	2	7
16	Lwinmax/Ltaskmean	0.37	73	0.67	0.84	5	15	1	6

Wall (start meas.)		shortest				dist.	TPR	TNR	Total
#	Metric	dist.	cut-off	TPR	TNR	rank	rank	rank	rank
1	DGP	0.53	0.26	0.67	0.58	7	1	14	6
2	EV	0.67	2088	0.33	0.98	10	9	3	7
3	DGI	0.46	20	0.67	0.69	2	2	9	1
4	UGR	0.46	26	0.67	0.69	3	3	10	3
5	VCP	0.79	25	0.33	0.58	16	10	15	16
6	CGI	0.52	28	0.67	0.60	6	4	13	8
7	UGP	0.46	0.85	0.67	0.69	4	5	11	4
8	UGRexp	0.44	21	0.67	0.71	1	6	8	2
9	DGImod	0.46	21	0.67	0.69	5	7	12	9
10	PGSV	0.67	2	0.33	0.96	11	11	4	11
11	L40°mean	0.67	1327	0.33	1.00	8	12	1	5
12	L180°mean	0.67	607	0.33	1.00	9	13	2	10
13	Lwinmean	0.67	7374	0.33	0.92	13	14	6	13
14	Lwinstd	0.67	7584	0.33	0.94	12	15	5	12
15	Lwinmean/Ltaskmean	0.71	26	0.33	0.75	15	16	7	14
16	Lwinmax/Ltaskmean	0.68	79	0.50	0.54	14	8	16	15

C.4.3 Performance analysis

Full (start meas.)		Spearman			ROC						All
#	Metric	sig.	ρ	low CI	sig.	AUC	low CI	dist.	TPR	TNR	rank
1	DGP	1	1	0	1	1	1	1	1	1	2
2	EV	1	1	1	1	1	1	1	1	1	1
3	DGI	1	0	0	1	1	1	0	1	1	4
4	UGR	1	0	0	1	1	1	0	1	1	4
5	VCP	0	0	0	0	0	0	0	0	0	7
6	CGI	1	0	0	1	1	1	0	1	1	4
7	UGP	1	0	0	1	1	1	0	1	1	4
8	UGRexp	1	0	0	1	1	1	1	1	1	3
9	DGImod	1	0	0	1	1	1	0	1	1	4
10	PGSV	1	0	0	0	1	0	0	0	1	5
11	L40°mean	1	1	0	1	1	1	0	1	1	3
12	L180°mean	1	1	1	1	1	1	1	1	1	1
13	Lwinmean	1	0	0	1	1	1	0	1	1	4
14	Lwinstd	1	0	0	1	1	1	0	1	1	4
15	Lwinmean/Ltaskmean	1	0	0	0	1	0	0	0	1	5
16	Lwinmax/Ltaskmean	1	0	0	1	1	1	0	1	1	4

Window (start meas.)		Spearman			ROC						All
#	Metric	sig.	ρ	low CI	sig.	AUC	low CI	dist.	TPR	TNR	rank
1	DGP	1	1	1	1	1	1	1	1	1	1
2	EV	1	1	1	1	1	1	1	1	1	1
3	DGI	1	1	1	1	1	1	1	1	1	1
4	UGR	1	1	1	1	1	1	1	1	1	1
5	VCP	1	1	0	1	0	0	0	0	1	2
6	CGI	1	1	1	1	1	1	1	1	1	1
7	UGP	1	1	1	1	1	1	1	1	1	1
8	UGRexp	1	1	1	1	1	1	1	1	1	1
9	DGImod	1	1	1	1	1	1	1	1	1	1
10	PGSV	1	1	1	1	1	1	1	1	1	1
11	L40°mean	1	1	1	1	1	1	1	1	1	1
12	L180°mean	1	1	1	1	1	1	1	1	1	1
13	Lwinmean	1	1	1	1	1	1	1	1	1	1
14	Lwinstd	1	1	1	1	1	1	1	1	1	1
15	Lwinmean/Ltaskmean	1	1	1	1	1	1	1	1	1	1
16	Lwinmax/Ltaskmean	1	1	1	1	1	1	1	1	1	1

Wall (start meas.)		Spearman			ROC						All
#	Metric	sig.	ρ	low CI	sig.	AUC	low CI	dist.	TPR	TNR	rank
1	DGP	0	0	0	0	0	0	0	1	1	3
2	EV	0	0	1	0	0	0	0	0	1	3
3	DGI	0	0	0	0	1	0	1	1	1	1
4	UGR	0	0	0	0	1	0	1	1	1	1
5	VCP	0	0	0	0	0	0	0	0	1	4
6	CGI	0	0	0	0	1	0	0	1	1	2
7	UGP	0	0	0	0	1	0	1	1	1	1
8	UGRexp	0	0	0	0	1	0	1	1	1	1
9	DGImod	0	0	0	0	1	0	1	1	1	1
10	PGSV	0	0	1	0	0	0	0	0	1	3
11	L40°mean	0	0	1	0	0	0	0	0	1	3
12	L180°mean	0	0	1	0	0	0	0	0	1	3
13	Lwinmean	0	0	1	0	0	0	0	0	1	3
14	Lwinstd	0	0	1	0	0	0	0	0	1	3
15	Lwinmean/Ltaskmean	0	0	1	0	0	0	0	0	1	3
16	Lwinmax/Ltaskmean	0	0	1	0	0	0	0	1	1	2

Parameters' analysis

D.1 Cut-off points of the glare parameters

Extraction of the BCD thresholds of the calculated parameters, based on the results of the ROC curve. The BCD threshold (identified as cut-off in the tables), corresponds to the point of the curve with the highest TPR and TNR, or the value of the parameter corresponding to the best prediction of 'glare' and 'no-glare'.

The cut-off points of the glare parameters were calculated for the dataset and its subsamples. The shaded parameters (blue) correspond to parameters that achieved a 'good' AUC (> 0.7).

Full sample

subdivision	#	parameter	any glare	disturbing
			glare	glare
			cutt-off	cutt-off
n=148				
full	1	Lavg	289	352
full	2	Ev	499	1294
full	3	Lb	104	219
full	4	Lt	260	303
full	5	Ls_omega	3705	4492
full	6	Ls_mean	3217	4034
full	7	omegas_total	0.08	0.10
full	8	omegas_mean	0.02	0.06
full	9	P_min	2.0	2.0
full	10	Ev_dir	107	420
full	11	Ev_ind	328	688
full	12	DGP	0.21	0.26
full	13	ls_mean/Lavg	12.0	13.2
full	14	ls_mean/Ev	3.7	7.0
full	15	ls_mean/Lt	12.7	14.8
full	16	Ev/Lt	2.7	2.9
full	17	Ev/Lb	4.5	4.5

Position 1

subdivision	#	parameter	any glare	disturbing
			glare	glare
			cutt-off	cutt-off
n=43				
P1	1	Lavg	806	939
P1	2	Ev	1543	1749
P1	3	Lb	116	242
P1	4	Lt	261	280
P1	5	Ls_omega	4126	4812
P1	6	Ls_mean	3296	5082
P1	7	omegas_total	0.32	0.74
P1	8	omegas_mean	0.09	0.11
P1	9	P_min	1.4	1.4
P1	10	Ev_dir	292	989
P1	11	Ev_ind	365	759
P1	12	DGP	0.26	0.28
P1	13	ls_mean/Lavg	9.0	20.3
P1	14	ls_mean/Ev	4.2	11.7
P1	15	ls_mean/Lt	13.5	14.8
P1	16	Ev/Lt	3.3	5.7
P1	17	Ev/Lb	5.2	6.8

Position 2

subdivision	#	parameter	any glare	disturbing
			glare	glare
			cutt-off	cutt-off
n=47				
P2	1	Lavg	334	543
P2	2	Ev	792	1357
P2	3	Lb	228	245
P2	4	Lt	260	310
P2	5	Ls_omega	4290	4834
P2	6	Ls_mean	2743	4890
P2	7	omegas_total	0.14	0.17
P2	8	omegas_mean	0.02	0.03
P2	9	P_min	2.1	2.3
P2	10	Ev_dir	78	89
P2	11	Ev_ind	717	770
P2	12	DGP	0.21	0.24
P2	13	ls_mean/Lavg	3.7	13.2
P2	14	ls_mean/Ev	1.7	5.1
P2	15	ls_mean/Lt	9.6	14.9
P2	16	Ev/Lt	3.0	3.8
P2	17	Ev/Lb	3.5	3.6

Position 3

subdivision	#	parameter	any glare	disturbing
			glare	glare
			cutt-off	cutt-off
n=46				
P3	1	Lavg	54	292
P3	2	Ev	360	1011
P3	3	Lb	89	72
P3	4	Lt	192	233
P3	5	Ls_omega	3812	3922
P3	6	Ls_mean	2137	2642
P3	7	omegas_total	0.06	0.06
P3	8	omegas_mean	0.00	0.03
P3	9	P_min	1.4	1.9
P3	10	Ev_dir	120	120
P3	11	Ev_ind	280	225
P3	12	DGP	0.21	0.21
P3	13	ls_mean/Lavg	10.1	25.1
P3	14	ls_mean/Ev	3.1	7.3
P3	15	ls_mean/Lt	11.1	11.7
P3	16	Ev/Lt	1.3	2.9
P3	17	Ev/Lb	4.1	4.9

Position 4

subdivision	#	parameter	any glare	disturbing
			glare	glare
			cutt-off	cutt-off
n=48				
P4	1	Lavg	124	352
P4	2	Ev	383	753
P4	3	Lb	74	168
P4	4	Lt	263	303
P4	5	Ls_omega	2670	7363
P4	6	Ls_mean	3541	3491
P4	7	omegas_total	0.07	0.10
P4	8	omegas_mean	0.02	0.03
P4	9	P_min	1.9	1.8
P4	10	Ev_dir	152	176
P4	11	Ev_ind	232	526
P4	12	DGP	0.21	0.22
P4	13	ls_mean/Lavg	12.5	20.9
P4	14	ls_mean/Ev	6.1	7.0
P4	15	ls_mean/Lt	11.7	19.3
P4	16	Ev/Lt	1.8	2.8
P4	17	Ev/Lb	4.5	4.5

Window

subdivision	#	parameter	any glare	disturbing
			glare	glare
			cutt-off	cutt-off
n=90				
window	1	Lavg	329	543
window	2	Ev	777	1743
window	3	Lb	228	242
window	4	Lt	260	310
window	5	Ls_omega	4092	4812
window	6	Ls_mean	3217	4890
window	7	omegas_total	0.23	0.32
window	8	omegas_mean	0.08	0.07
window	9	P_min	2.1	2.3
window	10	Ev_dir	107	581
window	11	Ev_ind	717	759
window	12	DGP	0.21	0.27
window	13	ls_mean/Lavg	3.7	16.4
window	14	ls_mean/Ev	1.7	4.2
window	15	ls_mean/Lt	13.5	14.8
window	16	Ev/Lt	3.0	3.8
window	17	Ev/Lb	3.6	5.3

Wall

subdivision	#	parameter	any glare	disturbing
			glare	glare
			cutt-off	cutt-off
n=94				
wall	1	Lavg	113	292
wall	2	Ev	360	1011
wall	3	Lb	89	168
wall	4	Lt	213	293
wall	5	Ls_omega	3164	3922
wall	6	Ls_mean	2388	2977
wall	7	omegas_total	0.06	0.10
wall	8	omegas_mean	0.00	0.03
wall	9	P_min	1.8	1.8
wall	10	Ev_dir	99	207
wall	11	Ev_ind	280	526
wall	12	DGP	0.20	0.22
wall	13	ls_mean/Lavg	12.0	20.9
wall	14	ls_mean/Ev	4.1	7.0
wall	15	ls_mean/Lt	11.1	11.7
wall	16	Ev/Lt	1.8	2.8
wall	17	Ev/Lb	4.6	4.5

Front

subdivision	#	parameter	any glare	disturbing
			glare	glare
			cutt-off	cutt-off
front	1	Lavg	334	352
front	2	Ev	821	859
front	3	Lb	214	219
front	4	Lt	236	361
front	5	Ls_omega	3812	5586
front	6	Ls_mean	3217	4096
front	7	omegas_total	0.08	0.10
front	8	omegas_mean	0.02	0.03
front	9	P_min	2.0	2.2
front	10	Ev_dir	107	120
front	11	Ev_ind	673	688
front	12	DGP	0.21	0.21
front	13	ls_mean/Lavg	5.3	13.2
front	14	ls_mean/Ev	1.7	3.8
front	15	ls_mean/Lt	9.6	12.5
front	16	Ev/Lt	2.8	2.9
front	17	Ev/Lb	3.6	4.3

Back

subdivision	#	parameter	any glare	disturbing
			glare	glare
			cutt-off	cutt-off
back	1	Lavg	213	352
back	2	Ev	499	1335
back	3	Lb	126	168
back	4	Lt	263	303
back	5	Ls_omega	4034	4492
back	6	Ls_mean	3491	4659
back	7	omegas_total	0.12	0.11
back	8	omegas_mean	0.06	0.08
back	9	P_min	1.4	1.4
back	10	Ev_dir	164	420
back	11	Ev_ind	397	526
back	12	DGP	0.20	0.26
back	13	ls_mean/Lavg	12.4	20.3
back	14	ls_mean/Ev	4.2	7.0
back	15	ls_mean/Lt	13.5	14.8
back	16	Ev/Lt	1.9	2.9
back	17	Ev/Lb	4.6	5.1

Model based on a metric

E.1 Assumptions of the linear regression

E.1.1 Independence of the dependent variable

Comparison of the regression models produced with and without the 7 subjects that did not perform a full set of observations (4) is provided below. The tables show the results of the regressions and the differences.

Linear regressions for all subjects

zone	metric	glare	r2	p	b0	b1	SE b0	SE b1
wall	dgp_calc	disturbing	0.18	0.22	-0.13	1.42	0.25	1.06
wall	dgp_calc	any_glare	0.32	0.09	0.33	1.70	0.21	0.88
wall	dgp_log_ev	disturbing	0.13	0.31	-0.55	4.04	0.69	3.69
wall	dgp_log_ev	any_glare	0.62	0.01	-0.72	7.79	0.40	2.17
wall	ugp_calc	disturbing	0.28	0.12	0.05	0.28	0.10	0.16
wall	ugp_calc	any_glare	0.58	0.01	0.51	0.38	0.07	0.11
window	dgp_calc	disturbing	0.47	0.03	-0.16	1.62	0.16	0.61
window	dgp_calc	any_glare	0.51	0.02	0.14	1.86	0.17	0.64
window	dgp_log_ev	disturbing	0.57	0.01	-1.62	10.87	0.58	3.37
window	dgp_log_ev	any_glare	0.60	0.01	-1.22	10.63	0.53	3.08
window	ugp_calc	disturbing	0.56	0.01	0.07	0.40	0.07	0.13
window	ugp_calc	any_glare	0.68	0.00	0.37	0.53	0.07	0.13

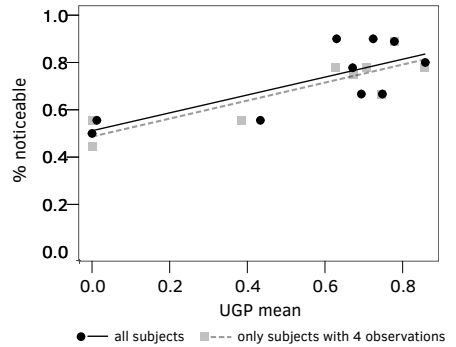
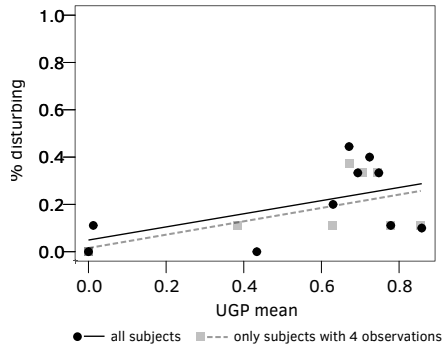
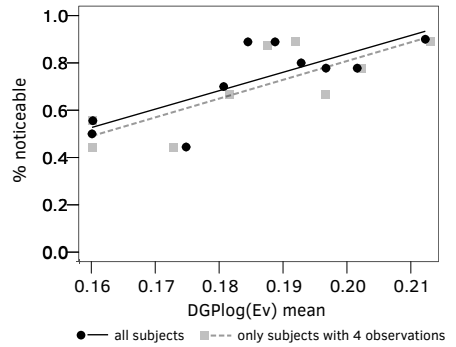
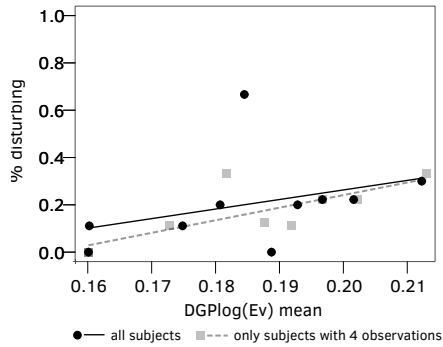
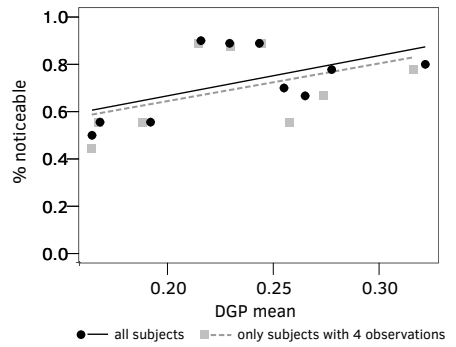
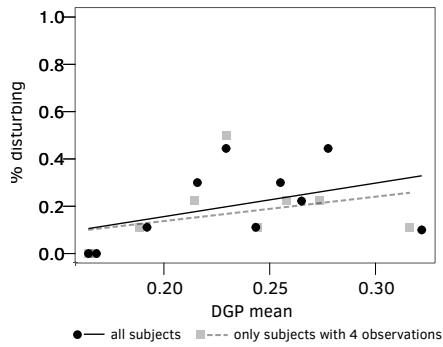
Linear regressions without subjects with less than 4 observations

zone	metric	glare	r2	p	b0	b1	SE b0	SE b1
wall	dgp_calc	disturbing	0.22	0.20	-0.15	1.46	0.24	1.04
wall	dgp_calc	any_glare	0.27	0.15	0.33	1.60	0.23	0.99
wall	dgp_log_ev	disturbing	0.51	0.03	-0.63	4.37	0.30	1.63
wall	dgp_log_ev	any_glare	0.59	0.02	-0.67	7.36	0.43	2.33
wall	ugp_calc	disturbing	0.20	0.22	0.05	0.26	0.12	0.19
wall	ugp_calc	any_glare	0.72	0.00	0.51	0.35	0.05	0.08
window	dgp_calc	disturbing	0.62	0.01	-0.17	1.64	0.12	0.48
window	dgp_calc	any_glare	0.65	0.01	0.07	2.15	0.15	0.59
window	dgp_log_ev	disturbing	0.60	0.01	-1.61	10.75	0.57	3.34
window	dgp_log_ev	any_glare	0.60	0.01	-1.84	14.27	0.75	4.40
window	ugp_calc	disturbing	0.56	0.02	0.06	0.40	0.07	0.13
window	ugp_calc	any_glare	0.68	0.01	0.35	0.59	0.08	0.15

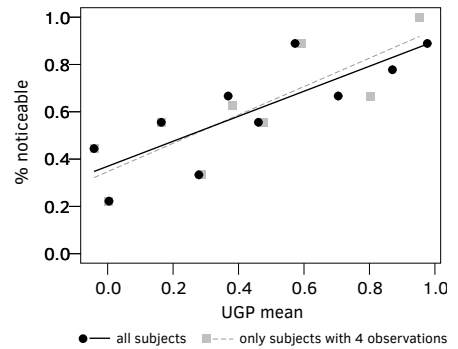
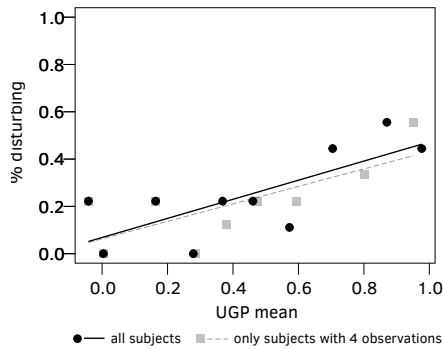
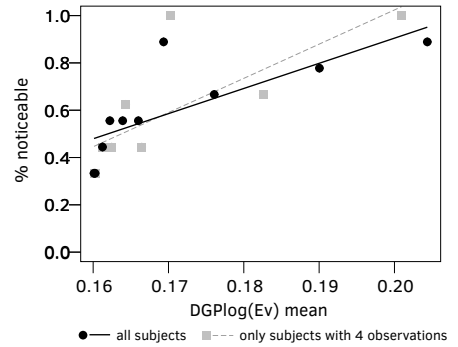
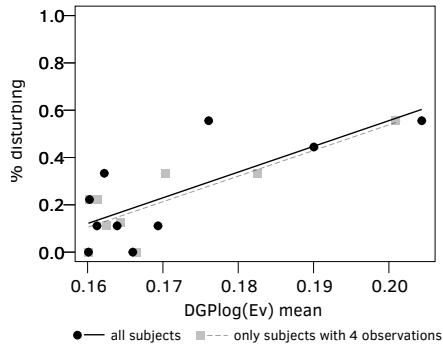
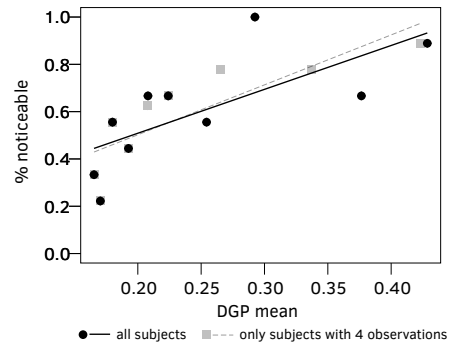
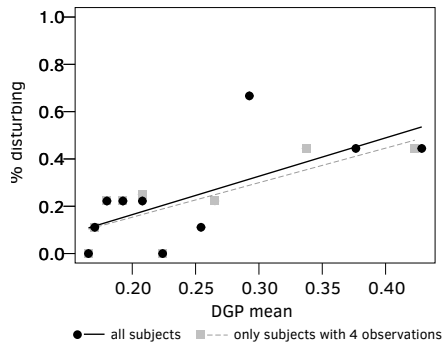
Difference between all subjects and without subjects with less than 4 observations

zone	metric	glare	r2	p	b0	b1	SE b0	SE b1
wall	dgp_calc	disturbing	-0.04	0.02	0.02	-0.04	0.01	0.02
wall	dgp_calc	any_glare	0.04	-0.06	0.00	0.10	-0.02	-0.10
wall	dgp_log_ev	disturbing	-0.38	0.27	0.08	-0.33	0.38	2.06
wall	dgp_log_ev	any_glare	0.03	-0.01	-0.05	0.43	-0.03	-0.16
wall	ugp_calc	disturbing	0.07	-0.10	0.00	0.02	-0.02	-0.03
wall	ugp_calc	any_glare	-0.14	0.01	0.00	0.03	0.02	0.03
window	dgp_calc	disturbing	-0.15	0.02	0.01	-0.02	0.04	0.13
window	dgp_calc	any_glare	-0.14	0.01	0.07	-0.29	0.02	0.05
window	dgp_log_ev	disturbing	-0.03	0.00	-0.01	0.12	0.01	0.03
window	dgp_log_ev	any_glare	0.00	-0.01	0.61	-3.64	-0.22	-1.31
window	ugp_calc	disturbing	0.00	-0.01	0.01	0.00	0.00	-0.01
window	ugp_calc	any_glare	0.00	0.00	0.02	-0.06	-0.01	-0.03

The differences between the regressions models produced with and without the 7 subjects is in general small for most metrics, with the corresponding regression lines showing parallel or almost parallel in most cases, with larger difference observed for the regression lines of the DGPllog(Ev) models, particularly for the 'any glare' definition of the window zone, model wall_dgplog(ev)_anyglare.



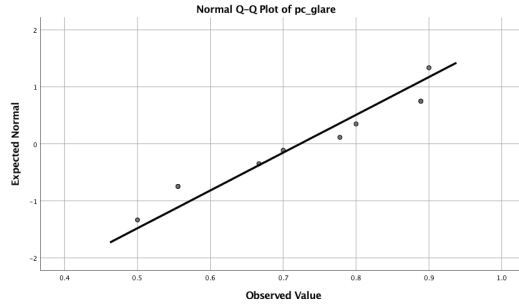
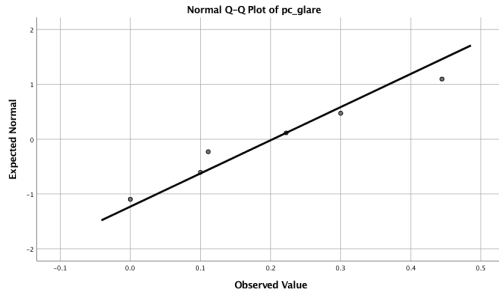
Linear regressions for DGP, DGPllog(Ev) and UGP with and without the subjects that made less than 4 observations, for 'any glare' (right) and 'disturbing glare' (left), in the wall zone.



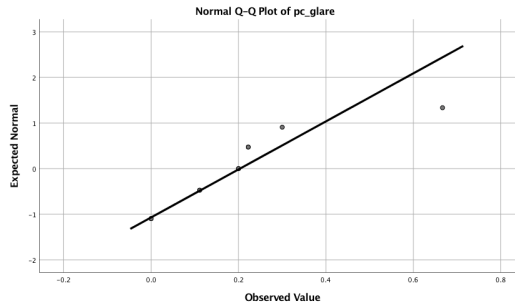
Linear regressions for DGP, DGPlg(Ev) and UGP with and without the subjects that made less than 4 observations, for 'any glare' (left) and disturbing glare, in the window zone.

E.1.2 Normality of the dependent variable

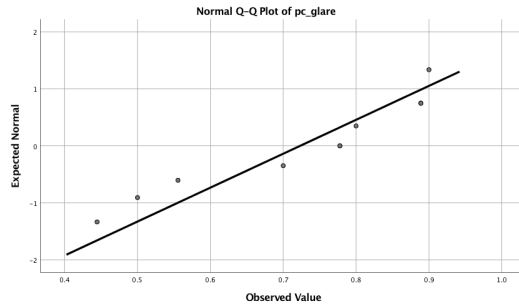
The Q-Q plots from the normality of the dependent variable test are provided below.



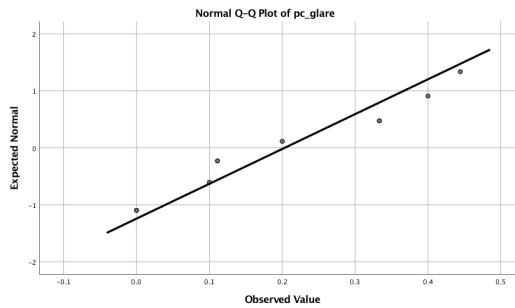
wall_dgp_calc_disturbing



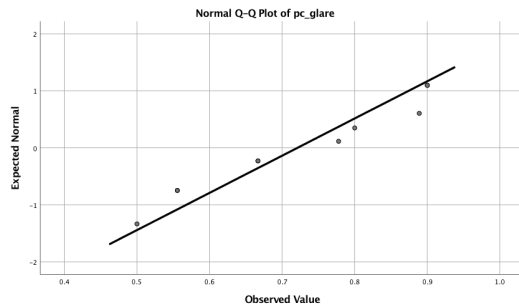
wall_dgp_calc_any_glare



wall_dgp_log_ev_disturbing

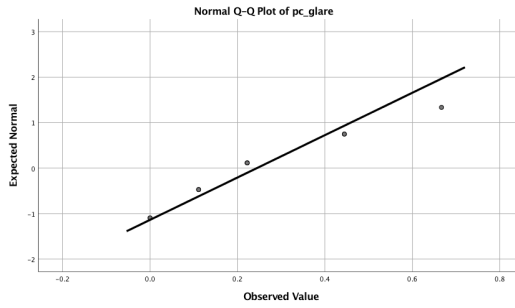


wall_dgp_log_ev_any_glare

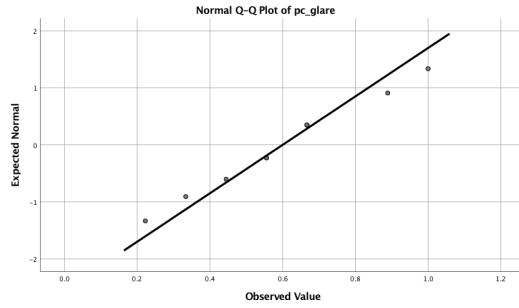


wall_ugp_calc_disturbing

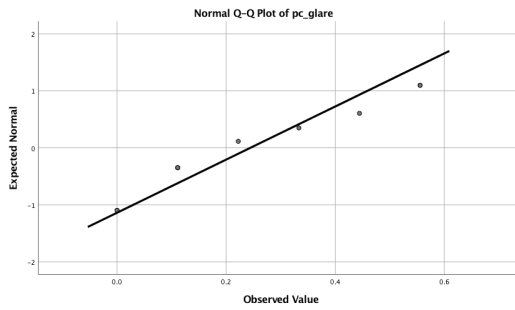
wall_ugp_calc_any_glare



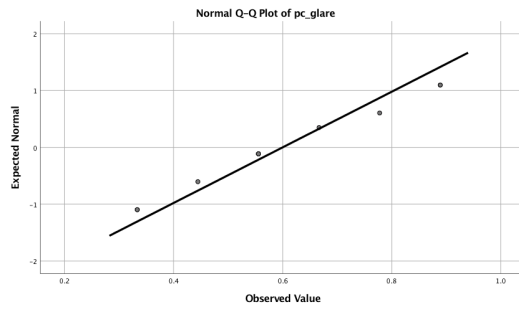
window_dgp_calc_disturbing



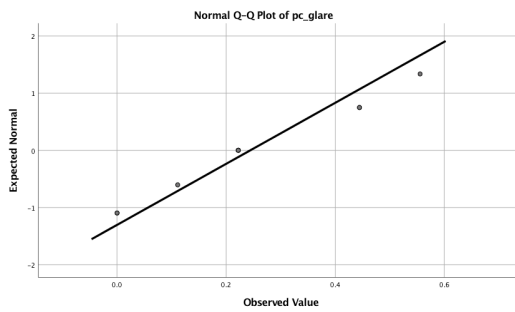
window_dgp_calc_any_glare



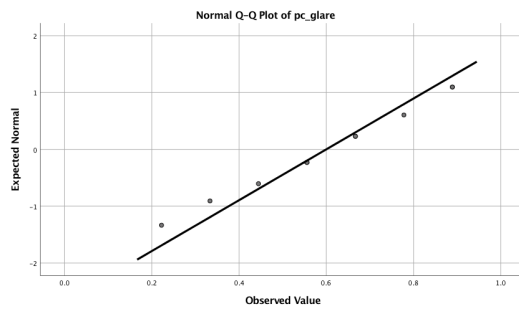
window_dgp_log_ev_disturbing



window_dgp_log_ev_any_glare



window_ugp_calc_disturbing



window_ugp_calc_any_glare

E.1.3 Linear regressions for different grouping approaches

Results for the linear regressions for the 7-group, 10-group and 13-group approaches of the model variables are provided below. The relevant columns of the tables are colour-coded from best to worst (brighter to darker blue). Additionally, values that produce very high values for the width of the 95% confidence interval of b_1 are signalled in grey.

Linear regression results for the wall zone and the 'any glare'

zone	parameter	glare	groups	r2	p	b0	b0	b0 lower	b0 upper	b1	b1	b1 lower	b1 upper
							SE	95% CI	95% CI		SE	95% CI	95% CI
wall	dgp_calc	any glare	7	0.33	0.175	0.30	0.27	-0.23	0.83	1.80	1.14	-0.43	4.04
wall	dgp_calc	any glare	10	0.32	0.091	0.33	0.21	-0.09	0.74	1.70	0.88	-0.03	3.43
wall	dgp_calc	any glare	13	0.24	0.093	0.29	0.24	-0.18	0.76	1.85	1.00	-0.12	3.81
wall	dgp_log_ev	any glare	7	0.61	0.039	-0.81	0.55	-1.89	0.28	8.26	2.97	2.43	14.09
wall	dgp_log_ev	any glare	10	0.62	0.007	-0.72	0.40	-1.51	0.07	7.79	2.17	3.54	12.04
wall	dgp_log_ev	any glare	13	0.40	0.021	-0.53	0.47	-1.45	0.39	6.78	2.52	1.84	11.72
wall	ugp_calc	any glare	7	0.68	0.022	0.50	0.08	0.35	0.65	0.40	0.12	0.16	0.64
wall	ugp_calc	any glare	10	0.58	0.010	0.51	0.07	0.37	0.65	0.38	0.11	0.16	0.60
wall	ugp_calc	any glare	13	0.54	0.004	0.53	0.06	0.41	0.65	0.35	0.10	0.16	0.54
wall	dgp_lowlight	any glare	7	0.47	0.091	0.51	0.11	0.30	0.73	1.03	0.49	0.06	2.00
wall	dgp_lowlight	any glare	10	0.50	0.022	0.50	0.08	0.34	0.67	1.08	0.38	0.34	1.83
wall	dgp_lowlight	any glare	13	0.32	0.042	0.50	0.11	0.29	0.71	1.10	0.48	0.16	2.03
wall	dgp_log_ev_lowlight	any glare	7	0.71	0.017	0.42	0.09	0.23	0.60	1.97	0.56	0.87	3.06
wall	dgp_log_ev_lowlight	any glare	10	0.71	0.002	0.45	0.07	0.32	0.58	1.76	0.40	0.97	2.55
wall	dgp_log_ev_lowlight	any glare	13	0.40	0.021	0.45	0.11	0.23	0.66	1.77	0.66	0.48	3.06

Linear regression results for the wall zone and the 'disturbing glare'

zone	parameter	glare	groups	r2	p	b0	b0	b0 lower	b0 upper	b1	b1	b1 lower	b1 upper
							SE	95% CI	95% CI		SE	95% CI	95% CI
wall	dgp_calc	disturbing	7	0.26	0.242	-0.12	0.25	-0.61	0.37	1.38	1.04	-0.66	3.43
wall	dgp_calc	disturbing	10	0.18	0.218	-0.13	0.25	-0.62	0.37	1.42	1.06	-0.66	3.49
wall	dgp_calc	disturbing	13	0.19	0.139	-0.10	0.20	-0.49	0.28	1.31	0.83	-0.30	2.93
wall	dgp_log_ev	disturbing	7	0.45	0.097	-0.75	0.47	-1.68	0.17	5.16	2.53	0.20	10.11
wall	dgp_log_ev	disturbing	10	0.13	0.306	-0.55	0.69	-1.89	0.80	4.04	3.69	-3.20	11.28
wall	dgp_log_ev	disturbing	13	0.27	0.069	-0.59	0.39	-1.36	0.18	4.27	2.12	0.12	8.43
wall	ugp_calc	disturbing	7	0.31	0.192	0.02	0.14	-0.25	0.29	0.33	0.22	-0.10	0.76
wall	ugp_calc	disturbing	10	0.28	0.119	0.05	0.10	-0.15	0.24	0.28	0.16	-0.03	0.59
wall	ugp_calc	disturbing	13	0.24	0.087	0.04	0.10	-0.14	0.23	0.29	0.15	-0.01	0.58
wall	dgp_lowlight	disturbing	7	0.42	0.117	0.01	0.11	-0.21	0.23	0.95	0.50	-0.03	1.92
wall	dgp_lowlight	disturbing	10	0.36	0.066	0.00	0.10	-0.20	0.21	0.98	0.46	0.08	1.88
wall	dgp_lowlight	disturbing	13	0.32	0.042	0.00	0.10	-0.19	0.19	0.99	0.43	0.14	1.84
wall	dgp_log_ev_lowlight	disturbing	7	0.62	0.037	-0.04	0.09	-0.23	0.14	1.57	0.56	0.48	2.66
wall	dgp_log_ev_lowlight	disturbing	10	0.73	0.002	-0.05	0.06	-0.16	0.06	1.61	0.34	0.94	2.28
wall	dgp_log_ev_lowlight	disturbing	13	0.33	0.039	-0.05	0.12	-0.28	0.18	1.62	0.69	0.26	2.98

Linear regression results for the window zone and the 'any glare'

zone	parameter	glare	groups	r2	p	b0	b0	b0 lower	b0 upper	b1	b1	b1 lower	b1 upper
							SE	95% CI	95% CI		SE	95% CI	95% CI
window	dgp_calc	any glare	7	0.48	0.086	0.12	0.24	-0.34	0.59	1.93	0.91	0.15	3.71
window	dgp_calc	any glare	10	0.51	0.020	0.14	0.17	-0.19	0.47	1.86	0.64	0.59	3.12
window	dgp_calc	any glare	13	0.39	0.022	0.13	0.19	-0.25	0.50	1.92	0.72	0.51	3.33
window	dgp_log_ev	any glare	7	0.63	0.033	-1.10	0.58	-2.25	0.04	9.94	3.40	3.28	16.60
window	dgp_log_ev	any glare	10	0.60	0.009	-1.22	0.53	-2.26	-0.18	10.63	3.08	4.59	16.68
window	dgp_log_ev	any glare	13	0.38	0.024	-1.08	0.65	-2.35	0.19	9.82	3.76	2.45	17.20
window	ugp_calc	any glare	7	0.80	0.006	0.38	0.06	0.26	0.50	0.51	0.11	0.29	0.73
window	ugp_calc	any glare	10	0.68	0.003	0.37	0.07	0.23	0.51	0.53	0.13	0.28	0.78
window	ugp_calc	any glare	13	0.70	0.000	0.37	0.06	0.26	0.48	0.53	0.11	0.32	0.74
window	dgp_lowlight	any glare	7	0.56	0.052	0.24	0.16	-0.07	0.55	1.61	0.63	0.37	2.85
window	dgp_lowlight	any glare	10	0.64	0.006	0.25	0.10	0.05	0.46	1.54	0.41	0.73	2.36
window	dgp_lowlight	any glare	13	0.49	0.008	0.24	0.12	0.00	0.48	1.60	0.49	0.64	2.56
window	dgp_log_ev_lowlight	any glare	7	0.81	0.006	0.08	0.12	-0.15	0.31	3.47	0.74	2.01	4.93
window	dgp_log_ev_lowlight	any glare	10	0.64	0.006	0.11	0.14	-0.16	0.38	3.30	0.88	1.57	5.04
window	dgp_log_ev_lowlight	any glare	13	0.39	0.023	0.11	0.20	-0.28	0.49	3.29	1.25	0.84	5.73

Linear regression results for the window zone and the 'disturbing glare'

zone	parameter	glare	groups	r2	p	b0	b0	b0 lower	b0 upper	b1	b1	b1 lower	b1 upper
							SE	95% CI	95% CI		SE	95% CI	95% CI
window	dgp_calc	disturbing	7	0.69	0.020	-0.19	0.14	-0.45	0.08	1.74	0.51	0.73	2.75
window	dgp_calc	disturbing	10	0.47	0.029	-0.16	0.16	-0.48	0.16	1.62	0.61	0.42	2.82
window	dgp_calc	disturbing	13	0.46	0.010	-0.18	0.15	-0.46	0.11	1.70	0.55	0.62	2.78
window	dgp_log_ev	disturbing	7	0.75	0.012	-1.70	0.51	-2.70	-0.71	11.36	2.95	5.58	17.15
window	dgp_log_ev	disturbing	10	0.57	0.012	-1.62	0.58	-2.75	-0.48	10.87	3.37	4.27	17.48
window	dgp_log_ev	disturbing	13	0.56	0.003	-1.61	0.50	-2.59	-0.63	10.83	2.91	5.13	16.52
window	ugp_calc	disturbing	7	0.58	0.046	0.06	0.09	-0.11	0.23	0.42	0.16	0.11	0.74
window	ugp_calc	disturbing	10	0.56	0.012	0.07	0.07	-0.07	0.20	0.40	0.13	0.16	0.65
window	ugp_calc	disturbing	13	0.49	0.007	0.05	0.07	-0.09	0.20	0.44	0.13	0.17	0.70
window	dgp_lowlight	disturbing	7	0.72	0.016	-0.05	0.09	-0.23	0.13	1.32	0.37	0.60	2.03
window	dgp_lowlight	disturbing	10	0.49	0.023	-0.04	0.11	-0.26	0.18	1.24	0.44	0.37	2.11
window	dgp_lowlight	disturbing	13	0.48	0.008	-0.05	0.10	-0.25	0.15	1.29	0.40	0.50	2.08
window	dgp_log_ev_lowlight	disturbing	7	0.52	0.068	-0.14	0.18	-0.49	0.20	2.59	1.12	0.40	4.77
window	dgp_log_ev_lowlight	disturbing	10	0.40	0.051	-0.13	0.17	-0.47	0.21	2.51	1.09	0.37	4.65
window	dgp_log_ev_lowlight	disturbing	13	0.40	0.020	-0.13	0.15	-0.42	0.15	2.53	0.93	0.71	4.35

Model based on modified metric

F.1 Invariance of r^2 for the model development approach

The model development approach that was used is based on the addition of a constant a_0 to a value x and the multiplication of a value x with a constant a_1 so that:

$$x_i^* = a_1 \cdot x_i + a_0$$

Below it is demonstrated that this operation does not affect r^2 .

The calculated r^2 corresponds to the quotient between the variance of the fitted values and the variance of the observed values of the dependent variable y .

$$r^2 = \frac{\sum_{i=1}^n (y_i - \hat{y}_i)^2}{\sum_{i=1}^n (y_i - \bar{y})^2}$$

where \hat{y} is the fitted value for the observation i , \bar{y} is the mean value of y , $y = b_0 + b_1 \cdot x$ where x is the independent variable, and b_0 and b_1 are the intercept and the slope of the fitted regression line, respectively.

$$\widehat{y}_i = b_0 + b_1 \cdot x_i$$

where

$$b_0 = \bar{y} - b_1 \cdot \bar{x}$$

$$b_1 = \frac{\sum_{i=1}^n x_i (y_i - \bar{y})}{\sum_{i=1}^n x_i (x_i - \bar{x})}$$

Adding a constant:

First it is shown what the effect on the r^2 is when a constant a_0 is added to x :

$$x_i^* = x_i + a_0$$

The only thing that changes in r^2 is \widehat{y}_i as y_i and \bar{y} only depend on the observed percentage of glare.

$$\widehat{y}_i^* = b_0^* + b_1^* \cdot x_i^*$$

$$b_0^* = \bar{y} - b_1^* \cdot \bar{x}^*$$

$$\bar{x}^* = \frac{1}{n} \sum_{i=1}^n x_i^* = \frac{1}{n} \sum_{i=1}^n (x_i + a_0) = \frac{1}{n} \sum_{i=1}^n x_i + \frac{1}{n} \sum_{i=1}^n a_0 = \bar{x} + a_0$$

$$b_0^* = \bar{y} - b_1^* \cdot (\bar{x} + a_0)$$

$$\begin{aligned}
b_1^* &= \frac{\sum_{i=1}^n x_i^* (y_i - \bar{y})}{\sum_{i=1}^n x_i^* (x_i^* - \bar{x}^*)} = \frac{\sum_{i=1}^n (x_i + a_0)(y_i - \bar{y})}{\sum_{i=1}^n (x_i + a_0)((x_i + a_0) - (\bar{x} + a_0))} = \\
&= \frac{\sum_{i=1}^n (x_i)(y_i - \bar{y}) + \sum_{i=1}^n (a_0)(y_i - \bar{y})}{\sum_{i=1}^n (x_i + a_0)(x_i - \bar{x})} = \frac{\sum_{i=1}^n (x_i)(y_i - \bar{y}) + a_0 \sum_{i=1}^n (y_i - \bar{y})}{\sum_{i=1}^n (x_i)(x_i - \bar{x}) + \sum_{i=1}^n (a_0)(x_i - \bar{x})} \\
&= \frac{\sum_{i=1}^n (x_i)(y_i - \bar{y}) + a_0 \left(\sum_{i=1}^n y_i - \sum_{i=1}^n \bar{y} \right)}{\sum_{i=1}^n (x_i)(x_i - \bar{x}) + a_0 \left(\sum_{i=1}^n x_i - \sum_{i=1}^n \bar{x} \right)} = \frac{\sum_{i=1}^n (x_i)(y_i - \bar{y}) + a_0 (n\bar{y} - n\bar{y})}{\sum_{i=1}^n (x_i)(x_i - \bar{x}) + a_0 (n\bar{x} - n\bar{x})} = \\
&= \frac{\sum_{i=1}^n (x_i)(y_i - \bar{y}) + a_0 \cdot 0}{\sum_{i=1}^n (x_i)(x_i - \bar{x}) + a_0 \cdot 0} = \frac{\sum_{i=1}^n (x_i)(y_i - \bar{y})}{\sum_{i=1}^n (x_i)(x_i - \bar{x})} = b_1
\end{aligned}$$

$$b_0^* = \bar{y} - b_1^* \cdot (\bar{x} + a_0) = \bar{y} - b_1 \cdot (\bar{x} + a_0) = b_0 - b_1 \cdot a_0$$

$$\widehat{y}_i^* = b_0^* + b_1^* \cdot x_i^* = b_0 - b_1 \cdot a_0 + b_1 \cdot (x_i + a_0) = b_0 + b_1 \cdot x_i = \widehat{y}_i$$

$$r^{*2} = \frac{\sum_{i=1}^n (y_i - \widehat{y}_i^*)^2}{\sum_{i=1}^n (y_i - \bar{y})^2} = \frac{\sum_{i=1}^n (y_i - \widehat{y}_i)^2}{\sum_{i=1}^n (y_i - \bar{y})^2} = r^2$$

The conclusion is then that r^2 does not change when a constant is added to x .

Multiplying with a constant:

First it is shown what is the effect of multiplying x with a constant a_1 :

$$x_i^* = a_1 \cdot x_i$$

The only thing that changes in r^2 is \widehat{y}_i as y_i and \bar{y} only depends on the observed percentage of glare.

$$\widehat{y}_i^* = b_0^* + b_1^* \cdot x_i^*$$

$$b_0^* = \bar{y} - b_1^* \cdot \bar{x}^*$$

$$\bar{x}^* = \frac{1}{n} \sum_{i=1}^n x_i^* = \frac{1}{n} \sum_{i=1}^n (a_1 \cdot x_i) = a_1 \cdot \frac{1}{n} \sum_{i=1}^n x_i = a_1 \cdot \bar{x}$$

$$b_0^* = \bar{y} - b_1^* \cdot (a_1 \cdot \bar{x})$$

$$\begin{aligned} b_1^* &= \frac{\sum_{i=1}^n x_i^* (y_i - \bar{y})}{\sum_{i=1}^n x_i^* (x_i^* - \bar{x}^*)} = \frac{\sum_{i=1}^n (a_1 \cdot x_i) (y_i - \bar{y})}{\sum_{i=1}^n a_1 \cdot x_i (a_1 \cdot x_i - a_1 \cdot \bar{x})} = \\ &= \frac{a_1 \cdot \sum_{i=1}^n (x_i) (y_i - \bar{y})}{a_1^2 \cdot \sum_{i=1}^n (x_i) (x_i - \bar{x})} = \frac{\sum_{i=1}^n (x_i) (y_i - \bar{y})}{a_1 \cdot \sum_{i=1}^n (x_i) (x_i - \bar{x})} = \frac{b_1}{a_1} \end{aligned}$$

$$b_0^* = \bar{y} - b_1^* \cdot (a_1 \cdot \bar{x}) = \bar{y} - \frac{b_1}{a_1} \cdot (a_1 \cdot \bar{x}) = \bar{y} - b_1 \cdot \bar{x} = b_0$$

$$\widehat{y}_i^* = b_0^* + b_1^* \cdot x_i^* = b_0 + \frac{b_1}{a_1} \cdot (a_1 \cdot x_i) = b_0 + b_1 \cdot x_i = \widehat{y}_i$$

$$r^{*2} = \frac{\sum_{i=1}^n (y_i - \widehat{y}_i^*)^2}{\sum_{i=1}^n (y_i - \bar{y})^2} = \frac{\sum_{i=1}^n (y_i - \widehat{y}_i)^2}{\sum_{i=1}^n (y_i - \bar{y})^2} = r^2$$

The conclusion is then that r^2 does not change when x is multiplied with a constant.

Model development:

A combination of adding a constant to x and multiplying x with a constant such as

$$x_i^* = a_1 \cdot x_i + a_0$$

then also does not influence r^2 .

F.2 Optimisation tests

Description of the tests that were done to test the parameters of the optimisation, followed by the tables providing the detailed inputs and outputs of the tests.

Run 1: initial bounds

The first run of the genetic algorithm was carried out for very wide ranges of c_1 , c_2 , c_3 and c_4 (lower bound of 0 and upper bound of 20), a population of 50, 1000 iterations and a convergence setting of 100.

The values obtained for the constants were significantly below the values of the defined upper bounds for most of the coefficients, suggesting that these could be lowered.

The produced equations with these constants were also tested and it was verified that they produced very inflated values for DGP and UGP in relation to their original ranges (0-1), mainly due to the extremely high values obtained for c_4 in the case of DGP and for c_1 , in the case of UGP.

Run 2: adjusted bounds

The upper bounds of the constants were adjusted to values similar to the ones obtained for the constants in Run 1. This specifically meant a reduction of the upper bound of the c_1 and of the c_3 for DGP and DGPlog(Ev) and of the c_1 and c_2 for UGP.

As the value of DGP can be highly influenced by the value of the constant c_4 , the upper bound of this constant was set to the DGP's equation original value of 0.16.

A reduction of the upper bounds produced either a somewhat better r^2 or the same r^2 that was previously found.

Run 3, 4 and 5: adjusted bounds – UGP

Further reduction of the upper bounds of the UGP's constants c_1 and c_2 was tested. Although small, it is verified that there is a tendency for improvement of the r_2 as the upper bounds of the constants are reduced. There is a tendency for c_1 to take a value as high as its defined upper bound, while little changes occur for the value of c_2 . The values obtained for constant c_2 are generally much lower than the defined upper bound, revealing that the upper bound for this constant can be reduced.

Run 6 and 7: adjusted bounds – DGP

A test of a fixed c_3 of 2 for DGP and DGPlog(Ev) was performed and produced a significant reduction of the r_2 .

It was verified that the values obtained for the constant c_3 are always below 3. Therefore a test was done to find if an upper bound of 4 rather than 5 for c_3 would deliver better results. An improvement of the r_2 was not verified.

Run 8 and 9: population size

A reduction of the population size produced either a reduction or no modifications on the value of the r_2 .

An increase of the population size did not change the r_2 in most cases; it produced a small improvement of the r_2 in one case and a somewhat worse r_2 for another case, revealing that there was no clear benefit in increasing the population size.

Run 10, 11 and 12: different seed

A change of seed corresponds to a change in the generation of the initial population and more specifically to a different starting point for the search. The ideal situation is one where the solution does not change depending on the seed.

Three different seeds were tested in addition to the original one. It was verified that the changes in the r_2 resulting from different seeds were either very small or not enough to change the general performance tendency of the metrics in the different cases.

Run 13: increased number of iterations

A 10-fold increase in the number of iterations with no convergence setting was tested, which means that the search was run for 10,000 iterations.

An increase of the number of iterations produced an improved r_2 for some cases, with some change in their constants, while there was no change for the worst for the rest of the cases. Although the improvements are small, there are benefits in running the optimisation for a wider number of iterations, as modifications of the r_2 were verified beyond iteration 1,000.

The tables below show the detailed inputs and outputs of the optimisation parameter tests.

Run 1 - initial constant bounds

zone	metric	glare	c1_ lbound	c1_ ubound	c2_ lbound	c2_ ubound	c3_ lbound	c3_ ubound	c4_ lbound	c4_ ubound	c1_ suggest	c2_ suggest	c3_ suggest	c4_ suggest
wall	DGP	disturbing	0	20	0	20	0	20	0	20	5.87	9.18	1.87	0.16
wall	DGPlog(Ev)	disturbing	0	20	0	20	0	20	0	20	5.87	9.18	1.87	0.16
wall	UGP	disturbing	0	20	0	20	0	0	0	0	0.26	0.25	0	0
wall	DGP	any glare	0	20	0	20	0	20	0	20	5.87	9.18	1.87	0.16
wall	DGPlog(Ev)	any glare	0	20	0	20	0	20	0	20	5.87	9.18	1.87	0.16
wall	UGP	any glare	0	20	0	20	0	0	0	0	0.26	0.25	0	0
window	DGP	disturbing	0	20	0	20	0	20	0	20	5.87	9.18	1.87	0.16
window	DGPlog(Ev)	disturbing	0	20	0	20	0	20	0	20	5.87	9.18	1.87	0.16
window	UGP	disturbing	0	20	0	20	0	0	0	0	0.26	0.25	0	0
window	DGP	any glare	0	20	0	20	0	20	0	20	5.87	9.18	1.87	0.16
window	DGPlog(Ev)	any glare	0	20	0	20	0	20	0	20	5.87	9.18	1.87	0.16
window	UGP	any glare	0	20	0	20	0	0	0	0	0.26	0.25	0	0
zone	metric	glare	popsize	max- itera- tions	iter_ stop	seed	itera- tions	fitness_ val	c1_ solu- tion	c2_ solu- tion	c3_ solu- tion	c4_ solu- tion		
wall	DGP	disturbing	50	1000	100	12345	511	0.441	0.39	7.72	2.01	19.65		
wall	DGPlog(Ev)	disturbing	50	1000	100	12345	1000	0.856	7.33	13.46	3.09	11.37		
wall	UGP	disturbing	50	1000	100	12345	147	0.287	5.69	0.0927	0.00	0.00		
wall	DGP	any glare	50	1000	100	12345	400	0.838	1.10	18.27	1.50	12.39		
wall	DGPlog(Ev)	any glare	50	1000	100	12345	264	0.814	5.79	11.62	3.10	13.97		
wall	UGP	any glare	50	1000	100	12345	107	0.588	19.75	0.1525	0.00	0.00		
window	DGP	disturbing	50	1000	100	12345	237	0.620	0.28	14.81	1.85	12.64		
window	DGPlog(Ev)	disturbing	50	1000	100	12345	328	0.720	9.50	16.07	2.48	5.69		
window	UGP	disturbing	50	1000	100	12345	265	0.658	10.59	0.0547	0.00	0.00		
window	DGP	any glare	50	1000	100	12345	690	0.931	0.18	17.70	0.79	2.78		
window	DGPlog(Ev)	any glare	50	1000	100	12345	481	0.916	1.29	14.50	2.97	10.22		
window	UGP	any glare	50	1000	100	12345	186	0.727	7.77	0.1812	0.00	0.00		

Run 2 - adjusted bounds

zone	metric	glare	c1_ lbound	c1_ ubound	c2_ lbound	c2_ ubound	c3_ lbound	c3_ ubound	c4_ lbound	c4_ ubound	c1_ suggest	c2_ suggest	c3_ suggest	c4_ suggest
wall	DGP	disturbing	0	15	0	20	0	5	0	0.16	5.87	9.18	1.87	0.16
wall	DGPlog(Ev)	disturbing	0	15	0	20	0	5	0	0.16	5.87	9.18	1.87	0.16
wall	UGP	disturbing	0	15	0	1	0	0	0	0	0.26	0.25	0	0
wall	DGP	any glare	0	15	0	20	0	5	0	0.16	5.87	9.18	1.87	0.16
wall	DGPlog(Ev)	any glare	0	15	0	20	0	5	0	0.16	5.87	9.18	1.87	0.16
wall	UGP	any glare	0	15	0	1	0	0	0	0	0.26	0.25	0	0
window	DGP	disturbing	0	15	0	20	0	5	0	0.16	5.87	9.18	1.87	0.16
window	DGPlog(Ev)	disturbing	0	15	0	20	0	5	0	0.16	5.87	9.18	1.87	0.16
window	UGP	disturbing	0	15	0	1	0	0	0	0	0.26	0.25	0	0
window	DGP	any glare	0	15	0	20	0	5	0	0.16	5.87	9.18	1.87	0.16
window	DGPlog(Ev)	any glare	0	15	0	20	0	5	0	0.16	5.87	9.18	1.87	0.16
window	UGP	any glare	0	15	0	1	0	0	0	0	0.26	0.25	0	0
zone	metric	glare	popsize	max- itera- tions	iter_ stop	seed	itera- tions	fitness_ val	c1_ solu- tion	c2_ solu- tion	c3_ solu- tion	c4_ solu- tion		
wall	DGP	disturbing	50	1000	100	12345	347	0.435	6.75	3.42	0.03	0.10		
wall	DGPlog(Ev)	disturbing	50	1000	100	12345	732	0.855	6.09	10.50	3.08	0.06		
wall	UGP	disturbing	50	1000	100	12345	111	0.287	10.94	0.09	0.00	0.00		
wall	DGP	any glare	50	1000	100	12345	742	0.838	1.08	18.19	1.49	0.06		
wall	DGPlog(Ev)	any glare	50	1000	100	12345	651	0.788	6.39	7.10	3.02	0.10		
wall	UGP	any glare	50	1000	100	12345	118	0.655	7.78	0.05	0.00	0.00		
window	DGP	disturbing	50	1000	100	12345	251	0.621	0.23	13.06	1.84	0.09		
window	DGPlog(Ev)	disturbing	50	1000	100	12345	127	0.720	9.09	15.43	2.48	0.08		
window	UGP	disturbing	50	1000	100	12345	100	0.660	7.27	0.05	0.00	0.00		
window	DGP	any glare	50	1000	100	12345	666	0.931	0.18	17.94	0.79	0.02		
window	DGPlog(Ev)	any glare	50	1000	100	12345	250	0.931	7.84	8.06	0.77	0.11		
window	UGP	any glare	50	1000	100	12345	348	0.781	8.49	0.01	0.00	0.00		

Run 3, 4 and 5 - adjusted bounds – UGP

zone	metric	glare	c1_lbound	c1_ubound	c2_lbound	c2_ubound	c3_lbound	c3_ubound	c4_lbound	c4_ubound	c1_suggest	c2_suggest	c3_suggest	c4_suggest
wall	UGP	disturbing	0	1	0	1	0	0	0	0	0.26	0.25	0	0
wall	UGP	any glare	0	1	0	1	0	0	0	0	0.26	0.25	0	0
window	UGP	disturbing	0	1	0	1	0	0	0	0	0.26	0.25	0	0
window	UGP	any glare	0	1	0	1	0	0	0	0	0.26	0.25	0	0
zone	metric	glare	popsize	max-iterations	iter_stop	seed	iterations	fitness_val	c1_solution	c2_solution	c3_solution	c4_solution		
wall	UGP	disturbing	50	1000	100	12345	111	0.287	0.99	0.09	0.00	0.00		
wall	UGP	any glare	50	1000	100	12345	118	0.655	0.99	0.05	0.00	0.00		
window	UGP	disturbing	50	1000	100	12345	100	0.660	0.62	0.05	0.00	0.00		
window	UGP	any glare	50	1000	100	12345	348	0.781	0.26	0.01	0.00	0.00		
zone	metric	glare	c1_lbound	c1_ubound	c2_lbound	c2_ubound	c3_lbound	c3_ubound	c4_lbound	c4_ubound	c1_suggest	c2_suggest	c3_suggest	c4_suggest
wall	UGP	disturbing	0	0.2	0	0.2	0	0	0	0	0.26	0.25	0	0
wall	UGP	any glare	0	0.2	0	0.2	0	0	0	0	0.26	0.25	0	0
window	UGP	disturbing	0	0.2	0	0.2	0	0	0	0	0.26	0.25	0	0
window	UGP	any glare	0	0.2	0	0.2	0	0	0	0	0.26	0.25	0	0
zone	metric	glare	popsize	max-iterations	iter_stop	seed	iterations	fitness_val	c1_solution	c2_solution	c3_solution	c4_solution		
wall	UGP	disturbing	50	1000	100	12345	189	0.287	0.09	0.09	0.00	0.00		
wall	UGP	any glare	50	1000	100	12345	152	0.655	0.04	0.05	0.00	0.00		
window	UGP	disturbing	50	1000	100	12345	171	0.662	0.07	0.05	0.00	0.00		
window	UGP	any glare	50	1000	100	12345	178	0.814	0.06	0.002	0.00	0.00		
zone	metric	glare	c1_lbound	c1_ubound	c2_lbound	c2_ubound	c3_lbound	c3_ubound	c4_lbound	c4_ubound	c1_suggest	c2_suggest	c3_suggest	c4_suggest
wall	UGP	disturbing	0	0.26	0	0.15	0	0	0	0	0.26	0.25	0	0
wall	UGP	any glare	0	0.26	0	0.15	0	0	0	0	0.26	0.25	0	0
window	UGP	disturbing	0	0.26	0	0.15	0	0	0	0	0.26	0.25	0	0
window	UGP	any glare	0	0.26	0	0.15	0	0	0	0	0.26	0.25	0	0
zone	metric	glare	popsize	max-iterations	iter_stop	seed	iterations	fitness_val	c1_solution	c2_solution	c3_solution	c4_solution		
wall	UGP	disturbing	50	1000	100	12345	193	0.287	0.22	0.09	0.00	0.00		
wall	UGP	any glare	50	1000	100	12345	115	0.655	0.21	0.05	0.00	0.00		
window	UGP	disturbing	50	1000	100	12345	102	0.662	0.26	0.05	0.00	0.00		
window	UGP	any glare	50	1000	100	12345	354	0.814	0.23	0.002	0.00	0.00		

Run 6 and 7 - adjusted bounds – DGP

zone	metric	glare	c1_ lbound	c1_ ubound	c2_ lbound	c2_ ubound	c3_ lbound	c3_ ubound	c4_ lbound	c4_ ubound	c1_ suggest	c2_ suggest	c3_ suggest	c4_ suggest
wall	DGP	disturbing	0	15	0	20	2	2	0	0.16	5.87	9.18	1.87	0.16
wall	DGPlog(Ev)	disturbing	0	15	0	20	2	2	0	0.16	5.87	9.18	1.87	0.16
wall	DGP	any glare	0	15	0	20	2	2	0	0.16	5.87	9.18	1.87	0.16
wall	DGPlog(Ev)	any glare	0	15	0	20	2	2	0	0.16	5.87	9.18	1.87	0.16
window	DGP	disturbing	0	15	0	20	2	2	0	0.16	5.87	9.18	1.87	0.16
window	DGPlog(Ev)	disturbing	0	15	0	20	2	2	0	0.16	5.87	9.18	1.87	0.16
window	DGP	any glare	0	15	0	20	2	2	0	0.16	5.87	9.18	1.87	0.16
window	DGPlog(Ev)	any glare	0	15	0	20	2	2	0	0.16	5.87	9.18	1.87	0.16
zone	metric	glare	popsize	max- itera- tions	iter_ stop	seed	itera- tions	fitness_ val	c1_ solu- tion	c2_ solu- tion	c3_ solu- tion	c4_ solu- tion		
wall	DGP	disturbing	50	1000	100	12345	357	0.441	0.72	14.10	2.00	0.07		
wall	DGPlog(Ev)	disturbing	50	1000	100	12345	205	0.404	10.89	0.14	2.00	0.12		
wall	DGP	any glare	50	1000	100	12345	209	0.779	0.55	14.89	2.00	0.09		
wall	DGPlog(Ev)	any glare	50	1000	100	12345	335	0.645	8.11	3.55	1.93	0.12		
window	DGP	disturbing	50	1000	100	12345	125	0.613	0.24	13.06	1.95	0.06		
window	DGPlog(Ev)	disturbing	50	1000	100	12345	141	0.697	10.36	1.01	2.00	0.14		
window	DGP	any glare	50	1000	100	12345	162	0.588	0.67	13.23	2.00	0.07		
window	DGPlog(Ev)	any glare	50	1000	100	12345	301	0.836	14.92	0.05	2.00	0.09		
zone	metric	glare	c1_ lbound	c1_ ubound	c2_ lbound	c2_ ubound	c3_ lbound	c3_ ubound	c4_ lbound	c4_ ubound	c1_ suggest	c2_ suggest	c3_ suggest	c4_ suggest
wall	DGP	disturbing	0	15	0	20	0	4	0	0.16	5.87	9.18	1.87	0.16
wall	DGPlog(Ev)	disturbing	0	15	0	20	0	4	0	0.16	5.87	9.18	1.87	0.16
wall	DGP	any glare	0	15	0	20	0	4	0	0.16	5.87	9.18	1.87	0.16
wall	DGPlog(Ev)	any glare	0	15	0	20	0	4	0	0.16	5.87	9.18	1.87	0.16
window	DGP	disturbing	0	15	0	20	0	4	0	0.16	5.87	9.18	1.87	0.16
window	DGPlog(Ev)	disturbing	0	15	0	20	0	4	0	0.16	5.87	9.18	1.87	0.16
window	DGP	any glare	0	15	0	20	0	4	0	0.16	5.87	9.18	1.87	0.16
window	DGPlog(Ev)	any glare	0	15	0	20	0	4	0	0.16	5.87	9.18	1.87	0.16
zone	metric	glare	popsize	max- itera- tions	iter_ stop	seed	itera- tions	fitness_ val	c1_ solu- tion	c2_ solu- tion	c3_ solu- tion	c4_ solu- tion		
wall	DGP	disturbing	50	1000	100	12345	727	0.383	1.59	12.76	1.18	0.07		
wall	DGPlog(Ev)	disturbing	50	1000	100	12345	1000	0.855	7.47	13.27	3.08	0.07		
wall	DGP	any glare	50	1000	100	12345	404	0.838	1.20	19.51	1.50	0.05		
wall	DGPlog(Ev)	any glare	50	1000	100	12345	119	0.788	8.86	10.65	3.03	0.14		
window	DGP	disturbing	50	1000	100	12345	361	0.568	3.13	13.69	1.56	0.12		
window	DGPlog(Ev)	disturbing	50	1000	100	12345	123	0.742	0.10	17.72	2.69	0.14		
window	DGP	any glare	50	1000	100	12345	453	0.931	0.20	15.91	0.80	0.10		
window	DGPlog(Ev)	any glare	50	1000	100	12345	365	0.931	13.07	1.64	0.78	0.10		

Run 8 and 9 - population size

zone	metric	glare	c1_ lbound	c1_ ubound	c2_ lbound	c2_ ubound	c3_ lbound	c3_ ubound	c4_ lbound	c4_ ubound	c1_ suggest	c2_ suggest	c3_ suggest	c4_ suggest
wall	DGP	disturbing	0	15	0	20	0	5	0	0.16	5.87	9.18	1.87	0.16
wall	DGPlog(Ev)	disturbing	0	15	0	20	0	5	0	0.16	5.87	9.18	1.87	0.16
wall	UGP	disturbing	0	1	0	1	0	0	0	0	0.26	0.25	0	0
wall	DGP	any glare	0	15	0	20	0	5	0	0.16	5.87	9.18	1.87	0.16
wall	DGPlog(Ev)	any glare	0	15	0	20	0	5	0	0.16	5.87	9.18	1.87	0.16
wall	UGP	any glare	0	1	0	1	0	0	0	0	0.26	0.25	0	0
window	DGP	disturbing	0	15	0	20	0	5	0	0.16	5.87	9.18	1.87	0.16
window	DGPlog(Ev)	disturbing	0	15	0	20	0	5	0	0.16	5.87	9.18	1.87	0.16
window	UGP	disturbing	0	1	0	1	0	0	0	0	0.26	0.25	0	0
window	DGP	any glare	0	15	0	20	0	5	0	0.16	5.87	9.18	1.87	0.16
window	DGPlog(Ev)	any glare	0	15	0	20	0	5	0	0.16	5.87	9.18	1.87	0.16
window	UGP	any glare	0	1	0	1	0	0	0	0	0.26	0.25	0	0
zone	metric	glare	popsi ze	max- itera- tions	iter_ stop	seed	itera- tions	fitness_ val	c1_ solu- tion	c2_ solu- tion	c3_ solu- tion	c4_ solu- tion		
wall	DGP	disturbing	25	1000	100	12345	322	0.430	7.95	3.94	0.10	0.09		
wall	DGPlog(Ev)	disturbing	25	1000	100	12345	352	0.854	5.83	8.44	3.04	0.08		
wall	UGP	disturbing	25	1000	100	12345	173	0.287	0.60	0.09	0.00	0.00		
wall	DGP	any glare	25	1000	100	12345	794	0.838	0.94	14.99	1.51	0.16		
wall	DGPlog(Ev)	any glare	25	1000	100	12345	200	0.769	11.25	11.90	2.97	0.02		
wall	UGP	any glare	25	1000	100	12345	106	0.655	0.54	0.05	0.00	0.00		
window	DGP	disturbing	25	1000	100	12345	312	0.568	2.61	12.13	1.57	0.11		
window	DGPlog(Ev)	disturbing	25	1000	100	12345	221	0.718	6.23	13.33	2.52	0.14		
window	UGP	disturbing	25	1000	100	12345	176	0.662	0.34	0.05	0.00	0.00		
window	DGP	any glare	25	1000	100	12345	348	0.808	4.47	15.73	0.39	0.04		
window	DGPlog(Ev)	any glare	25	1000	100	12345	290	0.931	6.13	3.00	0.77	0.14		
window	UGP	any glare	25	1000	100	12345	343	0.778	0.21	0.01	0.00	0.00		
zone	metric	glare	c1_ lbound	c1_ ubound	c2_ lbound	c2_ ubound	c3_ lbound	c3_ ubound	c4_ lbound	c4_ ubound	c1_ suggest	c2_ suggest	c3_ suggest	c4_ suggest
wall	DGP	disturbing	0	15	0	20	0	5	0	0.16	5.87	9.18	1.87	0.16
wall	DGPlog(Ev)	disturbing	0	15	0	20	0	5	0	0.16	5.87	9.18	1.87	0.16
wall	UGP	disturbing	0	1	0	1	0	0	0	0	0.26	0.25	0	0
wall	DGP	any glare	0	15	0	20	0	5	0	0.16	5.87	9.18	1.87	0.16
wall	DGPlog(Ev)	any glare	0	15	0	20	0	5	0	0.16	5.87	9.18	1.87	0.16
wall	UGP	any glare	0	1	0	1	0	0	0	0	0.26	0.25	0	0
window	DGP	disturbing	0	15	0	20	0	5	0	0.16	5.87	9.18	1.87	0.16
window	DGPlog(Ev)	disturbing	0	15	0	20	0	5	0	0.16	5.87	9.18	1.87	0.16
window	UGP	disturbing	0	1	0	1	0	0	0	0	0.26	0.25	0	0
window	DGP	any glare	0	15	0	20	0	5	0	0.16	5.87	9.18	1.87	0.16
window	DGPlog(Ev)	any glare	0	15	0	20	0	5	0	0.16	5.87	9.18	1.87	0.16
window	UGP	any glare	0	1	0	1	0	0	0	0	0.26	0.25	0	0

>>>

Run 8 and 9 - population size

zone	metric	glare	popsize	max-iterations	iter_stop	seed	iterations	fitness_val	c1_solution	c2_solution	c3_solution	c4_solution		
wall	DGP	disturbing	100	1000	100	12345	356	0.436	9.49	4.82	0.02	0.06		
wall	DGPlog(Ev)	disturbing	100	1000	100	12345	1000	0.856	7.97	15.04	3.09	0.06		
wall	UGP	disturbing	100	1000	100	12345	100	0.287	0.49	0.09	0.00	0.00		
wall	DGP	any glare	100	1000	100	12345	578	0.838	1.12	19.49	1.49	0.09		
wall	DGPlog(Ev)	any glare	100	1000	100	12345	185	0.822	9.75	3.21	2.75	0.12		
wall	UGP	any glare	100	1000	100	12345	139	0.655	0.44	0.05	0.00	0.00		
window	DGP	disturbing	100	1000	100	12345	485	0.568	3.51	15.38	1.56	0.03		
window	DGPlog(Ev)	disturbing	100	1000	100	12345	185	0.720	6.83	11.55	2.48	0.07		
window	UGP	disturbing	100	1000	100	12345	173	0.662	0.59	0.05	0.00	0.00		
window	DGP	any glare	100	1000	100	12345	1000	0.931	0.19	18.86	0.79	0.06		
window	DGPlog(Ev)	any glare	100	1000	100	12345	185	0.931	8.39	0.47	0.79	0.06		
window	UGP	any glare	100	1000	100	12345	301	0.781	0.47	0.01	0.00	0.00		

Run 10, 11 and 12 - different seed

zone	metric	glare	c1_lbound	c1_ubound	c2_lbound	c2_ubound	c3_lbound	c3_ubound	c4_lbound	c4_ubound	c1_suggest	c2_suggest	c3_suggest	c4_suggest
wall	DGP	disturbing	0	15	0	20	0	5	0	0.16	5.87	9.18	1.87	0.16
wall	DGPlog(Ev)	disturbing	0	15	0	20	0	5	0	0.16	5.87	9.18	1.87	0.16
wall	UGP	disturbing	0	0.26	0	0.15	0	0	0	0	0.26	0.25	0	0
wall	DGP	any glare	0	15	0	20	0	5	0	0.16	5.87	9.18	1.87	0.16
wall	DGPlog(Ev)	any glare	0	15	0	20	0	5	0	0.16	5.87	9.18	1.87	0.16
wall	UGP	any glare	0	0.26	0	0.15	0	0	0	0	0.26	0.25	0	0
window	DGP	disturbing	0	15	0	20	0	5	0	0.16	5.87	9.18	1.87	0.16
window	DGPlog(Ev)	disturbing	0	15	0	20	0	5	0	0.16	5.87	9.18	1.87	0.16
window	UGP	disturbing	0	0.26	0	0.15	0	0	0	0	0.26	0.25	0	0
window	DGP	any glare	0	15	0	20	0	5	0	0.16	5.87	9.18	1.87	0.16
window	DGPlog(Ev)	any glare	0	15	0	20	0	5	0	0.16	5.87	9.18	1.87	0.16
window	UGP	any glare	0	0.26	0	0.15	0	0	0	0	0.26	0.25	0	0
zone	metric	glare	popsiz	max-iterations	iter_stop	seed	iterations	fitness_val	c1_solution	c2_solution	c3_solution	c4_solution		
wall	DGP	disturbing	50	1000	100	31254	440	0.436	7.69	3.91	0.01	0.11		
wall	DGPlog(Ev)	disturbing	50	1000	100	31254	788	0.856	6.20	11.67	3.09	0.07		
wall	UGP	disturbing	50	1000	100	31254	226	0.287	0.08	0.09	0.00	0.00		
wall	DGP	any glare	50	1000	100	31254	802	0.838	0.99	17.50	1.49	0.05		
wall	DGPlog(Ev)	any glare	50	1000	100	31254	184	0.791	6.88	10.13	3.03	0.08		
wall	UGP	any glare	50	1000	100	31254	109	0.655	0.07	0.05	0.00	0.00		
window	DGP	disturbing	50	1000	100	31254	596	0.568	2.72	11.92	1.56	0.08		
window	DGPlog(Ev)	disturbing	50	1000	100	31254	251	0.720	7.21	12.20	2.48	0.10		
window	UGP	disturbing	50	1000	100	31254	141	0.662	0.07	0.05	0.00	0.00		
window	DGP	any glare	50	1000	100	31254	651	0.931	0.13	17.95	0.79	0.07		
window	DGPlog(Ev)	any glare	50	1000	100	31254	137	0.931	9.29	10.64	0.77	0.07		
window	UGP	any glare	50	1000	100	31254	368	0.814	0.23	0.00	0.00	0.00		
zone	metric	glare	c1_lbound	c1_ubound	c2_lbound	c2_ubound	c3_lbound	c3_ubound	c4_lbound	c4_ubound	c1_suggest	c2_suggest	c3_suggest	c4_suggest
wall	DGP	disturbing	0	15	0	20	0	5	0	0.16	5.87	9.18	1.87	0.16
wall	DGPlog(Ev)	disturbing	0	15	0	20	0	5	0	0.16	5.87	9.18	1.87	0.16
wall	UGP	disturbing	0	0.26	0	0.15	0	0	0	0	0.26	0.25	0	0
wall	DGP	any glare	0	15	0	20	0	5	0	0.16	5.87	9.18	1.87	0.16
wall	DGPlog(Ev)	any glare	0	15	0	20	0	5	0	0.16	5.87	9.18	1.87	0.16
wall	UGP	any glare	0	0.26	0	0.15	0	0	0	0	0.26	0.25	0	0
window	DGP	disturbing	0	15	0	20	0	5	0	0.16	5.87	9.18	1.87	0.16
window	DGPlog(Ev)	disturbing	0	15	0	20	0	5	0	0.16	5.87	9.18	1.87	0.16
window	UGP	disturbing	0	0.26	0	0.15	0	0	0	0	0.26	0.25	0	0
window	DGP	any glare	0	15	0	20	0	5	0	0.16	5.87	9.18	1.87	0.16
window	DGPlog(Ev)	any glare	0	15	0	20	0	5	0	0.16	5.87	9.18	1.87	0.16
window	UGP	any glare	0	0.26	0	0.15	0	0	0	0	0.26	0.25	0	0

>>>

Run 10, 11 and 12 - different seed

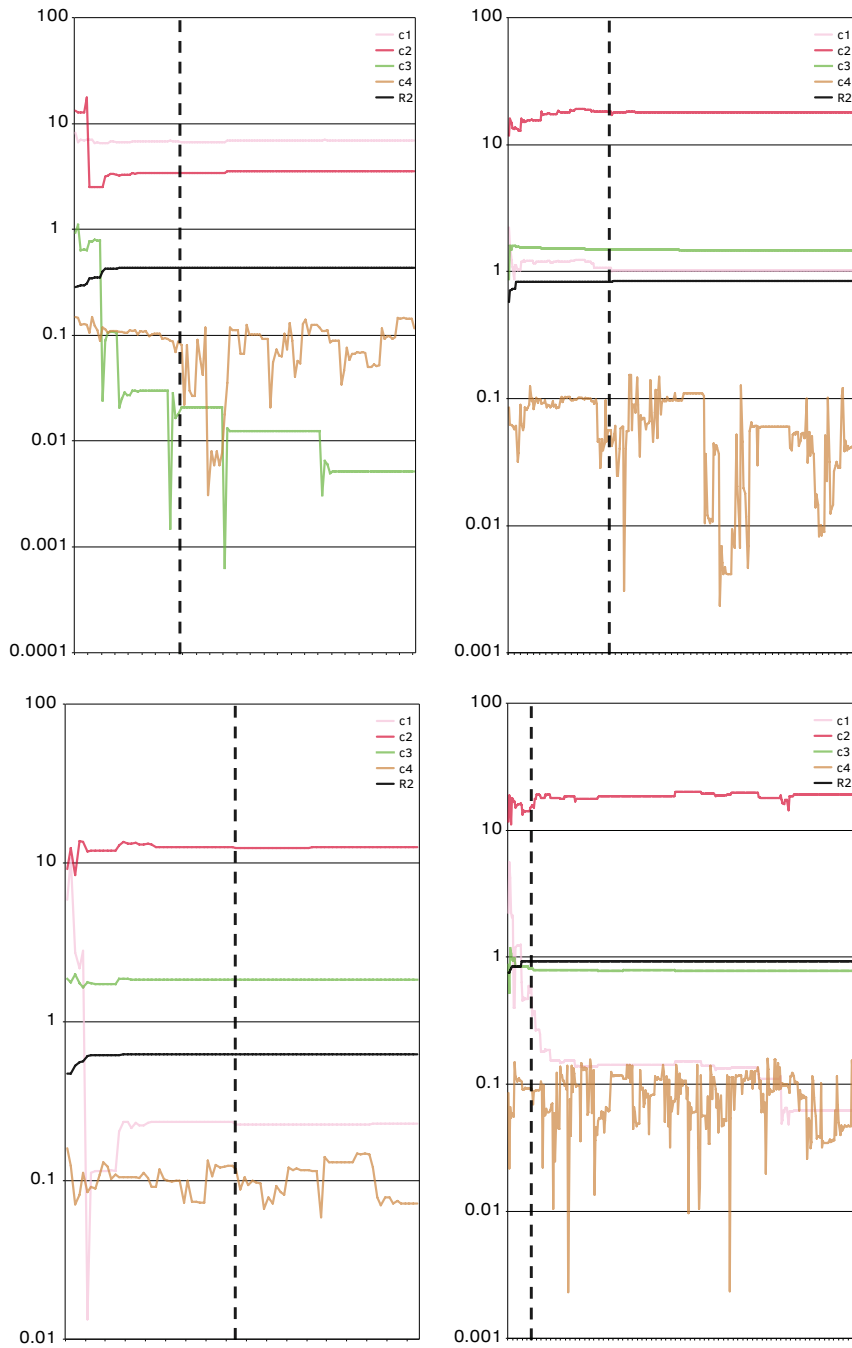
zone	metric	glare	popsize	max-iterations	iter_stop	seed	iterations	fitness_val	c1_solution	c2_solution	c3_solution	c4_solution		
wall	DGP	disturbing	50	1000	100	24153	738	0.435	8.09	4.09	0.03	0.09		
wall	DGPlog(Ev)	disturbing	50	1000	100	24153	233	0.776	12.57	8.01	2.93	0.07		
wall	UGP	disturbing	50	1000	100	24153	125	0.287	0.16	0.09	0.00	0.00		
wall	DGP	any glare	50	1000	100	24153	279	0.732	1.51	16.13	1.13	0.07		
wall	DGPlog(Ev)	any glare	50	1000	100	24153	376	0.791	8.78	12.94	3.03	0.08		
wall	UGP	any glare	50	1000	100	24153	332	0.655	0.00	0.05	0.00	0.00		
window	DGP	disturbing	50	1000	100	24153	485	0.568	3.00	13.15	1.56	0.04		
window	DGPlog(Ev)	disturbing	50	1000	100	24153	329	0.720	5.87	9.92	2.48	0.06		
window	UGP	disturbing	50	1000	100	24153	186	0.662	0.18	0.05	0.00	0.00		
window	DGP	any glare	50	1000	100	24153	379	0.931	0.27	18.69	0.80	0.07		
window	DGPlog(Ev)	any glare	50	1000	100	24153	332	0.931	8.56	0.91	0.78	0.08		
window	UGP	any glare	50	1000	100	24153	218	0.781	0.14	0.01	0.00	0.00		
zone	metric	glare	c1_lbound	c1_ubound	c2_lbound	c2_ubound	c3_lbound	c3_ubound	c4_lbound	c4_ubound	c1_suggest	c2_suggest	c3_suggest	c4_suggest
wall	DGP	disturbing	0	15	0	20	0	5	0	0.16	5.87	9.18	1.87	0.16
wall	DGPlog(Ev)	disturbing	0	15	0	20	0	5	0	0.16	5.87	9.18	1.87	0.16
wall	UGP	disturbing	0	0.26	0	0.15	0	0	0	0	0.26	0.25	0	0
wall	DGP	any glare	0	15	0	20	0	5	0	0.16	5.87	9.18	1.87	0.16
wall	DGPlog(Ev)	any glare	0	15	0	20	0	5	0	0.16	5.87	9.18	1.87	0.16
wall	UGP	any glare	0	0.26	0	0.15	0	0	0	0	0.26	0.25	0	0
window	DGP	disturbing	0	15	0	20	0	5	0	0.16	5.87	9.18	1.87	0.16
window	DGPlog(Ev)	disturbing	0	15	0	20	0	5	0	0.16	5.87	9.18	1.87	0.16
window	UGP	disturbing	0	0.26	0	0.15	0	0	0	0	0.26	0.25	0	0
window	DGP	any glare	0	15	0	20	0	5	0	0.16	5.87	9.18	1.87	0.16
window	DGPlog(Ev)	any glare	0	15	0	20	0	5	0	0.16	5.87	9.18	1.87	0.16
window	UGP	any glare	0	0.26	0	0.15	0	0	0	0	0.26	0.25	0	0
zone	metric	glare	popsize	max-iterations	iter_stop	seed	iterations	fitness_val	c1_solution	c2_solution	c3_solution	c4_solution		
wall	DGP	disturbing	50	1000	100	52134	612	0.436	4.69	2.38	0.02	0.09		
wall	DGPlog(Ev)	disturbing	50	1000	100	52134	817	0.856	7.78	14.64	3.09	0.03		
wall	UGP	disturbing	50	1000	100	52134	157	0.287	0.16	0.09	0.00	0.00		
wall	DGP	any glare	50	1000	100	52134	839	0.838	1.03	18.07	1.49	0.03		
wall	DGPlog(Ev)	any glare	50	1000	100	24153	376	0.791	8.78	12.94	3.03	0.08		
wall	UGP	any glare	50	1000	100	52134	207	0.655	0.10	0.05	0.00	0.00		
window	DGP	disturbing	50	1000	100	52134	132	0.612	0.27	16.25	1.82	0.04		
window	DGPlog(Ev)	disturbing	50	1000	100	52134	350	0.720	7.59	12.83	2.48	0.12		
window	UGP	disturbing	50	1000	100	52134	230	0.662	0.10	0.05	0.00	0.00		
window	DGP	any glare	50	1000	100	52134	481	0.931	0.19	18.75	0.79	0.08		
window	DGPlog(Ev)	any glare	50	1000	100	52134	236	0.931	10.08	1.65	0.78	0.03		
window	UGP	any glare	50	1000	100	52134	291	0.781	0.11	0.01	0.00	0.00		

Run 13 - increased iterations

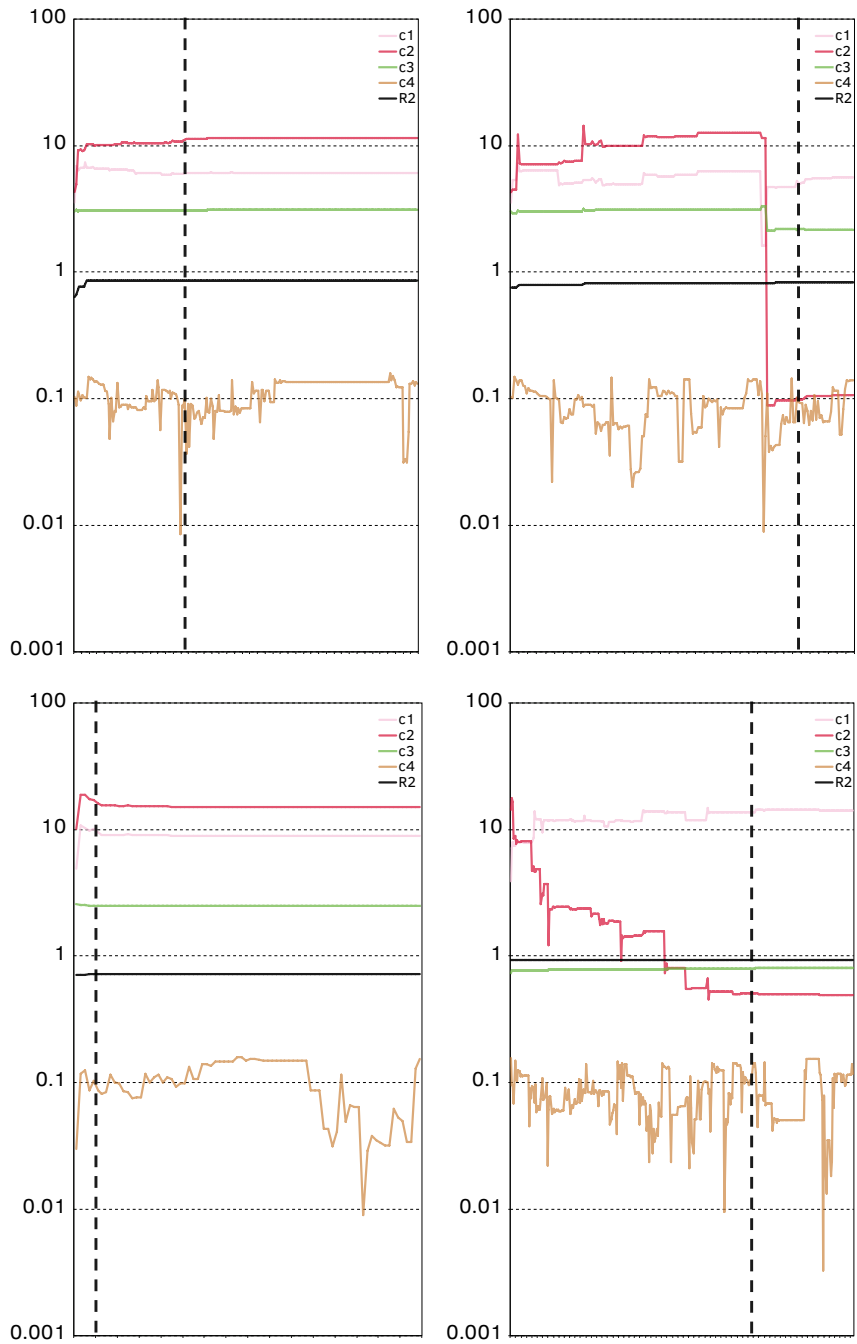
zone	metric	glare	c1_ lbound	c1_ ubound	c2_ lbound	c2_ ubound	c3_ lbound	c3_ ubound	c4_ lbound	c4_ ubound	c1_ suggest	c2_ suggest	c3_ suggest	c4_ suggest
wall	DGP	disturbing	0	15	0	20	0	5	0	0.16	5.87	9.18	1.87	0.16
wall	DGPlog(Ev)	disturbing	0	15	0	20	0	5	0	0.16	5.87	9.18	1.87	0.16
wall	UGP	disturbing	0	0.26	0	0.15	0	0	0	0	0.26	0.25	0	0
wall	DGP	any glare	0	15	0	20	0	5	0	0.16	5.87	9.18	1.87	0.16
wall	DGPlog(Ev)	any glare	0	15	0	20	0	5	0	0.16	5.87	9.18	1.87	0.16
wall	UGP	any glare	0	0.26	0	0.15	0	0	0	0	0.26	0.25	0	0
window	DGP	disturbing	0	15	0	20	0	5	0	0.16	5.87	9.18	1.87	0.16
window	DGPlog(Ev)	disturbing	0	15	0	20	0	5	0	0.16	5.87	9.18	1.87	0.16
window	UGP	disturbing	0	0.26	0	0.15	0	0	0	0	0.26	0.25	0	0
window	DGP	any glare	0	15	0	20	0	5	0	0.16	5.87	9.18	1.87	0.16
window	DGPlog(Ev)	any glare	0	15	0	20	0	5	0	0.16	5.87	9.18	1.87	0.16
window	UGP	any glare	0	0.26	0	0.15	0	0	0	0	0.26	0.25	0	0
zone	metric	glare	popsi ze	max- itera- tions	iter_ stop	seed	itera- tions	fitness_ val	c1_ solu- tion	c2_ solu- tion	c3_ solu- tion	c4_ solu- tion		
wall	DGP	disturbing	50	10000	4177	12345	10000	0.437	6.94	3.54	0.01	0.12		
wall	DGPlog(Ev)	disturbing	50	10000	1328	12345	10000	0.856	6.12	11.50	3.09	0.13		
wall	UGP	disturbing	50	10000	7196	12345	10000	0.287	0.21	0.09	0.00	0.00		
wall	DGP	any glare	50	10000	5059	12345	10000	0.838	1.02	18.06	1.49	0.04		
wall	DGPlog(Ev)	any glare	50	10000	72	12345	10000	0.833	5.59	0.11	2.17	0.14		
wall	UGP	any glare	50	10000	1799	12345	10000	0.655	0.12	0.05	0.00	0.00		
window	DGP	disturbing	50	10000	1000	12345	10000	0.622	0.23	12.59	1.83	0.07		
window	DGPlog(Ev)	disturbing	50	10000	813	12345	10000	0.720	8.91	15.07	2.48	0.15		
window	UGP	disturbing	50	10000	4219	12345	10000	0.662	0.04	0.05	0.00	0.00		
window	DGP	any glare	50	10000	772	12345	10000	0.931	0.06	19.19	0.78	0.13		
window	DGPlog(Ev)	any glare	50	10000	818	12345	10000	0.931	14.08	0.49	0.80	0.12		
window	UGP	any glare	50	10000	6919	12345	10000	0.814	0.13	0.00	0.00	0.00		

F.3 Constants' plots

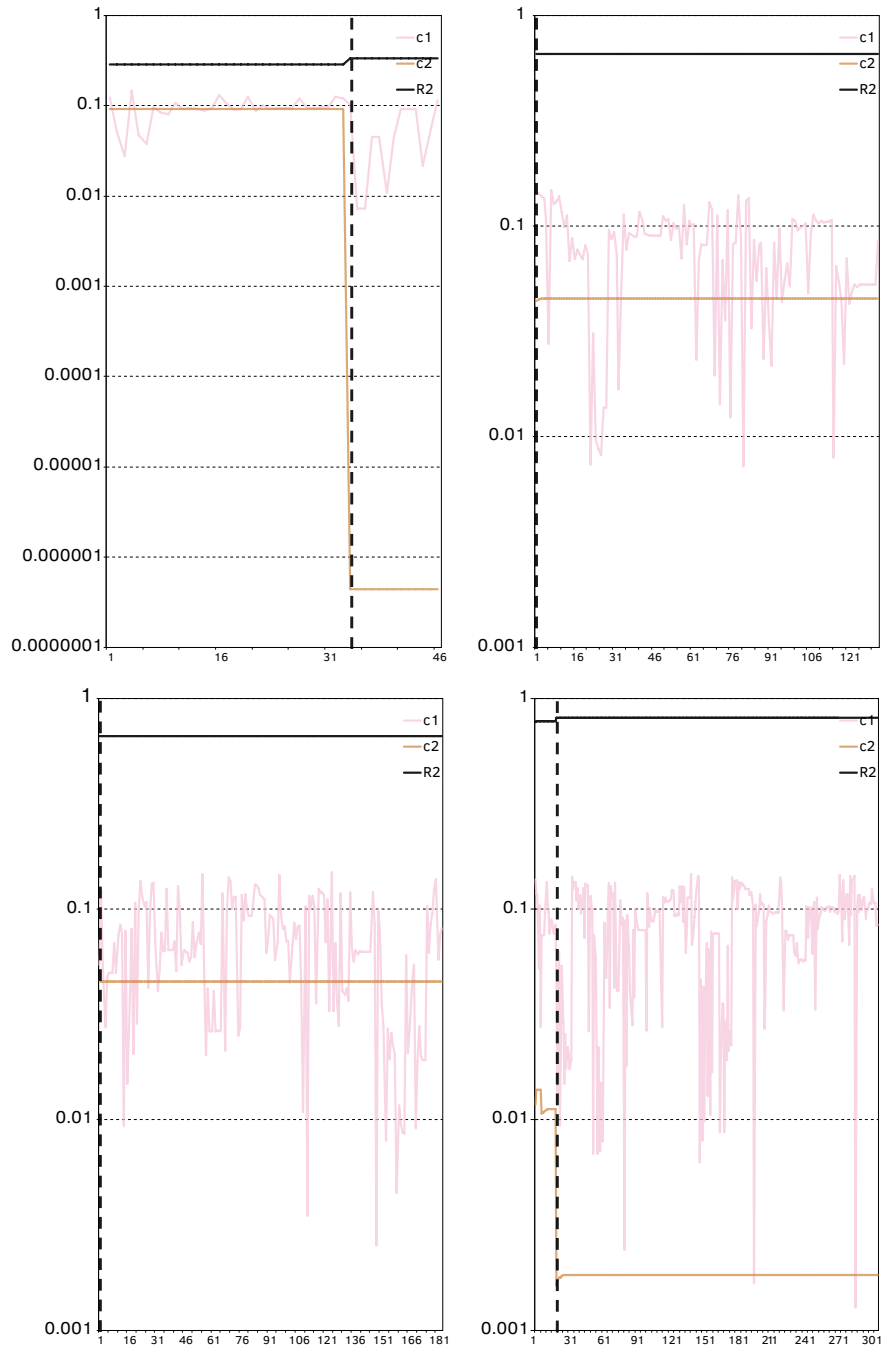
The plots show the constants obtained for every improvement of the r_2 , for a variable DGP and $DGP\log(E_v)$ of c_4 and for a variable c_1 of the UGP. As an improved r_2 is not always found for every iteration, the number of data points in these plots (x-axis) is lower than the total number of iterations. The vertical black line shows the iteration from which the r_2 stabilises to its best result.



Constants' plots for DGP; top-left: wall/disturbing; top-right: wall/any glare; bottom-left: window/disturbing and bottom-right: window/any glare.



Constants' plots for DGPlot(Ev); top-left: wall/disturbing; top-right: wall/any glare; bottom-left: window/disturbing and bottom-right: window/any glare.



Constants' plots for UGP; top-left: wall/disturbing; top-right: wall/any glare; bottom-left: window/disturbing and bottom-right: window/any glare.

F.4 Optimisation 1: inputs and outputs

CaptionHere DGP and DGPlag(Ev) with a c4 of 0.16 and UGP with c1 of 0.26

zone	metric	glare	c1_ lbound	c1_ ubound	c2_ lbound	c2_ ubound	c3_ lbound	c3_ ubound	c4_ lbound	c4_ ubound	c1_ suggest	c2_ suggest	c3_ suggest	c4_ suggest
wall	DGP	disturbing	0	15	0	20	0	5	0.16	0.16	5.87	9.18	1.87	0.16
wall	DGPlag(Ev)	disturbing	0	15	0	20	0	5	0.16	0.16	5.87	9.18	1.87	0.16
wall	UGP	disturbing	0.26	0.26	0	0.15	0	0	0	0	0.26	0.25	0	0
wall	DGP	any glare	0	15	0	20	0	5	0.16	0.16	5.87	9.18	1.87	0.16
wall	DGPlag(Ev)	any glare	0	15	0	20	0	5	0.16	0.16	5.87	9.18	1.87	0.16
wall	UGP	any glare	0.26	0.26	0	0.15	0	0	0	0	0.26	0.25	0	0
window	DGP	disturbing	0	15	0	20	0	5	0.16	0.16	5.87	9.18	1.87	0.16
window	DGPlag(Ev)	disturbing	0	15	0	20	0	5	0.16	0.16	5.87	9.18	1.87	0.16
window	UGP	disturbing	0.26	0.26	0	0.15	0	0	0	0	0.26	0.25	0	0
window	DGP	any glare	0	15	0	20	0	5	0.16	0.16	5.87	9.18	1.87	0.16
window	DGPlag(Ev)	any glare	0	15	0	20	0	5	0.16	0.16	5.87	9.18	1.87	0.16
window	UGP	any glare	0.26	0.26	0	0.15	0	0	0	0	0.26	0.25	0	0
zone	metric	glare	popsize	max- iterations	iter_ stop	seed	itera- tions	fitness_ val	c1_ solu- tion	c2_ solu- tion	c3_ solu- tion	c4_ solu- tion		
wall	DGP	disturbing	50	10000	685	12345	10000	0.437	7.14	3.65	0.00	0.16		
wall	DGPlag(Ev)	disturbing	50	10000	5988	12345	10000	0.856	5.29	9.94	3.09	0.16		
wall	UGP	disturbing	50	10000	2472	12345	10000	0.287	0.26	0.09	0.00	0.00		
wall	DGP	any glare	50	10000	5151	12345	10000	0.838	1.05	18.52	1.49	0.16		
wall	DGPlag(Ev)	any glare	50	10000	1617	12345	10000	0.814	6.64	13.41	3.10	0.16		
wall	UGP	any glare	50	10000	5781	12345	10000	0.655	0.26	0.05	0.00	0.00		
window	DGP	disturbing	50	10000	3643	12345	10000	0.622	0.25	13.76	1.82	0.16		
window	DGPlag(Ev)	disturbing	50	10000	2297	12345	10000	0.720	7.86	13.29	2.48	0.16		
window	UGP	disturbing	50	10000	5227	12345	10000	0.662	0.26	0.05	0.00	0.00		
window	DGP	any glare	50	10000	2484	12345	10000	0.931	0.05	19.24	0.78	0.16		
window	DGPlag(Ev)	any glare	50	10000	2626	12345	10000	0.931	11.76	0.40	0.80	0.16		
window	UGP	any glare	50	10000	3185	12345	10000	0.814	0.26	0.00	0.00	0.00		

F.5 Optimisation 2: inputs and outputs

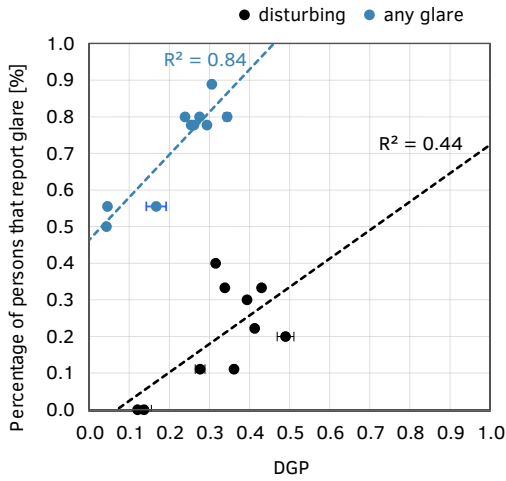
DGP and DGPllog(Ev), with a c4 of 0.

position	parameter	glare	c1_lbound	c1_ubound	c2_lbound	c2_ubound	c3_lbound	c3_ubound	c4_lbound	c4_ubound	c1_suggest	c2_suggest	c3_suggest	c4_suggest
wall	DGP	disturbing	0	15	0	20	0	5	0	0	5.87	9.18	1.87	0
wall	DGPllog(Ev)	disturbing	0	15	0	20	0	5	0	0	5.87	9.18	1.87	0
wall	DGP	any glare	0	15	0	20	0	5	0	0	5.87	9.18	1.87	0
wall	DGPllog(Ev)	any glare	0	15	0	20	0	5	0	0	5.87	9.18	1.87	0
window	DGP	disturbing	0	15	0	20	0	5	0	0	5.87	9.18	1.87	0
window	DGPllog(Ev)	disturbing	0	15	0	20	0	5	0	0	5.87	9.18	1.87	0
window	DGP	any glare	0	15	0	20	0	5	0	0	5.87	9.18	1.87	0
window	DGPllog(Ev)	any glare	0	15	0	20	0	5	0	0	5.87	9.18	1.87	0

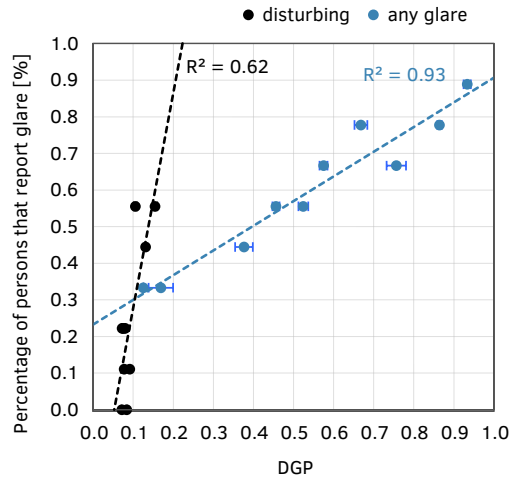
position	parameter	glare	popsiz	max-iterations	iter_stop	seed	iterations	fitness_val	c1_solution	c2_solution	c3_solution	c4_solution		
wall	DGP	disturbing	50	10000	139	12345	10000	0.437	6.60	3.37	0.00	0		
wall	DGPllog(Ev)	disturbing	50	10000	7923	12345	10000	0.856	5.37	10.09	3.09	0		
wall	DGP	any glare	50	10000	2941	12345	10000	0.838	0.96	16.98	1.49	0		
wall	DGPllog(Ev)	any glare	50	10000	2242	12345	10000	0.823	7.13	2.34	2.75	0		
window	DGP	disturbing	50	10000	729	12345	10000	0.568	2.95	12.92	1.56	0		
window	DGPllog(Ev)	disturbing	50	10000	4431	12345	10000	0.720	7.74	13.08	2.48	0		
window	DGP	any glare	50	10000	4350	12345	10000	0.931	0.08	17.70	0.78	0		
window	DGPllog(Ev)	any glare	50	10000	2517	12345	10000	0.931	12.77	0.43	0.80	0		

F.6 Additional scatter plots

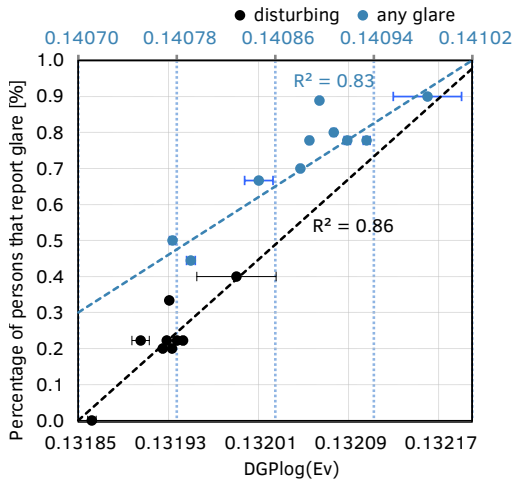
Additional scatter plots showing results of the 'disturbing' and 'any glare' optimised equations, in the same plot for optimisation 1.



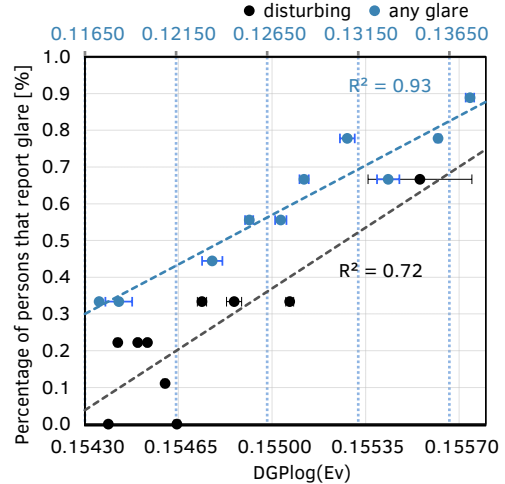
DGP, Wall



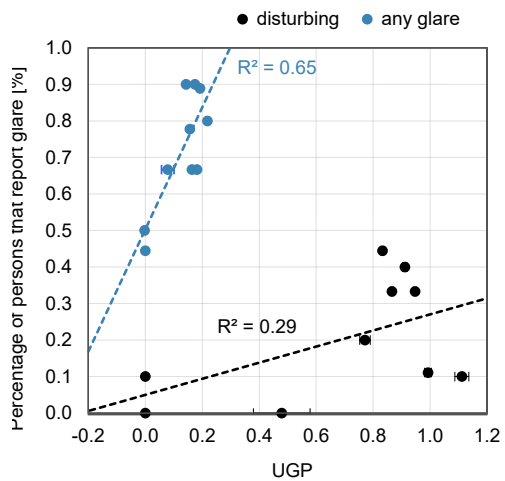
DGP, Window



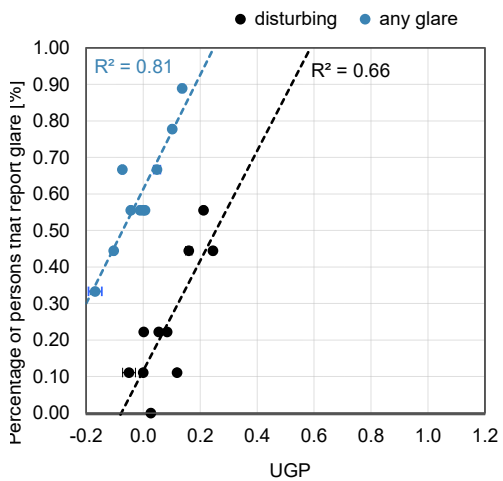
DGPlog(Ev), Wall



DGPlog(Ev), Window



UGP, Wall



UGP, Window

F.7 Descriptive statistics for the developed equations

Descriptive statistics for DGPnew and UGPnew for the 12 analysis cases, for the data of Study I

Equation	N	Mean	Std. Error of Mean	95% Confidence Interval (mean)		Std. Deviation	Minimum	Maximum	Range
				Lower	Upper				
DGPnew, any glare, wall	94	0.723	0.012	0.119	0.698	0.747	0.514	0.897	0.384
DGPnew, any glare, window	90	0.600	0.018	0.176	0.563	0.636	0.317	0.885	0.568
DGPnew, disturbing, wall	94	0.201	0.009	0.182	0.220	0.092	0.039	0.383	0.343
DGPnew, disturbing, window	90	0.244	0.014	0.136	0.217	0.273	0.109	0.556	0.448
UGPnew, any glare, wall	94	0.691	0.012	0.667	0.715	0.116	0.421	0.858	0.436
UGPnew, any glare, window	90	0.567	0.015	0.538	0.597	0.141	0.166	0.826	0.660
UGPnew, disturbing, wall	94	0.169	0.007	0.154	0.184	0.072	0.009	0.270	0.262
UGPnew, disturbing, window	90	0.211	0.014	0.182	0.239	0.137	-0.139	0.479	0.619

Descriptive statistics for DGPlg(Ev)new, DGPnew and for UGPnew by level of glare, for the data of Study I.

Levels 'disturbing' and 'intolerable' are grouped as there is only a few cases of 'intolerable' glare for the dataset.

Descriptive statistics for the four DGplog(Ev)new equations, by level of glare

Equation	N	Mean	Std. Deviation	Std. Error	95% Confidence (mean)		Minimum	Maximum
DGplog(Ev)new, any glare, wall					Lower	Upper		
imperceptible	26	0.660	0.129	0.025	0.608	0.712	0.473	0.831
noticeable	49	0.728	0.140	0.020	0.688	0.768	0.465	1.268
disturbing&intolerable	19	0.801	0.173	0.040	0.717	0.884	0.589	1.471
Equation	N	Mean	Std. Deviation	Std. Error	95% Confidence (mean)		Minimum	Maximum
DGplog(Ev)new, any glare, window					Lower	Upper		
imperceptible	36	0.521	0.167	0.028	0.465	0.577	0.318	0.851
noticeable	32	0.621	0.158	0.028	0.564	0.678	0.319	0.866
disturbing&intolerable	22	0.699	0.164	0.035	0.626	0.772	0.320	0.887
Equation	N	Mean	Std. Deviation	Std. Error	95% Confidence Interval for Mean		Minimum	Maximum
DGplog(Ev)new, disturbing, wall					Lower	Upper		
imperceptible	26	0.149	0.110	0.022	0.104	0.193	-0.016	0.286
noticeable	49	0.205	0.117	0.017	0.172	0.239	-0.024	0.637
disturbing&intolerable	19	0.269	0.151	0.035	0.197	0.342	0.096	0.866
Equation	N	Mean	Std. Deviation	Std. Error	95% Confidence (mean)		Minimum	Maximum
DGplog(Ev)new, disturbing, window					Lower	Upper		
imperceptible	36	0.182	0.106	0.018	0.146	0.217	0.080	0.522
noticeable	32	0.233	0.116	0.021	0.191	0.275	0.083	0.566
disturbing&intolerable	22	0.364	0.240	0.051	0.258	0.471	0.098	1.020

Descriptive statistics for the four DGpnew, by level of glare

Equation	N	Mean	Std. Deviation	Std. Error	95% Confidence Interval for Mean		Minimum	Maximum
DGpnew, any glare, wall					Lower	Upper		
imperceptible	26	0.674	0.133	0.026	0.620	0.728	0.514	0.872
noticeable	49	0.732	0.119	0.017	0.698	0.766	0.514	0.897
disturbing&intolerable	19	0.769	0.064	0.015	0.738	0.800	0.534	0.853
Equation	N	Mean	Std. Deviation	Std. Error	95% Confidence Interval for Mean		Minimum	Maximum
DGpnew, any glare, window					Lower	Upper		
imperceptible	36	0.521	0.167	0.028	0.464	0.577	0.317	0.850
noticeable	32	0.621	0.158	0.028	0.564	0.678	0.317	0.866
disturbing&intolerable	22	0.699	0.164	0.035	0.626	0.772	0.318	0.885
Equation	N	Mean	Std. Deviation	Std. Error	95% Confidence Interval for Mean		Minimum	Maximum
DGpnew, disturbing, wall					Lower	Upper		
imperceptible	26	0.169	0.103	0.020	0.127	0.210	0.040	0.309
noticeable	49	0.205	0.094	0.013	0.178	0.232	0.039	0.383
disturbing&intolerable	19	0.235	0.045	0.010	0.213	0.257	0.132	0.307
Equation	N	Mean	Std. Deviation	Std. Error	95% Confidence Interval for Mean		Minimum	Maximum
DGpnew, disturbing, window					Lower	Upper		
imperceptible	36	0.189	0.107	0.018	0.153	0.225	0.109	0.491
noticeable	32	0.251	0.131	0.023	0.204	0.298	0.109	0.556
disturbing&intolerable	22	0.326	0.147	0.031	0.261	0.391	0.113	0.529

The original DGP equation was developed based on the percentage of persons that report glare when glare is voted as 'disturbing' and therefore the DGP thresholds for the different levels of glare are more directly comparable to the means obtained for the 'disturbing glare' equations of the DGPnew.

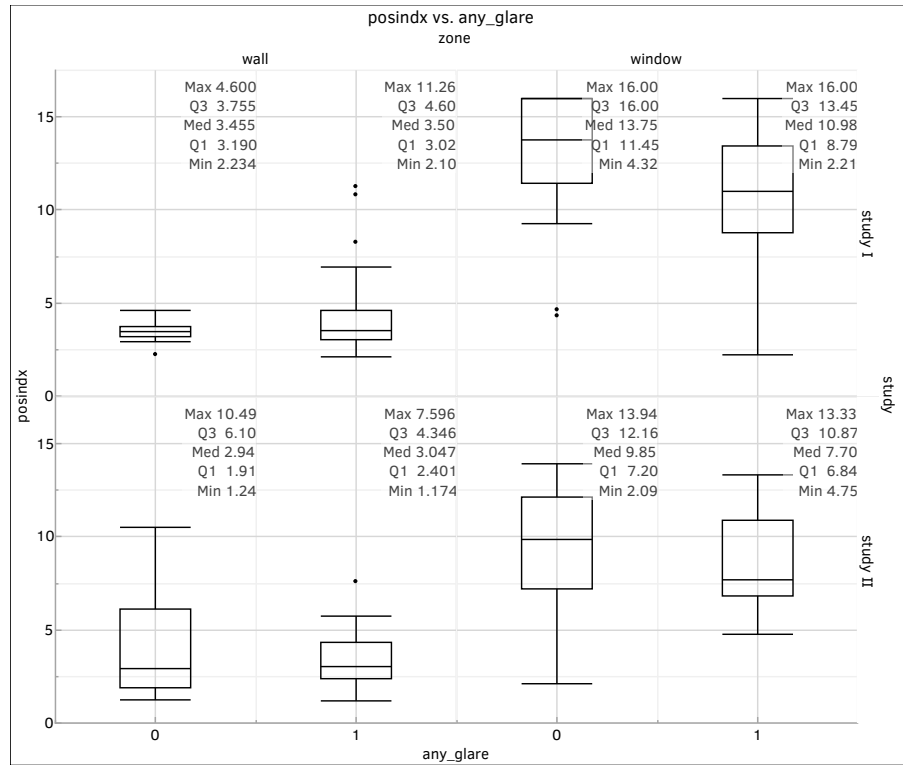
Descriptive statistics for the four UGPnew, by level of glare

Equation	N	Mean	Std. Deviation	Std. Error	95% Confidence Interval for Mean		Minimum	Maximum
UGPnew, any glare, wall					Lower	Upper		
imperceptible	26	0.646	0.129	0.025	0.595	0.698	0.466	0.846
noticeable	49	0.700	0.115	0.016	0.667	0.733	0.479	0.858
disturbing&intolerable	19	0.731	0.080	0.018	0.692	0.769	0.421	0.816
UGPnew, any glare, window					Lower	Upper		
imperceptible	36	0.520	0.139	0.023	0.473	0.567	0.166	0.767
noticeable	32	0.576	0.115	0.020	0.535	0.617	0.380	0.792
disturbing&intolerable	22	0.631	0.156	0.033	0.562	0.700	0.272	0.826
UGPnew, disturbing, wall					Lower	Upper		
imperceptible	26	0.141	0.080	0.016	0.109	0.173	0.035	0.263
noticeable	49	0.174	0.071	0.010	0.154	0.194	0.043	0.270
disturbing&intolerable	19	0.194	0.048	0.011	0.171	0.217	0.009	0.245
UGPnew, disturbing, window					Lower	Upper		
imperceptible	36	0.151	0.121	0.020	0.110	0.192	-0.139	0.424
noticeable	32	0.224	0.114	0.020	0.183	0.265	0.061	0.448
disturbing&intolerable	22	0.289	0.151	0.032	0.222	0.356	-0.040	0.479

Design guidelines

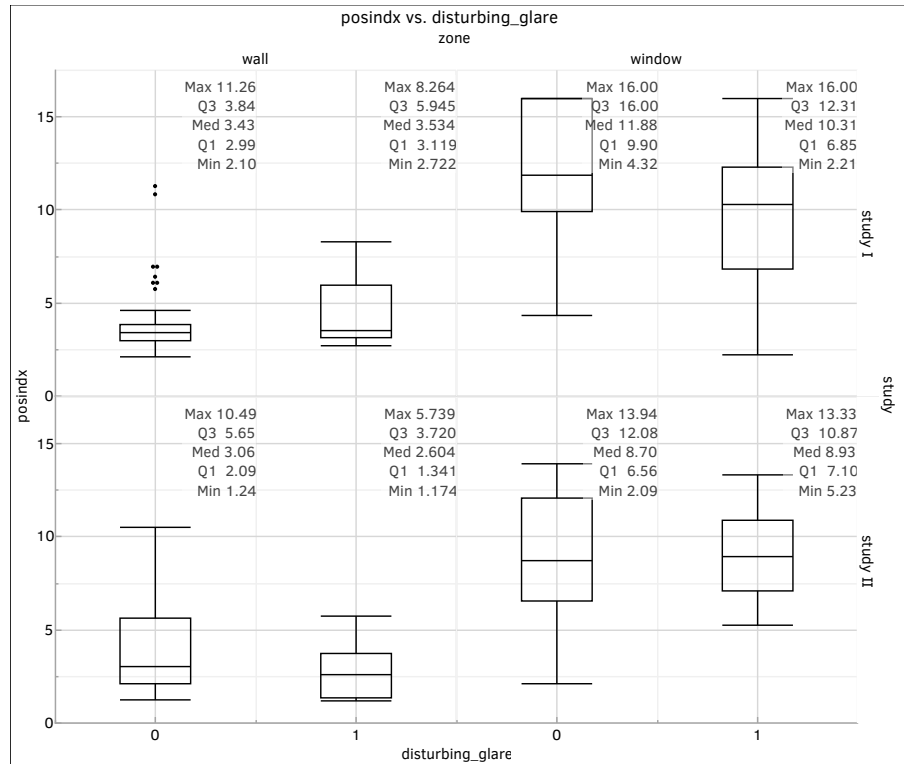
Descriptive statistics for the Position Index (P) for situations where a glare source was identified ($L_s > 2,000 \text{ cd/m}^2$), for the 'any glare' definition; 0 = no glare identified by the subjects, 1 = glare identified by the subjects.

The median P when glare is identified is as low as 3 in the wall zone and 7.7 in the window zone.



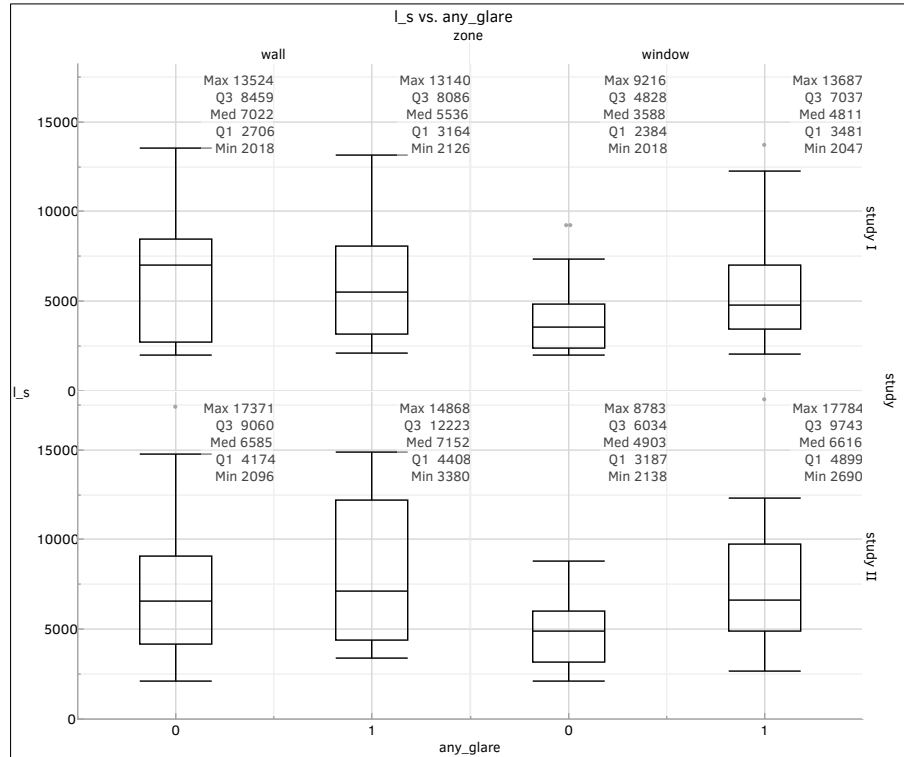
Descriptive statistics for the Position Index (P) for situations where a glare source was identified ($L_s \geq 2,000 \text{ cd/m}^2$), for the 'disturbing glare' definition; 0 = no glare identified by the subjects, 1 = glare identified by the subjects.

The median P when glare is identified is as low as 2.6 for wall zone and 8.9 for window zone.

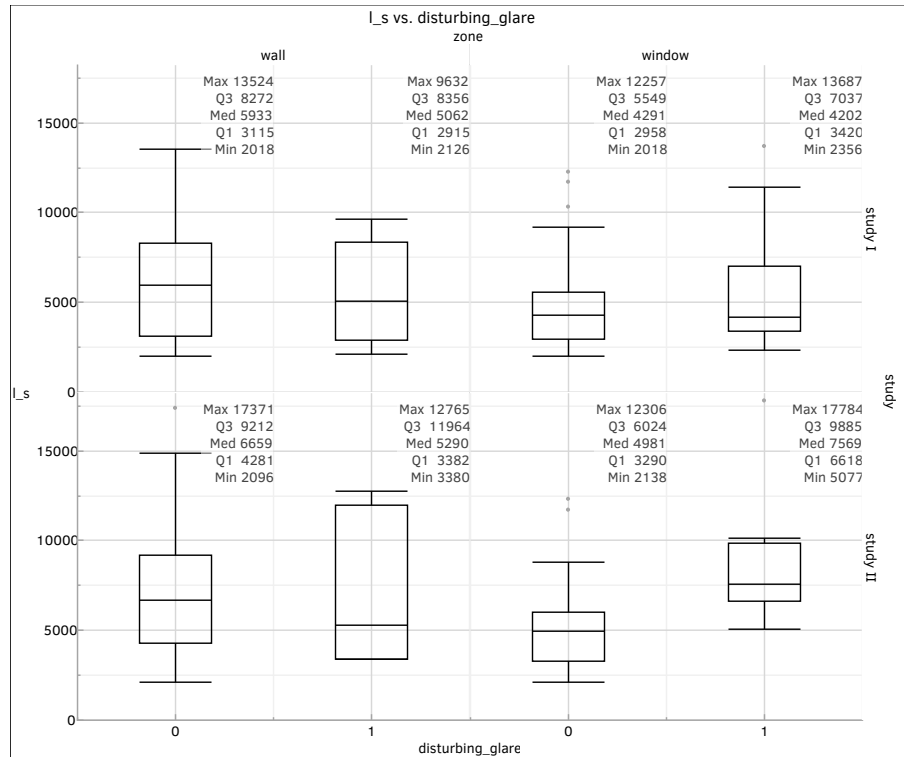


Descriptive statistics for the glare source luminance (Ls) and 'any glare' definition, for situations where a glare source was identified (Ls >= 2,000 cd/m2) and for the situations without sun in the field of view; 0 = no glare identified by the subjects, 1 = glare identified by the subjects.

The median Ls when glare is identified is 5,540 – 7,152 cd/m2 in the wall zone and 4,800 – 6,616 cd/m2 in the window zone.

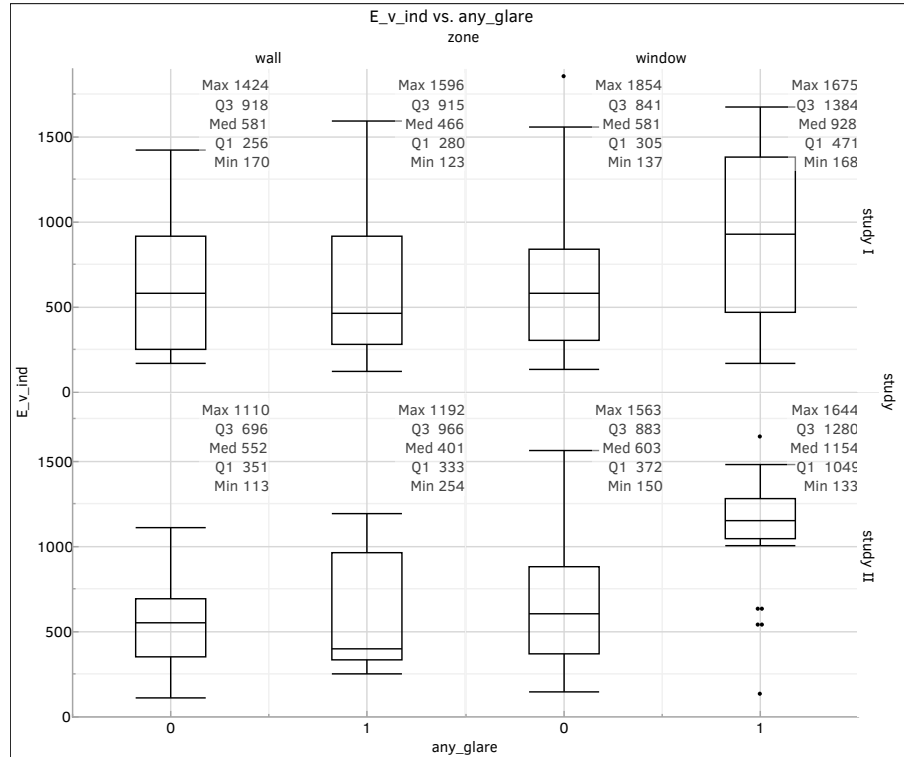


Descriptive statistics for the glare source luminance (Ls) and 'disturbing glare' definition, for situations where a glare source was identified (Ls >= 2,000 cd/m²) and for situations without sun in the field of view; 0 = no glare identified by the subjects, 1 = glare identified by the subjects. The median Ls when glare is identified is 5,062 – 5,290 cd/m² in the wall zone and 4,202 – 7,569 cd/m² in the window zone.

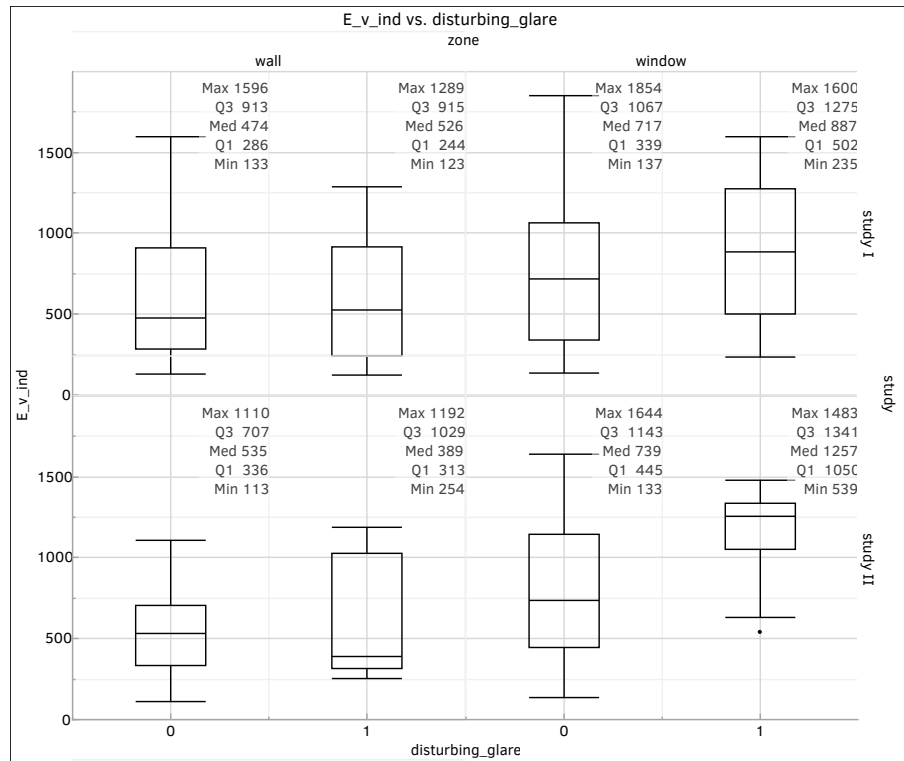


Descriptive statistics for the vertical illuminance of the background (E_{ind}) for situations where a glare source was identified (L_s ≥ 2,000 cd/m²), for the 'any glare' definition; 0 = no glare identified by the subjects, 1 = glare identified by the subjects.

The median E_{ind} when glare is identified is 466 - 401 lux in the wall zone and 471 - 1,154 lux in the window zone.



Descriptive statistics for the vertical illuminance of the background (E_{ind}) for situations where a glare source was identified (L_s ≥ 2,000 cd/m²), for the 'disturbing glare' definition; 0 = no glare identified by the subjects, 1 = glare identified by the subjects. The median E_{ind} when glare is identified is 526 – 389 lux in the wall zone and 887 – 1,257 lux in the window zone.



Data and code repository

Part of the analysis in this dissertation was carried out using open source software and scripting.

The research data that can be made public and the scripts that were produced for the statistical analysis are available in the TU Delft repository, 4TU.ResearchData (https://data.4tu.nl/categories/_/13362).

References

- Baker, N., Steemers, K., 2002. *Daylight Design of Buildings: A Handbook for Architects and Engineers*. Routledge, London.
- Barrett, P., Davies, F., Zhang, Y., Barrett, L., 2015. The impact of classroom design on pupils' learning: Final results of a holistic, multi-level analysis. *Building and Environment* 89, 118–133. <https://doi.org/10.1016/j.buildenv.2015.02.013>
- Bettonvil, F., 2005. Fisheye lenses. *Journal of the International Meteorological Organization* 33, 9–14.
- Boubekri, M., Boyer, L.L., 1992. Effect of window size and sunlight presence on glare: *Lighting Research & Technology*. <https://doi.org/10.1177/096032719202400203>
- Boyce, P.R., 2014. *Human Factors in Lighting*, 3rd ed. CRC Press, Boca Raton, London, New York.
- Carlucci, S., Causone, F., De Rosa, F., Pagliano, L., 2015. A review of indices for assessing visual comfort with a view to their use in optimization processes to support building integrated design. *Renewable and Sustainable Energy Reviews* 47, 1016–1033. <https://doi.org/10.1016/j.rser.2015.03.062>
- Champely, S., Ekstrom, C., Dalgaard, P., Gill, J., Weibelzahl, S., Anandkumar, A., Ford, C., Volcic, R., De Rosario, H., 2020. Package 'pwr,' Basic functions for Power Analysis. CRAN, Vienna.
- Charmant, J., 2019. Kinovea 8.15. <https://www.kinovea.org/download.html>
- Chauvel, P., Collins, J.B., Dogniaux, R., Longmore, J., 1982. Glare from windows: current views of the problem. *Lighting Research and Technology* 14, 31–46. <https://doi.org/10.1177/096032718201400103>
- CIE, 2002. CIE collection on glare. Commission Internationale de l'Éclairage, Technical committee TC 3.01 Discomfort Glare from Small and Large Sources, Division 1 and 3, Vienna, Austria.
- CIE, 1995. Discomfort Glare in Interior Lighting (No. CIE 117-1995). Commission Internationale de l'Éclairage, Technical Committee TC 3.13, Division 3, Vienna.
- CIE, 1983. Discomfort Glare in the Interior Working Environment (No. 55), TC-3.4. Vienna.
- Cohen, J., 1988. *Statistical Power Analysis for the Behavioral Sciences*. LEA. <https://doi.org/10.4324/9780203771587>
- Collingridge, D., 2014. Validating a Questionnaire. MethodSpace. URL <http://www.methodspace.com/validating-a-questionnaire/> (accessed 6.16.17).
- Comité Européen de Normalisation, 2018. NEN EN 17037 (en), Daglicht in gebouwen, Daylight in Buildings.
- Cook, R.D., Weisberg, S., 1982. *Residuals and Influence in Regression*. New York: Chapman and Hall.
- Coutelier, B., Dumortier, D., 2002. Luminance calibration of the Nikon Coolpix 990 digital camera. Application to glare evaluation. Presented at the 3rd AIVC and EPIC 2002 Conference, Energy efficient and healthy buildings in sustainable cities, AIVC, Lyon.
- Cumming, G., 2014. The New Statistics: Why and How. *Psychol Sci* 25, 7–29. <https://doi.org/10.1177/0956797613504966>
- Debevec, P., 1998. Rendering synthetic objects into real scenes: bridging traditional and image-based graphics with global illumination and high dynamic range photography, in: *Proceedings of the 25th Annual Conference on Computer Graphics and Interactive Techniques, SIGGRAPH '98*. Association for Computing Machinery, New York, NY, USA, pp. 189–198. <https://doi.org/10.1145/280814.280864>
- Debevec, P.E., Malik, J., 2008. Recovering High Dynamic Range Radiance Maps from Photographs, in: *ACM SIGGRAPH 2008 Classes, SIGGRAPH '08*. ACM, New York, NY, USA, p. 31:1-31:10. <https://doi.org/10.1145/1401132.1401174>
- DeLong, E.R., DeLong, D.M., Clarke-Pearson, D.L., 1988. Comparing the areas under two or more correlated receiver operating characteristic curves: a nonparametric approach., in: *Biometrics*. pp. 837–845.
- Department for Education and Skills, 2003. *Guidelines for environmental design in schools*, 2nd ed, Building Bulletin. England.
- Design for Climate & Comfort Lab, 2021. Spectral materials database [WWW Document]. <http://spectraldb.com/>.

- Dilaura, D.L., Houser, K.W., Mistrick, R.G., Steffy, G.R., 2011. *The Lighting Handbook: Reference and Application*, 10th ed. Illuminating Engineering Society of North America, New York.
- DIN, 1995. DIN 5032-6, Lichtmessung, Teil 6: Photometer, Begriffe, Eigenschaften und deren Kennzeichnung.
- DslrDashboard, 2017. qDslrDashboard V3.5.3. URL <https://dslrdashboard.info/v3-5-3-desktop-download-available/> (accessed 12.27.19).
- Dubois, M.-C., 2001. *Impact of Shading Devices on Daylight Quality in Offices* (Doctoral Thesis). Lund University, Lund.
- Dubois, M.-C., Gentile, N., Laike, T., Bournas, I., Alenius, M., 2019. *Daylighting and lighting under a Nordic sky*. Studentlitteratur AB.
- Education Funding Agency, 2014. *EFA daylight design guide* (Departmental Advice No. Version 2). London.
- Einhorn, H.D., 1979. Discomfort glare: a formula to bridge differences. *Lighting Research & Technology* 11, 90–94. <https://doi.org/10.1177/14771535790110020401>
- Einhorn, H.D., 1969. A new method for the assessment of discomfort glare. *Lighting Research & Technology* 1, 235–247. <https://doi.org/10.1177/14771535690010040201>
- Fan, D., Painter, B., Mardaljevic, J., 2009. A data collection method for long-term field studies of visual comfort in real-world daylit office environments.
- Fechner, G.T., 1860. *Elemente der Psychophysik*, Teil I, Originally published in 1860. Available in English as *Elements of psychophysics*, Rinehart and Winston, New York, 1966. Breitkopf und Härtel.
- Field, A., 2009. *Discovering Statistics with SPSS*, Third. ed. Sage, London.
- Fisekis, K., Davies, M., Kolokotroni, M., Langford, P., 2003. Prediction of discomfort glare from windows. *Lighting Research and Technology* 35, 360–369. <https://doi.org/10.1191/1365782803li0950a>
- Fotios, S., 2018. Correspondence: New methods for the evaluation of discomfort glare. *Lighting Research & Technology* 50, 489–491. <https://doi.org/10.1177/1477153518773577>
- Fotios, S., 2015. Research Note: Uncertainty in subjective evaluation of discomfort glare. *Lighting Research and Technology* 47, 379–383. <https://doi.org/10.1177/1477153515574985>
- Gall, D., Vandahl, C., Jordanow, W., Jordanowa, S., 2000. *Tageslicht und künstliche Beleuchtung: Bewertung von Lichtschutzeinrichtungen*. Schriftenreihe der Bundesanstalt für Arbeitsschutz und Arbeitsmedizin Fb.
- Hamedani, Z., Solgi, E., Skates, H., Hine, T., Fernando, R., Lyons, J., Dupre, K., 2019. Visual discomfort and glare assessment in office environments: A review of light-induced physiological and perceptual responses. *Building and Environment* 153, 267–280. <https://doi.org/10.1016/j.buildenv.2019.02.035>
- Hansen, P., Wienold, J., Andersen, M., 2017. HDR images for glare evaluation: comparison between DSLR cameras, an absolute calibrated luminance camera and a spot luminance meter, in: *Proceedings of the Conference at the CIE Midterm Meeting*. Presented at the CIE conference on Smarter Lighting for Better Life, CIE, Jeju, Korea. <https://doi.org/10.25039/x044.2017>
- Harvey, P., 2019. ExifTool [WWW Document]. URL <https://exiftool.org/> (accessed 12.27.19).
- Heschong Mahone Group, Inc., 2012. *Daylight Metrics*. PIER Daylighting Plus Research Programme. (Technical No. CEC-500-2012-053), Public Interest Energy Research. California Energy Commission, Gold River, California.
- Heschong Mahone Group, Inc., 2003a. *Daylighting In Schools: Reanalysis Report* (Technical No. P500- 03- 082- A-3), Public Interest Energy Research. California Energy Commission, Fair Oaks, California.
- Heschong Mahone Group, Inc., 2003b. *Windows and Classrooms: A Study of Student Performance and the Indoor Environment* (Technical No. P500- 03- 082- A-7), Public Interest Energy Research. California Energy Commission, Fair Oaks, California.
- Hirning, M.B., 2014. *The application of luminance mapping to discomfort glare : a modified glare index for green buildings* (Doctoral Thesis). Queensland University of Technology.
- Hirning, M.B., Isoardi, G.L., Cowling, I., 2014. Discomfort glare in open plan green buildings. *Energy and Buildings* 70, 427–440. <https://doi.org/10.1016/j.enbuild.2013.11.053>
- Hopkinson, R.G., 1972. Glare from daylighting in buildings. *Applied Ergonomics* 3, 206–215. [https://doi.org/10.1016/0003-6870\(72\)90102-0](https://doi.org/10.1016/0003-6870(72)90102-0)
- Hopkinson, R.G., 1956. Glare Discomfort and Pupil Diameter. *J. Opt. Soc. Am.*, JOSA 46, 649–656. <https://doi.org/10.1364/JOSA.46.000649>
- Hopkinson, R.G., 1949. *Studies of Lighting and Vision in Schools*. Transactions of the Illuminating Engineering Society 14, 244–268. <https://doi.org/10.1177/147715354901400802>
- Hopkinson, R.G., Collins, J.B., 1970. *The ergonomics of lighting*. Macdonald & Co, London.

- Hopkinson, R.G., Petherbridge, P., Longmore, J., 1966. Daylighting. Heinemann, London.
- IBM Corporation, 2016. IBM SPSS Statistics for Macintosh, 24.0. Armonk, NY.
- IESNA, 2012. IES LM-83-12 Approved Method: IES Spatial Daylight Autonomy (sDA) and Annual Sunlight Exposure (ASE), 1st ed. Illuminating Engineering Society, New York, NY.
- IESNA, 2000. The IESNA Lighting Handbook, Reference and Application, 9 edition. ed. Illuminating Engineering Society of North America, New York, NY.
- Inanici, M.N., 2006. Evaluation of high dynamic range photography as a luminance data acquisition system. *Lighting Research and Technology* 38, 123–134. <https://doi.org/10.1191/1365782806li1640a>
- International Energy Agency, 2018. Energy Efficiency 2018. Analysis and outlooks to 2040., Market Report Series. IEA/OECD, France.
- International WELL Building Institute, 2015. WELL Building Standard Educational Facilities Pilot Addendum. International WELL Building Institute pbc, New York, NY.
- Iwata, T., 1992. Experimental study on discomfort glare caused by windows, part 2 : Subjective response to glare from actual windows. *Journal of Architecture, Planning and Environmental Engineering* 439, 19–29.
- Iwata, T., Kimura, K.-I., Shukuya, M., Takano, K., 1990. Discomfort caused by wide-source glare. *Energy and Buildings* 15, 391–398. [https://doi.org/10.1016/0378-7788\(90\)90013-9](https://doi.org/10.1016/0378-7788(90)90013-9)
- Iwata, T., Tokura, M., 1997. Position Index for a glare source located below the line of vision. *Lighting Research and Technology* 29, 172–178. <https://doi.org/10.1177/14771535970290030801>
- Jacobs, A., 2012. Glare Measurement with HDR Photography. Presented at the 11th International Radiance Workshop, radiance-online.org, Copenhagen.
- Jacobs, A., 2007. High Dynamic Range Imaging and its Application in Building Research. *Advances in Building Energy Research* 1, 177–202. <https://doi.org/10.1080/17512549.2007.9687274>
- Jakubiec, J.A., 2016. Building a Database of Opaque Materials for Lighting Simulation, in: Proceedings of the 32nd International Conference on Passive and Low Energy Architecture. Presented at the PLEA 2016 Cities, Buildings, People: Towards Regenerative Environments, PLEA, Los Angeles.
- Jakubiec, J.A., Reinhart, C., 2013. Predicting Visual Comfort Conditions In A Large Daylit Space Based On Long-term Occupant Evaluations: A Field Study, in: Building Simulation 2013. Presented at the 13th Conference of International Building Performance Simulation Association, IBPSA, France, Chambéry, pp. 3408–3415.
- Jakubiec, J.A., Van Den Wymelenberg, K., Inanici, M., Mahic, A., 2016. Accurate measurement of daylight interior scenes using high dynamic range photography, in: Proceedings of the CIE 2016. Presented at the CIE 2016, Lighting Quality & Energy Efficiency, CIE, Melbourne, pp. 42–52.
- Jones, N.L., Reinhart, C.F., 2017. Experimental validation of ray tracing as a means of image-based visual discomfort prediction. *Building and Environment, Advances in daylighting and visual comfort research* 113, 131–150. <https://doi.org/10.1016/j.buildenv.2016.08.023>
- Karlsen, L., Heiselberg, P., Bryn, I., Johra, H., 2015. Verification of simple illuminance based measures for indication of discomfort glare from windows. *Building and Environment* 92, 615–626. <https://doi.org/10.1016/j.buildenv.2015.05.040>
- Kent, M.G., Fotios, S., Cheung, T., 2019. Stimulus range bias leads to different settings when using luminance adjustment to evaluate discomfort due to glare. *Building and Environment* 153, 281–287. <https://doi.org/10.1016/j.buildenv.2018.12.061>
- Kim, W., Kim, J.T., 2010. A distribution chart of glare sensation over the whole visual field. *Building and Environment* 45, 922–928. <https://doi.org/10.1016/j.buildenv.2009.09.013>
- Konica Minolta Sensing Americas, Inc, 2020. T-10A and T-10MA Illuminance Meters [WWW Document]. Konica Minolta. URL https://sensing.konicaminolta.us/us/products/t-10a_t-10ma-illuminance-meters/ (accessed 10.15.21).
- Konis, K., 2014. Predicting visual comfort in side-lit open-plan core zones: Results of a field study pairing high dynamic range images with subjective responses. *Energy and Buildings* 77, 67–79. <https://doi.org/10.1016/j.enbuild.2014.03.035>
- Konstantzos, I., Tzempelikos, A., 2017. Daylight glare evaluation with the sun in the field of view through window shades. *Building and Environment, Advances in daylighting and visual comfort research* 113, 65–77. <https://doi.org/10.1016/j.buildenv.2016.09.009>
- Köster, H., 2004. Dynamic daylighting architecture: basics, systems, projects. Birkhäuser, Basel.
- Larson, G.W., Shakespeare, R.A., 1998. Rendering with Radiance: Art and Science of Lighting Visualization. Morgan Kaufmann Publishers, San Francisco.

- Lee, E.S., Selkowitz, S.E., 2006. The New York Times Headquarters daylighting mockup: Monitored performance of the daylighting control system. *Energy and Buildings, Special Issue on Daylighting Buildings* 38, 914–929. <https://doi.org/10.1016/j.enbuild.2006.03.019>
- Li, D.H.W., Lam, T.N.T., Wong, S.L., 2006. Lighting and energy performance for an office using high frequency dimming controls. *Energy Conversion and Management* 47, 1133–1145. <https://doi.org/10.1016/j.enconman.2005.06.016>
- Lighting Research Center, 2004. Guide for Daylighting Schools (Technical No. DE-FC26-02NT41497), Daylight Dividends. Rensselaer Polytechnic Institute, New York, NY.
- Luckiesh, M., Guth, S.K., 1949. Brightnesses in Visual Field at Borderline Between Comfort and Discomfort (BCD). *Illuminating Engineering* 44, 650–670.
- Luckiesh, M., Guth, S.K., 1946. Discomfort glare and angular distance of glare source. *Illum Eng* 41, 485–492.
- Luckiesh, M., Holladay, L.L., 1925. Glare and Visibility. *Transactions of the Illuminating Engineering Society* 20.
- Mahić, A., Galiciano, K., Van Den Wymelenberg, K., 2017. A pilot daylighting field study: Testing the usefulness of laboratory-derived luminance-based metrics for building design and control. *Building and Environment, Advances in daylighting and visual comfort research* 113, 78–91. <https://doi.org/10.1016/j.buildenv.2016.11.024>
- Mardaljevic, J., Andersen, M., Roy, N., Christoffersen, J., 2012. Daylighting Metrics: Is there a relation between Useful Daylight Illuminance and Daylight Glare Probability?, in: *Proceedings of the First Building Simulation and Optimization Conference*. Presented at the BSO12, IBPSA-England, Loughborough, pp. 189–196.
- Marty, C., Fontoynt, M., Christoffersen, J., Dubois, M.-C., Wienold, J., Osterhaus, W., 2003. User assessment of visual comfort: Review of existing methods (Technical No. ECCO-Ingelux-200305-01), ECCO-build. Vaulx-en-Velin.
- Mathôt, S., 2016. Open Sesame. cogsci, Groningen.
- Mathôt, S., Schreij, D., Theeuwes, J., 2012. OpenSesame: An open-source, graphical experiment builder for the social sciences. *Behav Res* 44, 314–324. <https://doi.org/10.3758/s13428-011-0168-7>
- Nabil, A., Mardaljevic, J., 2006. Useful daylight illuminances: A replacement for daylight factors. *Energy and Buildings, Special Issue on Daylighting Buildings* 38, 905–913. <https://doi.org/10.1016/j.enbuild.2006.03.013>
- Nabil, A., Mardaljevic, J., 2005. Useful daylight illuminance: a new paradigm for assessing daylight in buildings. *Lighting Research & Technology* 37, 41–57. <https://doi.org/10.1191/1365782805li128oa>
- Nazzari, A.A., 2000. A New Daylight Glare Evaluation Method. *Journal of Light & Visual Environment* 24, 19–27. https://doi.org/10.2150/jlve.24.2_19
- New Buildings Institute, University of Idaho, University of Washington, 2021. Daylighting Pattern Guide [WWW Document]. Daylighting Pattern Guide. URL <http://patternguide.advancedbuildings.net/home>
- Onaygil, S., Güler, Ö., 2003. Determination of the energy saving by daylight responsive lighting control systems with an example from Istanbul. *Building and Environment* 38, 973–977. [https://doi.org/10.1016/S0360-1323\(03\)00034-9](https://doi.org/10.1016/S0360-1323(03)00034-9)
- Osterhaus, W., Bailey, I., 1992. Large area glare sources and their effect on visual discomfort and visual performance at computer workstations. Presented at the Industry Applications Society Annual Meeting, Lawrence Berkeley National Laboratory, Houston.
- Parque Escolar EPE, 2017. Especificações técnicas de arquitetura para projeto do edifício escolar. Direção Geral de Projeto e Gestão de Ativos, Lisboa.
- Petherbridge, P., Hopkinson, R.G., 1950. Discomfort Glare and the Lighting of Buildings. *Transactions of the Illuminating Engineering Society* 15, 39–79. <https://doi.org/10.1177/147715355001500201>
- Pierson, C., Wienold, J., Bodart, M., 2018. Daylight Discomfort Glare Evaluation with Evalglare: Influence of Parameters and Methods on the Accuracy of Discomfort Glare Prediction. *MDPI Buildings* 94, 1–33. <https://doi.org/10.3390/buildings8080094>
- Porsch, T., Schmidt, F., 2010. Assessment of daylight glare parameters with imaging luminance measuring devices (ILMD) and image processing.
- R Core Team, 2020. R: A language and environment for statistical computing. R Foundation for Statistical Computing, Vienna.
- Reinhard, E., Heidrich, W., Debevec, P., Pattanaik, S., Ward, G., Myszkowski, K., 2010. High Dynamic Range Imaging: Acquisition, Display, and Image-Based Lighting. Morgan Kaufmann.
- Rijksdienst voor Ondernemend Nederland, 2014. Programma van Eisen Frisse Scholen 2015. Utrecht.

- Rodriguez, R.G., Yamín Garretón, J.A., Pattini, A.E., 2017. An epidemiological approach to daylight discomfort glare. *Building and Environment, Advances in daylighting and visual comfort research* 113, 39–48. <https://doi.org/10.1016/j.buildenv.2016.09.028>
- Roisin, B., Bodart, M., Deneyer, A., D'Herdt, P., 2008. Lighting energy savings in offices using different control systems and their real consumption. *Energy and Buildings* 40, 514–523. <https://doi.org/10.1016/j.enbuild.2007.04.006>
- RStudio Team, 2020. RStudio: Integrated Development for R. RStudio, PBC, Boston, MA.
- SAS Institute Inc., 2019. JMP Pro 14, 14.1. Cary, NC.
- Scrucca, L., 2013a. GA version 3.2.1.
- Scrucca, L., 2013b. GA: A Package for Genetic Algorithms in R. *Journal of Statistical Software* 53, 1–37. <https://doi.org/10.18637/jss.v053.i04>
- Shin, J.Y., Yun, G.Y., Kim, J.T., 2012. View types and luminance effects on discomfort glare assessment from windows. *Energy and Buildings, Sustainable and healthy buildings* 46, 139–145. <https://doi.org/10.1016/j.enbuild.2011.10.036>
- Siegel, S., 1956. *Nonparametric statistics for the behavioral sciences*. McGraw-Hill, New York.
- Šimundić, A.-M., 2009. Measures of Diagnostic Accuracy: Basic Definitions. *EIJFCC* 19, 203–211.
- Society of Light and Lighting, 2018. *The SLL lighting handbook*. CIBSE Publications, London.
- Society of Light and Lighting, 2011. *SLL Lighting Guide 5: Lighting for Education*. Chartered Institution of Building Services Engineers.
- Society of Light and Lighting, National Physical Laboratory (Eds.), 2001. *LG 11 Surface reflectance and colour: its specification and measurement for designers, Lighting guide*. The Society of Light and Lighting, London.
- Spectra Partners, 2021. *Sphere Standard* [WWW Document]. Spectra Partners. URL <http://www.spectrapartners.nl/products/optical-radiation-standard/sphere-standard> (accessed 5.3.21).
- Stockman, A., 2020. *Luminous efficiency functions* [WWW Document]. Colour & Vision Research Laboratory, Institute of Ophthalmology, UCL. URL <http://www.cvrl.org/> (accessed 10.6.21).
- Stumpf, J., Tchou, C., Jones, A., Hawkins, T., Wenger, A., Debevec, P., 2004. Direct HDR Capture of the Sun and Sky, in: *Proceedings of the 3rd International Conference on Computer Graphics, Virtual Reality, Visualisation and Interaction in Africa, AFRIGRAPH '04*. ACM, New York, NY, pp. 145–149. <https://doi.org/10.1145/1029949.1029977>
- Suk, J.Y., Schiler, M., Kensek, K., 2016. Absolute glare factor and relative glare factor based metric: Predicting and quantifying levels of daylight glare in office space. *Energy and Buildings* 130, 8–19. <https://doi.org/10.1016/j.enbuild.2016.08.021>
- Technoteam, 2019. *LMK 6: video photometer* [WWW Document]. URL <http://www.technoteam.de/apool/tnt/content/e5183/e5432/e5733/e6645/>
- Technoteam, 2017. *LMK Labsoft 4 Standard Monochrome*. Technoteam Bildverarbeitung GmbH, Ilmenau.
- Technoteam, 2016. *LMK mobile air: camera photometer*. Technoteam Bildverarbeitung GmbH, Ilmenau.
- The Collaborative for High Performance Schools, 2006. *High performance schools best practices manual. Volume II. Design*. <https://chps.net/best-practices-manual>.
- The Society of Light and Lighting, 2012. *The SLL Code for Lighting*. CIBSE Publications, London.
- The Society of Light and Lighting, 2011. *Lighting Guide 5: Lighting for education*. CIBSE Publications, London.
- Tokura, M., Iwata, T., 1996. Experimental study on discomfort glare caused by windows - part 3: development of a method for evaluating discomfort glare from a large light source. *Journal of Architecture, Planning and Environmental Engineering* 489, 17–25.
- USGBC, 2019. *The WELL building standard v1 with Q3 addenda*. International WELL Building Institute pbc.
- USGBC, 2013. *LEED v4, Reference Guide for Building Design and Construction*. USGBC.
- Van Den Wymelenberg, K., 2012. *Evaluating Human Visual Preference and Performance in an Office Environment Using Luminance-based Metrics* (Doctoral Thesis).
- Van Den Wymelenberg, K., Inanici, M., 2015. Evaluating a New Suite of Luminance-Based Design Metrics for Predicting Human Visual Comfort in Offices with Daylight. *LEUKOS* 0, 1–26. <https://doi.org/10.1080/15502724.2015.1062392>
- Van Den Wymelenberg, K., Inanici, M., 2014. A Critical Investigation of Common Lighting Design Metrics for Predicting Human Visual Comfort in Offices with Daylight. *LEUKOS* 10, 145–164. <https://doi.org/10.1080/15502724.2014.881720>

- Van Den Wymelenberg, K., Inanici, M., Johnson, P., 2010. The Effect of Luminance Distribution Patterns on Occupant Preference in a Daylit Office Environment. *LEUKOS* 7, 103–122. <https://doi.org/10.1582/LEUKOS.2010.07.02003>
- Veitch, J.A., Newsham, G.R., 1998. Determinants of Lighting Quality I: State of the Science. *Journal of the Illuminating Engineering Society* 27, 92–106. <https://doi.org/10.1080/00994480.1998.10748215>
- Velds, M., 2002. User acceptance studies to evaluate discomfort glare in daylit rooms. *Solar Energy, Daylighting* 73, 95–103. [https://doi.org/10.1016/S0038-092X\(02\)00037-3](https://doi.org/10.1016/S0038-092X(02)00037-3)
- Velds, M., 1999. Assessment of lighting quality in office rooms with daylighting systems (Doctoral Thesis). Technische Universiteit Delft, Delft.
- Wagdy, A., Garcia-Hansen, V., Isoardi, G., Pham, K., 2019. A Parametric Method for Remapping and Calibrating Fisheye Images for Glare Analysis. *Buildings* 9, 219. <https://doi.org/10.3390/buildings9100219>
- Ward, G., 2018a. Radiance Reference: Manual Pages: findglare. Lawrence Berkeley National Laboratory, https://floyd.lbl.gov/radiance/man_html/findglare.1.html.
- Ward, G., 2018b. Radiance 5.0.a.12 Darwin. NREL, Denver.
- Ward, G., 1991. Real Pixels, in: Arvo, J. (Ed.), *Graphics Gems II*. Academic Press Inc., pp. 80–83.
- Ward, G.J., 1994. The RADIANCE Lighting Simulation and Rendering System, in: *Proceedings of the 21st Annual Conference on Computer Graphics and Interactive Techniques, SIGGRAPH '94*. ACM, New York, NY, USA, pp. 459–472. <https://doi.org/10.1145/192161.192286>
- Waters, C.E., Mistrick, R.G., Bernecker, C.A., 1995. Discomfort Glare from Sources of Nonuniform Luminance. *Journal of the Illuminating Engineering Society* 24, 73–85. <https://doi.org/10.1080/00994480.1995.10748120>
- Wienold, J., 2019. Evalglare 2.09. EPFL, Lausanne.
- Wienold, J., 2017a. Evalglare 2.02. EPFL, Lausanne.
- Wienold, J., 2017b. pftopic. Fraunhofer Institute for Solar Energy Systems, Freiburg.
- Wienold, J., 2014. Daylight Glare analysis and metrics. Presented at the 13th Radiance Workshop, radiance-online.org, London, UK.
- Wienold, J., 2012a. Evalglare – A Radiance based tool for glare evaluation. Presented at the 11th International Radiance Workshop, radiance-online.org, Copenhagen.
- Wienold, J., 2012b. Evalglare Manual, Version 1.0. Fraunhofer Institute for Solar Energy Systems, Freiburg.
- Wienold, J., 2010. Daylight glare in offices (Doctoral Thesis). Fraunhofer Verlag, Stuttgart.
- Wienold, J., 2009. Dynamic daylight glare evaluation, in: *Building Simulation 2009*. Presented at the Eleventh International IBPSA Conference, IBPSA, Glasgow, pp. 944–951.
- Wienold, J., 2007. Dynamic simulation of blind control strategies for visual comfort and energy balance analysis, in: *Proceedings: Building Simulation 2007*. Presented at the 10th International Building Performance Simulation Association Conference and Exhibition, pp. 1197–1204.
- Wienold, J., Christoffersen, J., 2006. Evaluation methods and development of a new glare prediction model for daylight environments with the use of CCD cameras. *Energy and Buildings, Special Issue on Daylighting Buildings* 38, 743–757. <https://doi.org/10.1016/j.enbuild.2006.03.017>
- Wienold, J., Iwata, T., Sarey Khanie, M., Erell, E., Kaftan, E., Rodriguez, R., Yamin Garretón, J., Tzempelikos, T., Konstantzos, I., Christoffersen, J., Kuhn, T., Pierson, C., Andersen, M., 2019. Cross-validation and robustness of daylight glare metrics. *Lighting Research & Technology* 51, 983–1013. <https://doi.org/10.1177/1477153519826003>
- Wienold, J., Kuhn, T., Christoffersen, J., Sarey Khanie, M., Andersen, M., 2017. Comparison of luminance based metrics in different lighting conditions, in: *CIE 2017 Midterm Meeting, Smarter Lighting for Better Life*. Presented at the CIE 2017 Midterm meeting, CIE, Republic of Korea, Jeju.
- Yamin Garretón, J.A., Colombo, E.M., Pattini, A.E., 2018. A global evaluation of discomfort glare metrics in real office spaces with presence of direct sunlight. *Energy and Buildings* 166, 145–153. <https://doi.org/10.1016/j.enbuild.2018.01.024>
- Yamin Garretón, J.A., Rodriguez, R.G., Ruiz, A., Pattini, A.E., 2015. Degree of eye opening: A new discomfort glare indicator. *Building and Environment, Interactions between human and building environment* 88, 142–150. <https://doi.org/10.1016/j.buildenv.2014.11.010>
- Zwinkels, J., 2016. Light, Electromagnetic Spectrum, in: Luo, M.R. (Ed.), *Encyclopedia of Color Science and Technology*. Springer, New York, NY, pp. 843–849. https://doi.org/10.1007/978-1-4419-8071-7_204

Biography

Raquel Viula

born in Funchal, Portugal

e-mail:

- r.j.a.v.viula@tudelft.nl
- raquel.viula@gmail.com web:
- <http://pt.linkedin.com/in/raquelviula>

Raquel is an architect and urban designer, graduated at the Faculty of Architecture, TU Lisbon, in 1997. Following her studies, she joined the award-winning practice of Paulo David Arquitecto where she worked on a range of building and interior design projects and collaborated with a range of other Portuguese architecture offices. In 2001 she moved to London to do a Masters in Advanced Environmental and Energy Studies at the University of East London, which she completed in 2003.

Between 2004 and 2010, Raquel worked as an Environmental Design Analyst at Foster + Partners in London, becoming an Associate Partner in 2009. At Foster + Partners Raquel worked in the Specialist Modelling Group, an in-house support team that provides advice to the design teams in the fields of geometry, parametric and performance-driven design and where she was in charge of the environmental performance simulation and analysis work. In this position she developed an expertise on the analysis of thermal, energy, solar, daylighting and airflow performance of buildings. She was also a founding member of the company's Sustainability Forum and the coordinator of the environmental design work of a range of projects.

In 2010, Raquel moved back to Portugal to work as an independent Environmental Design Consultant. In this position she provided strategic advice regarding a project's environmental design concept and design advice based on performance simulation and analysis, to a range of architectural design firms.

Raquel joined Broadway Malyan in Lisbon as a Sustainability Advisor in 2014. In this role, she provided advice towards the integration of sustainability in the design process, by developing project support tools to align the design process with the requirements of LEED, BREEAM and Estidama green building certification systems and with the UK's Government Soft Landings recommendations and guidance.

In 2014 she earned an individual scholarship from the Portuguese Foundation for Science and Technology to pursue doctoral studies at the TU Delft in The Netherlands, starting her PhD research in the Building Physics and Services group of the Faculty of Architecture and the Built Environment in 2015. In parallel, Raquel has been working with fellow PhD colleagues in a cross-country research project, DAYKE, an investigation on the knowledge of daylighting among future architecture professionals and the aspects contributing to the development of that knowledge.

In 2018, Raquel moved to Göteborg in Sweden where she currently lives and plans to continue her professional career.

Personal awards

- Scholarship by the Portuguese Foundation for Science and Technology (FCT), to pursue doctoral studies at the TU Delft in the Netherlands.
- 1st Prize in Architectural competition (FPM41, Lisbon), with Barbas Lopes Arquitectos.
- 2nd Prize in Architecture competition (NEST – Allerød, Denmark), with OpenLab Architects.
- Scholarship by the Centre for Science and Technology of Madeira (CITMA), to pursue Master studies.

Publications

Viula, R. Bokel, R. Tenpierik, M. (2021). Discomfort glare from daylight in classrooms: proposal for a revised predictive model. *Lighting Research & Technology*. (Manuscript under consideration).

Viula, R., & Hordijk, T. (2019). Testing the predictive power of visual discomfort from glare metrics in the near-window and near-wall zones of the daylit classroom environment. In *Proceedings of the 29th CIE Session, Washington D.C., USA, June 14 – 22, 2019* (pp. 282-294). Commission Internationale de l'Eclairage.

Viula, R., & Hordijk, T. (2019). A method for estimating fisheye lens' field-of view angle and projection for HDR luminance capture. In *Proceedings of the 29th CIE Session, Washington D.C., USA, June 14 – 22, 2019* (pp. 1108-1112). Commission Internationale de l'Eclairage.

Viula, R. & Hordijk, T., 2017, Metrics to predict visual discomfort in a daylit classroom, *Proceedings of the Lux Europa 2017 Conference: Lighting for a modern society*. Kobav, M.B. (ed.). Ljubljana: Lighting Engineering Society of Slovenia, p. 389-394.

Other publications

Giuliani, F., Sokol, N., Lo Verso, V. R. M., Viula, R., Caffaro, F., Paule, B., Diakite, A., & Sutter, Y. (2021) A study about daylighting knowledge and education in Europe. Results from the first phase of the DAYKE project, *Architectural Science Review*, 64:1-2, 169-181

Giuliani, F., Sokol, N., Lo Verso, V.R.M., Caffaro, F., Diakite, A.; Viula, R., Paule, B., 2018, Daylighting education in practice: verification of a new goal within a European knowledge investigation. In *proceedings of the 34th international conference on Passive and Low Energy Architecture (PLEA): smart and healthy within the two-degree limit*, Ng, E., Fong, S., Ren, C. (ed.), Vol. 2, p. 886-891.

Giuliani, F., Sokol, N., Viula, R., Lo Verso, V.R.M., Coch Roura, H. & Caffaro, F., 2017, First outcomes of an investigation about daylighting knowledge and education in Europe, Proceedings of the Lux Europa 2017 Conference: Lighting for a modern society. Kobav, M.B. (ed.). Ljubljana: Lighting Engineering Society of Slovenia, p. 469-474.

Discomfort glare from daylight in classrooms

Raquel Viula

Provision of daylight without the risk of discomfort glare is one of the aspects that determine the quality of the classroom environment. Although discomfort glare from daylight is under investigation for a long time, a knowledge gap concerning the applicability of the existing metrics to the spatial conditions of the classroom is identified in this work. An investigation on the applicability of existing metrics to the prediction of discomfort glare in classrooms has been carried out based on two experimental studies. The analysis shows that the existing metrics have poor predictive ability particularly in the sitting positions away from the window light source. A study is then carried out to investigate how can more appropriate predictive models of discomfort glare be developed, based on three different methods. A modification of the Daylight Glare Probability (DGP) equation produced a significantly better discomfort glare model than any of the metrics that have been studied in this work. Following this finding, a new metric, $DGP_{log}(E_{v, new})$, is proposed. The produced metric suggests that discomfort glare in the classroom is better identified based on a range of equations for different sitting positions or that new variables that account for sitting position need to be included in a predictive model of discomfort glare for these spaces. A set of architectural design guidelines towards a discomfort glare free classroom is then proposed, based on the newly produced model and on the collected data.

A+BE | Architecture and the Built Environment | TU Delft BK